frontiers | Research Topics

Case reports in cardio-oncology 2022

Edited by
Carlo Gabriele Tocchetti and Reto Asmis

Published in
Frontiers in Cardiovascular Medicine
Frontiers in Oncology

FRONTIERS EBOOK COPYRIGHT STATEMENT

The copyright in the text of individual articles in this ebook is the property of their respective authors or their respective institutions or funders. The copyright in graphics and images within each article may be subject to copyright of other parties. In both cases this is subject to a license granted to Frontiers.

The compilation of articles constituting this ebook is the property of Frontiers.

Each article within this ebook, and the ebook itself, are published under the most recent version of the Creative Commons CC-BY licence. The version current at the date of publication of this ebook is CC-BY 4.0. If the CC-BY licence is updated, the licence granted by Frontiers is automatically updated to the new version.

When exercising any right under the CC-BY licence, Frontiers must be attributed as the original publisher of the article or ebook, as applicable.

Authors have the responsibility of ensuring that any graphics or other materials which are the property of others may be included in the CC-BY licence, but this should be checked before relying on the CC-BY licence to reproduce those materials. Any copyright notices relating to those materials must be complied with.

Copyright and source acknowledgement notices may not be removed and must be displayed in any copy, derivative work or partial copy which includes the elements in question.

All copyright, and all rights therein, are protected by national and international copyright laws. The above represents a summary only. For further information please read Frontiers' Conditions for Website Use and Copyright Statement, and the applicable CC-BY licence.

ISSN 1664-8714
ISBN 978-2-8325-3114-3
DOI 10.3389/978-2-8325-3114-3

About Frontiers

Frontiers is more than just an open access publisher of scholarly articles: it is a pioneering approach to the world of academia, radically improving the way scholarly research is managed. The grand vision of Frontiers is a world where all people have an equal opportunity to seek, share and generate knowledge. Frontiers provides immediate and permanent online open access to all its publications, but this alone is not enough to realize our grand goals.

Frontiers journal series

The Frontiers journal series is a multi-tier and interdisciplinary set of open-access, online journals, promising a paradigm shift from the current review, selection and dissemination processes in academic publishing. All Frontiers journals are driven by researchers for researchers; therefore, they constitute a service to the scholarly community. At the same time, the *Frontiers journal series* operates on a revolutionary invention, the tiered publishing system, initially addressing specific communities of scholars, and gradually climbing up to broader public understanding, thus serving the interests of the lay society, too.

Dedication to quality

Each Frontiers article is a landmark of the highest quality, thanks to genuinely collaborative interactions between authors and review editors, who include some of the world's best academicians. Research must be certified by peers before entering a stream of knowledge that may eventually reach the public - and shape society; therefore, Frontiers only applies the most rigorous and unbiased reviews. Frontiers revolutionizes research publishing by freely delivering the most outstanding research, evaluated with no bias from both the academic and social point of view. By applying the most advanced information technologies, Frontiers is catapulting scholarly publishing into a new generation.

What are Frontiers Research Topics?

Frontiers Research Topics are very popular trademarks of the *Frontiers journals series*: they are collections of at least ten articles, all centered on a particular subject. With their unique mix of varied contributions from Original Research to Review Articles, Frontiers Research Topics unify the most influential researchers, the latest key findings and historical advances in a hot research area.

Find out more on how to host your own Frontiers Research Topic or contribute to one as an author by contacting the Frontiers editorial office: frontiersin.org/about/contact

Case reports in cardio-oncology: 2022

Topic editors

Carlo Gabriele Tocchetti — University of Naples Federico II, Italy

Reto Asmis — Wake Forest University, United States

Citation

Tocchetti, C. G., Asmis, R., eds. (2023). *Case reports in cardio-oncology: 2022*. Lausanne: Frontiers Media SA. doi: 10.3389/978-2-8325-3114-3

Table of contents

07 Editorial: Case reports in cardio-oncology: 2022
Michael S. Ewer, Syed Wamique Yusuf, Reto Asmis and Jun-ichi Abe

11 Case Report: The Neuromusclar Triad of Immune Checkpoint Inhibitors: A Case Report of Myositis, Myocarditis, and Myasthenia Gravis Overlap Following Toripalimab Treatment
Yue-Bei Luo, Weiting Tang, Qiuming Zeng, Weiwei Duan, Shuyu Li, Xiaosu Yang and Fangfang Bi

16 Case Report: A Primary Right Ventricular Vascular Malformation Presenting as a Mass
Hongduan Liu, Xin Li, Cuiwei Zhang, Chengming Fan, Liming Liu and Juyi Wan

21 Case Report: An Unusual Cause for Recurrent Hemopericardium in a Patient With Dyspnea
Uyên Châu Nguyên, Astrid I. P. Vernemmen, Patrique Segers, Axel zur Hausen, Rob G. H. Driessen, Maurice J. H. M. Pluijmen and Sebastiaan C. A. M. Bekkers

27 Capecitabine and Warfarin Interaction: A Case Report With Review of Literature and Management Options
Khalefa Althiab, Manal Aljohani, Sultan Alraddadi and Mohammed Algarni

34 Case Report: Cardiac Tamponade in Association With Cytokine Release Syndrome Following CAR-T Cell Therapy
Shohei Moriyama, Mitsuhiro Fukata, Taku Yokoyama, Shohei Ueno, Takuya Nunomura, Yasuo Mori, Koji Kato, Toshihiro Miyamoto and Koichi Akashi

41 Successful Therapy for Myocarditis Concomitant With Complete Heart Block After Pembrolizumab Treatment for Head and Neck Squamous Cell Carcinoma: A Case Report With Literature Review
Lina Su, Chuanfen Liu, Wenjie Wu, Yuxia Cui, Manyan Wu and Hong Chen

49 Case Report: Torsade de Pointes Induced by the Third-Generation Epidermal Growth Factor Receptor–Tyrosine Kinase Inhibitor Osimertinib Combined With Litsea Cubeba
Xia-yan Zhang, Cha-bin Wu, Cai-xia Wu, Li Lin, Yue-juan Zhou, Yan-yan Zhu, Wei-qiang Tian and Song-mei Luo

55 Surgical treatment of giant right ventricular fibroma for a newborn: A case report
Yuhang Liu, Ning Wang and Ping Wen

59 Case report: Primary cardiac angiosarcoma with multiple metastases
Xuan Li, Lan Lan and Huijuan Hu

65 Case report: Minimally invasive excision of multifocal cardiac papillary fibroelastomas involving right atrium and aortic valve
Peng Teng, Peng Hu, Shuai Yuan and Liang Ma

70 Successful immune checkpoint inhibitor rechallenge after immune-related pericarditis: Clinical case series
Adrian M. Chye, Ina I. C. Nordman and Aaron L. Sverdlov

76 Genetics and clinical phenotype of Erdheim–Chester disease: A case report of constrictive pericarditis and a systematic review of the literature
Lorenzo Bartoli, Francesco Angeli, Andrea Stefanizzi, Michele Fabrizio, Pasquale Paolisso, Luca Bergamaschi, Alessandro Broccoli, Pier Luigi Zinzani, Nazzareno Galiè, Paola Rucci, Alberto Foà and Carmine Pizzi

85 Case report: A primary calcified cardiac mass in right atrium partially obstructs the tricuspid valve in a patient on hemodialysis
Hongduan Liu, Xiaokang Tu, Hao Zhang, Chengming Fan, Haoyu Tan, Long Song, Qin Wu and Liming Liu

90 Case report: Recurrent syncope as initial symptom in a patient with neck lymphoma
Yanfang Wu, Deyan Yang, Luxi Sun, Xiqi Xu, Peng Gao, Kangan Cheng, Taibo Chen, Zhongwei Cheng, Yongtai Liu and Quan Fang

96 Rare pulmonary embolism in a pregnant patient: A primary diffused pulmonary artery myxofibrosarcoma case report
Kanghui Xiang, Lu Liu, Hui-Jun Li and Guang-Wei Zhang

101 Diagnosis of rapidly progressed primary cardiac lymphoma in liver transplant recipient: A case report
Jianghua Li, Qiyun Liu, Quanzhou Peng and Shaohong Dong

106 Case report: Evaluation of myocardial microcirculation in patients with breast cancer after anthracycline chemotherapy by using intravoxel incoherent motion imaging
Shilan Li, Di Tian, Xin Li, Jia Li, Qingwei Song, Yunlong Xia and Zhiyong Li

112 Overdrive pacing in the acute management of osimertinib-induced ventricular arrhythmias: A case report and literature review
Yanyu Zhang, Xingtong Wang, Yilin Pan, Beibei Du, Kumaraswamy Nanthakumar and Ping Yang

118 The surgical strategy of hormonally active primary cardiac paraganglioma sarcoma: A case report
Xiangyu Wang, Haiyuan Liu, Shuaipeng Zhang, Shaojun Huang and Chengxin Zhang

124 Immune myocarditis related to sintilimab treatment in a patient with advanced lung adenocarcinoma: A case report
Yunling Lin, Xun Yuan and Lianglong Chen

130 A case report of primary cardiac angiosarcoma with *DNMT3A* gene mutation
Kun Tian, Yating Liu, Haiying Zhu, Tao Wang, Tianxing Chen, Xiaxia Pei and Feixue Song

138 Cardiac venous malformation concurrent with multiple hepatic venous malformations: A case report
Shijie Zhang, Zhenqiang Xu, Chengwei Zou and Gang Zhang

143 A case report of melanotic neuroectodermal tumor of infancy complicated with congenital heart disease and hypothyroidism
Hua-Chu Zuo, Jin-Yue Huang, Xiao-Li Hu and Lin-Sheng Zhao

152 Takotsubo cardiomyopathy Afatinib-related in a non-small cell lung cancer patient: Case report
German E. Ramos, Christian Caglevic, Juan F. Bulnes, Sergio E. Panay, Mario I. Zapata, Andrés J. Daniele and Manuel E. Rodríguez

160 Extranodal natural killer/T-cell lymphoma invading a patient's heart: A rare case report and literature review
Yifei Xiang, Xueqin Lin, Xiaoling Cai, Shuang Qu and Kai-Yang Lin

166 Anti-immunoglobulin-like transcript 3 induced acute myocarditis—A case report
Osnat Itzhaki Ben Zadok, Arthur Shiyovich, Ashraf Hamdan, Moshe Yeshurun, Inbar Nardi Agmon, Pia Raanani, Ran Kornowski and Liat Shargian

170 Case report: Metastatic melanoma masquerading as apical hypertrophic cardiomyopathy
Muddasir Ashraf, Arshad Jahangir, M. Fuad Jan, Lakshmi Muthukumar, Gary Neitzel and A. Jamil Tajik

176 Case report: Persistent ST-segment elevation due to cardiac metastasis from lung cancer
Jiawei Zhou, Chengchuang Zhan, Jing Zhou, Chao Wei and Cao Zou

181 Case report: The diagnostic challenge of primary cardiac intimal sarcoma
Naili Ye, Lan Lan, Huijuan Hu, Jinping Liu and Haibo Xu

186 A case report of sudden cardiac arrest and torsade de pointes induced by the second-generation tyrosine kinase inhibitor dasatinib combined with fluconazole
Yuting Yuan, Chunjian Wang and Hongying Yao

191 Surgical resection of a giant cardiac angiosarcoma and reconstruction of involved right heart structures: A case report
Andreea Blindaru, Alexandru Vasilescu, Andrei Danet, Oana Zimnicaru, Maximilian Cristu, Stefan Tudorica, Tudor Borjog, Oana Patrascu and Catalin Constantin Badiu

195 Case report: Diagnosis, management and evolution of a bulky and invasive cardiac mass complicated by complete atrioventricular block
Yohann Bohbot, Jérôme Garot, Isabelle Danjon, Dominique Thébert, Louis Nahory, Philippe Gros, Fiorella Salerno and Philippe Garot

200 Case report: Early acute myocarditis after radiation therapy for breast cancer: A case presentation and review of literature
Mohammadbagher Sharifkazemi, Mahsa Elahi and Masoud Sayad

208 Late-onset doxorubicin-induced congestive heart failure in an elderly cancer survivor: A case report
Hirotaka Suto, Makiko Suto, Yumiko Inui and Atsuo Okamura

214 Intracardiac biopsy of cardiac tumors with echocardiographic guidance: Case report
Jinyun Zhu, Ning Zhang, Qunchao Ma, Luhang Jin and Xiaohong Pan

222 Case report: Non-thrombotic iliac vein lesion: an unusual cause of unilateral leg swelling in a patient with endometrial carcinoma
Jan Zeman, Ritika Kompella, JuYong Lee and Agnes S. Kim

227 Case report: Successful treatment of mediastinal unicentric castleman disease using cardiopulmonary bypass
Wei Ran, Zhu Cuilin, Piao Hulin and Liu Kexiang

231 The broad spectrum of cardiotoxicities from immunotherapies
Martina Iengo, Ester Topa, Alessandra Cuomo, Giancarlo Marone, Remo Poto, Gilda Varricchi, Leonardo Cristinziano, Maria Rosaria Galdiero, Anne Lise Ferrara, Stefania Loffredo, Luigi Formisano, Teresa Troiani, Valentina Mercurio and Carlo Gabriele Tocchetti

frontiers | Frontiers in Cardiovascular Medicine

TYPE Editorial
PUBLISHED 13 July 2023
DOI 10.3389/fcvm.2023.1235015

Check for updates

OPEN ACCESS

EDITED AND REVIEWED BY
June-Wha Rhee,
City of Hope National Medical Center, United States

*CORRESPONDENCE
Reto Asmis
reto.asmis@gmail.com

RECEIVED 05 June 2023
ACCEPTED 21 June 2023
PUBLISHED 13 July 2023

CITATION
Ewer MS, Yusuf SW, Asmis R and Abe J-i (2023) Editorial: Case reports in cardio-oncology: 2022.
Front. Cardiovasc. Med. 10:1235015.
doi: 10.3389/fcvm.2023.1235015

COPYRIGHT
© 2023 Ewer, Yusuf, Asmis and Abe. This is an open-access article distributed under the terms of the Creative Commons Attribution License (CC BY). The use, distribution or reproduction in other forums is permitted, provided the original author(s) and the copyright owner(s) are credited and that the original publication in this journal is cited, in accordance with accepted academic practice. No use, distribution or reproduction is permitted which does not comply with these terms.

Editorial: Case reports in cardio-oncology: 2022

Michael S. Ewer[1], Syed Wamique Yusuf[1], Reto Asmis[2]* and Jun-ichi Abe[1]

[1]MD Anderson Department of Cardiology, Internal Medicine Division, The University of Texas, Houston, TX, United States, [2]Department of Internal Medicine, Wake Forest School of Medicine, Winston-Salem, NC, United States

KEYWORDS

cardiooncology, cardiotoxicity after chemotherapy, history of cardio-oncology, adverse cardiac events, cardiac monitoring of cancer patients

Editorial on the Research Topic
Case reports in cardio-oncology: 2022

One of the early references to an effect of cancer on the circulatory system was the observation by Armand Trousseau in the 1860s that vascular inflammation could be an early manifestation of the presence of a malignancy (1). Recurrent or migratory non-infectious vascular disease would become an important clinical sign that continues to draw the attention of clinicians to the possibility of occult malignancy. Cancer and cardiovascular disease are the two most common causes of mortality worldwide (2). Improvements in cancer therapy have led to the increasing number of cancer survivors. In the USA, an estimated 18 million individuals with a history of cancer were alive on January 1, 2022 (3). A sizeable number of these patients have cardiotoxicity related to radiation and or chemotherapy. In addition, amongst older patients diagnosed with cancer, heart and vascular disease are the most frequent concomitant conditions (4). Hence, in clinical practice, it is not uncommon for a clinician to face a patient who has a concomitant diagnosis of both cancer and cardiovascular disease.

Cardiovascular disease attributable to malignancy and, in more recent times, to the treatment of malignancy, has expanded. Interventions to mitigate preventable acute and long-term cardiovascular sequelae of the disease or its treatment have evolved into a discipline now referred to as cardio-oncology.

The era of cardio-oncology emerged with the introduction of therapeutic agents, most notably in the late 1960s and early 1970s with the introduction and expansion of anthracyclines (5). Exposure to anthracyclines resulted in cardiac failure that was dose-dependent when given in sufficiently high dosages, resulted in severe cardiac failure and death (6). Several important characteristics emerged: first, the toxicity could be quantified by ultrastructural changes in the myocyte when studied by electron microscopy (7). Dosages could be individualized, as not all exposed individuals showed equal sensitivity to the cardiotoxic effects, and some could tolerate doses several times greater than others. Additionally, risk factors for augmented sensitivity to these agents were explored and identified. Initially, entities such as hypertension and valvular lesions were noted to be risk factors, but the more modern view emerged that any entity that had either damaged the heart or that made it more susceptible to ongoing damage was a risk factor. Throughout the 1980s cardiac biopsies were undertaken to assess toxicity and were

graded according to the toxicity scale initially proposed by Billingham and later modified by Mackay that allowed dosages to be individualized (8).

As non-invasive techniques improved, cardiac ejection fraction became the parameter of choice for cardiac surveillance, and both cardiac ultrasound and nuclear imaging in the form of multi-gated (MUGA) scans were widely used. However, it was recognized that while the cardiac biopsy showed and clearly quantified the injury to the myocyte, the ejection fraction could only detect the effects of the injury when compensatory reserves were sufficiently impaired. By the early 1980s, it was evident that ejection fraction reduction was a late consequence of anthracycline injury and was clearly not an optimal parameter for the guidance of anthracycline therapy (9). At that time sufficient interest had accumulated regarding risk assessment of cancer patients that the first mention of a cardio-oncologist ("oncologic cardiologist") appeared in a major journal (9). Later, the fact that myocyte apoptosis-released troponin helped to solidify the concept that the anthracycline injury occurred early and could be quantified at the time of injury despite the fact that the impact of the injury might only come to the forefront years or even decades later (10).

As different therapeutic strategies entered the oncologic armamentarium other adverse events became recognized. Coronary spasm associated with 5-fluorouracil, while recognized, did not reach the threshold of requiring pre-evaluation or on-going surveillance. The approach to other modalities including radiation was largely reactive at that time; if a patient experienced an event or a hypertensive crisis, referral to a cardiologist might ensue to optimize management. By the 1990s, the taxanes had entered standard chemotherapy regimens, but cardiovascular sequelae were not a major concern; the associated bradycardia was generally transient and did not require the expertise of a cardiologist. Cyclophosphamide caused hemorrhagic myocarditis, but this was usually seen when high dosages were administered; high-dose usage and hemorrhagic myocarditis, while recognized, was uncommon, and the cardiologist's role was generally one of providing supportive care.

With the development of the monoclonal antibody trastuzumab, cardiac concerns regarding that agent, and later other novel agents, came to the forefront. An early report noted that, in patients with metastatic disease treated with an anthracycline, cyclophosphamide, and trastuzumab, class III or IV cardiac failure occurred in 27 percent (11). As reports of cardiac events following administration of trastuzumab appeared, there was great concern regarding the observed toxicity. It was speculated that it could be direct toxicity, but also might be the result of a synergistic effect, or a surveillance artifact (12). At that time, most thought that the reported toxicity was mechanistically similar to that seen with the anthracyclines and, therefore, would suggest that great caution was needed when using this highly effective medicine. Concerns were raised, especially in view of the intended role of trastuzumab in the adjuvant breast cancer setting, where many women could be exposed to this agent who, in fact, did not have residual cancer.

In 2005, it became clear that the cardiotoxicity of trastuzumab was fundamentally different from that of the anthracyclines and the concept of a new form of cardiotoxicity, now often referred to as Type II, was introduced (13). Trastuzumab did not show the ultrastructural changes characteristic of the anthracyclines and the decreased cardiac contractility was often transient. While some found the categorization of Type II agents, i.e., agents that do not directly cause myocyte injury as do anthracyclines, to be superficial or overly simplistic, the categorization had two huge effects: first, it became universally recognized that some forms of cardiac dysfunction following cancer treatment behaved differently from that seen with the anthracyclines. Perhaps more importantly, it allowed some of the major clinical trials to continue despite the recognition of decreasing ejection fractions; the results of those trials ultimately led to the approval of trastuzumab in the adjuvant setting, a huge breakthrough that resulted in a major life-sparing innovation in the treatment of HER2 positive breast cancer.

Questions regarding the cardiotoxicity of trastuzumab, and later of other monoclonal antibodies and tyrosine-kinase inhibitors, continued to raise concerns. The ability to mine expanding databases further added to the confusion regarding the true clinical risk of these newer agents as well as to questions about the ideal way to screen patients prior to their receiving anti-cancer treatment as well as what surveillance during and following treatment should be undertaken. As more studies were entered into the literature, the idea that some reports might have included false positive data and confounding factors, i.e., real changes in cardiac function related to factors other than a specific anti-cancer treatment might explain the disparity between the number of reported events and the clinical perception by many oncologists regarding the safety of some of these newer agents (14, 15). Concerns were sufficiently large that cardiac surveillance exploded and monitoring guidelines continue to suggest that surveillance was essential despite little evidence that extensive monitoring provided meaningful clinical benefit. In many instances guidelines were not followed (16). Additionally, both early and late sequalae of radiation were recognized and, while cardioprotective strategies to protect the heart from radiation exposure were developed, long-term late expression of radiation injury remains an important consideration in the surveillance of patients previously exposed to radiation (17).

A new era ensued with new concerns of cardiac damage as the vitally important and innovative group of anti-cancer agents, the immune checkpoint inhibitors, was introduced. These agents were associated with a rare but often lethal form of myocardial inflammation that continues to receive considerable attention. Risk factors are gradually emerging, but it is now clear that combinations of these agents have resulted in increased incidences of toxicity. Estimates of serious events suggest that clinically relevant myocardial inflammation occurs in about 1% of treated patients, but sub-clinical inflammation may occur in a greater proportion of patients. Treatment strategies usually include steroid administration, but other interventions are emerging (18).

As we move forward, the combined efforts of cardiologists and oncologists to optimize survival and quality of life of cancer patients will continue and will become increasingly important as remissions expand for increasingly long periods and cures become more common. The goal of cardio-oncology will be a more focused approach to help achieve an optimal balance between the risks of cancer treatment that impact the cardiovascular system and that include secondary burdens that affect quality of life with true short and long-term benefits of these interventions. Our ability to integrate new information and to apply new analytical techniques to achieve this balance will be one of the future goals of cardo-oncology, and one that is highly likely to continue to be important and potentially hugely meaningful.

As we explained above, cardio-oncology is a rapidly evolving field that focuses on the intersection between cardiovascular diseases and cancer. It has become increasingly important because advancements in cancer treatment have improved cancer survival rates, but they can also lead to cardiovascular complications. Therefore, it is crucial that cardio-oncologists understand and learn to mitigate the cardiovascular side effects of cancer therapies, optimize treatment strategies, and improve the overall outcomes and quality of life for cancer patients. To accomplish this goal, a multidisciplinary approach with collaboration between oncologists and cardiologists is essential. Both specialists bring their unique expertise, enabling comprehensive patient care. Working together, they can tailor cancer therapies to minimize cardiac risks and develop cardiovascular management strategies for cancer patients.

Cardio-oncology is a relatively new discipline, and this strengthens the importance of case reports. Such reports provide valuable insights into previously unknown or under-recognized cardiovascular complications of cancer treatments; many cardiotoxic sequalae, especially those that had not been anticipated from pharmacologic considerations or not seen in pre-clinical or early clinical studies, were first brought to our attention through case reports. These reports serve as the foundation for generating new knowledge, often through augmented surveillance and retrospective analysis. This, together with our understanding of the mechanisms, risk factors, and management strategies for such complications is crucial as we strive to place such events in perspective. Case reports also help in developing guidelines and best practice algorithms for cardio-oncology. We understand that there is a discussion to eliminate *Case Reports* because this section may negatively affect the impact factor of the journal. However, we would like to challenge this perception as we believe that Case Reports are critically important to the still young and evolving field of Cardio-Oncology and provide us with state-of-the art information. We are facing many new drugs and interventions. By focusing on cardio-oncology cases and obtaining more knowledge from each case, we can improve our understanding and ultimately improve patient outcomes, enhance survivorship, and optimize cancer treatment strategies for individuals with concurrent cancer and cardiovascular disease.

Author contributions

MSE wrote the first complete draft, all other authors contributed text and to the editing of the final article. All authors contributed to the article and approved the submitted version.

Conflict of interest

The authors declare that the research was conducted in the absence of any commercial or financial relationships that could be construed as a potential conflict of interest.

Publisher's note

All claims expressed in this article are solely those of the authors and do not necessarily represent those of their affiliated organizations, or those of the publisher, the editors and the reviewers. Any product that may be evaluated in this article, or claim that may be made by its manufacturer, is not guaranteed or endorsed by the publisher.

References

1. Callander N, Rapaport SI. Trousseau's syndrome. *West J Med.* (1993) 158 (4):364–71. PMCID: PMC1022062

2. Fuster V, Voûte J. MDGs: chronic diseases are not on the agenda. *Lancet.* (2005) 366(9496):1512–4. doi: 10.1016/S0140-6736(05)67610-6

3. American Cancer Society, Cancer Treatment and survivorship facts & Figures. Available at: https://www.cancer.org/content/dam/cancer-org/research/cancer-facts-and-statistics/cancer-treatment-and-survivorship-facts-and-figures/2022-cancer-treatment-and-survivorship-fandf-acs.pdf (Accessed June 04, 2023).

4. Coebergh JW, Janssen-Heijnen ML, Post PN, Razenberg PP. Serious co-morbidity among unselected cancer patients newly diagnosed in the southeastern part of The Netherlands in 1993–1996. *J Clin Epidemiol.* (1999) 52(12):1131–6. doi: 10.1016/s0895-4356(99)00098-0

5. Ewer MS, Von Hoff DD, Benjamin RS. A historical perspective of anthracycline cardiotoxicity. *Heart Fail Clin.* (2011) 7(3):363–72. doi: 10.1016/j.hfc.2011.03.001

6. Von Hoff DD, Layard MW, Basa P, Davis HL Jr, Von Hoff AL, Rozencweig M, et al. Risk factors for doxorubicin-induced congestive heart failure. *Ann Intern Med.* (1979) 91(5):710–7. doi: 10.7326/0003-4819-91-5-710

7. Billingham ME, Mason JW, Bristow MR, Daniels JR. Anthracycline cardiomyopathy monitored by morphologic changes. *Cancer Treat Rep.* (1978) 62 (6):865–72. PMID: 667860

8. Mackay B, Ewer MS, Carrasco CH, Benjamin RS. Assessment of anthracycline cardiomyopathy by endomyocardial biopsy. *Ultrastruct Pathol.* (1994) 18(1–2):203–11. doi: 10.3109/01913129409016291

9. Ewer MS, Ali MK, Mackay B, Wallace S, Valdivieso M, Legha SS, et al. A comparison of cardiac biopsy grades and ejection fraction estimations in patients receiving Adriamycin. *J Clin Oncol.* (1984) 2(2):112–7. doi: 10.1200/JCO.1984.2.2.112

10. Cardinale D, Colombo A, Bacchiani G, Tedeschi I, Meroni CA, Veglia F, et al. Early detection of anthracycline cardiotoxicity and improvement with heart failure

therapy. *Circulation*. (2015) 131(22):1981–8. doi: 10.1161/CIRCULATIONAHA.114.013777

11. Slamon DJ, Leyland-Jones B, Shak S, Fuchs H, Paton V, Bajamonde A, et al. Use of chemotherapy plus a monoclonal antibody against HER2 for metastatic breast cancer that overexpresses HER2. *N Engl J Med*. (2001) 344(11):783–92. doi: 10.1056/NEJM200103153441101

12. Ewer MS, Gibbs HR, Swafford J, Benjamin RS. Cardiotoxicity in patients receiving transtuzumab (Herceptin): primary toxicity, synergistic or sequential stress, or surveillance artifact? *Semin Oncol*. (1999) 26(4 Suppl 12):96–101. PMID: 10482200

13. Ewer MS, Lippman SM. Type II chemotherapy-related cardiac dysfunction: time to recognize a new entity. *J Clin Oncol*. (2005) 23(13):2900–2. doi: 10.1200/JCO.2005.05.827

14. Ewer MS, Herson J. False positive cardiotoxicity events in cancer-related clinical trials: risks related to imperfect noninvasive parameters. *Chemotherapy*. (2018) 63(6):324–9. doi: 10.1159/000495147

15. Chavez-MacGregor M, Niu J, Zhang N, Elting LS, Smith BD, Banchs J, et al. Cardiac monitoring during adjuvant trastuzumab-based chemotherapy among older patients with breast cancer. *J Clin Oncol*. (2015) 33(19):2176–83. doi: 10.1200/JCO.2014.58.9465

16. Lyon AR, López-Fernández T, Couch LS, Asteggiano R, Aznar MC, Bergler-Klein J, et al. 2022 ESC guidelines on cardio-oncology developed in collaboration with the European hematology association (EHA), the European society for therapeutic radiology and oncology (ESTRO) and the international cardio-oncology society (IC-OS). *Eur Heart J*. (2022) 43(41):4229–361; Erratum in: *Eur Heart J*. (2023);44(18):1621. doi: 10.1093/eurheartj/ehac244

17. Raghunathan D, Khilji MI, Hassan SA, Yusuf SW. Radiation-Induced cardiovascular disease. *Curr Atheroscler Rep*. (2017) 19(5):22. doi: 10.1007/s11883-017-0658-x

18. Palaskas N, Lopez-Mattei J, Durand JB, Iliescu C, Deswal A. Immune checkpoint inhibitor myocarditis: pathophysiological characteristics, diagnosis, and treatment. *J Am Heart Assoc*. (2020) 9(2):e013757. doi: 10.1161/JAHA.119.013757

frontiers in Cardiovascular Medicine

CASE REPORT
published: 16 August 2021
doi: 10.3389/fcvm.2021.714460

Case Report: The Neuromusclar Triad of Immune Checkpoint Inhibitors: A Case Report of Myositis, Myocarditis, and Myasthenia Gravis Overlap Following Toripalimab Treatment

Yue-Bei Luo†, Weiting Tang†, Qiuming Zeng, Weiwei Duan, Shuyu Li, Xiaosu Yang and Fangfang Bi**

Department of Neurology, Xiangya Hospital, Central South University, Changsha, China

The neuromuscular adverse events of immune checkpoint inhibitor (ICI) treatment include myositis, polymyalgia rheumatica, myocarditis, and myasthenia syndrome. We report a 47-year old female presenting with external ophthalmoplegia, generalized muscle weakness, and third-degree atrioventricular block 4 weeks after toripalimab treatment for metastatic thymoma. Creatine kinase was elevated to 25,200 U/l and cardiac troponin I to 2.796 ng/ml. Autoantibody profiling shows positive anti-ryanodine receptor and anti-acetylcholine receptor antibodies and negative myositis specific antibodies. Repetitive nerve stimulation did not reveal decrement of compound muscle action potentials. Pulse methylprednisolone and immunoglobulin infusion, together with temporary pacemaker insertion normalized her muscle enzyme levels and cardiac rhythm. This is the first report of overlaping neuromuscular adverse event of toripalimab.

Keywords: myositis, myasthenia gravis, myocarditis, PD-1, toripalimab

OPEN ACCESS

Edited by:
Carlo Gabriele Tocchetti, University of Naples Federico II, Italy

Reviewed by:
Yuebing Li, Neurological Institute, Cleveland Clinic, United States
Valentina Damato, Università Cattolica del Sacro Cuore, Italy

****Correspondence:***
Fangfang Bi
fangfangbi@csu.edu.cn
Xiaosu Yang
sjnk_yxs@163.com

†These authors have contributed equally to this work

Specialty section:
This article was submitted to Cardio-Oncology, a section of the journal Frontiers in Cardiovascular Medicine

Received: *10 June 2021*
Accepted: *22 July 2021*
Published: *16 August 2021*

Citation:
Luo Y-B, Tang W, Zeng Q, Duan W, Li S, Yang X and Bi F (2021) Case Report: The Neuromusclar Triad of Immune Checkpoint Inhibitors: A Case Report of Myositis, Myocarditis, and Myasthenia Gravis Overlap Following Toripalimab Treatment. Front. Cardiovasc. Med. 8:714460. doi: 10.3389/fcvm.2021.714460

INTRODUCTION

Immune checkpoint inhibitors (ICIs) such as antibodies targeting programmed cell death 1 (PD-1), PD-1 ligand (PD-L1), and cytotoxic T lymphocyte associated antigen 4 (CTLA-4) are the major advances in cancer therapy in the recent two decades. These drugs eliminate cancer cells by "releasing the brakes" on T cell activation pathway, i.e., enhancing immune surveillance. This modulatory mechanism inevitably leads to pleiotropic immune-related adverse events (irAEs) which include neuromuscular involvement manifesting as myositis, polymyalgia rheumatica, myocarditis myasthenia syndrome, and peripheral neuropathy.

Toripalimab (Junshi Bioscience) is a new PD-1 monoclonal antibody approved by the National Medical Products Administration of China in 2018. A phase I trial registered with U.S. National Library of Medicine (identifier NCT03474640) is underway in the United States. Here we describe a case presenting with polymyositis, myocarditis, and myasthenia gravis (MG) after toripalimab treatment.

CASE DESCRIPTION

A 47-year-old woman was admitted to the Emergency Department of Xiangya Hospital because of progressive diplopia, myalgia, and limb weakness for 7 days. The patient presented with non-fluctuating diplopia, myalgia, and weakness throughout the four limbs without prodromal infections. The symptoms rapidly deteriorated and she also developed dysphagia and dyspnea. She was treated with 240 mg toripalimab for bone metastasis of thymoma 4 weeks earlier. Type B2 thymoma was diagnosed 2 years ago, with immunohistochemistry showing CD5 (++), CD17 (–), TdT (++), p63 (+ + +), CK5/6 (+ + +), TTF (–), NapsinA (–), CR (–), and WT1 (–). She had no prior history of muscle weakness. On physical examination, she was alert and had a slurred speech. She also had bilateral ptosis, and her eyes were fixed in the mid-position without any noticeable horizontal or vertical movement. Pupillary light reflexes were normal. Muscle strength of proximal limbs was graded 3/5 and distal 3+/5. Deep tendon reflexes were absent. Cardiac troponin I level was increased to 2.796 ng/ml (normal range <0.04 ng/ml), and creatine kinase to 25,200 U/L (40–200 U/l). Electrocardiogram showed sinus tachycardia and right bundle branch block. Electromyography showed muscle unit potentials with reduced amplitude and short duration, as well as increased fibrillation and positive sharp weave in her biceps brachii, extensor digitorum communis and quadriceps femoris. Repetitive stimulation of the facial, accessory and ulnar nerves did not reveal significant decrement or increment. Intramuscular neostigmine of 1 mg did not improve her muscle weakness. The patient soon developed type II respiratory failure, therefore was incubated and mechanically ventilated. She was treated with intravenous immunoglobulin (0.4 g/kg/d for 5 days) and was later transferred to Neurology Intensive Care Unit. Subsequent screening for MG antibodies showed positive ryanodine receptor antibody (RyR-Ab) and acetylcholine receptor antibody (AChR-Ab, 7.11 nmol/l, normal range <0.45 nmol/l). Myositis specific and myositis related antibody profiling revealed weakly positive anti-fibrillarin, anti-NOR-90, and Ro-52 antibodies. A regime of pulse methylprednisolone of 500 mg, succeeded by 250 mg each for 5 days was initiated. On the same day, she developed third-degree atrioventricular block with multiple asystole events and temporal pacemaker was inserted. ECG monitoring showed her heart beat gradually returned to sinus rhythm and the pacemaker was removed 12 days later. After 10 days of pulse methylprednisolone, oral prednisolone (60 mg/d) was used for 4 weeks, then tapering to a dose of 50 mg/d. Repeated MG antibody test 40 days after disease onset demonstrated negative RyR-Ab, but still increased AChR-Ab level (9.66 nmol/l). Sixty-nine days after onset, distal limb strength of this patient improved to grade 4-/5 and proximal to 3/5. Despite the normalized CK level and increased muscle strength, she still had difficulty weaning from the ventilator. She was transferred to local hospital for pulmonary and extremity rehabilitation. Telephone follow-up 1 month after the referral indicated that she was off mechanical ventilator support and on non-invasive ventilation. **Figure 1** shows chronological changes of main laboratory markers and treatment.

DISCUSSION

Neuromuscular irAEs represent a group of serious side effects of ICIs that requires prompt investigation and care. So far reported skeletal muscle irAEs of ICIs assume the forms of polymyositis, dermatomyositis, inclusion body myositis, antisynthetase syndrome, immune-mediated necrotizing myopathy, granulomatous myositis, and orbital myositis. The majority of ICI-related myositis cases assume the polymyositis phenotype, as our case does, although a definitive diagnosis requires pathological evidence. Patients usually present with acute onset myalgia and proximal weakness with moderately to severely elevated CK levels within 2 months of ICI initiation. Bulbar, extraocular muscle and axial involvement is also common. Myopathology ranges from necrotizing myopathy with few infiltrates to granulomatous inflammation within muscle tissues. Other types of myositis are anecdotal. ICI-related DM patients manifest characteristic DM skin changes such as periorbital heliotrope rashes. Whether the pathognomic perifascicular atrophy is present in this group of patients needs further exploration as unambiguous muscle biopsy evidence is lacking (1, 2). In a single case with lung adenocarcinoma, Nivolumab leads to development of myopathy and interstitial pneumonia, with anti-PL-7 seropositivity (3). Pembrolizumab is reported to cause painless orbital myositis with hyperCKaemia in a renal cancer case (4). In terms of the myositis specific antibodies that develop after ICI treatment, TIF1-γ and HMGCR antibodies are the only two reported antibodies (1, 5, 6). Notably, TIF1-γ antibody is closely correlated with tumors in idiopathic inflammatory myopathies. A definitive link between ICIs and HMGCR antibody remains undetermined, as the reported case has a pre-existing statin induced myopathy that resolves after statin discontinuation 2 weeks prior to ICI treatment. Patients with pre-existing myositis are inclined to flares following ICI treatment (7, 8). Proposed mechanisms include loss of self-tolerance by disrupted balance between Treg and T effector cells, shared antigens between tumor and tissue, and epitope spreading in which release of tumor-origin and self antigens initiates inflammatory cascade (9, 10).

Admittedly, our patient does not show any response to neostigmine and her repetitive stimulation lacks the characteristic amplitude decrement. It is also estimated that 20–37% of thymoma patients with elevated AChR levels do not develop MG (11, 12), which challenges the diagnosis of MG in this case. However, neither myositis nor myocarditis could account for the early and severe involvement of extraocular and respiratory muscles of this patient. Previous studies estimate that approximately 0.12–0.4% patients receiving ICI treatment develop or experience flares of MG (13, 14). The characteristic amplitude decrement of compound muscle action potentials occurs in 29–53% of these patients. Up to 66% of ICI-related MG cases have elevated anti-AChR antibody titer (13). They have more frequent anti-striated muscle antibodies than the idiopathic cases (66.7 vs. 39.5%) (13, 15). This group of patients also have a higher propensity to develop respiratory failure and a worse outcome. Anti-RyR antibody positive MG patients typically present with ocular, bulbar and axial weakness instead of limb

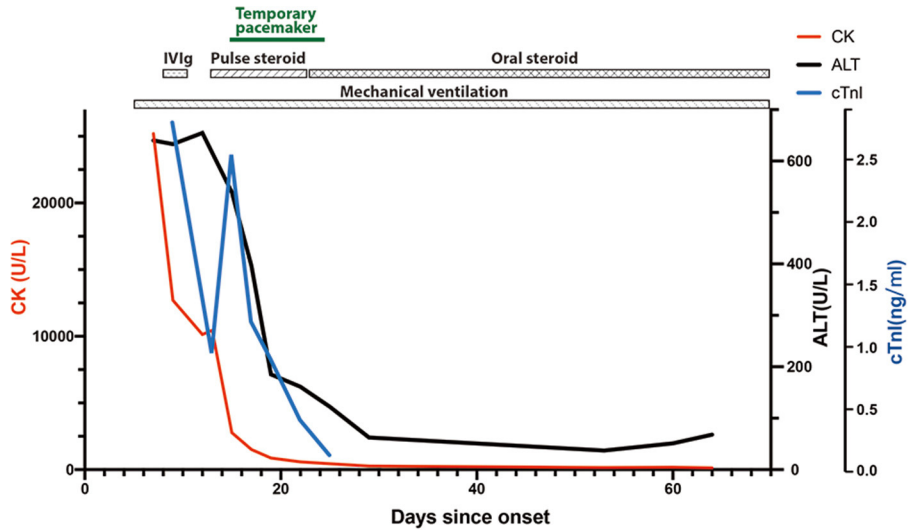

FIGURE 1 | Illustration of the main laboratory markers and treatment of this patient.

weakness. Our case falls into class V of MG according to MGFA classification. This patient displays a generalized involvement of virtually all modalities of striated muscles, including extraocular, facial, bulbar, respiratory, axial, limb and cardiac muscles. While it is difficult to dissect the specific roles of each of the neuromuscular triad in phenotype development, there is no doubt that they synergistically contribute to the aggressive disease progression.

Adverse cardiac events related to ICIs include myocarditis, pericardial diseases, myocardial infarction, and vasculitis. The severity of myocarditis cases following ICI therapy range from sub-clinical to fatal. Patients may present with dyspnea, palpitation, syncope, or chest pain. Despite the overall elevated troponin levels, approximately half of cases demonstrate abnormal left ventricular ejection fraction (16, 17). In comparison, 89% cases have arrhythmias including atrial fibrillation, premature ventricular contraction, conduction block and ventricular tachycardia. On cardiovascular magnetic resonance, 48% of patients show late gadolinium enhancement (LGE), whose patterns include transmural, sub-epicardial, mid-myocardial, and diffuse (17). LGE was present in anteroseptal, inferoseptal, inferior, and inferolateral wall. Endomyocardial biopsy findings are characterized by myocardial infiltration consisting of T lymphocytes and macrophages (18). Notably, a previous analysis of irAEs in Chinese patients shows that toripalimab causes myocarditis more frequently than other ICIs (19). The National Comprehensive Cancer Network recommends permanent discontinuation of ICIs in Grade 3 (severe) and 4 (life-threatening) myocarditis cases (20).

Overall, the myositis-myocarditis-myasthenia gravis overlap represents a serious neuromuscular irAE of PD-1 monoantibodies, and are considerably more deleterious compared with their idiopathic counterparts. Meta-analysis shows that myositis, myocarditis and myasthenia gravis account for one fifth of irAE-related death (21). When the neuromuscular triad is present, the disease progression is particularly malignant. Permanent discontinuation of ICIs is therefore recommended for severe myositis or myocarditis, and also for myositis-myocarditis overlap (22, 23). Patients require more aggressive treatments including pulse steroid, immunoglobulin infusion and plasmapheresis. A second immunomodulatory drug is in option if the patient shows poor response to the above therapies (24).

It should be noted that thymic epithelial tumors (TETs) are associated with higher incidence of ICI-related irAEs compared with other types of cancers (25, 26). This may be explained by the critical role of thymus in T lymphocyte education and the compromised immune tolerance of TETs. Toripalimb is a recombinant humanized IgG4 monoantibody against PD-1 molecule that has a promising therapeutic potential for advance solid tumors. It is reported to cause more aggressive myocarditis (grade 3–5) (19). In conclusion, we report a case presenting with the neuromuscular triad irAE after toripalimab treatment. Clinicians should carefully consider the type and nature of tumors and be aware of the potential irAEs in each ICIs when planning immunotherapy.

DATA AVAILABILITY STATEMENT

The original contributions presented in the study are included in the article/**Supplementary Material**, further inquiries can be directed to the corresponding author/s.

ETHICS STATEMENT

The studies involving human participants were reviewed and approved by the Ethic Committee of the Xiangya Hospital of Central South University. The patients/participants provided their written informed consent to participate in this study.

AUTHOR CONTRIBUTIONS

Y-BL and FB initiated the study. Y-BL and WT collected clinical data and wrote the manuscript. FB and XY reviewed the manuscript. QZ, WD, WT, SL, XY, and FB provided medical care for the patient and participated in literature reviewing. All authors contributed to the article and approved the submitted version.

FUNDING

This work was supported by National Natural Science Foundation of China (grant number 81601094).

SUPPLEMENTARY MATERIAL

The Supplementary Material for this article can be found online at: https://www.frontiersin.org/articles/10.3389/fcvm.2021.714460/full#supplementary-material

REFERENCES

1. Osaki M, Tachikawa R, Ohira J, Hara S, Tomii K. Anti-transcriptional intermediary factor 1-gamma antibody-positive dermatomyositis induced by nivolumab for lung adenocarcinoma: a case report. *Invest New Drugs.* (2021) 39:251–5. doi: 10.1007/s10637-020-00974-7
2. Liewluck T, Kao JC, Mauermann ML. PD-1 inhibitor-associated myopathies: emerging immune-mediated myopathies. *J Immunother.* (2018) 41:208–11. doi: 10.1097/CJI.0000000000000196
3. Shikano K, Kaneko K, Kaburaki K, Isobe K, Kawabe K, Homma S, et al. Nivolumab-induced anti-aminoacyl-tRNA synthetase antibody-positive polymyositis complicated by interstitial pneumonia in a patient with lung adenocarcinoma. *Scand J Rheumatol.* (2020) 49:82–3. doi: 10.1080/03009742.2019.1596309
4. Garibaldi M, Calabro F, Merlonghi G, Pugliese S, Ceccanti M, Cristiano L, et al. Immune checkpoint inhibitors (ICIs)-related ocular myositis. *Neuromuscul Disord.* (2020) 30:420–3. doi: 10.1016/j.nmd.2020.02.013
5. Berger M, Legeay AL, Souci S, Streichenberger N, Thomas L, Dalle S. Pembrolizumab-induced dermatomyositis in a patient with metastatic melanoma. *Eur J Cancer.* (2018) 104:227–30. doi: 10.1016/j.ejca.2018.08.021
6. von Itzstein MS, Khan S, Popat V, Lu R, Khan SA, Fattah FJ, et al. Statin intolerance, anti-HMGCR antibodies, and immune checkpoint inhibitor-associated myositis: a "two-hit" autoimmune toxicity or clinical predisposition? *Oncologist.* (2020) 25:e1242–5. doi: 10.1634/theoncologist.2019-0911
7. Mackintosh D, Islam MF, Ng J, Basham J. Immune checkpoint inhibitor use in antisynthetase syndrome. *Asia Pac J Clin Oncol.* (2019) 15:266–9. doi: 10.1111/ajco.13141
8. Abdel-Wahab N, Shah M, Lopez-Olivo MA, Suarez-Almazor ME. Use of immune checkpoint inhibitors in the treatment of patients with cancer and preexisting autoimmune disease: a systematic review. *Ann Intern Med.* (2018) 168:121–30. doi: 10.7326/M17-2073
9. Solimando AG, Crudele L, Leone P, Argentiero A, Guarascio M, Silvestris N, et al. Immune checkpoint inhibitor-related myositis: from biology to bedside. *Int J Mol Sci.* (2020) 21:3054. doi: 10.3390/ijms21093054
10. Johnson DB, Balko JM, Compton ML, Chalkias S, Gorham J, Xu Y, et al. Fulminant myocarditis with combination immune checkpoint blockade. *N Engl J Med.* (2016) 375:1749–55. doi: 10.1056/NEJMoa1609214
11. Ohta M, Itoh M, Hara H, Itoh N, Nishitani H, Hayashi K, et al. Anti-skeletal muscle and anti-acetylcholine receptor antibodies in patients with thymoma without myasthenia gravis: relation to the onset of myasthenia gravis. *Clin Chim Acta.* (1991) 201:201–5. doi: 10.1016/0009-8981(91)90371-i
12. Sakuraba M, Onuki T, Nitta S. Measurement of antiacetylcholine receptor antibody in patients with thymoma without myasthenia gravis complications. *Jpn J Thorac Cardiovasc Surg.* (2001) 49:690–2. doi: 10.1007/BF02913506
13. Safa H, Johnson DH, Trinh VA, Rodgers TE, Lin H, Suarez-Almazor ME, et al. Immune checkpoint inhibitor related myasthenia gravis: single center experience and systematic review of the literature. *J Immunother Cancer.* (2019) 7 319. doi: 10.1186/s40425-019-0774-y
14. Suzuki S, Ishikawa N, Konoeda F, Seki N, Fukushima S, Takahashi K, et al. Nivolumab-related myasthenia gravis with myositis and myocarditis in Japan. *Neurology.* (2017) 89:1127–34. doi: 10.1212/WNL.0000000000004359
15. Choi Decroos E, Hobson-Webb LD, Juel VC, Massey JM, Sanders DB. Do acetylcholine receptor and striated muscle antibodies predict the presence of thymoma in patients with myasthenia gravis? *Muscle Nerve.* (2014) 49:30–4. doi: 10.1002/mus.23882
16. Mahmood SS, Fradley MG, Cohen JV, Nohria A, Reynolds KL, Heinzerling LM, et al. Myocarditis in patients treated with immune checkpoint inhibitors. *J Am Coll Cardiol.* (2018) 71:1755–64. doi: 10.1016/j.jacc.2018.02.037
17. Zhang L, Awadalla M, Mahmood SS, Nohria A, Hassan MZO, Thuny F, et al. Cardiovascular magnetic resonance in immune checkpoint inhibitor-associated myocarditis. *Eur Heart J.* (2020) 41:1733–43. doi: 10.1093/eurheartj/ehaa051
18. Moslehi J, Lichtman AH, Sharpe AH, Galluzzi L, and Kitsis RN. Immune checkpoint inhibitor-associated myocarditis: manifestations and mechanisms. *J Clin Invest.* (2021) 131. doi: 10.1172/JCI145186
19. Li L, Li G, Rao B, Dong AH, Liang W, Zhu JX, et al. Landscape of immune checkpoint inhibitor-related adverse events in Chinese population. *Sci Rep.* (2020) 10:15567. doi: 10.1038/s41598-020-72649-5
20. Thompson JA, Schneider BJ, Brahmer J, Andrews S, Armand P, Bhatia S, et al. NCCN guidelines insights: management of immunotherapy-related toxicities, version 1.2020. *J Natl Compr Canc Netw.* (2020) 18:230–41. doi: 10.6004/jnccn.2020.0012
21. Wang DY, Salem JE, Cohen JV, Chandra S, Menzer C, Ye F, et al. Fatal toxic effects associated with immune checkpoint inhibitors: a systematic review and meta-analysis. *JAMA Oncol.* (2018) 4:1721–8. doi: 10.1001/jamaoncol.2018.3923
22. Steven NM, Fisher BA. Management of rheumatic complications of immune checkpoint inhibitor therapy - an oncological perspective. *Rheumatology.* (2019) 58:vii29–39. doi: 10.1093/rheumatology/kez536
23. Kostine M, Finckh A, Bingham CO, Visser K, Leipe J, Schulze-Koops H, et al. EULAR points to consider for the diagnosis and management of rheumatic immune-related adverse events due to cancer immunotherapy with checkpoint inhibitors. *Ann Rheum Dis.* (2021) 80:36–48. doi: 10.1136/annrheumdis-2020-217139
24. Brahmer JR, Lacchetti C, Schneider BJ, Atkins MB, Brassil KJ, Caterino JM, et al. Management of immune-related adverse events in patients treated with immune checkpoint inhibitor therapy: american society of clinical oncology clinical practice

guideline. *J Clin Oncol*. (2018) 36:1714–68. doi: 10.1200/JCO.2017.77.6385

25. Jakopovic M, Bitar L, Seiwerth F, Marusic A, Krpina K, Samarzija M. Immunotherapy for thymoma. *J Thorac Dis*. (2020) 12:7635–41. doi: 10.21037/jtd-2019-thym-12
26. Rajan A, Heery CR, Thomas A, Mammen AL, Perry S, O'Sullivan Coyne G, et al. Efficacy and tolerability of anti-programmed death-ligand 1 (PD-L1) antibody (Avelumab) treatment in advanced thymoma. *J Immunother Cancer*. (2019) 7:269. doi: 10.1186/s40425-019-0723-9

Conflict of Interest: The authors declare that the research was conducted in the absence of any commercial or financial relationships that could be construed as a potential conflict of interest.

Publisher's Note: All claims expressed in this article are solely those of the authors and do not necessarily represent those of their affiliated organizations, or those of the publisher, the editors and the reviewers. Any product that may be evaluated in this article, or claim that may be made by its manufacturer, is not guaranteed or endorsed by the publisher.

Copyright © 2021 Luo, Tang, Zeng, Duan, Li, Yang and Bi. This is an open-access article distributed under the terms of the Creative Commons Attribution License (CC BY). The use, distribution or reproduction in other forums is permitted, provided the original author(s) and the copyright owner(s) are credited and that the original publication in this journal is cited, in accordance with accepted academic practice. No use, distribution or reproduction is permitted which does not comply with these terms.

frontiers in Cardiovascular Medicine

CASE REPORT
published: 01 October 2021
doi: 10.3389/fcvm.2021.736199

Case Report: A Primary Right Ventricular Vascular Malformation Presenting as a Mass

Hongduan Liu[1,2], *Xin Li*[2], *Cuiwei Zhang*[3], *Chengming Fan*[1], *Liming Liu*[1] *and Juyi Wan*[2*]

[1] *Department of Cardiovascular Surgery, The Second Xiangya Hospital, Central South University, Changsha, China,*
[2] *Department of Cardiovascular Surgery, The Affiliated Hospital of Southwest Medical University, Luzhou, China,*
[3] *Department of Pathology, The Affiliated Hospital of Southwest Medical University, Luzhou, China*

Primary right ventricular vascular malformation is a rare primary benign anomaly in heart in nature. Due to the extremely low incidence and the progress on the classification of vascular malformation, a few cases were reported in the literatures. In the current case study, a 55-year-old women presented with a cardiac mass that was identified in right ventricle during a routine medical checkup. Magnetic resonance imaging demonstrated a well-circumscribed mass attached to the interventricular septum. Median sternotomy for the surgical resection of the mass and a cardiopulmonary bypass were performed. The intraoperative transesophageal echocardiogram showed that the mass had been successfully removed. The patient recovered well and was discharged from hospital 9 days after the surgery. The pathological diagnosis was primary cardiac arteriovenous malformation. No mass recurrence was shown by echocardiography during the 13 months' follow-up.

Keywords: cardiac surgery, cardiac tumor, echocardiography, vascular malformation, hemangioma

OPEN ACCESS

Edited by:
Reto Asmis,
Wake Forest School of Medicine,
United States

Reviewed by:
Samer Kassem,
Monza Polyclinic, Italy
Jiancheng Han,
Capital Medical University, China

***Correspondence:**
Juyi Wan
wanjuyi@yeah.net

Specialty section:
This article was submitted to Cardio-Oncology, a section of the journal Frontiers in Cardiovascular Medicine

Received: *04 July 2021*
Accepted: *06 September 2021*
Published: *01 October 2021*

Citation:
Liu H, Li X, Zhang C, Fan C, Liu L and Wan J (2021) Case Report: A Primary Right Ventricular Vascular Malformation Presenting as a Mass. Front. Cardiovasc. Med. 8:736199. doi: 10.3389/fcvm.2021.736199

INTRODUCTION

The primary cardiac arteriovenous malformation (AVM) is a rare benign vascular malformation in nature, which develops from vascular endothelial hyperplasia (1). In terms of the proportion of cardiac AVM is an extreme rarity in heart and its clinical information is limited. Herein, a case of primary cardiac AVM presenting as right ventricular mass was reported and the multimodality imaging, classification and the differential diagnosis of AVM were presented.

CASE PRESETATION

A 55-year-old female was referred to our hospital because a cardiac tumor in right ventricle was detected by transthoracic echocardiography during a medical checkup. The patient was asymptomatic, with a history of diabetes for 5 years and hypertension for 1 year. No cough, dyspnea, dizziness and fever were presented when she was admitted. The blood pressure was 112/56 mmHg with Irbesartan intake and the heart rate was 84 beats per min. No cardiac murmur was heard and no edema was detected in the lower limb. There were no family history of cardiovascular disease following medical history and physical examination. Laboratory tests were negative.

Electrocardiography was normal. Transesophageal echocardiography showed the cardiac mass (15 x 14 mm) located in right ventricle, attached to the interventricular septum (IVS) abutting the apex (**Figure 1**; **Supplementary Video 1**). A well-circumscribed homogenous "shadow," representing a nodule measuring 16 × 13 mm, with equal T1- and T2-weighted signal intensity in the right ventricle, located adjacent to the IVS, was revealed using moderate enhancement for the first perfusion scan and delayed myocardial enhancement MRI subsequently (**Figure 2**). Coronary angiography (CA) showed stenosis (30%) in the right coronary artery and no obvious stenosis in the left coronary; a discernible tumor-feeding artery was not detected.

Initially, the clinical diagnosis was right ventricular myxoma or fibroelastoma. Median sternotomy for the surgical resection of the mass was performed to avoid the risk of pulmonary embolization and determine the tumor characteristics. A cardiopulmonary bypass was carried out using ascending aortic and superior and inferior vena cava cannulation. Upon cardiac arrest, the right atrium was opened, and it was confirmed that the semispherical mass, with soft texture and broad base, originated from the IVS (**Figure 3A**). Because no significant boundary was detected preoperatively, the mass along with a small portion of IVS was resected (**Figure 3B**). The resected specimen comprised a reddish mass enveloped with blood. Signs of ventricular septal defect were not found with TTE (**Supplementary Figure 1**). The histopathological examination revealed that the tumor was a cardiac AVM (**Figures 4A,B**). The patient's postoperative course was uneventful. She was shown to have recovered well and without recurrence at the 13-month follow-up.

DISSCUSION AND CONCLUSION

The AVM was considered as a benign vascular tumor, some of which was termed as plexiform hemangioma in the past (2). However, the classification was changed since the International Society for the Study of Vascular Anomalies (ISSVA) grouped the vascular anomalies into two major categories, vascular tumors (mainly hemangiomas) and vascular malformations; According to this classification, AVM is a vascular malformation subtype (3, 4). In our case, the right ventricular mass was identified as the AVM which is extreme rare in the limited literature.

The differential diagnosis of a mass attached to the right ventricle includes myxoma, lipoma, fibroelastoma, and hemangioma. Categorization of the symptoms depends on their location and the pathological classification of the mass. Some cases are characterized by pericardial effusion, right ventricular outlet obstruction, and even sudden cardiac death (5–7). The location of cardiac benign masses varies, typically involving the atrium, ventricle, aortic valve, mitral valve, or epicardium (8, 9). In the present case, the patient was asymptomatic, and the mass was attached to the IVS in the right ventricle, abutting the apex. Initially, fibroelastoma and cardiac myxoma were suspected.

Appropriate screening imaging modalities for cardiac mass include echocardiography, CT, and MRI, all of which can be used to eliminate the problem of a differential diagnosis (10, 11). In the current study, a diagnosis of benign tumor was made, based on the MRI and echocardiographic findings. Enhanced myocardial echocardiography and ^{18}F-fluorodeoxyglucose-positron emission tomography can also be utilized to provide detailed information to resolve a differential diagnosis (12, 13). In addition, CA can be used to determine whether a coronary artery is feeding the tumor; however, it should only be considered if performing CA is consistent with the patient's age and symptoms (14). Although echocardiography, CT or MRI can be helpful in the diagnosis and differential diagnosis, the histopathology is still needed for the final diagnosis. In the current case study, a right ventricular mass was identified using TE and intraoperative TEE, which showed its location, diameter, and morphology; it also showed that the IVS was intact following the resection. TEE and MRI clearly showed the mass' margin and feeding artery to the mass, which informed the surgeons of the confidence to completely remove it. In the event that the patient presents with symptoms caused by the mass or in cases when the prognosis is uncertain in relation to the tumor, surgical resection should be performed to reduce the risk of embolism (15). Conservative management is an option when the biopsy returns a pathological classification of vascular malformation, except in the case of concomitant aortic valve insufficiency (9).

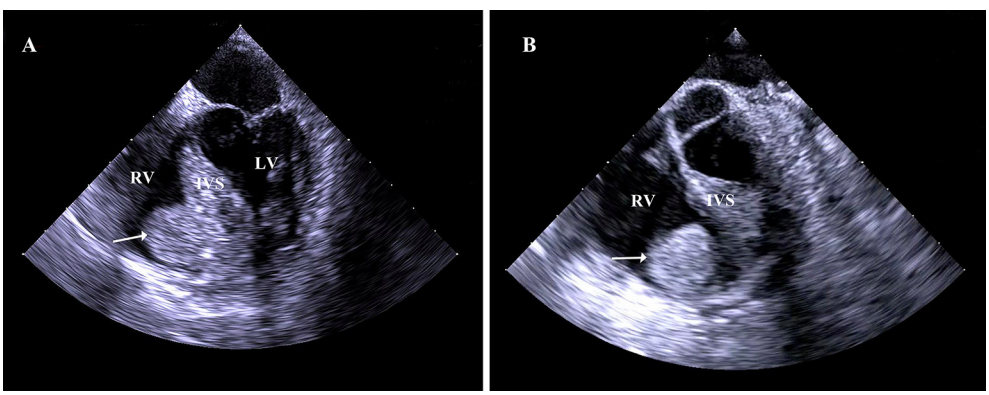

FIGURE 1 | (A,B) Transesophageal echocardiography showed the cardiac mass (15 x 14 mm) located in right ventricle, attached to the interventricular septum abutting the apex. RV, right ventricle; IVS, interventricular septum; LV, left ventricle.

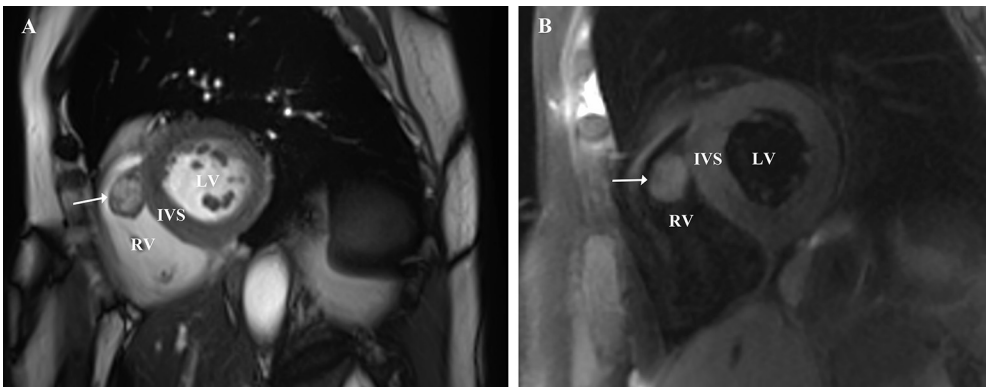

FIGURE 2 | (A,B) Magnetic resonance imaging demonstrated that a well-circumscribed homogenous nodule, measuring 16 × 13 mm, with medium signal intensity on T1-weighted images and medium signal intensity on T2- weighted images in the right ventricle, located adjacent to the IVS, was revealed uniform moderate enhancement for the first perfusion scan and uniform significantly delayed enhancement subsequently. RV, right ventricle; IVS, interventricular septum; LV, left ventricle.

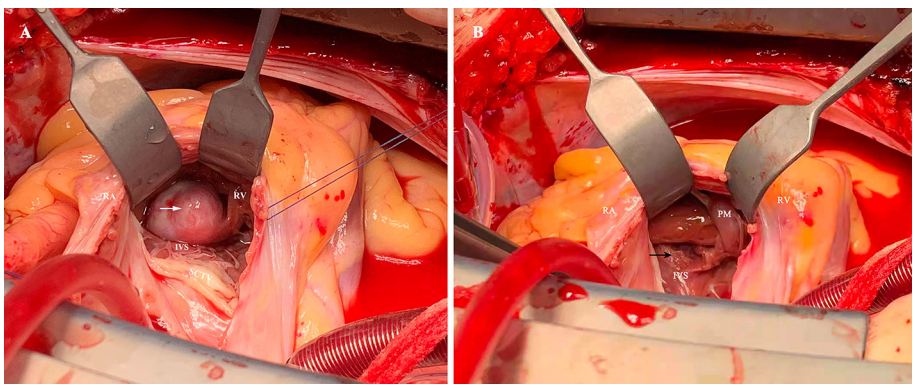

FIGURE 3 | (A) The mass located in the right ventricle and was attached to the interventricular septum (white arrow). **(B)** The mass were removed completely and the IVS was intact without perforation (black arrow). RA, right atrium; RV, right ventricle; IVS, interventricular septum; SCTV, septal cusp of tricuspid valve; PM, papillary muscles.

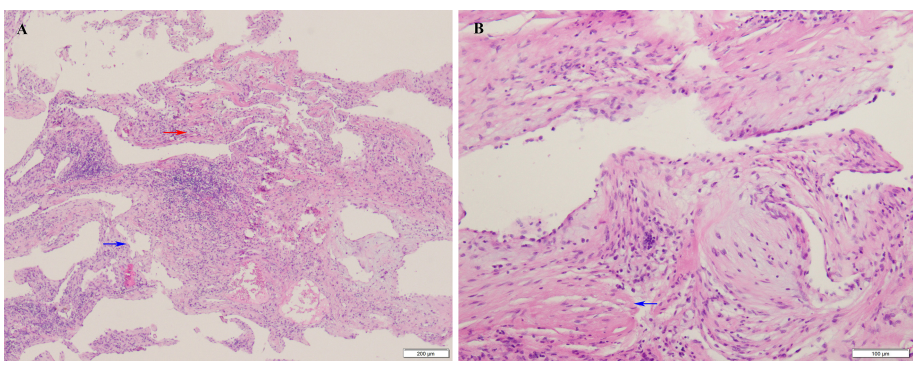

FIGURE 4 | (A) Histopathology revealed that there are a lot of branches of vessels, thick-walled arteries (red arrow) and thin-walled veins (blue arrow), which was identified as cardiac arteriovenous malformation. **(B)** Histopathology showed the anomalous arteries with thick wall are composed of smooth muscle (blue arrow).

The ISSVA classification standards have been published; however, there is a lack of consensus regarding the understanding of whether vascular anomalies are tumors or malformations (16). Initially, they were classified according to factors such as vascular distortion and structure. Recently, an analysis of WT-1 and GLUT-1 expression is used to distinguish

between vascular malformation and vascular tumors (17, 18). Elsewhere, a MSOT-based, non-invasive assessment of hemoglobin levels was used to differentiate between vascular malformation subtypes (19). In addition, advances in molecular genetics are ensuring greater insight into the genetic basis for vascular anomalies and providing potential molecular targets for pharmacotherapy. Thus, in future, vascular malformations may be treated using novel pharmacotherapeutic approaches rather than surgery (3).

Right ventricular AVM is extremely rare which might be resulted in sudden death. Currently, echocardiography is the primary and most common method for detecting ventricular AVM as it effectively indicates its location, diameter, and morphology. Likewise, multiple imaging plays a key role in solving the problem of a differential diagnosis, while providing invaluable information to assist with complete resection of the mass. Although echocardiography, CT or MRI can be helpful in the diagnosis, it is still challenging. After all, the histopathology is still the "gold standard" in the final diagnosis.

DATA AVAILABILITY STATEMENT

The original contributions presented in the study are included in the article/**Supplementary Material**, further inquiries can be directed to the corresponding author/s.

ETHICS STATEMENT

The study protocol was approved by the Ethics Committee of the Affiliated Hospital of South West University, Luzhou, China. The patients/participants provided informed consent to participate in this study. Written informed consent was obtained from the individual(s) for the publication of any potentially identifiable images or data included in this article.

AUTHOR CONTRIBUTIONS

HL drafted the manuscript. HL and JW designed the study. XL, HL, and JW performed the surgery and were responsible for the collection of data or analysis. JW, CF, and LL revised the manuscript. CZ provided the pathological outcome. All have authors read and approved the final manuscript.

FUNDING

This study was supported in part by the following funding sources: Sichuan Province science and technology projects (2018JY0405, 2021YFH0148, and 2020YJ0190), Science and Technology Strategic Cooperation Programs of Luzhou Municipal People's Government and Southwest Medical University (2019LZXNYDJ30).

SUPPLEMENTARY MATERIAL

The Supplementary Material for this article can be found online at: https://www.frontiersin.org/articles/10.3389/fcvm.2021.736199/full#supplementary-material

Supplementary Video 1 | Transesophageal echocardiography showed the cardiac mass located in right ventricle, attached to the interventricular septum abutting the apex.

Supplementary Figure 1 | Postoperative transthoracic echocardiography showed that there was no shunt across the IVS. IVS, interventricular septum.

REFERENCES

1. McCuaig CC. Update on classification and diagnosis of vascular malformations. *Curr Opin Pediatr.* (2017) 29:448–54. doi: 10.1097/MOP.0000000000000518
2. Fan J, Liao X, Zhou X, A. case report of primary cardiac capillary hemangioma. *Cancer Biol Ther.* (2016) 17:11–3. doi: 10.1080/15384047.2015.1109391
3. Martinez-Lopez A, Salvador-Rodriguez L, Montero-Vilchez T, Molina-Leyva A, Tercedor-Sanchez J, Arias-Santiago S. Vascular malformations syndromes: an update. *Curr Opin Pediatr.* (2019) 31:747–53. doi: 10.1097/MOP.0000000000000812
4. ISSVA Classification of Vascular Anomalies ©2018 International Society for the Study of Vascular Anomalies. (2018). Available online at: https://www.issva.org/UserFiles/file/ISSVA-Classification-2018.pdf (accessed September 23, 2016).
5. Rathore K, Yussouf R, Teh M, Jindal S, Wong D, Newman M. Left atrial anastomosing hemangioma causing recurrent pericardial effusion. *Ann Thorac Surg.* (2020) 109:e157–9. doi: 10.1016/j.athoracsur.2019.06.082
6. Wildgruber M, Sadick M, Muller-Wille R, Wohlgemuth WA. Vascular tumors in infants and adolescents. *Insights Imaging.* (2019) 10:30. doi: 10.1186/s13244-019-0718-6
7. Aguilera B, Suárez-Mier M, Argente T. Cardiac arteriovenous malformation causing sudden death. *Cardiovasc Pathol.* (2004) 13:296–8. doi: 10.1016/j.carpath.2004.06.002
8. Kotoulas C, Georgiou C, Grapatsas K, Kotoulas S, Theodosiadis N, Panagiotou I. Cavernous hemangioma of the left atrium: a rare tumor. *J Card Surg.* (2020) 35:202–3. doi: 10.1111/jocs.14373
9. Cotier P, Bruneval P, Amemiya K. Vascular malformation in a bicuspid aortic valve. *Cardiovasc Pathol.* (2019) 38:39–41. doi: 10.1016/j.carpath.2018.10.006
10. Gao Y, Wu W, Zhang L, Sun Z, Xie Y, Li Y, et al. Multimodality imaging in preparation for resection of a right atrial cavernous hemangioma. *Echocardiography.* (2020) 37:465–6. doi: 10.1111/echo.14615
11. Vodovar N, Seronde MF, Laribi S, Gayat E, Lassus J, Boukef R, et al. Post-translational modifications enhance NT-proBNP and BNP production in acute decompensated heart failure. *Eur Heart J.* (2014) 35:3434–1. doi: 10.1093/eurheartj/ehu314
12. Xiachuan Q, Xuebin L, Yongjie W. Case of cardiac hemangioma diagnosed by myocardial contrast echocardiography. *Circ Cardiovasc Imaging.* (2019) 12:e008811. doi: 10.1161/CIRCIMAGING.118.008811
13. Matsuba T, Hisashi Y, Yotsumoto G, Imoto Y, A. rare cardiac haemangioma in the right ventricle diagnosed accurately using (1)(8)F-fluorodeoxyglucose-positron emission tomography. *Eur J Cardiothorac Surg.* (2015) 47:e223–5. doi: 10.1093/ejcts/ezu540
14. Chen X, Lodge AJ, Dibernardo LR, Milano CA. Surgical treatment of a cavernous haemangioma of the heart. *Eur J Cardiothorac Surg.* (2012) 41:1182–3. doi: 10.1093/ejcts/ezr153

15. Rekik S, Hentati M, Boudawara T, Abdennadher M, Frikha I, Kammoun S. Myofibroblastic tumor of the right ventricle causing bilateral pulmonary embolism in a 31 year-old woman. *Int J Cardiol.* (2009) 131:e131–3. doi: 10.1016/j.ijcard.2007.07.082
16. Pahl KS, Kim K, Sams C, Alvarez H, Smith SV, Blatt J. Inconsistency in classifying vascular anomalies: what's in a name? *Pediatr Blood Cancer.* (2018) 65. doi: 10.1002/pbc.26836
17. Al Dhaybi R, Powell J, McCuaig C, Kokta V. Differentiation of vascular tumors from vascular malformations by expression of Wilms tumor 1 gene: evaluation of 126 cases. *J Am Acad Dermatol.* (2010) 63:1052–7. doi: 10.1016/j.jaad.2009.12.017
18. Rastogi K, Singh L, Khan NA, Goyal S, Khatri A, Gupta N. Benign vascular anomalies: a transition from morphological to etiological classification. *Ann Diagn Pathol.* (2020) 46:151506. doi: 10.1016/j.anndiagpath.2020.151506
19. Masthoff M, Helfen A, Claussen J, Karlas A, Markwardt NA, Ntziachristos V, et al. Use of multispectral optoacoustic tomography to diagnose vascular malformations. *JAMA Dermatol.* (2018) 154:1457–62. doi: 10.1001/jamadermatol.2018.3269

Conflict of Interest: The authors declare that the research was conducted in the absence of any commercial or financial relationships that could be construed as a potential conflict of interest.

Publisher's Note: All claims expressed in this article are solely those of the authors and do not necessarily represent those of their affiliated organizations, or those of the publisher, the editors and the reviewers. Any product that may be evaluated in this article, or claim that may be made by its manufacturer, is not guaranteed or endorsed by the publisher.

Copyright © 2021 Liu, Li, Zhang, Fan, Liu and Wan. This is an open-access article distributed under the terms of the Creative Commons Attribution License (CC BY). The use, distribution or reproduction in other forums is permitted, provided the original author(s) and the copyright owner(s) are credited and that the original publication in this journal is cited, in accordance with accepted academic practice. No use, distribution or reproduction is permitted which does not comply with these terms.

frontiers in Cardiovascular Medicine

CASE REPORT
published: 15 November 2021
doi: 10.3389/fcvm.2021.755106

Case Report: An Unusual Cause for Recurrent Hemopericardium in a Patient With Dyspnea

Uyên Châu Nguyên[1], Astrid I. P. Vernemmen[2], Patrique Segers[3], Axel zur Hausen[2], Rob G. H. Driessen[1,4], Maurice J. H. M. Pluijmen[1] and Sebastiaan C. A. M. Bekkers[1]*

[1] Department of Cardiology, Maastricht University Medical Center, Maastricht, Netherlands, [2] Department of Pathology, Maastricht University Medical Center, Maastricht, Netherlands, [3] Department of Cardiothoracic Surgery, Maastricht University Medical Center, Maastricht, Netherlands, [4] Department of Intensive Care Medicine, Maastricht University Medical Center, Maastricht, Netherlands

The case concerns a female presenting with dyspnoea resulting from recurrent hemopericardium. Pericardiocentesis, coronary angiography, and extensive laboratory and imaging studies did not reveal the underlying etiology of the hemopericardium. Only after repeat and exploratory surgery, diffuse venous pericardial hemorrhages with localized thrombi typical of angiosarcoma were discovered.

Keywords: hemopericardium, cardiac angiosarcoma, right heart sarcoma, dyspnea, pericardial effusion

OPEN ACCESS

Edited by:
Cezar Angi Iliescu, University of Texas MD Anderson Cancer Center, United States

Reviewed by:
Maria Sol Andres, Royal Brompton Hospital, United Kingdom
Bernhard Maisch, University of Marburg, Germany

****Correspondence:***
Uyên Châu Nguyên
u.nguyen@maastrichtuniversity.nl

Specialty section:
This article was submitted to Cardio-Oncology, a section of the journal Frontiers in Cardiovascular Medicine

Received: *07 August 2021*
Accepted: *15 October 2021*
Published: *15 November 2021*

Citation:
Nguyên UC, Vernemmen AIP, Segers P, zur Hausen A, Driessen RGH, Pluijmen MJHM and Bekkers SCAM (2021) Case Report: An Unusual Cause for Recurrent Hemopericardium in a Patient With Dyspnea. Front. Cardiovasc. Med. 8:755106. doi: 10.3389/fcvm.2021.755106

INTRODUCTION

Dyspnea is a common symptom in pericardial effusive disease. The etiology of pericardial effusion varies widely but often remains unknown. Primary cardiac tumors are extremely rare (1, 2) and often go undetected until a late stage of the disease.

The present case highlights the importance of considering angiosarcoma of the heart as a potential diagnosis in patients presenting with recurrent pericardial effusion, even in the absence of malignant cells in the pericardial fluid and absence of macroscopic lesions on non-invasive imaging.

CASE DESCRIPTION AND DIAGNOSTIC ASSESSMENT

Part 1

A 52-year-old woman presented at the emergency room (ER) in a regional hospital with progressive dyspnea, a dry cough and fatigue during several weeks despite taking oral antibiotics because of a suspected pneumonia. Three days prior to presentation she had experienced a severe dull thoracic and epigastric pain accompanied by nausea and vomiting that had resolved spontaneously. Besides taking ferrofumarate and cholecalciferol for iron-deficiency anemia and vitamin D deficiency, she had no previous medical history.

On presentation, physical examination revealed a regular tachycardia of 116 beats per minute (bpm), a blood pressure of 120/75 mmHg, an oxygen saturation of 100% while breathing ambient air, and a core temperature of 38.0°C (100.4°F). Cardiac, pulmonary, and abdominal examinations were unremarkable. There were no signs of deep venous thrombosis and the Wells-score was 4.5 (3). The electrocardiogram (ECG) showed sinus tachycardia, normal electrical heart axis and normal PR- and QRS-intervals, but inverted T-waves in both antero- and inferolateral leads (**Figure 1**). A low hemoglobin level (5 mmol/L), elevated c-reactive protein (102 mg/ml), troponin-I (1036 ng/L, cut-off is <20) and NT-pro-BNP (366 ng/L, normally < 100) levels were the most prominent abnormal laboratory results.

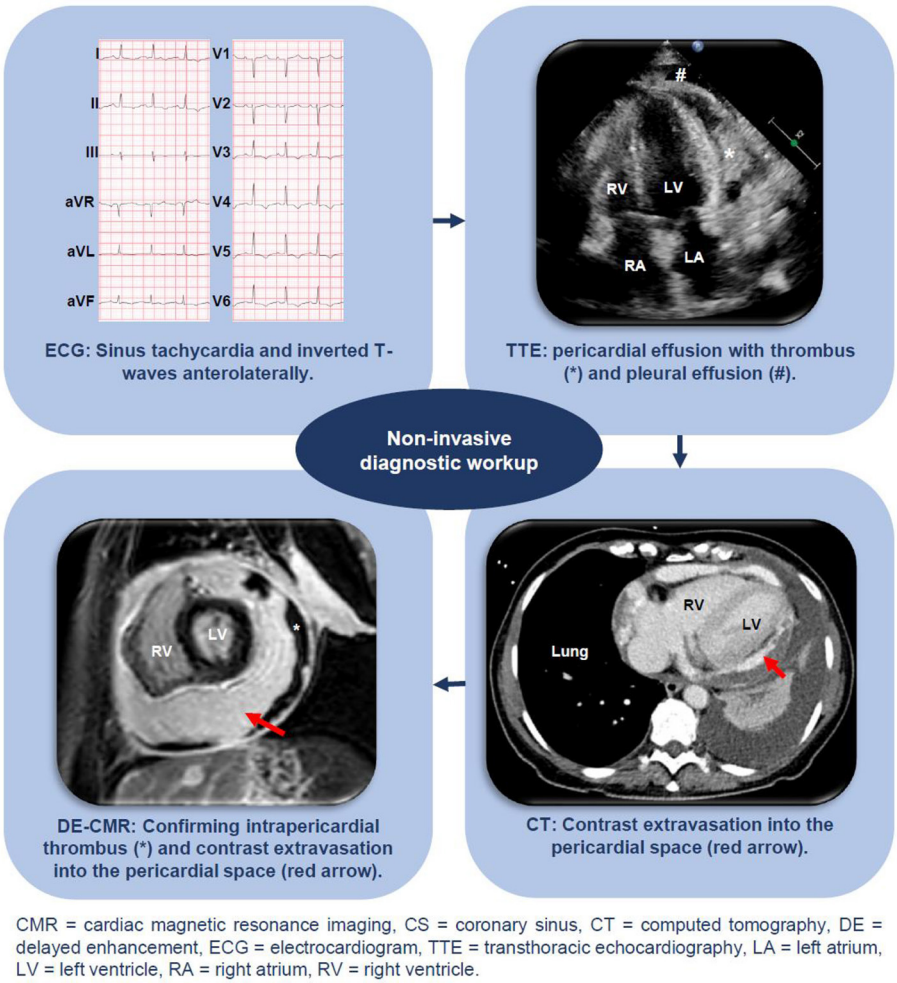

FIGURE 1 | Non-invasive diagnostic workup including ECG, echocardiography, DE-CMR, and CT.

Computed tomography angiography of the thorax (CTA) ruled out pulmonary embolism, but demonstrated pericardial and pleural effusion. Subsequent transthoracic echocardiography (TTE) confirmed circumferential pericardial effusion of ∼4.5 cm with signs of haemodynamic compromise (dilated and poor collapsing inferior caval vein, early systolic right atrial (RA) collapse and >25% respiratory variation in peak mitral E-wave). Urgent evacuation of ∼1 L of hemorrhagic fluid after pericardiocentesis immediately ameliorated symptoms. Investigation of this pericardial fluid did not reveal a tuberculous, bacterial, viral, or malignant etiology. A respiratory viral panel by polymerase chain reaction (influenzas A and B and respiratory syncytial virus) and a serum HIV antibody test were negative. After recurrent pericardial effusion was ruled out 1 week later, she was discharged home. While unconfirmed, a discharge diagnosis of post-infectious/post-viral pneumonia related pericardial and pleural effusion was made.

Already 5 days later, she presented again with progressive dyspnea, coughing, and nausea. A further decrease in hemoglobin (4.7 mmol/L) was noted and TTE showed recurrent circumferential pericardial effusion (∼3 cm) but now a dense structure suggesting thrombus in the pericardial sac (**Figure 1**). Coronary angiography (CAG) was performed after which coronary artery disease including dissection could be ruled out.

Part 2

She was transferred to a tertiary university center and received a blood transfusion. Additional viral serology (adenovirus, coxsackievirus, echovirus, borrelia burgdorferi, cytomegalovirus, Epstein-Barr virus, and parvovirus), immunological testing (systemic lupus erythematosus, rheumatoid arthritis, vasculitis, complement screening, and M-protein), a tuberculosis test and blood culture analyses were normal. To re-assess the possibility of a malignant cause, a repeat CTA of the thorax and abdomen was performed. While macroscopic malignancies could be ruled out, the scan showed contrast extravasation into the pericardial space, suggesting active bleeding. After a multidisciplinary consultation between cardiologists and cardiothoracic surgeons, and given the

observation that the patient remained hemodynamically stable, it was decided that urgent surgery was not yet indicated and that there was still sufficient time for additional diagnostic workup. On cine cardiac magnetic resonance imaging (CMR), left (LV) and right ventricular (RV) systolic function were preserved and pleural and pericardial effusion confirmed. During contraction, the LV apex remained remarkably "fixed" to the pericardium (**Supplementary Video 1**). On the delayed enhancement (DE) images, the high intra-pericardial signal again suggested contrast-extravasation into the pericardial sac, whereas an extensive, hypo-enhanced circumferential layer against the inner parietal pericardium suggested thrombus (**Figure 1**). No intramyocardial abnormalities were observed.

It was concluded that ongoing, albeit slow, intra-pericardial bleeding was present. Since other diagnostic clues were missing at this time, an initial post-viral and subsequent recurrent traumatic or reactive pericardial effusion after pericardiocentesis were still considered causative and urgent surgery was yet indicated.

Part 3

Since focal bleeding from a traumatic ventricular lesion after initial pericardiocentesis could not be excluded, it was decided to first perform a limited thoracotomy *via* a left-sided submammary incision. After evacuating 2.5 L hemorrhagic pericardial fluid with thrombi, careful inspection did not reveal a focal bleeding site. Because of persistent bleeding, the incision was extended further but again no focal bleeding source was discernable. Instead, multiple active venous hemorrhages on the entire epicardium were visible and hemostasis was attempted by placing multiple fibrin sealant patches Tachosil (Baxter healthcare cooperation, Illinois, USA). In addition, multiple biopsies of the pericardium and pericardial fluid and thrombi were sent for pathological examination.

The patient was subsequently transferred to the intensive care unit (ICU), but went into cardiogenic shock the following day. TTE showed recurrent pericardial effusion with a thrombus compressing the RA. A conventional emergency sternotomy was carried out. After thrombus removal, again diffuse hemorrhages were observed and a single bleeding focus in the RA was sutured.

Unfortunately, within 3 days she had to be operated two more times to relief recurrent cardiac tamponade and a left-sided hemothorax. Repeatedly, extensive diffuse venous epicardial hemorrhages were found that were difficult to manage, causing her to remain hemodynamically unstable in the ICU. After 9 days, pathology of the pericardium revealed an epithelioid angiosarcoma. Given the disease extent and unfavorable prognosis, it was decided to refrain from additional aggressive therapy. She died the same day, 28 days after the initial presentation. A timeline is showcased in **Figure 2**.

Part 4

After obtaining consent from relatives, gross autopsy revealed a diffusely thickened residual pericardium with an irregular surface with multiple thrombi and hemorrhages. The pericardium was extensively adhered to ribs, myocardium, ascending aorta, and aortic arch. A nodular epicardial surface was found with diffuse hemorrhages and thrombi. The heart was only minimally enlarged (419 [normal 233–403] g). Microscopy showed an atypical vascular proliferation with focal papillary structures consisting of large epithelioid cells with high amounts of eosinophilic cytoplasm. The nuclei of these epithelioid cells were pleomorphic and hyperchromatic with numerous, sometimes atypical, mitoses. Because these epithelioid cells stained positive for the immunohistochemical vascular markers ERG, CD31 and CD34 but not for CD68, HHV-8 and keratin markers CK AE1/AE3, CK 5/6, and CK7, a diagnosis of epithelioid angiosarcoma was made. The angiosarcoma was predominantly localized in the pericardium and epicardium without deeply infiltrating the myocardium leading to epicarditis and pericarditis. A single longitudinal thickened lesion was found at the RA appendage that had been surgically sutured. Microscopic evaluation of this lesion revealed transmural invasion of the angiosarcoma (**Figure 3**).

Additionally, lympho-vascular invasion with intracapillary tumor cells in the lungs (hemangiosis carcinomatosa) and focal invasion from the pericardium into the left lung was found, explaining the hemothorax.

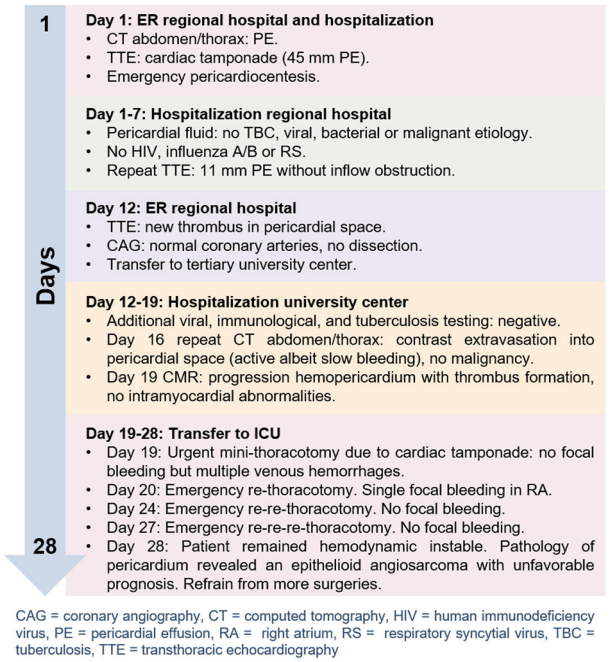

FIGURE 2 | Figure showcasing the timeline of events.

DISCUSSION AND PATIENT PERSPECTIVE

Dyspnea, fatigue, thoracic pain, nausea, anorexia, and vomiting are common symptoms in pericardial effusive disease. The etiology of pericardial effusion often remains unknown but may be caused by malignancies that are mostly metastatic, complications of myocardial infarction, infections or iatrogenic. Differentiating between primary cardiac malignancies and other causes of pericardial

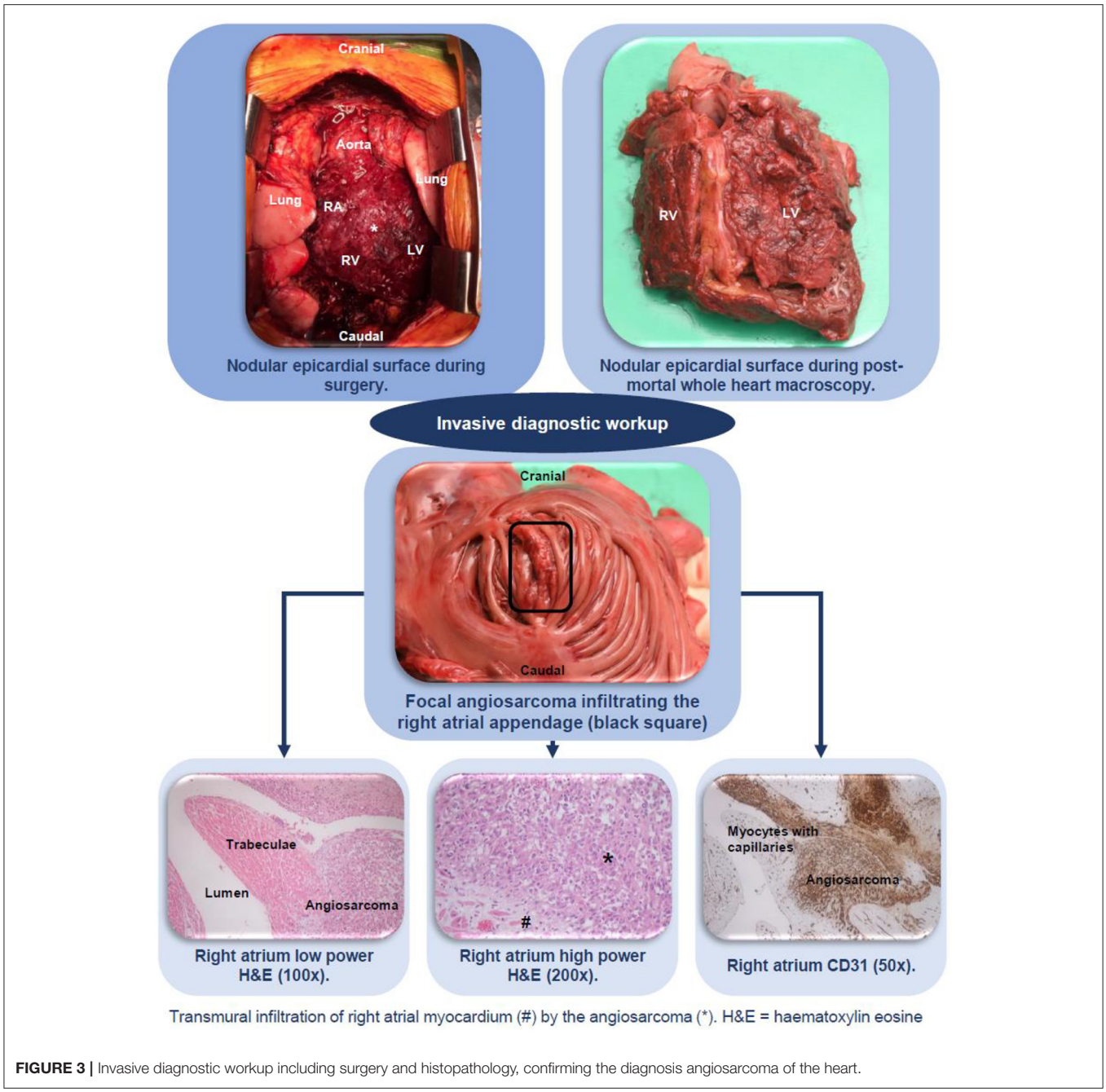

FIGURE 3 | Invasive diagnostic workup including surgery and histopathology, confirming the diagnosis angiosarcoma of the heart.

effusion should be accomplished using non-invasive imaging, CAG, cytological and ideally histological investigation of pericardial effusion and tissue specimen, respectively (4).

Primary cardiac tumors are extremely rare with an autopsy incidence of <0.06% (1, 2) of which one quarter turns out to be malignant. Angiosarcoma is the most common primary cardiac malignancy (5) and has been first reported in 1934 by Barnes et al. (6). Cardiac angiosarcomas are aggressive tumors and are often fatal and metastases are found in the majority of patients (66–89%) at time of diagnosis (7).

Angiosarcomas are soft-tissue sarcomas of endothelial cell origin that may show features of vascular and/or lymphatic differentiation. The majority of angiosarcomas arise in the RA (8) in contrast to intimal or unclassified sarcomas, which typically arise from the left atrium or inter-atrial septum (9). Common sites of extension are the right coronary artery, myocardium of the LV and RV, superior and inferior caval vein, pericardium, and mediastinum.

Early diagnosis of cardiac angiosarcoma is difficult. Non-specific symptoms and disease rarity often prevent clinicians from inclusion in the initial differential diagnosis (2).

Previous cases have described angiosarcomas as irregulated lobulated masses extending into the pericardium and adjacent vessels and have demonstrated non-invasive imaging modalities to be useful (10).

CAG is generally recommended to rule out coronary artery disease and dissection (4). Pericardiocentesis is indicated in case of hemodynamic compromise (4), and to obtain material for cytological examination, although initially rarely yielding a conclusive diagnosis of angiosarcoma (11).

Histological investigation is often needed to finally diagnose angiosarcoma and tissue specimen can be obtained *via* thoracotomy or imaging-guided biopsy, although biopsies are often non-diagnostic while carrying considerable procedural risk. In the current European guidelines, a diagnostic epicardial/pericardial biopsy is a class IIA/B indication and only recommended after more than 3 weeks of illness (4).

Because cardiac angiosarcomas are rare, no evidence-based guidelines exist for its treatment. Complete surgical resection is indicated in case of a solitary lesion and if resection preserves cardiac integrity (12). Unfortunately, this is often not possible (12) because of its diffuse infiltrative nature. There is insufficient evidence that chemotherapy, radiotherapy or cardiac transplantation may improve survival (13, 14). As a result, prognosis of cardiac angiosarcomas remains poor with survival ranging from 6 to 9 months after diagnosis (13).

Cardiac angiosarcoma turned out to be a devil in disguise in our case and we were misled by the non-diagnostic results of the initial pericardiocentesis, CAG, and imaging results. Only after repeat and exploratory surgery, the diffuse venous pericardial hemorrhages with localized thrombi typical of angiosarcoma were discovered. At that time, the angiosarcoma was already disseminated with focal transmural invasion and only palliative options remained.

In retrospect, pathologically confirming angiosarcoma would have been possible several days earlier (day 12) if we had considered biopsy (either surgical or image-guided) immediately after transfer to our center. Whether this would have changed the outcome is doubtful, given that the tumor was already widely disseminated. Though, earlier diagnosis may have omitted repetitive surgery.

With the present case we would like to stress the importance of considering cardiac angiosarcoma as a potential diagnosis in recurrent pericardial effusion, even when malignant cells are absent in the pericardial fluid and macroscopic lesions on non-invasive imaging cannot (yet) be seen. An atypical clinical course of recurrent pericardial effusion may be typical for angiosarcoma of the heart.

DATA AVAILABILITY STATEMENT

The raw data supporting the conclusions of this article will be made available by the authors, without undue reservation.

ETHICS STATEMENT

Ethical review and approval was not required for the study on human participants in accordance with the local legislation and institutional requirements. Written informed consent for participation was not required for this study in accordance with the national legislation and the institutional requirements.

AUTHOR CONTRIBUTIONS

UN and SB contributed to conception and design of the study and wrote the first drafts of the manuscript. AV, PS, AH, RD, and MP wrote sections of the manuscript. All authors contributed to manuscript revision, read, and approved the submitted version.

SUPPLEMENTARY MATERIAL

The Supplementary Material for this article can be found online at: https://www.frontiersin.org/articles/10.3389/fcvm.2021.755106/full#supplementary-material

Supplementary Video 1 | Chamber cine CMR video.

REFERENCES

1. Lam KY, Dickens P, Chan AC. Tumors of the heart. A 20-year experience with a review of 12,485 consecutive autopsies. *Arch Pathol Lab Med*. (1993) 117:1027–31.
2. Krishnan T, Pettersson G, Mukherjee R, Singhal N. Cardiac angiosarcoma: a diagnostic and therapeutic challenge. *J Cardiol Cases*. (2020) 22:90–3. doi: 10.1016/j.jccase.2020.04.010
3. Wells PS, Anderson DR, Rodger M, Stiell I, Dreyer JF, Barnes D, et al. Excluding pulmonary embolism at the bedside without diagnostic imaging: management of patients with suspected pulmonary embolism presenting to the emergency department by using a simple clinical model and d-dimer. *Ann Intern Med*. (2001) 135:98–107. doi: 10.7326/0003-4819-135-2-200107170-00010
4. Adler Y, Charron P, Imazio M, Badano L, Barón-Esquivias G, Bogaert J, et al. (2015). ESC guidelines for the diagnosis and management of pericardial diseases: the task force for the diagnosis and management of pericardial diseases of the European Society of Cardiology (ESC)Endorsed by: the European Association for Cardio-Thoracic Surgery (EACTS). *Eur Heart J*. (2015) 36:2921–64. doi: 10.1093/eurheartj/ehv318
5. Burke A. *Atlas of Tumor Pathology: Tumors of the Heart and Great Vessels*. Washington, DC: American Registry of Pathology (1996).
6. Barnes AR, Beaver DC, Snell AM. Primary sarcoma of the heart: report of a case with electrocardiographic and pathological studies. *Am Heart J*. (1934) 9:480–91. doi: 10.1016/S0002-8703(34)90096-X
7. Janigan DT, Husain A, Robinson NA. Cardiac angiosarcomas. A review and a case report. *Cancer*. (1986) 57:852–9.
8. Look Hong NJ, Pandalai PK, Hornick JL, Shekar PS, Harmon DC, Chen YL, et al. Cardiac angiosarcoma management and outcomes: 20-year single-institution experience. *Ann Surg Oncol*. (2012) 19:2707–15. doi: 10.1245/s10434-012-2334-2
9. Gopal AS, Arora NS, Messineo FC. Right ventricular myxoma. *N Engl J Med*. (2000) 342:295. doi: 10.1056/NEJM200001273420418
10. Holloway BJ, Agarwal PP. AJR teaching file: right atrial mass in a woman with dyspnea on exertion. *AJR Am J Roentgenol*. (2009) 192(3 Suppl.):S49–52. doi: 10.2214/AJR.07.7066
11. Randall MB, Geisinger KR. Angiosarcoma of the heart: pericardial fluid cytology. *Diagn Cytopathol*. (1990) 6:58–62. doi: 10.1002/dc.2840060113

12. Bouma W, Lexis CP, Willems TP, Suurmeijer A, van der Horst I, Ebels T, et al. Successful surgical excision of primary right atrial angiosarcoma. *J Cardiothorac Surg*. (2011) 6:47. doi: 10.1186/1749-8090-6-47
13. Herrmann MA, Shankerman RA, Edwards WD, Shub C, Schaff HV. Primary cardiac angiosarcoma: a clinicopathologic study of six cases. *J Thorac Cardiovasc Surg*. (1992) 103:655–64. doi: 10.1016/S0022-5223(19)34948-7
14. Gowdamarajan A, Michler RE. Therapy for primary cardiac tumors: is there a role for heart transplantation? *Curr Opin Cardiol*. (2000) 15:121–5. doi: 10.1097/00001573-200003000-00010

Conflict of Interest: The authors declare that the research was conducted in the absence of any commercial or financial relationships that could be construed as a potential conflict of interest.

Publisher's Note: All claims expressed in this article are solely those of the authors and do not necessarily represent those of their affiliated organizations, or those of the publisher, the editors and the reviewers. Any product that may be evaluated in this article, or claim that may be made by its manufacturer, is not guaranteed or endorsed by the publisher.

Copyright © 2021 Nguyên, Vernemmen, Segers, zur Hausen, Driessen, Pluijmen and Bekkers. This is an open-access article distributed under the terms of the Creative Commons Attribution License (CC BY). The use, distribution or reproduction in other forums is permitted, provided the original author(s) and the copyright owner(s) are credited and that the original publication in this journal is cited, in accordance with accepted academic practice. No use, distribution or reproduction is permitted which does not comply with these terms.

frontiers in Cardiovascular Medicine

CASE REPORT
published: 31 January 2022
doi: 10.3389/fcvm.2021.707361

Capecitabine and Warfarin Interaction: A Case Report With Review of Literature and Management Options

Khalefa Althiab[1,2,3,4], *Manal Aljohani*[1,2,3,4]*, *Sultan Alraddadi*[1,2,3,4] and *Mohammed Algarni*[2,3,4,5]

[1] Department of Pharmacy Service, King Abdulaziz Medical City, Riyadh, Saudi Arabia, [2] Ministry of National Guard Health Affair, Riyadh, Saudi Arabia, [3] King Abdullah International Medical Research Center, Riyadh, Saudi Arabia, [4] King Saud bin Abdulaziz University for Health Sciences, Riyadh, Saudi Arabia, [5] Adult Oncology Department, King Abdulaziz Medical City, Riyadh, Saudi Arabia

Capecitabine is an orally active prodrug of 5-fluorouracil with improved safety and efficacy that is extensively used as an antineoplastic agent. It is converted to 5-Fluorouracil in the liver and tumor tissues. *In vitro* assays did not reveal any significant potential for interaction between capecitabine and its metabolites with warfarin. However, several reports provided clinical evidence of such interaction resulting in an elevated international normalized ratio (INR) and bleeding. Here, we report another case of capecitabine and warfarin concurrent administration that resulted in sub- or supra- therapeutic INR without any bleeding episode or venous-thromboembolic event through the follow-up period. Moreover, a review of available management options is also presented in this paper.

Keywords: warfarin, capecitabine, drug interaction, international normalized ratio (INR), case report

OPEN ACCESS

Edited by:
Reto Asmis,
Wake Forest School of Medicine,
United States

Reviewed by:
Christian Cadeddu Dessalvi,
University of Cagliari, Italy
Chiara Lestuzzi,
Santa Maria degli Angeli Hospital
Pordenone, Italy

***Correspondence:**
Manal Aljohani
aljohaniMa6@ngha.med.sa

Specialty section:
This article was submitted to Cardio-Oncology, a section of the journal Frontiers in Cardiovascular Medicine

Received: *09 May 2021*
Accepted: *07 December 2021*
Published: *31 January 2022*

Citation:
Althiab K, Aljohani M, Alraddadi S and Algarni M (2022) Capecitabine and Warfarin Interaction: A Case Report With Review of Literature and Management Options. Front. Cardiovasc. Med. 8:707361. doi: 10.3389/fcvm.2021.707361

INTRODUCTION

Fluoropyrimidines such as 5-fluorouracil (5-FU) and capecitabine mainstay for several solid malignancies. Capecitabine is approved for colorectal cancer and metastatic breast cancer as mono-therapy and adjuvant therapy (1). Capecitabine is an orally administered prodrug of 5-FU, with almost 100% oral bioavailability, which mimics 5-FU continuous infusion with improved safety and efficacy. Its advantages over 5-FU led to a reduction in the economic burden on both patient and health care systems and infectious complications due to intravenous access. The conversion of capecitabine to 5-FU is catalyzed via thymidine phosphorylase which is found in the liver and several tumors in high levels compared to other healthy tissue (2, 3). Capecitabine is dosed based on the body surface area at 1,250 mg/m^2 taken twice daily for 14 days, followed by a 7-day rest period over a 21-days cycle (1). On the other hand, warfarin is an oral anticoagulant that antagonizes vitamin K and inhibits the synthesis of clotting factors II, VII, IX, and X in addition to the naturally occurring endogenous anticoagulant proteins C and S. It is indicated for the prevention and treatment of venous thrombosis, pulmonary embolism, atrial fibrillation, myocardial infarction, and prosthetic cardiac valve component embolism (4). Warfarin is a medication with narrow therapeutic index and associated with numerous drug-drug and drug-food interactions, through pharmacodynamic or pharmacokinetic mechanisms (4, 5). It consists of a pair of enantiomers that are extensively and differently metabolized by human cytochrome P450 (CYP 450) isoenzymes. CYP2C9 is the predominant *S*-warfarin enantiomer metabolizing enzyme, while CYP1A2 and CYP3A4 are the major hepatic enzymes contributing to *R*-warfarin enantiomer metabolism (5, 6). Although *S*-warfarin is 5–8 times more potent as a vitamin K antagonist than *R*-warfarin, however,

the later has a longer half-life (37.4–88.6 h) compared to that of *S*-warfarin (21.2–42.6 h), and further prolongation of the half-life by decreased metabolism may have greater clinical significance (7). Besides that, *R*-warfarin is a noncompetitive inhibitor of *S*-warfarin's metabolism by CYP2C9, indicating that *S*-warfarin's pharmacokinetic properties may be altered by *R*-warfarin. There is a potential drug-drug interaction between capecitabine and warfarin, alike to that observed between 5-FU and warfarin, speculated to be most likely due to the same mechanism (2, 3, 5). *In vitro* assays of human liver microsome did not reveal any significant potential for interaction between capecitabine or its metabolites and substrates of the CYP 450 isoenzymes 1A2, 2A6, 2C9, 2C19, 2D6, 2E1, or 3A4. However, several post-marketing case reports provided clinical evidence of significant interaction between capecitabine and warfarin, leading to an elevation of international normalized ratio (INR), requiring a black box warning in the package insert. The mechanism of action for the interaction is not well-understood and could be related to down-regulation of CYP2C9 by capecitabine or its metabolites or a pharmacodynamic interaction with warfarin.

CASE REPORT

A 73-year-old female, new to our institution with a past medical history of traumatic intracranial hemorrhage due to fall, poor mobility, wheelchair-bound, old stroke, cardiomyopathy of undetermined etiology with an ejection fraction of 35–40%, and non-valvular atrial fibrillation (NVAF), which was stable on warfarin 2 mg orally daily for many years, her therapeutic range is 2–3. In January 2020, she was diagnosed with right colonic adenocarcinoma, and later on that month, she underwent a right hemicolectomy. Pathology showed cecal adenocarcinoma moderately differentiated at stage T4N2b. At that time, she was offered adjuvant therapy, but she refused. Few months later, her follow up scans showed liver deposits highly suspicious of metastasis from colonic origin. For colorectal cancer capecitabine is dosed at 1,250 mg/m^2. However, due to her Eastern Cooperative Oncology Group (ECOG) performance status of three points and taking in account the drug-drug interaction with warfarin, she was started on capecitabine 1000 mg/m^2, twice daily for 2 weeks, followed by 1 week off. Before her first visit to the Adult Medical Oncology clinic at King Abdulaziz Medical City (KAMC), Riyadh, Saudi Arabia, she already finished three cycles of capecitabine. No other concurrent medications were administered. Her laboratory test showed an elevated INR of 6.98 without any bleeding or bruises. To evaluate the degree of the interaction between capecitabine and warfarin and manage warfarin doses, she was referred to the clinical pharmacist-managed anticoagulation clinic (ATC). Before the referral, the average of all her laboratory results were within normal ranges, including kidney and liver functions. Except for red blood cells and hemoglobin which were 2.5 × 10^12/L and 93 g/L, respectively. The patient interview revealed that before the initiation of capecitabine at a certain point in time, she was shifted from warfarin to rivaroxaban but did not tolerate its gastrointestinal side effects and shifted back to warfarin. Since the patient is on long-term warfarin treatment, the caregivers (patient's daughters) were trained to make "self-manage" adjustment of warfarin doses after performing her coagulation profile testing in a private laboratory. After the capecitabine initiation, the family noticed the patient's INR elevations, reaching up to 5.0 but without any history of minor or major bleeding episodes. They started to monitor the INR every 2 weeks and withholding warfarin on the second day of each cycle and resume it again 1–3 days after the last dose of capecitabine, depending on the INR result. This management resulted in either sub- or supratherapeutic INR. A discussion of the case between the clinical pharmacist and her oncologist, the most responsible physician, resulted in a plan to shift the patient to apixaban after being reviewed by a cardiologist. However, she refused to change warfarin due to her previous gastrointestinal side effects with rivaroxaban. Coagulation profile monitoring was carried out on a weekly basis. The management of warfarin doses on capecitabine period and free period is presented in **Table 1**. The last recorded INR while writing this paper was 2.45, without any major or minor bleeding episodes or venous-thromboembolic events.

DISCUSSION

With the increased concomitant use of capecitabine and warfarin, this is another case that confirms the clinical interaction between these two medications. Bleeding events secondary to the interaction have occurred several days to several months after the initiation of capecitabine; these events can occur up to months after the last dose of capecitabine (7, 8). The exact mechanism of this interaction is yet, unknown but may be related to hepatic metabolism. Capecitabine is a prodrug that is converted in a 3-step pathway via thymidine phosphorylase in the liver and the tumor site, releasing its only active metabolite 5-fluorouracil (2, 3). Of importance, gastrointestinal toxicity is an essential common adverse effect of 5-FU that includes nausea, vomiting, and diarrhea. This toxic adverse effect causes cell death of the gastrointestinal epithelium, which could alter warfarin's absorption (7).

Six cases reported concerning the adverse interaction between capecitabine and warfarin are summarized in **Table 2**. The first two cases in the literature reporting severe coagulopathy with bleeding due to drug-drug interaction between capecitabine and warfarin were of two female patients. The first was a 91-year-old woman diagnosed with adenocarcinoma of the rectum with lung and liver metastases. After 4 cycles of capecitabine, she developed left femoral vein thrombosis, for which she was anticoagulated with warfarin dosed at 2.5 mg/day. After 6 weeks of concurrent administration, the patient was admitted due to vagino-rectal bleeding with an INR of $>$ 10. The second was of a 72-years-old female who had recurrent metastatic breast cancer to the bone. She was controlled on chronic warfarin 2.5 mg/day to treat her pulmonary embolism for 3 years before capecitabine's initiation. After the completion of two cycles, she presented with a 3-day history of loose black stools and INR of $>$ 10 (9). Another two reported cases were of two men with metastatic colon cancer; both were on long-term warfarin with therapeutic INR for a long

TABLE 1 | Warfarin doses with INR trend during capecitabine cycles.

Management	Recorded INR test		Warfarin dose (mg/day)		Number of days warfarin was withheld
	No.	Result	Capecitabine period (14 days)	Capecitabine free period (7 days)	
Self-managed	1	1.66	2	2	12–15*
	2	1.49	2	2	12–15*
	3	1.24	2	2	12–15*
	4	1.34	2	2	12–15*
	5	6.96	2	2	12–15*
Anticoagulation clinic	6	2.47	1	2	0
	7	3.80	1	2	2
	8	1.57	0.5	2	0
	9	2.28	0.5	2	0
	10	1.55	1	2	0
	11	2.35	1	2	0
	12	2.21	1	2	0
	13	2.29	1	2	0
	14	2.40	1	2	0
	15	2.28	1	2	0
	16	2.72	1	2	0
	17	2.03	1	2	0
	18	2.75	1	2	0
	19	1.87	1	2	0
	20	2.07	1	2	0
	21	2.43	1	2	0
	22	2.45	1	2	0

**Number of days withheld self-reported estimate by the patient's caregiver.*

time before they began capecitabine. Both patients were admitted due to gastrointestinal bleeding in a shocked state, with an INR of > 10. One of these patients was an 81-year-old who was admitted on the fifth day of the first cycle. The second was a 79-year-old who was admitted on the fourth day of the second cycle (10). The fifth case reported was a 67-year-old female who had been well-controlled on long-term warfarin (5 mg/day). After 4.5 weeks of capecitabine initiation for her metastatic breast cancer, she developed hemorrhagic blisters, purpura and ecchymoses, and an INR of 8.56 (11). All of the previously mentioned cases were managed as inpatient settings withholding both medications, administration of vitamin K, and blood products transfusion ± omeprazole infusion. The last case was a 59-year-old female with metastatic breast cancer to bone and lung receiving a chronic mini-dose of warfarin dosed as 1 mg/day as prophylaxis against catheter-associated thrombosis. Before capecitabine initiation, her weekly INR monitoring reports were always below 2. Three weeks after the capecitabine initiation, her INR markedly rose to 8.87 without any signs and symptoms of bleeding. After her coagulation profile was normalized, she was switched to subcutaneous low-molecular-weight heparin (LMWH), and her chemotherapy was restarted without any further consequences (5).

Only two studies addressed the effects of capecitabine and warfarin interaction, as summarized in **Table 3**. In an observational study, medical records of 69 patients who used capecitabine and warfarin concurrently within 7 days or less of the later use were reviewed. Most patients were diagnosed with breast cancer (49%) or colon cancer (32%). Indications for warfarin use were deep vein thrombosis/pulmonary embolism ($n = 38$), venous access device prophylaxis ($n = 17$), and other indications ($n = 14$). Among the 17 patients who received low-dose warfarin for venous access device prophylaxis, only one bleeding event occurred, and one patient (5.9%) had at least one INR > 3.0. No bleeding events occurred among the 52 patients who received warfarin for indications other than venous access device prophylaxis, although 35 patients (67.3%) had at least one INR > 3.0 and 23 patients (44.2%) had at least one INR > 5.0. Compared with the use of warfarin alone, the study did not find big differences in the rates of bleeding events and elevated INR in patients receiving concomitant capecitabine and warfarin (12). Moreover, a retrospective study of 77 participants analyzed the alerted coagulation profile while on capecitabine with or without warfarin. Tumors were pancreatic or gallbladder (63.6%), colon (23.4%), hepatocellular (5.4%), breast (3.5%), carcinoid and gastric (1.2% each). Liver metastases were present in 32 patients. Only 21 patients were on anticoagulation therapy with warfarin, with an average weekly dose of 18.8 mg, for central-vein thrombosis prophylaxis (48%), deep vein thrombosis (33%), and atrial fibrillation/flutter (19%). Twelve patients were already

TABLE 2 | Summary of reported cases of adverse events between capecitabine and warfarin.

Patient characteristics		Therapy indication		Co-administration			Bleeding	
Case no. (Ref)	**Age/ Gender**	**Warfarin**	**Capecitabine**	**Sequence**	**Duration**	**Reported INR**	**Description**	**Management**
1 (9)	91/F	DVT	Rectal with liver metastases	Capecitabine for 4 cycles before warfarin	6 weeks	>10	Vagino-rectal bleeding	- Holding both agents - IV vitamin K - No further chemotherapy received
2 (9)	72/F	PE	Recurrent metastatic breast cancer	Warfarin for 3 years before Capecitabine	8 weeks	>10	Melena	- Holding both agents - IV hydration and vitamin K - Fresh frozen plasma - Packed red blood cells - No further chemotherapy received
3 (10)	81/M	NR	Metastatic colon cancer	Warfarin before Capecitabine (time interval NR)	1 week	>10	Gastrointestinal in a shocked condition	- Holding both agents - IV vitamin K - Fresh frozen plasma - Packed red blood cells - Omeprazole infusion
4 (10)	79/M	NR	Metastatic colon cancer	Warfarin before Capecitabine (time interval NR)	4 weeks	>10	Gastrointestinal in a shocked condition	- Holding both agents - IV vitamin K - Fresh frozen plasma - Packed red blood cells - Omeprazole infusion
5 (11)	67/F	PE	Metastatic breast cancer	Warfarin for 1 year before Capecitabine	4.5 weeks	8.56	Hemorrhagic blisters, purpura, and ecchymoses	- Holding both agents - IV vitamin K
6 (5)	59/F	CRT prophylaxis	Metastatic breast cancer	Warfarin before Capecitabine (time interval NR)	3 weeks	8.87	No signs and symptoms of bleeding	- Holding both agents - IV vitamin K - Switched to LMWH

INR, international normalized ratio; DVT, deep vein thrombosis; PE, pulmonary embolism, NR, not reported; CRT, catheter-related thrombosis; LMWH, low-molecular-weight heparin.

on warfarin before capecitabine initiation, and nine started warfarin while previously on capecitabine therapy. Eleven patients had an INR > 3 (range, 3.23–11.5); consequently, the incidence of an INR > 3 at 130 days of treatment with capecitabine was 32% with warfarin vs. 4% without warfarin ($P = 5.1 \times 10^{-14}$). After the discontinuation of capecitabine, INR results returned to their normal ranges. Seven patients developed gastrointestinal bleeding that required hospitalization for aggressive management; four of them were on concurrent administration of capecitabine and warfarin. The incidence of bleeding at 130 days of treatment with capecitabine was 18% with warfarin vs. 2% without ($P = 4 \times 10^{-13}$). Overall, six patients needed warfarin dose reduction by 1–2.5 mg (13).

Management

Cancer patients are at higher risk of developing venous thromboembolism (VTE) than non-cancer patients, with an incident of 6.5-fold higher. Thromboembolic event(s) can occur at any time either preceding the diagnosis of cancer, more often, at the time of diagnosis or during treatment resulting in the second leading cause of death among cancer patients. Such population requires comprehensive management, which includes identifying patients that require effectual treatment or pharmacologic prophylaxis to reduce the risk of recurrence (14, 15).

Erratic INR control is seen in patients with cancer making vitamin K antagonists not an option to anticoagulate such population, particularly while receiving chemotherapy. Maintaining therapeutic INR could be challenged by nutritional factors and drug-drug interactions with other concomitant medications, including chemotherapy agents (16). Such management of both agents' concurrent administration is challenging; warfarin dose reduction or switching to an alternative as low-molecular-weight heparin (LMWH) or direct-acting oral anticoagulants (DOACs) are the currently available options. Available anticoagulation options for cancer patients other than warfarin are presented in **Table 4**.

Frequent INR Monitoring and Warfarin Dose Reduction

Generally speaking, more frequent testing is optimal to keep patients within target therapeutic INR, especially during the initial warfarin therapy, if a patient's INR becomes supratherapeutic or subtherapeutic, or if an interacting medication is introduced (18), A case report of a chronically anticoagulated patient with warfarin for a mechanical mitral valve replacement was diagnosed with stage IV metastatic colon cancer. Before initiating capecitabine, therapeutic INR was maintained with an average dose of 10.35 mg/day. While on chemotherapy, the patient was anticoagulated with warfarin;

TABLE 3 | Summary of studies reporting the adverse events between capecitabine and warfarin.

Study type/number of patients		Therapy indication		Reported INR	Reported bleeding cases	Study outcome(s)
Type of study (Ref.)	**No. of patients receiving capecitabine and warfarin concomitantly**	**Warfarin (%)**	**Capecitabine (%)**			
An observational study (12)	69	1. DVT/PE (55.07) 2. Venous access device prophylaxis (24.64) 3. Other (20.29)	1. Breast (49) 2. Colon (32)	- 36 patients had at least one INR >3.0 - 23 patients had at least one INR >5.0	One bleeding event in a patient who was on warfarin for venous access device prophylaxis	The study did not find significant differences in the rates of bleeding events and elevated INR in patients receiving concomitant capecitabine and warfarin
A retrospective study (15)	21	1. Central-vein thrombosis prophylaxis (48) 2. DVT (33) 3. AF (19)	1. Pancreatic or gallbladder (63.6) 2. Colon (23.4) 3. HCC (5.4) 4. Breast (3.5) 5. Carcinoid (1.2) 6. Gastric (1.2)	11 patients had an INR >3	GI bleeding was encountered in 7 patients	There is a clinically significant interaction between warfarin and capecitabine

INR, international normalized ratio; DVT, deep vein thrombosis; PE, pulmonary embolism; AF, atrial fibrillation/flutter; HCC, hepatocellular carcinoma; GI, gastrointestinal.

with each cycle, warfarin's dose was adjusted according to the INR result. After completing 3-consecutive cycles of concomitant administration of capecitabine and warfarin, a total reduction of > 85% of the warfarin dose was achieved to maintain therapeutic INR (19). On the other hand, a retrospective study showed that only six out of 21 patients who used capecitabine and warfarin concurrently required warfarin dose reduction by 1–2.5 mg. It is worth mentioning that four of the patients who developed bleeding had an INR of 1.0–1.1 within 4 weeks prior to initiating capecitabine. Only 1 of them developed an elevated INR of 5.9 within 4 weeks after the initiation of capecitabine (13). When managing patients receiving concomitant capecitabine and warfarin, it is crucial to keep in mind the presence of high unpredictable inter-individual variables and the importance of closely monitoring the patients for signs and symptoms of bleeding. Once or twice per week, if applicable, INR monitoring is highly recommended to adjust warfarin's doses accordingly. In our approach, we were targeting to monitor INR twice-weekly; however, we were limited by the patient's age and the complete blood count status that did not allow more frequent INR monitoring (i.e., twice weekly). However, the patient and the caregivers were satisfied with both the monitoring and the INR results.

LOW-MOLECULAR-WEIGHT HEPARIN

Five clinical trials comparing LMWHs vs. warfarin revealed that they are effective in VTE reduction in cancer patients. Additionally, a meta-analysis of 15 randomized controlled trials confirmed their efficacy. A Cochrane review in 2016 showed a reduction in the risk of symptomatic VTE by roughly half (RR, 0.54; 95%CI, 0.38–0.75) when comparing LMWH prophylaxis with no thromboprophylaxis (20). The absence of drug-drug interaction with capecitabine makes them a considerable option in cancer patients. Also, LMWHs seem to have a more favorable profile in such population. However, several factors may limit their use, including quality of life reduction associated with long-term daily administration of subcutaneous injections, weight-based dosing, the need for dose adjustments in renal impairment, and they are not an option in patients who developed heparin-induced thrombocytopenia (HIT) (14). A study was conducted in patients with active cancer receiving chemotherapy with NVAF to evaluate the safety and efficacy of DOAC vs. LMWH and their associated relevant bleeding-free survival. A total of 302 patients with NVAF and active cancer were included. Among all, 192 (63.5%) were treated with dabigatran, rivaroxaban, apixaban, and edoxaban in 20, 24, 80, and 68 patients, respectively. On the other hand, 110 were treated with LMWH. Systemic embolism and stroke rates were higher in the LMWH group, as reported in seven patients compared to three patients in the DOACs; there were significant differences in relation to major bleeding events (21).

DIRECT-ACTING ORAL ANTICOAGULANTS

With the current expansion of treatment and prophylaxis options of VTE, of note, direct-acting oral anticoagulants (DOACs) can be used in cancer patients. Clinical trials of comparing DOACs to warfarin showed that they are non-inferior. The clinical decision of the selected DOACs must be individualized to fit the patients' clinical profile after an in-depth discussion about risks vs. benefits, including patients' risk of bleeding, the presence of any drug-drug interaction with other medications via CYP 3A4 metabolic pathway and P-glycoprotein transport, as well as the patients renal and hepatic functions (14, 15). Although, Clinical data suggest that capecitabine or its metabolites in

TABLE 4 | Available anticoagulation options for cancer patients (15, 17).

Pharmacologic prophylaxis options		
UFH	5,000 Units every 8 h	
Dalteparin[a,b]	5,000 Units once daily subcutaneous	
Enoxaparin[c]	40 mg once daily subcutaneous	
Fondaparinux[d]	2.5 mg once daily subcutaneous	
Apixaban[e]	2.5 mg orally twice daily	
Rivaroxaban	10 mg orally once daily	
Treatment of established VTE management options		
UFH	80 Units/kg IV bolus followed by 18 Units/kg/h IV*	
Dalteparin[a,b,g]	Initially, 200 Units/kg subcutaneous once daily for 30 days	
	Followed by 150 Units/kg subcutaneous once daily	
Enoxaparin[c]	1 mg/kg every 12 hours; or	
	1.5 mg/kg once daily	
Tinzaparin	175 Units/kg once daily subcutaneous	
Fondaparinux[d]	Weight-based dosing regimen	< 50 kg: 5 mg once daily subcutaneous
		50-100 kg: 7.5 mg once daily subcutaneous
		> 100 kg: 10 mg once daily subcutaneous
Apixaban[e]	Initially, 10 mg orally twice daily after that	
	Followed by 5 mg orally twice daily after that	
Rivaroxaban[f]	Initially, 15 mg orally every 12 h for 21 days	
	Followed by 20 mg orally once daily after that	
Edoxaban[h]	Weight-based dosing regimen	≥ 60 mg orally once daily
		≤ 60 kg: 30 mg orally once daily[i]

aPTT, Activated Partial Thromboplastin; VTE, venous thromboembolism.
[a]FDA approved LMWH for an extended therapy to prevent recurrent thrombosis in patients with cancer.
[b]In renal impairment cancer patients with CrCl ≤ 30 mL/min, monitor anti-factor Xa levels and adjust the dose accordingly to achieve target range 0.5–1.5 international unit.
[c]Mainly renally cleared; avoid in patients with CrCl ≤ 30 mL/min or adjust the dose according to anti-factor Xa levels.
[d]In renal impairment patients with CrCl ≤ 30 mL/min, use is contraindicated by manufacture labeling.
[e]In severe hepatic impairment, Child-Pugh Class C apixaban is not recommended.
[f]Doses to be taken with food.
[g]Maximum daily 18,000 units per day, therapy beyond 6 months not established.
[h]In moderate to severe hepatic impairment (Child-Pugh Class B and C) edoxaban is not recommended.
[i]If the patients' CrCl 30–50 mL/min, or the patient needs concomitant use of a P-glycoprotein inhibitor.
**After which adjust the dose based on aPTT.*

human may interact mainly with CYP2C9, and to a lesser extent on CYP3A4 or CYP1A2 (22). Up to our knowledge, there is not documented drug-drug interaction nor reported cases between capecitabine or its metabolites and DOACs. Another critical factor to consider, patients receiving chemotherapy frequently suffer from gastrointestinal symptoms, primarily vomiting, diarrhea, and mucositis. Consequently, such patients are at a greater risk of gastrointestinal bleeding and at a higher risk of an altered absorption due to diarrhea episodes that could alter their bioavailability (14). DOACs have been tested extensively in the general population; however, the available data on their safety and efficacy in patients with active cancer and AF remains low. Moreover, the number of cancer patients in the pivotal clinical trials was small; they were mainly excluded from the trial, not to cancer itself, but due to their short life expectancy. Furthermore, cancer-specific information, including the type of cancer, stage, and the concomitant use of chemotherapy, was not collected (16).

CONCLUSION

There is clinical evidence of drug-drug interaction resulting in potentiation of coumarin derivatives' effect when co-administered with fluoropyrimidine-based chemotherapy, as reported in several case reports in the literature. Such interaction could occur at any time after the concurrent administration in cancer patients with or without liver metastases. It is reasonable to speculate that such interaction may be due to a similar mechanism as with fluorouracil. This interaction could result from the inhibition of CYP450 2C9 by capecitabine or its metabolites. Awareness of this potentially serious interaction between capecitabine and warfarin will further improve anticoagulation control in cancer patients. Close monitoring of coagulation parameters throughout treatment and to be continued for at least 1 month after the last dose of capecitabine is required in patients receiving both agents concomitantly. Available management options include warfarin dose adjustments, low-molecular-weight heparin, or direct-acting oral anticoagulants.

DATA AVAILABILITY STATEMENT

The original contributions presented in the study are included in the article/supplementary material, further inquiries can be directed to the corresponding author/s.

ETHICS STATEMENT

Written informed consent was obtained from the individual(s) for the publication of any potentially identifiable images or data included in this article.

AUTHOR CONTRIBUTIONS

KA and MAlg were involved in the case management. MAlj and KA wrote the manuscript in consultation with SA and MAlg. All authors contributed to the article and approved the submitted version.

REFERENCES

1. Hoffman-LaRoche Inc. *Warning: Xeloda-Warfarin Interaction Drug Label* (2015). Available online at: https://www.accessdata.fda.gov/drugsatfda_docs/label/2015/020896s037lbl.pdf (accessed October 13, 2020).
2. Walko CM, Lindley C. Capecitabine: a review. *Clin Ther.* (2005) 27:23–44. doi: 10.1016/j.clinthera.2005.01.005
3. Shah SR, Martin R, Dowell JE, Ussery SMG. Comparison of the 5-fluorouracil-warfarin and capecitabine-warfarin drug interactions. *Pharmacotherapy.* (2010) 30:1259–65. doi: 10.1592/phco.30.12.1259

4. Kuruvilla M, Gurk-Turner C. A Review of warfarin dosing and monitoring. *Baylor Univ Med Cent Proc.* (2001) 14:305–6. doi: 10.1080/08998280.2001.11927781
5. Giunta G. Adverse interaction between capecitabine and warfarin resulting in altered coagulation parameters: a review of the literature starting from a case report. *Case Rep Med.* (2010) 2010:426804. doi: 10.1155/2010/426804
6. Enantiomers S, Yumazaki H. Shim T. Human liver cytochrome P450 enzymes involved in the 7-hydroxylation of R-and S-warfarin enantiomers. *Biochem Pharmacol.* (1997) 54:1195–203. doi: 10.1016/S0006-2952(97)00304-3
7. Kolesar JM, Johnson CL, Freeberg BL, Berlin JD, Schiller JH. Warfarin-5-FU interaction - A consecutive case series. *Pharmacotherapy.* (1999) 19:1445–9. doi: 10.1592/phco.19.18.1445.30897
8. Ikenishi M, Ueda M, Kuroda A, Tsukazaki H, Nakao M, Takeuchi M, et al. A study on drug interaction between warfarin and capecitabine with special reference to the co-administered term or the discontinuation term of capecitabine gan to kagaku ryoho. *Cancer Chemother.* (2015) 42:833–9.
9. Copur MS, Ledakis P, Bolton M, Morse AK, Werner T, Norvell M, et al. An adverse interaction between warfarin and capecitabine: a case report and review of the literature. *Clin Colorectal Cancer.* (2001) 1:182–4. doi: 10.3816/CCC.2001.n.019
10. Buyck HCE, Buckley N, Leslie MD, Plowman PN. Capecitabine-induced potentiation of warfarin. *Clin Oncol.* (2003) 15:297–8. doi: 10.1016/S0936-6555(03)00111-0
11. Isaacs K, Haim N. Adverse interaction between capecitabine and warfarin resulting in altered coagulation parameters and bleeding: case report and review of the literature. *J Chemother.* (2005) 17:339–42. doi: 10.1179/joc.2005.17.3.339
12. Ulcickas Yood M, Quesenberry Jr CP, Hensley Alford S, Tsai AL, Wells KE, Yood SM, et al. An observational study examining the impact of capecitabine on warfarin antithrombotic activity and bleeding complications. *Curr Med Res Opin.* (2006) 22:307–14. doi: 10.1185/030079906X89694
13. Shah HR, Ledbetter L, Diasio R, Saif MW. A retrospective study of coagulation abnormalities in patients receiving concomitant capecitabine and warfarin. *Clin Colorectal Cancer.* (2006) 5:354–8. doi: 10.3816/CCC.2006.n.006
14. Grandoni F, Alberio L. Direct oral anticoagulant drugs: On the treatment of cancer-related venous thromboembolism and their potential anti-neoplastic effect. *Cancers (Basel).* (2019) 11:46. doi: 10.3390/cancers11010046
15. Key NS, Khorana AA, Kuderer NM, Bohlke K, Lee AY, Arcelus JI, et al. Venous thromboembolism prophylaxis and treatment in patients with cancer: ASCO clinical practice guideline update. *J Clin Oncol.* (2020) 38:496–520. doi: 10.1200/JCO.19.01461
16. Sanz AP, Gómez JLZ. AF in cancer patients: a different need for anticoagulation? *Eur Cardiol Rev.* (2019) 14:65–7. doi: 10.15420/ecr.2018.32.2
17. Agnelli G, Becattini C, Meyer G, Muñoz A, Huisman MV, Connors JM, et al. Apixaban for the treatment of venous thromboembolism associated with cancer. *N Engl J Med.* (2020) 382:1599–607. doi: 10.1056/NEJMoa1915103
18. Horstkotte D, Piper C, Wiemer M. Optimal frequency of patient monitoring and intensity of oral anticoagulation therapy in valvular heart disease. *J Thromb Thrombolysis.* (1998) 5(Suppl. 1):19–24. doi: 10.1023/A:1013228718768
19. Janney LM, Waterbury NV. Report C Capecitabine – Warfarin Interaction. *Ann Pharmacother.* (2005) 39:1546–51. doi: 10.1345/aph.1G153
20. Di Nisio M, Porreca E, Candeloro M, De Tursi M, Russi I, Rutjes AW. Primary prophylaxis for venous thromboembolism in ambulatory cancer patients receiving chemotherapy. *Cochr Database Syst Rev.* (2016) 12:CD008500. doi: 10.1002/14651858.CD008500.pub4
21. Olivera PE, Velasquez CA, Campoy D, Artaza G, Canals T, Flores K, et al. Effectiveness and safety of direct oral anticoagulants vs. low molecular weight heparin as anticoagulant therapy in patients with active cancer therapy and non valvular atrial fibrillation. *Blood.* (2019) 134(Suppl_1):3661. doi: 10.1182/blood-2019-128300
22. Camidge R, Reigner B, Cassidy J, Grange S, Abt M, Weidekamm E, et al. Significant effect of capecitabine on the pharmacokinetics and pharmacodynamics of warfarin in patients with cancer. *J Clin Oncol.* (2005) 23:4719–25. doi: 10.1200/JCO.2005.09.129

Conflict of Interest: The authors declare that the research was conducted in the absence of any commercial or financial relationships that could be construed as a potential conflict of interest.

Publisher's Note: All claims expressed in this article are solely those of the authors and do not necessarily represent those of their affiliated organizations, or those of the publisher, the editors and the reviewers. Any product that may be evaluated in this article, or claim that may be made by its manufacturer, is not guaranteed or endorsed by the publisher.

Copyright © 2022 Althiab, Aljohani, Alraddadi and Algarni. This is an open-access article distributed under the terms of the Creative Commons Attribution License (CC BY). The use, distribution or reproduction in other forums is permitted, provided the original author(s) and the copyright owner(s) are credited and that the original publication in this journal is cited, in accordance with accepted academic practice. No use, distribution or reproduction is permitted which does not comply with these terms.

frontiers in Cardiovascular Medicine

CASE REPORT
published: 21 March 2022
doi: 10.3389/fcvm.2022.848091

Case Report: Cardiac Tamponade in Association With Cytokine Release Syndrome Following CAR-T Cell Therapy

Shohei Moriyama[1], Mitsuhiro Fukata[1], Taku Yokoyama[1], Shohei Ueno[1], Takuya Nunomura[2], Yasuo Mori[1], Koji Kato[1], Toshihiro Miyamoto[3] and Koichi Akashi[1]*

[1] Department of Hematology, Oncology and Cardiovascular Medicine, Kyushu University Hospital, Fukuoka, Japan, [2] Department of Hematology, Hiroshima Red Cross Hospital & Atomic-bomb Survivors Hospital, Hiroshima, Japan, [3] Department of Hematology, Faculty of Medicine, Institute of Medical Pharmaceutical and Health Sciences, Kanazawa University, Ishikawa, Japan

OPEN ACCESS

Edited by:
Chun Liu,
Stanford University, United States

Reviewed by:
Peter P. Rainer,
Medical University of Graz, Austria
Houli Zhao,
Zhejiang University, China

***Correspondence:**
Mitsuhiro Fukata
fukata.mitsuhiro.555@m.kyushu-u.ac.jp

Specialty section:
This article was submitted to Cardio-Oncology, a section of the journal Frontiers in Cardiovascular Medicine

Received: *03 January 2022*
Accepted: *03 March 2022*
Published: *21 March 2022*

Citation:
Moriyama S, Fukata M, Yokoyama T, Ueno S, Nunomura T, Mori Y, Kato K, Miyamoto T and Akashi K (2022) Case Report: Cardiac Tamponade in Association With Cytokine Release Syndrome Following CAR-T Cell Therapy. Front. Cardiovasc. Med. 9:848091. doi: 10.3389/fcvm.2022.848091

Chimeric antigen receptor T (CAR-T) cell therapy has been shown to have substantial efficacy against refractory hematopoietic malignancies. However, it frequently causes cytokine release syndrome (CRS) as a treatment-specific adverse event. Although cardiovascular events associated with CAR-T cell therapy have been increasingly reported recently, pericardial disease is a rare complication and its clinical course is not well characterized. Here, we report a case of acute pericardial effusion with cardiac tamponade after CAR-T cell therapy.

Case Summary: A 59-year-old man with refractory diffuse large B-cell lymphoma underwent CAR-T cell therapy. Grade 2 CRS was observed on day 0; it progressed to grade 4 on day 7 and was accompanied by a fever over 39°C, hypoxia requiring intubation, hypotension requiring the use of a vasopressor agent, and supraventricular tachycardia. Although cardiac function was preserved, marked pericardial effusion with the collapse of the right heart was detected on echocardiography. Since pericardiocentesis was considered to have a high complication risk due to severe myelosuppression, medications for CRS were prioritized. Tocilizumab, an interleukin-6 inhibitor, and high-dose methylprednisolone (1 g/day for 3 days) were administered for the management of severe CRS. On day 8, the pericardial effusion decreased, and the hemodynamic status markedly stabilized. CRS did not exacerbate after the steroid dose was reduced. Further, lymphoma size reduced after the induction of CAR-T cell therapy, and tumor regrowth was not noted at 3 months after CAR-T cell infusion.

Conclusion: Interleukin-6 pathway inhibitors and corticosteroid therapy should be considered in the context of CRS for significant pericardial effusion after CAR-T cell therapy in the acute phase.

Keywords: cardiac tamponade, pericardial effusion, CAR-T, CRS, pericarditis

INTRODUCTION

Chimeric antigen receptor T (CAR-T) cell therapy is a novel immunotherapy for cancer treatment. Clinical trials of CAR-T cell therapy for refractory large B-cell lymphoma have shown a high response rate and long-term response (1, 2). However, CAR-T cells induce cytokine release syndrome (CRS), which is caused by a rapid increase in inflammatory cytokines released from activated immune cells and could be fatal (3). Cardiovascular complications such as heart failure, arrhythmia, and pericardial disease due to CAR-T cell therapy have been reported and shown to be strongly related to CRS. However, the clinical features and management of CRS have not yet been well defined (4, 5). Herein, we describe a case of acute pericardial effusion with cardiac tamponade associated with CRS after CAR-T cell therapy.

CASE DESCRIPTION

A 59-year-old man was diagnosed with diffuse large B-cell lymphoma (DLBCL), not otherwise specified. DLBCL relapsed after first-line chemotherapy with rituximab, cyclophosphamide, doxorubicin, vincristine, and prednisolone. Despite the multiple salvage chemotherapies and local radiation therapy, it aggravated and systemic multiple lymphoma lesions developed. Part of the lesions in the mediastinum was adjacent to the right side of the pericardium (**Figure 1**). The patient was referred to our hospital for anti-CD19 CAR-T cell therapy with axicabtagene ciloleucel as part of a phase 2 clinical trial (JapicCTI-183914; https://rctportal.niph.go.jp/en/detail?trial_id=JapicCTI-183914) (6). He had a history of a duodenal ulcer but not cardiovascular disease. The cumulative anthracycline dose administered was 440 mg/m^2. The radiation therapy was performed for supraclavicular lesion with a dose of 46Gy 8 months ago and sacral lesion with a dose of 30Gy 3 months ago, and both site did not include the heart. An electrocardiogram obtained before the administration of CAR-T therapy showed normal sinus rhythm **(Figure 2A)**, and echocardiography showed normal left ventricular systolic and diastolic functions with no pericardial or pleural effusion (**Figure 2B**, **Supplementary Movie 1**).

Following conditioning chemotherapy with cyclophosphamide and fludarabine, CAR-T cells (2.0×10^6 cells/kg) were administered. Empiric administration of antibiotics was initiated on day 0. The patient developed fever (≥38°C) on the day of CAR-T cell infusion (day 0) and hypoxia requiring oxygen on day 1. He was diagnosed with grade 2 CRS (7), and tocilizumab (8 mg/kg) was administered for the same on day 2 **(Figure 3A)**. Fever due to bacterial infection was ruled out based on negative blood culture results. He developed supraventricular tachycardia on day 5, and landiolol was administered. Computed tomography on day 5 showed marked pleural effusion and slight pericardial effusion (**Supplementary Figure 1**). Because grade 2 CRS persisted, tocilizumab (8 mg/kg) was readministered on day 6. However, exacerbation of hypoxia and severe hypotension with tachycardia was observed on day 7 (CRS grade 3), and the patient was transferred to the intensive care unit.

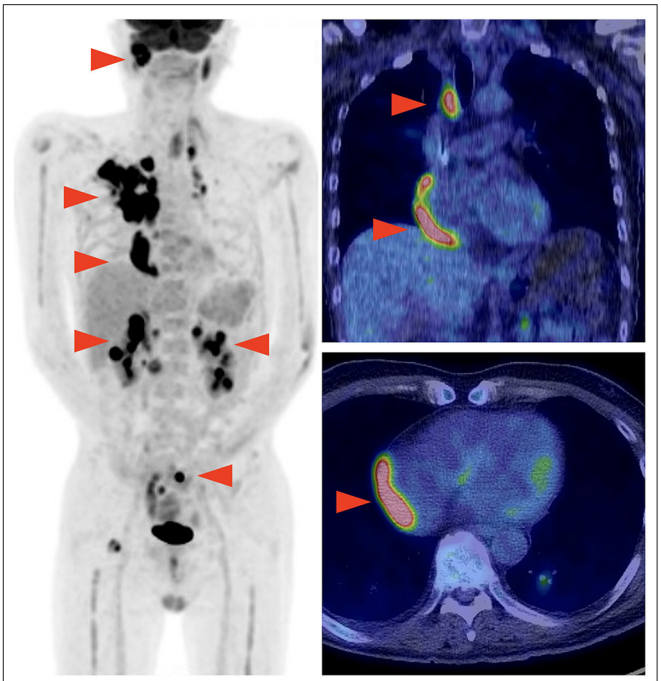

FIGURE 1 | Positron emission tomography-computed tomography performed before chimeric antigen receptor T (CAR-T) cell therapy showing multiple lymphoma lesions including the site adjacent to the right pericardium.

The time course of the vital signs and medications on day 7 is shown in **Figure 3B**. His blood pressure was 67/40 mmHg with noradrenalin (0.2 μg/kg/min), heart rate was 115 beats per minute, body temperature was 38.9°C, and percutaneous oxygen saturation was 86% with oxygen (10 L/min) administered through a face mask with a reservoir bag. The patient was intubated soon after admission to the intensive care unit because of his deteriorating respiratory condition (CRS grade 4). Jugular venous distension and pretibial pitting edema were observed. Furthermore, heart sounds were distant. Pericardial friction rubs were not evident. Serum C-reactive protein (CRP) was elevated to 9.9 mg/dL (**Figure 3A**, **Supplementary Figure 2**). Serum troponin T (0.038 ng/mL; normal range: ≤0.014 ng/mL) and brain natriuretic peptide (323.3 pg/mL; normal range: ≤18.4 pg/mL) levels were also elevated. An electrocardiogram revealed supraventricular tachycardia **(Figure 4A)**. Echocardiography revealed preserved bilateral ventricular systolic functions but marked pericardial effusion (maximum echo-free space: 15 mm at end-diastole). The right heart chamber collapsed in the early diastolic phase, and the inferior vena cava was distended with a reduced respiratory diameter change (**Figure 4B**, **Supplementary Movies 2**, **3**). Based on these findings, the patient was diagnosed with severe CRS and cardiac tamponade.

Although pericardiocentesis would have been effective for hemodynamic stabilization, immediate pericardiocentesis was

Abbreviations: CAR-T, Chimeric antigen receptor; CRS, Cytokine release syndrome; DLBCL, Diffuse large B-cell lymphoma; IL-6, Interleukin-6.

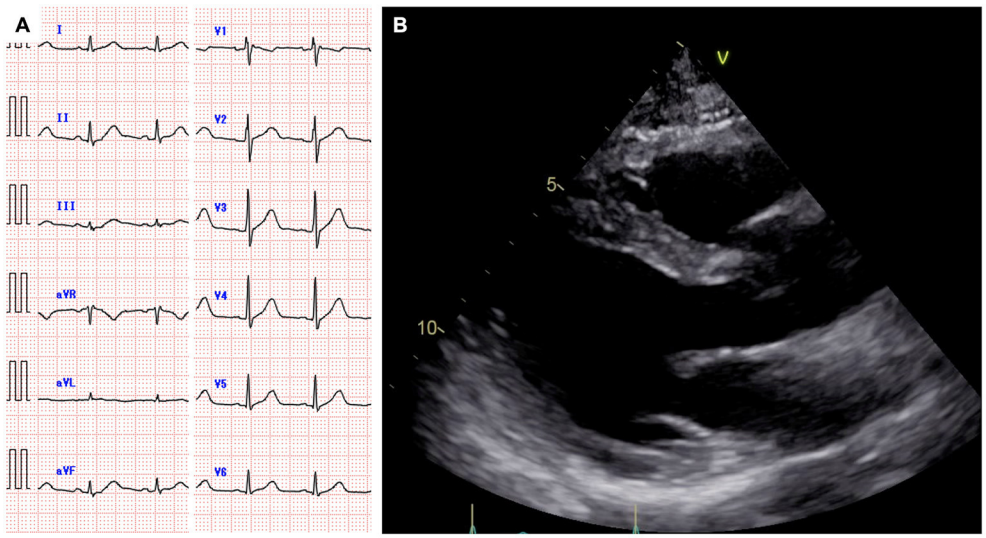

FIGURE 2 | Electrocardiogram showing normal sinus rhythm **(A)**. Echocardiography showing normal cardiac function and no pericardial effusion **(B)**.

deferred, because of the high complication risk associated with the procedure owing to severe myelosuppression (white blood cell count, 590/μL; platelet count 31,000/μL). The negative blood culture results and the rapid increase in pericardial effusion despite the administration of antibiotics suggested that the cause of pericardial effusion was not a bacterial infection. Therefore, immunosuppressive medications were prioritized for CRS management. Since blood pressure remained low (<80/<50 mmHg) after the administration of tocilizumab followed by dexamethasone (10 mg/body), intravenous high-dose methylprednisolone (1 g/body) was administered. The patient's blood pressure increased 2 h after the administration of methylprednisolone. Amiodarone and landiolol were initiated for the treatment of recurrent supraventricular tachycardia. On the next day (day 8), pericardial effusion decreased, and echocardiography showed attenuation of the degree of right heart chamber collapse and recovery of respiratory diameter change of inferior vena cava (**Figure 4C**, **Supplementary Movies 4**, **5**). The patient's blood pressure and heart rate improved further and stabilized. Serum CRP consistently decreased after the administration of high-dose methylprednisolone, and the steroids dose was gradually reduced until discontinuation on day 29 (**Supplementary Figure 2**). Echocardiography after the discontinuation of steroid therapy showed no pericardial effusion and normal biventricular systolic function. Supraventricular tachycardia was occasionally observed up to 1 month after CAR-T cell infusion. Computed tomography on day 91 showed a partial response of the primary disease to CAR-T cell therapy. The patient was eventually discharged on day 112. There was no cardiovascular adverse event after discharge. At 6 months after the CAR-T cell therapy, the lymphoma aggravated rapidly and the treatment for this patient was transferred to best supportive care.

DISCUSSION

Anti-CD19 CAR-T cell therapy has been approved for the management of adult non-Hodgkin lymphoma and leukemia in young adults or children globally and is expected to be expanded to other malignancies in the future. Refractory DLBCL was reported to have an abysmal prognosis, with a median overall survival of 6.3 months and a response rate of 26% even after chemotherapy and hematopoietic stem cell transplantation before the CAR-T cell therapy era (8). Anti-CD19 CAR-T cell therapy has markedly improved the prognosis of patients with refractory large B-cell lymphoma, with a response rate increase to 52–82% and longer overall survival (1, 2, 9). However, this novel therapy frequently causes CRS by over-activation of the immune system and subsequent elevation of cytokines such as interferon-gamma, tumor necrosis factor-alpha, and interleukin (IL)-6 (10). In recent years, there has been an increase in the number of reports on cardiovascular events after CAR-T cell therapy with or without overlapping CRS (4, 5). To our knowledge, this is the first report of a case of cardiac tamponade associated with CRS after CAR-T cell therapy.

Raza et al. reported that the rate of cardiotoxicity after CAR-T cell therapy in adult patients with lymphoma or multiple myeloma was 12% (11). In their study, when analyzing limited patients who developed grade 2-4 CRS, cardiovascular events were found to have occurred in 31% of the patients, whereas no cardiovascular events were observed in patients without or grade 1 CRS (11). Lefebvre et al. reported that major adverse cardiovascular events occurred in 17% of patients at 30 days, 19% at 6 months, and 21% at 12 months. The time from CAR-T cell infusion to the onset of cardiovascular events is similar to that of CRS which occurring in most cases within 30 days of CAR-T cell infusion (12). The relatively

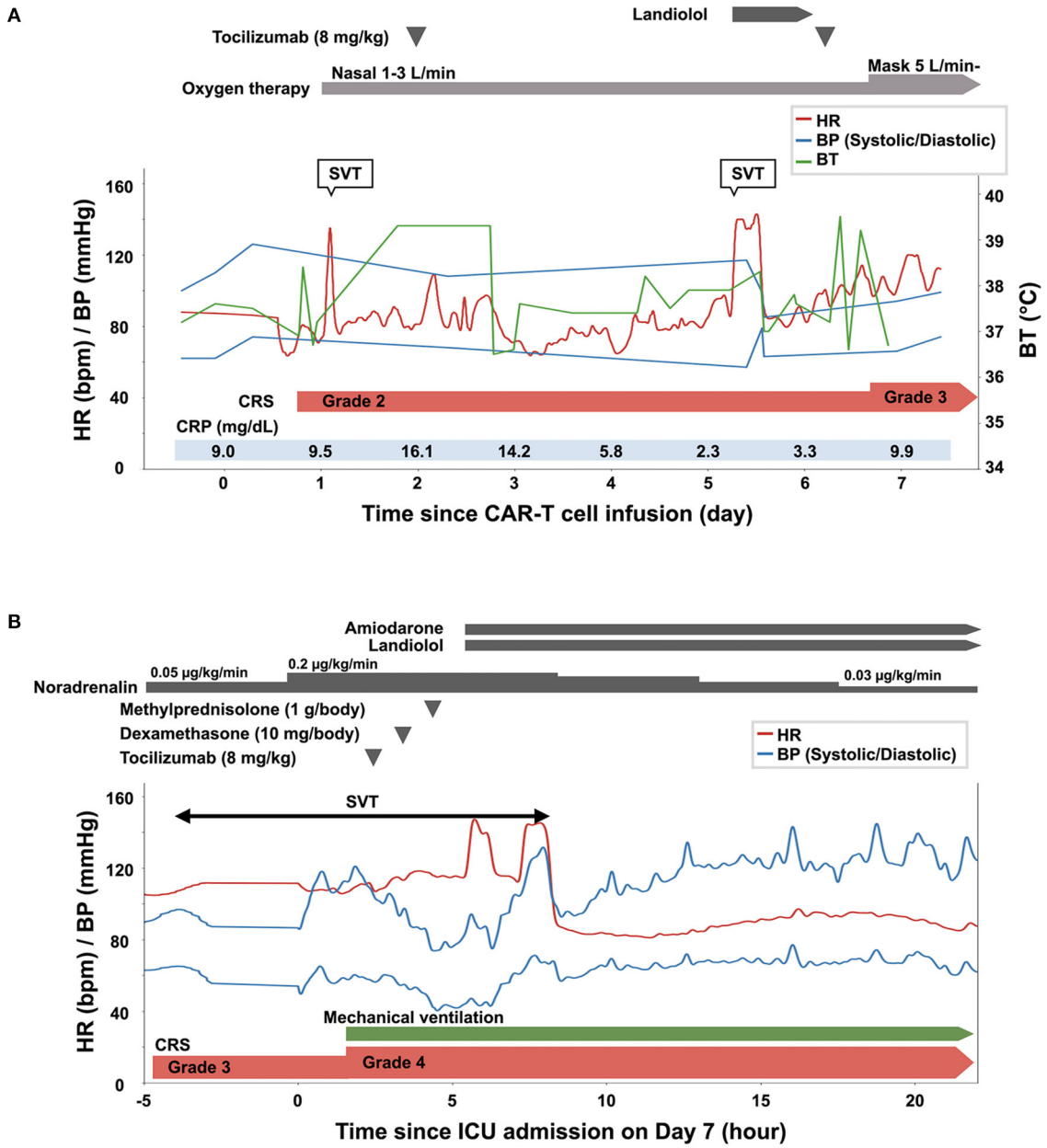

FIGURE 3 | Clinical course of the patient from the day of the infusion of chimeric antigen receptor T (CAR-T) cells (day 0) until day 6 **(A)**, and on day 7 **(B)**. BP, blood pressure; BT, body temperature; CRP, C-reactive protein; CRS, cytokine release syndrome; ICU, intensive care unit; SVT, supraventricular tachycardia.

high incidence of cardiovascular events in cases with high-grade CRS and the simultaneous development of CRS and cardiovascular events suggest a causal relationship between CRS and cardiovascular toxicity in the early period following CAR-T cell infusion. In our case, fever was observed immediately after CAR-T cell infusion, followed by refractory hypotension and hypoxia in a week. This clinical course is consistent with the typical manifestation of high-grade CRS after CAR-T cell therapy in a previous report (13). Additionally, in this case, the development of CRS preceded pericardial effusion, and cardiac tamponade was observed with the exacerbation of CRS. CRP, a surrogate marker for IL-6 bioactivity with time lag by 1 to 2 days, peaked on the next day of the development of cardiac tamponade (7, 14). Taken together, the developmental course of pericardial effusion and its evident response to steroid therapy suggested a relationship between CRS and the development of cardiac tamponade.

Pericarditis or pericardial effusion after CAR-T cell therapy is rare, with a total incidence rate of 0.4%, and two-thirds of patients with pericardial disease have concurrent CRS (5).

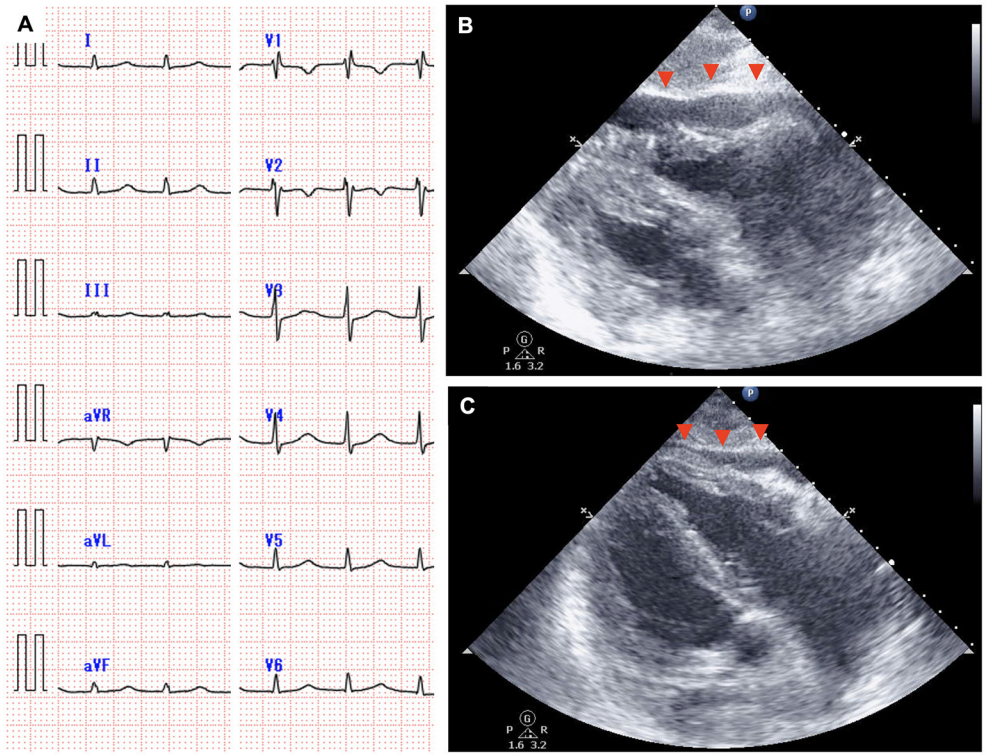

FIGURE 4 | An electrocardiogram obtained on day 7 showing narrow QRS tachycardia with the absence of the P wave **(A)**, and echocardiography showing rapidly accumulated pericardial effusion with the collapse of the right heart chamber [**(B)**, arrowhead]. Pericardial effusion decreased and the collapse of the right heart chamber resolved on day 8 [**(C)**, arrowhead].

The underlying mechanism of pericardial disease after CAR-T cell therapy has not been well clarified. Cytokine-induced fluid retention and/or systemic high vascular permeability is a possible cause of rapid accumulation of pericardial fluid (15, 16). The clinical features of severe CRS resemble those of capillary leak syndrome (4, 5, 15, 16). Pericardial effusion is reported to occur in 11% of patients with idiopathic capillary leak syndrome and can be life-threatening (17, 18). Since the levels of inflammatory cytokines such as IL-6 and vascular endothelial growth factor significantly increased in the serum of patients with severe capillary leak syndrome, this cytokine-related capillary leak may induce the accumulation of pericardial fluid (19, 20). Hemodynamic deterioration in this case was accompanied by the dilatation of inferior vena cava, which is quite different from hypovolemic state in case of capillary leak syndrome (17). This clinical feature suggests the cause of pericardial effusion in this case includes a different mechanism other than capillary leakage. The difference in mediators between idiopathic capillary leak syndrome and CAR-T cell-induced CRS has not been fully elucidated. Accumulation of evidence from studies on the cytokine profiles and their signaling pathways in cases of CAR-T cell-induced CRS would help understand the mechanism of organ damage by CRS due to CAR-T cell therapy. An additional possible cause is locally accelerated pericardial inflammation. In this case, CAR-T cell immunoreaction to lymphoma lesion adjacent to the pericardium might have accelerated the accumulation of pericardial fluid. In addition, the highest engineered T-cell concentration was detected in the pericardium or the myocardium, and the levels of some cytokines in the pericardial fluid were higher than the corresponding levels in blood in a case of cardiogenic shock after T-cell receptor-engineered T-cell immunotherapy (21). Direct T-cell toxicity in the pericardium or the myocardium has not been demonstrated in anti-CD19 CAR-T cell therapy to date; however, it needs to be elucidated in the future (4).

IL-6 plays an important role in the pathogenesis of CRS, and tocilizumab, an IL-6 receptor antagonist, has been approved as first-line therapy for CRS (22, 23). For severe CRS with a poor response to tocilizumab, additional administration of corticosteroids is recommended (23). In previous reports, more than 50% of patients with CRS showed amelioration after tocilizumab administration, and no tocilizumab-related adverse reactions were detected (1, 2). Furthermore, corticosteroid therapy did not suppress the response to CAR-T cell therapy clinically; however, it decreased the number of CAR-T cells in the serum and bone marrow (1, 14, 24). Therefore, its use may have to be limited to life-threatening conditions associated with severe CRS. Consideration of infection before and after

the administration of tocilizumab or corticosteroids is also important because of the immunocompromised state of the patients (23). In this case, given the negative findings of bacterial infection and the considerable risk of pericardiocentesis due to severe myelosuppression, the administration of high-dose corticosteroids in addition to tocilizumab took precedence over pericardiocentesis, and the patient's hemodynamic condition drastically improved. Nevertheless, for all cases of cardiac tamponade, the best precautions to perform prompt pericardiocentesis should be taken in case of hemodynamic deterioration. Pericardiocentesis should be considered even if the patient has severe thrombocytopenia if the response to high-dose steroid therapy in addition to tocilizumab is unfavorable (25).

CONCLUSION

We described the case of a 59-year-old man with refractory DLBCL who was treated with anti-CD19 CAR-T cell therapy and developed severe CRS and cardiac tamponade. Appropriate immunosuppressive therapy for CRS reduces pericardial effusion without the need for pericardiocentesis. When hemodynamic instability occurs in the acute phase after CAR-T cell therapy, CRS-related cardiovascular complications including cardiac tamponade as well as severe CRS need to be considered. In cases in which pericardiocentesis poses a considerable risk, urgent strengthening of the treatment for CRS is worth considering.

DATA AVAILABILITY STATEMENT

The original contributions presented in the study are included in the article/**Supplementary Material**, further inquiries can be directed to the corresponding author.

ETHICS STATEMENT

Written informed consent was obtained from the patient for the publication of any potentially identifiable images or data included in this article.

AUTHOR CONTRIBUTIONS

SM drafted the manuscript and all authors contributed significantly to the manuscript. All authors reviewed the draft manuscript and provided critique and feedback on the manuscript. All authors read and approved the final version of the manuscript.

FUNDING

This work was supported by JSPS KAKENHI Grant Number JP17K11577.

ACKNOWLEDGMENTS

We gratefully acknowledge past and present staffs in our hospital for their clinical work and Editage for language editing.

SUPPLEMENTARY MATERIAL

The Supplementary Material for this article can be found online at: https://www.frontiersin.org/articles/10.3389/fcvm.2022.848091/full#supplementary-material

Supplemental Figure 1 | Computed tomography performed on day 5 showing bilateral pleural effusion and slight pericardial effusion.

Supplemental Figure 2 | Serum C-reactive protein (CRP) levels from the day of the infusion of chimeric antigen receptor T (CAR-T) cells until day 14. CRS, cytokine release syndrome.

REFERENCES

1. Neelapu SS, Locke FL, Bartlett NL, Lekakis LJ, Miklos DB, Jacobson CA, et al. Axicabtagene Ciloleucel CAR T-cell therapy in refractory large B-cell lymphoma. *N Engl J Med.* (2017) 377:2531–44. doi: 10.1056/NEJMoa1707447
2. Schuster SJ, Bishop MR, Tam CS, Waller EK, Borchmann P, McGuirk JP, et al. Tisagenlecleucel in adult relapsed or refractory diffuse large B-cell lymphoma. *N Engl J Med.* (2019) 380:45–56. doi: 10.1056/NEJMoa1804980
3. Neelapu SS. Managing the toxicities of CAR T-cell therapy. *Hematol Oncol.* (2019) 37 Supplement 1:48–52. doi: 10.1002/hon.2595
4. Ghosh AK, Chen DH, Guha A, Mackenzie S, Walker JM, Roddie C, et al. cell therapy-related cardiovascular outcomes and management. *JACC Cardiooncol.* (2020) 2:97–109. doi: 10.1016/j.jaccao.2020.02.011
5. Goldman A, Maor E, Bomze D, Liu JE, Herrmann J, Fein J, et al. Adverse cardiovascular and pulmonary events associated with chimeric antigen receptor T-cell therapy. *J Am Coll Cardiol.* (2021) 78:1800–13. doi: 10.1016/j.jacc.2021.08.044
6. Kato K, Makita S, Goto H, Kanda J, Fujii N, Shimada K, et al. Phase 2 study of axicabtagene ciloleucel in Japanese patients with relapsed or refractory large B-cell lymphoma. *Int J Clin Oncol.* (2022) 27:213–23. doi: 10.1007/s10147-021-02033-4
7. Lee DW, Gardner R, Porter DL, Louis CU, Ahmed N, Jensen M, et al. Current concepts in the diagnosis and management of cytokine release syndrome. *Blood.* (2014) 124:188–95. doi: 10.1182/blood-2014-05-552729
8. Crump M, Neelapu SS, Farooq U, Van Den Neste E, Kuruvilla J, Westin J, et al. Outcomes in refractory diffuse large B-cell lymphoma: Results from the international SCHOLAR-1 study. *Blood.* (2017) 130:1800–8. doi: 10.1182/blood-2017-03-769620
9. Locke FL, Ghobadi A, Jacobson CA, Miklos DB, Lekakis LJ, Oluwole OO, et al. Long-term safety and activity of axicabtagene ciloleucel in refractory large B-cell lymphoma (ZUMA-1): a single-arm, multicentre, phase 1–2 trial. *Lancet Oncol.* (2019) 20:31–42. doi: 10.1016/S1470-2045(18)30864-7
10. Fischer JW, Bhattarai N. CAR-T cell therapy: Mechanism, management, and mitigation of inflammatory toxicities. *Front Immunol.* (2021) 12:693016. doi: 10.3389/fimmu.2021.693016
11. Alvi RM, Frigault MJ, Fradley MG, Jain MD, Mahmood SS, Awadalla M, et al. Cardiovascular events among adults treated with chimeric antigen receptor T-cells (CAR-T). *J Am Coll Cardiol.* (2019) 74:3099–108. doi: 10.1016/j.jacc.2019.10.038
12. Lefebvre B, Kang Y, Smith AM, Frey NV, Carver JR, Scherrer-Crosbie M. Cardiovascular effects of CAR T cell therapy: A retrospective study. *JACC Cardiooncol.* (2020) 2:193–203. doi: 10.1016/j.jaccao.2020.04.012
13. Fitzgerald JC, Weiss SL, Maude SL, Barrett DM, Lacey SF, Melenhorst JJ, et al. Cytokine release syndrome after chimeric antigen receptor T cell therapy for acute lymphoblastic leukemia. *Crit Care Med.* (2017) 45:e124–31. doi: 10.1097/CCM.0000000000002053
14. Davila ML, Riviere I, Wang X, Bartido S, Park J, Curran K, et al. Efficacy and toxicity management of 19-28z CAR T cell therapy

in B cell acute lymphoblastic leukemia. *Sci Transl Med.* (2014) 6:224ra25. doi: 10.1126/scitranslmed.3008226
15. Fajgenbaum DC, June CH. Cytokine storm. *N Engl J Med.* (2020) 383:2255–73. doi: 10.1056/NEJMra2026131
16. Maude SL, Laetsch TW, Buechner J, Rives S, Boyer M, Bittencourt H, et al. Tisagenlecleucel in children and young adults with B-cell lymphoblastic leukemia. *N Engl J Med.* (2018) 378:439–48. doi: 10.1056/NEJMoa1709866
17. Eo TS, Chun KJ, Hong SJ, Kim JY, Lee IR, Lee KH, et al. Clinical presentation, management, and prognostic factors of idiopathic systemic capillary leak syndrome: a systematic review. *J Allergy Clin Immunol Pract.* (2018) 6:609–18. doi: 10.1016/j.jaip.2017.07.021
18. Khan HR, Khan S, Srikanth A, Smith WHT. A case report of capillary leak syndrome with recurrent pericardial and pleural effusions. *Eur Heart Case Rep.* (2020) 4:1–5. doi: 10.1093/ehjcr/ytaa013
19. Lesterhuis WJ, Rennings AJ, Leenders WP, Nooteboom A, Punt CJ, Sweep FC, et al. Vascular endothelial growth factor in systemic capillary leak syndrome. *Am J Med.* (2009) 122:e5–7. doi: 10.1016/j.amjmed.2009.01.020
20. Nagao Y, Harada H, Yamanaka H, Fukuda K. Possible mediators for systemic capillary leak syndrome. *Am J Med.* (2011) 124:e7–9. doi: 10.1016/j.amjmed.2010.04.024
21. Linette GP, Stadtmauer EA, Maus MV, Rapoport AP, Levine BL, Emery L, et al. Cardiovascular toxicity and titin cross-reactivity of affinity-enhanced T cells in myeloma and melanoma. *Blood.* (2013) 122:863–71. doi: 10.1182/blood-2013-03-490565
22. Le RQ, Li L, Yuan W, Shord SS, Nie L, Habtemariam BA, et al. FDA approval summary: Tocilizumab for treatment of chimeric antigen receptor T cell-induced severe or life-threatening cytokine release syndrome. *Oncologist.* (2018) 23:943–7. doi: 10.1634/theoncologist.2018-0028
23. Neelapu SS, Tummala S, Kebriaei P, Wierda W, Gutierrez C, Locke FL, et al. Chimeric antigen receptor T-cell therapy — Assessment and management of toxicities. *Nat Rev Clin Oncol.* (2018) 15:47–62. doi: 10.1038/nrclinonc.2017.148
24. Gardner RA, Finney O, Annesley C, Brakke H, Summers C, Leger K, et al. Intent-to-treat leukemia remission by CD19 CAR T cells of defined formulation and dose in children and young adults. *Blood.* (2017) 129:3322–31. doi: 10.1182/blood-2017-02-769208
25. El Haddad D, Iliescu C, Yusuf SW, William WN, Khair TH, Song J, et al. Outcomes of cancer patients undergoing percutaneous pericardiocentesis for pericardial effusion. *J Am Coll Cardiol.* (2015) 66:1119–28. doi: 10.1016/j.jacc.2015.06.1332

Conflict of Interest: KK received research funding from Chugai Pharmaceutical, Takeda Pharmaceutical, Kyowa Kirin, AbbVie, Novartis, Eisai, Janssen, Celgene, Ono Pharmaceutical, Daiichi Sankyo, and honorarium from Chugai Pharmaceutical, Takeda Pharmaceutical, Kyowa Kirin, Novartis. KA received research funding from Chugai Pharmaceutical, Takeda Pharmaceutical, Kyowa Kirin, AbbVie, Eisai, Ono Pharmaceutical, Asahi Kasei, Shionogi, Sumitomo Dainippon Pharma, Otsuka Pharmaceutical, Taiho Pharmaceutical, Astellas Pharma, and honorarium from AbbVie, Eisai.

The remaining authors declare that the research was conducted in the absence of any commercial or financial relationships that could be construed as a potential conflict of interest.

Publisher's Note: All claims expressed in this article are solely those of the authors and do not necessarily represent those of their affiliated organizations, or those of the publisher, the editors and the reviewers. Any product that may be evaluated in this article, or claim that may be made by its manufacturer, is not guaranteed or endorsed by the publisher.

Copyright © 2022 Moriyama, Fukata, Yokoyama, Ueno, Nunomura, Mori, Kato, Miyamoto and Akashi. This is an open-access article distributed under the terms of the Creative Commons Attribution License (CC BY). The use, distribution or reproduction in other forums is permitted, provided the original author(s) and the copyright owner(s) are credited and that the original publication in this journal is cited, in accordance with accepted academic practice. No use, distribution or reproduction is permitted which does not comply with these terms.

frontiers | Frontiers in Cardiovascular Medicine

CASE REPORT
published: 12 May 2022
doi: 10.3389/fcvm.2022.898756

Successful Therapy for Myocarditis Concomitant With Complete Heart Block After Pembrolizumab Treatment for Head and Neck Squamous Cell Carcinoma: A Case Report With Literature Review

Lina Su[1†], *Chuanfen Liu*[1†], *Wenjie Wu*[2], *Yuxia Cui*[1], *Manyan Wu*[1] *and Hong Chen*[1*]

[1] *Department of Cardiology, Peking University People's Hospital, Beijing, China,* [2] *Department of Oral and Maxillofacial Surgery, Peking University School and Hospital of Stomatology, Beijing, China*

OPEN ACCESS

Edited by:
Carlo Gabriele Tocchetti, University of Naples Federico II, Italy

Reviewed by:
Daniela Di Lisi, Azienda Ospedaliera Universitaria Policlinico Paolo Giaccone, Italy
Daniel Antwi-Amoabeng, CHRISTUS St. Patrick Hospital, United States

***Correspondence:**
Hong Chen
chenhongbj@medmail.com.cn

[†]*These authors have contributed equally to this work*

Specialty section:
This article was submitted to Cardio-Oncology, a section of the journal Frontiers in Cardiovascular Medicine

Received: *17 March 2022*
Accepted: *15 April 2022*
Published: *12 May 2022*

Citation:
Su L, Liu C, Wu W, Cui Y, Wu M and Chen H (2022) Successful Therapy for Myocarditis Concomitant With Complete Heart Block After Pembrolizumab Treatment for Head and Neck Squamous Cell Carcinoma: A Case Report With Literature Review. Front. Cardiovasc. Med. 9:898756. doi: 10.3389/fcvm.2022.898756

Immune checkpoint inhibitors (ICIs) have revolutionized cancer therapy over the past decade. Despite their beneficial effects on treating numerous types of tumors, cardiotoxicity resulting from ICIs is a rare side effect but a concerning one due to its high mortality rate. We herein describe a case of an 80-year-old woman with recurrent head and neck squamous cell cancer (HNSCC), who presented with myocarditis complicated by complete atrioventricular block (CAVB) after second infusion of pembrolizumab. After quickly ruling out myocardial infarction and viral myocarditis, the strong relationship between the onset time and pembrolizumab therapy suggested that ICI-induced myocarditis was the most possible diagnosis. Though CAVB frequently presents with fulminant myocarditis in the setting of ICI-related cardiotoxicity, the patients kept a stable hemodynamic status and had normal myocardial function with just a slightly low global longitudinal strain (GLS) at−16.4%, which implied myocardial injury but was highly related to good prognosis based on the existing literature. Besides, elderly patients are vulnerable to adverse outcomes of steroid therapy, notably opportunistic infections. To balance beneficial effects and adverse effects of immune suppression, she accepted high-dose steroids without pulse methylprednisolone. Excitingly, she had a dramatic clinical and laboratory improvement, and heart block quickly returned to normal sinus rhythm. Another interesting finding was that the patient's tumor remained stable during the half-year follow-up from the termination of immunotherapy. Besides, we here firstly review previously reported cases in terms of their clinical characteristics and prognosis of ICI-induced myocarditis with CAVB, in particular the reversibility of heart block. In conclusion, ICI-induced myocarditis can be life-threatening and it therefore warrants efforts to increase awareness, facilitate early detection, and initiate prompt intervention. Importantly, CAVB secondary to ICIs-induced myocarditis may not always present with fulminant myocarditis and more than 50% of these surviving patients might recover to

normal sinus rhythm. For patients with ICI-induced myocarditis with contraindication for cardiac magnetic resonance (CMR), speckle-tracking echocardiography is a reliable and sensitive alternative to CMR for detecting myocardial injury, and GLS may be an important prognostic indicator.

Keywords: immune checkpoint inhibitors, myocarditis, complete atrioventricular (AV) block, head and neck squamous cancer cells (HNSCC), global longitudinal peak strain

INTRODUCTION

Immune checkpoint inhibitors (ICIs) have transformed the treatment landscape of many different types of cancers in recent years (1). Pembrolizumab, a humanized monoclonal IgG4 antibody, binds to programmed death receptor-1 (PD-1) and blocks its interaction with programmed death ligand-1 (PD-L1), thereby triggering the patients' immune system to recognize and combat cancer cells (2). Based on the survival results from the phase III clinical trial Keynote 048, pembrolizumab has been approved as the preferred first-line treatment for patients with recurrent or metastatic head and neck squamous cell carcinoma (HNSCC) who have no surgical or radiotherapeutic option (3). Despite favorable benefits, immune-related adverse events (irAEs) have occured in 70–90% of patients treated with ICIs (2). The most common irAEs have been found in the skin, colon, liver, lungs, pituitary gland, and thyroid (2). Cardiotoxicity resulting from ICIs is uncommon but potentially fatal. The incidence of ICI-induced myocarditis ranges from 0.01 to 1.1%, with a mortality rate of up to 50% (4). However, due to the low incidence of cardiac irAEs, data on presentation, diagnosis, treatment, and outcomes are limited (1). We herein present a case of recurrent HNSCC who presented with myocarditis complicated by complete atrioventricular block (CAVB).

CASE PRESENTATION

An 80-year-old woman was diagnosed with primary intraosseous squamous cell carcinoma of the mandible and underwent radical resection in December 2020. Adjuvant therapy was recommended, while the patient could not tolerate chemotherapy or radiotherapy. Five months after the primary surgery, the right mandibular mass recurred and was confirmed as recurrent HNSCC. Immunohistochemistry showed a PD-L1 expression level with a tumor proportion score of 15% and a combined positive score of 15. Given the patient's advanced age and vulnerability, radical resection and adjuvant chemoradiotherapy were not advantageous. Scholars have recommended PD-1 inhibitor monotherapy or PD-1 inhibitors combined with epidermal growth factor receptor (EGFR) inhibitors for the treatment of recurrent HNSCC with no surgical or chemoradiotherapeutic option (5, 6). The patient received pembrolizumab (200 mg) and nimotuzumab (200 mg), with an intravenous delivery every 3 weeks. She had no previous history of cardiovascular diseases.

At 10 h after the second administration of pembrolizumab plus nimotuzumab in the stomatology department, the patient complained of palpitation, faintness, and general fatigue, with no typical symptoms of anginal pectoris. She denied recent prodromal infection. Except for pembrolizumab and nimotuzumab, she did not receive any other medicine. The electrocardiogram (ECG) showed CAVB with a ventricular escape rate at 37 bpm (**Figure 1A**), which was normal prior to therapy with combined pembrolizumab. The high-sensitivity troponin I (hsTnI) assay showed a moderate elevation of 440 pg/mL (normal $<$ 10.4 pg/mL). Serum electrolytes were within normal range, which did not support electrolyte disturbance-induced CAVB.

The patient was then urgently transferred to the cardiology department. Vital signs upon admission indicated heart rate of 37 bpm, blood pressure of 128/54 mmHg, respiratory rate of 18 rpm, temperature of 36°C, and oxygen saturation of 98% in room air. The physical examination revealed a vegetable mass in the right mandibular region. There was no rash, cyanosis, edema or bibasilar rales in the lungs. Except for the abnormal heart rate, cardiovascular examination revealed no other abnormality. She was awake and oriented, with no focal neurologic deficit.

Repeat ECG showed CAVB with a ventricular escape rate at 37 bpm. The initial work-up showed elevated levels of hsTnI of 1,026.5 pg/mL (normal $<$ 10.4 pg/mL), creatine kinase (CK) of 510 U/L (normal $<$ 165 U/L), CK-MB of 39.8 U/L (normal $<$ 5 U/L), and brain natriuretic peptide (BNP) of 2,171 pg/mL (normal $<$ 125 pg/mL). Moreover, her white blood cell was 11.8 $\times$ $10^9/\mu$L (normal 4 to 10 $\times$ $10^9/\mu$L), while her C-reactive protein level and erythrocyte sedimentation rate were both within normal limits. Urgent transthoracic echocardiography and chest computed tomography showed unremarkable results.

Considering the possibility of myocardial infarction and the potential high risk of cardiac arrest, the patient underwent urgent coronary angiography, which did not reveal any significant stenosis, and a dual-chamber pacemaker was subsequently implanted. The pacemaker was programmed with DDD pacing mode and ECG recorded a ventricular pacing rhythm with a wide QRS complex (**Figure 1B**). Further diagnostic work-up was performed. Hepatitis B, human immunodeficiency virus (HIV), Epstein–Barr virus, and cytomegalovirus were negative on the basis of serology while thyroid hormone was unremarkable. Therefore, neither viral myocarditis nor thyroid disorder could be considered as the cause of myocarditis. Myocardial contrast echocardiography showed that the perfusion of myocardium was normal (**Figure 1C**), with a normal left ventricular ejection fraction (LVEF) of 65%. However, speckle tracking echocardiography revealed a slightly decreased left ventricular global longitudinal strain (GLS) of−16.4%. Longitudinal strain

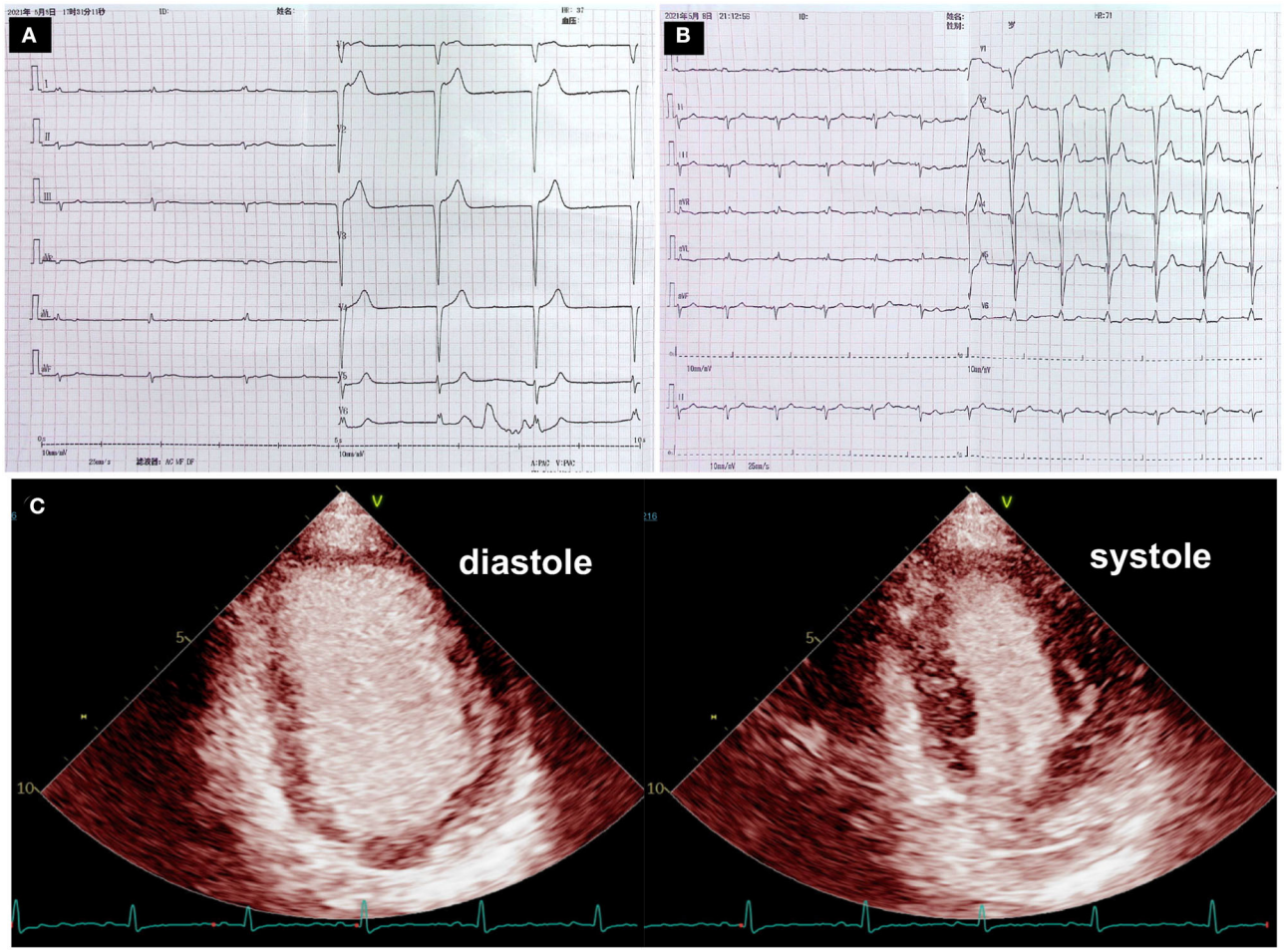

FIGURE 1 | Electrocardiogram and myocardial contrast echocardiography. **(A)** Electrocardiogram at the onset showed complete atrioventricular block with a ventricular escape at a rate of 37 beats per minute. **(B)** Echocardiogram after pacemaker implantation indicated a ventricular pacing rhythm with a wide QRS complex. **(C)** Myocardial contrast echocardiography examinations showed homogenous and equal enhancement intensity in the basal, middle and apical segments.

was mainly impaired in the basal segments of the anterior and lateral walls (**Figure 2A**).

Nimotuzumab is marketed and has been administered to over 38,000 patients with limited adverse events (7). Until now, no reports have been published yet regarding myocarditis caused by nimotuzumab. Thus, the strong relationship between the onset time and pembrolizumab therapy suggested that pembrolizumab-induced myocarditis was the most likely diagnosis. In the light of hemodynamic stability as well as advanced age and vulnerability, high-dose glucocorticoids were initiated (1 mg/kg/day intravenous methylprednisolone) without pulse steroids within 24 h after onset. Excitingly, the patient's symptoms rapidly resolved, and repeat ECG revealed the recovery of atrioventricular conduction (**Figure 2B**) on the 5th day of admission. The treatment response to steroids further supported the diagnosis of pembrolizumab induced myocarditis. The patient was then discharged on the 7th day of admission, and the dosage of glucocorticoids was gradually tapered during the regular outpatient follow-up. The levels of hsTnI, BNP, and CK were gradually reduced to normal limits within 3 weeks after onset. On the 6th month of follow-up, the patient had a normal active life, and the mandibular mass showed no marked enlargement after discontinuation of pembrolizumab therapy. The overview of the clinical course of this patient is illustrated in **Figure 2C**.

LITERATURE REVIEW

The largest retrospective study of the WHO VigiBase demonstrated that cardiac irAEs comprise 2,215 (2.09%) of 106,025 irAEs (8). Among the cardiac irAEs, myocarditis was the most common form accounting for 14.1%, followed by pericardial disease (13.6%), conduction abnormalities (6.87%) and stress cardiomyopathy (0.72%) (8). Case reports of ICI-induced CAVB were often assessed to be secondary to myocarditis involving the conduction system. One multicenter trial, involving 30 cases of ICI-associated myocarditis, showed that atrioventricular conduction

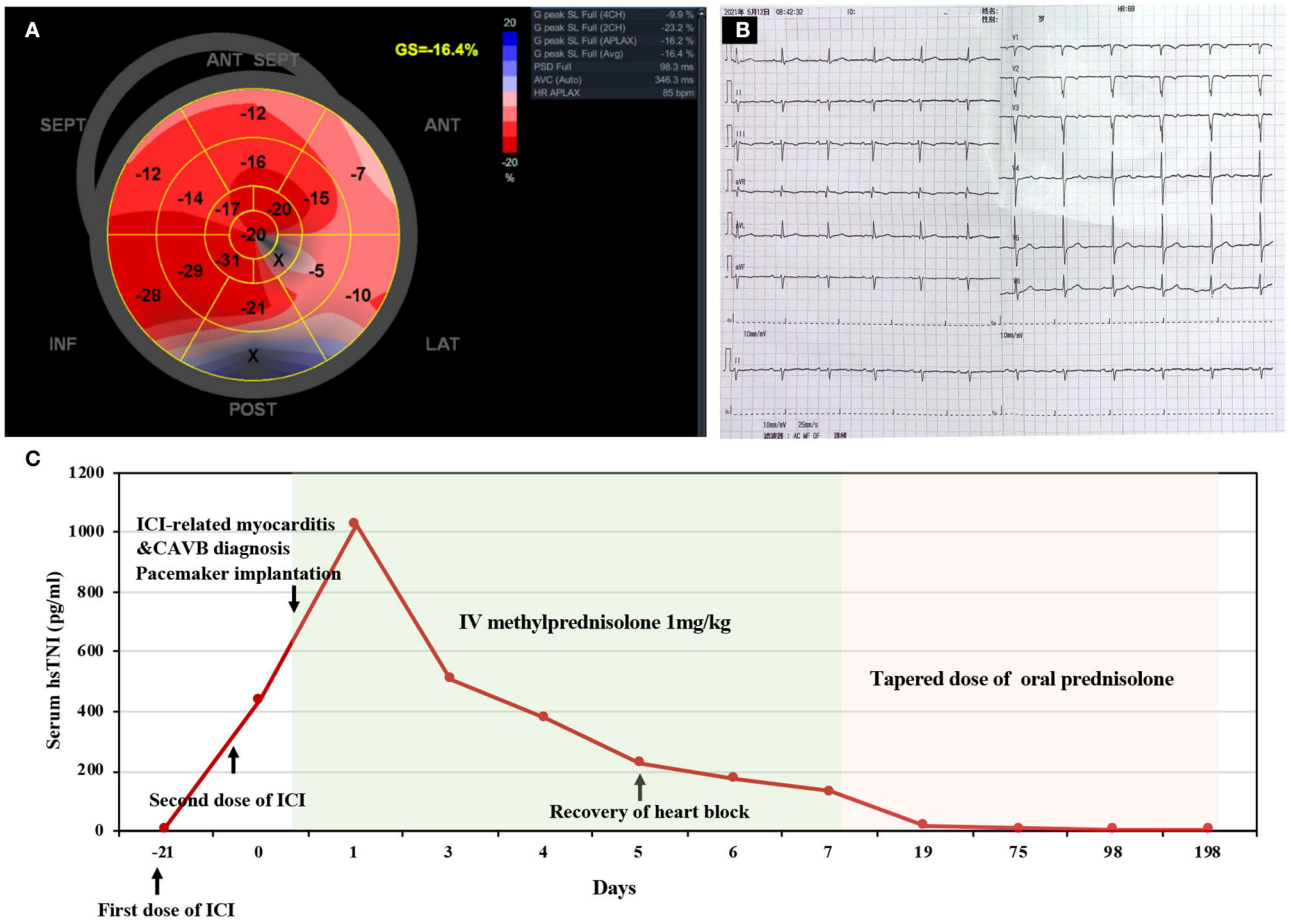

FIGURE 2 | Speckle tracking echocardiography, repeat electrocardiogram, and timeline of disease diagnosis and treatment. **(A)** Global longitudinal strain (GLS) bull's-eye plot showed a slightly decreased GLS of−16.4% and mainly impaired strain in the basal segments of anterior and lateral wall. **(B)** Electrocardiogram on the 5th day of admission showed sinus rhythm with a normal rate of 69 beats per minute. **(C)** Timeline of disease diagnosis and treatment. ICI, immune checkpoint inhibitor; CAVB, complete atrioventricular block; IV, intravenous.

disorders were observed in 17% of patients with ICI-induced myocarditis (9). Albeit, the clinical characteristics and prognosis of CAVB secondary to ICI-induced myocarditis are less well defined.

We searched PubMed for articles published from inception to March 31th, 2022 in the English language. Search terms included "immune checkpoint" and "myocarditis". Case reports on human myocarditis concurrent with CAVB caused by ICIs were selected. Totally, we reported 30 cases of ICI-induced myocarditis concurrent with CAVB, with a fatality rate of 60% (see **Table 1** for details). The median age of patients was 67 (interquartile range, 63–74) years old and 63% of the patients were male. The median time from ICI administration to the onset of myocarditis was 21 days (interquartile range, 15–26 days). Among these cases, 63% of the patients occurred after the first ICI infusion and 23% occurred after the second ICI infusion. Besides, Most of the patients (87%) had no previous history of cardiovascular diseases and 30% presented EF-reduced heart failure. Of these patients with improved outcomes other than our case, they all received pulse methylprednisolone in the presence or absence of other immunosuppressive therapy. Additionally, 7 out of 12 (58%) surviving patients recovered from conduction disorders after immunosuppressive treatment.

DISCUSSION

Cardiotoxicity caused by ICIs is a rare adverse event, while its high mortality rate makes it worthy of further investigation (4). Patients can present with myocarditis, heart failure, arrhythmia, pericardial involvement, myocardial infarction, Takotsubo cardiomyopathy, vasculitis, etc. (2). Among these cardiac irAEs, myocarditis is the most common form with an incidence of 0.27–1.14% (38). The mechanism of ICI-induced myocarditis is still under research. Histopathological analyses of patients with ICI-induced myocarditis revealed that the infiltration of predominant $CD8^+$ T lymphocytes and a few macrophages might be the main cause of ICI-induced myocarditiss (39). This inflammation sometimes

TABLE 1 | Published cases of immune checkpoint inhibitor-induced myocarditis concurrent with complete heart block.

No	Ref.	Age	Sex	CVD	Tumor	ICIs	ICIs cycles/days	EF%	Pulse GC	OIT	Pacing	Outcome
1	(10)	63	M	–	Melanoma	IP+NI	1/15	50	+	INFI	TP	Death
2	(10)	65	F	–	Melanoma	IP+NI	1/12	73	–	–	–	Death
3	(11)	68	M	–	Sarcoma	IP+NI	1/14	35	+	MYCO	PP	Improved
4	(12)	63	M	HTN	Melanoma	NI	2/21	N	–	–	TP	Death
5	(13)	66	M	–	CMML	IP	1/7	70	+	–	–	Death
6	(14)	76	F	–	Lung cancer	NI	7/98	15	+	IVIG+PLAS+INFI	CRT-D	Improved
7	(15)	69	F	–	Lung cancer	NI	3/38	N	+	–	TP	Improved†
8	(16)	79	M	–	Gastric cancer	PE	2/35	N	+	IVIG+PLAS+MTX	TP	Death†
9	(17)	64	F	–	Glioblastoma	NI	2/22	37	+	INFI+ATG+MMF	TP	Improved†
10	(18)	73	M	–	Lung cancer	PE	1/16	70	+	–	PP	Improved†
11	(19)	67	M	–	Melanoma	IP+NI	1/16	20	+	ATG	PP	Death
12	(20)	67	F	–	Myeloma	PE	1/16	30	–	INFI	–	Death
13	(21)	67	M	HTN	Melanoma	IP+NI	1/16	N	+	IVIG INFI	–	Death
14	(22)	33	M	–	Lymphoma	NI	8/150	NM	–	MMF+IVIG	–	Death
15	(23)	70	F	–	Thymoma	PE	1/16	N	+	PLAS	PP	Improved
16	(24)	81	M	–	Renal cancer	IP+NI	1/21	62	+	PLAS	TP	Death
17	(25)	88	M	–	Melanoma	NI	1/22	N	+	INFI+MMF	PP	Death
18	(26)	48	F	–	Thymoma	PE	1/13	45	+	INFI	PP	Death
19	(27)	66	M	–	Gastric cancer	NI	1/24	NM	+	IVIG+PLAS	TP	Death
20	(28)	47	F	–	Thymoma	TO	1/28	NM	+	–	TP	Improved†
21	(29)	57	M	–	Renal cancer	IP+NI	1/12	50	+	ABAT+MMF	PP	Improved
22	(30)	79	F	–	Melanoma	IP+NI	2/25	NM	NM	–	P	Death
23	(31)	73	F	–	Melanoma	NI	1/18	N	–	–	PP	Death
24	(32)	57	M	–	Lung cancer	IP+NI	2/60	N	+	TCZ	P	Improved
25	(33)	70	M	HTN	Renal cancer	IP+NI	1/14	N	+	MMF+PLAS	TP	Death
26	(34)	66	M	–	Lung cancer	SI	2/25	N	+	IVIG	PP	Improved†
27	(35)	59	M	–	Renal cancer	IP+NI	1/21	N	+	IVIG+PLAS	–	Improved†
28	(36)	78	M	CHD	Lung cancer	IP+NI	1/15	45	–	–	–	Death
29	(37)	74	M	–	Gastric cancer	NI	12/240	10	+	IVIG+PLAS	TP	Death
30	ours	80	F	–	HNSCC	PE	2/21	65	–	–	PP	Improved†

CVD, cardiovascular disease; ICIs, immune checkpoint inhibitors; EF, ejection fraction; OIT, other immunosuppressive therapy; GC, glucocorticoids; M, male; F, female; HTN, hypertension; CMML, chronic myelomonocytic leukemia; HNSCC, head and neck squamous cell cancer; CHD, coronary heart disease; IP, ipilimumab; NI, nivolumab; PE, pembrolizumab; SI, sintilimab; TO, toripalimab; INFI, infliximab; MMF, mycophenolate mofetil; PLAS, plasmapheresis; IVIG, intravenous immunoglobulins; MTX, methotrexate; ATG, anti-thymocyte globulin; ABAT, abatacept; TP, temporary pacemaker; PP, permanent pacemaker; P, pacemaker; CRT-D, cardiac resynchronization therapy defibrillator; TCZ, tocilizumab; N, normal; NM, not mention.
† Recovery to sinus rhythm from complete heart block.

involves the cardiac conduction system, leading to conduction disorders (39). Therefore, conduction abnormalities frequently present with myocarditis. Furthermore, compared to the mortality rate (50%) of ICI-induced myocarditis in the existing literature, CAVB appeared a trend of increasing the mortality of ICI-induced myocarditis based on the mortality (60%) we reviewed.

The most widely recommended therapy for ICI-associated myocarditis is discontinuation of ICI therapy and administration of high-dose corticosteroids (1–2 mg/kg/day) as soon as possible, which is mainly initiated with pulse methylprednisolone (500–1,000 mg/day) for 3 days and subsequently gradually tapered and off (38). For cases who are unresponsive to corticoids, escalation to other immunosuppressive therapies should be evaluated, frequently involving plasmapheresis, intravenous immunoglobin, mycophenolate, and infliximab (38). Notably, steroid therapy may be accompanied by several adverse effects, particularly in elderly patients, who are vulnerable to adverse outcomes of steroid therapy, notably opportunistic infections. Thus, it is imperative to balance treatment effects of irAEs and adverse effects according to risk stratification. In most cases with cardiac irAEs, myocarditis concomitant with CAVB was clinically categorized as fulminant myocarditis, and pulse methylprednisolone thereby was initiated early after the onset (**Table 1**). In this report, the patient received high-dose steroids rather than pulse methylprednisolone therapy while clinical and laboratory results were noticeably improved. Importantly, repeated ECG

revealed recovery of conduction disorder on the 5th day after its onset. This successful treatment indicated that CAVB does not always portend worse outcomes and may not need aggressive immunosuppressive therapy in such cases. Additionally, suspicion of ICI-induced myocarditis in our patients was raised early, and intravenous corticoids were quickly administrated after ruling out myocardial infarction and viral myocarditis based on medical history and quick-easy examination. As a consequence, early initiation of steroid treatment also contributed to good clinical outcomes.

Despite the limited available data, numerous risk factors for developing cardiac irAEs have been reported, including combination ICI therapy, underlying cardiovascular disease, previous cancer therapy-induced cardiac dysfunction, and underlying autoimmune diseases (38). Additionally, it should be noted that thymic epithelial tumors are associated with a higher incidence of irAEs than other types of cancers (23). Among these patients, cardiac biomarkers and electrocardiograms should warrant intensive monitoring. To our knowledge, we report the first case of CAVB secondary to ICI-induced myocarditis complicated with recurrent HNSCC, and the above-mentioned risk factors were not found in this patient.

Among patients with ICI-induced myocarditis, more than half of patients had a normal LVEF, while they could still develop severe cardiac events (40). GLS has been found as a sensitive marker of cardiac injury with traditional cytotoxic therapy. A recent study on patients with cardiac irAEs showed that each percent reduction in GLS was correlated with a 1.5-fold increase in major adverse cardiovascular events (MACEs) in patients with a reduced EF and a 4.4-fold increase with a preserved EF (41). Importantly, GLS lower than 16% was significantly associated with a higher incidence of MACEs in patients with the preserved LVEF (41). In our case, the patient underwent myocardial contrast (MCE) echocardiography and speckle-tracking echocardiography. Although the slightly decreased GLS with normal MCE demonstrated that myocardial injury was irrelevant to myocardial ischemia, a GLS higher than 16% with a preserved LVEF highly indicated that the patient had a lower risk of subsequent cardiac events based on the existing literature. In support of our speculation, the patient showed an exceedingly good outcome after steroid therapy.

Another interesting finding was that the patient's tumor remained stable during the half-year follow-up after termination of immunotherapy. Of note, current literature has shown that patients with recurrent or metastatic HNSCC who are not amenable to curative therapies have poor survival (6). Despite receipt of aggressive chemotherapy or anti-EGFR monotherapy, the median progression-free survival only ranges from 3 to 4 months in these patients (6). Conceivably, the patient may obtain prolonged disease stabilization from pembrolizumab. However, in the setting of cardiac irAEs, ICIs are frequently recommended for discontinuation.

There are several limitations in the present case report. First, endomyocardial biopsy was not performed due to the patient's refusal given procedural risks. Second, cardiac magnetic resonance (CMR) has been regarded as an gold-standard noninvasive imaging to confirm myocarditis. But our patient refused to further perform CMR due to the improved clinical course. Third, the patient underwent permanent pacing early, but conduction disorder disappeared rapidly after steroid therapy. Although permanent pacing was performed in the majority of the aforementioned cases with concurrence of myocarditis and CAVB (**Table 1**), we here firstly reviewed that more than half of surviving patients with conduction disorders secondary to ICIs might recover to normal sinus rhythm under immunosuppressive therapy. Consequently, temporary pacemakers should be recommended first. Nevertheless, given the paucity of data on the reversibility of heart block related to ICIs, the indication for and timing of permanent pacemaker placement remains elusive.

In general, ICI-induced myocarditis can be life-threatening and it therefore warrants efforts to increase awareness, facilitate early detection, and initiate prompt intervention. Importantly, CAVB may not always present with fulminant myocarditis and more than 50% of these surviving patients could recover to normal sinus rhythm. When CMR is contraindicated in patients with ICI-related myocarditis, speckle-tracking echocardiography is a reliable and sensitive alternative to CMR for detecting myocardial injury, and GLS may be an important prognostic indicator.

DATA AVAILABILITY STATEMENT

The original contributions presented in the study are included in the article/supplementary material, further inquiries can be directed to the corresponding author/s.

ETHICS STATEMENT

Written information consent was obtained from the individual(s) for the publication of any potentially identifiable images or data included in this article.

AUTHOR CONTRIBUTIONS

LS and CL contributed to data analysis, article drafting, and figure editing. WW provided the history of this patient's tumor and revised the related sections in the manuscript. YC searched the literature. MW collected clinical records. HC revised the manuscript. All authors contributed to the article and approved the submitted version.

FUNDING

This study was financially supported by the National Natural Science Foundation of China (No. 81970301).

REFERENCES

1. Neilan TG, Rothenberg ML, Amiri-Kordestani L, Sullivan RJ, Steingart RM, Gregory W et al. Myocarditis associated with immune checkpoint inhibitors: an expert consensus on data gaps and a call to action. *Oncologist.* (2018) 23:874–8. doi: 10.1634/theoncologist.2018-0157
2. Shalata W, Abu-Salman A, Steckbeck R, Mathew Jacob B, Massalha I, Yakobson A. Cardiac toxicity associated with immune checkpoint inhibitors: a systematic review. *Cancers (Basel).* (2021) 13:5218. doi: 10.3390/cancers13205218
3. Machiels JP, Rene Leemans C, Golusinski W, Grau C, Licitra L, Gregoire V et al. Squamous cell carcinoma of the oral cavity, larynx, oropharynx and hypopharynx: EHNS-ESMO-ESTRO Clinical Practice Guidelines for diagnosis, treatment and follow-up. *Ann Oncol.* (2020) 31:1462–75. doi: 10.1016/j.annonc.2020.07.011
4. Ball S, Ghosh RK, Wongsaengsak S, Bandyopadhyay D, Ghosh GC, Aronow WS et al. Cardiovascular toxicities of immune checkpoint inhibitors: JACC review topic of the week. *J Am Coll Cardiol.* (2019) 74:1714–27. doi: 10.1016/j.jacc.2019.07.079
5. Burtness B, Harrington KJ, Greil R, Soulieres D, Tahara M, de Castro G. Jr, et al. Pembrolizumab alone or with chemotherapy versus cetuximab with chemotherapy for recurrent or metastatic squamous cell carcinoma of the head and neck (KEYNOTE-048): a randomised, open-label, phase 3 study. *Lancet.* (2019) 394:1915–28. doi: 10.1016/S0140-6736(19)32591-7
6. Sacco AG, Chen R, Worden FP, Wong DJL, Adkins D, Swiecicki P et al. Pembrolizumab plus cetuximab in patients with recurrent or metastatic head and neck squamous cell carcinoma: an open-label, multi-arm, non-randomised, multicentre, phase 2 trial. *Lancet Oncol.* (2021) 22:883–92. doi: 10.1016/S1470-2045(21)00136-4
7. Bernhard W, Barreto K, El-Sayed A, Gonzalez C, Viswas RS, Toledo D et al. Pre-clinical study of IRDye800CW-nimotuzumab formulation, stability, pharmacokinetics, and safety. *BMC Cancer.* (2021) 21:270. doi: 10.1186/s12885-021-08003-3
8. Upadhrasta S, Elias H, Patel K, Zheng L. Managing cardiotoxicity associated with immune checkpoint inhibitors. *Chronic Dis Transl Med.* (2019) 5:6–14. doi: 10.1016/j.cdtm.2019.02.004
9. Escudier M, Cautela J, Malissen N, Ancedy Y, Orabona M, Pinto J et al. Clinical features, management, and outcomes of immune checkpoint inhibitor-related cardiotoxicity. *Circulation.* (2017) 136:2085–7. doi: 10.1161/CIRCULATIONAHA.117.030571
10. Johnson DB, Balko JM, Compton ML, Chalkias S, Gorham J, Xu Y et al. Fulminant myocarditis with combination immune checkpoint blockade. *N Engl J Med.* (2016) 375:1749–55. doi: 10.1056/NEJMoa1609214
11. Reddy N, Moudgil R, Lopez-Mattei JC, Karimzad K, Mouhayar EN, Somaiah N et al. Progressive and reversible conduction disease with checkpoint inhibitors. *Can J Cardiol.* (2017) 33:1335 e13–5. doi: 10.1016/j.cjca.2017.05.026
12. Behling J, Kaes J, Munzel T, Grabbe S, Loquai C. New-onset third-degree atrioventricular block because of autoimmune-induced myositis under treatment with anti-programmed cell death-1 (nivolumab) for metastatic melanoma. *Melanoma Res.* (2017) 27:155–8. doi: 10.1097/CMR.0000000000000314
13. Berg DD, Vaduganathan M, Nohria A, Davids MS, Alyea EP, Torre M et al. Immune-related fulminant myocarditis in a patient receiving ipilimumab therapy for relapsed chronic myelomonocytic leukaemia. *Eur J Heart Fail.* (2017) 19:682–5. doi: 10.1002/ejhf.806
14. Frigeri M, Meyer P, Banfi C, Giraud R, Hachulla AL, Spoerl D et al. Immune checkpoint inhibitor-associated myocarditis: a new challenge for cardiologists. *Can J Cardiol.* (2018) 34:92 e1–3. doi: 10.1016/j.cjca.2017.09.025
15. Fukasawa Y, Sasaki K, Natsume M, Nakashima M, Ota S, Watanabe K et al. Nivolumab-Induced Myocarditis Concomitant with Myasthenia Gravis. *Case Rep Oncol.* (2017) 10:809–12. doi: 10.1159/000479958
16. Nasr F, El Rassy E, Maalouf G, Azar C, Haddad F, Helou J et al. Severe ophthalmoplegia and myocarditis following the administration of pembrolizumab. *Eur J Cancer.* (2018) 91:171–3. doi: 10.1016/j.ejca.2017.11.026
17. Tay RY, Blackley E, McLean C, Moore M, Bergin P, Gill S et al. Successful use of equine anti-thymocyte globulin (ATGAM) for fulminant myocarditis secondary to nivolumab therapy. *Br J Cancer.* (2017) 117:921–4. doi: 10.1038/bjc.2017.253
18. Katsume Y, Isawa T, Toi Y, Fukuda R, Kondo Y, Sugawara S et al. Complete atrioventricular block associated with pembrolizumab-induced acute myocarditis: the need for close cardiac monitoring. *Intern Med.* (2018) 57:3157–62. doi: 10.2169/internalmedicine.0255-17
19. Jain V, Mohebtash M, Rodrigo ME, Ruiz G, Atkins MB, Barac A. Autoimmune myocarditis caused by immune checkpoint inhibitors treated with antithymocyte globulin. *J Immunother.* (2018) 41:332–5. doi: 10.1097/CJI.0000000000000239
20. Martinez-Calle N, Rodriguez-Otero P, Villar S, Mejias L, Melero I, Prosper F et al. Anti-PD1 associated fulminant myocarditis after a single pembrolizumab dose: the role of occult pre-existing autoimmunity. *Haematologica.* (2018) 103:e318–21. doi: 10.3324/haematol.2017.185777
21. Saibil SD, Bonilla L, Majeed H, Sotov V, Hogg D, Chappell MA et al. Fatal myocarditis and rhabdomyositis in a patient with stage IV melanoma treated with combined ipilimumab and nivolumab. *Curr Oncol.* (2019) 26:e418–21. doi: 10.3747/co.26.4381
22. Charles J, Giovannini D, Terzi N, Schwebel C, Sturm N, Masson D et al. Multi-organ failure induced by Nivolumab in the context of allo-stem cell transplantation. *Exp Hematol Oncol.* (2019) 8:8. doi: 10.1186/s40164-019-0132-2
23. Szuchan C, Elson L, Alley E, Leung K, Camargo AL, Elimimian E et al. Checkpoint inhibitor-induced myocarditis and myasthenia gravis in a recurrent/metastatic thymic carcinoma patient: a case report. *Eur Heart J Case Rep.* (2020) 4:1–8. doi: 10.1093/ehjcr/ytaa051
24. Hardy T, Yin M, Chavez JA, Ivanov I, Chen W, Nadasdy T et al. Acute fatal myocarditis after a single dose of anti-PD-1 immunotherapy, autopsy findings: a case report. *Cardiovasc Pathol.* (2020) 46:107202. doi: 10.1016/j.carpath.2020.107202
25. Giancaterino S, Abushamat F, Duran J, Lupercio F, DeMaria A, Hsu JC. Complete heart block and subsequent sudden cardiac death from immune checkpoint inhibitor-associated myocarditis. *HeartRhythm Case Rep.* (2020) 6:761–4. doi: 10.1016/j.hrcr.2020.07.015
26. Portoles Hernandez A, Blanco Clemente M, Escribano Garcia D, Velasco Calvo R, Nunez Garcia B, Oteo Dominguez JF et al. Checkpoint inhibitor-induced fulminant myocarditis, complete atrioventricular block and myasthenia gravis-a case report. *Cardiovasc Diagn Ther.* (2021) 11:1013–9. doi: 10.21037/cdt-21-147
27. Komatsu M, Hirai M, Kobayashi K, Hashidate H, Fukumoto J, Sato A et al. A rare case of nivolumab-related myasthenia gravis and myocarditis in a patient with metastatic gastric cancer. *BMC Gastroenterol.* (2021) 21:333. doi: 10.1186/s12876-021-01904-4
28. Luo YB, Tang W, Zeng Q, Duan W, Li S, Yang X et al. Case Report: The neuromusclar triad of immune checkpoint inhibitors: a case report of myositis, myocarditis, and myasthenia gravis overlap following toripalimab treatment. *Front Cardiovasc Med.* (2021) 8:714460. doi: 10.3389/fcvm.2021.714460
29. Jespersen MS, Fano S, Stenor C, Moller AK. A case report of immune checkpoint inhibitor-related steroid-refractory myocarditis and myasthenia gravis-like myositis treated with abatacept and mycophenolate mofetil. *Eur Heart J Case Rep.* (2021) 5:ytab342. doi: 10.1093/ehjcr/ytab342
30. Barham W, Guo R, Park SS, Herrmann J, Dong H, Yan Y. Case report: simultaneous hyperprogression and fulminant myocarditis in a patient with advanced melanoma following treatment with immune checkpoint inhibitor therapy. *Front Immunol.* (2020) 11:561083. doi: 10.3389/fimmu.2020.561083
31. Wang F, Sun X, Qin S, Hua H, Liu X, Yang L et al. A retrospective study of immune checkpoint inhibitor-associated myocarditis in a single center in China. *Chin Clin Oncol.* (2020) 9:16. doi: 10.21037/cco.2020.03.08
32. Doms J, Prior JO, Peters S, Obeid M. Tocilizumab for refractory severe immune checkpoint inhibitor-associated myocarditis. *Ann Oncol.* (2020) 31:1273–5. doi: 10.1016/j.annonc.2020.05.005
33. Gonzalez-Ferrero T, Vargas-Osorio K, Gonzalez-Juanatey JR. Fulminant myocarditis with myositis after treatment with immune checkpoint inhibitors. *Med Clin (Barc).* (2022) 158:140–1. doi: 10.1016/j.medcli.2021.04.014
34. Xing Q, Zhang ZW, Lin QH, Shen LH, Wang PM, Zhang S et al. Myositis-myasthenia gravis overlap syndrome complicated with myasthenia

crisis and myocarditis associated with anti-programmed cell death-1 (sintilimab) therapy for lung adenocarcinoma. *Ann Transl Med.* (2020) 8:250. doi: 10.21037/atm.2020.01.79
35. Yanase T, Moritoki Y, Kondo H, Ueyama D, Akita H, Yasui T. Myocarditis and myasthenia gravis by combined nivolumab and ipilimumab immunotherapy for renal cell carcinoma: a case report of successful management. *Urol Case Rep.* (2021) 34:101508. doi: 10.1016/j.eucr.2020.101508
36. Vartanov A, Kalotra A, Varughese J, Gautam S, Kandel S, Hosmer W. Immunotherapy-associated complete heart block in a patient with NSCLC: a case report and literature review. *Respir Med Case Rep.* (2021) 33:101390. doi: 10.1016/j.rmcr.2021.101390
37. Naganuma K, Horita Y, Matsuo K, Miyama Y, Mihara Y, Yasuda M et al. An autopsy case of late-onset fulminant myocarditis induced by nivolumab in gastric cancer. *Intern Med.* (2022). doi: 10.2169/internalmedicine.9161-21
38. Hu JR, Florido R, Lipson EJ, Naidoo J, Ardehali R, Tocchetti CG et al. Cardiovascular toxicities associated with immune checkpoint inhibitors. *Cardiovasc Res.* (2019) 115:854–68. doi: 10.1093/cvr/cvz026
39. Tajiri K, Ieda M. Cardiac complications in immune checkpoint inhibition therapy. *Front Cardiovasc Med.* (2019) 6:3. doi: 10.3389/fcvm.2019.00003
40. Mahmood SS, Fradley MG, Cohen JV, Nohria A, Reynolds KL, Heinzerling LM et al. Myocarditis in patients treated with immune checkpoint inhibitors. *J Am Coll Cardiol.* (2018) 71:1755–64. doi: 10.1016/j.jacc.2018.02.037
41. Awadalla M, Mahmood SS, Groarke JD, Hassan MZO, Nohria A, Rokicki A et al. Global longitudinal strain and cardiac events in patients with immune checkpoint inhibitor-related myocarditis. *J Am Coll Cardiol.* (2020) 75:467–78. doi: 10.1016/j.jacc.2019.11.049

Conflict of Interest: The authors declare that the research was conducted in the absence of any commercial or financial relationships that could be construed as a potential conflict of interest.

Publisher's Note: All claims expressed in this article are solely those of the authors and do not necessarily represent those of their affiliated organizations, or those of the publisher, the editors and the reviewers. Any product that may be evaluated in this article, or claim that may be made by its manufacturer, is not guaranteed or endorsed by the publisher.

Copyright © 2022 Su, Liu, Wu, Cui, Wu and Chen. This is an open-access article distributed under the terms of the Creative Commons Attribution License (CC BY). The use, distribution or reproduction in other forums is permitted, provided the original author(s) and the copyright owner(s) are credited and that the original publication in this journal is cited, in accordance with accepted academic practice. No use, distribution or reproduction is permitted which does not comply with these terms.

frontiers | Frontiers in Cardiovascular Medicine

CASE REPORT
published: 31 May 2022
doi: 10.3389/fcvm.2022.903354

Case Report: Torsade de Pointes Induced by the Third-Generation Epidermal Growth Factor Receptor–Tyrosine Kinase Inhibitor Osimertinib Combined With Litsea Cubeba

Xia-yan Zhang[1], Cha-bin Wu[1,2], Cai-xia Wu[1,3], Li Lin[4], Yue-juan Zhou[1], Yan-yan Zhu[1], Wei-qiang Tian[1] and Song-mei Luo[1]*

[1] Department of Pharmacy, Lishui Central Hospital, Lishui, China, [2] Department of Pharmacy, Longquan Hospital of TCM, Lishui, China, [3] Department of Pharmacy, Traditional Chinese Medicine Hospital of Qingyuan, Lishui, China, [4] Department of Cardiovascular Medicine, Lishui Central Hospital, Lishui, China

OPEN ACCESS

Edited by:
Daniel M. Johnson,
The Open University, United Kingdom

Reviewed by:
Toru Maruyama,
Kyushu University, Japan
Luis Alberto Gonano,
Universidad Nacional de La Plata, Argentina

***Correspondence:**
Yan-yan Zhu
zhuyanyan304@126.com

Specialty section:
This article was submitted to Cardio-Oncology, a section of the journal Frontiers in Cardiovascular Medicine

Received: *24 March 2022*
Accepted: *25 April 2022*
Published: *31 May 2022*

Citation:
Zhang X-y, Wu C-b, Wu C-x, Lin L, Zhou Y-j, Zhu Y-y, Tian W-q and Luo S-m (2022) Case Report: Torsade de Pointes Induced by the Third-Generation Epidermal Growth Factor Receptor–Tyrosine Kinase Inhibitor Osimertinib Combined With Litsea Cubeba. Front. Cardiovasc. Med. 9:903354. doi: 10.3389/fcvm.2022.903354

Torsades de Pointes (TdP) occurred in a 68-year-old female with epidermal growth factor receptor (EGFR) mutant lung cancer administered osimertinib, the third-generation EGFR tyrosine kinase inhibitor (TKI). Electrocardiogram (ECG) recorded at Tdp showed QT prolongation (QTc = 515 ms), to which a Traditional Chinese Medicine (TCM) named "Litsea Cubeba" may have contributed. After discontinuation of osimertinib and Litsea Cubeba, magnesium supplementation, potassium supplementation, lidocaine infusion, and the pacemaker frequency adjustment, Tdp terminated. However, QT prolongation sustained at discharge (QTc = 528 ms), partly because of the emergency use of amiodarone. Osimertinib may prolong the QT interval leading to TdP, especially when multiple risk factors to lengthen QT interval are incidentally overlapped. Thus, regular monitoring of ECG and appropriate management of concomitant drugs are highly recommended.

Keywords: torsade de pointes, osimertinib, Litsea Cubeba, QT prolongation, adverse events

INTRODUCTION

Osimertinib is an oral, irreversible, third-generation epidermal growth factor receptor (EGFR) tyrosine kinase inhibitor (TKI), recommended as a first-line treatment for EGFR-mutated advanced or metastasis non-small cell lung cancer (NSCLC) (1, 2). Since vascular and cardiac potassium channels are regulated largely by EGFR tyrosine kinase (3), cardiotoxicity such as congestive heart failure and QT prolongation has been reported to be common with Osimertinib. Of the 1,479 patients treated with TAGRISSO in clinical trials (4, 5), 0.8% were found to have a QTc >500 ms, and 3.1% of patients had an increase from baseline QTc >60 ms, but no QTc-related arrhythmias were reported. Thus, osimertinib-induced QT prolongation leading to the possible development of

Torsades de Pointes (TdP) has received less attention. Here we present a 68-year-old woman with advanced NSCLC (T1N2M0, IIIa) had sudden TdP, which was caused by osimertinib combined with Traditional Chinese Medicine (TCM) named "Litsea Cubeba."

CASE DESCRIPTION

A 68-year-old woman, who had a history of lung adenocarcinoma for 1 year, was admitted to our hospital with "syncope" on January 02, 2022. In April 2020, she visited our hospital due to waist pain and back pain. The Chest CT on 15 April 2020 showed space-occupying lesions in the left upper lung, which was considered to be the lung cancer, accompanied by pleural effusion in both sides. The PET-CT on 20 April 2020 showed subpleural solid nodules in the left upper lung with FDG metabolism slightly elevated, which was considered to be Pulmonary CA. The target scan of pulmonary nodules on 23 April 2020 showed Subpleural solid nodule in the left upper lung and ground-glass nodule in the left lower dorsal segment. Then she underwent left total pneumonectomy in the first affiliated hospital of Zhejiang University, with post-operative pathology showing the stage was T1N2M0, stage IIIA. Genetic testing showed that exon 21 EGFR-L858R was positive with a mutation frequency of 1.65%. She was given lcotinib (Conmana) 125 mg tid for targeted therapy, and had a dose reduction or discontinuation due to diarrhea and itch according to the instructions of dosage adjustment. On 13 October 2021, re-examination of PET-CT showed vertebral metastasis in the S1 vertebral body. On 20 October 2021, a second genetic testing: exon 20 EGFR -T790M was positive with a mutation frequency of 0.75%. Then, the treatment was adjusted to osimertinib (TAGRISSO) 80 mg qd in 1 November 2021.

Her transthoracic ultrasound cardiography (UCG) was not examined at the initiation of osimertinib, but it showed a left ventricular end-diastolic diameter (LVEDD) of 54 mm and a left ventricular ejection fraction (LVEF) of 60% in 10 months before the initiation on 1 January 2021 and showed a LVEDD of 57 mm and an LVEF of 62% 10 days after the initiation on 11 November 2021. She had >1 year history of atrial fibrillation with third degree atrioventricular blocker, but no provable electrocardiogram (ECG) evidence could be provided. And we found no indications in her ECG [QTc (QT interval corrected by Bazetts's formula, $QTc = QT/RR^{0.5}$): 481 ms, HR: 76 bpm, **Figure 1A**] examined 19 months before. Because of some personal reasons, her ECG examination was postponed to 5 days after the initiation of osimertinib, which showed atrial fibrillation with third degree atrioventricular block (QTc: 464 ms, HR: 40 bpm, **Figure 1B**). Then a pacemaker (VVI, Medtronic, E10A1) was implanted in 10 November 2021, and her ECG was normal (QTc: 488 ms, HR: 60 bpm, **Figure 1C**). In 1 January 2022, 60 days after administration of osimertinib, she had some tea made of leaves and fruits (≈10 g) from TCM named "Litsea Cubeba" due to heatstroke. In 2 January 2022, she suddenly fainted when cooking at home at around 7:00 and woke up approximately 30 min later, feeling a little dizzy and chest tightness. She fainted again when walking around 14:00 and woke up after about 1 h, then she was sent to our hospital for emergency treatment. UCG showed a LVEDD of 57 mm and an LVEF of 57%. The ECG indicated TdP (QTc: 532 ms, HR: 60 bpm, **Figure 1D**). A loading dose of amiodarone of 0.15 g was intravenously injected immediately, followed by continuous infusion at 1 mg/min. In the meantime, intravenous administration of potassium and magnesium (500 ml 5% GS supplement of 25% magnesium sulfate 10 ml and 10% muriate 15 ml) and omeprazole (40 mg in 0.9% NS 100 ml) were carried out. She was transferred to cardiovascular medicine for further treatment at 20:51.

The vital signs were temperature (T) 36.3°C, blood pressure (BP) 89/69 mmHg, heart rate (HR) 59 bpm, and respiratory rate (RR) 20 bpm during the initial examination. Chest CT on admission showed a little fiber focus in the middle lobe of the right lung and small calcifications in the lower lobe of the right lung. Electrolytes: potassium 3.5 mmol/L, calcium 2.21 mmol/L; blood routine: white blood cells 10.7×10^9/L, neutrophils 9.5×10^9/L; BNP: 248 pg/mL.

Half an hour after admission (21:20), her condition suddenly deteriorated. Tdp (QTc: 515 ms, HR: 110 bpm, **Figure 1E**) with loss of consciousness occurring repeatedly. Cardiopulmonary resuscitation of repeated chest compressions was carried out. Supplement of potassium and magnesium (15 ml of 10% potassium chloride and 20 ml of 25% magnesium sulfate were added to 500 ml of 5% glucose) were intravenously injected immediately and had a dosage adjustment according to serum electrolytes (**Table 1**). Meanwhile, 50 mg of lidocaine was intravenously injected at the first dose, resulting in no reduction of premature beats. Then an additional 150 mg was injected, followed by continuous infusion at 1 mg/min. Furthermore, pacemaker frequency was adjusted to 100 bpm and gradually reduced to 70 bpm based on her ECG monitoring (**Table 1**). Finally, TdP terminated at 22:20 and was not recurrent afterward. As she had >10 year history of stable diabetes, subcutaneous injection of insulin Degludec and insulin Aspart injection (Ryzodeg) was continued. She also had >1 year history of stable hypertension treated with valsartan (80 mg qd po), but valsartan (80 mg qd po) was discontinued due to the low blood pressure during her hospitalization. Her ECG did not return to normal (QTc:528 ms, HR:69 bpm, **Figure 1F**) at discharge, partly because of amiodarone use. She was discharged on the ninth hospital day.

DISCUSSION

Over the past 10 years, overall survival among cancer patients has been extended due to the development of efficacious treatment regimens, while many of these treatments can cause QTc prolongation (6). QTc prolongation is an unusual but important cardiac adverse reaction of anti-tumor drugs, especially chemotherapeutic agents, EGFR-TKI, and immune checkpoint inhibitors, which can lead to TdP, a potentially life-threatening form of malignant arrhythmia with clinical manifestations characterized by syncope, tetany, or sudden death. In a scientific statement from the American Heart Association and the American College of Cardiology Foundation published

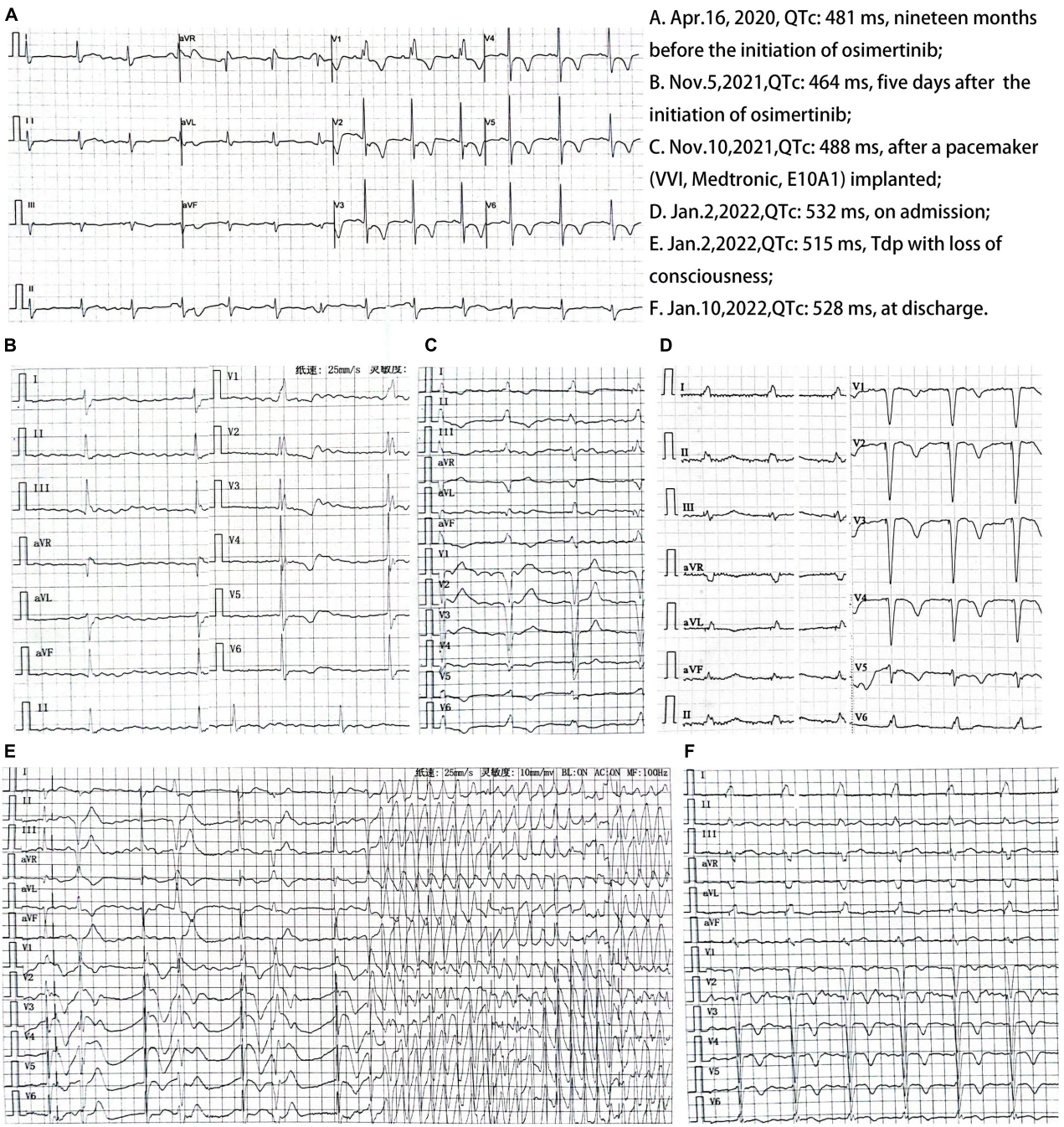

FIGURE 1 | Twelve-lead electrocardiogram (ECG).

in Drew et al. (7), the normal QTc interval is recommended to be 470 ms for males and 480 ms for females. QTc interval >500 ms is considered highly abnormal in both males and females, and may be associated with a substantially elevated risk of TdP (8). Usually, the risk of TdP increase 5∼7% for every 10 ms extention in the QTc interval (9). But the link between changes in QT and TdP is highly variable. For some individuals, TdP may occur with modest QT prolongation, whereas others may experience no effects even with markedly prolonged QT (10). That is because Tdp is also associated with increased dispersion of ventricular repolarization. For example, amiodarone can markedly increase QT, but typically has a homogenous effect on the ventricular myocardium and rarely causes TdP (7, 11).

Osimertinib, an oral, third-generation EGFR-TKI that can specifically bind mutated T790M, has been approved for the treatment of NSCLC patients with T790M mutation. According

TABLE 1 | Serum electrolyte and pacing frequency adjustment in hospital.

Date	Electrolytes			Pacing frequency adjustment (beats/min)
	Potassium (mmol/L)	Magnesium (mmol/L)	Calcium (mmol/L)	
January 2, 2022	3.5	NA	2.21	60
January 3, 2022	5.0	1.64	2.01	100
January 4, 2022	NA	NA	NA	90
January 5, 2022	NA	NA	NA	80
January 6, 2022	4.66	0.83	2.14	80
January 7, 2022	NA	NA	NA	70
January 11, 2022	4.99	0.67	2.40	70

NA, not available.

TABLE 2 | Review of case reports of Tdp due to osimertinib.

Authors	Age, sex	EGFR mt	Heart diseases	Prior treatment	Osimertinib response	Time to Tdp	QTc				Suspicious concomitant drugs	Tdp outcome
							Baseline	Tdp occurr	Tdp Terminated	Tdp Discharge		
Bain (22)	85, M	L861Q + T790M	ND	Gefitinib	ND	6 months	484 ms	647 ms	631*/496 ms#	ND	Moxifloxacin	Improved
Ikebe (23)	84, F	Dell 9	None	SRT	PR	2 months	467 ms	524 ms	ND	464 ms	ND	Improved
Matsuura (24)	60, F	ND	QT prolongation without syncope	ND	ND	2 months	486 ms	532 ms	ND	475 ms$	General anesthesia	Improved
This case	68, F	ND	HTN, DB, AF, VVI-IP	Lcotinib	PR	2 months	481 ms	515 ms	510 ms	528 ms	Litsea Cubeba	Improved

*AF, atrial fibrillation; DB, diabetes; EGFR mt, epidermal growth factor receptor mutation; F, female; HTN, hypertension; M, male; ND, not documented; PR, partial response; SRT, stereotactic thoracic radiotherapy; TdP, torsade de pointes; VVI-IP, a pacemaker (VVI, Medtronic, E10A1) implanted; *7 h after Tdp occurr, #91 h after Tdp occurr, $12 day after discharge.*

to a United States retrospective clinical study from 2016 to 2018, osimertinib significantly increased the risk of cardiotoxicity compared with other EGFR-TKIs, and QT prolongation was the second common AE next to cardiac failure (12). In that study, the median onset of QT interval prolonged following osimertinib initiation was 23 days (IQR:14∼55). A Japanese retrospective study of 3,578 patients treated with osimertinib from 2016 to 2018 also reported that QT prolongation was observed in 45 patients (1.3%; Grade ≥3, 0.1% [5/3578]), while other cardiac disorders (including cardiac disorders, cardiac failure, and cardiomyopathy) were observed in 101 patients (2.3%) (13). In that study, the median onset of QT interval prolonged was 56 days (range:4∼548) after the first dose. Most prolonged QTc induced by osimertinib is mild to moderate (grade 1–2) adverse events, as 0.9% patients have prolonged QTc over 500 ms and 3.6% patients has prolonged QTc above 60 ms from baseline in clinical trials (4, 5). As per the osimertinib package insert, if the QT interval is >500 ms the osimertinib should be withheld until the QT interval is <480 ms or recovers to baseline. If the baseline QT is >480 ms, then osimertinib should be resumed at one-half the dose (14). The mechanism of osimertinib-induced QT interval prolongation may associate with potassium channels which plays an important role in repolarization. EGFR are linked to many potassium channels, i.e., Kv1.3 (15), Kv10.1 (16), Kv4.3 (17), and Kir2.3 (18), which are modulated by EGFR kinase *via* phosphorylation of tyrosine in their specific residues. Osimertinib has been proved as a weak inhibitor of the cardiac potassium ion channel, Kv11.1, inhibiting hERG encoded potassium channel function with an *in vitro* IC50 of 0.69 mM (19). Spontaneous release of Ca^{2+} *via* cardiac ryanodine receptors (RyR2), through a process termed store overload-induced Ca^{2+} release (SOICR), is a common mechanism underlying arrhythmia. It has been reported that some class I kinase inhibitors (silmitasertib, sunitinib) can increase the activity of RyR2, ultimately increasing the propensity for SOICR (20), which suggests that RyR2 may contribute to arrhythmia induced by Osimertinib. Besides, animal model suggests that down-regulation of PI3K signaling directly or indirectly *via* tyrosine kinase inhibition prolongs the QT interval by affecting multiple ion channels, i.e., decrease the delayed rectifier K^+ currents (I_{Kr} and I_{Ks}), the L-type calcium ion (Ca^{2+}) current ($I_{Ca,\ L}$) and the peak sodium ion (Na^+) current (I_{Na}) and increase the persistent Na^+ current I_{NaP} (21).

No Tdp associated with osimertinib has occurred in clinical trials (4, 5), and only three cases of Tdp caused by osimertinib have been reported (**Table 2**). In addition, Kondo (25) reported

a case of an 85-year-old female patient treated with osimertinib for advanced lung cancer expressing EGFR mutations (T790M), which lengthened QT interval causing abortive sudden cardiac death (SCD). Cardiac arrest in that case was supposed to be due to possible development of TdP based on several predisposing factors lengthening QT interval. However, the case was not presented in **Table 2**, because the ECG was not retrieved from AED, resulting in no ostensive proof of Tdp. Here we present a 68-year-old woman with advanced NSCLC who underwent QT prolongation leading to Tdp when combined with a TCM named "Litsea Cubeba." In this case, Tdp happened along with QTc interval prolonged from 464 to 515 ms in 61 days after osimertinib administration.

Litsea Cubeba is a traditional herb and its plant parts, such as bark, leaf, root, and fruits, have been utilized in TCM for various diseases, including carminative (relieves flatulence), diuretic (aids urine passage), expectorant (aids secretion of sputum), stomachache, antiasthmatic, dyspepsia, gastroenteritis, diabetes, edema, cold, arthritis, pain, traumatic injury, and so on (26). In this case, the patient diagnosed herself with heatstroke based on a series of symptoms such as dizziness, nausea, and vomiting. Then she had some tea made of leaves and fruits (≈10 g) from Litsea Cubeba. Litsea cubeba encompasses a varied number of active compounds, such as alkaloids, monoterpenes, sesquiterpenes, diterpenes, flavonoids, amides, lignans, steroids, and fatty acids. According to TCM systems pharmacology database and analysis platform (TCMSP),[1] there are at least 11 compounds that can target potassium voltage-gated channel subfamily H member 2 (KCNH2), one of the important potassium channels that regulate vascular tonus and QT interval in ECG. Thus, Litsea Cubeba may affect QT interval and partly contributed to the Tdp.

Besides, risk factors for the development of TdP in hospitalized patients include: QTc >500 ms, use of QT-prolonging drugs, heart disease (congestive heart failure and myocardial infarction), advanced age, female sex, electrolyte disturbance (hypokalemia, hypomagnesemia, hypocalcemia, etc.), treatment with diuretics, impaired hepatic drug metabolism (hepatic dysfunction or drug-drug interactions), bradycardia, genetic polymorphisms, and so on (7). In this case, the patient had at least third risk factors, i.e., advanced age, female sex, concurrent use of more than 1 QT-prolonging drug, history of atrial fibrillation with third degree atrioventricular blocker, might partly contribute to the TdP.

CONCLUSION

We have described a 68-year-old female patient with EGFR mutant advanced lung cancer treated with standard regimen of osimertinib, underwent QT prolongation leading to Tdp when combined with a TCM named "Litsea Cubeba." Magnesium supplementation, potassium supplementation, and the antiarrhythmic drug lidocaine was given, so as the pacemaker frequency was adjusted to 70∼100 bpm. Then, Tdp terminated, but QT prolongation sustained at discharge.

Although osimertinib-induced QT prolongation is mild to moderate and not frequent (3∼10%), TdP may be induced by standard dose of osimertinib, especially when multiple risk factors to lengthen QT interval are incidentally overlapped. Concomitant drugs that can increase QT prolongation should be avoided while taking osimertinib. Besides, we recommend that clinicians consider an ECG at baseline when initiating osimertinib and at periodic intervals to monitor for QT prolongation. Dose reduction or treatment interruption should be performed for serious adverse events of QTc prolongation or even serious arrhythmia.

DATA AVAILABILITY STATEMENT

The original contributions presented in the study are included in the article/supplementary material, further inquiries can be directed to the corresponding author.

ETHICS STATEMENT

The studies involving human participants were reviewed and approved by the Ethics Committee of Lishui Central Hospital. The patients/participants provided their written informed consent to participate in this study. Written informed consent was obtained from the individual(s) for the publication of any potentially identifiable images or data included in this article.

AUTHOR CONTRIBUTIONS

X-YZ contributed to manuscript writing. C-BW, C-XW, and Y-JZ contributed to data collection. LL contributed to the clinical treatment. Y-YZ contributed to the initial concept of the manuscript preparation. W-QT contributed to the review of the manuscript. S-ML contributed to the editing of the manuscript. All authors collaborated and carried out case report manuscript, read, and approved the final manuscript.

FUNDING

This work was supported by the Natural Science Foundation of Zhejiang Provincial (grant numbers LYY19H280004 and LY18H300007), Research Fund of Zhejiang Pharmaceutical Association (grant number 2014ZYY33), Research Fund of Wu Jieping Medical Foundation, Clinical Pharmacy Branch of Chinese Medical Association (grant numbers 320.6750.2020-04-43 and LCYX-Q014), and Foundation of Lishui Science and Technology Bureau (grant number 2015sjzc19).

ACKNOWLEDGMENTS

We thank the ward staffs of Lishui Central Hospital for their clinical assistance.

[1] https://tcmsp-e.com/tcmsp.php

REFERENCES

1. Mok TS, Wu YL, Ahn MJ, Garassino MC, Kim HR, Ramalingam SS, et al. Osimertinib or platinum-pemetrexed in EGFR T790M-positive lung cancer. *N Engl J Med.* (2017) 376:629–40. doi: 10.1056/NEJMoa1612674
2. Soria JC, Ohe Y, Vansteenkiste J, Reungwetwattana T, Chewaskulyong B, Lee KH, et al. Osimertinib in untreated EGFR-mutated advanced non-small-cell lung cancer. *N Engl J Med.* (2018) 378:113–25. doi: 10.1056/NEJMoa1713137
3. Schiefer M, Hendriks LEL, Dinh T, Lalji U, Dingemans AC. Current perspective: osimertinib-induced QT prolongation: new drugs with new side-effects need careful patient monitoring. *Eur J Cancer.* (2018) 91:92–8. doi: 10.1016/j.ejca.2017.12.011
4. Cheng Y, He Y, Li W, Zhang HL, Zhou Q, Wang B, et al. Osimertinib versus comparator EGFR TKI as first-line treatment for EGFR-mutated advanced NSCLC: FLAURA China, A randomized study. *Target Oncol.* (2021) 16:165–76. doi: 10.1007/s11523-021-00794-6
5. Goss G, Tsai CM, Shepherd FA, Bazhenova L, Lee JS, Chang GC, et al. Osimertinib for pretreated EGFR Thr790Met-positive advanced non-small-cell lung cancer (AURA2): a multicentre, open-label, single-arm, phase 2 study. *Lancet Oncol.* (2016) 17:1643–52. doi: 10.1016/S1470-2045(16)30508-3
6. Roden DM. A current understanding of drug-induced QT prolongation and its implications for anticancer therapy. *Cardiovasc Res.* (2019) 115:895–903. doi: 10.1093/cvr/cvz013
7. Drew BJ, Ackerman MJ, Funk M, Gibler WB, Kligfield P, Menon V, et al. Prevention of torsade de pointes in hospital settings: a scientific statement from the American heart association and the American college of cardiology foundation. *Circulation.* (2010) 121:1047–60. doi: 10.1161/CIRCULATIONAHA.109.19270
8. Yap YG, Camm AJ. Drug induced QT prolongation and torsades de pointes. *Heart.* (2003) 89:1363–72. doi: 10.1136/heart.89.11.1363
9. Trinkley KE, Page RLII, Lien H, Yamanouye K, Tisdale JE. QT interval prolongation and the risk of torsades de pointes: essentials for clinicians. *Curr Med Res Opin.* (2013) 29:1719–26. doi: 10.1185/03007995.2013.840568
10. Al-Khatib SM, LaPointe NM, Kramer JM, Califf RM. What clinicians should know about the QT interval. *JAMA.* (2003) 289:2120–7. doi: 10.1001/jama.289.16.2120
11. Torres V, Tepper D, Flowers D, Wynn J, Lam S, Keefe D, et al. QT prolongation and the antiarrhythmic efficacy of amiodarone. *J Am Coll Cardiol.* (1986) 7:142–7. doi: 10.1016/s0735-1097(86)80272-8
12. Anand K, Ensor J, Trachtenberg B, Bernicker EH. Osimertinib-induced cardiotoxicity: a retrospective review of the FDA adverse events reporting system (FAERS). *JACC CardioOncol.* (2019) 1:172–8. doi: 10.1016/j.jaccao.2019.10.006
13. Ohe Y, Kato T, Sakai F, Kusumoto M, Endo M, Saito Y, et al. Real-world use of osimertinib for epidermal growth factor receptor T790M-positive non-small cell lung cancer in Japan. *Jpn J Clin Oncol.* (2020) 50:909–19. doi: 10.1093/jjco/hyaa067
14. Astrazeneca pharmaceuticals. *Tagrisso (Osimertinib) [Package Insert]*. Silver Spring, MD: U.S. Food and Drug Administration (2022).
15. Teisseyre A, Palko-Labuz A, Sroda-Pomianek K, Michalak K. Voltage-gated potassium channel Kv1.3 as a target in therapy of cancer. *Front Oncol.* (2019) 9:933. doi: 10.3389/fonc.2019.00933
16. Wu W, Dong MQ, Wu XG, Sun HY, Tse HF, Lau CP, et al. Human ether-à-go-go gene potassium channels are regulated by EGFR tyrosine kinase. *Biochim Biophys Acta.* (2012) 1823:282–9. doi: 10.1016/j.bbamcr.2011.10.010
17. Zhang YH, Wu W, Sun HY, Deng XL, Cheng LC, Li X, et al. Modulation of human cardiac transient outward potassium current by EGFR tyrosine kinase and Src-family kinases. *Cardiovasc Res.* (2012) 93:424–33. doi: 10.1093/cvr/cvr347
18. Zhang DY, Zhang YH, Sun HY, Lau CP, Li GR. Epidermal growth factor receptor tyrosine kinase regulates the human inward rectifier potassium K(IR)2.3 channel, stably expressed in HEK 293 cells. *Br J Pharmacol.* (2011) 164:1469–78. doi: 10.1111/j.1476-5381.2011.01424.x
19. Jin T, Hu B, Chen S, Wang Q, Dong X, Zhang Y, et al. An *in vitro* assay of hERG K^+ channel potency for a new EGFR inhibitor FHND004. *Front Pharmacol.* (2018) 9:577. doi: 10.3389/fphar.2018.00577
20. Chakraborty AD, Gonano LA, Munro ML, Smith LJ, Thekkedam C, Staudacher V, et al. Activation of RyR2 by class I kinase inhibitors. *Br J Pharmacol.* (2019) 176:773–86. doi: 10.1111/bph.14562
21. Lu Z, Wu CY, Jiang YP, Ballou LM, Clausen C, Cohen IS, et al. Suppression of phosphoinositide 3-kinase signaling and alteration of multiple ion currents in drug-induced long QT syndrome. *Sci Transl Med.* (2012) 4:131ra50. doi: 10.1126/scitranslmed.3003623
22. Bian S, Tang X, Lei W. A case of torsades de pointes induced by the third-generation EGFR-TKI, osimertinib combined with moxifloxacin. *BMC Pulm Med.* (2020) 20:181. doi: 10.1186/s12890-020-01217-4
23. Ikebe S, Amiya R, Minami S, Ihara S, Higuchi Y, Komuta K. Osimertinib-induced cardiac failure with QT prolongation and torsade de pointes in a patient with advanced pulmonary adenocarcinoma. *Int Cancer Conf J.* (2020) 10:68–71. doi: 10.1007/s13691-020-00450-2
24. Matsuura C, Kato T, Koyama K. Successful management of refractory torsades de pointes due to drug-induced long QT syndrome guided by point-of-care monitoring of ionized magnesium. *Cureus.* (2021) 13:e13939. doi: 10.7759/cureus.13939
25. Kondo M, Kisanuki M, Kokawa Y, Gohara S, Kawano O, Kagiyama S, et al. Case report: QT prolongation and abortive sudden death observed in an 85-year-old female patient with advanced lung cancer treated with tyrosine kinase inhibitor osimertinib. *Front Cardiovasc Med.* (2021) 8:655808. doi: 10.3389/fcvm.2021.655808
26. Kamle M, Mahato DK, Lee KE, Bajpai VK, Gajurel PR, Gu KS, et al. Ethnopharmacological properties and medicinal uses of *Litsea cubeba*. *Plants (Basel).* (2019) 8:150. doi: 10.3390/plants8060150

Conflict of Interest: The authors declare that the research was conducted in the absence of any commercial or financial relationships that could be construed as a potential conflict of interest.

Publisher's Note: All claims expressed in this article are solely those of the authors and do not necessarily represent those of their affiliated organizations, or those of the publisher, the editors and the reviewers. Any product that may be evaluated in this article, or claim that may be made by its manufacturer, is not guaranteed or endorsed by the publisher.

Copyright © 2022 Zhang, Wu, Wu, Lin, Zhou, Zhu, Tian and Luo. This is an open-access article distributed under the terms of the Creative Commons Attribution License (CC BY). The use, distribution or reproduction in other forums is permitted, provided the original author(s) and the copyright owner(s) are credited and that the original publication in this journal is cited, in accordance with accepted academic practice. No use, distribution or reproduction is permitted which does not comply with these terms.

frontiers | Frontiers in Cardiovascular Medicine

TYPE Case Report
PUBLISHED 19 July 2022
DOI 10.3389/fcvm.2022.908287

Check for updates

OPEN ACCESS

EDITED BY
Reto Asmis,
Wake Forest School of Medicine,
United States

REVIEWED BY
Colin McMahon,
University College Dublin, Ireland
Mohamed Rahouma,
NewYork-Presbyterian, United States

*CORRESPONDENCE
Ping Wen
13504115999@163.com

SPECIALTY SECTION
This article was submitted to Cardio-Oncology, a section of the journal Frontiers in Cardiovascular Medicine

RECEIVED 30 March 2022
ACCEPTED 23 June 2022
PUBLISHED 19 July 2022

CITATION
Liu Y, Wang N and Wen P (2022) Surgical treatment of giant right ventricular fibroma for a newborn: A case report.
Front. Cardiovasc. Med. 9:908287.
doi: 10.3389/fcvm.2022.908287

COPYRIGHT
© 2022 Liu, Wang and Wen. This is an open-access article distributed under the terms of the Creative Commons Attribution License (CC BY). The use, distribution or reproduction in other forums is permitted, provided the original author(s) and the copyright owner(s) are credited and that the original publication in this journal is cited, in accordance with accepted academic practice. No use, distribution or reproduction is permitted which does not comply with these terms.

Surgical treatment of giant right ventricular fibroma for a newborn: A case report

Yuhang Liu, Ning Wang and Ping Wen*

Dalian Women and Children's Medical Center (Group), Dalian, China

This report describes the surgical treatment of giant right ventricular fibroma in a newborn. Cardiac uhrasonography and CT showed a large mass in the right ventricle wall, which narrowed the right ventricular inflow tract. The newborn patient gradually developed symptoms such as shortness of breath, oliguria, and pericardial effusion. We performed tumor excision, but due to severe damage to the right ventricular wall and right heart failure, the patient relied on cardiopulmonary bypass. Then, we immediately restored the opening of the ductus arteriosus, enlarged the foramen ovale, and used various vasoactive drugs to ensure the smooth resuscitation of the patient. This is a kind of operation for the youngest patients. The perioperative treatment experience indicated the feasibility of excision of giant right ventricular fibroma for newborn patients.

KEYWORDS

cardiac tumor, fibroma, case report, histology, newborn

Introduction

Primary heart tumor in children is quite rare. As reported, the incidence is about 0.03–0.32%, about 25% of the cases are fibroma, followed by benign heart tumor (1, 2). Cardiac fibromas are generally solitary and large at the free end of the left ventricle, while rare at the right ventricle or atrium. They may be aggressive tumors with high mortality and generally show progressive growth, with rare spontaneous regression. Therefore, in the case of any tumor-induced symptom or expected life-threatening complication, excision is the preferred treatment method. In this case, the operation was performed for a newborn (birth weight: 3.2 Kg) 6 days after birth for improving hemodynamic disorder due to giant right ventricular fibroma.

Case summary

The study protocol was approved by the Dalian Women and Children's Medical Center (Group) Institutional Ethics Committee. The legal guardian signed informed consent for the operation and clinical record review. The patient is a test-tube baby, which means that the baby was a result of *in-vitro* fertilization. Fetal cardiac uhrasonography showed solid mass occupying the right ventricular wall and pericardial effusion; therefore, the patient was transferred to Cardiac care unit (CCU) after birth, early vital signs were stable and physical examination

showed no obvious abnormalities. Cardiac uhrasonography: A hypoechoic mass of about 36 mm×23 mm on the right ventricular wall, narrowing of the right ventricular inflow tract (Figure 1), a small amount of pericardial effusion, patent foramen ovale (2 mm), and patent ductus arteriosus (2 mm). Cardiac CT angiography (CTA): An elliptical low-density shadow of 35 mm×23 mm on the right ventricular wall, with the right ventricle compressed (Figures 2A,B). The patient gradually had shortness of breath, rapid heart rate and oliguria, and cardiac echocardiography indicated increased pericardial effusion during observation. Tumor excision and ligation of ductus arteriosus were performed on Day 6 after birth. During the operation, the tumor was found to be yellow and hard, with a clear boundary with the myocardial tissue. Part of the myocardial tissue was enlarged along the boundary between the tumor and the myocardial tissue, and the marginal myocardial tissue was cut from multiple locations for pathological examination to ensure complete tumor resection, the fibroma was completely removed (Figures 3A–C), and the right ventricular wall wound was directly sutured. After the first cardiopulmonary bypass, the patient had severe hypotension and hypoxemia, making the condition unsustainable. The cardiopulmonary bypass was arranged again; given severe damage to the right ventricular wall due to tumor excision, and right heart failure, the ductus arteriosus was opened, the foramen ovale was enlarged, and various vascular drugs such as dopamine, adrenaline and prostaglandin were given; the patient was barely out of cardiopulmonary bypass, and transferred to the ICU with delayed sternal closure. The patient's vital signs were gradually stable, the chest was closed on Day 3, the respirator was removed on Day 6, and the patient was discharged on Day 14 after an operation. At present, the heart function has returned to normal, with a satisfactory prognosis. Pathologic results confirmed the presence of fibroma (Figures 4A,B).

The patient underwent TTE, CT, and electrocardiography at the outpatient clinic every 3 months after surgery. So far the recovery has been good and the tumor has not returned.

Discussion

Although cardiac fibroma is histopathologically benign, it may still be an aggressive tumor, with high mortality

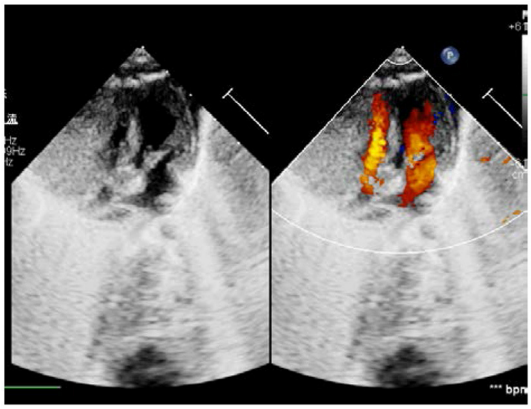

FIGURE 1
Ultrasonic Cardiogram: Neoplastic mass on the right ventricular wall and constricted right cardiac cavity.

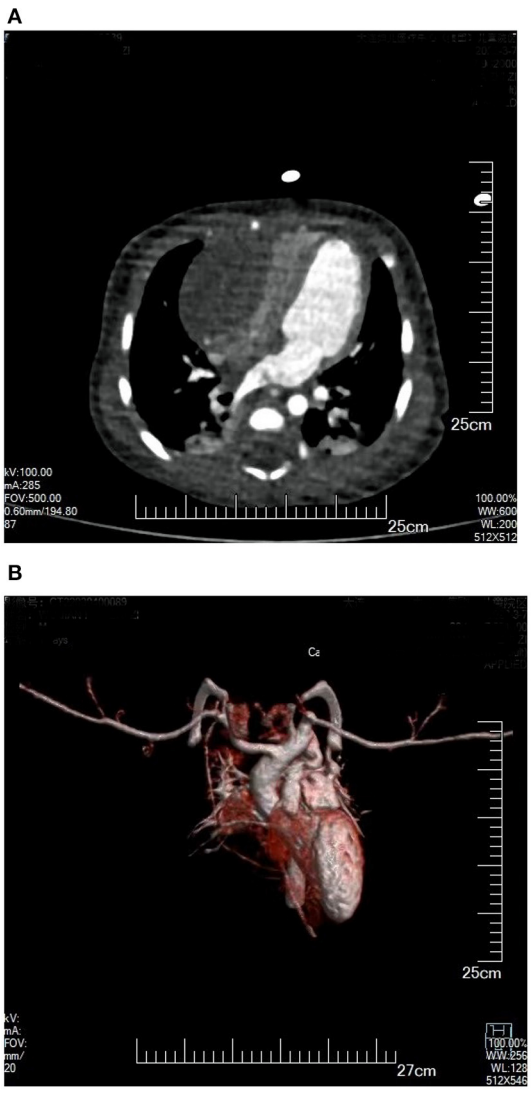

FIGURE 2
(A) Plain CT scan: Enormous space-occupying mass on a right ventricular wall, with compressed right ventricle cavity. **(B)** 3D reconstruction of cardiac blood flow: The right ventricular inflow tract was compressed by tumor, without obvious blood flow filling.

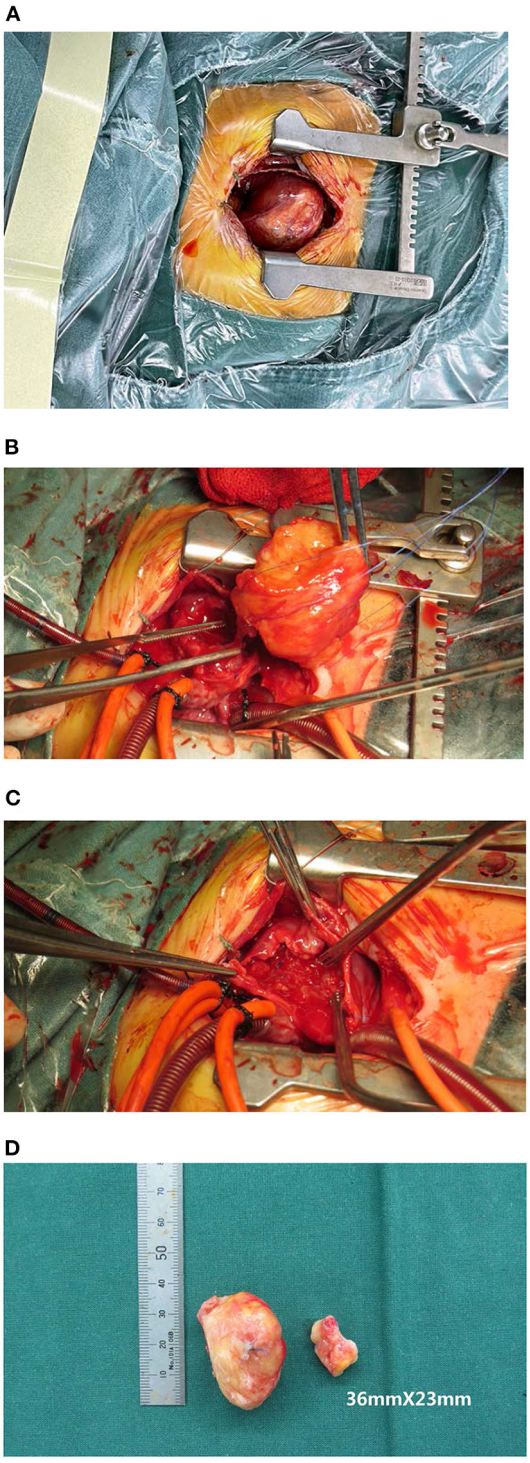

FIGURE 3
(A) Tumor appearance before an operation; **(B)** Removal of a tumor; **(C)** During operation, right ventricular wall wound after tumor removal; **(D)** Tumor specimen appearance.

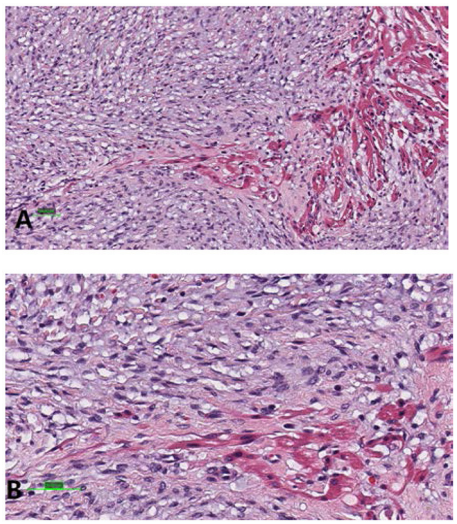

FIGURE 4
Examination under a light microscope **(A);** Magnification: 20x, and **(B)** 40x (hematoxylin and eosin staining).

(approximately 20–33%) among primary cardiac tumors. Cardiac fibroma generally has no clear boundary with cardiac muscle tissues, therefore, there would be high rates of ventricular arrhythmia (64–89%) and sudden cardiac death (10–30%) (3, 4). In addition, cardiac fibroma is generally progressive, with rare natural regression. Therefore, in the case of any tumor-induced symptom or expected life-threatening complication, excision is the preferred treatment method. In this case, we expected to perform tumor excision when the patient was older, but on Day 6 after birth, the follow-up in ICU found clinical symptoms; we had to operate during the neonatal period.

The excision of a large tumor is likely to cause insufficient myocardial quality, thus leading to severe impairment of cardiac function. A literature review indicated that most deaths were caused by the failure in withdrawal of cardiopulmonary bypass and heart failure. Some researchers adopted extracorporeal membrane oxygenation (ECMO), but the long-term use resulted in a high rate of serious complications; while some performed subtotal excision of a tumor to avoid damage to the basic structure, but there was a high recurrence rate. In this case, the patient had severe right heart failure after the operation; we enlarged the foramen ovale, to make full right-to-left shunt and ensure smooth blood circulation; maintained the ductus arteriosus open, to increase pulmonary blood supply, which ensured basic oxygen supply, made the patient successfully live without cardiopulmonary bypass after an operation, and recover without ECMO.

Conclusion

In conclusion, we performed excision of giant right ventricular fibroma for a newborn who had severe right heart failure after an operation but discharged after treatment. This is a kind of operation for the youngest patients worldwide. A large cardiac fibroma may lead to early blood flow obstruction or arrhythmias, which should be excised as soon as possible. It is possible to operate during the neonatal period.

Data availability statement

The original contributions presented in the study are included in the article/supplementary material, further inquiries can be directed to the corresponding author/s.

Ethics statement

This study protocol was approved by the Dalian Women and Children's Medical Center (Group) Institutional Ethics Committee. Written informed consent was obtained from the patient's legal guardian/next of kin for the publication of this case report. Written informed consent was obtained from the patient's legal guardian/next of kin for the publication of any potentially identifiable images or data included in this article.

Author contributions

PW designed the study and performed the experiments. YL and NW performed the experiments, analyzed the data, and wrote the manuscript. PW was major contributor in writing the manuscript. All authors contributed to the article and approved the submitted version.

Conflict of interest

The authors declare that the research was conducted in the absence of any commercial or financial relationships that could be construed as a potential conflict of interest.

Publisher's note

All claims expressed in this article are solely those of the authors and do not necessarily represent those of their affiliated organizations, or those of the publisher, the editors and the reviewers. Any product that may be evaluated in this article, or claim that may be made by its manufacturer, is not guaranteed or endorsed by the publisher.

References

1. Alice H, Irene E, Van G, Francois R, Jean-Benoit T. Large right ventricular fibroma in a 6-month-old infant. *Pediatr Cardiol.* (2012) 33:1458-1460.

2. Miyake CY, Del Nido PJ, Alexander ME, Cecchin F, Berul CI, Triedman JK, et al. Cardiac tumors and associated arrhythmias in pediatric patients, with observations on surgical therapy for ventricular tachycardia. *J Am Coll Cardiol.* (2011) 58:1903–1909.

3. Lkegami H, Lemaire A, Gowda S, Fyfe B, Ali M, Mark J, et al. Case report: surgical resection of right ventricular cardiac fibroma in an adult patient. *J Cardiothorac Surg.* (2021)16:136.

4. Torimitsu S, Nemoto T, Wakayama M, Okubo Y, Yokose T, Kitahara K, et al. Literature survey on epidemiology and pathology of cardiac fibroma. Eur J Med Res. (2012) 17:5.

frontiers | Frontiers in Cardiovascular Medicine

TYPE Case Report
PUBLISHED 28 July 2022
DOI 10.3389/fcvm.2022.941967

Check for updates

OPEN ACCESS

EDITED BY
Reto Asmis,
Wake Forest School of Medicine,
United States

REVIEWED BY
Sameh M. Said,
University of Minnesota Twin Cities,
United States
Ana Paula Nunes Alves,
Federal University of Ceara, Brazil

*CORRESPONDENCE
Huijuan Hu
59698684@qq.com

SPECIALTY SECTION
This article was submitted to Cardio-Oncology, a section of the journal Frontiers in Cardiovascular Medicine

RECEIVED 12 May 2022
ACCEPTED 27 June 2022
PUBLISHED 28 July 2022

CITATION
Li X, Lan L and Hu H (2022) Case report: Primary cardiac angiosarcoma with multiple metastases. *Front. Cardiovasc. Med.* 9:941967. doi: 10.3389/fcvm.2022.941967

COPYRIGHT
© 2022 Li, Lan and Hu. This is an open-access article distributed under the terms of the Creative Commons Attribution License (CC BY). The use, distribution or reproduction in other forums is permitted, provided the original author(s) and the copyright owner(s) are credited and that the original publication in this journal is cited, in accordance with accepted academic practice. No use, distribution or reproduction is permitted which does not comply with these terms.

Case report: Primary cardiac angiosarcoma with multiple metastases

Xuan Li, Lan Lan and Huijuan Hu*

Department of Radiology, Zhongnan Hospital of Wuhan University, Wuhan, China

This reports outlines a rare case of primary right atrial angiosarcoma with multiple metastases. Multimodality imaging and histopathology confirmed the diagnosis of primary cardiac angiosarcoma and multiple metastases. We present the details of the presentation, multimodality imaging findings, and clinical management. The patient was followed up by cardiac MRI (CMRI) 2 months after therapy, the cardiac tumor and pulmonary metastases decreased markedly. Up to now, the patient has undergone four cycles of chemotherapy and immunotherapy.

KEYWORDS

cardiac angiosarcoma, metastasis, PET/CT, MRI, treatment

Introduction

Primary cardiac angiosarcoma (PCA) is extremely rare, and accounts for 33% of all primary malignant cardiac neoplasms (1). It originates from mesenchymal angioblasts and histologically it is composed of irregularly shaped vascular channels lined by anaplastic epithelial cells with large areas of intratumoral hemorrhage and necrosis (2). Clinical manifestations are not specific and depend on their infiltration into the myocardium and adjacent structures, as well as the extent of metastases (3). Patients usually visit a hospital because of chest pain, arrhythmia, peripheral edema, dyspnea, orthopnea, congestive heart failure, and pericardial tamponade (4). The most common location is the right atrium (RA). The prognosis of PCA is considerably poor, with a median survival of 14 months, reduced to 6 months in metastatic disease (5).

Case presentation

A 28-year-old man was admitted to the orthopedics department on 13 January 2022 with low back pain for one month. On admission, the patient had neither previous cardiovascular antecedents nor family history. He also denied medication use. The patient's body temperature was normal, 36.6°C with a blood pressure of 102/68 mmHg, and a heart rate of 96 bpm. The patient body mass index was 20.2.

The biochemical investigation showed no alteration in the following serum levels: total bilirubin, alkaline phosphatase, urea, creatinine, potassium, glucose, and sodium. Hemoglobin level was 144 g/l, hematocrit level was 43.2%, and serum leukocyte and platelet levels were 9.2×10^9/L and 165×10^9/L, respectively.

Physical examination revealed pain in the sternocostal and lumbosacral region, other body systems showed no abnormalities. Electrocardiography was normal.

Radiological investigations

A CT examination from the chest to the pelvis was performed, which revealed a right atrial mass, multiple small ground-glass pulmonary nodules, and bone destructions (Figures 1A–D). Transthoracic echocardiography (TTE) showed an ill-defined hypoechoic mass of approximately 3.8 cm × 2.3 cm, attached to the lateral wall of the right atrium. Cardiac MRI (CMRI) exhibited a right atrial tumor and multiple pulmonary lesions. On steady-state free precession (SSFP) cine imaging planned in the four chambers, the tumor showed isointense (Figure 2A). On T2-short tau inversion recovery (STIR) sequence images, the tumor displayed high-signal intensity (Figure 2B). On enhanced MRI, the tumor showed arterial heterogeneous enhancement and progressive but incomplete enhancement in the delayed phase (dynamic acquisition) (Figures 2C,D). The patient was referred for 18F-fluorodeoxyglucose (FDG) positron emission tomography-CT (PET-CT) for further characterization of the cardiac mass and systemic evaluation. PET-CT images demonstrated that the right atrial tumor had intensely increased FDG uptake (standardized uptake value, SUVmax, 8.4) with signs of pulmonary and bony metastases (Figure 3). These preoperative images characterized the mass as highly suspicious for a malignant cardiac tumor with multiple metastases.

Management

To get a definitive diagnosis, the patient underwent the sacral biopsy, but the result was a benign vascularized lesion, which was in contradiction with the presentations on images, so the left lower lung nodule resection was performed. The histopathology examination and immunohistochemical staining supported the diagnosis of angiosarcoma positive for CD31, CD34, ETS-related gene (ERG), and Ki67 (LI: 60%) (Figures 4A,B). Combined with multimodality images, the final diagnosis was primary right atrial angiosarcoma with multiple metastases. The case was discussed in a multidisciplinary heart team meeting. Because of the presence of widespread metastases, curative treatment was considered to be impossible. The clinician suggested palliative chemotherapy and immunotherapy, and the patient agreed with the suggestion. Thus, the patient underwent chemotherapy and immunotherapy with epirubicin (10 mg, QD), ifosfamide (.5 g, QD), and

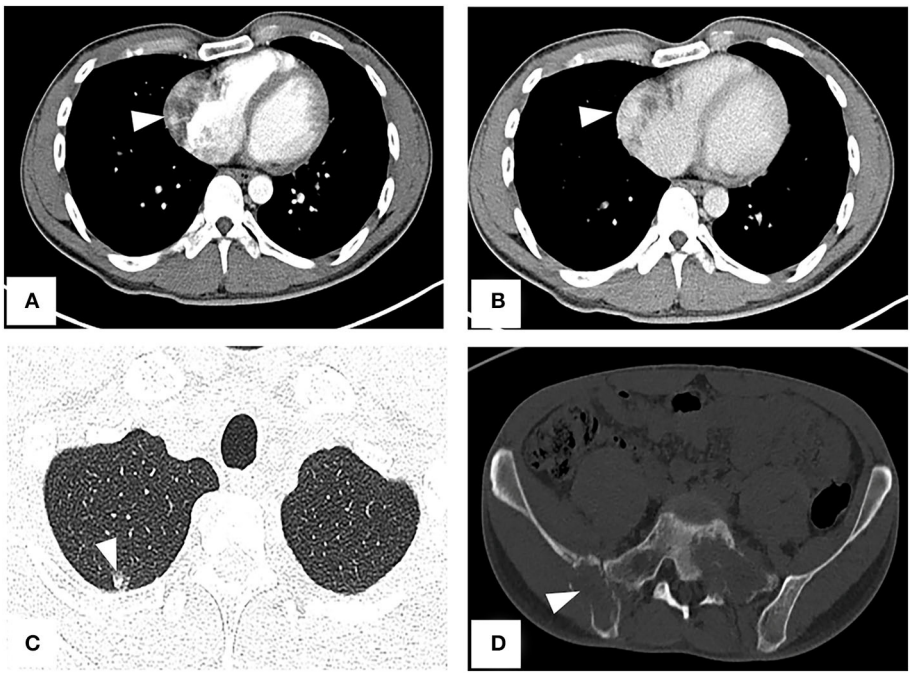

FIGURE 1
CT from chest to pelvis with enhancement shows right atrial tumor, small ground-glass pulmonary nodule, and bone destructions. **(A)** Arterial phase imaging reveals a filling defect in the right atrium (arrowhead). **(B)** Venous phase imaging shows the tumor inhomogeneously enhancing (arrowhead). **(C)** A lung window image shows a metastatic nodule in the upper right lung. **(D)** Bone destructions in the right ilium and sacrum.

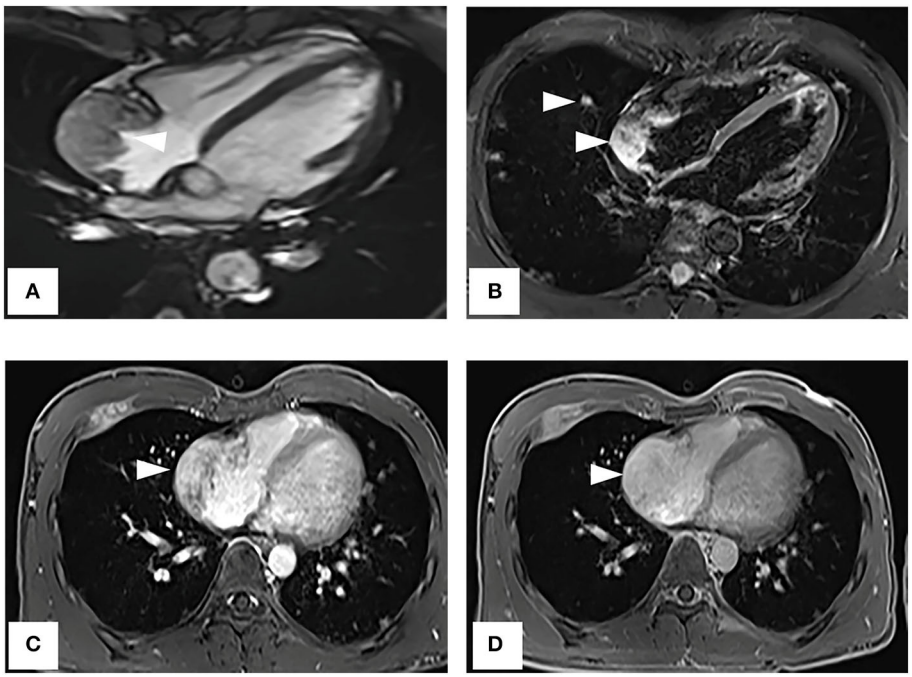

FIGURE 2
Cardiac magnetic resonance imaging. **(A)** On SSFP cine imaging planned in the four chambers, the tumor shows isointense (arrowhead). **(B)** On T2-short tau inversion recovery sequence images, the tumor displays high-signal intensity (arrowhead). **(C,D)** On enhanced MR imaging, the tumor shows arterial heterogeneous enhancement and progressive but incomplete enhancement in the delayed phase (dynamic acquisition).

pembrolizumab (100 mg, QD). Simultaneously the patient underwent palliative radiotherapy (20 Gy/5f) at the sites of the 10th thoracic vertebra. Up to now, the patient has undergone four cycles of treatment.

Follow-up period

Repeat CMRI and chest CT showed significant regression of the tumor and pulmonary metastases (Figures 5A,B). Now, the patient continues the chemotherapy and immunotherapy.

Discussion

PCA is one of the most common primary cardiac malignancies (3), originated preferentially in the right atrium (approximately 90%), while <5% occur in the left atrium or ventricles (6). PCA commonly affects male patients those 30–40 years of age as in this case (7). The clinical symptoms are non-specific, depending on location and size, such as chest pain, chest tightness, shortness of breath, arrhythmia, pericar-dial effusion, or right heart failure (8, 9). The overall prognosis is extremely poor due to the aggressive and frequent presence of metastases at the time of diagnosis (3, 8–10).

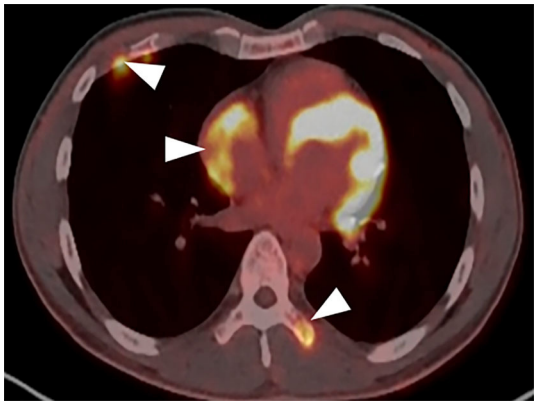

FIGURE 3
PET-CT demonstrates the tumor intensely increased FDG uptake with bony metastases (arrowhead).

Echocardiography has become an initial imaging technique because of its wide availability and high sensitivity, non-invasiveness, and cost-effectiveness (8, 11, 12), but it has some limitations, such as operator dependence, and the views may be limited in some patients (13).

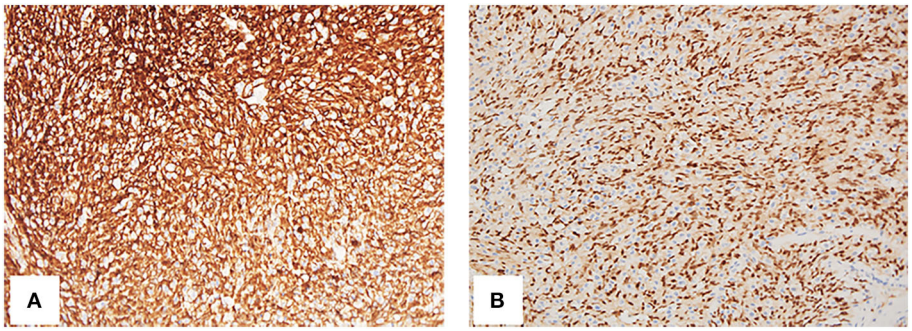

FIGURE 4
Histology of resection from the left lower lung nodule. The spindle cells are CD34 (**A**, 200×) and ERG (ETS-related gene) (**B**, 200×) positive.

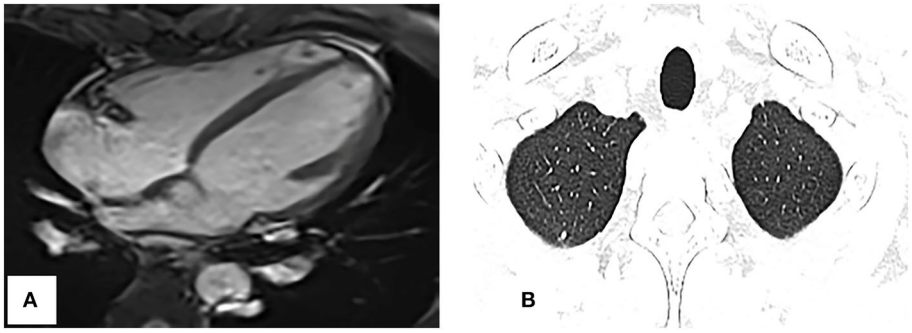

FIGURE 5
Repeat cardiac magnetic resonance imaging and thoracic CT. **(A)** SSFP cine imaging planned in the four chambers shows the tumor markedly reduced. **(B)** Thoracic CT shows the pulmonary nodules obviously decreased too, compared with Figure 1C.

There is more efficiency in using CT for tissue characterization and systemic metastases, especially in the lungs (3). PCA often presents as homogeneous or inhomogeneous density on unenhanced CT scans and heterogeneous centripetal enhancement on enhanced images (14).

Cardiac MRI is considered to be the most sophisticated imaging method to display the cardiac tumor size, location, and signal characteristics (15). T1-weighted images show tumor as predominantly isointense to the myocardium and high signal on T2-weighted images. Late gadolinium-enhanced (LGE) is avid and may predominate along prominent vascular channels to give a characteristic "sunray" pattern (2). In our case, CMRI clearly showed the tumor-infiltrating the free wall of the RA with obvious heterogeneous enhancement indicative of malignancy.

Positron emission tomography/CT has advantages in non-invasively characterizing cardiac tumors and disease staging, scarce case reports have described the use of FDG PET-CT in differentiating the benign and malignant mass, metastatic workup, preoperative staging, and assessment of response to treatment in primary cardiac angiosarcomas (16–19). Rahbar et al. (20) in their study of various cardiac tumors proposed that malignancy was determined with a sensitivity of 100% and specificity of 86% (accuracy, 96%) after a cutoff with high sensitivity (SUVmax of 3.5) was chosen to avoid false-negatives. In our case, the SUV max of the tumor is 8.4, which is highly suspicious of malignancy.

Although multimodality images can help diagnosis, definitive diagnosis and classification depend on the pathological examination, which is the gold standard based on immunohistochemistry as evidence for chemotherapy and radiotherapy. Immunohistochemically, angiosarcomas are usually positive for vimentin, CD31, CD34, and factor VIII-related antigens (21). ERG was the most sensitive vascular marker, with diffusely reactive in all cases of cardiac angiosarcoma and its superior sensitivity to CD31 and CD34 (22). In our patient, CD31, CD34, and ERG were positive, which supported the diagnosis of angiosarcoma.

The most common organ for metastasis of primary angiosarcoma is the lungs and bone, occasionally in the liver and spleen, and extremely rarely in the brain (14, 23). Pulmonary metastases manifested different sized multiple hemorrhagic nodules (24), which was a characteristic CT

appearance, consisting of a central area of soft-tissue attenuation surrounded by a halo of ground-glass attenuation. This halo sign was previously established as a common finding correlated with pulmonary angiosarcoma, and it also helps in detecting metastatic pulmonary lesions (23). In this report, this case had typical halo signs on thoracic CT.

Due to the rarity of these tumors, the optimal management strategy is still argued. Current treatment options include surgery, radiotherapy, and chemotherapy. Surgical resection remains the gold standard for the treatment of primary malignant cardiac tumors. The limits of surgical resection have been related to the degree of extensive involvement of nearby structures and other cardiac chambers (25). In addition, targeted medicines and immunotherapy have been studied as promising treatments for angiosarcoma (26). Although the benefits of adjuvant therapy and other strategies are still unknown, there is a tendency to use more aggressive treatment for younger patients (25). Because of widespread metastases, our patient received adjuvant immunotherapy and chemotherapy, which has a good effect. Close follow-up is mandatory because of the poor prognosis.

There were limitations in this study. First, the patient did not conduct surgical resection, and no pathology of the tumor was obtained. We speculated the diagnosis according to histopathologic findings of lower left lung and multimodality images. Second, at present adjuvant immunotherapy and chemotherapy is very effective, but we should follow up closely to observe the future effect.

Conclusion

Evaluation and diagnosis of PCA can be complex and should include multimodality imaging, multidisciplinary discussion is important. The case demonstrates the typical presentation of primary cardiac angiosarcoma and its associated features on multimodality imaging. More experience is needed to better understand the imaging characteristics of angiosarcoma.

Data availability statement

The original contributions presented in the study are included in the article/supplementary material, further inquiries can be directed to the corresponding author.

Ethics statement

The studies involving human participants were reviewed and approved by Medical Ethics Committee of Zhongnan Hospital of Wuhan University. The informed consent was waived.

Author contributions

XL contributed to MRI scanning of the patient and collecting clinical data. HH contributed to editing, revising, and approving the manuscript. LL contributed to interpreting the data. XL, HH, and LL contributed to the writing and revision of the manuscript. All authors have read and approved the final manuscript.

Conflict of interest

The authors declare that the research was conducted in the absence of any commercial or financial relationships that could be construed as a potential conflict of interest.

Publisher's note

All claims expressed in this article are solely those of the authors and do not necessarily represent those of their affiliated organizations, or those of the publisher, the editors and the reviewers. Any product that may be evaluated in this article, or claim that may be made by its manufacturer, is not guaranteed or endorsed by the publisher.

References

1. Liu CW, Zhao YX, Yin ZY. H T, Ren JH, Wei JL, et al. Right atrial epithelioid angiosarcoma with multiple pulmonary metastasis confirmed by multimodality imaging-guided pulmonary biopsy: a case report and literature review. *Medicine (Baltimore).* (2018) 97:e11588. doi: 10.1097/MD.0000000000011588

2. Hoey ET, Shahid M, Ganeshan A, Baijal S, Simpson H, Watkin RW, et al. Assessment of cardiac tumours: part 2, spectrum of appearances of histologically malignant lesions and tumour mimics. *Quant Imaging Med Surg.* (2014) 4:489–97. doi: 10.3978/j.issn.2223-4292.2014.11.25

3. Patel SD, Peterson A, Bartczak A, Lee S, Chojnowski S, Gajewski P, et al. Primary cardiac angiosarco- ma-A review. *Med Sci Monit.* (2014) 20:103–9. doi: 10.12659/MSM.889875

4. Chen TW, Loong HH, Srikanthan A, Zer A, Barua R, Butany J, et al. Primary cardiac sarcomas: a multi-national retrospective review. *Cancer Med.* (2019) 8:104–10. doi: 10.1002/cam4.1897

5. Randhawa JS, Budd GT. Randhawa M, Ahluwalia M, Jia X, Daw H, et al. Primary cardiac sarcoma: 25-year cleveland clinic experience. *Am J Clin Oncol.* (2016) 39:593–9. doi: 10.1097/COC.0000000000000106

6. Masaoki Saito T. Miku Oda, Toshinori Minamishima, Ken Kongoji, Aya Isomura, et al. Rapidly progressive respiratory failure with multiple halo signs on computed tomography in a patient with primary cardiac angiosarcoma derived from the right atrium: a case report. *BMC Pulm Med.* (2020) 20:321. doi: 10.1186/s12890-020-01366-6

7. Xu C, Sun W, Fang L, He L, Yang F, Zhang J, et al. The value of multimodal imaging in the diagnosis of primary cardiac angiosarcoma. *Echocardiography*. (2021) 38:1474–7. doi: 10.1111/echo.15156

8. Maleszewski JJ, Bois MC, Bois JP, Young PM, Stulak JM, Klarich KW. Neoplasia and the heart: pathological review of effects with clinical and radiological correlation. *J Am Coll Cardiol*. (2018) 72:202–27. doi: 10.1016/j.jacc.2018.05.026

9. Chen Y, Li Y, Zhang N, Shang J, Li X, Liu J, et al. Clinical and imaging features of primary cardiac angiosarcoma. *Diagnostics (Basel)*. (2020) 10:776. doi: 10.3390/diagnostics10100776

10. Jagdish Butany Vi. Ather Naseemuddin, Girish M Nair, Charles Catton, Teri Yau. Cardiac tumours: diagnosis and management. *Lancet Oncol*. (2005) 6:219–28. doi: 10.1016/S1470-2045(05)70093-0

11. Inês Gonçalves C. Catarina Vieira, Diana Freitas, Luisa Pinto. Primary cardiac angiosarcoma: a rare and fatal diagnosis. *Cureus*. (2021) 13:e20816. doi: 10.7759/cureus.20816

12. Capotosto L, Elena G, Massoni F, De Sio S, Carnevale A, Ricci S, et al. Cardiac tumors: echocardiographic diagnosis and forensic correlations. *Am J Forensic Med Pathol*. (2016) 37:306–16. doi: 10.1097/PAF.0000000000000271

13. Chen YC. Localization of angiosarcoma by perioperative transesophageal echocardiography. *Int JCardiovasc Imaging*. (2017) 33:1749–51. doi: 10.1007/s10554-017-1183-2

14. Ji GM, Li SQ. Huang Y, Wang RN, et al. Clinical and imaging manifestations of primarycardiac angiosarcoma. *BMC Med Imaging*. (2019) 19:16. doi: 10.1186/s12880-019-0318-4

15. Nijjar PS, Masri SC, Tamene A, Kassahun H, Liao K, Valeti U. Benefits and limitations of multimodality imaging in the diagnosis of a primary cardiac lymphoma. *Tex Heart Inst J*. (2014) 41:657–9. doi: 10.14503/THIJ-13-3595

16. Bilski M, Kaminski G, Dziuk M. Metabolic activity assessment of cardiac angiosarcoma by 18FDG PET-CT. *Nucl Med Rev Cent East Eur*. (2012)15:83-4. doi: 10.5603/NMR.2012.0015

17. Manohar K, Kashyap R, Bhattacharya A, Mittal B R. Initial staging and treatment monitoring of right atrial sarcoma with F-18 fluorodeoxyglucose positron emission tomography/computed tomography. *Indian J Nucl Med*. (2013) 28:188–9. doi: 10.4103/0972-3919.119525

18. Hod N, Shalev A, Levin D, Anconina R, Ezroh Kazap D. Lantsberg S. FDG PET/CT of cardiac angiosarcoma with pulmonary metastases. *Clin Nucl Med*. (2018) 43:744–6. doi: 10.1097/RLU.0000000000002215

19. Jain A, Simon S, Elangovan I. (18)F- fluoro-deoxyglucose position emission tomography-computed tomography in initial assessment and diagnosis of right atrial angiosarcoma with widespread visceral metastases: a rare case report and review of the literature. *Indian J Nucl Med*. (2015) 30:51–4. doi: 10.4103/0972-3919.147541

20. Rahbar K, Seifarth H, Schäfers M, Stegger L, Hoffmeier A, Spieker T, et al. Differentiation of malignant and benign cardiac tumors using 18F-FDG PET/CT. *J Nucl Med*. (2012) 53:856–63. doi: 10.2967/jnumed.111.095364

21. Clarissa Pessoa Fernandes F. Fábio Wildson Gurgel Costa, Régia Maria do Socorro Vidal Patrocínio, Mário Rogério Lima Mota, Ana Paula Negreiros Nunes Alves, et al. Clinical, histological, and immunohistochemical features of a mandibular metastasis from a primary cardiac angiosarcoma. *Oral Surg Oral Med Oral Pathol Oral Radiol*. (2013) 116:e121–7. doi: 10.1016/j.oooo.2012.12.017

22. Leduc C, Jenkins SM, Sukov WR, Rustin JG, Maleszewski JJ. Cardiac angiosarcoma: histopathologic, immunohistochemical, and cytogenetic analysis of 10 cases. *Hum Pathol*. (2017) 60:199–207. doi: 10.1016/j.humpath.2016.10.014

23. Yogi A, Miyara T, Ogawa K, Iraha S, Matori S, Haranaga S, et al. Pulmonary metastases from angiosarcoma: a spectrum of CT findings. *Acta Radiol*. (2016) 57:41–6. doi: 10.1177/0284185115571789

24. Tateishi U, Hasegawa T, Kusumoto M, Yamazaki N, Iinuma G, Muramatsu Y, et al. Metastatic angiosarcoma of the lung: spectrum of CT findings. *AJR Am J Roentgenol*. (2003) 180:1671–4. doi: 10.2214/ajr.180.6.1801671

25. Pietras CM, Spittell PC. Nuttall GA, Eleid MF, Said SM. Pulmonary venous obstruction from a large left atrial sarcoma: resection combined with mitral valve bypass. *Ann Thorac Surg*. (2016) 102:e237–9. doi: 10.1016/j.athoracsur.2016.02.041

26. Cao J, Wang JL, He CY, Fang MY. Angiosarcoma: a review of diagnosis and current treatment. *Am J Cancer Res*. (2019) 9:2303–13.

frontiers | Frontiers in Cardiovascular Medicine

TYPE Case Report
PUBLISHED 03 August 2022
DOI 10.3389/fcvm.2022.908567

Check for updates

OPEN ACCESS

EDITED BY
Carlo Gabriele Tocchetti,
University of Naples Federico II, Italy

REVIEWED BY
Goverdhan Puri,
Post Graduate Institute of Medical Education and Research (PGIMER), India
Gelsomina Mansueto,
University of Naples Federico II, Italy
Randolph Wong,
Prince of Wales Hospital, China

*CORRESPONDENCE
Liang Ma
ml1402@zju.edu.cn

SPECIALTY SECTION
This article was submitted to Cardio-Oncology, a section of the journal Frontiers in Cardiovascular Medicine

RECEIVED 30 March 2022
ACCEPTED 12 July 2022
PUBLISHED 03 August 2022

CITATION
Teng P, Hu P, Yuan S and Ma L (2022) Case report: Minimally invasive excision of multifocal cardiac papillary fibroelastomas involving right atrium and aortic valve.
Front. Cardiovasc. Med. 9:908567.
doi: 10.3389/fcvm.2022.908567

COPYRIGHT
© 2022 Teng, Hu, Yuan and Ma. This is an open-access article distributed under the terms of the Creative Commons Attribution License (CC BY). The use, distribution or reproduction in other forums is permitted, provided the original author(s) and the copyright owner(s) are credited and that the original publication in this journal is cited, in accordance with accepted academic practice. No use, distribution or reproduction is permitted which does not comply with these terms.

Case report: Minimally invasive excision of multifocal cardiac papillary fibroelastomas involving right atrium and aortic valve

Peng Teng[1], Peng Hu[1], Shuai Yuan[2] and Liang Ma[1]*

[1]Department of Cardiovascular Surgery, The First Affiliated Hospital, College of Medicine, Zhejiang University, Hangzhou, China, [2]Department of Echocardiography and Vascular Ultrasound Center, The First Affiliated Hospital, College of Medicine, Zhejiang University, Hangzhou, China

Background: Cardiac papillary fibroelastomas (CPFs) are rare benign cardiac tumors most commonly found on left-sided cardiac valves. Right atrial CPFs are extremely rare, accounting for only 2% of all CPFs. Median sternotomy is a typical approach for surgical excision of CPFs in most cases. Herein, we report an extremely rare case of multifocal CPFs involving the right atrium and aortic valve that were surgically excised *via* minimally invasive right anterolateral thoracotomy.

Case Summary: A 59-year-old Chinese man was admitted because of an incidental finding of a right atrial mass on transthoracic echocardiography during a routine check-up. The mass was initially diagnosed as a myxoma, and the patient was scheduled for minimally invasive excision *via* right anterolateral thoracotomy. An additional mass on the non-coronary cusp of the aortic valve was identified using intraoperative transesophageal echocardiography. The patient still underwent complete tumor excision *via* right anterolateral thoracotomy. Both neoplasms were pathologically diagnosed as CPFs.

Conclusions: This case highlights the need for a comprehensive cardiac evaluation of cardiac tumors because CPFs can manifest as multifocal lesions. Moreover, minimally invasive surgery is highly feasible as the CPF can be easily excised, and the valve can usually be preserved.

KEYWORDS

cardiac papillary fibroelastoma, minimally invasive, multifocal, right atrium, aortic valve, cardiac tumor

Introduction

Cardiac papillary fibroelastomas (CPFs) are rare and considered one of the most common benign cardiac tumors (1). The incidence of CPFs is approximately 1,380/100 million individuals and constitutes 11.5% of all primary cardiac tumor (2). Although CPFs may arise on any endocardium-lined surface, more than three-quarters of CPFs occur on valvular surfaces, with left-sided valves being more commonly affected than those on the right. Right atrial CPFs are extremely rare and account for only 2% of all

CPFs (3). Multifocal CPFs with simultaneous involvement of the right atrium (RA) and the aortic valve (AV) have seldom been reported. Moreover, most cases of multifocal CPFs were treated with surgical excision *via* a median sternotomy. Herein, we present a case of minimally invasive excision of multifocal CPFs involving the RA and the AV.

Case presentation

History of presentation and investigation

A 59-year-old Chinese male was admitted because of incidental findings of a right atrial mass on transthoracic echocardiography (TTE) during a routine check-up. No medical history has been reported to date. The laboratory results and physical examination findings were unremarkable. TTE revealed an irregular hyperechoic mobile mass (1.2 × 0.9 cm in size) with a stalk arising from the RA adjacent to the aortic root (Figure 1A). TTE also revealed thickened leaflets of AV, which was considered to be a degenerative change. No wall motion or other structural valve abnormalities were reported. Coronary computed tomography angiography (CTA) demonstrated no obvious stenosis of the coronary artery.

Diagnosis

The right atrial mass was initially diagnosed as myxoma or papillary fibroelastoma.

Management

The patient was scheduled for minimally invasive excision of the right atrial mass *via* right anterolateral thoracotomy. Intraoperative transesophageal echocardiography (TEE) after anesthesia detected an additional mobile mass (1.3 × 0.8 cm in size) on the ventricular side of the non-coronary cusp of the AV (Figure 1B). Both right atrial and aortic valvular masses were considered CPFs due to their stippled edge and good mobility with stalks. Considering the high probability of AV preservation in cases of primary surgical indication for CPF based on our experience, we proceeded with the surgery *via* right anterolateral thoracotomy, without conversion to media sternotomy. Cardiopulmonary bypass was established through the femoral artery and vein cannulation. A 5 cm right mini-thoracotomy incision was made in the fourth interspace, which started medially to the anterior axillary line. Cardioplegia was achieved by antegrade perfusion of cold blood cardioplegia solution through a Y-shaped cannula. After transverse aortotomy, the tumor was located on the ventricular side of the noncoronary cusp of the AV (Figure 2A) and was easily excised by shaving its stalk. AV leaflet inspection confirmed their anatomical preservation. The aorta was then closed, and the heart resumed beating automatically. Then the tip of the cannula in the inferior vena cava was laid in the right atrium, 1 cm above the inferior atriocaval junction. No caval veins were snared and after transverse right atriotomy, a vacuum-assisted venous drainage controller was used to maintained the negative pressure ranging from−20 to−30 mmHg, or according to the blood level in the right atrium. The right atrial tumor (Figure 2B) was successfully excised on a beating heart by shaving its stalk (Supplementary Video 1). TEE revealed trivial AV regurgitation and complete excision of the masses. As only still echo images were regular archived, we retrospectively found abnormal thickness of non-coronary cusp of AV on coronary CTA, representing the CPF which was misdiagnosed as degenerative thickening of leaflet (Figure 1C). The postoperative course was uneventful and the patient was discharged on postoperative day six. After a 2-year follow-up, TTE showed no signs of CPF recurrence.

Abbreviations: CPF, cardiac papillary fibroelastoma; TTE, transthoracic echocardiography; CTA, computed tomographic angiography; TEE, transesophageal echocardiography; RA, right atrium; AV, aortic valve.

Macroscopic observation and histopathological examination

When immersed in water, both tumors showed "the sea anemone" phenomenon, which strongly suggested the presence of CPFs (Figure 3A). Both tumors were fixed with formalin, embedded with paraffin and stained with hematoxylin and eosin. Histopathological examination demonstrated bundles of papillary projections with a collagenous core surrounded by a single layer of endothelium, and a final diagnosis of multifocal CPFs was made (Figures 3B,C).

Discussion

Our study reported an extremely rare case of multifocal CPFs involving the RA and AV that was successfully treated with complete tumor excision *via* right anterolateral thoracotomy, of which the surgical approach has seldom been reported. This case highlights two important points: (1) CPFs could present as multifocal involvement and should be comprehensively evaluated by multimodality imaging, and (2) a minimally invasive approach is suitable for surgical excision of multifocal CPFs based on the fact that the valve can usually be preserved when tumor excision is the primary surgical indication (4).

Despite CPF being one of the top three common primary benign cardiac tumors, the other two being myxomas and lipomas (2, 5) quite a few scholars consider it to be the most

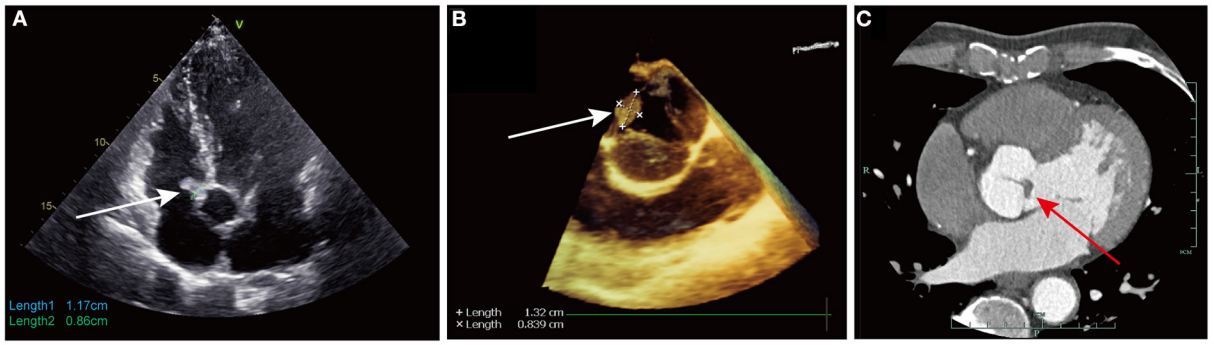

FIGURE 1
(A) Transthoracic echocardiography showed an irregular hyperechoic mobile mass (1.2 × 0.9 cm in size, white arrow) with a stalk arising from the right atrium adjacent to the aortic root; **(B)** Transesophageal echocardiography showed an additional mobile mass (1.3 × 0.8 cm in size, white arrow) on the ventricular side of the non-coronary cusp of aortic valve; **(C)** Coronary computed tomography angiography showed abnormal thickness of non-coronary cusp of aortic valve, which represented the cardiac papillary fibroelastoma (red arrow) on the aortic valve.

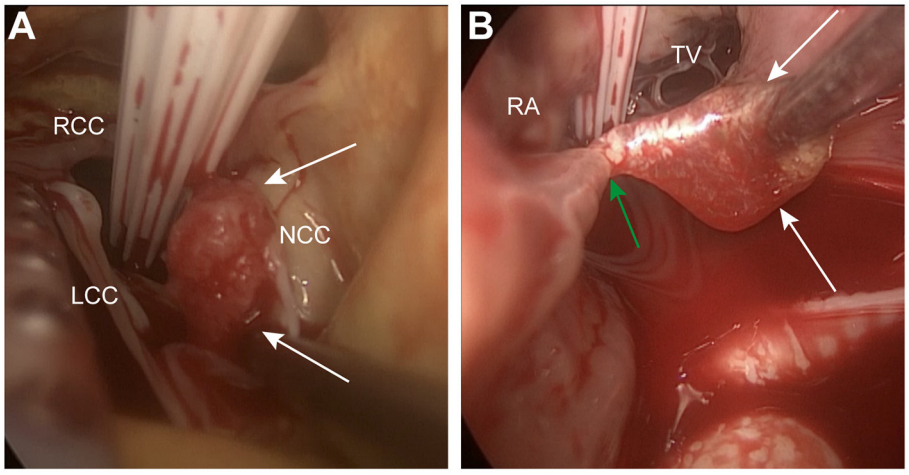

FIGURE 2
(A) CPF was located on the ventricular side of non-coronary cusp of aortic valve (white arrows); **(B)** CPF (white arrows) was located in the RA adjacent to aortic root with a stalk (green arrow). CPF, cardiac papillary fibroelastoma; NCC, non-coronary cusp; RCC, right-coronary cusp; LCC, left-coronary cusp; RA, right atrium; TV, tricuspid valve.

common (6). Moreover, it is the most common primary cardiac valvular tumor, whereas non-valvular involvement is infrequent. Right-sided CPFs only account for ∼10% of cases, and the tricuspid valve is the most common right-sided location (7). Right atrial CPFs are rare, accounting for only 2% of all CPFs, which makes our case of multifocal CPFs involving the RA and AV extremely rare.

CPFs are commonly found incidentally in asymptomatic individuals (8). When symptoms develop, the most common are systemic (9) or pulmonary embolization (10), followed by coronary ostium obstruction (5), heart failure, and even sudden cardiac death due to the detachment of tumor fragments or thrombi related to the tumor. Right-sided CPFs tend to be larger at presentation than left-sided CPFs (4), possibly due to their tendency to present late as they have fewer clinical implications. Typical CPF exhibit a "frond-like" appearance because of its papillary projections arising from the fibrous stalk attached to the endocardium, which makes it look like a sea anemone when immersed in water. On TEE, the borders may appear slightly stippled or shimmering caused by vibration at the tumor-blood interface because of its finger-like projections. TEE is more sensitive than TTE because of the typical small size of CPFs, and about one-quarter of patients with CPFs might be detected on TEE but not TTE (4), similar to our case where the CPF on the AV was misdiagnosed by preoperative TTE.

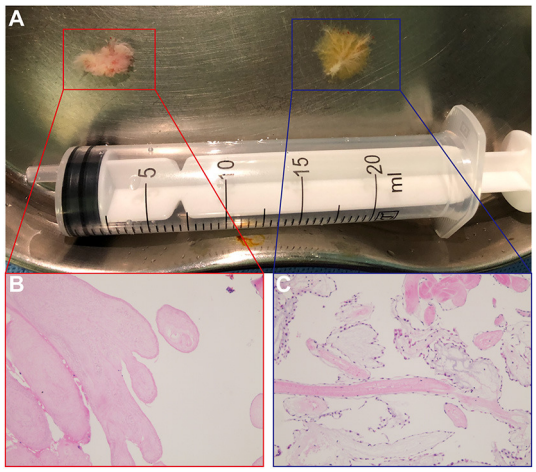

FIGURE 3
(A) Macroscopic inspection of the tumors when immersed in water showed a "sea anemone" phenomenon. On the left is the tumor on the aortic valve, and on the right is the tumor in the right atrium. **(B,C)** Histopathologic examination of the tumors [panel **(B)** represents the tumor on the aortic valve and panel **(C)** represents the tumor in the right atrium] with hematoxylin-eosin staining (100×) confirmed the diagnosis of cardiac papillary fibroelastomas.

Histologically, CPFs are composed of thickened, broad papillae of varying lengths, lined by endothelial cells, with avascular connective tissue stroma, myxoid, fibrosis or collagen. Immunohistochemically, the cells covering the surface are positive for factor VIII-related antigen and CD 34, in keeping with their presumed vascular endothelial origin, but also the S-100 protein may be positive (11).

Surgical indications for CPFs remain controversial. The mainstream view recommends surgical excision in patients who are good surgical candidates with a large (≥1 cm) or mobile left-sided CPF (12). Asymptomatic right-sided CPFs can be managed more conservatively, unless they are associated with embolization. Surgical excision *via* median sternotomy is considered the standard surgical approach, particularly in cases of multifocal CPFs (13). However, based on the experience of our center and other studies (4), valves are usually spared when tumor excision of the CPFs is the primary surgical indication. Therefore, we highlight the importance and feasibility of minimally invasive excision *via* right anterolateral thoracotomy, as most patients with CPFs are asymptomatic and surgical damage should be minimized. In our case, both CPFs were easily excised by simple shave excision, and valvular function was unaffected. However, long-term antiplatelet treatment is recommended for patients who are not candidates for surgery or who refuse surgery.

Conclusions

CPFs can present as multifocal lesions and should be comprehensively evaluated using multimodal imaging. TEE is more sensitive than TTE for cardiac mass detection. As valves are usually spared when CPF excision is the primary surgical indication, a minimally invasive approach *via* right anterolateral thoracotomy is recommended to minimize surgical damage, especially in asymptomatic patients.

Data availability statement

The original contributions presented in the study are included in the article/Supplementary material, further inquiries can be directed to the corresponding author.

Ethics statement

Written informed consent was obtained from the participant/s for the publication of this case report. Written informed consent was obtained from the individual(s) for the publication of any potentially identifiable images or data included in this article.

Author contributions

LM: conceptualization. PT and PH: data collection and analysis. PT: writing. SY: writing, review, and editing. All authors have approved the manuscript for publication.

Funding

This study was funded by the Key Research and Development Program of Zhejiang Province, China (Project Number: 2019C03008) and the Natural Science Foundation of Zhejiang Province, China (Project Number: LQ22H020005).

Conflict of interest

The authors declare that the research was conducted in the absence of any commercial or financial relationships that could be construed as a potential conflict of interest.

Publisher's note

All claims expressed in this article are solely those of the authors and do not necessarily represent those of their affiliated organizations, or those of the publisher, the editors and the reviewers. Any product that may be evaluated in this article, or claim that may be made by its manufacturer, is not guaranteed or endorsed by the publisher.

Supplementary material

The Supplementary Material for this article can be found online at: https://www.frontiersin.org/articles/10.3389/fcvm.2022.908567/full#supplementary-material

SUPPLEMENTARY VIDEO 1
The video of minimally invasive tumor excision *via* right anterolateral thoracotomy recorded by endoscope.

References

1. Jallad N, Parikh R, Daoko J, Albareqdar E, Al-Dehneh A, Goldstein J, et al. Concurrent primary cardiac tumors of differing histology and origin: case report with literature review. *Tex Heart Inst J.* (2009) 36:591–3.

2. Tyebally S, Chen D, Bhattacharyya S, Mughrabi A, Hussain Z, Manisty C, et al. Cardiac tumors: JACC cardiooncology state-of-the-art review. *JACC CardioOncol.* (2020) 2:293–311. doi: 10.1016/j.jaccao.2020.05.009

3. Gowda RM, Khan IA, Nair CK, Mehta NJ, Vasavada BC, Sacchi TJ. Cardiac papillary fibroelastoma: a comprehensive analysis of 725 cases. *Am Heart J.* (2003) 146:404–10. doi: 10.1016/S0002-8703(03)00249-7

4. Tamin SS, Maleszewski JJ, Scott CG, Khan SK, Edwards WD, Bruce CJ, et al. Prognostic and bioepidemiologic implications of papillary fibroelastomas. *J Am Coll Cardiol.* (2015) 65:2420–9. doi: 10.1016/j.jacc.2015.03.569

5. Tadic S, Ilic A, Stefanovic M, Stojsic-Milosavljevic A, Popov T, Bjelobrk M, et al. Case report: multimodality imaging as a lifeline for fatal localization of valsalva sinus fibroelastoma. *Front Cardiovasc Med.* (2021) 8:683534. doi: 10.3389/fcvm.2021.683534

6. Maleszewski JJ, Bois MC, Bois JP, Young PM, Stulak JM, Klarich KW. Neoplasia and the heart: pathological review of effects with clinical and radiological correlation. *J Am Coll Cardiol.* (2018) 72:202–27. doi: 10.1016/j.jacc.2018.05.026

7. Ahmad A, El-Am EA, Kurmann RD, Sorour AA, Bois MC, Maleszewski JJ, et al. Clinical and echocardiographic characteristics of patients with pathology proven right-sided papillary fibroelastomas. *Int J Cardiol.* (2022) 349:123–6. doi: 10.1016/j.ijcard.2021.11.083

8. Ikegami H, Andrei AC, Li Z, McCarthy PM, Malaisrie SC. Papillary fibroelastoma of the aortic valve: analysis of 21 cases, including a presentation with cardiac arrest. *Tex Heart Inst J.* (2015) 42:131–5. doi: 10.14503/THIJ-14-4262

9. Eftekhari H, Islam A, Slawsky M. Aortic valve fibroelastoma presenting with myocardial infarction. *Catheter Cardiovasc Interv.* (2011) 77:716–9. doi: 10.1002/ccd.22879

10. Ahmad A, Arghami A, El-Am EA, Foley TA, Kurmann RD, Klarich KW. Case report: a tale of a cardiac mass: looks like a papillary fibroelastoma, acts like a non-bacterial thromboendocarditis. *Front Cardiovasc Med.* (2021) 8:782926. doi: 10.3389/fcvm.2021.782926

11. Mansueto G, Capasso E, Buccelli C, Niola M. Pulmonary eosinophilic inflammatory infiltration post-intensive care in a nearly drowned young man with papillary fibroelastoma: a rare complication discovered by forensic autopsy. *Front Med.* (2017) 4:253. doi: 10.3389/fmed.2017.00253

12. Sasaki A, Sato M, Jikuya T. Surgical treatment for papillary fibroelastoma of the aortic valve. *Gen Thorac Cardiovasc Surg.* (2009) 57:481–3. doi: 10.1007/s11748-009-0429-x

13. Mandryk Y, Czesla M, Flora C, Massoudy P. Concomitant tumourous lesions in the left atrium and aortic valve suspected to be myxoma. *Eur J Cardiothorac Surg.* (2020) 57:1011–2. doi: 10.1093/ejcts/ezz314

frontiers | Frontiers in Cardiovascular Medicine

TYPE Case Report
PUBLISHED 09 August 2022
DOI 10.3389/fcvm.2022.964324

Check for updates

OPEN ACCESS

EDITED BY
Reto Asmis,
Wake Forest School of Medicine,
United States

REVIEWED BY
Alessandro Inno,
Ospedale Sacro Cuore Don
Calabria, Italy
Nikhil Agrawal,
University of Texas Health Science
Center at Houston, United States

*CORRESPONDENCE
Aaron L. Sverdlov
Aaron.Sverdlov@newcastle.edu.au

SPECIALTY SECTION
This article was submitted to
Cardio-Oncology,
a section of the journal
Frontiers in Cardiovascular Medicine

RECEIVED 08 June 2022
ACCEPTED 22 July 2022
PUBLISHED 09 August 2022

CITATION
Chye AM, Nordman IIC and
Sverdlov AL (2022) Successful immune
checkpoint inhibitor rechallenge after
immune-related pericarditis: Clinical
case series.
Front. Cardiovasc. Med. 9:964324.
doi: 10.3389/fcvm.2022.964324

COPYRIGHT
© 2022 Chye, Nordman and Sverdlov.
This is an open-access article
distributed under the terms of the
Creative Commons Attribution License
(CC BY). The use, distribution or
reproduction in other forums is
permitted, provided the original
author(s) and the copyright owner(s)
are credited and that the original
publication in this journal is cited, in
accordance with accepted academic
practice. No use, distribution or
reproduction is permitted which does
not comply with these terms.

Successful immune checkpoint inhibitor rechallenge after immune-related pericarditis: Clinical case series

Adrian M. Chye[1,2,3,4], Ina I. C. Nordman[1,5] and
Aaron L. Sverdlov[1,5,6,7]*

[1]Calvary Mater Newcastle, Newcastle, NSW, Australia, [2]Garvan Institute of Medical Research, Darlinghurst, NSW, Australia, [3]Faculty of Medicine, St Vincent's Clinical School, University of New South Wales, Sydney, NSW, Australia, [4]St Vincent's Hospital, Darlinghurst, NSW, Australia, [5]School of Medicine and Public Health, University of Newcastle, Newcastle, NSW, Australia, [6]Cardiovascular Department, John Hunter Hospital, Hunter New England Local Health District, New Lambton Heights, NSW, Australia, [7]Newcastle Centre of Excellence in Cardio-Oncology, New Lambton Heights, NSW, Australia

Pericardial diseases secondary to immune checkpoint inhibitors (ICI) are rare. Here, we describe two cases of immune-related pericarditis caused by ICI for treatment of advanced NSCLC. Select patients can be successfully rechallenged with ICI after immune-related pericardial disease.

KEYWORDS

immune checkpoint inhibitors, immune-related adverse events, cardiotoxicity, pericarditis, lung cancer

Introduction

Immune checkpoint inhibitors (ICI) are a pillar of cancer therapy and have shown remarkable benefit in a range of cancer types including advanced non-small cell lung cancer (NSCLC) (1, 2). ICI are associated with a wide range of immune-related adverse events (irAE), which can affect any organ system. Cardiac irAE are rare, potentially life-threatening and include a spectrum of disorders including myocarditis, cardiomyopathy, arrhythmias and pericardial disease (3). The safety and efficacy of ICI rechallenge after cardiac irAE remains unclear. We report two rare cases (Table 1) of ICI-related pericardial disease in patients with metastatic NSCLC who were successfully rechallenged with ICI.

Learning objectives

- Clinicians should be aware of the rare and potentially life-threatening cardiac irAE related to immune checkpoint inhibitors.
- Rechallenge with immune checkpoint inhibitors following a full recovery from immune-related pericardial disease may be considered with involvement of a cardiologist or cardio-oncologist, taking into consideration the usefulness of rechallenge and predicted risk of irAE.

- Following rechallenge, patients should be monitored closely for recurrent and/or new irAE.
- If relapses occur, secondary prevention of immune-related pericardial disease can be considered with concomitant colchicine.

Case 1

A 69-year-old male ex-smoker was diagnosed with stage IV NSCLC of squamous-cell carcinoma subtype. He initially received palliative radiotherapy to the left lower lobe bronchus obstructing primary lesion. Subsequently, he received platinum doublet chemotherapy with four cycles of carboplatin and paclitaxel, and achieved stable disease post-treatment, and was then commenced on anti-programmed death-1 (PD-1) inhibitor Nivolumab.

Following 6 months (12 cycles, 2-weekly) of Nivolumab, he presented to hospital with acute pericardial chest pain, lethargy and dyspnoea, consistent with acute pericarditis. A computed tomography (CT) Pulmonary Angiogram showed a mild pericardial effusion and left pleural effusion (Figure 1). An echocardiogram demonstrated a small pericardial effusion, with no evidence of tamponade, consistent with NCI-CTCAE grade 2. He was treated with a pulse of glucocorticoids (prednisolone 50 mg daily for 1 week) and colchicine for 3 weeks. Two weeks later a repeat echocardiogram showed resolution of the pericardial effusion. He was recommenced on Nivolumab and received a further 6 cycles until disease progression, without recurrence of pericardial disease. He subsequently progressed through vinorelbine therapy and died 5 months later. There was no recurrence of the pericardial effusion at any stage.

In this case, the pericardial effusion was attributed to a cardiac irAE rather than malignant invasion/malignant effusion due to the absence of corresponding malignant disease progression prior to development of the effusion, rapid response to glucocorticoid treatment, as well as lack of recurrence of effusion when metastatic disease progressed.

A CT pulmonary angiogram demonstrated a pericardial effusion in a patient with metastatic NSCLC undergoing Nivolumab therapy.

Case 2

A 67-year-old female was diagnosed with stage IV NSCLC of adenocarcinoma subtype, which lacked a driver mutation and programmed death ligand 1 (PD-L1) expression was >90. She achieved a partial response from frontline Pembrolizumab, an anti-PD-1 therapy.

She presented with acute pericardial chest pain following 6 cycles (3 weekly) of Pembrolizumab. A CT pulmonary angiogram showed an interval pericardial effusion (Figure 2). An echocardiogram demonstrated a pericardial effusion with tricuspid valve velocity variation with respiration consistent with early tamponade and thickened pericardium, consistent with NCI-CTCAE grade 3. She was haemodynamically stable and did not require pericardiocentesis or surgical intervention. Pericardial disease was treated with NSAIDs, colchicine and glucocorticoids (prednisone 50 mg daily tapered over 4 weeks), with prompt resolution of symptoms. Colchicine was ceased due to diarrhea. A follow-up echocardiogram demonstrated complete resolution of the pericardial effusion. Acute pericarditis and pericardial effusion were attributed to a cardiac irAE rather than from direct malignant invasion due to the rapid response with high-dose glucocorticoid treatment, and simultaneous tumor regression in known sites of disease. She was rechallenged with pembrolizumab after multi-disciplinary consultation with the cardio-oncologist.

Following cycle 9 of pembrolizumab, she represented with pericardial chest pain and was diagnosed with recurrent pericarditis. Her symptoms quickly resolved with reinstitution of NSAIDs, colchicine and glucocorticoids. Pembrolizumab was subsequently resumed concomitantly with colchicine. Following cycle 15 of pembrolizumab on concurrent colchicine therapy, a third episode of pericarditis occurred. Her symptoms again rapidly resolved with addition of NSAIDs and glucocorticoids. Pembrolizumab combined with colchicine was resumed. The patient continued to benefit from pembrolizumab with exceptional response for >18 months. The timeline of pembrolizumab treatment related to pericardial disease is shown in Figure 3.

A CT pulmonary angiogram demonstrated an interval pericardial effusion in a patient with metastatic NSCLC undergoing frontline therapy with pembrolizumab.

The development of recurrent pericarditis in relation to pembrolizumab treatment and the use of anti-inflammatory therapies including prednisone and colchicine.

Discussion

Pericardial diseases including acute pericarditis, pericardial effusion and tamponade caused by ICI have been increasingly recognized, but very few cases have been rechallenged with ICI therapy (4–7). Overall, the incidence of pericardial disease in the setting of ICI treatment is relatively rare, in the order of 1.57 events per 100 person-years (8). We present here, two rare cases of pericardial disease caused by ICI with anti-PD-1 monotherapy who were successfully rechallenged.

Abbreviations: CT, computed tomography; PD-1, programmed cell death protein 1; PD-L1, programmed cell death ligand 1; ICI, immune checkpoint inhibitor; IrAE, immune-related adverse event; NSCLC, non-small cell lung cancer.

TABLE 1 Characteristics of patients who developed pericardial disease due to immune checkpoint inhibitors.

Case	Age, yrs, sex, race	Cardiac irAE	Primary cancer and mutations	Other Medical history	CVRF	Cancer Stage before immunotherapy	Immuno-therapeutic agent	Onset of cardiac irAE	Other cancer treatment	Clinical presentation	Typical pericarditis chest pain	Typical ECG changes of pericarditis	Presence of pericardial Rub	Echocardiography findings: new or worsening effusion, evidence of tamponade or constriction	Exclusion of malignant effusion	Treated with high-dose steroids	Recovery	Naranjo Score	Recurrence of Side effect	Associated irAE	Progression of primary malignancy	Death/ cause of death
1	69, male, white	Pericarditis and small pericardial effusion	Squamous cell carcinoma of the lung	COPD, Base of tongue SCC treated with radical chemoradiotherapy	Ex-smoker	IV	Nivolumab	24 weeks	Chemo-therapy and radiotherapy	Pleuritic chest pain, shortness of breath and lethargy	(+)	(-)	(-)	New small pericardial effusion, no evidence of tamponade or constriction	Tap not done, however effusion responded to steroids, colchicine	Prednsolone 50mg daily then tapered	Yes, after holding the mediciation and starting steroids	3	(-), even after drug reintroduced	Nil	(+)	(+), non-cardiac, after 5 months
2	67, female, white	Pericarditis and pericardial effusion with early tamponade, thickened pericardium	Adenocarcinoma of the lung, PD-L1 >90%, no driver mutations detected	COPD, pulmonary embolism	Hypertension (well controlled on amlodipine and valsartan)	IV	Pembroli-zumab	18 weeks	Nil	Pleuritic chest pain	(+)	(+)	(+)	New moderate pericardial effsion, early tamponade with tricspid valve velocity variation with respiration, no evidence of constriction	Tap not done, however effusion responded to steroids, colchicine	Prednsolone 50mg daily then tapered	Yes, after holding the mediciation and starting steroids	6	(+) 9 weeks after first reintroduction and 27 weeks after second reintroduction	Nil	(-)	(-)

(–), negative; (+), positive; CK, creatine kinase; COPD, chronic obstructive pulmonary disease; CVRF, cardiovascular risk factors; ECG, electrocardiogram; irAE, immune related adverse event; IV, intravenous; PD-L1, programmed death ligand 1.

10.3389/fcvm.2022.964324

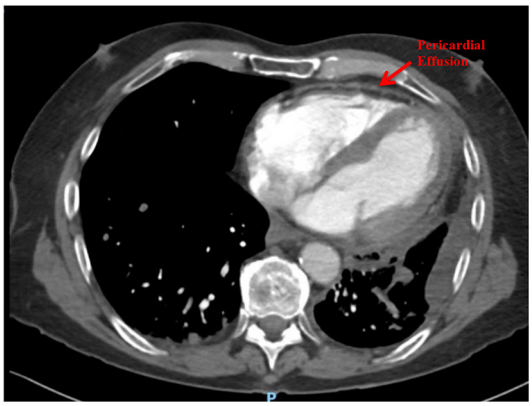

FIGURE 1
Pericardial effusion after 12 cycles of Nivolumab (Case 1).

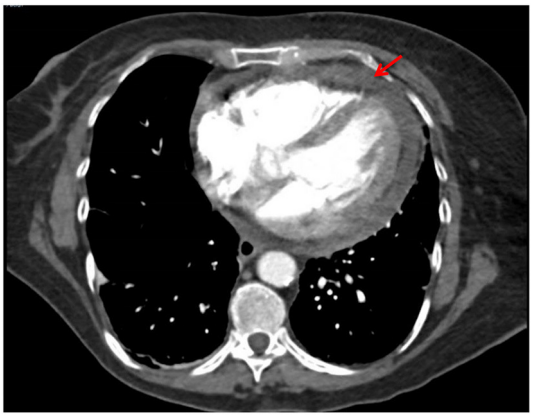

FIGURE 2
Pericardial effusion after 6 cycles of pembrolizumab (Case 2).

The precise mechanisms by which ICI-related pericardial disease occurs is poorly understood. There is also a paucity of data evaluating the optimal management of ICI-related pericardial disease. Numerous bodies including the American Society of Clinical Oncology (ASCO) and the European Society for Medical Oncology (ESMO) have endeavored to develop standardized guidelines for managing irAE. The scope of these guidelines is restricted as they group all cardiac toxicities together, and do not address the disorder of pericardial disease specifically. ASCO guidelines recommend rapid initiation of high-dose glucocorticoids for cardiac toxicity, holding ICI and permanently discontinuing ICI if greater than grade 1 toxicity occurs (9). ESMO suggest treating cardiac toxicity with high-dose glucocorticoids and escalation to other immunosuppressive drugs if not responsive to glucocorticoids (10).

ICI-related pericardial disease is treated with high-dose glucocorticoids (prednisolone 1–2 mg/kg), urgent pericardiocentesis if haemodynamic compromise is present, and permanent discontinuation of ICI. The safety, efficacy, and appropriateness of rechallenging with ICI following ICI-related pericardial disease is a key question that is yet to be answered. In routine clinical practice, ICI is permanently discontinued in patients who have developed cardiac irAE. We propose that patients with ICI-related pericardial disease with resolution or near resolution of irAE, ICI re-challenge can be considered on a case-by-case basis with multi-disciplinary expertise. The multi-disciplinary team should consider the potential benefit of a rechallenge, patient comorbidities, patient preference and predicted risk of new and recurrent irAE. Patients should be closely monitored for recurrent or new irAE if ICI is indeed resumed.

Furthermore, Case 2 demonstrates that if relapses of ICI-related pericarditis do occur, it can be managed with temporary discontinuation of ICI and short courses of glucocorticoids. Recurrent pericarditis in this case was immunosuppression-sensitive and each relapse was followed by a full recovery. Following cardio-oncology consultation, discussion with the patient and careful consideration of the risk-benefit ratio of resuming treatment, ICI was reinstituted. Secondary prevention for ICI resumption with long-term concomitant colchicine was used as a strategy to reduce the risk of recurrent pericarditis.

A systematic review of case reports and series, which included 20 publications with a total of 28 cases of ICI-associated pericardial disease, suggested that majority of cases are severe, and the re-challenge was only done in minority (7 out of 28 patients) in the absence of further pericardial effusion (11). Our case series demonstrates that re-challenge is possible even in the case of recurrent pericarditis/pericardial effusion, provided it is not severe. This may potentially help avoid unnecessary discontinuation of life-saving ICI therapy in patients with mild pericardial disease, even if it recurs.

One limitation of our case series was that pericardial effusion cytology or pericardial biopsy were not performed on either patient, due to non-life-threatening nature of the pericardial effusions and rapid response to treatment.

Conclusion

Clinicians across disciplines should be aware of the rare but potentially life-threatening complication of ICI-related pericardial disease to enable prompt diagnosis and treatment. Rechallenge with ICI following resolution of pericardial disease on prior ICI treatment may be considered, but should be balanced with the usefulness of rechallenge, patient comorbidities and the risk of recurrent irAE. If relapses occur, secondary prevention of ICI-related pericardial disease can be considered with concomitant colchicine. Questions remain regarding the pathogenesis of irAE, optimal management of cardiac irAE and in what circumstances ICI may be resumed

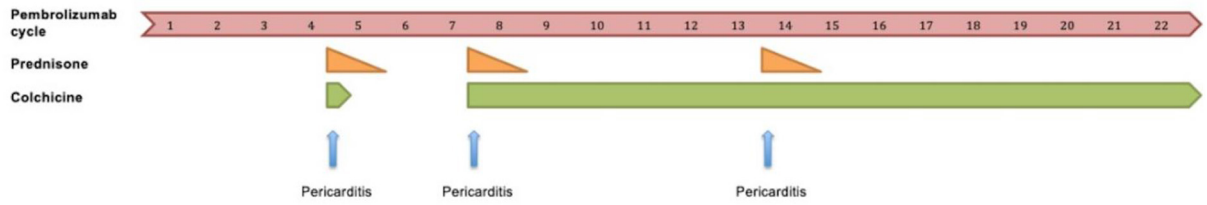

FIGURE 3
Clinical course of patient with recurrent pericarditis (Case 2).

after irAE. Further prospective clinical trials are needed to address these gaps in our knowledge.

Data availability statement

The original contributions presented in the study are included in the article/supplementary material, further inquiries can be directed to the corresponding author.

Ethics statement

Written informed consent was obtained from the individual(s) for the publication of any potentially identifiable images or data included in this article. Written informed consent was obtained from the participant/s for the publication of this case report.

Author contributions

AC wrote the manuscript in consultation with IN and AS. All authors were involved in the case management, contributed to the article, and approved the submitted version.

Funding

AS is supported by a Future Leader Fellowship (Award Reference No. 106025) from the National Heart Foundation of Australia. This work, in part, was supported by the Cardiovascular Medicine Department at the Hunter New England Local Health Service, Australia. The funder had no role in the current work.

Acknowledgments

The authors thank the patients for being involved in this clinical case series.

Conflict of interest

AS has received speaker honorarium/advisory board/consultancy fees from Bayer, Novartis, BMS, AstraZeneca, and Boehringer Ingelheim and research grants from BMS, Roche, Vifor, Biotronik, and RaceOncology.

The remaining authors declare that the research was conducted in the absence of any commercial or financial relationships that could be construed as a potential conflict of interest.

Publisher's note

All claims expressed in this article are solely those of the authors and do not necessarily represent those of their affiliated organizations, or those of the publisher, the editors and the reviewers. Any product that may be evaluated in this article, or claim that may be made by its manufacturer, is not guaranteed or endorsed by the publisher.

References

1. Reck M, Rodríguez-Abreu D, Robinson AG, Hui R, Csoszi T, Fülöp A, et al. Pembrolizumab versus chemotherapy for PD-L1–positive non–small-cell lung cancer. *New Engl J Med.* (2016) 375:1823–33. doi: 10.1056/NEJMoa1606774

2. Herbst RS, Baas P, Kim DW, Felip E, Pérez-Gracia JL, Han JY, et al. Pembrolizumab versus docetaxel for previously treated, PD-L1-positive, advanced non-small-cell lung cancer (KEYNOTE-010): a randomised controlled trial. *Lancet.* (2016) 387:1540–50. doi: 10.1016/S0140-6736(15)01281-7

3. Escudier M, Cautela J, Malissen N, Ancedy Y, Orabona M, Pinto J, et al. Clinical features, management, and outcomes of immune checkpoint inhibitor–related cardiotoxicity. *Circulation.* (2017) 136:2085–7. doi: 10.1161/CIRCULATIONAHA.117.030571

4. Atallah-Yunes SA, Kadado AJ, Soe MH. Pericardial effusion due to pembrolizumab-induced immunotoxicity: A case report and literature review. *Curr Probl Cancer*. (2019) 43:504–10. doi: 10.1016/j.currproblcancer.2019.01.001

5. Oristrell G, Bañeras J, Ros J, Muñoz E. Cardiac tamponade and adrenal insufficiency due to pembrolizumab: a case report. *Eur Heart J Case Rep*. (2018) 2:yty038–yty. doi: 10.1093/ehjcr/yty038

6. Chahine J, Collier P, Maroo A, Tang WHW, Klein AL. Myocardial and pericardial toxicity associated with immune checkpoint inhibitors in cancer patients. *JACC Case Rep*. (2020) 2:191–9. doi: 10.1016/j.jaccas.2019.11.080

7. Altan M, Toki MI, Gettinger SN, Carvajal-Hausdorf DE, Zugazagoitia J, Sinard JH, et al. Immune checkpoint inhibitor–Associated Pericarditis. *J Thorac Oncol*. (2019) 14:1102–8. doi: 10.1016/j.jtho.2019.02.026

8. Gong J, Drobni ZD, Zafar A, Quinaglia T, Hartmann S, Gilman HK, et al. Pericardial disease in patients treated with immune checkpoint inhibitors. *J ImmunoTher Cancer*. (2021) 9:e002771. doi: 10.1136/jitc-2021-002771

9. Brahmer JR, Lacchetti C, Schneider BJ, Atkins MB, Brassil KJ, Caterino JM, et al. Management of immune-related adverse events in patients treated with immune checkpoint inhibitor therapy: American Society of Clinical Oncology Clinical Practice Guideline. *J Clin Oncol*. (2018) 36:1714–68. doi: 10.1200/JCO.2017.77.6385

10. Haanen JBAG, Carbonnel F, Robert C, Kerr KM, Peters S, Larkin J, et al. Management of toxicities from immunotherapy: ESMO Clinical Practice Guidelines for diagnosis, treatment and follow-up†. *Ann Oncol*. (2017) 28(suppl_4):iv119-iv42. doi: 10.1093/annonc/mdx225

11. Inno A, Maurea N, Metro G, Carbone A, Russo A, Gori S. Immune checkpoint inhibitors-associated pericardial disease: a systematic review of case reports. *Cancer Immunol Immunother*. (2021) 70:3041–53. doi: 10.1007/s00262-021-02938-z

frontiers | Frontiers in Cardiovascular Medicine

TYPE Case Report
PUBLISHED 11 August 2022
DOI 10.3389/fcvm.2022.876294

Check for updates

OPEN ACCESS

EDITED BY
Reto Asmis,
Wake Forest School of Medicine,
United States

REVIEWED BY
Andrei Tica,
University of Craiova, Romania
Aldo Bonaventura,
ASST Sette Laghi, Italy

*CORRESPONDENCE
Carmine Pizzi
carmine.pizzi@unibo.it

†These authors have contributed equally to this work and share first authorship

‡These authors have contributed equally to this work and share last authorship

SPECIALTY SECTION
This article was submitted to Cardio-Oncology, a section of the journal Frontiers in Cardiovascular Medicine

RECEIVED 15 February 2022
ACCEPTED 18 July 2022
PUBLISHED 11 August 2022

CITATION
Bartoli L, Angeli F, Stefanizzi A, Fabrizio M, Paolisso P, Bergamaschi L, Broccoli A, Zinzani PL, Galiè N, Rucci P, Foà A and Pizzi C (2022) Genetics and clinical phenotype of Erdheim–Chester disease: A case report of constrictive pericarditis and a systematic review of the literature.
Front. Cardiovasc. Med. 9:876294.
doi: 10.3389/fcvm.2022.876294

COPYRIGHT
© 2022 Bartoli, Angeli, Stefanizzi, Fabrizio, Paolisso, Bergamaschi, Broccoli, Zinzani, Galiè, Rucci, Foà and Pizzi. This is an open-access article distributed under the terms of the Creative Commons Attribution License (CC BY). The use, distribution or reproduction in other forums is permitted, provided the original author(s) and the copyright owner(s) are credited and that the original publication in this journal is cited, in accordance with accepted academic practice. No use, distribution or reproduction is permitted which does not comply with these terms.

Genetics and clinical phenotype of Erdheim–Chester disease: A case report of constrictive pericarditis and a systematic review of the literature

Lorenzo Bartoli[1,2†], Francesco Angeli[1,2†], Andrea Stefanizzi[1,2], Michele Fabrizio[1,2], Pasquale Paolisso[3,4], Luca Bergamaschi[1,2], Alessandro Broccoli[2,5], Pier Luigi Zinzani[2,5], Nazzareno Galiè[1,2], Paola Rucci[6], Alberto Foà[1,2‡] and Carmine Pizzi[1,2*‡]

[1]Institute of Cardiology, Sant'Orsola-Malpighi Hospital, IRCCS, Bologna, Italy, [2]Department of Experimental, Diagnostic and Specialty Medicine-DIMES, University of Bologna, Bologna, Italy, [3]Cardiovascular Center Aalst, OLV-Clinic, Aalst, Belgium, [4]Department of Advanced Biomedical Sciences, University of Naples Federico II, Naples, Italy, [5]Institute of Hematology "L. e A. Seràgnoli", Sant'Orsola-Malpighi Hospital, IRCCS, Bologna, Italy, [6]Division of Hygiene and Biostatistics, Department of Biomedical and Neuromotor Sciences, Alma Mater Studiorum, University of Bologna, Bologna, Italy

Background: Erdheim–Chester disease (ECD) is a rare form of histiocytosis. An increasing number of genetic mutations have been associated with this syndrome, confirming its possible neoplastic origin. Recently, a connection between the BRAF mutational status and a specific phenotype was described; however, no studies have yet evaluated the correlations between other mutations and the clinical features of the disease.

Objectives: This study aims to clarify the association between the clinical phenotype and genetic mutations identified in the neoplastic cell lines of ECD.

Methods: We describe a case of ECD characterized by pericardial involvement and a KRAS mutation shared with chronic myelomonocytic leukemia. Hence, through a meta-analysis of individual participant data of all genetically and clinically described cases of ECD in the literature, we aimed to elucidate the association between its clinical phenotype and baseline genetic mutations.

Results: Of the 760 studies screened, our review included 133 articles published from 2012 to April 2021. We identified 311 ECD patients whose genotype and phenotype were described. We found five main genes (BRAF, KRAS, NRAS, PIK3CA, and MAP2K1) whose mutation was reported at least three times. Mutation of BRAF led to a neurological disease (183 of 273 patients, 67%; $p < 0.001$); KRAS- and NRAS-mutated patients mainly showed cutaneous (five of six patients, 83.3%, $p < 0.004$) and pleural (four of nine patients, 44%, $p = 0.002$) involvement, respectively; PIK3CA was not associated with specific

organ involvement; and MAP2K1 mutations caused the disease to primarily involve the peritoneum and retroperitoneum (4 of 11, 36.4%, $p = 0.01$).

Conclusion: This work implies a possible influence of baseline mutation over the natural history of ECD, underscoring the importance of a thorough genetic analysis in all cases with the ultimate goal of identifying a possible targeted therapy for each patient.

KEYWORDS

Erdheim-Chester disease, constrictive pericarditis, genotype, phenotype, precision medicine, case-report

Introduction

Erdheim–Chester disease (ECD) is a rare non-Langerhans cell histiocytosis (1, 2), with less than 1,000 cases described so far (2). It is known that ECD affects multiple organs with a wide spectrum of clinical presentations, ranging from an asymptomatic to a life-threatening condition. The most common symptom is bone pain (50%) as bilateral symmetric osteosclerosis evaluated by 18F-fluorodeoxyglucose (18F-FDG) positron emission tomography/computed tomography (PET/CT) or technetium-99 m (Tc-99m) bone scan is considered a pathognomonic feature, reported by about 80–95% of patients (3, 4). The other organs often infiltrated are the skin (xanthelasmas), central nervous system (CNS; resulting in ataxia, dysarthria, cognitive impairment, headache, peripheral neuropathy, and, sometimes, mood lability), respiratory system, pituitary gland (mostly central diabetes insipidus), retroperitoneum (renal failure requiring dialysis), and retro-orbital tissue (exophthalmos, retro-orbital pain, oculomotor nerve palsy, or vision loss; 2–4). About 50–70% of patients with ECD exhibit cardiovascular involvement. The most common findings include pericardial infiltration and effusion, and right atrioventricular pseudotumor and peri-arterial sheathing, involving mainly the thoracic and abdominal aorta, renal vessels, and coronary arteries (2–4).

Supplementary Box 1 summarizes the multiorgan involvement in ECD and the potential "red flags." An increasing number of genetic mutations have been associated with ECD. Specifically, recurrent activating mutations involving the mitogen-activated protein kinase and phosphatidylinositol 3-kinase (PI3K)-AKT pathways have been discovered. BRAF V600E is the most frequent mutation encountered (5), although other genes may be affected, such as NRAS, KRAS, PI3KCA, ARAF, MAP2K1, ALK, and NTRK1 (6–9).

These findings suggest that ECD is a clonal neoplastic disorder, and the most common signaling pathways involved could represent the first molecular targets in histiocytic disorders (7, 8, 10–12).

Last, an association between ECD and leukemic/myelodysplastic disorders that share most of the clonal mutations has been described (13), confirming the possible neoplastic origin probably due to a clonal hematopoiesis phenomenon (14–16).

In terms of clinical presentation, an association between the BRAF mutational status and cardiac, as well as neurological, disorders has been reported. Nevertheless, no studies have yet evaluated the correlations between other gene mutations and the specific ECD phenotype.

We report a case of constrictive pericarditis in a man with xanthelasmas and monocytosis; the final diagnosis was ECD associated with chronic myelomonocytic leukemia (CMML) harboring the same clonal mutation in the KRAS gene. Furthermore, we report the results of a meta-analysis of individual participant data (IPD) of all available ECD cases, aiming to elucidate the association between the ECD clinical phenotype and genetic mutations in neoplastic cell lines.

Case report

In the early 2000s, a 55-year-old man developed bilateral eyelid and thorax xanthelasmas (**Figure 1A**). The eyelid lesions relapsed rapidly after two surgical excisions.

In 2011, blood tests revealed monocytosis, and in the following years, splenomegaly was detected. No further diagnostic or therapeutic approaches were applied due to the lack of systemic and specific organ symptoms, as well as blood test alterations.

In 2017, the patient underwent left pleurodesis due to left pleuritis after a series of ineffective conservative treatments. Bioptic and cytologic materials revealed non-specific inflammation.

The patient remained asymptomatic until October 2019, when he developed fatigue and breathlessness. An electrocardiogram demonstrated sinus tachycardia. Right pleural effusion was detected on chest X-ray. Echocardiography

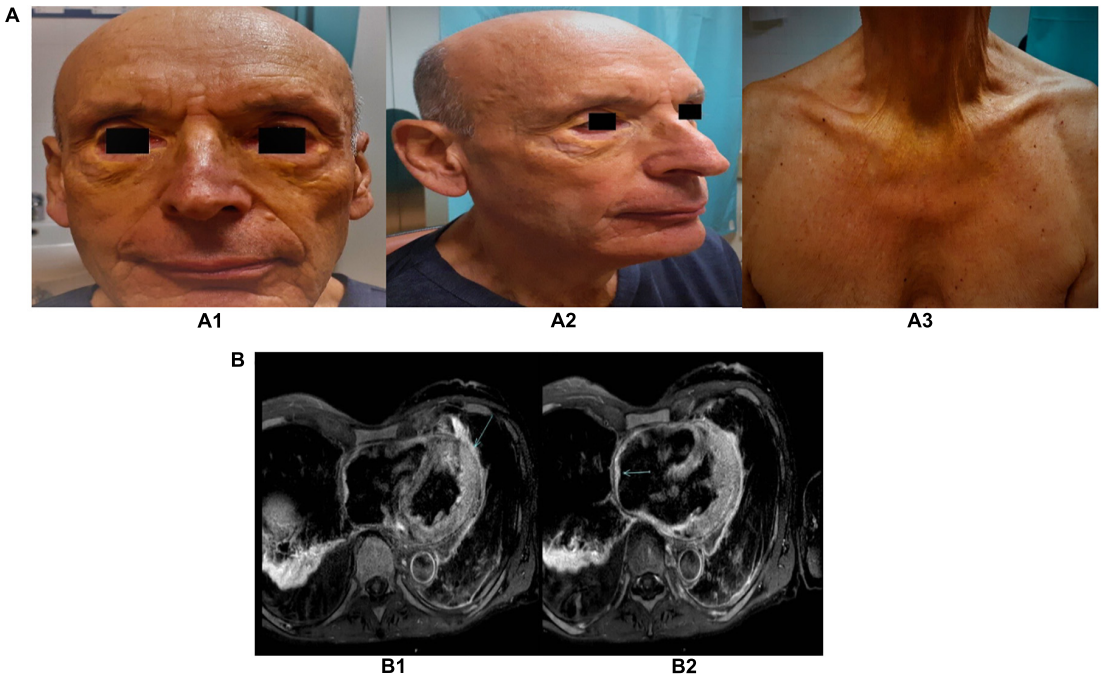

FIGURE 1
(A) Pictures of the xanthelasmas of the eyelid and thorax. Several yellowish plaque/papules on both upper and lower eyelids, cheeks **(A1,A2)**, and anterior region of the thorax **(A3)**. **(B)** Cardiac magnetic resonance images. Post-gadolinium T2-weighted sequences, showing a gadolinium-enhanced pericardial nodule **(B1)** and the pseudotumor of the right atrial roof **(B2)**.

showed findings consistent with constrictive pericarditis; therefore, he was admitted to our cardiology unit.

Blood tests confirmed monocytosis with dysmorphic, broken, and vacuolated monocytes on a blood smear. In addition, anemia and elevated C-reactive protein were observed. Notably, despite the history of xanthelasmas, cholesterol levels were low without lipid-lowering therapy.

A chest CT scan detected nodular pleuro-pericardial lesions. Right heart catheterization and cardiac magnetic resonance (MR; **Supplementary Video 1**) confirmed the diagnosis of constrictive pericarditis. Furthermore, cardiac MR revealed right atrial posterior wall and pericardial thickening. It also confirmed nodular pericardial and pleural lesions showing hyperemia and edema in T2-weighted sequences (**Figure 1B**).

Given the multiorgan involvement, including the right atrium and pericardium, which are reported to be commonly affected in cardiac malignancies (17), we hypothesized a hematologic systemic disease. Specifically, the presence of xanthelasma, pleuro-pericardial involvement, and right atrial posterior wall thickening raised the suspicion of ECD.

Methods

To investigate the possible bone involvement, we performed a bilateral femoral X-ray and MR scan.

Subsequently, a whole-body 99mTc-3,3-diphosphono-1,2-propanodicarboxylic acid (99mTc-DPD) bone scintigraphy and 18F-FDG PET/TC were performed to evaluate disease extension and to guide a subsequent biopsy.

We performed blood tests to exclude endocrinopathy, namely, adrenal and pituitary involvement. The CNS was evaluated by a head MR scan. To demonstrate pulmonary, perivascular, and perinephric infiltrates, CT scans of the neck, chest, abdomen, and pelvis were acquired.

The presence of peripheral monocytes and splenomegaly led us to perform a bone marrow biopsy. To detect the typical components of histiocytic infiltrates, tissue was taken from the xanthelasmas of upper lateral and lower medial left eyelids, and a bone biopsy from regions with maximum osteosclerosis on the previous femoral MR.

Moreover, immunohistochemistry (IHC) was performed to evaluate the presence of the typical BRAF V600E mutation. Targeted capture next-generation sequencing (NGS) was executed to identify ECD-related mutations in the skin biopsy, blood plasma, and bone marrow. The panels used for genetic analysis, the genes specifically evaluated by these techniques, and methods used are reported in the section "**Supplementary material**."

Last, we performed a meta-analysis of IPD of all ECD cases in the literature. Design and reporting were carried out according to PRISMA-IPD Statement (18) (**Supplementary Tables 1, 2**). Our methods are reported in the **Supplementary material**.

Results

Bilateral femoral X-ray and MR revealed osteosclerosis. In addition, MR images showed a symmetrical increase in the red bone marrow. On the other hand, both whole-body 99mTc-DPD scintigraphy and 18F- FDG PET/CT were negative for bone tracer uptake. 18F-FDG PET/CT showed bone marrow glucose uptake consistent with a myeloproliferative disease and there was a mild uptake by the known pleural and pericardial nodular lesions (19).

The head MR scan excluded CNS, pituitary, or retro-orbital involvement. The CT scans of the neck, chest, abdomen, and pelvis only showed marked splenomegaly, without any further sign of organ involvement. The hypothalamic–pituitary–adrenal axis and thyroid and sex hormones were within the normal range.

A right femur biopsy did not show any relevant histiocytic and/or inflammatory component. Conversely, the skin specimen presented diffuse histiocytic infiltrates, with histopathologic and immunohistochemical features, consistent with ECD (CD 68+, CD163+, S100-, and CD1a-; **Supplementary Figures 1A, A1, A2, and A3**).

The bone marrow biopsy showed a monocytic component (CD14+, CD68PGM1+, and CD163+) compatible with CMML, a rare myeloproliferative disorder (**Supplementary Figures 1B, B1, B2, and B3**).

Next-generation sequencing analysis of the skin biopsy, blood, and bone marrow, and immunofluorescence of the skin biopsy excluded the presence of typical BRAFV600E mutation but showed a clonal mutation involving KRAS gene (p. Gly12Asp, c.35G > A9), shared by both histiocytes and leukemic cells (**Supplementary Figures 1A, A4, 1B, B4**). Moreover, adjunctive mutations were reported on the peripheral blood and bone marrow, namely, ASXL1 (p. Leu815Pro), SETBP1 (p.Val1101Ile a), EZH2 (p.Asp185His), and TP53 (p.Pro72Arg).

The final diagnosis was ECD and concomitant chronic myelomonocytic leukemia with a shared clonal mutation.

Treatment and follow-up

A treatment with corticosteroid was started, and clinical conditions rapidly improved. A chest X-ray at 3 months showed the resolution of pleural effusion. Blood tests indicated a progressive increase in the blood cell count with no signs of inflammation markers. Cutaneous lesions showed a progressive reduction, leading to complete disappearance.

At the 6-month follow-up, the patient was completely asymptomatic. A cardiac MR scan demonstrated resolution of pericardial constriction (**Supplementary Video 1**), and neither hyperemia nor edema was observed at T2-weighted images. Similarly, a contrast-enhanced chest CT scan demonstrated complete resolution of pleuro-pericardial effusion and nodular lesions.

Meta-analysis of individual participant data

Of 760 studies screened, our review of the literature selected 133 articles. The first article included was published in September 2012, and it was the first molecularly characterized case report of ECD (20). In the end, we identified 311 ECD patients whose genotype and phenotype were described (flow diagram of IPD search). The major traits of ECD are summarized in **Figure 2**, which illustrates the main clinical and radiographic findings of ECD (**Figure 2A**), the clinical features of specific subgroups (**Figure 2B**), and the influences of the main mutation over clinical phenotypes (**Figure 2C**).

We identified five main genes (BRAF, KRAS, NRAS, PIK3CA, and MAP2K1) whose mutation was reported at least three times in the literature. We merged all the others (Kit, JAK2, PDGFRA, ARAF, CSF1R, and FLT3-ITD) in the same group "other genes."

BRAF was the most frequently mutated gene (**Table 1**). Its mutation is linked to neurological disease (67.9%), with one-third of the patients showing pituitary involvement, while in less than 10%, the pleura and peritoneum were affected (**Tables 2**, **3**, and **Figure 2C**).

KRAS mutation is closely related to the skin (both xanthelasma-like and nodular lesions). Furthermore, there was a lower incidence of bone tracer uptake at PET-FDG and bone scan (in case of bone involvement) and a higher frequency of concomitant hematologic neoplasia. The CNS, retroperitoneum, and mesentery were never affected. Finally, patients with KRAS-mutated ECD frequently showed multigene involvement (**Tables 1–3** and **Figure 2C**). These features were also observed in our case report.

Erdheim–Chester disease patients carrying NRAS mutations did not present pericardial or pituitary disease but had a high frequency of pleural involvement (**Tables 2**, **3**, and **Figure 2C**).

Patients with MAP2K1-mutated ECD showed more frequent abdominal involvement, with both peritoneal and retroperitoneal fibrosis and/or hairy kidney features. Moreover, they tended to show reticuloendothelial system involvement, and they never had xanthelasma lesions (**Tables 2**, **3**, and **Figure 2C**).

PIK3CA mutation affected young patients without a specific organ involvement. Notably, the lung, skin, serosa, pituitary gland, and reticuloendothelial system were never affected (**Tables 1–3** and **Figure 2C**).

Furthermore, we noticed peculiar characteristics of three different populations: pediatric individuals, patients with

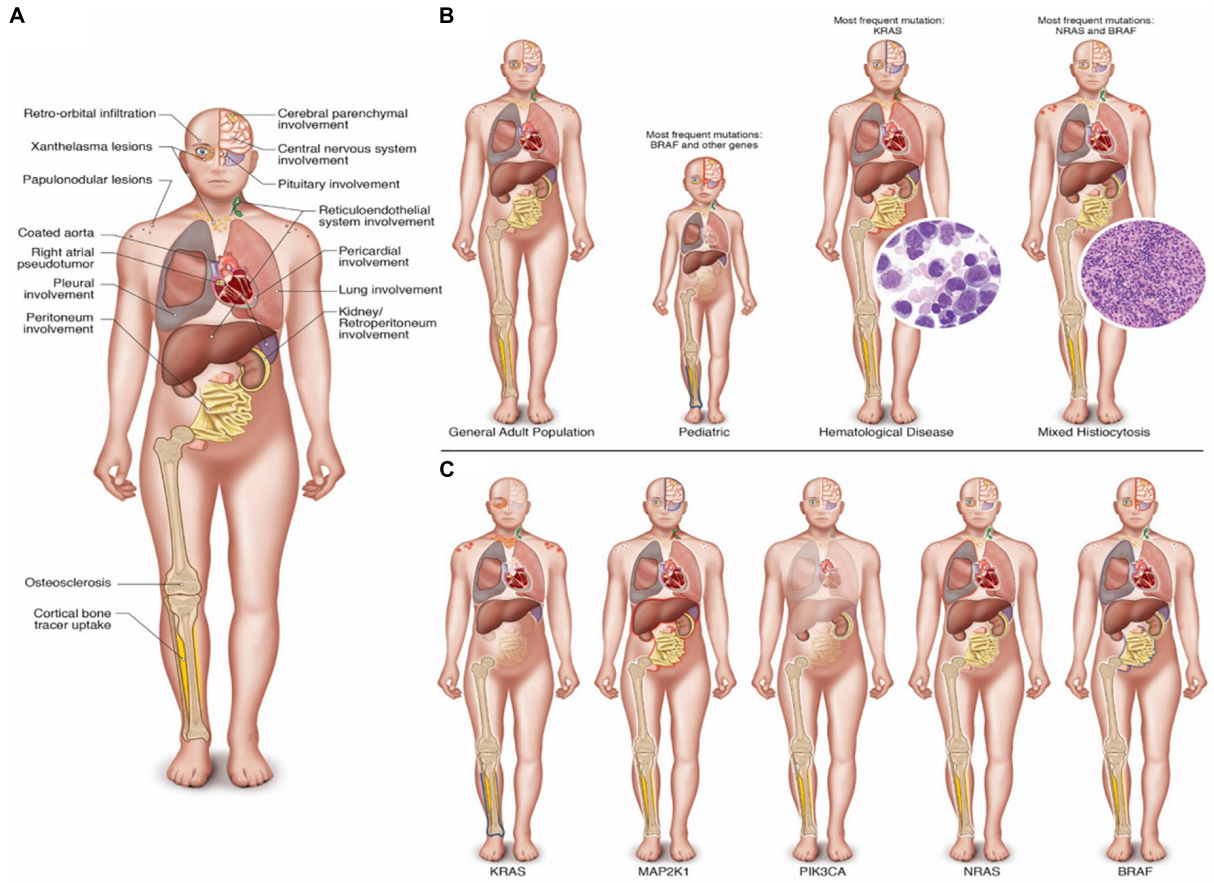

FIGURE 2
(Central Illustration): **(A)** Main clinical and radiographic findings in ECD. **(B)** Clinical and radiographic findings in specific subgroups of ECD. Characteristics of the general adult population, the pediatric population, patients with associated hematologic disorder, in mixed histiocytosis and the respective most frequently associated genetic mutations reported in the literature. **(C)** Clinical and radiographic findings of ECD in patients with mutation of KRAS, MAP2K1, PIK3CA, NRAS, and BRAF. Note: In **(B,C)**, clinical and radiological features of the specific subgroups were depicted transparent if they were never reported in the literature. Instead, they were reported with a blue halo if there was a statistically significant low frequency involvement; a white halo if there was a normal frequency involvement; and finally with a red halo if there was a statistically significant common involvement in the respective group.

concomitant hematologic disease, and subjects with mixed histiocytosis (defined as the simultaneous presence of another histiocytic disease).

In pediatric patients, the most frequently mutated gene was BRAF. These patients frequently exhibited CNS involvement with a lower incidence of serosal and bone disease (with lower tracer uptake at PET-FDG or bone scan), while cardiovascular involvement and abdominal involvement were never observed (**Supplementary Table 3** and **Figure 2B**).

Patients with an associated hematologic neoplasia are older, with a higher frequency of pulmonary, reticuloendothelial, and serosal manifestations, while CNS involvement is sporadic. Notably, subjects with KRAS or NRAS-mutated ECD frequently shared the genetic mutation between histiocytes and hematologic neoplasia (**Supplementary Table 4** and **Figure 2B**).

Finally, patients with mixed histiocytosis showed clinical features similar to those of the conventional ECD cohort with, a higher incidence of skin involvement, such as papulonodular lesions (**Supplementary Table 5** and **Figure 2B**).

Discussion

Our clinical case demonstrated that targeted therapy is driven by a precise diagnosis.

The goal of precision medicine is "to provide the best available care for each individual," (21) and an accurate diagnostic approach is crucial to allow the best therapeutic option. This concept is pivotal in entities with a heterogeneous clinical presentation, such as ECD.

In fact, our clinical case differs from the classical presentation of this disease. The patient developed bilateral eyelid and thorax xanthelasmas, pleuritis, and constrictive pericarditis without typical ECD findings, such as tracer uptake

TABLE 1 General characteristics of Erdheim–Chester patients according to different genotypes.

	NRAS	KRAS	BRAF	MAP2K1	PIK3CA	Other	*P* value
	n = 9	*n* = 6	*n* = 273	*n* = 11	*n* = 3	*n* = 8	
Male gender, *n* (%)	8 (88.9)	2 (33.3)	172 (65.6)	10 (90.9)	3 (100)	6 (75.0)	ns
Age, mean ± SD	59.9 ± 9.8	59.8 ± 9.4	52.2 ± 17.7	51.9 ± 11.6	31 ± 1.7	43.6 ± 28.1	ns
Pediatric patient, *n* (%)	0 (0.0)	0 (0.0)	16 (5.9)	0 (0.0)	0 (0.0)	2 (25.0)	ns
Multigene involvement, *n* (%)	0 (0.0)	3 (50) *	14 (5.1)	1 (9.1)	0 (0.0)	4 (50.0) *	**0.001**
Concomitant myeloid	3	4	26	1	0	2	**0.001**
or lymphoid neoplasms, *n* (%)	(33.3)	(66.7) *	(9.5)	(9.1)	0	(25)	
Type of concomitant neoplasm, *n* (%)							
Acute	1 (33.3)	0 (0.0)	6 (23.1)	0 (0.0)	0 (0.0)	1 (50.0)	ns
Chronic	3 (100.0)	4 (100.0)	22 (84.6)	1 (100.0)	0 (0.0)	1 (50.0)	ns
Lymphoid	0 (0.0)	0 (0.0)	3 (11.5)	0 (0.0)	0 (0.0)	0 (0.0)	ns
Myeloid	3 (100.0)	4 (100.0)	19 (73.1)	1 (0.0)	0 (0.0)	2 (100.0)	ns
Myelodysplasia	0 (0.0)	0 (0.0)	4 (15.4)	0 (0.0)	0 (0.0)	0 (0.0)	ns
Mixed Histiocytosis	1 (11.1)	0 (0.0)	24 (8.8)	1 (9.1)	0 (0.0)	0 (0.0)	ns
Shared mutation between ECD and neoplasm	3 (100.0) *	4 (100.0) *	1 (7.7)	0 (0.0)	0 (0.0)	2 (100.0) *	**0.004**

*Categories for which there is a statistically significant difference. Statistically significant *p*-values are in bold.

TABLE 2 Clinical characteristics of Erdheim–Chester patients according to different genotypes.

	NRAS	KRAS	BRAF	MAP2K1	PIK3CA	Other	*P* value
	n = 9	*n* = 6	*n* = 273	*n* = 11	*n* = 3	*n* = 8	
Cardiovascular involvement, *n* (%)	5	3	131	6	1	2	ns
	(55.6)	(50)	(47.8)	(54.5)	(33.3)	(25)	
Central nervous system involvement, *n* (%)	3	0	183	5	1	2	<**0.001**
	(33.3)	0	(67) *	(45.5)	(33.3)	(25)	
Bone involvement, *n*(%)	6	4	232	10	3	6	ns
	(66.7)	(66.7)	(85)	(90.9)	(100)	(75)	
Cortical bone tracer uptake, *n*(%)	3	1	161	9	3	5	**0.001**
	(100)	(33.3) *	(94.7)	(90)	(100)	(100)	
Lung involvement, *n* (%)	4	2	62	1	0	3	ns
	(44.4)	(33.3)	(22.7)	(9.1)	(0.0)	(37.5)	
Kidney/retroperitoneum involvement, *n* (%)	6	0	155	10	1	4	**0.009**
	(66.7)	0	(56.7)	(90.9) *	(33.3)	(50)	
Skin involvement, *n* (%)	3	5	77	3	0	4	**0.004**
	(33.3)	(83.3) *	(28.2)	(27.3)	(0.0)	(50)	
Serosal involvement, *n* (%)	5	3	79	4	0	3	ns
	(55.6)	(50)	(28.9)	(36.4)	(0.0)	(37.5)	
Reticuloendothelial system involvement, *n* (%)	1	1	14	3	0	2	**0.01**
	(11.1)	(16,6)	(5.1)	(27.3) *	(0.0)	(25)	

*Categories for which there is a statistically significant difference. Statistically significant *p*-values are in bold.

on the bone scan or FDG-PET, CNS involvement, coated aorta, and the hairy kidney/retroperitoneal fibrosis, which usually raise the suspicion of ECD.

Furthermore, the hematologic neoplasm and the presence of histiocytes and leukemic cells of KRAS mutation were confounding factors in the diagnostic process.

Precision medicine means to match clinical, diagnostic, and genetic features of a disease. Therefore, to further promote the use of precision medicine and considering the growing body of evidence that ECD is a clonal hematopoietic disorder (3), we hypothesized that extremely variable clinical features may relate to the primitive mutations that generate neoplastic germlines. These germlines give birth to both histiocytic and, if present, hematologic neoplastic cells, and the baseline genetic mutations could greatly influence the clinical phenotype and the natural history of the disease.

TABLE 3 Specific cardiac and non-cardiac involvements of Erdheim–Chester patients according to different genotypes.

	NRAS	KRAS	BRAF	MAP2K1	PIK3CA	Other	*P* value
	n = 9	*n* = 6	*n* = 273	*n* = 11	*n* = 3	*n* = 8	
Coated aorta, *n* (%)	5 (55.6)	0 (0.0)	84 (32.3)	5 (45.5)	1 (33.3)	1 (12.5)	ns
Peri-myocardial formations[a], *n* (%)	1 (11.1)	1 (16.7)	65 (24.6)	1 (9.1)	0 (0.0)	1 (12.5)	ns
Pericardial involvement, *n* (%)	0 (0.0)	2 (33.3)	51 (19.6)	1 (9.1)	0 (0.0)	2 (25.0)	ns
Cerebral parenchymal involvement, *n* (%)	2 (22.2)	0 (0.0)	115 (42.1) *	1 (9.1) *	1 (33.3)	0 (0.0)	**0.008**
Pituitary involvement, *n* (%)	0 (0.0)	0 (0.0)	91 (33.3) *	3 (27.3)	0 (0.0)	0 (0.0)	**0.009**
Retro-orbital infiltration, *n* (%)	1 (11.1)	0 (0.0)	52 (19)	1 (9.1)	1 (33.3)	2 (25.0)	ns
Pleural involvement, *n* (%)	4 (44.4) *	2 (33.3)	25 (9.2) *	1 (9.1)	0 (0.0)	3 (37.5)	**0.002**
Peritoneal involvement, *n* (%)	2 (22.2)	0 (0.0)	24 (8.8) *	4 (8.8) *	0 (0.0)	2 (25.0)	**0.01**
Xanthelasma lesions, *n* (%)	3 (33.3)	3 (50.0) *	38 (14.6)	0 (0.0)	0 (0.0)	4 (50.0) *	**0.005**
Papulonodular lesions, *n* (%)	0 (0.0)	3 (50.0) *	24 (9.2)	2 (18.2)	0 (0.0)	1 (12.5)	**0.01**

[a]Presence of at least one between myocardial, right atrium and atrio-ventricular junction infiltration.
*Categories for which there is a statistically significant difference. Statistically significant *p*-values are in bold.

To test this hypothesis, we performed an individual meta-analysis of all case reports and case series of patients with a diagnosis of ECD and known mutational status. The results of our work, which is the most comprehensive to date, support our hypothesis since each mutation demonstrated a trend toward organ-specific involvement.

Not surprisingly, the clinical features of our case matched with the results of our analysis since they could be explained by the KRAS mutated status and the concomitant hematologic neoplasm.

Our results, which help in the diagnostic process and promote a thorough genetic analysis of ECD, may have also a positive therapeutic and prognostic impact following a precision model of therapy for Mendelian disease, focused on treating the underlying mechanism using a genetic therapy.

This approach is increasingly used and continuously developing: BRAF and MEK/ERK inhibitors have been already used extensively in ECD (7, 8, 10–12), while others have been used in sporadic case reports. Moreover, a new molecule targeting KRAS has been successfully administrated for the first time in a phase I trial in lung cancer (4, 22) and has recently been approved by the Food and Drug Administration for therapeutic use (23). Our work suggests a possible influence of baseline mutation over the natural history of the disease, underscoring the importance of a thorough genetic analysis in all ECD cases with the ultimate goal of identifying a targeted therapy for each patient.

Study limitations

Our sample size is small (311 patients), except for BRAF, which had a small number of cases for other mutations. This is due to the rarity of this syndrome. Also, there is lack of systematic or thorough genetic analysis in all cases found in the literature, so a high number of patients could not be included in our study owing to the absence of a known mutation.

On the contrary, some studies were excluded because they did not provide the clinical phenotype of the study population, or because a clear link between the genotype and phenotype of individual patients was not always possible (i.e., aggregate data).

Since our meta-analysis focused only on those cases whose both genotype and clinical phenotype were available, confounding and selection bias cannot be excluded.

Finally, there was a risk of including low-quality articles or studies with heterogenous data. Nevertheless, data from individual patients retrieved from different articles were harmonized for statistical analysis, and the methodological quality of the studies was assessed using the method proposed

by Murad et al. (see **Supplementary material**). Thus, of the 131 studies included, 106 and 27 showed good and moderate overall quality, respectively. No study revealed a low methodological quality.

Data availability statement

The original contributions presented in the study are included in the article/**Supplementary material**, further inquiries can be directed to the corresponding authors.

Ethics statement

Written informed consent was obtained from the individual(s) for the publication of any potentially identifiable images or data included in this article. Written informed consent was obtained from the participant/s for the publication of this case report.

Author contributions

LBa and FA contributed to the conception or design of the work and drafted the manuscript. AS, MF, PP, LBe, and PR contributed to the acquisition, analysis, or interpretation of data for the work. AB, PZ, NG, AF, and CP critically revised the manuscript. All authors gave final approval and agreed to be accountable for all aspects of work ensuring integrity and accuracy.

Funding

PP was supported by a research grant from the CardioPaTh Ph.D. Program.

Conflict of interest

The authors declare that the research was conducted in the absence of any commercial or financial relationships that could be construed as a potential conflict of interest.

Publisher's note

All claims expressed in this article are solely those of the authors and do not necessarily represent those of their affiliated organizations, or those of the publisher, the editors and the reviewers. Any product that may be evaluated in this article, or claim that may be made by its manufacturer, is not guaranteed or endorsed by the publisher.

Supplementary material

The Supplementary Material for this article can be found online at: https://www.frontiersin.org/articles/10.3389/fcvm.2022.876294/full#supplementary-material

SUPPLEMENTARY FIGURE 1
(A) Biopsy of the eyelid. Images of hematoxylin-eosin stain **(A1)**, CD 68 **(A2)**, and CD163 **(A3)** immunohistochemistry. The illustrations show foamy, CD68+ and CD163+ histiocytes, typical of Erdheim-Chester disease. In the last image **(A4)**, demonstration of a KRAS exon 2 mutation (p.Gly12Asp) by NGS (S5 Gene Studio) in the specimen. **(B)** Biopsy of the bone marrow (BM). Images of hematoxylin-eosin **(B1)**, and May–Grünwald **(B2)** stain and CD14 immunohistochemistry **(B3)**. The illustrations show granulocytic proliferation in an hypercellular bone marrow, with monocytes (CD14+), erythroid precursors and abundant hypolobulated and small megakaryocytes, suggestive of chronic myelomonocytic leukemia. The last image **(B4)** shows the detection by NGS (S5 Gene Studio) in both BM and peripheral blood of the same KRAS mutation already detected in the eyelid specimen.

SUPPLEMENTARY VIDEO 1
In the video frames real T1 cine sequences showing evident respiratory shift of the interventricular septum due to enhanced ventricular interdependence, which completely resolves at follow-up.

References

1. Diamond EL, Dagna L, Hyman DM, Cavalli G, Janku F, Estrada-Veras J, et al. Consensus guidelines for the diagnosis and clinical management of Erdheim-Chester disease. *Blood.* (2014) 124:483–92. doi: 10.1182/blood-2014-03-561381

2. Goyal G, Heaney ML, Collin M, Cohen-Aubart F, Vaglio A, Durham BH, et al. Erdheim-Chester disease: Consensus recommendations for evaluation, diagnosis, and treatment in the molecular era. *Blood.* (2020) 135:1929–45. doi: 10.1182/blood.2019003507

3. Estrada-Veras JI, O'Brien KJ, Boyd LC, Dave RH, Durham B, Xi L, et al. The clinical spectrum of Erdheim-Chester disease: An observational cohort study. *Blood Adv.* (2017) 1:357–66. doi: 10.1182/bloodadvances.2016001784

4. Cohen-Aubart F, Emile JF, Carrat F, Helias-Rodzewicz Z, Taly V, Charlotte F, et al. Phenotypes and survival in Erdheim-Chester disease: Results from a 165-patient cohort. *Am J Hematol.* (2018) 93:E114–7. doi: 10.1002/ajh.25055

5. Haroche J, Charlotte F, Arnaud L, von Deimling A, Hélias-Rodzewicz Z, Hervier B, et al. High prevalence of BRAF V600E mutations in Erdheim-Chester disease but not in other non-langerhans cell histiocytoses. *Blood.* (2012) 120:2700–3. doi: 10.1182/blood-2012-05-430140

6. Emile JF, Diamond EL, Hélias-Rodzewicz Z, Cohen-Aubart F, Charlotte F, Hyman DM, et al. Recurrent RAS and PIK3CA mutations in Erdheim-Chester disease. *Blood.* (2014) 124:3016–9. doi: 10.1182/blood-2014-04-570937

7. Diamond EL, Durham BH, Haroche J, Yao Z, Ma J, Parikh SA, et al. Diverse and targetable kinase alterations drive histiocytic neoplasms. *Cancer Discov.* (2016) 6:154–65. doi: 10.1158/2159-8290.CD-15-0913

8. Durham BH, Lopez Rodrigo E, Picarsic J, Abramson D, Rotemberg V, De Munck S, et al. Activating mutations in CSF1R and additional receptor tyrosine kinases in histiocytic neoplasms. *Nat Med.* (2019) 25:1839–42. doi: 10.1038/s41591-019-0653-6

9. Tzankov A, Kremer M, Leguit R, Orazi A, van der Walt J, Gianelli U, et al. Histiocytic cell neoplasms involving the bone marrow: Summary of the workshop cases submitted to the 18th meeting of the European association for haematopathology (EAHP) organized by the European bone marrow working group, Basel 2016. *Ann Hematol.* (2018) 97:2117–28. doi: 10.1007/s00277-018-3436-0

10. Haroche J, Amoura Z, Charlotte F, Salvatierra J, Wechsler B, Graux C, et al. Imatinib mesylate for platelet-derived growth factor receptor-beta-positive Erdheim-Chester histiocytosis. *Blood.* (2008) 111:5413–5. doi: 10.1182/blood-2008-03-148304

11. Diamond EL, Subbiah V, Lockhart AC, Blay JY, Puzanov I, Chau I, et al. Vemurafenib for BRAF V600-mutant Erdheim– Chester disease and langerhans cell histiocytosis: Analysis of data from the histology– independent, phase 2, open-label VE-BASKET study. *JAMA Oncol.* (2018) 4:384–8. doi: 10.1001/jamaoncol.2017.5029

12. Bhatia A, Ulaner G, Rampal R, Hyman DM, Abdel-Wahab O, Durham BH, et al. Single-agent dabrafenib for BRAFV600E-mutated histiocytosis. *Haematologica.* (2018) 103:e177–80. doi: 10.3324/haematol.2017.185298

13. Papo M, Diamond EL, Cohen-Aubart F, Emile JF, Roos-Weil D, Gupta N, et al. High prevalence of myeloid neoplasms in adults with non-langerhans cell histiocytosis. *Blood.* (2017) 130:1007–13. doi: 10.1182/blood-2017-01-761718

14. Milne P, Bigley V, Bacon CM, Néel A, McGovern N, Bomken S, et al. Hematopoietic origin of langerhans cell histiocytosis and Erdheim-Chester disease in adults. *Blood.* (2017) 130:167–75. doi: 10.1182/blood-2016-12-757823

15. Durham BH, Roos-Weil D, Baillou C, Cohen-Aubart F, Yoshimi A, Miyara M, et al. Functional evidence for derivation of systemic histiocytic neoplasms from hematopoietic stem/progenitor cells. *Blood.* (2017) 130:176–80. doi: 10.1182/blood-2016-12-757377

16. Cohen Aubart F, Roos-Weil D, Armand M, Marceau-Renaut A, Emile JF, Duployez N, et al. High frequency of clonal hematopoiesis in Erdheim-Chester disease. *Blood.* (2021) 137:485–92. doi: 10.1182/blood.2020005101

17. Foà A, Paolisso P, Bergamaschi L, Rucci P, Di Marco L, Pacini D, et al. Clues and pitfalls in the diagnostic approach to cardiac masses: Are pseudo-tumours truly benign? *Eur J Prev Cardiol.* (2021) 29:zwab032. doi: 10.1093/eurjpc/zwab032

18. Stewart LA, Clarke M, Rovers M, Riley RD, Simmonds M, Stewart G, et al. Preferred reporting items for systematic review and meta-analyses of individual participant data: The PRISMA-IPD statement. *JAMA.* (2015) 313:1657–65. doi: 10.1001/jama.2015.3656

19. D'Angelo EC, Paolisso P, Vitale G, Foà A, Bergamaschi L, Magnani I, et al. Diagnostic accuracy of cardiac computed tomography and 18-F fluorodeoxyglucose positron emission tomography in cardiac masses. *JACC Cardiovasc Imaging.* (2020) 13:2400–11. doi: 10.1016/j.jcmg.2020.03.021

20. Blombery P, Wong SQ, Lade S, Prince HM. Erdheim-Chester disease harboring the BRAF V600E mutation. *J Clin Oncol.* (2012) 30:e331–2. doi: 10.1200/JCO.2012.43.2260

21. National Research Council. *Toward precision medicine: Building a knowledge network for biomedical research and a new taxonomy of disease.* Washington, DC: The National Academies Press (2011).

22. Hong DS, Fakih MG, Strickler JH, Desai J, Durm GA, Shapiro GI, et al. KRAS G12C inhibition with sotorasib in advanced solid tumors. *N Engl J Med.* (2020) 383:1207–17. doi: 10.1056/NEJMoa1917239

23. FDA. *FDA approves first targeted therapy for lung cancer mutation previously considered resistant to drug therapy. FDA press announcement 2021.* Silver Spring, MD: FDA (2021).

frontiers | Frontiers in Cardiovascular Medicine

TYPE Case Report
PUBLISHED 16 August 2022
DOI 10.3389/fcvm.2022.950628

Check for updates

OPEN ACCESS

EDITED BY
Syed Wamique Yusuf,
University of Texas MD Anderson Cancer Center, United States

REVIEWED BY
Guoxing Weng,
Shengli Clinical Medical College of Fujian Medical University, China
Mu Chen,
Shanghai Jiao Tong University, China

*CORRESPONDENCE
Liming Liu
liulimingjia@csu.edu.cn

†These authors have contributed equally to this work and share first authorship

SPECIALTY SECTION
This article was submitted to Cardio-Oncology, a section of the journal Frontiers in Cardiovascular Medicine

RECEIVED 23 May 2022
ACCEPTED 02 August 2022
PUBLISHED 16 August 2022

CITATION
Liu H, Tu X, Zhang H, Fan C, Tan H, Song L, Wu Q and Liu L (2022) Case report: A primary calcified cardiac mass in right atrium partially obstructs the tricuspid valve in a patient on hemodialysis.
Front. Cardiovasc. Med. 9:950628.
doi: 10.3389/fcvm.2022.950628

COPYRIGHT
© 2022 Liu, Tu, Zhang, Fan, Tan, Song, Wu and Liu. This is an open-access article distributed under the terms of the Creative Commons Attribution License (CC BY). The use, distribution or reproduction in other forums is permitted, provided the original author(s) and the copyright owner(s) are credited and that the original publication in this journal is cited, in accordance with accepted academic practice. No use, distribution or reproduction is permitted which does not comply with these terms.

Case report: A primary calcified cardiac mass in right atrium partially obstructs the tricuspid valve in a patient on hemodialysis

Hongduan Liu†, Xiaokang Tu†, Hao Zhang, Chengming Fan, Haoyu Tan, Long Song, Qin Wu and Liming Liu*

Department of Cardiovascular Surgery, The Second Xiangya Hospital, Central South University, Changsha, China

Primary cardiac calcification is a rare benign mass in patients with end-stage renal disease. A few cases have been reported in the literatures. In this case study, during a routine checkup for hemodialysis, a transthoracic echocardiography on a 19-year-old male showed a cardiac mass in the right atrium that was partially obstructing the tricuspid valve. Cardiac magnetic resonance imaging showed a well-circumscribed, homogeneous "shadow" in the right atrium; it measured 29 × 27 mm, had equal T1- and T2-weighted signal intensities, and was adjacent to the tricuspid valve. According to 18F-fluorodeoxyglucose positron emission tomography combined with computed tomography, there was a dense circular shadow in the right atrium abutting the tricuspid valve, but there was no increase in glucose metabolism. Median sternotomy was performed for the surgical resection of the mass, and a cardiopulmonary bypass was completed. The mass was completely removed. The patient recovered well and was discharged 10 days after the surgery. Histological examination showed that the mass contained multiple calcified nodules. No mass recurrence was found by echocardiography during the 12th-month follow-up.

KEYWORDS

cardiac surgery, chronic kidney disease, calcified cardiac tumor, tricuspid valve, hemodialysis

Introduction

Most primary cardiac tumors are myxomas, lipomas, and fibroelastomas, of which calcification is found in cardiac myxoma, thrombosis, and osteosarcoma, respectively (1, 2). A cardiac calcified amorphous tumor (CCAT), a rare non-neoplastic intracavitary cardiac tumor, is characterized by calcification deposits in an amorphous background with fibrin materials and focal inflammation (3). Solely calcified cardiac masses without inflammation are extremely rare non-neoplastic cardiac masses that mimic malignancy on imaging. In particular, calcified cardiac masses are highly unusual in patients with end-stage renal disease (ESRD) who are on hemodialysis. Herein, a rare case of an

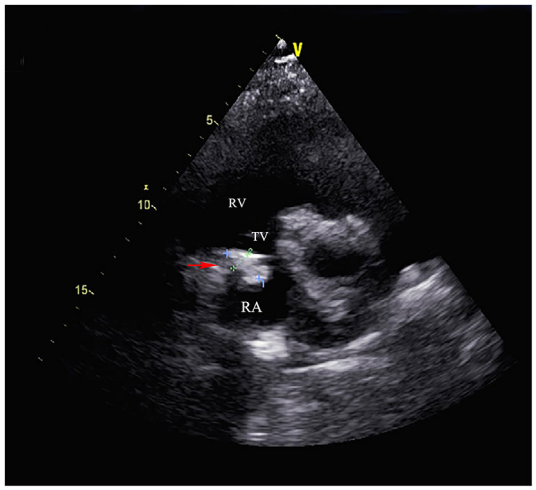

FIGURE 1
Transthoracic echocardiography showed the cardiac mass (30 mm x 28 mm) located in the right atrium and the anterior tricuspid valve was partially obstructed by the mass but the flow velocity of tricuspid valve did not accelerate. (RA, right atrium; RV, right ventricle; TV, tricuspid valve).

atypical cardiac calcified mass partially obstructing the tricuspid valve in a patient on hemodialysis is presented.

Case presentation

A 19-year-old male was referred to our hospital because a cardiac mass in the right atrium was detected by transthoracic echocardiography (TEE). The patient presented with cough and resting dyspnea and had a history of hypertension and ESRD, requiring hemodialysis for 2 years and hyperparathyroidism for 1 year. Two years ago, the urine culture was positive for C.parapsilosis, and then the fluconazole had been administrated until the urine culture was negative. Nephrotic syndrome and uremia of chronic kidney failure (CKD) were diagnosed by a kidney biopsy due to nocturia and elevated creatinine. Hemodialysis was being performed three times a week. An arteriovenous fistula was performed without central venous catheterization in the left upper extremity 1 year ago to improve the routine hemodialysis. Physical examination showed a normal temperature, 123/78 mmHg blood pressure, and 105 bpm heart rate. There was no cardiac murmur or family history of cardiovascular disease. Mild edema was found in the lower limb. Creatine was 1,015 μmol/L, N-terminal pro-B-type natriuretic peptide was 1,796 pg/ml, hemoglobin was 112 g/L, and parathyroid hormone level was above 2,000 pmmol/L. Laboratory data revealed a calcium level of 2.37 mmol/L and phosphorus level of 2.36 mmol/L. The other laboratory test results were normal.

Electrocardiography showed sinus tachycardia. TTE detected the cardiac mass (30 x 28 mm) in right atrium. The LVEF was 39% and FS was 19. The anterior tricuspid valve was partially obstructed by the mass, but the flow velocity of tricuspid valve did not accelerate (Figure 1). Cardiac magnetic resonance imaging (cMRI) showed that a well-circumscribed, homogenous "shadow" in the right atrium; it measured 29 mm × 27 mm, had equal T1- and T2-weighted signal intensities, was adjacent to the tricuspid valve (Figure 2). According to 18F-fluorodeoxyglucose (FDG) positron emission tomography combined with computed tomography (PET–CT), a dense circular shadow was in the right atrium abutting the tricuspid valve (32 × 34 mm). There was no increase in glucose metabolism, and the tumor was considered benign (Figure 3). There was no calcium deposited in the coronary arteries or other organs. The initial clinical diagnosis was a right atrial myxoma or fibroelastoma. Median sternotomy was performed to remove the mass and eliminate the obstruction of the tricuspid valve. A cardiopulmonary bypass was conducted using ascending aortic and superior and inferior vena cava cannulation. Without cardiac arrest, the right atrium was opened, and the mass, with a firm-hard texture, was confirmed to be partially embedded in the right atrium (Figure 4A). It was removed together with the implantation base. Histopathological examination revealed that the mass consisted of abundant calcific deposits without malignant cells (Figure 4B). The patient's postoperative course was uneventful, involving only three-times-a-week hemodialysis. The postoperative echocardiography showed that the LVEF was 55% and there was no residual of the mass. The patient was found to have recovered well and without recurrence at the 12th-month follow-up.

Discussion and conclusion

Primary cardiac tumors with calcification occur in cardiac myxoma, thrombosis, and osteosarcoma, among others. A CCAT is characterized by a calcified nodule in an amorphous background with fibrous degeneration and focal inflammation (3). Solely calcified cardiac mass without thrombus or inflammation are extremely rare (4). A past study showed that inflammation does not occur in CCATs in non-ESRD (5). This is consistent with our findings: the mass consisted only of abundant calcific deposits. The novelty of our case is that the mass presented in a patient with ESRD who was on hemodialysis.

The etiology of the CCATs is unknown (6), but some cases are associated with the hemodialysis in ESED (7–11). Metabolic disorders of calcium and phosphorus, which are common comorbidities among patients with CKD requiring hemodialysis, may result in calcification deposits in the mass, vascular calcification, and calciphylaxis (12–14). Hyperparathyroidism is the main comorbidity of CKD,

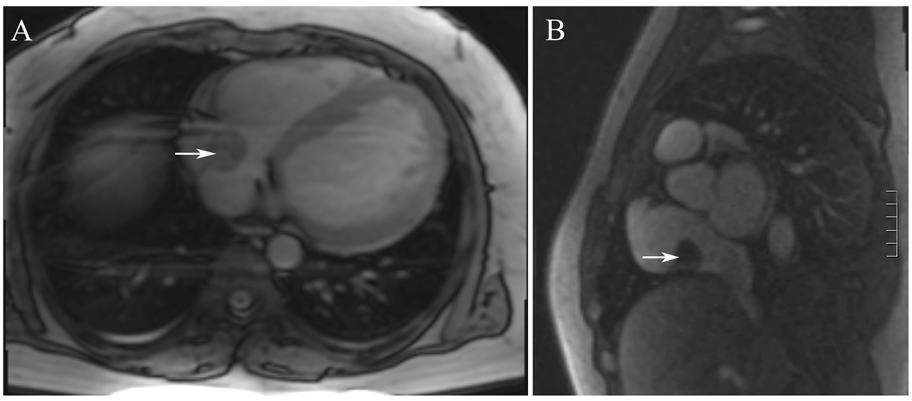

FIGURE 2
(A,B) The cardiac magnetic resonance imaging showed that showed that a well-circumscribed, homogenous "shadow" in the right atrium; it measured 29 mm × 27 mm, had equal T1- and T2-weighted signal intensities, was adjacent to the tricuspid valve.

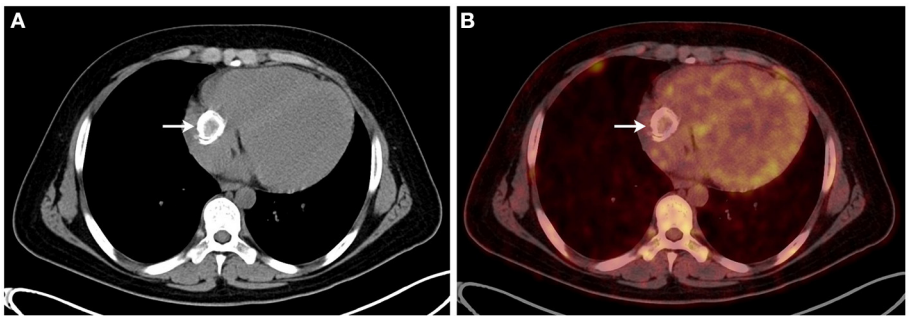

FIGURE 3
(A,B) The 18F-fluorodeoxyglucose positron emission tomography combined with computed tomography showed that a dense circular shadow was in the right atrium abutting the tricuspid valve (32 × 34 mm), and there was no increase in glucose metabolism.

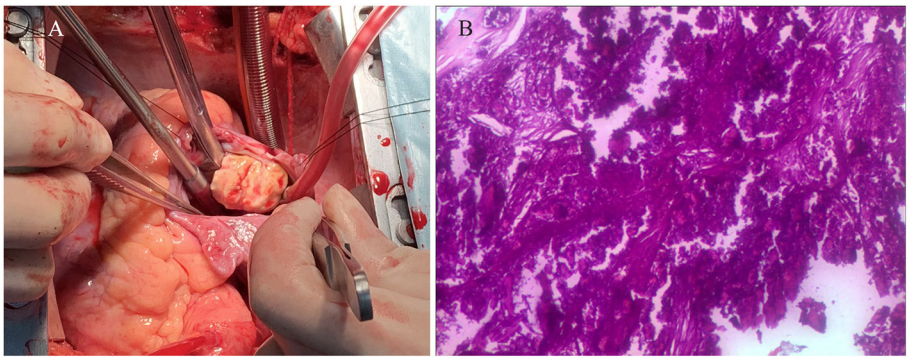

FIGURE 4
(A) The intraoperative image showed that the mass, with a firm-hard texture, was confirmed to be partially embedded in the right atrium. **(B)** The histopathological examination revealed that the mass consisted of abundant calcific deposits without malignant cells.

especially among patients requiring hemodialysis (15). As a result, metabolic disorders of calcium and phosphorus may result in calcium deposition in the vascular system via the disruption and alteration of the calcium regulatory mechanisms (16). Our study presents an extremely rare case: a calcified right atrial mass in a patient with ESED and hyperparathyroidism who was on hemodialysis.

Categorization of the symptoms depends on their location, obstruction, or embolization. Most patients are asymptomatic, and symptoms include shortness of breath, syncope (17), stroke (18), and central retinal arterial occlusion (6). In our case, cough, resting dyspnea, and lower limb edema were presented, which may have been related to low partially obstruction of the tricuspid valve and uremia. Calcified primary cardiac tumors have been found in all four chambers, usually in the mitral valve and annulus (7, 19, 20). CCATs presented most frequently in the right atrium and ventricle in non-ERSD patients, whereas CCTAs in the mitral annulus are significantly more common in patients with ESRD than in patients without ESRD (19). By contrast, the present study shows an exceptional case where a calcified cardiac mass is presented in the right atrium abutting the tricuspid valve in a ESRD on hemodialysis.

Appropriate screening imaging modalities for cardiac mass include echocardiography, computed tomography (CT), cMRI, and PET-CT; they can be used to make differential diagnoses among myxomas, fibroelastomas, thrombi, and among others. All of these can eliminate the problem of differential diagnoses (4). Although PET-CT and FDG uptake can provide valuable information about inflammation for the differential diagnoses (5), histopathology is still needed to make a final diagnosis, especially for CCATs. In the current study, a clinial diagnosis of a benign tumor was made, based on the cMRI, echocardiographic, and PET-CT findings. If a patient presents with symptoms caused by a mass or in cases where the histopathology is uncertain in relation to the tumor, surgical resection should be performed to alleviate the symptoms, reduce the risks, and clarify the nature of the mass.

In conclusion, CCAT is a rare non-neoplastic primary cardiac tumor characterized by calcification deposits with fibrin materials and inflammation. Solely calcified cardiac masses without inflammation are an exceptional subtype of CCATs. Abnormal calcium metabolism due to renal dysfunction and the inflammation associated with hemodialysis may contribute to the occurrence of the CCATs. Conventional imaging modalities, such as TTE, CT, and cMRI cannot specifically define the CCATs. Surgical resection is an appropriate measure for relieving symptoms, reducing the risks, and clarifying the pathological diagnoses of patients with CCATs.

Data availability statement

The original contributions presented in the study are included in the article/supplementary material, further inquiries can be directed to the corresponding author.

Ethics statement

The studies involving human participants were reviewed and approved by Ethics Committee of the Second Xiangya Hospital. The patients/participants provided their written informed consent to participate in this case study. Written informed consent was obtained from the individual(s) for the publication of any potentially identifiable images or data included in this article.

Author contributions

HL drafted the manuscript. HL and XT designed the study. HL, HZ, and LL performed the surgery. LS, CF, HT, and LL revised the manuscript. HL, XT, and QW were responsible for the collection of data or analysis. All authors read and approved the final manuscript.

Conflict of interest

The authors declare that the research was conducted in the absence of any commercial or financial relationships that could be construed as a potential conflict of interest.

Publisher's note

All claims expressed in this article are solely those of the authors and do not necessarily represent those of their affiliated organizations, or those of the publisher, the editors and the reviewers. Any product that may be evaluated in this article, or claim that may be made by its manufacturer, is not guaranteed or endorsed by the publisher.

References

1. Nowrangi SK, Ammash NM, Edwards WD, Breen JF, Edmonson JH. Calcified left ventricular mass: unusual clinical, echocardiographic, and computed tomographic findings of primary cardiac osteosarcoma. *Mayo Clin Proc.* (2000) 75:743–7. doi: 10.1016/S0025-6196(11)64623-5

2. Chaowalit N, Dearani JA, Edwards WD, Pellikka PA. Calcified right ventricular mass and pulmonary embolism in a previously healthy young woman. *J Am Soc Echocardiogr.* (2005) 18:275–7. doi: 10.1016/j.echo.2004.10.007

3. Reynolds C, Tazelaar HD, Edwards WD. Calcified amorphous tumor of the heart (cardiac CAT). *Hum Pathol.* (1997) 28:601–6. doi: 10.1016/S0046-8177(97)90083-6

4. Tian F, Zhang L, Wang J, Li Y, Xie M. Multimodality imaging of a left atrial calcified amorphous tumor. *Echocardiography.* (2020) 37:147–9. doi: 10.1111/echo.14559

5. Saku K, Tahara N, Takaseya T, Shintani Y, Takagi K, Shojima T, et al. Multimodal imaging of cardiac-calcified amorphous tumor. *J Nucl Cardiol.* (2020) 27:682–5. doi: 10.1007/s12350-018-01510-0

6. Choi EK, Ro JY, Ayala AG. Calcified amorphous tumor of the heart: case report and review of the literature. *Methodist Debakey Cardiovasc J.* (2014) 10:38–40. doi: 10.14797/mdcj-10-1-38

7. Kubota H, Fujioka Y, Yoshino H, Koji H, Yoshihara K, Tonari K, et al. Cardiac swinging calcified amorphous tumors in end-stage renal failure patients. *Ann Thorac Surg.* (2010) 90:1692–4. doi: 10.1016/j.athoracsur.2010.04.097

8. Seo H, Fujii H, Aoyama T, Sasako Y. Cardiac calcified amorphous tumor in a hemodialysis patient. *Asian Cardiovasc Thorac Ann.* (2016) 24:461–3. doi: 10.1177/0218492315574795

9. Takeuchi T, Dohi K, Sato Y, Kanemitsu S, Sugiura S, Uchida K, et al. Calcified amorphous tumor of the heart in a hemodialysis patient. *Echocardiography.* (2016) 33:1926–8. doi: 10.1111/echo.13335

10. Tanaka A, Mizuno M, Suzuki Y, Oshima H, Sakata F, Ishikawa H, et al. Calcified amorphous tumor in the left atrium in a patient on long-term peritoneal dialysis. *Intern Med.* (2015) 54:481–5. doi: 10.2169/internalmedicine.54.2967

11. Kanemitsu S, Bessho S, Sakamoto S, Yamamoto N, Ito H, Shimpo H. Calcified amorphous tumor with caseous calcification of mitral annulus in hemodialysis patients. *Gen Thorac Cardiovasc Surg.* (2020) 68:1513–6. doi: 10.1007/s11748-020-01363-w

12. Combalia A, Munoz-Mahamud E, Cofan F. Giant calcified mass in a hemodialysis patient. *Kidney Int.* (2019) 95:719. doi: 10.1016/j.kint.2018.08.006

13. Niu Z, Su G, Li T, Yu H, Shen Y, Zhang D, et al. Vascular calcification: new insights into BMP type I receptor A. *Front Pharmacol.* (2022) 13:887253. doi: 10.3389/fphar.2022.887253

14. Kim J, Konkel K, Jones SC, Reyes M, McCulley L. Teriparatide-associated calciphylaxis: a case series. *Osteoporos Int.* (2022) 33:499–504. doi: 10.1007/s00198-021-06139-3

15. Mathur A, Ahn JB, Sutton W, Chu NM, Gross AL, Segev DL, et al. Secondary hyperparathyroidism (CKD-MBD) treatment and the risk of dementia. *Nephrol Dial Transplant.* (2022). doi: 10.1093/ndt/gfac167. [Epub ahead of print].

16. Atta MG. A molecular target of vascular calcification in chronic kidney disease. *J Clin Invest.* (2022) 132:e156257. doi: 10.1172/JCI156257

17. Lewin M, Nazarian S, Marine JE, Yuh DD, Argani P, Halushka MK. Fatal outcome of a calcified amorphous tumor of the heart (cardiac CAT). *Cardiovasc Pathol.* (2006) 15:299–302. doi: 10.1016/j.carpath.2006.05.004

18. Formelli B, Farina A, Pescini F, Palumbo V, D'Alfonso MG, Oddo A, et al. Cardiac calcified amorphous tumor as a rare cause of ischemic stroke: clinical case. *Circ Cardiovasc Imaging.* (2020) 13:e009623. doi: 10.1161/CIRCIMAGING.119.009623

19. Yoshimura S, Kawano H, Minami T, Tsuneto A, Nakata T, Koga S, et al. Cardiac calcified amorphous tumors in a patient with hemodialysis for diabetic nephropathy. *Intern Med.* (2017) 56:3057–60. doi: 10.2169/internalmedicine.9057-17

20. Obase K, Kojima S, Nakaji S, Miura T, Eishi K. Aortic regurgitation resulted from traumatic leaflet tear due to calcified amorphous tumour. *Eur Heart J Cardiovasc Imaging.* (2020) 21:1431. doi: 10.1093/ehjci/jeaa124

frontiers | Frontiers in Cardiovascular Medicine

TYPE Case Report
PUBLISHED 17 August 2022
DOI 10.3389/fcvm.2022.932798

Check for updates

OPEN ACCESS

EDITED BY
Carlo Gabriele Tocchetti,
University of Naples Federico II, Italy

REVIEWED BY
Cheng Wang,
The Second Xiangya Hospital, Central South University, China
Stergios Soulaidopoulos,
Aristotle University of Thessaloniki, Greece

*CORRESPONDENCE
Deyan Yang
swallow_sums@163.com

SPECIALTY SECTION
This article was submitted to Cardio-Oncology, a section of the journal Frontiers in Cardiovascular Medicine

RECEIVED 30 April 2022
ACCEPTED 29 July 2022
PUBLISHED 17 August 2022

CITATION
Wu Y, Yang D, Sun L, Xu X, Gao P, Cheng K, Chen T, Cheng Z, Liu Y and Fang Q (2022) Case report: Recurrent syncope as initial symptom in a patient with neck lymphoma. *Front. Cardiovasc. Med.* 9:932798. doi: 10.3389/fcvm.2022.932798

COPYRIGHT
© 2022 Wu, Yang, Sun, Xu, Gao, Cheng, Chen, Cheng, Liu and Fang. This is an open-access article distributed under the terms of the Creative Commons Attribution License (CC BY). The use, distribution or reproduction in other forums is permitted, provided the original author(s) and the copyright owner(s) are credited and that the original publication in this journal is cited, in accordance with accepted academic practice. No use, distribution or reproduction is permitted which does not comply with these terms.

Case report: Recurrent syncope as initial symptom in a patient with neck lymphoma

Yanfang Wu, Deyan Yang*, Luxi Sun, Xiqi Xu, Peng Gao, Kangan Cheng, Taibo Chen, Zhongwei Cheng, Yongtai Liu and Quan Fang

Department of Cardiology, Peking Union Medical College Hospital, Chinese Academy of Medical Sciences and Peking Union Medical College, Beijing, China

Syncope may have many different causes, requiring careful identification. Recurrent syncope is uncommon as an initial symptom of neck lymphoma. Head and neck tumors involving the carotid artery cause syncope associate with carotid sinus syndrome. We report the case of a 72-year-old man who suffered from recurrent syncope due to compression of the right carotid sinus by diffuse large B-cell lymphoma and was successfully treated with immunochemotherapy. Syncope may be an early or sole sign of a neck or head tumor. We should be aware of the possibility of an underlying malignancy in patients with unexplained syncope after initial evaluation.

KEYWORDS

syncope, carotid sinus syndrome, neck malignancy, lymphoma, chemotherapy

Introduction

Syncope is defined as a transient loss of consciousness due to cerebral hypoperfusion, characterized by a rapid onset, short duration, and spontaneous complete recovery (1). The pathophysiological mechanism is a fall in systemic blood pressure, which is caused by low total peripheral resistance, low cardiac output, or both. For patients with recurrent syncope, diagnosis and treatment are urgently required. While etiology may be broad, syncope resulting from head and neck malignancy is rare. We describe a patient with recurrent syncope due to neck lymphoma causing compression of the carotid sinus who was successfully treated with immunochemotherapy.

Case presentation

A 72-year-old man was admitted to our hospital with recurrent syncope over the past month. Syncope occurred while sitting, standing, or walking, with prodromes

such as dizziness and palpitations. The syncope lasted 1 to 3 min. The patient developed persistent post-auricular and occipital pain in the morning. When the pain was at its peak, syncope was induced. A new, non-tender neck mass demonstrating progressive enlargement was observed. The patient had an occasional choking cough and dysphagia but no dyspnea. The patient did not complain any chest pain, exertional dyspnea or palpitation. The patient had a history of hyperthyroidism, but after that he take thyroxine tablet because of hypothyroidism. He had a history of smoking for 40 years and a family history of coronary atherosclerotic heart disease. In the physical examination, a soft mass with no tenderness was palpable in the right neck, which was misdiagnosed as an enlarged thyroid gland. Meanwhile, an enlarged lymph node (5 cm of max diameter) was palpable in the left inguinal region, with poor mobility and no tenderness. The cardiopulmonary physical examination was normal. During hospitalization, there were many episodes of syncope. Continuous tracking with a Holter monitor captured one episode of syncope, which occurred with sinus rhythm and a heart rate of 70 beats per minute. Transthoracic echocardiography showed impaired relaxation (mitral E/A ratio, 0.8) with left atrial enlargement and normal systolic function. A 2-h electroencephalogram showed that there was no epileptic seizure during the episode of syncope. Neuroimaging with computed tomography (CT) and magnetic resonance angiography were normal. Carotid artery ultrasonography revealed atherosclerotic plaques in bilateral carotid arteries with no stenosis. Considering the risk of carotid plaque embolization, carotid sinus massage was not performed. Supine and standing blood pressure measurements were not accompanied by any abnormal decrease in blood pressure. An upright tilt-table test was then performed, showing a decrease in arterial blood pressure (>20 mmHg) that reproduced syncope for a duration of 20 s without any change in heart rate, consistent with reflex syncope of the vasodepressor type.

Neck ultrasonography showed a hypo-echoic region with abundant blood flow in the lower middle part of the right neck, approximately 9.0 cm × 8.2 cm × 4.4 cm, surrounding the right common carotid artery, which had normal internal blood flow (**Figure 1A**). Positron emission tomography (PET)/CT showed a large soft tissue mass in the right neck, approximately 8.6 cm × 5.0 cm × 11.0 cm, surrounding the adjacent large vessels (**Figure 1B**). The mass had a non-uniform increase in radioactive uptake, with a maximum standard uptake value (SUVmax) of 59.1. Lymph nodes in the right neck (SUVmax, 30.6), in the left hilar and mediastinal regions (SUVmax, 5.3–48.6), and along the left external iliac vessels and bilateral inguinal vessels (especially left inguinal) (SUVmax 2.3–43.2) demonstrated increased metabolism. Due to the high bleeding risk of the right neck mass, the left inguinal lymph node was biopsied instead. Histopathological examination showed highly invasive B-cell lymphoma with a morphology consistent with diffuse large B-cell lymphoma (**Figure 2**).

The patient was referred to the hematology department for further treatment. After the assessment of the involved site, he was diagnosed as having diffuse large B-cell lymphoma (Ann Arbor stage, IV; International Prognostic index, 2) and secondary carotid sinus syndrome (CSS). He received immunochemotherapy, i.e., rituximab (600 mg), plus cyclophosphamide (1.2 g), doxorubicin (60 mg), vincristine (4 mg), and prednisone (100 mg/day × 5 day) (R-CHOP). After four cycles of R-CHOP immunochemotherapy, PET/CT revealed that the original large mass in the neck had disappeared (**Figure 3**). The patient no longer complained of either syncope or pain from the post-auricular and occipital regions. Choking when eating was also relieved (**Table 1**).

Discussion

Carotid sinus syndrome has a prevalence of 8.8% in patients aged 40 years and above with unexplained syncope after the initial evaluation (2). CSS is associated with many types of space-occupying lesions of the head and neck (3–7). Head and neck malignancy was reported as being the most frequent malignancy associated with syncope. All previously reported cases had carotid sinus compression or infiltration. Our patient, whose right carotid sinus was surrounded by neck lymphoma, presented with recurrent episodes of syncope as the initial symptom.

The pathophysiological mechanisms involved in syncope-associated CSS are complex (6). The carotid baroreceptor, located at the bifurcation of the carotid artery, is sensitive to mechanical pressure. When the arterial wall is stretched by a tumor, information is transmitted by the carotid sinus nerve to the brainstem centers in the caudal nucleus of the solitary tract. Interneurons activate the efferent pathways, resulting in the stimulation of the parasympathetic system and inhibition of the sympathetic system, which leads to a decrease in blood pressure and heart rate. Two hypotheses have been proposed to explain the association between syncope and neck lymphoma (4, 8): first, the lymphoma may invade the carotid sinus and cause direct compression, or invade the glossopharyngeal nerve, resulting in increased activity in the reflex arc; second, syncope may present as autonomic failure, similar to other B-cell lymphoma symptoms. Our patient had a large mass in the right neck surrounding the right common carotid artery that was the probable cause of syncope. The precipitating factor may be head movements. However, in clinical practice, obtaining a clear history of carotid sinus stimulation is challenging. Claassen et al. (9) reported that a turn of the head to look sideways can contribute to syncope in a healthy 70-year-old woman for the first time. In this case, we didn't see a clear-cut relationship between head movements and symptom episodes, such as syncope caused by the head tilting to the right side, or cessation of syncope resulting from the head turning to the

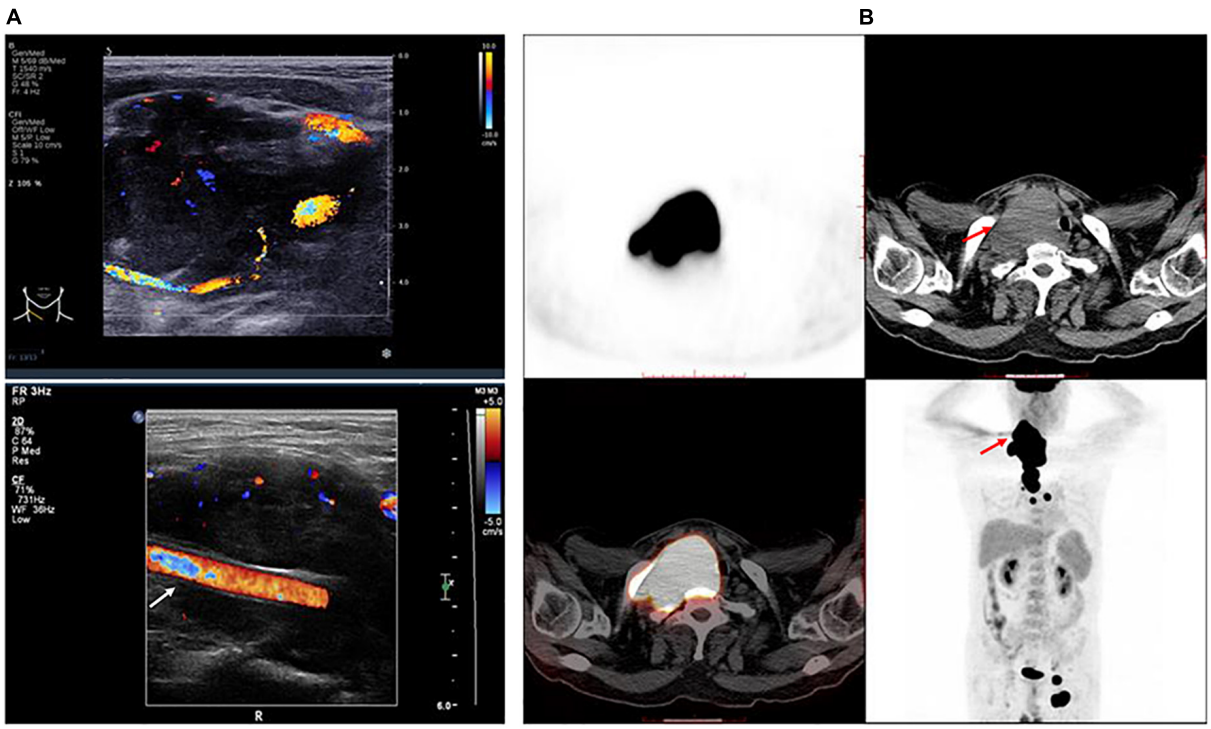

FIGURE 1
Features of the tumor. **(A)** Right neck ultrasonography shows a hypo-echoic region with abundant blood flow surrounding the right common carotid artery, which has normal internal blood flow. White arrow indicates the right common carotid artery. **(B)** The trunk positron emission tomography/computed tomography shows a large mass in the right neck surrounding the adjacent large vessels, which had a non-uniform increase in radioactive uptake. Red arrow indicates the tumor.

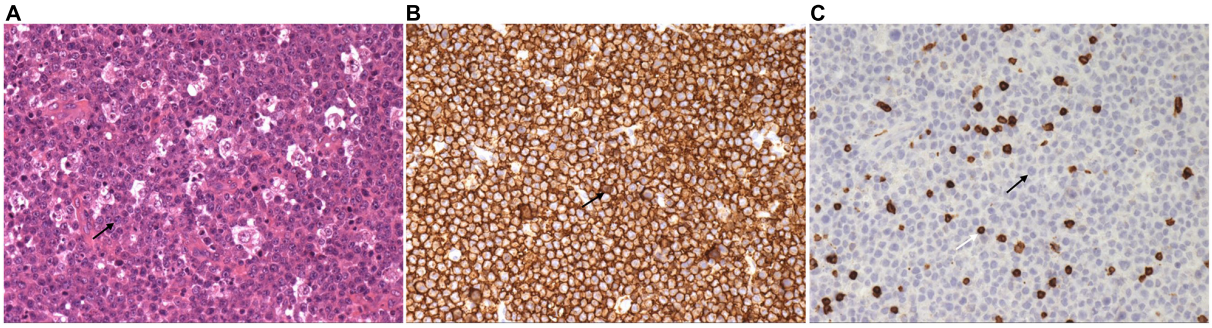

FIGURE 2
Left inguinal lymph node biopsy shows diffuse large B-cell lymphoma. **(A)** Large, round, or ovoid tumor cells are seen, with some cells having an irregularly shaped nuclear membrane. Single large or multiple small nucleoli can be seen in the tumor cells, and nuclear division is more common (H and E, × 200). **(B)** Immunohistochemistry stain of CD 20 shows the tumor cells were uniformly and strongly positive (× 200). **(C)** Immunohistochemistry stain of CD 3 shows the tumor cells are negative, but the T lymphocytes in the background are positive (× 200). Black arrow indicates the tumor cell. White arrow indicates the T lymphocyte.

left side. Although a history of syncope following mechanical manipulation of the carotid sinuses is important, the absence of history does not exclude CSS.

In this case, considering the risk of carotid plaque embolization, carotid sinus massage was not performed. The current European Society of Cardiology guidelines recommend that carotid sinus massage should be avoided in patients with prior transient ischemic attack, stroke or carotid stenosis >70%, seeking to minimize neurological complications. Data was limited about the risk of neurological complications caused by carotid sinus massage in patients with carotid plaque or carotid atherosclerosis. In two prospective study with

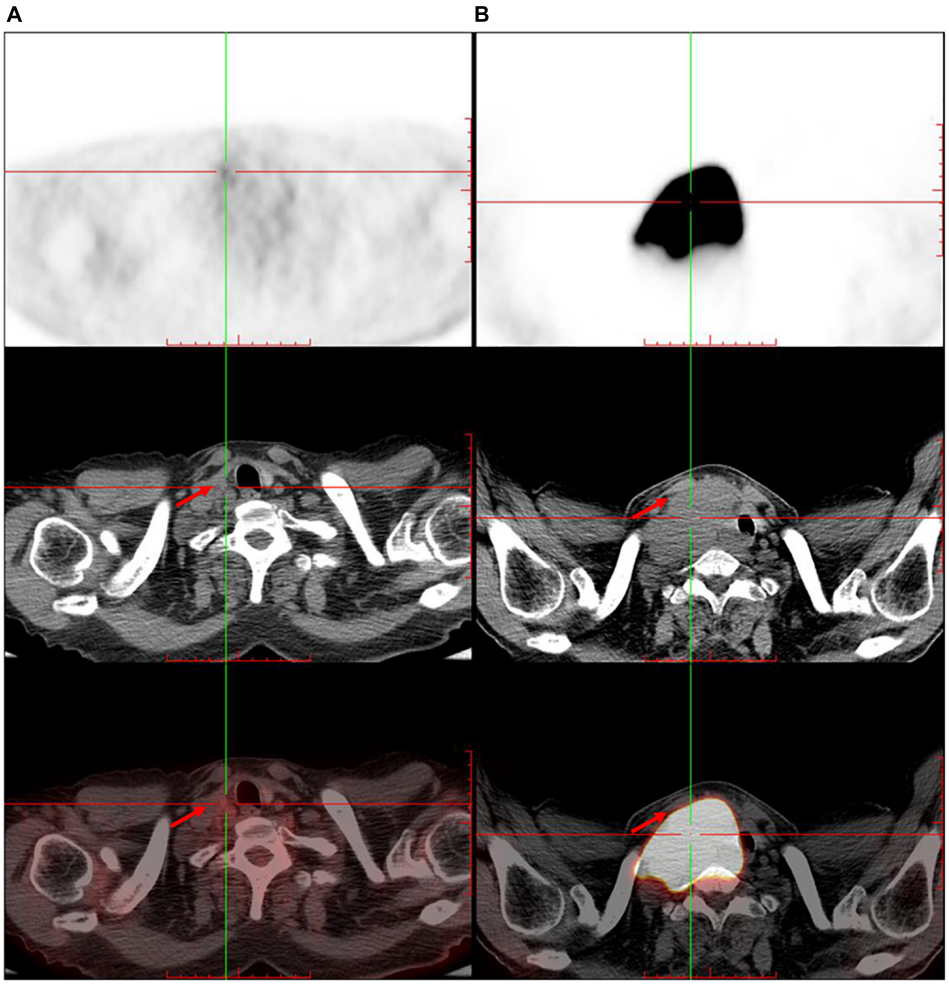

FIGURE 3
The trunk positron emission tomography/computed tomography shows significant shrinkage of the original large mass in the right neck after four cycles of immunochemotherapy. **(A)** After immunochemotherapy for four cycles. **(B)** Before the immunochemotherapy. Red arrow indicates the tumor.

excluding patients with carotid stenosis or history of stoke, the incidence of neurological complications is low. In a prospective series of 1,000 consecutive patients aged 50 or over, only 1% had neurological symptoms during or after carotid sinus massage, such as visual disturbance, sensation of numbness, or leg weakness (10). Most complications were transient, only 0.1% patients had persistent neurological complications. Subsequently, in a prospective study with 1,401 patients (49.5% aged 80 or over), there were no neurological complications occurred during or after carotid sinus massage (11). Although the incidence of neurological complications is low, given the severity of stroke, we should inform the risk-benefit analysis when consenting patients. Therefore, carotid sinus massage should be recommended in patients with high clinical suspicion of carotid sinus syndrome after informing the risk-benefit analysis, regardless of carotid atherosclerosis, but not in patients with carotid stenosis. However, syncope associated with head and neck malignancy is often not reproducible with carotid sinus massage (7).

Additionally, our patient had persistent pain from the post-auricular region to the occipital region, which could have induced syncope. Some case reports described glossopharyngeal neuralgia, a cause of syncope in the head-and-neck tumor patient, characterized by acute unilateral head or neck pain preceding each syncopal episode (12, 13). The syncope produced by glossopharyngeal neuralgia is not completely understood. In our patient, the major mechanism may involve invasion of the glossopharyngeal nerve by malignancy (14). With glossopharyngeal afferent impulses precipitated by mechanical touch, swallowing, or taste in the posterior oropharynx, spillover impulses into the glossopharyngeal reflex arc would result in symptomatic syncope.

TABLE 1 Time line.

One month prior to presentation	• Syncope occurred while walking with prodromes such as dizziness and palpitations. Syncope occurred once a day. • cTnI: <0.1 ng/ml; BNP: 225 pg/ml. ECG: sinus rhythm and a heart rate of 65 beats per minute. Arterial blood pressure monitoring: mean blood pressure 121/76 mmHg (range: 87–161/59–98 mmHg). • Pulmonary artery computed tomography angiography: no thrombosis was observed in pulmonary artery and its branches. • Neuroimaging with CT, magnetic resonance angiography and electroencephalogram: normal. • Magnetic resonance imaging of cervical spine: hyperostosis of cervical 4–7 with narrow intervertebral space and left foramen.
Half 1 month prior to presentation	• Syncope occurred every 2–3 days. The patient developed persistent post-auricular and occipital pain in the morning. When the pain was at its peak, syncope was induced. A new, non-tender neck mass demonstrating progressive enlargement was observed. The patient had an occasional choking cough and dysphagia but no dyspnea. • Seven days-Holter monitor: long intervals and conduction block were not observed without episodes of syncope.
At presentation	Syncope occurred while sitting with prodromes such as dizziness, along with fecal incontinence. After 5–6 min, the patient regained consciousness. • cTnI: <0.017 ng/ml. ECG: sinus rhythm and a heart rate of 98 beats per minute. Continuous tracking with a Holter monitor captured one episode of syncope, which occurred with sinus rhythm and a heart rate of 70 beats per minute. Transthoracic echocardiography: impaired relaxation (mitral E/A ratio, 0.8) with left atrial enlargement and normal systolic function. • A 2-h electroencephalogram: no epileptic seizure during the episode of syncope. Carotid artery ultrasonography: atherosclerotic plaques in bilateral carotid arteries with no stenosis. • Supine and standing blood pressure measurements: normal. Upright tilt-table test: a decrease in arterial blood pressure (>20 mmHg) that reproduced syncope for a duration of 20 s without any change in heart rate. • Neck ultrasonography: a hypo-echoic region with abundant blood flow in the lower middle part of the right neck, surrounding the right common carotid artery. PET/CT: a large soft tissue mass in the right neck, surrounding the adjacent large vessels. Histopathological examination of left inguinal lymph node: diffuse large B-cell lymphoma. • Treatment: rituximab (600 mg), plus cyclophosphamide (1.2 g), doxorubicin (60 mg), vincristine (4 mg), and prednisone (100 mg/day × 5 day) (R-CHOP).
Four months later	• After four cycles of R-CHOP immunochemotherapy, PET/CT revealed that the original large mass in the neck had disappeared. • The patient no longer complained of either syncope or pain from the post-auricular and occipital regions. Choking when eating was also relieved.

cTnI, cardiac troponin I; BNP, type B natriuretic peptide; ECG, electrocardiogram; BP, blood pressure; CT, computed tomography; PCT, positron emission tomography.

Management depends on the type of syncope and its cause. Syncope in patients with head and neck tumors, frequently due to vaso-depression, is under-recognized as in our case (8). Cardiac pacing rarely ameliorates these symptoms. Head and neck tumor debulking and other tumor-targeted treatments may be the best options for relieving syncope. Our patient had no further episodes of syncope after immunochemotherapy for the lymphoma. Similarly, most of the previously reported lymphoma cases also described the successful treatment of syncope after chemotherapy. Symptoms can rapidly respond to treatment of the underlying tumor. In cases with glossopharyngeal neuralgia, antiepileptic drugs or surgical resection of the glossopharyngeal nerve may be an option.

Conclusion

In conclusion, we report a case of neck lymphoma with recurrent syncope as the initial symptom that was successfully relieved by immunochemotherapy. Syncope may be an early or sole sign of neck or head tumor. Hence, we should be aware of the possibility of an underlying malignancy in patients with unexplained syncope after initial evaluation. The diagnostic approach for syncope should include a complete medical history—particularly for tumors—and a detailed physical examination of the head and neck.

Data availability statement

The original contributions presented in this study are included in the article/supplementary material, further inquiries can be directed to the corresponding author.

Ethics statement

Written informed consent was obtained from the participant for the publication of this case report. Written informed consent was obtained from the individual for the publication of any potentially identifiable images or data included in this article.

Author contributions

YW drafted the original manuscript and contributed to the case collection. DY identified by the case and revised the manuscript. LS contributed to the case collection. XX, PG, KC, TC, ZC, YL, and QF contributed to major diagnosis and

treatment. All authors contributed to the article and approved the submitted version.

Funding

The work was supported by the project of Postgraduate Education and Teaching Reform of Peking Union Medical College in 2019 (10023201900111).

Acknowledgments

We are grateful for the hard work of the whole electrophysiology team in the Peking Union Medical College Hospital.

Conflict of interest

The authors declare that the research was conducted in the absence of any commercial or financial relationships that could be construed as a potential conflict of interest.

Publisher's note

All claims expressed in this article are solely those of the authors and do not necessarily represent those of their affiliated organizations, or those of the publisher, the editors and the reviewers. Any product that may be evaluated in this article, or claim that may be made by its manufacturer, is not guaranteed or endorsed by the publisher.

References

1. Brignole M, Moya A, de Lange FJ, Deharo JC, Elliott PM, Fanciulli A, et al. 2018 ESC Guidelines for the diagnosis and management of syncope. *Eur Heart J.* (2018) 39:1883–948. doi: 10.1093/eurheartj/ehy037

2. Solari D, Maggi R, Oddone D, Solano A, Croci F, Donateo P, et al. Clinical context and outcome of carotid sinus syndrome diagnosed by means of the 'method of symptoms'. *Europace.* (2014) 16:928–34. doi: 10.1093/europace/eut283

3. Tannebaum RD. Adult retropharyngeal abscess: A case report and review of the literature. *J Emerg Med.* (1996) 14:147–58. doi: 10.1016/0736-4679(95)02113-2

4. Kim K, Kaur H, Chan M, Balasubramanian M, Gupta S, Jorge VM. An unusual initial presentation of diffuse large B-cell lymphoma as recurrent syncope. *Case Rep Hematol.* (2019) 2019:1082543. doi: 10.1155/2019/1082543

5. Sharudin SN, Huda Al, Firdas AN, Hitam S, Hamid Z, Nordin NJ, et al. Lymphoma with superimposed tuberculosis and fungal infection mimicking parapharyngeal abscess complicated with recurrent neurocardiogenic syncope: A case report. *Malays J Pathol.* (2020) 42:287–91.

6. Casini A, Tschanz E, Dietrich PY, Nendaz M. Recurrent syncope due to esophageal squamous cell carcinoma. *Case Rep Oncol.* (2011) 4:433–8. doi: 10.1159/000331664

7. Macdonald DR, Strong E, Nielsen S, Posner JB. Syncope from head and neck cancer. *J Neurooncol.* (1983) 1:257–67. doi: 10.1007/BF00165610

8. Bauer CA, Redleaf MI, Gartlan MG, Tsue TT, McColloch TM. Carotid sinus syncope in head and neck cancer. *Laryngoscope.* (1994) 104:497–503. doi: 10.1288/00005537-199404000-00018

9. Claassen JA, Jansen RW. Carotid sinus syndrome: Looking sideways is sufficient cause for syncope. *J Am Geriatr Soc.* (2006) 1:188–9. doi: 10.1111/j.1532-5415.2005.00575_17.x

10. Richardson DA, Bexton R, Shaw FE, Steen N, Bond J, Kenny RA. Complications of carotid sinus massage–a prospective series of older patients. *Age Ageing.* (2000) 5:413–7. doi: 10.1093/ageing/29.5.413

11. Ungar A, Rivasi G, Rafanelli M, Toffanello G, Mussi C, Ceccofiglio A, et al. Safety and tolerability of tilt testing and carotid sinus massage in the octogenarians. *Age Ageing.* (2016) 45:242–8. doi: 10.1093/ageing/afw004

12. Krasoudakis A, Anyfantakis D, Hadjipetrou A, Kastanakis M, Symvoulakis EK, Marathianos S. Glossopharyngeal neuralgia associated with cardiac syncope: Two case reports and literature review. *Int J Surg Case Rep.* (2015) 12:4–6. doi: 10.1016/j.ijscr.2015.05.007

13. Banerjee C, Viers A, Vender J. Glossopharyngeal neuralgia/neuropathy with hemodynamic instability and associated syncope treated with stereotactic radiosurgery. *World Neurosurg.* (2020) 139:314–7. doi: 10.1016/j.wneu.2020.04.130

14. Papay FA, Roberts JK, Wegryn TL, Gordon T, Levine HL. Evaluation of syncope from head and neck cancer. *Laryngoscope.* (1989) 99:382–8. doi: 10.1288/00005537-198904000-00004

frontiers | Frontiers in Oncology

TYPE Case Report
PUBLISHED 25 August 2022
DOI 10.3389/fonc.2022.956236

Check for updates

OPEN ACCESS

EDITED BY
Carlo Gabriele Tocchetti,
University of Naples Federico II, Italy

REVIEWED BY
Jesus Arriaga-Caballero,
Centro del pie del diabético, Mexico
Yi-yan Lu,
Aerospace Center Hospital, China

*CORRESPONDENCE
Guang-Wei Zhang
gwzhang@cmu.edu.cn

†These authors share first authorship

SPECIALTY SECTION
This article was submitted to Cardio-Oncology, a section of the journal Frontiers in Oncology

RECEIVED 30 May 2022
ACCEPTED 18 July 2022
PUBLISHED 25 August 2022

CITATION
Xiang K, Liu L, Li H-J and Zhang G-W (2022) Rare pulmonary embolism in a pregnant patient: A primary diffused pulmonary artery myxofibrosarcoma case report.
Front. Oncol. 12:956236.
doi: 10.3389/fonc.2022.956236

COPYRIGHT
© 2022 Xiang, Liu, Li and Zhang. This is an open-access article distributed under the terms of the Creative Commons Attribution License (CC BY). The use, distribution or reproduction in other forums is permitted, provided the original author(s) and the copyright owner(s) are credited and that the original publication in this journal is cited, in accordance with accepted academic practice. No use, distribution or reproduction is permitted which does not comply with these terms.

Rare pulmonary embolism in a pregnant patient: A primary diffused pulmonary artery myxofibrosarcoma case report

Kanghui Xiang[1,2,3,4†], Lu Liu[5†], Hui-Jun Li[6] and Guang-Wei Zhang[7*]

[1]Department of Medical Oncology, The First Hospital of China Medical University, Shenyang, China, [2]Key Laboratory of Anticancer Drugs and Biotherapy of Liaoning Province, The First Hospital of China Medical University, Shenyang, China, [3]Liaoning Province Clinical Research Center for Cancer, The First Hospital of China Medical University, Shenyang, China, [4]Key Laboratory of Precision Diagnosis and Treatment of Gastrointestinal Tumors, Ministry of Education, The First Hospital of China Medical University, Shenyang, China, [5]Department of Cardiac Surgery, The First Hospital of China Medical University, Shenyang, China, [6]Shenyang Medical and Film Science and Technology Co. Ltd., Shenyang, China, [7]Smart Hospital Management Department, The First Hospital of China Medical University, Shenyang, China

A 37-year-old female patient presented with shortness of breath, cough, and chest pain complaints from the 12th week of her first pregnancy. At the 28th week, labor induction had to be performed because of severe dyspnea and hyoxemia. Thereafter, a diffused pulmonary embolism was detected by echocardiography and CT angiography, without histological diagnosis. Pulmonary endarterectomy was performed, and it was found during operation that a huge, lobular mass originated in the posterior wall and extended throughout the vasculature of both lungs, and a mucinous pellicle covered the entire pulmonary endothelium. Pathology revealed a low-grade myxofibrosarcoma with positive vimentin and SMA, partially positive CD-34.

KEYWORDS

pulmonary embolism, low-grade myxofibrosarcoma, pregnancy, operation, ECMO - extracorporeal membrane oxygenation

Introduction

Low-grade myxofibrosarcoma (LGMFS) is a low-grade malignant mesenchymal tumor, which usually arises in the extremities of 60–80-year-old patients and rarely originates in the pulmonary artery of young patients. Thereby, it is often misdiagnosed as chronic pulmonary thromboembolism. Furthermore, surgical operation for these patients is still a challenge. Here, we report a rather rare case with incidence of LGMFS during pregnancy.

Case report

A 37-year-old female patient presented with shortness of breath, cough, and chest pain complaints from the 12th week of her first pregnancy. However, no special examination or treatment was performed. Thereafter, these symptoms were gradually worsened. At the 28th week of pregnancy, labor induction had to be performed because of severe dyspnea and hyoxemia. Two weeks later, she was admitted to our hospital for continually aggravated symptoms. She reported an apparent distress at rest but no syncope, palpitations, lower-extremity edema, weight loss, fever, rashes, or arthritis. There was a history of hysteromyoma defined by transvaginal ultrasound but no history of tobacco, estrogen, appetite suppressant, or illicit drug use, deep-venous thrombosis, or familial pulmonary hypertension or thromboembolic disease. No positive sign was found in physical examination.

Chest radiography showed patchy alveolar opacities in both lower lobes, right-ventricular enlargement, and prominent central pulmonary artery. Echocardiography revealed a lobulated mass occupying attached by a pedicle to the posterior wall of the main pulmonary artery, a right-ventricular enlargement with an estimated pulmonary artery systolic pressure of 79 mmHg and normal left ventricular size and function. Subsequently, diffuse pulmonary embolism was detected by CT angiography (Figure 1). Electrocardiography (ECG) evidenced Wolff–Parkinson–White syndrome. Lower-extremity duplex ultrasonography was negative. Laboratory analysis results showed white blood cell count (WBC) 13.66 KU/l, erythrocyte sedimentation rate (ESR) 66 mm/h, C-reactive protein (CRP) 86.3 mg/l, and D-dimer 1,378 μg/l. Moreover, cancer antigen (CA)-125, CA-15-3, CA-19-9, and carcinoembryonic antigen (CEA) results were normal.

The operation was performed at undiagnosed conditions, due to severe dyspnea and hyoxemia. Femoral cannulation of cardiopulmonary bypass (CPB) was performed for preparation of possible ECMO. When the pulmonary trunk was incised, it was found that a huge, lobular mass originated in the posterior wall and extended throughout the vasculature of both lungs, and a mucinous pellicle covered the entire pulmonary endothelium (Figure 2). Because the tumor has invaded into subsegmental and distal arteries, it was impossible for a complete resection. Deep hypothermic circulatory arrest (DHCA) was used for better exposure to resect more tumor tissue in distal pulmonary arteries. The patient suffered from a severe pneumorrhagia, immediately following aortic cross-clamp opening. Therefore, it was difficult for withdrawal of CPB and the patient had to undergo ECMO support. Seven and 10 days after operation, ECMO and tracheal intubation were removed, respectively. Pathology revealed a LGMFS with positive vimentin and SMA, partially positive CD-34, and negative CK-3, CK-5, desmin, and s-100. HE staining showed that spindle cells proliferated and were crowded, with myxoid stroma around them. The percentage of Ki-67-positive cells was about 30% (Figure 3). A subtotal resection was confirmed by postoperative CT angiography and echocardiography (Figure 4). Twenty-two days postoperatively, the patient was discharged with a good recovery, followed by chemotherapy (pazopanib) and lung radiotherapy. Two years after operation, the patient reported that she had no obvious respiratory symptoms, but unfortunately refused CT or echocardiography examination, and thereafter was lost to follow-up due to poor compliance.

Discussion

Pulmonary thromboembolism is a common complication after pregnancy (1). The patient had similar medical histories and significantly increased D-dimer, which supported that diagnosis. However, echocardiography found a lobulated mass occupying in the pulmonary trunk, increasing three probabilities of diagnosis, namely, benign myxoma, malignant sarcoma, and myxoma combined with thromboembolism. In addition, uterine leiomyosarcoma cannot be also excluded, due to a past

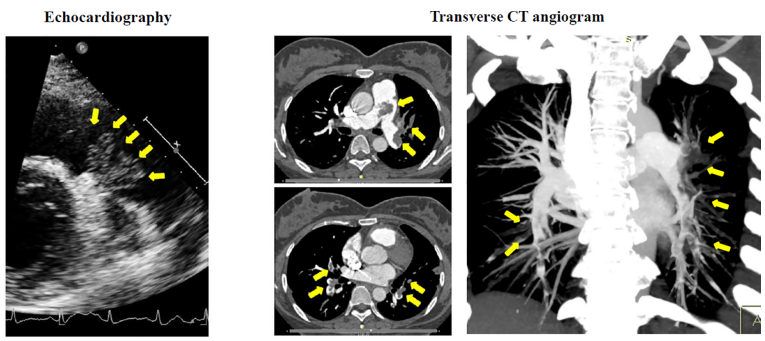

FIGURE 1
Preoperative echocardiography demonstrated a large lobulated mass (arrows) attached by a pedicle to the posterior wall of pulmonary truck. Transverse CT angiogram revealed a diffused occlusion of both pulmonary arteries (arrows).

FIGURE 2
It is proved during operation that a huge, lobular mass originated in the pulmonary trunk, diffuse growth into both pulmonary arteries was observed, and the entire pulmonary endothelium was covered by a thin mucinous pellicle.

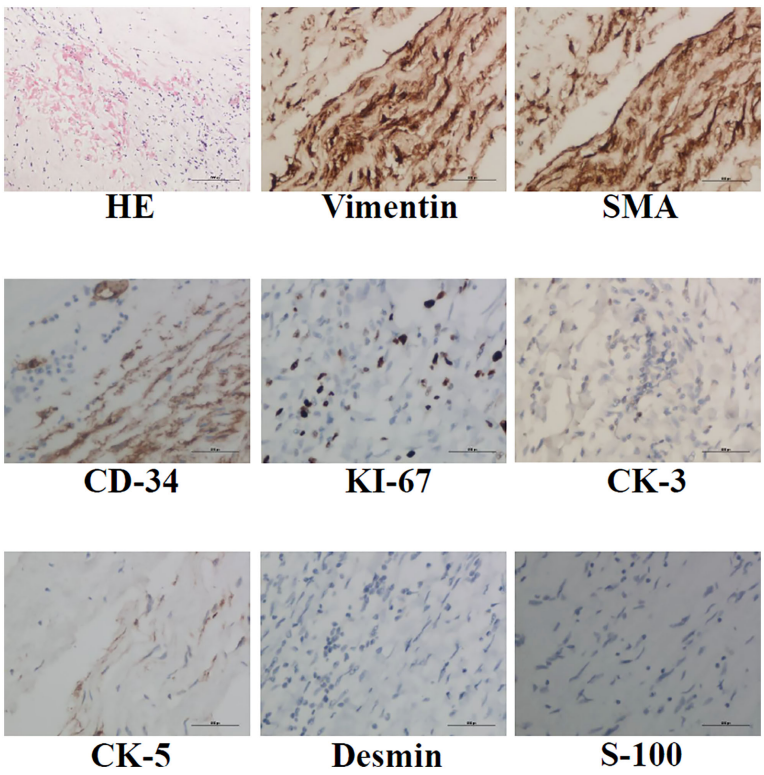

FIGURE 3
HE, anti-vimentin, SMA, CD-34, CK-3, CK-5, desmin and s-100 immunohistochemistry staining was performed to identify LGMFS.

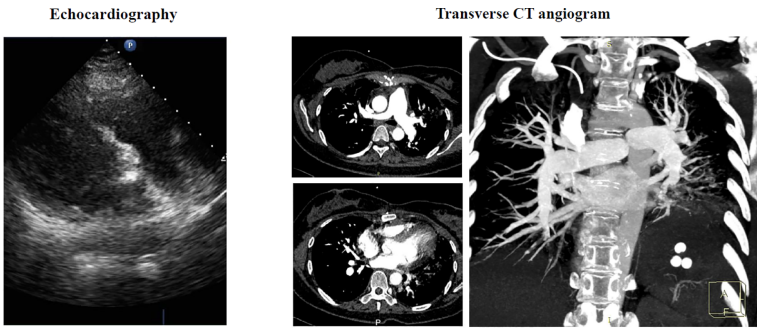

FIGURE 4
Postoperative echocardiography and transverse CT angiogram showed that most tumor tissue of both lungs has been resected with a little residual occlusion.

history of hysteromyoma. In CT scan views, however, there is no a significant wall eclipsing sign as described by Gan et al. (2), no contrast enhancement of the mass and extravascular spread of the lesion as described by Scheffel et al. (3), or no other characteristic signs of malignant sarcoma. Therefore, the diagnosis was rather confused before operation.

Because of the similar clinical presentations and no specific biomarker, it is very difficult to differentiate pulmonary artery tumor and thromboembolism without histological diagnosis, which is often impossible preoperatively (2), so that most pulmonary artery tumor patients were misdiagnosed with thromboembolism before surgical intervention, consequently receiving inappropriate therapeutic strategies such as long-term anticoagulant treatment (2, 3). Therefore, regardless of whether it is benign or malignant, it is suggested that the patients with a severe pulmonary embolism should undergo operation (4, 5). This is because the median survival of time of untreated patients after diagnosis of malignant tumor is only several months (range 1.5–5.5 months) (6, 7), which can be significantly increased by surgical treatment, even to 5–10 years reported by Tavora et al. (8).

Due to better prognosis in patients with complete resections than incomplete resections (8), it is advocated that DHCA should be used to for a clear exposure for a more complete resection of LGMFS in distal pulmonary arteries. The pulmonary artery hypertension from chronic embolism and endothelial injury from surgical procedure severely damages heart and lung function, which usually needs ECMO support (9). Thus, femoral cannulation is a reasonable choice, fulfilling a direct conversion from CPB to ECMO without re-cannulating. It is suggested that chemotherapy and lung radiotherapy were performed after surgical resection to prevent recurrence, although the role of these methods is still controversial and the outcome is uncertain (10, 11).

It has been reported that vimentin and SMA are used for identification of myxofibrosarcoma. In this patient, besides the tumor cells being vimentin and SMA positive, these cells partially expressed CD-34, perhaps representing a novel myxofibrosarcoma cell line or suggesting a conversion from myxofibrosarcoma cells to endothelial cells. Similar reports are absent.

Data availability statement

The raw data supporting the conclusions of this article will be made available by the authors, without undue reservation.

Ethics statement

Written informed consent was obtained from the individual(s) for the publication of any potentially identifiable images or data included in this article.

Author contributions

KX carried out data collection and immunohistochemical analysis. LL and G-WZ participated in clinical treatment. H-JL and G-WZ drafted the manuscript. All authors read and approved the final manuscript.

Conflict of interest

Author H-JL was employed by Shenyang Medical and Film Science and Technology Co. Ltd., Shenyang, China.

The remaining authors declare that the research was conducted in the absence of any commercial or financial relationships that could be construed as a potential conflict of interest.

Publisher's note

All claims expressed in this article are solely those of the authors and do not necessarily represent those of their affiliated organizations, or those of the publisher, the editors and the reviewers. Any product that may be evaluated in this article, or claim that may be made by its manufacturer, is not guaranteed or endorsed by the publisher.

References

1. Donnelly JC, D'Alton ME. Pulmonary embolus in pregnancy. *Semin Perinatol* (2013) 37(4):225–33. doi: 10.1053/j.semperi.2013.04.002

2. Gan HL, Zhang JQ, Huang XY, Yu W. The wall eclipsing sign on pulmonary artery computed tomography angiography is pathognomonic for pulmonary artery sarcoma. *PLoS One* (2013) 8(12):e83200. doi: 10.1371/journal.pone.0083200

3. Scheffel H, Stolzmann P, Plass A, Weber A, Pretre R, Marincek B, et al. Primary intimal pulmonary artery sarcoma: a diagnostic challenge. *J Thorac Cardiovasc Surg* (2008) 135(4):949–50. doi: 10.1016/j.jtcvs.2007.11.041

4. Athanassiadi K, Grothusen C, Mengel M, Haverich A. Primary leiomyosarcoma of the pulmonary artery: Is aggressive treatment justified for a long survival? *J Thorac Cardiovasc Surg* (2006) 132(2):435–6. doi: 10.1016/j.jtcvs.2006.02.057

5. Huo L, Moran CA, Fuller GN, Gladish G, Suster S. Pulmonary artery sarcoma: A clinicopathologic and immunohistochemical study of 12 cases. *Am J Clin Pathol* (2006) 125(3):419–24. doi: 10.1309/9H8RHUV1JL1WE0QF

6. Kruger I, Borowski A, Horst M, de Vivie ER, Theissen P, Gross-Fengels W. Symptoms, diagnosis, and therapy of primary sarcomas of the pulmonary artery. *Thorac Cardiovasc Surg* (1990) 38(2):91–5. doi: 10.1055/s-2007-1014001

7. Nonomura A, Kurumaya H, Kono N, Nakanuma Y, Ohta G, Terahata S, et al. Primary pulmonary artery sarcoma. report of two autopsy cases studied by immunohistochemistry and electron microscopy, and review of 110 cases reported in the literature. *Acta Pathol Jpn* (1988) 38(7):883–96. doi: 10.1111/j.1440-1827.1988.tb02360.x

8. Tavora F, Miettinen M, Fanburg-Smith J, Franks TJ, Burke A. Pulmonary artery sarcoma: a histologic and follow-up study with emphasis on a subset of low-grade myofibroblastic sarcomas with a good long-term follow-up. *Am J Surg Pathol* (2008) 32(12):1751–61. doi: 10.1097/PAS.0b013e31817d7fd0

9. Omar HR, Miller J, Mangar D, Camporesi EM. Experience with extracorporeal membrane oxygenation in massive and submassive pulmonary embolism in a tertiary care center. *Am J Emerg Med* (2013) 31(11):1616–7. doi: 10.1016/j.ajem.2013.08.013

10. DeAndrade DS, Kilic A, Christie NA, Sultan I. Aggressive invasive recurrence of a right atrial myxofibrosarcoma. *J Card Surg* (2019) 34(4):223–5. doi: 10.1111/jocs.14014

11. Vanni S, De Vita A, Gurrieri L, Fausti V, Miserocchi G, Spadazzi C, et al. Myxofibrosarcoma landscape: diagnostic pitfalls, clinical management and future perspectives. *Ther Adv Med Oncol* (2022) 14:17588359221093973. doi: 10.1177/17588359221093973

frontiers | Frontiers in Oncology

TYPE Case Report
PUBLISHED 23 September 2022
DOI 10.3389/fonc.2022.1014371

Check for updates

OPEN ACCESS

EDITED BY
Reto Asmis,
Wake Forest School of Medicine,
United States

REVIEWED BY
Jian Zhu,
General Hospital of Central Theater Command, China
Su Yao,
Guangdong Provincial People's Hospital, China

*CORRESPONDENCE
Jianghua Li
75090935@qq.com
Shaohong Dong
dsh266@outlook.com

SPECIALTY SECTION
This article was submitted to Cardio-Oncology, a section of the journal Frontiers in Oncology

RECEIVED 08 August 2022
ACCEPTED 09 September 2022
PUBLISHED 23 September 2022

CITATION
Li J, Liu Q, Peng Q and Dong S (2022) Diagnosis of rapidly progressed primary cardiac lymphoma in liver transplant recipient: A case report. *Front. Oncol.* 12:1014371. doi: 10.3389/fonc.2022.1014371

COPYRIGHT
© 2022 Li, Liu, Peng and Dong. This is an open-access article distributed under the terms of the Creative Commons Attribution License (CC BY). The use, distribution or reproduction in other forums is permitted, provided the original author(s) and the copyright owner(s) are credited and that the original publication in this journal is cited, in accordance with accepted academic practice. No use, distribution or reproduction is permitted which does not comply with these terms.

Diagnosis of rapidly progressed primary cardiac lymphoma in liver transplant recipient: A case report

Jianghua Li[1]*, Qiyun Liu[1], Quanzhou Peng[2] and Shaohong Dong[1]*

[1]Department of Cardiology, Shenzhen Cardiovascular Minimally Invasive Medical Engineering Technology Research and Development Center, Shenzhen People's Hospital, Shenzhen, China, [2]Department of Pathology, Shenzhen People's Hospital, Shenzhen, China

Primary cardiac lymphomas (PCLs) are extremely rare and affect the heart. Patients with PCLs usually have delayed diagnosis and treatment. As a consequence, their prognosis is quite unfavorable, and their median survival is approximately 7 months. Herein, we report a 64-year-old man who underwent liver transplantation, presented with chest pain and exertional dyspnea, developed a huge cardiac mass within 2 months and passed away on day 3 of hospitalization. Histological examination revealed diffuse large B-cell lymphoma (DLBCL), which is a rare cardiac tumor with a poor prognosis. In this case, DLBCL was only detected postmortem. The extension of the mass and its relationship with the heart were explored with non-invasive cardiac imaging. Despite the rarity of DLBCL, it should be considered in the differential diagnosis of cardiac tumors.

KEYWORDS

immunocompromised patient, primary cardiac lymphoma (PCL), case report, MRI, echocardiography, lymph node biopsy

Introduction

Primary cardiac lymphomas (PCLs) are an extremely rare type of non-Hodgkin's lymphoma (NHL) and account for less than 0.01% of all heart tumors (1). PCLs originate in the heart or pericardium and are often diagnosed postmortem (2).

PCLs are frequently observed in immunosuppressed patients (3). The right heart is more susceptible than the left heart (4), and the presentation of patients can be diverse, including congestive heart failure, cardiac tamponade, pericardial effusions, and even death (4). Diffuse large B-cell lymphoma (DLBCL) is the most common pathological of PCLs. Here, we present a case of PCL diagnosed in a subject who passed away on day 3 of

hospitalization. This case will enhance the concept that differential diagnosis of cardiac tumors should be considered in clinical practice.

Case description

As shown in Table 1, a 64-year-old man presented with progressive atypical chest pain and exertional shortness of breath for 2 months. He had a history of liver cancer in 2010 and had undergone liver transplantation. Since then, he had regularly consumed immunosuppressive drugs. In addition, he was diagnosed with hypertension 2 years ago and paroxysmal atrial fibrillation 0.5 years before. He underwent transthoracic echocardiography (TTE), coronary artery computed tomography, left ventriculography, and coronary angiography (data not shown) in another hospital 2 months before the current hospitalization. No remarkable abnormality was found.

No other substantial medical history was reported, and his medication list was as follows: 150 mg/day of irbesartan, 15 mg/day of rivaroxaban, 200 mg/day of amiodarone, and 1 mg/day of tacrolimus. The patient was referred to our hospital for further comprehensive examination due to progressive chest tightness. He denied pleuritic chest pain and had no reports of cough, sputum production, fever, or night sweats.

He had a regular rhythm at a rate of 67 bpm, normal blood pressure (114/80 mmHg), a respiratory rate within normal limits (16 breaths/min), oxygen saturation of 97% in room air, and tympanic temperature of 36.5°C. No remarkable murmur was found in cardiac auscultation. Respiratory and abdominal examinations had no positive findings.

His N-terminal pro-B-type natriuretic peptide (NT-proBNP) concentration was 9,100 pg/ml with a normal renal function. His arterial blood gas test indicated 76 and 30.6 mmHg of PaO_2 and $PaCO_2$, respectively. C-reactive protein increased to 81.8 mg/L (normal value of <5), and his erythrocyte sedimentation rate was 36 mm/h (normal values of 0–15). Hepatitis B surface antigen (HbsAg) and hepatitis B core antibody (HbcAb) were positive. HBV DNA was 4.37×10^4 ($<1 \times 10^2$), and CA125 was 51.13 U/ml (normal value of <35). His anti-HIV test result was negative. He was diagnosed with acute heart failure because of the high NT-proBNP level, and a negative clinical response was obtained with the intravenously administered diuretic.

On day 2 of hospitalization, TTE and transesophageal echocardiography (TEE) showed a mass measuring 62 mm × 39 mm originating from the right atrium and right ventricle (Figure 1). It was a lobulated, poorly mobile mass that partially occupied the right atrium and partly occupied and occluded the tricuspid, hampering the blood flow to the right ventricle, even though a chest CT scan showed no mass in the right heart 2 months before (Figure 2A). In the following magnetic resonance imaging (MRI), the visualization of the mass and its extension improved, demonstrating a large poorly mobile heterogeneous mass obliterating the right atrium cavity. It also revealed the mass infiltration of the surrounding myocardium, with mild pericardial and pleural effusion (Figures 2B,C). Myocardial contrast echocardiography and left ventricular opacification revealed that a large filling defect invaded the anterior wall of the right atrium and right ventricle (Figures 2D-F). The patient was then subjected to a lymph node biopsy to examine the mass.

Unfortunately, on day 3, before his chest contrast-enhanced computed tomography artery scan was scheduled, he passed away because of hemodynamic collapse. The tissue collected from the lymph node showed a diffuse infiltrate consisting predominantly of large atypical lymphoid cells (Figure 2G) and blasts of B-cell lineage (CD20, B-cell marker) (Figure 2H); other immunohistochemical pictures, such as BCL6, CD3, CD5, MUM1, CD10, CD30, and c-Myc, were all negative (Figures 2I-O). The presence of Epstein–Barr virus (EBV) infection was identified using *in situ* hybridization (ISH) for the detection of EBV-encoded small RNA (EBER) in biopsy tissue samples, which was negative as well (Figure 2P). A diagnosis of DLBCL was made (Figures 2G-I). In this case, standard biosecurity and institutional safety procedures have been followed.

TABLE 1 Timeline of the case: The crucial events in this case.

Timeline of the case

12 years before	Diagnosed with liver cancer, received liver transplantation, and consumed immunosuppressive drugs.
2 months before	Presented atypical chest pain and exertional shortness of breath, and no certain cause was found.
Day 1	Diagnosed with acute heart failure for remarkably increased NT-proBNP concentration, and a negative clinical response was obtained with the intravenously administered diuretic.
Day 2	TTE and TEE were performed; a lobulated, poorly mobile mass was detected; and MRI and lymph node biopsy were performed to evaluate the cardiac mass.
Day 3	The patient underwent hemodynamic collapse and died.

NT-proBNP, N-terminal pro-B-type natriuretic peptide; TTE, transthoracic echocardiography; TEE, transesophageal echocardiography.

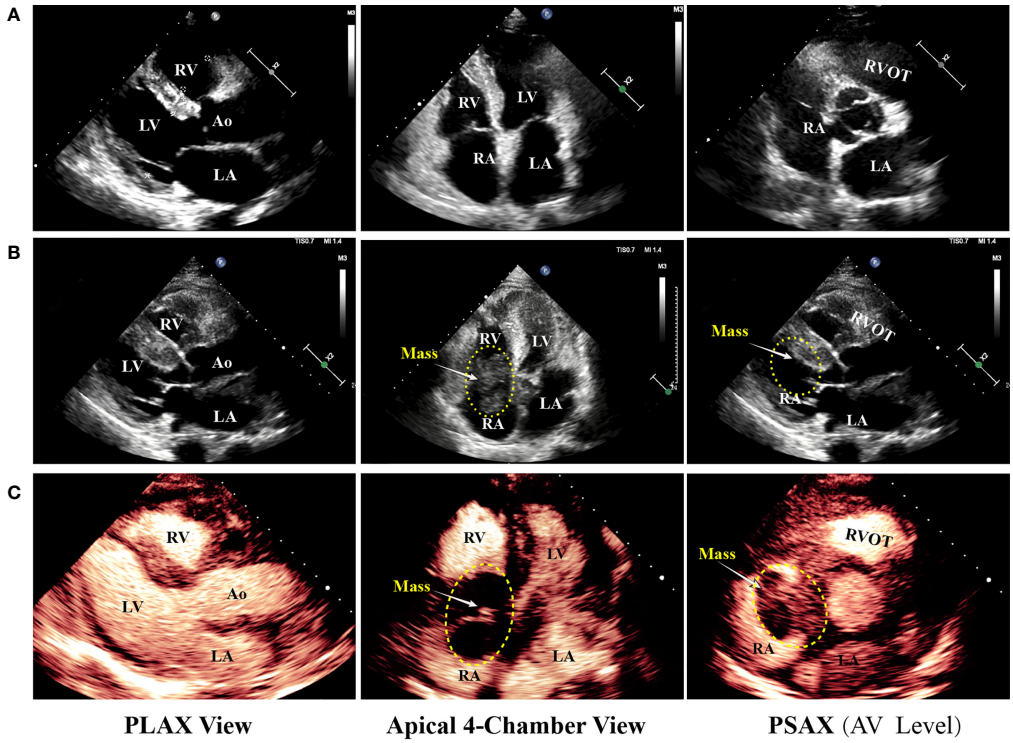

FIGURE 1
Echocardiography progression of the patient. **(A)** The patient underwent echocardiography 2 months prior to the present hospitalization, and no remarkable abnormality was revealed. **(B, C)** Regular TTE and myocardial contrast echocardiography showing tumor extending from the right atrium to the right ventricle through the tricuspid valve. LA, left atrium; LV, left ventricle; RA, right atrium; RV, right ventricle; Ao, aorta; RVOT, right ventricular outflow tract; PLAX, parasternal long axis; PSAX, parasternal short axis; AV, aortic valve.

Discussion

Our patient is an extremely rare case with a cardiac mass who passed away within 3 days and was diagnosed with PCL postmortem. PCLs are rare cardiac neoplasms that are more frequently found in immunocompromised patients with a median age of 63 years at diagnosis, and the right heart is predominantly affected (3). DLBCL often presents dyspnea, followed by constitutional symptoms and chest pain, and is the most common pathological variant of PCL. Approximately 47% of patients diagnosed with PCL have congestive heart failure resistant to standard heart failure treatment (5).

Multiple cardiovascular advanced imaging modalities can help to morphologically examine the cardiac mass. Echocardiography (Figures 1, 2E,F) is usually the first-line diagnostic test, and its sensitivity in detecting masses is more than 90%. Furthermore, MRI is superior to TTE and TEE in the examination of myocardial and pericardial thickening (1). In addition, a CT scan can help characterize the extent of the mass. For patients with cardiac tumors, the prognosis depends on the type of neoplasms. Patients with PCL have a median survival of 7 months (4), and most patients pass away within a couple of months after diagnosis. Given the severe prognosis of PCLs, early diagnosis and treatment are crucial for these patients.

In our case, 2 months prior to the present hospitalization, the patient was admitted to another hospital and subjected to a CT scan, left ventriculography, and coronary angiography. No remarkable occlusion was detected. However, 2 months later, a large neoplasm in his right atrium was found by TTE, TEE, and MRI. The mass caused cardiac failure and serious hemodynamic abnormality. Unfortunately, the patient underwent hemodynamic collapse and expired on day 3 in our center.

The most common causes of death are intractable heart failure, sepsis, lymphoma progression, arrhythmias, and sudden cardiac death (4). Some potential mechanisms contribute to this unfavorable outcome. First, the obstruction of blood flow and cardiac valve dysfunction may lead to circulation collapse (6); furthermore, arrhythmia is often caused by neoplasm infiltration into the conduction system of the heart. Excessive pericardial effusion usually results in circulatory failure. In the presented case, our patient did not exhibit a notable atrioventricular block or remarkable pericardial effusion but experienced tricuspid valve occlusion and sudden death. Under this condition,

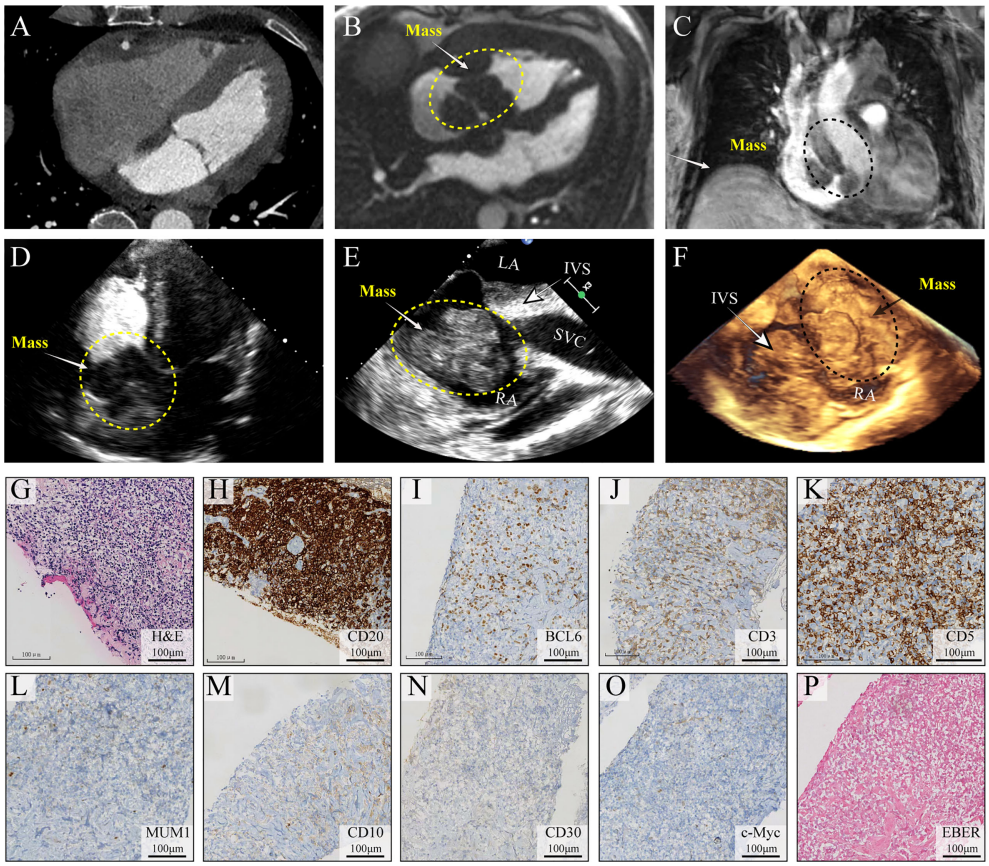

FIGURE 2
Multimodality medical imaging diagnosis and histopathological examination of the mass. **(A)** Computed tomography obtained 2 months before showed no mass in the right heart. **(B, C)** Cine MRI demonstrated a large infiltrating mass extending in the right atrium and ventricle, occupying most of the right atrium. **(D–F)** Left ventricular opacification, TEE, and 3D ultrasonic imaging of the morphological feature of the mass. **(G–O)** Histological examination of the lymph node, H&E, CD20, BCL6, CD3, CD5, MUM1, CD10, CD30, and c-Myc, **(P)** EBV infection was identified using *in situ* hybridization (ISH) for the detection of EBV-encoded small RNA (EBER) EBER staining. IVS, interventricular septum; TEE, transesophageal echocardiography; EBV, Epstein–Barr virus.

traditional diuretics should be cautiously used for this group of patients.

Histopathological examination is the gold standard for the pathological variant of PCL confirmation. More invasive diagnostic procedures, such as cardiac catheterization with echocardiography-guided transvenous biopsy, are required. DLBCL is the most common pathological type of PCL. Its incidence is relatively high in immunocompromised individuals, especially for subjects with AIDS or transplant recipients. In our case, the patient underwent liver translation and received an immunosuppressive agent daily. According to studies that reevaluated reported PCL cases over the past several decades, management has been very variable, and no accepted standard of care has been established (3, 7). According to reports, surgical procedures were given in as many as 29% of the PCL cases that had been investigated (8). However, data from the SEER Program imply that surgical resection is not associated with improved survival in PCL. Chemotherapy was the most common treatment option and was linked to improved survival (9). Consistent with a previous experience, our finding showed an unexpected rapid disease progression. Delayed diagnosis is often correlated with poor outcome because of tumor invasion. Although PCL has no standardized therapy, a chemotherapy regimen with rituximab, cyclophosphamide, hydroxydaunorubicin, vincristine, and prednisone is recommended for this group of patients. Radiotherapy and surgery are given as complementary treatments.

Conclusions

PCL is a rare cardiac tumor, and its aggressive form is DLBCL. Its early diagnosis and treatment are essential owing to

its poor prognosis. Immunocompromised patients are susceptible to this kind of cardiac tumor. The extension of a mass and its relationship with the heart should be explored through non-invasive cardiac imaging. Despite the rarity of DLBCL, its differential diagnosis as a cardiac tumor should be considered.

Data availability statement

The original contributions presented in the study are included in the article/supplementary material. Further inquiries can be directed to the corresponding authors.

Ethics statement

This study was reviewed and approved by the Institutional ethics committee of Shenzhen People's Hospital. The patients/participants provided their written informed consent to participate in this study. Written informed consent was obtained from the individual(s) for the publication of any potentially identifiable images or data included in this article.

Author contributions

JL wrote the manuscript with support from QL and QP. JL and SD contributed to the conception of the study. All authors contributed to manuscript revision, read, and approved the submitted version.

Funding

This study was supported by the Medical Scientific Research Foundation of Guangdong Province of China (No. A2018530), Sanming Project of Medicine in Shenzhen (No. SZSM201412012), and Shenzhen Key Medical Discipline Construction Fund (No. szxk003). Shenzhen People's Hospital Research Cultivation Project (SYLCYJ202119) to JL.

Conflict of interest

The authors declare that the research was conducted in the absence of any commercial or financial relationships that could be construed as a potential conflict of interest.

Publisher's note

All claims expressed in this article are solely those of the authors and do not necessarily represent those of their affiliated organizations, or those of the publisher, the editors and the reviewers. Any product that may be evaluated in this article, or claim that may be made by its manufacturer, is not guaranteed or endorsed by the publisher.

References

1. Ceresoli GL, Ferreri AJ, Bucci E, Ripa C, Ponzoni M, Villa E. Primary cardiac lymphoma in immunocompetent patients: Diagnostic and therapeutic management. *Cancer* (1997) 80:1497–506. doi: 10.1002/(SICI)1097-0142(19971015)80:8<1497::AID-CNCR18>3.0.CO;2-0

2. Morgan HP, El-Nayir M, Jenkins C, Campbell PG. Complete heart block as a herald sign for cardiac lymphoma. *BMJ Case Rep* (2021) 14. doi: 10.1136/bcr-2020-239356

3. Petrich A, Cho SI, Billett H. Primary cardiac lymphoma: An analysis of presentation, treatment, and outcome patterns. *Cancer* (2011) 117:581–9. doi: 10.1002/cncr.25444

4. Singh B, Ip R, Ibrahim Al-Rajjal A, Kafri Z, Al-Katib A, Hadid T. Primary cardiac lymphoma: Lessons learned from a long survivor. *Case Rep Cardiol* (2016) 2016:7164829. doi: 10.1155/2016/7164829

5. Skalec K, Litwin L, Drozdz K, Gac P, Jazwiec P, Chabowski M, et al. Primary cardiac lymphoma (PCL) - diagnostic difficulties. *Kardiochirurgia i torakochirurgia polska = Polish J cardio-thoracic Surg* (2015) 12:266–8. doi: 10.5114/kitp.2015.54468

6. Zhu J, Jiang W, Dong YQ, Zhu SB. A high-grade pleomorphic sarcoma in left atrium. *J Thorac Oncol* (2015) 10:535–6. doi: 10.1097/JTO.0000000000000377

7. Carras S, Berger F, Chalabreysse L, Callet-Bauchut E, Cordier JF, Salles G, et al. Primary cardiac lymphoma: Diagnosis, treatment and outcome in a modern series. *Hematological Oncol* (2017) 35:510–9. doi: 10.1002/hon.2301

8. Chalabreysse L, Berger F, Loire R, Devouassoux G, Cordier JF, Thivolet-Bejui F. Primary cardiac lymphoma in immunocompetent patients: A report of three cases and review of the literature. *Virchows Archiv* (2002) 441:456–61. doi: 10.1007/s00428-002-0711-0

9. Yin K, Brydges H, Lawrence KW, Wei Y, Karlson KJ, McAneny DB, et al. Primary cardiac lymphoma. *J Thorac Cardiovasc Surg* (2022) 164:573–580.e1. doi: 10.1016/j.jtcvs.2020.09.102

frontiers | Frontiers in Cardiovascular Medicine

TYPE Case Report
PUBLISHED 23 September 2022
DOI 10.3389/fcvm.2022.900309

Check for updates

OPEN ACCESS

EDITED BY
Carmine Pizzi,
University of Bologna, Italy

REVIEWED BY
Lian-Ming Wu,
Shanghai Jiao Tong University, China
Francesco Angeli,
University of Bologna, Italy

*CORRESPONDENCE
Zhiyong Li
zjy_lzy@163.com

SPECIALTY SECTION
This article was submitted to Cardio-Oncology, a section of the journal Frontiers in Cardiovascular Medicine

RECEIVED 20 March 2022
ACCEPTED 06 July 2022
PUBLISHED 23 September 2022

CITATION
Li S, Tian D, Li X, Li J, Song Q, Xia Y and Li Z (2022) Case report: Evaluation of myocardial microcirculation in patients with breast cancer after anthracycline chemotherapy by using intravoxel incoherent motion imaging. *Front. Cardiovasc. Med.* 9:900309. doi: 10.3389/fcvm.2022.900309

COPYRIGHT
© 2022 Li, Tian, Li, Li, Song, Xia and Li. This is an open-access article distributed under the terms of the Creative Commons Attribution License (CC BY). The use, distribution or reproduction in other forums is permitted, provided the original author(s) and the copyright owner(s) are credited and that the original publication in this journal is cited, in accordance with accepted academic practice. No use, distribution or reproduction is permitted which does not comply with these terms.

Case report: Evaluation of myocardial microcirculation in patients with breast cancer after anthracycline chemotherapy by using intravoxel incoherent motion imaging

Shilan Li[1], Di Tian[1], Xin Li[1], Jia Li[2], Qingwei Song[1], Yunlong Xia[3] and Zhiyong Li[1]*

[1]Department of Radiology, The First Affiliated Hospital of Dalian Medical University, Dalian, China, [2]Department of Oncology, The First Affiliated Hospital of Dalian Medical University, Dalian, China, [3]Department of Cardiology, The First Affiliated Hospital of Dalian Medical University, Dalian, China

Introduction: Anthracycline chemotherapy drugs can produce cardiotoxicity in patients with breast cancer, leading to myocardial cell death and fibrosis, further developing into cardiac failure. However, the condition of myocardial microcirculation was unknown in breast cancer after anthracycline chemotherapy. As a result, intravoxel incoherent motion (IVIM) imaging was used to non-invasively observe the condition of myocardial microcirculation in a patient with breast cancer after anthracycline chemotherapy.

Case report: A 43-year-old female patient with a right breast lump was reported. Preoperative ultrasound-guided needle biopsy showed invasive carcinoma of the right breast with fibroadenoma. Sentinel lymph node biopsy combined with simplified radical surgery for right breast cancer was performed. Postoperative pathological findings reported breast cancer (pT2N2M0 IIIA). The patient underwent eight sessions of the EC-TH chemotherapy scheme, and the EC and the TH schemes were adopted for the first four sessions and the last four sessions, respectively. During chemotherapy, during which there was the occurrence of Grade II myelosuppression, chest CT and abdomen CT showed no metastasis, and ECG and cardiac ultrasound reports returned to normal. Cardiac cine magnetic resonance and IVIM imaging were performed at the beginning of the first chemotherapy session (baseline) and after the third, fifth, and eighth chemotherapy sessions, respectively. We found that the fast apparent diffusion coefficient (ADC_{fast}) and f parameters appeared to show a downward trend from the baseline to the fifth chemotherapy session, where the $IVIM_{fast}$ values declined from 163 $\times$ 10^{-3} mm^2/s to 148 $\times$ 10^{-3} mm^2/s and finally to 134 $\times$ 10^{-3} mm^2/s and f values declined from 45% to 36% and then to 30%, respectively. ADC_{fast} and f values showed an inclination from the fifth and eighth chemotherapy sessions.

Conclusion: Our case report showed that IVIM technology can likely detect non-invasive myocardial microcirculation early and quantitatively after

anthracycline chemotherapy in patients with breast cancer. That is, IVIM technology seems to be helpful for cardiovascular risk monitoring and prognosis assessment of myocardial microcirculation in patients with breast cancer after anthracycline chemotherapy.

KEYWORDS

breast cancer, anthracycline, cardiotoxicity, IVIM, microcirculation

Introduction

Breast cancer is the most common malignant tumor in women, ranking as the highest incidence of cancer among women and the main cause of cancer-related deaths in women (1). Radical surgical treatment and postoperative adjuvant chemotherapy can greatly reduce breast cancer mortality. Anthracycline is a major component of first-line chemotherapy for breast cancer because it is a chemical substance with anti-tumor activity produced by microorganisms (2). However, anthracyclines induce cardiotoxicity, and early stages of cardiotoxicity are associated with inflammation, vacuolation, and edema of the myocardial cells, leading to myocardial cell fibrosis and cardiac failure (3–5). Early cardiotoxicity precedes cardiac function after chemotherapy in patients with breast cancer, which highlights the importance of early recognition of cardiac injury and the establishment of cardioprotective treatment mechanisms to prevent cardiac failure.

IVIM is a new non-invasive technology that can analyze the characteristics of the myocardial tissue from the perspective of microcirculation, and early cardiac toxicity after anthracycline chemotherapy in patients with breast cancer was observed by using the IVIM technique, providing a new idea for future research and hoping to be better applied in clinical practice in the future. Therefore, the IVIM technology was initially used to observe the laboratory parameters of patients with breast cancer after anthracycline chemotherapy, and a case regarding is reported below.

Case report

A 43-year-old woman accidentally found a right breast lump on March 2014, with a diameter of 2 × 2 cm and stabbing pain. The mass was not related to the menstrual cycle. There was no redness, swelling, or rupture of the skin near the lump. No erosion, stabbing pain, pruritus, or discharge of the nipple was observed. In 2016, the tumor became progressively enlarged, and a mass of 3 × 2 cm was found under the right axilla. In March 2017, there was pain in the right axilla with obvious tenderness. Physical examination determined with touch indicated a tough mass of 5 × 3 cm in the right breast (between 7 and 9 o'clock), and the lump was characterized by unpolished surface, obscure boundary, and poor activity. A soft mass of 4 × 2 cm was touched in the right axilla, and no obvious abnormality was found during the rest of the physical examination. Ultrasound examination suggested multiple solid masses in the right breast. The dimensions of the tumor determined between 6 and 11 o'clock were 5.3 × 3.4 cm, which was classified as BI-RADS 4C-5; the dimensions of the mass identified at 10 o'clock were 1.2 × 0.5 cm, which was classified as BI-RADS 4a. The dimensions of enlarged lymph nodes in the right axilla were 1.2 × 0.6 cm. Ultrasound-guided needle biopsy showed an invasive carcinoma of the right breast with fibroadenoma. Surgical treatment was performed on 9 March 2017. Intraoperative sentinel lymph node biopsy found metastatic cancer, and simplified radical mastectomy was performed for right breast cancer. Postoperative pathology showed non-specific invasive carcinoma of the right breast (invasive ductal carcinoma SBR II-III) and mucinous carcinoma of high to medium grade (intraductal carcinoma) of the dimension 3.5 × 1.5 × 3.0 cm, as seen in Figure 1A. The other three lesions were non-special invasive carcinoma (invasive ductal carcinoma SBR II), with the dimensions of 0.7 × 0.7 × 0.5 cm, 1.0 × 0.6 × 0.5 cm, and 1.0 × 0.8 × 0.5 cm. No metastasis was found in the right axillary lymph node (0/15). Positive immunohistochemical staining for ER, PR, HER-2, AR, P53, and Ki 67 (Figure 1B) was performed. The postoperative stage was pT2N2M0 IIIA, Lumina I B. The chemotherapy regimen was EC-TH chemotherapy, with 8 sessions of chemotherapy completed from April 7, 2017 to September 25, 2017.

During the follow-up, corresponding examinations were made according to the patient's condition. Between the baseline and eighth chemotherapy sessions, ECG, cardiac ultrasonography and breast ultrasound, chest CT and upper abdomen CT, and ECT were performed in the following order: Chest CT, upper abdomen CT, and cardiac ultrasound were performed at baseline; ECG examination was performed after the first chemotherapy and the third chemotherapy. On the fifth chemotherapy session, none of the above examinations were performed. Chest CT, upper abdomen CT, cardiac ultrasonography, and breast ultrasound were performed during the eight chemotherapy session. Breast ultrasound results showed (1) a right breast surgery, (2) multiple cystic nodules in the left breast, and (3) no enlarged lymph nodes under both axilla and supraclavicular, and the rest of the examination

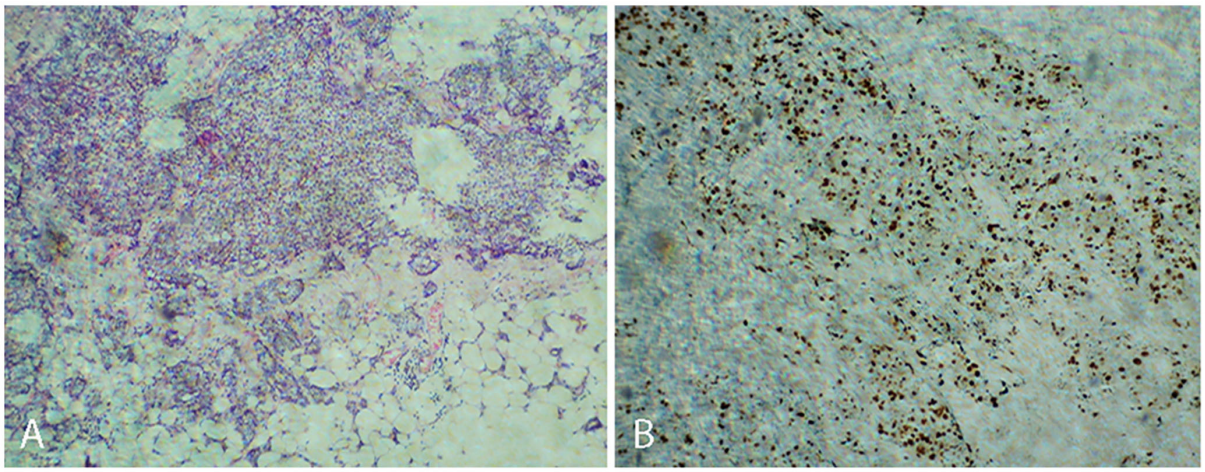

FIGURE 1
Non-specific invasive carcinoma of the right breast (invasive ductal carcinoma SBR II-III) **(A)**. Positive immunohistochemical staining for Ki 67 **(B)**.

results were normal. Degree II myelosuppression occurred during chemotherapy, and hematology returned to normal after treatment with granulocyte colony-stimulating factor (G-CSF).

In this case, CMR examinations were performed at the beginning of the first chemotherapy (baseline) and after the third, fifth, and eighth chemotherapy sessions, using a 3.0 T magnetic resonance imager (platform HDxt; General Electric Medical Systems, Waukesha, WI) equipped with an 8-channel phased-array cardiac coil. Standard 2-, 3-, and 4-chamber and left ventricle (LV) short-axis cine images from apical to basal were acquired with fast imaging employing a steady-state acquisition sequence. IVIM imaging was performed with the echo planar imaging (EPI) sequence. LV structural and functional parameters were measured by the Qmass package (Medis® Suite MR), as seen in Table 1. IVIM parameters were obtained by using GE Functool 9.4.05a software, as seen in Table 2. Cine images of 4-chamber, 2-chamber, left ventricle (LV) short-axis and IVIM images of baseline are shown in Figure 2. IVIM images of the third, fifth, and eighth chemotherapy sessions are shown in Figure 3.

TABLE 1 The situation at the baseline and after the third, fifth, and eighth chemotherapy sessions.

	Baseline	Third	Fifth	Eighth
Left atrium (anterior and posterior diameter, cm)	6.21	6.73	6.45	6.54
Right atrium (vertical atrial septum, cm)	6.12	6.67	6.47	6.58
Left ventricular transverse diameter (cm)	4.73	6.81	7.12	6.71
Right ventricular transverse diameter (cm)	4.93	5.12	5.20	5.11
LVEF (%)	56.91	62.48	63.16	71.70
LVEDV (ml)	128.31	151.82	136.88	160.94
LVESV (ml)	55.30	56.97	50.42	61.64
CO (L)	4.53	6.07	4.76	6.16
LV ED mass (g)	65.49	78.4	73.17	84.91
BMI (kg/m^2)	24.8	26.98	26.98	26.98

TABLE 2 IVIM parameters at the baseline and after the third, fifth, and eighth chemotherapy sessions.

	Baseline	Third	Fifth	Eighth
ADC_{slow} ($\times 10^{-3}$ mm^2/s)	2.88	2.25	2.55	3.5
ADC_{fast} ($\times 10^{-3}$ mm^2/s)	163	148	134	171
f (%)	45%	36%	30%	31%

Discussion

Water molecules include water molecules both at the intracellular and intercellular levels and at the intravascular level in the human body. However, diffusion-weighted imaging (DWI) cannot distinguish microcirculation perfusion and extravascular dispersion by using a single b-value model. Le Bihan first proposed the intravoxel incoherent motion technique for reflecting the movement of water molecules in tissues and microcirculation (6). With the progress of IVIM technology in sequence design and data processing (7–9), Callot et al. (10) attempted to use IVIM imaging on living animals and found it to be feasible. The technology observes the movement of water molecules in tissue cells and microvessels without any contrast agent, and ADC_{fast} and f parameters reflect the condition of

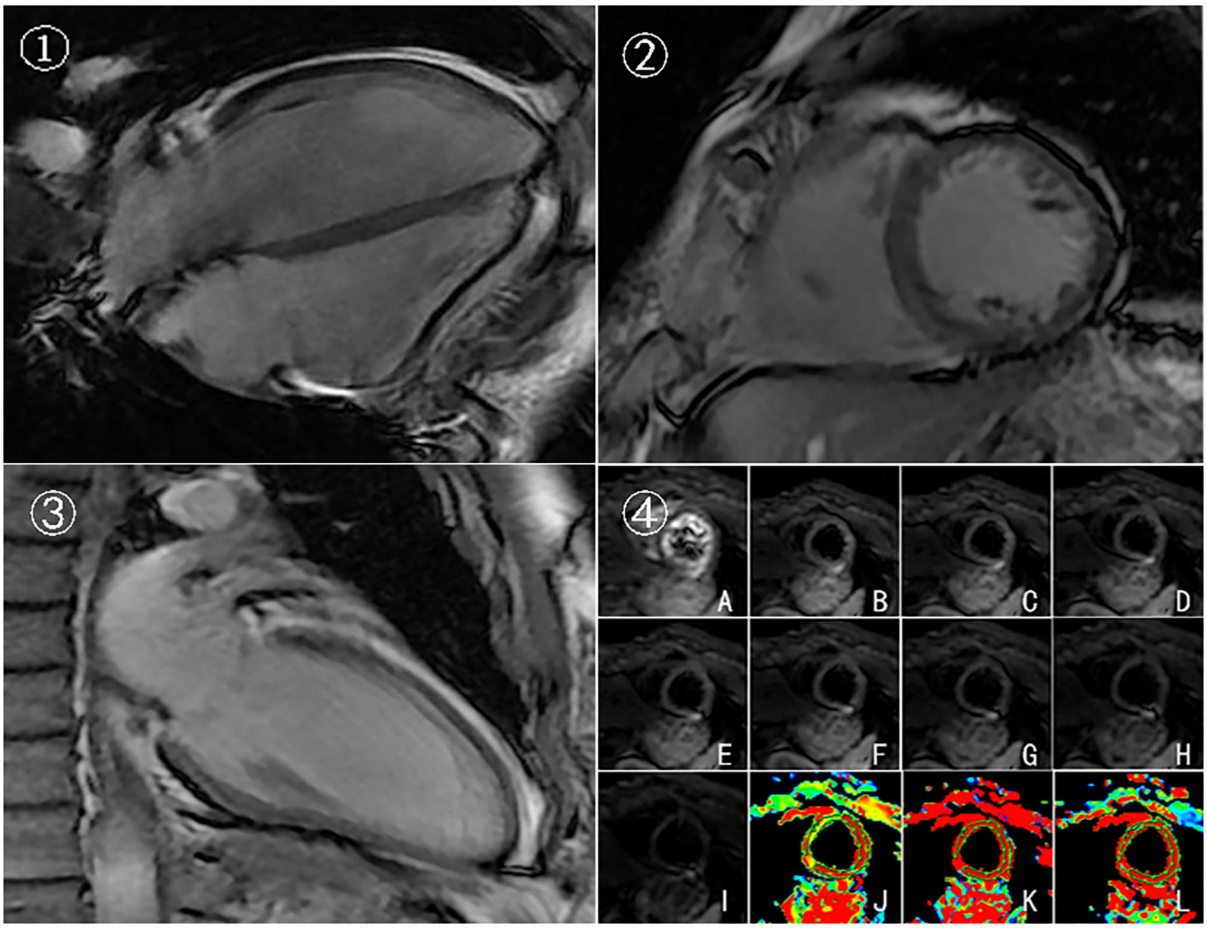

FIGURE 2
Cine images and IVIM images of baseline. 4-chamber(①), left ventricle (LV) short-axis ②, 2-chamber③, and IVIM images ④ of baseline. (A–I) Original images of IVIM at the left ventricular short-axis view (corresponding to b = 0, 20, 50, 80,100, 120, 200, 300, and 500 s/mm^2, respectively). (J–L) Pseudocolor images were produced using the bi-exponential mode of the IVIM imaging system (corresponding to ADC_{slow}, ADC_{fast}, and f values, respectively).

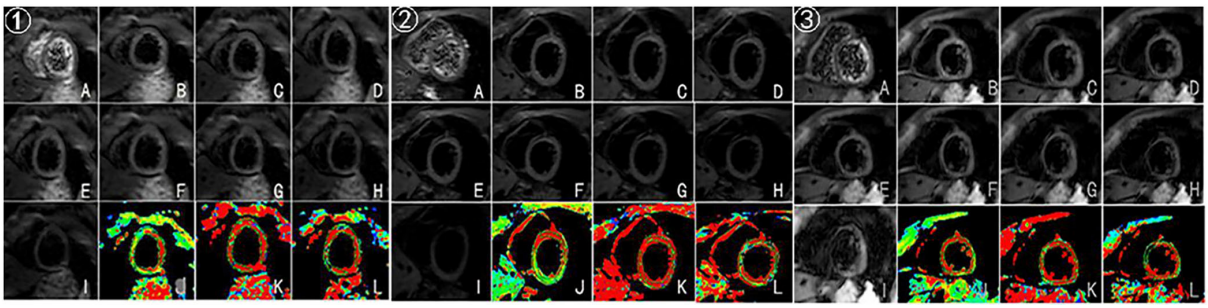

FIGURE 3
(A–I) Original images of IVIM at the left ventricular short-axis view (corresponding to b = 0, 20, 50, 80,100, 120, 200, 300, and 500 s/mm^2, respectively). (J–L) Pseudocolor images were produced using the bi-exponential mode of the IVIM imaging system (corresponding to ADC_{slow}, ADC_{fast}, and f values, respectively). ①, ②, ③ represent IVIM images after the third, fifth, and eighth chemotherapy sessions.

microcirculation perfusion. Further, Delattre et al. (11) and Mou et al. (12) applied it to the human body and proved that it was feasible.

Using the ICC test, Mou et al. (12) found that the IVIM parameters were consistent in intra-observer and inter-observer values in 30 healthy volunteers (at least one slice successful

acquisition). This study found that the intra- and inter-observer consistencies of ADC_{slow}, ADC_{fast}, and f values were 0.87, 0.89, 0.93, 0.97, 0.93, and 0.96, respectively. In addition, Moulin et al. (13) evaluated the inter-measurement reproducibility of IVIM parameters by Lin's concordance coefficient and the Bland-Altman analysis on 10 healthy volunteers. In this study, f values and ADC_{slow} showed high repeatability (Pc = 0.963; Pc = 0.762) and ADC_{fast} showed low repeatability (Pc = 0.652). Li found that intra-observer and inter-observer consistencies were good in 80 healthy volunteers (14).

Cardiotoxicity induced by anthracyclines was first proposed by Lefrak et al. (15). Cardiotoxicity includes arrhythmias, cardiac failure, and myocardial injury. It may occur months to years after the completion of primary treatment and can severely impair life quality and overall survival of the patient. Besides, it can be classified as acute, chronic, and delayed (16). Cardiotoxicity from anthracyclines is a dose-dependent toxicity, the risk of which increases exponentially with cumulative doses, which irreversibly results in myocardial cell structural changes and cell death in the chronic and delayed stages (17). Therefore, early and effective detection of cardiotoxicity of anthracyclines is an effective means to guide clinical medication and minimize cardiotoxicity. CMR is the gold standard for evaluating cardiac function due to its multi-mode imaging and high repeatability. CMR has high sensitivity and accuracy for cardiac injury caused for various reasons, especially in the early stage. In the early stages of cardiac injury, CMR can detect edema, inflammation, and fibrosis of cardiomyocytes, playing an important role in the diagnosis of early cardiotoxicity in patients with cancer (18). However, so far, no studies were reported on myocardial microcirculation after chemotherapy for patients with cancer using IVIM imaging.

In this case, the EC-TH (Epirubicin, Cyclophosphamide, Docetaxel, Trastuzumab) scheme was used. The selection of EC-TH, in this case, was related to the patient's postoperative pathology. Since lymph node metastasis occurred in the pathology of this case, postoperative adjuvant chemotherapy was required, so EC-TH was selected according to the recommendation of international guidelines (19). The details of medication are as follows: EPI(Epirubicin) 70 mg d1-2 ivgtt and CTX(Cyclophosphamide) 900 mg d1 ivgtt Q21d before the fifth chemotherapy. The TH regimen was used from the fifth to the eighth chemotherapy sessions, and the details of the medication are as follows: TXT, 160 mg and Herceptin, 500 mg ivgtt.

In this case, baseline and the third, fifth, and eighth sessions of chemotherapy were selected because, after the first and second chemotherapy sessions, the time of drug action on the myocardium was shorter, so IVIM was chosen after the third chemotherapy to observe the myocardial microcirculation. Besides, the choice of the fifth chemotherapy is related to the chemotherapy regimen of this case, the EC-TH was used in this case, anthracycline was used for the first four sessions, and docetaxel and trastuzumab were used for the last four sessions in order to observe the effect of drugs on cardiac microcirculation. The eighth session was observed for the overall situation after chemotherapy. The early stages of cardiotoxicity include cellular vacuolation and edema, which could lead to microcirculation dysfunction; however, the IVIM technology can be used to observe the early stage of cardiotoxicity from the perspective of microcirculation. ADC_{fast} and f values showed a downward trend from the baseline to the fifth chemotherapy, and it may be because anthracycline was used before the fifth chemotherapy, so the case showed that anthracycline causes damage to myocardial microcirculation. In terms of histological features, early stages of cardiotoxicity include cellular vacuolation and edema, which could lead to microcirculation dysfunction. In addition, ADC_{fast} and f values showed an upward trend from the fifth chemotherapy to the eighth chemotherapy session in the case. Possible reasons for this could be the following: early myocardial damage may be recovered after the withdrawal of anthracyclines, because cardiotoxicity of anthracyclines can be classified into acute, chronic, and delayed according to time. Among these classifications of cardiac damage, the acute is reversible, and clinical manifestations of chronic and delayed cardiotoxicity will manifest as cardiac failure and cardiac dysfunction (20); however, the cardiac function of the case remained normal from baseline to the eighth chemotherapy, suggesting that the patient may be in early myocardial toxicity rather than a phase of chronic and delayed cardiotoxicity. In addition, due to individual differences and because the case was of a middle-aged woman without cardiovascular disease, good physical and mental conditions were observed. The specific reasons remain to be studied.

Conclusion

Anthracyclines can induce cardiotoxicity. Early stages of cardiotoxicity include cellular vacuolation and edema, which could lead to microcirculation dysfunction. However, CMR is the gold standard for evaluating cardiac structure and function, and the IVIM technology is likely to non-invasively observe early myocardial microcirculation, that is, early and effective detection of anthracycline cardiotoxicity can help to guide clinical medication to minimize cardiotoxicity and improve overall survival.

Data availability statement

The original contributions presented in the study are included in the article/supplementary material, further inquiries can be directed to the corresponding author.

Ethics statement

The studies involving human participants were reviewed and approved by Ethics Committee of the First Affiliated Hospital of Dalian Medical University(PJ-KS-KY-2022-69). Written informed consent to participate in this study was provided by the participants' legal guardian/next of kin. Written informed consent was obtained from the individual(s) for the publication of any potentially identifiable images or data included in this article.

Author contributions

All authors listed have made a substantial, direct, and intellectual contribution to the work and approved it for publication.

Conflict of interest

The authors declare that the research was conducted in the absence of any commercial or financial relationships that could be construed as a potential conflict of interest.

Publisher's note

All claims expressed in this article are solely those of the authors and do not necessarily represent those of their affiliated organizations, or those of the publisher, the editors and the reviewers. Any product that may be evaluated in this article, or claim that may be made by its manufacturer, is not guaranteed or endorsed by the publisher.

References

1. Bray F, Ferlay J, Soerjomataram I, Siegel RL, Torre LA, Jemal A. Global cancer statistics 2018: GLOBOCAN estimates of incidence and mortality worldwide for 36 cancers in 185 countries. *CA Cancer J Clin.* (2018) 68:394–424. doi: 10.3322/caac.21492

2. Rosa GM, Gigli L, Tagliasacchi MI, Di Iorio C, Carbone F, Nencioni A, et al. Update on cardiotoxicity ofanti-cancer treatments. *Eur J Clin Invest.* (2016) 46:264–84. doi: 10.1111/eci.12589

3. Santoni M, Guerra F, Conti A, Lucarelli A, Rinaldi S, Belvederesi L, et al. Incidence and risk of cardiotoxicity in cancer patients treated with targeted therapies. *Cancer Treat Rev.* (2017) 59:123–31. doi: 10.1016/j.ctrv.2017.07.006

4. Kajihara H, Yokozaki H, Yamahara M, Kadomoto Y, Tahara E. Anthracycline induced myocardial damage. An analysis of 16 autopsy cases. *Pathol Res Pract.* (1986) 181:434–41. doi: 10.1016/S0344-0338(86)80079-6

5. Cottin Y, Ribuot C, Maupoil V, Godin D, Arnould L, Brunotte F, et al. Early incidence of adriamycin treatment on cardiac parameters in the rat. *Can J Physiol Pharmacol.* (1994) 72:140–5. doi: 10.1139/y94-022

6. Le Bihan D, Breton E, Lallemand D, Grenier P, Cabanis E, Laval-Jeantet M, et al. MR imaging of intravoxel incoherent motions: application to diffusion and perfusion in neurologic disorders. *Radiology.* (1986) 161:401–7. doi: 10.1148/radiology.161.2.3763909

7. Edelman RR, Gaa J, Wedeen VJ, Loh E, Hare JM, Prasad P, et al. *In vivo* measurement of water diffusion in the human heart. *Magn Reson Med.* (1994) 32:423–8. doi: 10.1002/mrm.1910320320

8. Reese TG, Tseng WY, Wedeen VJ. Cardiac diffusion MRI without motion effects. *Magn Reson Med.* (2002) 48:105–14. doi: 10.1002/mrm.10188

9. Fischer SE, Stuber M, Scheidegger MB, Boesiger P. Limitations of stimulated echo acquisition mode (STEAM) techniques in cardiac applications. *Magn Reson Med.* (1995) 34:80–91. doi: 10.1002/mrm.1910340113

10. Decking UK, Balaban RS, Wen H. *In vivo* study of microcirculation in canine myocardium using the IVIM method. *Magn Reson Med.* (2003) 50:531–40. doi: 10.1002/mrm.10568

11. Delattre BM, Viallon M, Wei H, Zhu YM, Feiweier T, Pai VM, et al. *In vivo* cardiac diffusion-weighted magnetic resonance imaging: quantification of normal perfusion and diffusion coefficients with intravoxel incoherent motion imaging. *Invest Radiol.* (2012) 47:662–70. doi: 10.1097/RLI.0b013e31826ef901

12. Mou A, Zhang C, Li M, Jin F, Song Q, Liu A, et al. Evaluation of myocardial microcirculation using intravoxel incoherent motion imaging. *J Magn Reson Imaging.* (2017) 46:1818–28. doi: 10.1002/jmri.25706

13. Moulin K, Croisille P, Feiweier T, Delattre BM, Wei H, Robert B, et al. *In vivo* free-breathing DTI and IVIM of the whole human heart using a real-time slice-followed SE-EPI navigator-based sequence: a reproducibility study in healthy volunteers. *Magn Reson Med.* (2016) 76:70–82. doi: 10.1002/mrm.25852

14. Li S, Mou A, Li X, Guo Y, Song Q, Liu A, et al. Myocardium microcirculation study in a healthy Chinese population using 30-T cardiac magnetic resonance intravoxel incoherent motion imaging. *Acta Radiol.* (2022) 63:596–605. doi: 10.1177/02841851211006311

15. Lefrak EA, Pitha J, Rosenheim S, Gottlieb JA. A clinicopathologic analysis of adriamycin cardiotoxicity. *Cancer.* (1973) 32:302–14. doi: 10.1002/1097-0142(197308)32:2<302::aid-cncr2820320205>3.0.co;2-2

16. Volkova M, Russell R. Anthracycline cardiotoxicity: prevalence, pathogenesis and treatment. *Curr Cardiol Rev.* (2011) 7:214–20. doi: 10.2174/157340311799960645

17. Jensen BV. Cardiotoxic consequences of anthracycline-containing therapy in patients with breast cancer. *Semin Oncol.* (2006) 33:S15–21. doi: 10.1053/j.seminoncol.2006.04.022

18. Wintersperger BJ, Flamm SD, Marwick TH. Cardiac MRI in the assessment of cardiac injury and toxicity from cancer chemotherapy: a systematic review. *Circ Cardiovasc Imaging.* (2013) 6:1080–91. doi: 10.1161/CIRCIMAGING.113.000899

19. Gradishar WJ, Anderson BO, Abraham J, Aft R, Agnese D, Allison KH, et al. Breast cancer, version 3.2020, NCCN clinical practice guidelines in oncology. *J Natl Compr Canc Netw.* (2020) 18:452–78. doi: 10.6004/jnccn.2020.0016

20. Appel JM, Sander K, Hansen PB, Møller JE, Krarup-Hansen A, Gustafsson F. Left ventricular assist device as bridge to recovery for anthracycline-induced terminal heart failure. *Congest Heart Fail.* (2012) 18:291–4. doi: 10.1111/j.1751-7133.2012.00291.x

frontiers | Frontiers in Cardiovascular Medicine

TYPE Case Report
PUBLISHED 29 September 2022
DOI 10.3389/fcvm.2022.934214

Check for updates

OPEN ACCESS

EDITED BY
Carlo Gabriele Tocchetti,
University of Naples Federico II, Italy

REVIEWED BY
Weichieh Lee,
Chi Mei Medical Center, Taiwan
Tamas Szili-Torok,
Erasmus Medical Center, Netherlands

*CORRESPONDENCE
Beibei Du
beibeidu2012@jlu.edu.cn

†These authors share first authorship

SPECIALTY SECTION
This article was submitted to Cardio-Oncology, a section of the journal Frontiers in Cardiovascular Medicine

RECEIVED 02 May 2022
ACCEPTED 13 September 2022
PUBLISHED 29 September 2022

CITATION
Zhang Y, Wang X, Pan Y, Du B, Nanthakumar K and Yang P (2022) Overdrive pacing in the acute management of osimertinib-induced ventricular arrhythmias: A case report and literature review.
Front. Cardiovasc. Med. 9:934214.
doi: 10.3389/fcvm.2022.934214

COPYRIGHT
© 2022 Zhang, Wang, Pan, Du, Nanthakumar and Yang. This is an open-access article distributed under the terms of the Creative Commons Attribution License (CC BY). The use, distribution or reproduction in other forums is permitted, provided the original author(s) and the copyright owner(s) are credited and that the original publication in this journal is cited, in accordance with accepted academic practice. No use, distribution or reproduction is permitted which does not comply with these terms.

Overdrive pacing in the acute management of osimertinib-induced ventricular arrhythmias: A case report and literature review

Yanyu Zhang[1,2†], Xingtong Wang[3†], Yilin Pan[1], Beibei Du[1*], Kumaraswamy Nanthakumar[4] and Ping Yang[1]

[1]Department of Cardiology, China-Japan Union Hospital of Jilin University, Jilin Provincial Cardiovascular Research Institute, Changchun, China, [2]Department of Cardiology, Inner Mongolia Autonomous Region Cancer Hospital, Hohhot, China, [3]National Key Discipline in Hematology, Department of Hematology, The First Hospital of Jilin University, Changchun, China, [4]The Hull Family Cardiac Fibrillation Management Laboratory, Toronto General Hospital, University Health Network, Toronto, ON, Canada

QT interval prolongation and ventricular arrhythmias (VAs) induced by osimertinib, a third-generation epidermal growth factor receptor tyrosine kinase inhibitor, are life-threatening complications. However, no consensus has been achieved regarding their management. Overdrive pacing has been shown to be effective in shortening the QT interval and terminating torsade de pointes (TdP). Here, we report a case of osimertinib-induced QT prolongation accompanied by frequent VAs and TdP. Osimertinib was immediately discontinued after it was identified as the etiology for QT prolongation and VAs. A temporary pacemaker and overdrive pacing were used after other anti-arrhythmia treatments had failed and successfully shortened the QTc interval and terminated VAs. Repeated Holter monitoring at 1 week showed no remaining VAs or TdP, and the pacemaker was removed. Routine electrocardiography (ECG) surveillance was conducted afterward, and three- and 6-month follow-ups showed good recovery and normal ECG results. Vigilance is required for rare vital arrhythmias in patients taking osimertinib, and ECG surveillance should be conducted.

KEYWORDS

osimertinib, QTc interval prolongation, ventricular tachycardia, temporary pacemaker, torsade de pointes (TdPs)

Introduction

Epidermal growth factor receptor (EGFR) mutation is one of the most common oncogenic drivers in non-small cell lung cancer (NSCLC). Osimertinib, the third-generation EGFR tyrosine kinase inhibitor (TKI), has substantially improved treatment efficacy for NSCLC with EGFR mutations (1). However, while remaining low in incidence, cardiotoxicities related to EGFR-TKIs, such as congestive heart failure, QT interval prolongation, and ventricular arrhythmias (VAs) have become a safety concern (2), as they are life-threatening complications.

No consensus has been achieved for the management of these cardiotoxicities (2, 3). Overdrive pacing, or pacing with a higher heart rate, has been shown to be effective in shortening QT intervals and terminating torsade de pointes (TdP) (4). However, overdrive pacing in the acute management of osimertinib-induced VAs has rarely been reported in the literature. Here, we report a case of osimertinib-induced QT prolongation, frequent VAs, and TdP for which a temporary pacemaker and overdrive pacing were used. Serial electrocardiography (ECG) and Holter monitoring results during hospitalization and follow-ups confirmed the in-hospital and long-term efficacy and safety of these treatments.

Case presentation

A 60-year-old woman was admitted to our hospital with palpitations and an onset of syncope. The patient had experienced palpitations 3 months previously while working and one episode of syncope later at home. The patient had regained consciousness after 10 seconds but took no action and sought no treatment. Two days preceding admission, the palpitations had become more frequent, and the patient reported feeling dizzy on several occasions. The symptoms were not related to exercise or emotional changes. Seventeen months previously, the patient had been diagnosed with peripheral lung adenocarcinoma and associated brain and bone metastases (Figure 1A). Genomic analysis had indicated *EGFR* gene mutations, and she had therefore been treated with the EGFR TKI osimertinib (80 mg, QD). The patient had no history of hypertension, diabetes or related family history. There was also no record of previous use of anti-arrhythmic agents.

The patient presented with tachycardia (122 bpm) and hypotension (81/68 mmHg) on physical examination. Electrocardiography (ECG) on admission showed prolonged QTc intervals (QTcB 577 ms) and frequent ventricular premature complexes (VPCs). Holter analysis also showed prolonged QTc intervals (longest QTcB 640 ms, Figure 1B), frequent VPCs, and ventricular tachycardias (VTs) (122 episodes/20 h, including multiple TdP) (Figure 1C). Echocardiography showed no structural or functional abnormalities. Laboratory assessments showed normal electrolyte concentrations (K^+ 3.9 mmol/L, Ca^{2+} 2.50 mmol/L, Mg^{2+} 0.93 mmol/L) and negative cardiac biomarkers. SCN5A and KCH2 mutations were not detected during genetic screening. An ECG that had been conducted prior to osimertinib treatment showed normal QTc intervals (QTcB 417 ms, Supplementary Figure 1A). After ruling out QT prolongation caused by myocardial ischemia or other QT-prolongation drugs, the patient was diagnosed with osimertinib-induced QT prolongation, VAs, and TdP (Probable causality, World Health Organization-Uppsala Monitoring Center [WHO-UMC] causality assessment scale).

Osimertinib was immediately discontinued after it was identified as the etiology for QT prolongation and VAs. Anti-arrhythmia treatments (intravenous magnesium, potassium magnesium aspartate, and oral propranolol) were administered; however, they did not relieve the patient's

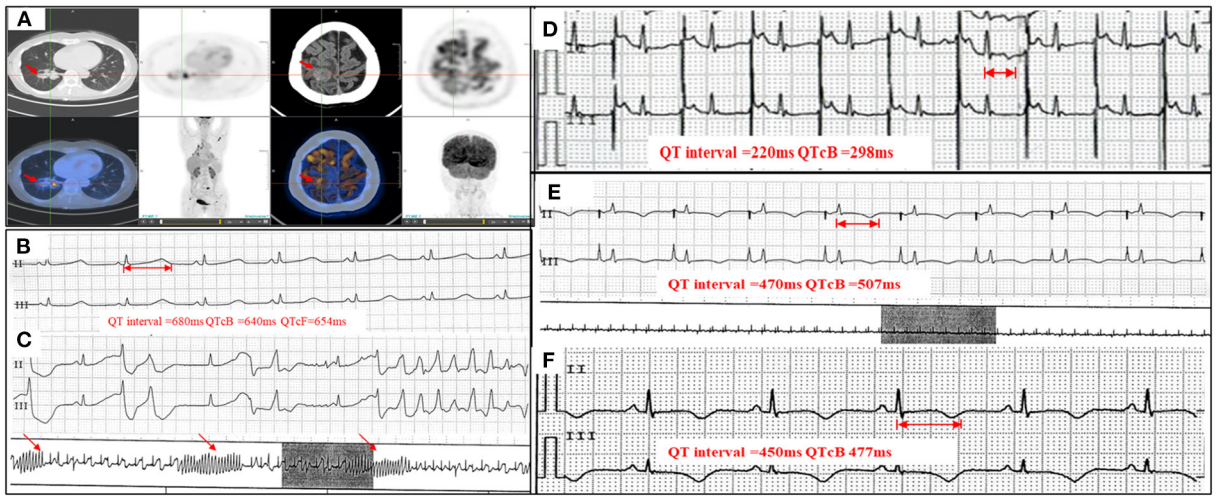

FIGURE 1
PET-CT, serial Holter monitoring, and ECG. **(A)** PET-CT showing peripheral pulmonary carcinoma and brain metastasis (arrowheads); **(B)** Holter monitoring on admission showing prolonged QTc interval (QTcB 640 ms); **(C)** Holter monitoring on admission showing frequent VTs and TdP (arrowheads); **(D)** ECG with a temporary pacemaker and overdrive pacing at 110 bpm (QTcB 298 ms); **(E)** Holter monitoring with a temporary pacemaker and pacing at 70 bpm (QTcB 507 ms); **(F)** ECG at discharge showing near-normal QTc interval (QTcB 477 ms). VT, ventricular tachycardia; TdP, torsade de pointes; QTcB, QTc interval calculated with Bazett formula; PET-CT, positron emission tomography – computed tomography; ECG, electrocardiogram.

symptoms. No defibrillation treatment was delivered for a stable hemodynamic status.

After a temporary pacemaker was implanted with the pacing lead placed at the patient's right atrium, overdrive pacing successfully shortened the QTc interval and terminated the VAs. The initial pacing rate of 110 bpm was gradually reduced to 60-−70 bpm within 1 week, and the QTc interval was shortened to 298–507 msec (Figures 1D,E). Repeat Holter monitoring at 1 week showed no VPCs or VTs. The pacemaker was then removed and following consultation with a hematologist, osimertinib was replaced by gefitinib (250 mg QD). At discharge, the patient's symptoms were relieved and her ECG showed normal results (QTc 477 ms) (Figure 1F, Supplementary Figure 1B). Routine ECG surveillance was conducted. Three- (Supplementary Figure 1C) and 6-month follow-ups showed good recovery and normal ECG results (Table 1).

TABLE 1 Time line.

17 months prior to presentation	• Diagnosed with peripheral lung adenocarcinoma with associated brain and bone metastases. • Osimertinib treatment started.
3 months prior to presentation	• Palpitations whilst working. • One episode of syncope at home.
2 days prior to presentation	• Frequent palpations, dizziness.
At presentation	• BP 81/68 mmHg, BMI 14.9 kg/m^2 (164 cm/40 kg) • ECG: HR 122 bpm, QTcB 532 msec, frequent VPCs. • Normal electrolyte concentrations. • Negative cardiac biomarkers. • Anti-arrhythmias medical treatment: including intravenous magnesium, potassium magnesium aspartate and lidocaine, and oral propranolol. • Osimertinib was discontinued.
2 days later	• Symptoms not relieved. • Holter monitoring: prolonged QTc interval (longest QTcB 640 ms), frequent VPCs and VTs (122 episodes/20 h, including multiple TdP) • Treatment: temporary pacemaker implantation. Overdrive pacing (at 110 bpm) shortened the QTc interval and terminated VAs. QTcB 298 ms.
9 days later	• With temporary pacemaker, the pacing rate was gradually reduced to 60–70 bpm; ECG: HR 70 bpm, QTcB 507 msec. • No palpitation and syncope. Holter monitoring: no VAs. Temporary pacemaker removed.
15 days later	• ECG: HR 67 bpm, QTcB 477 ms • No palpitation and syncope
3 months later	• No palpitation and syncope, good recovery • ECG: HR 68 bpm, QTcB 479 ms
6 months later	• No palpitation and syncope, good recovery

BP, Blood pressure; HR, Heart rate; BMI, Body mass index; ECG, Electrocardiograph; QTcB, Corrected QT interval by Bazett formula; TdP, Torsade de pointes; VPCs, Ventricular premature complexes; VT, Ventricular tachycardias; VAs, Ventricular arrhythmias.

Discussion

This study reported a case of osimertinib-induced QT prolongation accompanied by frequent VAs and TdP in a patient being treated for NSCLC.

EGFR mutation is one of the most common oncogenic drivers in NSCLC. As such, EGFR-TKIs (including gefitinib, erlotinib, and osimertinib, etc.) are used to inhibit EGFR tyrosine kinase and have enhanced the treatment for NSCLC over the past two decades (5). In particular, osimertinib, a third-generation EGFR-TKI, has been shown to increase treatment efficacy even when compared with that of first- or second-generation EGFR TKIs (6). Osimertinib has thus become the first-line treatment for advanced EGFR-mutant NSCLC patients, especially for those with brain metastases or acquired T790M resistance mutation (1).

Despite their low incidence, cardiotoxicities including congestive heart failure, QT prolongation, and vital arrhythmias have become a safety concern for patients taking EGFR TKIs. Osimertinib-induced QT prolongation was first reported during the phase I trials for the drug (7), after which analyses in two phase III randomized controlled trials also confirmed that osimertinib notably increased the risk of cardiac toxicities, with a risk ratio of 2.62 for QT prolongation (8). The initial FDA risk-benefit assessment reported a low incidence (0.7%) of osimertinib-induced substantial QTc prolongation (QTc $\geq$ 500 msec), with no QTc-related VAs reported (9). Further, when Anand et al. reviewed the pharmacovigilance database of the FDA Adverse Events Reporting System (FAERS), and compared the cardiotoxicities of different EGFR-TKIs, a total of 315 cardiac adverse events (AE) were noted. Cardiac failure and QT prolongation were the cardiotoxicities most commonly caused by osimertinib. Of patients treated with osimertinib, 33/2,454 (1.3%) developed QT prolongation at a median time of 23 days. A comparison with first- and second-generation EGFR-TKIs has shown that osimertinib is more likely than the others to induce QT prolongation (reported odds ratio 6.6) (2). In a recent retrospective cohort study, Kunimasa et al. compared QT intervals in 72 patients with serial ECGs before and after osimertinib administration and found that QTc intervals were prolonged by approximately 20 ms over a median time of 116 days. However, no fatal arrhythmias were reported in this study (10).

In addition to QT prolongation, VT or TdP were also reported in a limited number of cases taking osimertinib (Table 2) (11–14). This indicates that osimertinib-induced vital arrhythmias are probably underestimated owing to the

TABLE 2 Summary of osimertinib-induced VAs cases reported.

Author [Ref]	Osimertinib treatment time (month)	QTc interval (ms)	Type of VAs	Anti-arrhythmias treatment	Follow-up
Matsuura et al. (11)	2	486	TdP	• Osimertinib discontinued; • Magnesium supplementation.	• Not mentioned
Ikebe et al. (12)	2	524	TdP	• Osimertinib discontinued; • Cardioversion;	• Died of cancer progression and cachexia 15 months after osimertinib discontinuation.
Bian et al. (13)	6	647	TdP	• Osimertinib discontinued; • Magnesium supplementation, potassium supplementation, and administration of antiarrhythmic drug lidocaine.	• QT interval got closer to normal gradually, but the patient experienced decreased blood pressure, pulse oxygen saturation, and was unconscious. In order to relieve the patient's pain, the patient was discharged without invasive salvage measures.
Kaira et al. (14)	3	>600	VF, Cardiac arrest	• Osimertinib discontinued; • Cardiovascular agents (not specified). • Cardiopulmonary resuscitation.	• Not mentioned.
Our case	17	640	VT, TdP	• Osimertinib discontinued • Intravenous magnesium, potassium magnesium aspartate, and oral propranolol; • Overdrive pacing by temporary pacemaker	• Osimertinib was replaced by gefitinib (250 mg QD). • QT interval getting closer to normal gradually, the three- and 6-month follow-ups showed good recovery and normal ECG results.

TdP, Torsade de pointes; VT, Ventricular tachycardias; VAs, Ventricular arrhythmias.

limitations of retrospective studies and the reporting system. Physicians should be vigilant to the occurrence of these rare vital arrhythmias in patients on osimertinib and conduct ECG surveillance for these patients.

However, the mechanism of osimertinib-induced cardiotoxicity is still unclear (15). In the preliminary IC50 inhibition *in-vitro* cell test, osimertinib showed weak inhibition of the cardiac potassium channel Kv11.1, which may be a potential mechanism of osimertinib-induced QT prolongation (16). However, further basic research is required for full clarification of the underlying mechanism.

As the treatment of VTs is based on the determination of their etiology, owing to the lack of understanding of the mechanism behind osimertinib-related arrhythmias, there has been no consensus for appropriate management. Magnesium supplementation, cardioversion, and β-blockers are generally used in the management of long QT syndrome (LQTS) related VT and Tdp (4). In the limited cases of osimertinib-induced VAs, point-of-care monitoring-guided magnesium supplementation, cardioversion, and antiarrhythmic drugs have been reportedly used (Table 2) (11–14); however, in this case, all treatment failed to improve this patient's symptoms. Although implantable cardioverter defibrillator (ICD) implantation is suggested in high-risk LQTS patients, it would have certainly led to frequent shocks for this particular patient, and was therefore deemed unsuitable. Additionally, the presence of polymorphic VT and TdP, indicated the ineligibility for radiofrequency ablation. Lastly, left cardiac sympathetic denervation (LCSD) is regarded as a bail-out strategy in the case that other treatments should fail.

Medically (isoprenaline infusion) or electrically (override pacing) speed up the heart can both help to decrease the QTc interval and terminate TdP temporarily. The efficacy of override pacing in comparison with isoprenaline is uncertain due to the lack of randomized comparison evidence (17). However, override pacing would be a better option when the risk of TdP

may persist over a more extended period, such as a long-acting drug. As the mean elimination half-life time of osimertinib is 48–59.7 h theoretically (18, 19), temporary pacemaker implantation and overdrive pacing can help to shorten the QTc interval and increase survival during this life-threatening time period.

On the other hand, osimertinib was replaced with gefitinib for chemotherapy after the occurrence of this life-threatening complication. No disease progression or TdP recurrence has been detected and favorable recovery has been archived in the follow-ups.

Conclusions

Osimertinib-induced QT interval prolongation and VAs are underestimated in NSCLC patients, and no consensus has been achieved on standard treatment. This case showed that ECG and Holter monitoring should be performed periodically in patients on osimertinib treatment. Temporary pacemaker implantation and overdrive pacing may be considered a safe and effective treatment for the acute management of osimertinib-induced VAs.

Data availability statement

The original contributions presented in the study are included in the article/Supplementary material, further inquiries can be directed to the corresponding author/s.

Ethics statement

Written informed consent was obtained from the participant for the publication of this case report.

Author contributions

YZ and BD identified the case. XW and YP conducted the literature search and prepared the first draft of the manuscript. KN and PY provided critical revision for the manuscript. All authors contributed to the articles and approved the submitted version.

Funding

This research was supported by grants from Jilin Provincial Science and Technology Department International Cooperation Project (No. 20210402016GH) and the National Natural Science Foundation of China (No. 82100337).

Conflict of interest

The authors declare that the research was conducted in the absence of any commercial or financial relationships that could be construed as a potential conflict of interest.

Publisher's note

All claims expressed in this article are solely those of the authors and do not necessarily represent those of their affiliated organizations, or those of the publisher, the editors and the reviewers. Any product that may be evaluated in this article, or claim that may be made by its manufacturer, is not guaranteed or endorsed by the publisher.

Supplementary material

The Supplementary Material for this article can be found online at: https://www.frontiersin.org/articles/10.3389/fcvm.2022.934214/full#supplementary-material

SUPPLEMENTARY FIGURE 1
Serial 12 leads ECGs before osimertinib treatment and in the recovery stage. **(A)** 12 leads ECG four months before osimertinib treatment showing normal QTc interval (QTcB 417 ms); **(B)** 12 leads ECG at discharge showing near-normal QTc interval (QTcB 477 ms); **(C)** 12 leads ECG at three month's follow-up showing near-normal QTc interval (QTcB 468 ms); QTcB, QTc interval calculated with Bazett formula.

References

1. Ramalingam SS, Vansteenkiste J, Planchard D, Cho BC, Gray JE, Ohe Y, et al. Overall survival with osimertinib in untreated, egfr-mutated advanced nsclc. *N Engl J Med.* (2020) 382:41–50. doi: 10.1056/NEJMoa1913662

2. Anand K, Ensor J, Trachtenberg B, Bernicker EH. Osimertinib-induced cardiotoxicity. *JACC: CardioOncology.* (2019) 1:172–8. doi: 10.1016/j.jaccao.2019.10.006

3. Salem J-E, Nguyen LS, Moslehi JJ, Ederhy S, Lebrun-Vignes B, Roden DM, et al. Anticancer drug-induced life-threatening ventricular arrhythmias: a world health organization pharmacovigilance study. *Eur Heart J.* (2021) 42:3915–28. doi: 10.1093/eurheartj/ehab362

4. Al-Khatib SM, Stevenson WG, Ackerman MJ, Bryant WJ, Callans DJ, Curtis AB, et al. 2017 Aha/Acc/Hrs guideline for management of patients with ventricular arrhythmias and the prevention of sudden cardiac death. *Circulation.* (2018) 138:e272–391. doi: 10.1016/j.hrthm.2017.10.036

5. Kim C, Liu SV. First-line egfr tki therapy in non-small-cell lung cancer: looking back before leaping forward. *Ann Oncol.* (2019) 30:1852–5. doi: 10.1093/annonc/mdz415

6. Wu L, Ke L, Zhang Z, Yu J, Meng X. Development of egfr tkis and options to manage resistance of third-generation egfr tki osimertinib: conventional ways and immune checkpoint inhibitors. *Front Oncol.* (2020) 10:602762. doi: 10.3389/fonc.2020.602762

7. Jänne PA, Yang JC-H, Kim D-W, Planchard D, Ohe Y, Ramalingam SS, et al. Azd9291 in egfr inhibitor–resistant non–small-cell lung cancer. *NEJM.* (2015) 372:1689–99. doi: 10.1056/NEJMoa1411817

8. Thein KZ, Swarup S, Ball S, Quirch M, Vorakunthada Y, Htwe KK, et al. Incidence of cardiac toxicities in patients with advanced non-small cell lung cancer treated with osimertinib: a combined analysis of two phase iii randomized controlled trials. *Ann Oncol.* (2018) 29:viii500. doi: 10.1093/annonc/mdy292.011

9. Odogwu L, Mathieu L, Goldberg KB, Blumenthal GM, Larkins E, Fiero MH, et al. Fda benefit-risk assessment of osimertinib for the treatment of metastatic non-small cell lung cancer harboring epidermal growth factor receptor T790m mutation. *Oncologist.* (2018) 23:353–9. doi: 10.1634/theoncologist.2017-0425

10. Kunimasa K, Kamada R, Oka T, Oboshi M, Kimura M, Inoue T, et al. Cardiac adverse events in egfr-mutated non-small cell lung cancer treated with osimertinib. *JACC CardioOncol.* (2020) 2:1–10. doi: 10.1016/j.jaccao.2020.02.003

11. Matsuura C, Kato T, Koyama K. Successful management of refractory torsades de pointes due to drug-induced long qt syndrome guided by point-of-care monitoring of ionized magnesium. *Cureus.* (2021) 13:e13939. doi: 10.7759/cureus.13939

12. Ikebe S, Amiya R, Minami S, Ihara S, Higuchi Y, Komuta K. Osimertinib-induced cardiac failure with qt prolongation and torsade de pointes in a patient with advanced pulmonary adenocarcinoma. *Int Cancer Confer J.* (2021) 10:68–71. doi: 10.1007/s13691-020-00450-2

13. Bian S, Tang X, Lei W. A case of torsades de pointes induced by the third-generation egfr-tki, osimertinib combined with moxifloxacin. *BMC Pulm Med.* (2020) 20:181. doi: 10.1186/s12890-020-01217-4

14. Kaira K, Ogiwara Y, Naruse I. Occurrence of ventricular fibrillation in a patient with lung cancer receiving osimertinib. *J Thorac Oncol.* (2020) 15:e54–e5. doi: 10.1016/j.jtho.2019.11.029

15. Ewer MS, Tekumalla SH, Walding A, Atuah KN. Cardiac safety of osimertinib: a review of data. *J Clin Oncol.* (2021) 39:328–37. doi: 10.1200/JCO.20.01171

16. Desai MY, Windecker S, Lancellotti P, Bax JJ, Griffin BP, Cahlon O, et al. Prevention, diagnosis, and management of radiation-associated cardiac disease: jacc scientific expert panel. *J Am Coll Cardiol.* (2019) 74:905–27. doi: 10.1016/j.jacc.2019.07.006

17. Thomas SH, Behr ER. Pharmacological treatment of acquired qt prolongation and torsades de pointes. *Br J Clin Pharmacol.* (2016) 81:420–7. doi: 10.1111/bcp.12726

18. Gao X, Le X, Costa DB. The safety and efficacy of osimertinib for the treatment of egfr t790m mutation positive non-small-cell lung cancer. *Expert Rev Anticancer Ther.* (2016) 16:383–90. doi: 10.1586/14737140.2016.1162103

19. Vishwanathan K, So K, Thomas K, Bramley A, English S, Collier J. Absolute bioavailability of osimertinib in healthy adults. *Clin Pharmacol Drug Development.* (2019) 8:198–207. doi: 10.1002/cpdd.467

frontiers | Frontiers in Cardiovascular Medicine

TYPE Case Report
PUBLISHED 30 September 2022
DOI 10.3389/fcvm.2022.941142

Check for updates

OPEN ACCESS

EDITED BY
Reto Asmis,
Wake Forest School of Medicine,
United States

REVIEWED BY
Michael Joseph Reardon,
Houston Methodist DeBakey Heart and Vascular Center, United States
Xiangbin Meng,
Peking University Third Hospital, China

*CORRESPONDENCE
Chengxin Zhang
zhangchengxin@ahmu.edu.cn

†These authors have contributed equally to this work and share first authorship

SPECIALTY SECTION
This article was submitted to Cardio-Oncology, a section of the journal Frontiers in Cardiovascular Medicine

RECEIVED 11 May 2022
ACCEPTED 06 September 2022
PUBLISHED 30 September 2022

CITATION
Wang X, Liu H, Zhang S, Huang S and Zhang C (2022) The surgical strategy of hormonally active primary cardiac paraganglioma sarcoma: A case report. *Front. Cardiovasc. Med.* 9:941142. doi: 10.3389/fcvm.2022.941142

COPYRIGHT
© 2022 Wang, Liu, Zhang, Huang and Zhang. This is an open-access article distributed under the terms of the Creative Commons Attribution License (CC BY). The use, distribution or reproduction in other forums is permitted, provided the original author(s) and the copyright owner(s) are credited and that the original publication in this journal is cited, in accordance with accepted academic practice. No use, distribution or reproduction is permitted which does not comply with these terms.

The surgical strategy of hormonally active primary cardiac paraganglioma sarcoma: A case report

Xiangyu Wang†, Haiyuan Liu†, Shuaipeng Zhang†, Shaojun Huang and Chengxin Zhang*

Department of Cardiovascular Surgery, First Affiliated Hospital of Anhui Medical University, Hefei, China

Cardiac paraganglioma is a kind of rare neuroendocrine tumor characterized by the persistent secretion of catecholamines. Under excessive exposure of catecholamines, some atypical symptoms are presented, including hypertension, arrhythmias, and headache. The case of surgical treatment of a 28-year-old woman with primary cardiac paraganglioma is presented for experience sharing and surgical skill improvements.

KEYWORDS

cardiac paraganglioma, catecholamine, primary cardiac oncology, neuroendocrine tumor, surgical skill

Case presentation

The patient was a 28-year-old woman admitted with the complaint of progressive hypertension complicated with chest pain, tightness, and palpitation for 5 years. In particular, the hypertension of systolic pressure at the 16th week during pregnancy ranging from 110–200 mmHg was managed through combined therapy with labetalol and amlodipine. However, the level of blood pressure was not controlled stably as expected after medical intervention, therefore, the pregnancy termination underwent further treatment of refractory hypertension. Both previous surgical procedures and family genetic disorders were denied.

When at admission, tachycardia was found by electrocardiogram (Figure 1A). Based on the findings from the contrast-enhanced CT, it was demonstrated that a mass of 46 × 42 mm with serious adhesion to the surrounding aorta located at the root of the aorta in the middle mediastinum and the left main coronary was also involved (Figure 1B).

In MRI, it was confirmed that both the root of the aorta and left main coronary were involved, however, the myocardium was free from involvement (Figure 1C). In accordance with the echocardiography, the mass was completely perfused through mini-vascular circulation (Figure 1D). After exclusion of adrenal pheochromocytoma with the absence of any abnormal images found in bilateral adrenals, the final diagnosis of primary cardiac paraganglioma was confirmed comprehensively in accordance with the objective results from imaging and lab tests indicating the elevated catecholamine. The α and β receptor blockers were selected as preoperative agents for hypertension control

and multidisciplinary consultants were performed, including gynecology and urology for preoperative assessment.

Surgical procedure

Peripheral cardiopulmonary bypass (CPB) was established *via* the femoral artery and vein. Once CPB started, the median sternotomy was selected. After surgical field exposure, it was found that the mass with the visual size of 65 mm located at the outflow tract of the right ventricle besides the main pulmonary artery was involved seriously. The blood supplement was distributed fully around the mass. Cardiac arrest was maintained using HTK cardioplegia after ascending aorta clamping when the temperature is lower than 35°C. Given the complicated mass-related anatomical changes, extended lesion resection, reconstruction of the pulmonary artery, and coronary artery bypass grafting (CABG) were processed simultaneously. The surgical separation of the mass began at the anterior wall of outflow of the right ventricle. The main pulmonary artery was opened to expose the pulmonary valve due to serious adhesion between the mass and the right ventricle. Then, the separation of the posterior wall of the main pulmonary artery was continued cautiously. Meanwhile, the proximal end of left main coronary was also damaged due to severe involvement by the mass. After the mass was removed completely, a bovine pericardial patch of reasonable size was used to repair the pulmonary artery (Figures 1E,F).

There were two grafts for CABG, great saphenous vein (SVG), and internal mammary artery (LIMA), respectively. First, circumflex (LCX) grafting was performed through end-to-side anastomosis with the proximal end of the great saphenous vein. Then, left anterior descending (LAD) grafting was continued with end-to-side anastomosis with the internal mammary artery. At last, the distal end of the great saphenous vein was sutured at the ascending aorta (AO).

After CABG was completed, regular rewarming was activated and when the temperature was higher than 33°C, the ascending aorta was de-aired and opened. The final closure of the chest was finished after weaning of CPB.

Postoperative management

The postoperative blood pressure was managed stably and dynamically using α-receptor and β-receptor blockers. Daily administration of vasoactive agents was adjusted and monitored as needed to prevent both organic function and perfusion affected dramatically after surgery. The urine norepinephrine on the 1st day after surgery was 1,953.4 mg/ml. The norepinephrine decreased to 616.7 ng/ml on the 5th day and to the normal level on the 9th day after surgery. The blood pressure was gradually stable and maintained on the 3rd day after surgery. Pathologically, the removed mass was confirmed as cardiac paraganglioma (Figure 2A).

The outcome and follow-up

The patient was discharged smoothly after clinical assessment where no recurred hypertension, arrhythmias, or any other discomfort complaints were found. During the latest follow-up, it was shown that, morphologically, all chambers and valves were normal and the heart function was stable without any serious abnormal changes (Figure 2B). The sinus rhythm was found by electrocardiogram rechecking (Figure 2C). Furthermore, it was demonstrated *via* the coronary angiography, the patency of grafts for both LIMA–LAD and AO–SVG–LCX was qualified without any obstructions (Figure 2D).

Discussion

Clinically, the incidence of cardiac paraganglioma is only about 0.6/100,000 (1). All chambers of the heart are potential locating targets for cardiac paraganglioma, however, among them, the left atrial is the predominated candidate (2). It has been demonstrated that genetic mutations are associated with the development of cardiac paraganglioma (3). Moreover, the major mutation is found in the gene SDHB accounting for more than 70% of mutations for cardiac paraganglioma (4). Therefore, it is recommended that all patients with suspected paraganglioma should take a gene test. Unfortunately, this patient refused a gene test due to private reasons. The symptoms of paraganglioma highly depend on the secretion products and the metabolites from tumors, including norepinephrine, epinephrine, and dopamine (5). In principle, the histology of cardiac paraganglioma classified as the extra-adrenal non-epithelial tumor is similar with that of the pheochromocytoma and is mainly considered as a noradrenergic-subtype with the presentation of norepinephrine-related symptoms, such as hypertension, diaphoresis, palpitations, and headache (6). Medically, rather than the secretion level, the location of cardiac paraganglioma is more challenging and significant.

Under persistent secretion of catecholamines, patients with cardiac paraganglioma are more at risk for severe or even fatal complications, including hypertensive crisis, refractory arrhythmias, or myocardial infarction. Hence, as previously reported, both α- and β-adrenoceptor blockers were used for this patient before the surgery to control and adjust the secretion of catecholamines reasonably (7). Moreover, if complicated tachycardia is presented because of the induction by catecholamines, the specific if currency inhibitor, ivabradine is recommended (8). Surgically, the feasibility of cardiac paraganglioma resection should be evaluated cautiously and

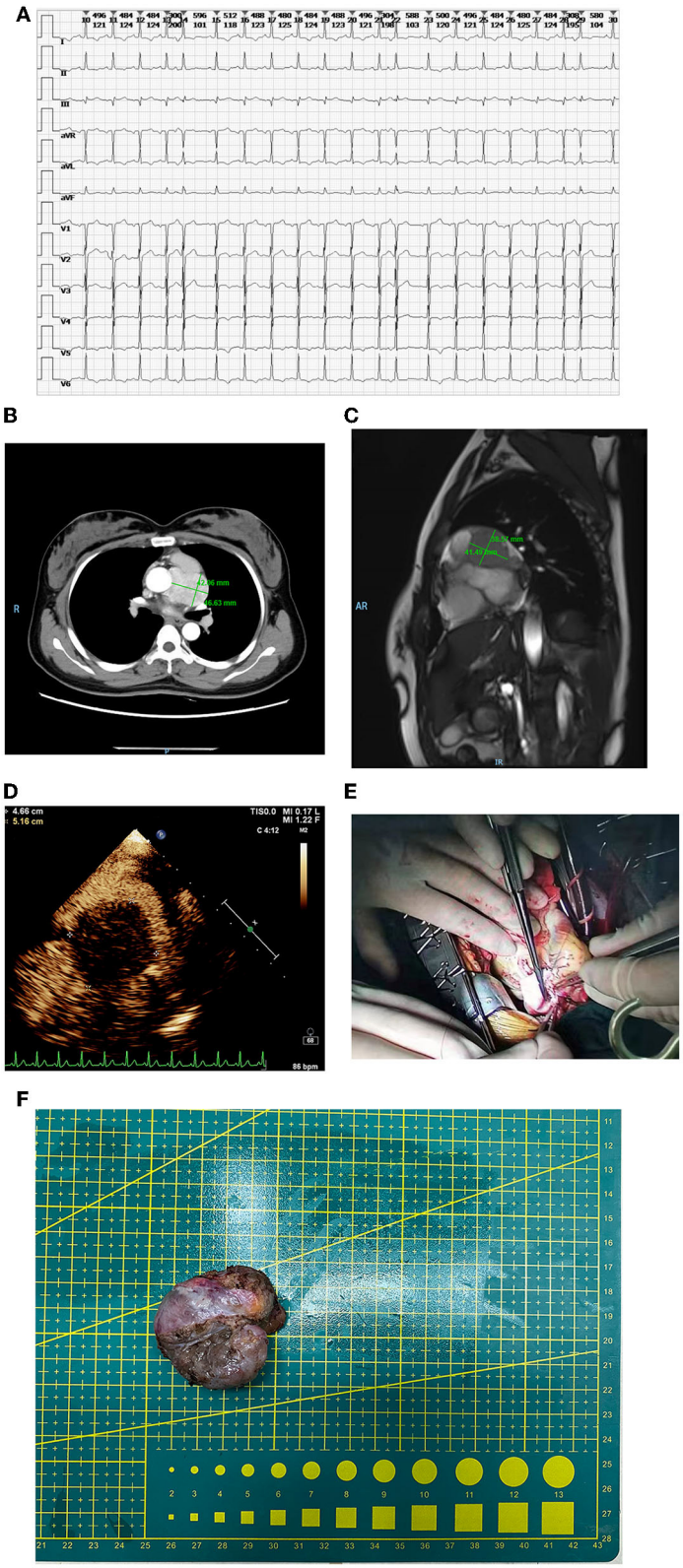

FIGURE 1
(A) Tachycardia in electrocardiogram at admission. **(B)** The mass in the contrast-enhanced CT. The size was 46 × 42 mm and serious adhesion between the aorta and the mass was found. Also, the involved left main coronary was observed. **(C)** The mass in the MRI. Both the root of the aorta and left main coronary were involved, however, the myocardium was free from involvement. **(D)** The mass in the echocardiography. The mass was fully perfused through mini-vascular circulation. **(E)** The repairing of the pulmonary artery. **(F)** The removed mass.

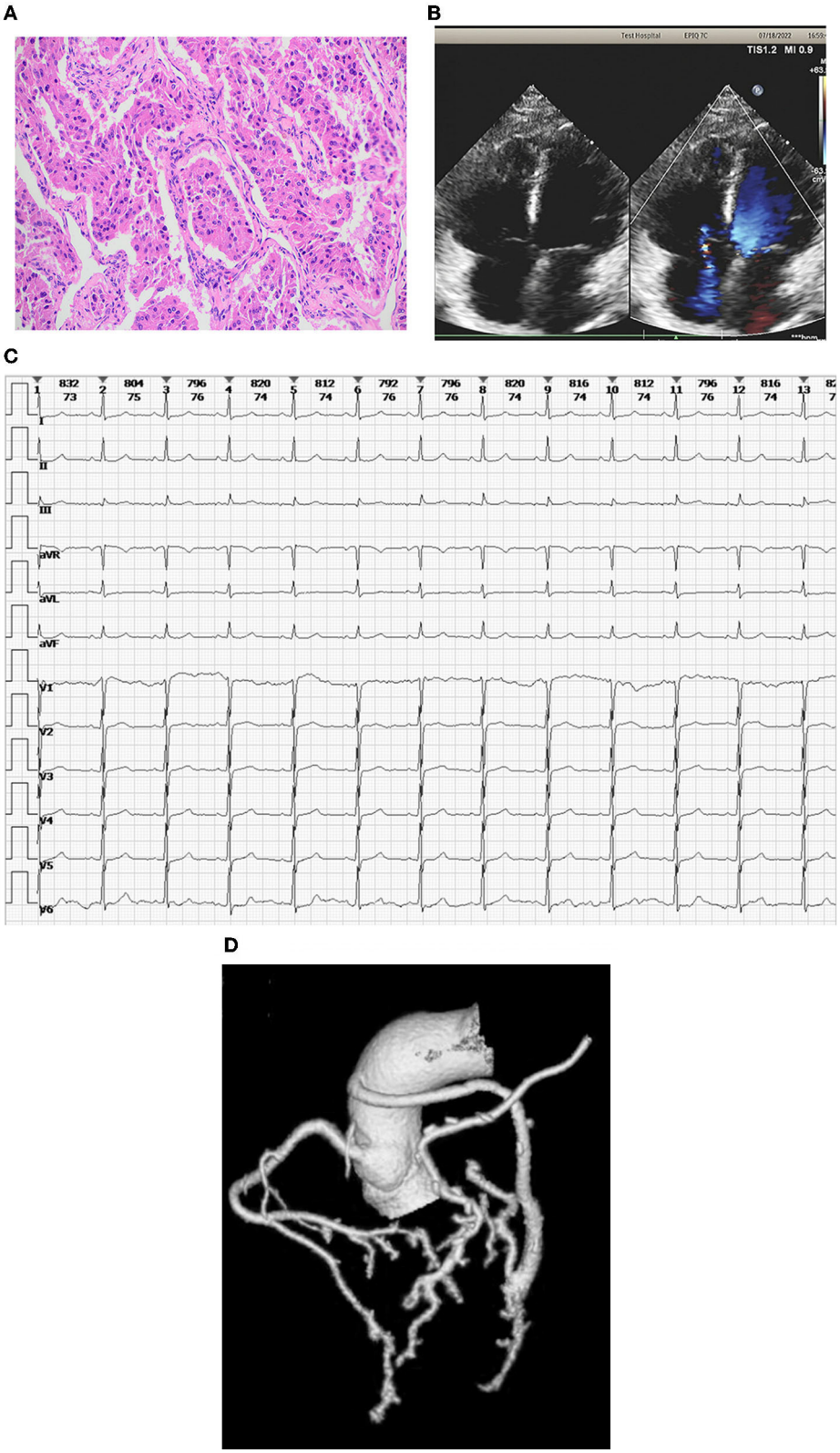

FIGURE 2
(A) Pathology of the removed mass. The pathological findings of the mass were confirmed as cardiac paraganglioma. **(B)** The echocardiography at the latest follow-up. Morphologically, all the chambers and valves were normal and the heart function was stable without any serious abnormal changes. **(C)** Sinus rhythm in electrocardiogram rechecking. **(D)** Coronary CT angiography shows a patent coronary vessel.

carefully prior to surgery. The anatomical changes due to the tumor and the structural relationship between the tumor and surrounding organs and tissues are critical in the decision-making of surgical procedures. For our patient, given the history of pregnancy, although underwent pregnancy termination, a differentiated diagnosis for obstetrical complications should also be needed. Besides, it has been found that paraganglioma without any intervention during pregnancy is closely associated with the high incidence of complications for both pregnant patients and fetuses. Therefore, earlier diagnosis and medical intervention during pregnancy are positive and valuable in improving outcomes and survival for both of them and the most suitable period for surgical resection is no longer than the 24th week of gestation (9, 10). During the surgery, surgical resection was processed under the assistance of CPB established with the peripheral femoral artery-vein path aiming to keep enough space for anastomosis due to serious involvement of the posterior wall of the main pulmonary artery. Following the mass resection, vascular reconstruction and repairing are performed with autologous, xenogeneic, and synthetic materials. In addition, it should be emphasized that the left main coronary of this patient was involved in cardiac paraganglioma, also, CABG is required to reconstruct the system of the coronary artery. Both SVG and LIMA, are the main prepared grafts (11).

Postoperation, management of blood pressure and organic perfusion during the transition period with the absence of excessive stimulation under catecholamines and prevention of recurrence of the tumor are major points influencing the outcome. The improvement for both postoperative survival and life quality is significant and qualified as long as no metastatic lesions are found (12). During the postoperative follow-up of 6 months, the recurred tumor and metastatic lesions or any other tumor-related discomforts and complaints have not been found.

Furthermore, the therapies for patients with metastatic paraganglioma are summarized as chemotherapy, radiotherapy, targeted therapy, and combination therapy. For instance, the combination therapy of cyclophosphamide, vincristine, and dacarbazine following the temozolomide monotherapy is considered the first-line conventional strategy for patients with progressive paraganglioma complicated with SDHB mutation (13). Also, Sunitinib is proved to be the indication of therapy for patients with progressive or even inoperable paraganglioma (14). Clinically, for this kind of rare and complicated tumor and in accordance with various different involved organs and/or tissues, a multidisciplinary team can be assembled to provide more suitable and optimal options in decision-making for postoperative management and dynamic observation during long-term follow-up (15).

Conclusion

Though it is uncommon, the symptoms and complications related to cardiac paraganglioma are severe and even life-threatening, especially for pregnant female patients. Surgical treatment is the most effective strategy against cardiac paraganglioma, nevertheless, the difficulty and feasibility of mass resection should be assessed fully before surgery. During the surgical procedures, completed mass resection and necessary tissue reconstruction are required and CABG should be potential as needed. Periodical follow-up after surgery is useful to evaluate any recurrence or metastasis. If necessary, further medical intervention, such as chemotherapy, radiotherapy, and targeted therapy, may be continued.

Data availability statement

The original contributions presented in the study are included in the article/supplementary material, further inquiries can be directed to the corresponding author/s.

Ethics statement

Written informed consent was obtained from the patient for the publication of this case report and any accompanying images and data.

Author contributions

All authors listed have made a substantial, direct, and intellectual contribution to the work and approved it for publication.

Conflict of interest

The authors declare that the research was conducted in the absence of any commercial or financial relationships that could be construed as a potential conflict of interest.

Publisher's note

All claims expressed in this article are solely those of the authors and do not necessarily represent those of their affiliated organizations, or those of the publisher, the editors and the reviewers. Any product that may be evaluated in this article, or claim that may be made by its manufacturer, is not guaranteed or endorsed by the publisher.

References

1. Neumann HPH, Young WF Jr, Eng C. Pheochromocytoma and paraganglioma. *N Engl J Med.* (2019) 381:552–65. doi: 10.1056/NEJMra1806651

2. Tella SH, Jha A, Taïeb D, Horvath KA, Pacak K. Comprehensive review of evaluation and management of cardiac paragangliomas. *Heart.* (2020) 106:1202–10. doi: 10.1136/heartjnl-2020-316540

3. Fishbein L, Leshchiner I, Walter V, Danilova L, Robertson AG, Johnson AR, et al. Comprehensive molecular characterization of pheochromocytoma and paraganglioma. *Cancer Cell.* (2017) 31:181–93. doi: 10.1016/j.ccell.2017.01.001

4. Martucci VL, Emaminia A. del Rivero J, Lechan RM, Magoon BT, Galia A, et al. Succinate dehydrogenase gene mutations in cardiac paragangliomas. *Am J Cardiol.* (2015) 115:1753–9. doi: 10.1016/j.amjcard.2015.03.020

5. van Berkel A, Lenders JW, Timmers HJ. Diagnosis of endocrine disease: biochemical diagnosis of phaeochromocytoma and paraganglioma. *Eur J Endocrinol.* (2014) 170:R109–19. doi: 10.1530/EJE-13-0882

6. Wang JG, Han J, Jiang T, Li YJ. Cardiac paragangliomas. *J Card Surg.* (2015) 30:55–60. doi: 10.1111/jocs.12455

7. Lenders JW, Duh QY, Eisenhofer G, Gimenez-Roqueplo AP, Grebe SKG, Murad MH, et al. Pheochromocytoma and paraganglioma: an endocrine society clinical practice guideline. *J Clin Endocrinol Metab.* (2014) 99:1915–42. doi: 10.1210/jc.2014-1498

8. Malaza G, Brofferio A, Lin F, Pacak K. Ivabradine in catecholamine-induced tachycardia in a patient with paraganglioma. *N Engl J Med.* (2019) 380:1284–6. doi: 10.1056/NEJMc1817267

9. Bancos I, Atkinson E, Eng C, Young Jr WF, Neumann HPH. Maternal and fetal outcomes in phaeochromocytoma and pregnancy: a multicentre retrospective cohort study and systematic review of literature. *Lancet Diabet Endocrinol.* (2021) 9:13–21. doi: 10.1016/S2213-8587(20)30363-6

10. Lenders JWM, Langton K, Langenhuijsen JF, Eisenhofer G. Pheochromocytoma and pregnancy. *Endocrinol Metab Clin North Am.* (2019) 48:605–17. doi: 10.1016/j.ecl.2019.05.006

11. Zubair MM, El Nihum LI, Haley SL, Al Abri Q, Lenihan DJ, MacGillivray TE, et al. Large, hormonally active primary cardiac paraganglioma: diagnosis and management. *Ann Thorac Surg.* (2022) 113:e167–70. doi: 10.1016/j.athoracsur.2021.05.042

12. Yadav PK, Baquero GA, Malysz J, Kelleman J, Gilchrist IC. Cardiac paraganglioma. *Circ Cardiovasc Interv.* (2014) 7:851–6. doi: 10.1161/CIRCINTERVENTIONS.114.001856

13. Nölting S, Grossman A, Pacak K. Metastatic phaeochromocytoma: spinning towards more promising treatment options. *Exp Clin Endocrinol Diabetes.* (2019) 127:117–28. doi: 10.1055/a-0715-1888

14. Sesti F, Feola T, Puliani G, Centello R, Di Vito V, Bagni O, et al. Sunitinib treatment for advanced paraganglioma: case report of a novel SDHD gene mutation variant and systematic review of the literature. *Front Oncol.* (2021) 11:677983. doi: 10.3389/fonc.2021.677983

15. Chan EY, Ali A, Umana JP, Nguyen DT, Hamilton DJ, Graviss EA, et al. Management of primary cardiac paraganglioma. *J Thorac Cardiovasc Surg.* (2022) 164:158–66. doi: 10.1016/j.jtcvs.2020.09.100

frontiers | Frontiers in Cardiovascular Medicine

TYPE Case Report
PUBLISHED 06 October 2022
DOI 10.3389/fcvm.2022.955527

Check for updates

OPEN ACCESS

EDITED BY
Carlo Gabriele Tocchetti,
University of Naples Federico II, Italy

REVIEWED BY
Leilei Cheng,
Fudan University, China
Jianqing She,
The First Affiliated Hospital of Xi'an Jiaotong University, China

*CORRESPONDENCE
Lianglong Chen
lianglongchen@126.com

SPECIALTY SECTION
This article was submitted to Cardio-Oncology, a section of the journal Frontiers in Cardiovascular Medicine

RECEIVED 28 May 2022
ACCEPTED 13 September 2022
PUBLISHED 06 October 2022

CITATION
Lin Y, Yuan X and Chen L (2022) Immune myocarditis related to sintilimab treatment in a patient with advanced lung adenocarcinoma: A case report.
Front. Cardiovasc. Med. 9:955527.
doi: 10.3389/fcvm.2022.955527

COPYRIGHT
© 2022 Lin, Yuan and Chen. This is an open-access article distributed under the terms of the Creative Commons Attribution License (CC BY). The use, distribution or reproduction in other forums is permitted, provided the original author(s) and the copyright owner(s) are credited and that the original publication in this journal is cited, in accordance with accepted academic practice. No use, distribution or reproduction is permitted which does not comply with these terms.

Immune myocarditis related to sintilimab treatment in a patient with advanced lung adenocarcinoma: A case report

Yunling Lin, Xun Yuan and Lianglong Chen*

Department of Cardiology, Fujian Medical University Union Hospital, Fujian Cardiovascular Medical Center, Fujian Institute of Coronary Heart Disease, Fuzhou, China

Immune checkpoint inhibitors (ICI) have improved clinical outcomes of patients with advanced lung cancer, but may lead to fatal cardiac injury. We describe a 66-year-old man with advanced lung adenocarcinoma who presented with chest pain and dyspnea 3 weeks after the first dose of sintilimab. The initial electrocardiogram (ECG) demonstrated ST-elevation in leads V5-V9, and a high-sensitivity troponin level was significantly elevated. However, coronary angiography did not reveal any significant stenosis. The patient was successfully treated with methylprednisolone and immunoglobulin. Cardiac MRI was carried out before discharge and late gadolinium enhancement (LGE) was found to be in the mid layer of the septal segment and the subepicardial layer of the inferolateral wall. Due to the high fatality, ICI-related myocarditis requires close surveillance, prompt management and long-term follow-up.

KEYWORDS

PD-1, myocarditis, sintilimab, lung adenocarcinoma, cardio-oncology, immune-related adverse events

Data from the National Cancer Center shows that lung cancer is the leading causes of cancer morbidity and mortality in China (1). Monoclonal antibodies targeting inhibitory immune checkpoints (ICI) have significantly improved results for patients with advanced-stage lung cancer (2). However, treatment with ICI is accompanied by immune-related adverse events (irAEs) (3). The immune-related adverse events that most often affect the colon, the liver, the lungs, and the skin, although some rare events may affect the heart as well. Cardiotoxicity induced by ICI may present with arrhythmias, cardiomyopathy, myocarditis, pericarditis and vasculitis. Myocarditis has emerged as an rare, but often fatal complication (4).

Sintilimab has shown positive results in people with relapsed/refractory (RR) Hodgkin's lymphoma, non-small cell lung cancer, esophagealcarcinoma (5–8). We report here a case of a 66-year-old man with advanced lung adenocarcinoma who developed acute myocarditis. The patient was treated successfully with IV methylprednisolone and immunoglobulin. We present the following case in accordance with the CARE reporting checklist.

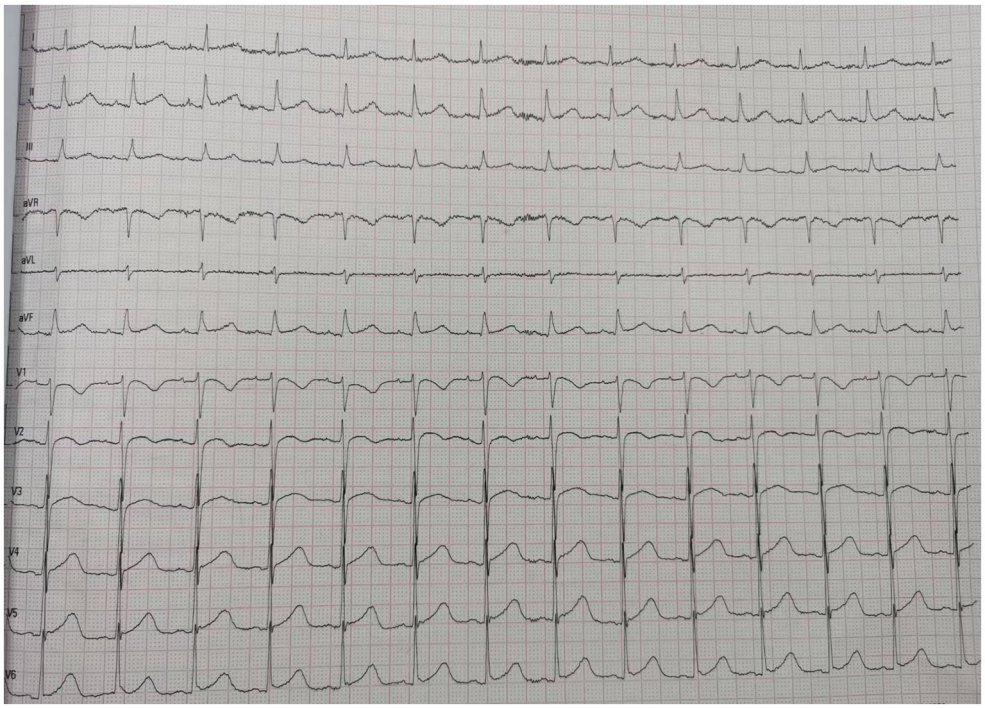

FIGURE 1
ECG before chemotherapy.

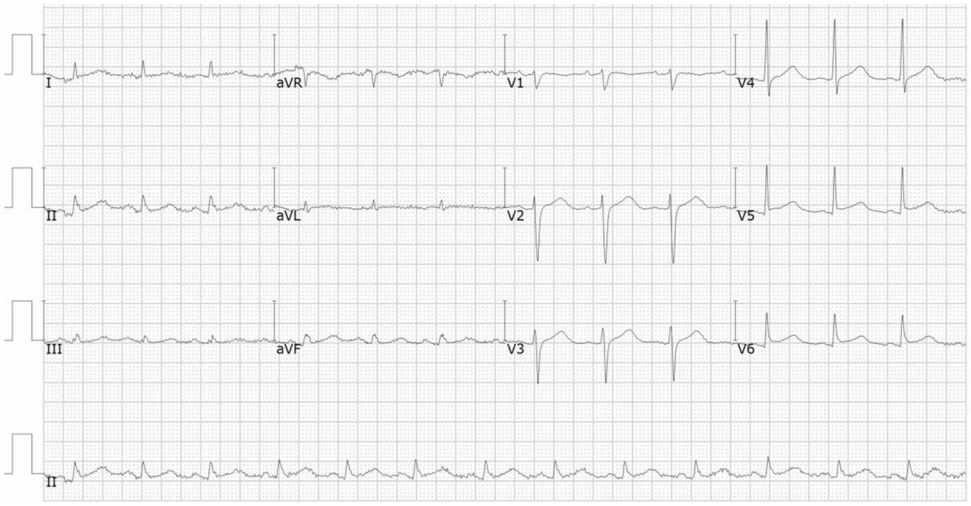

FIGURE 2
ECG on admission showed ST-segment elevation in leads V5 and V6.

A 66-year-od man with advanced lung adenocarcinoma was admitted to the local chest pain center with progressive chest pain, dyspnea. He had been diagnosed with advanced lung adenocarcinoma 4 month earlier. He had no history of autoimmune or cardiovascular diseases. Cardiac screening tests including cardiac biomarkers, ECG (Figure 1), and echocardiography showed normal results before chemotherapy. The patient was treated with four cycles of albumin paclitaxel

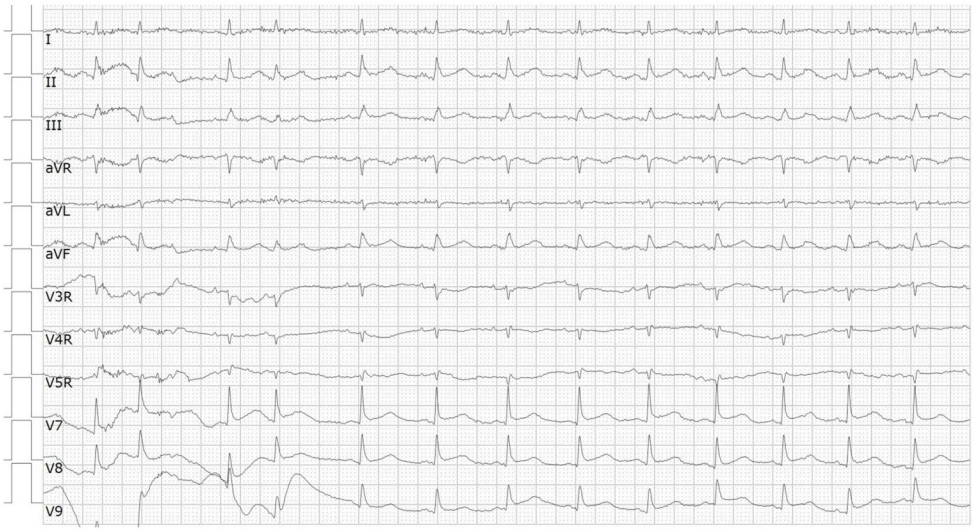

FIGURE 3
ECG on admission showed ST-segment elevation in leads V7 through V9.

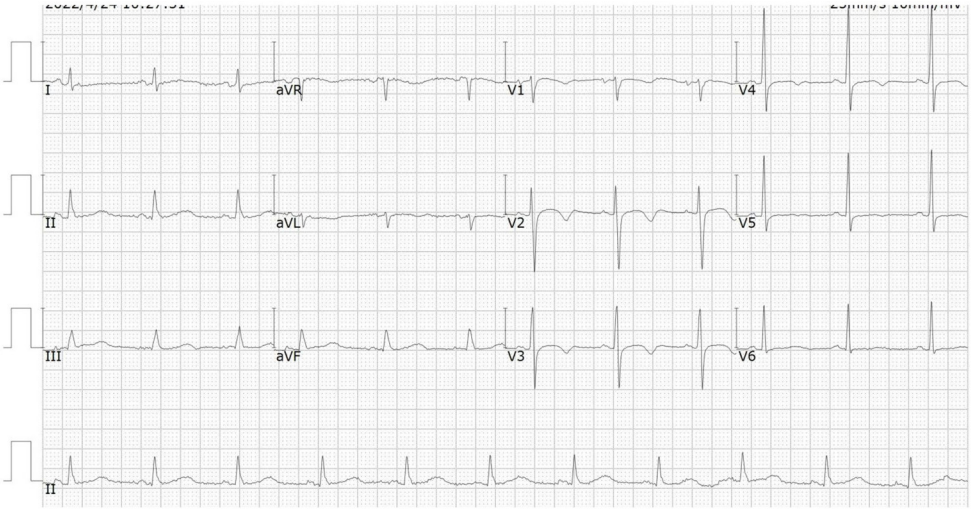

FIGURE 4
ECG at day 4 showed the elevated ST-segment had fallen back.

plus carboplatin. The CT scan showed that the patient was not responding to chemotherapy. Then he started albumin paclitaxel plus carboplatin for chemotherapy combined with sintilimab (200 mg/injection). 3 weeks after sintilimab initiation, the patient presented with chest pain, shortness of breath and was admitted to the hospital. His vital signs were unstable on arrival (temperature 36.7°C, heart rate, 84 beats/min; respiratory rate 17 breaths/min, blood pressure 84/52 mmHg. The admission ECG showed sinus rhythm with ST-segment elevation in leads V5 through V9 (Figures 2, 3); laboratory test showed that cardiac troponin-I was 9.4 ng/mL (normal range, 0.00–0.03 ng/mL), CK 922IU/L (normal range, 22-270IU/L), CK-MB 109 IU/L (normal range, 2-25 IU/L);NT-proBNP 8290pg/ml (normal range, 0-349pg/ml). Transthoracic echocardiography showed anterior hypokinaesia, severe left ventricular function impairment with a left ventricular ejection fraction of 35%, mild pericardial effusion (Supplementary Videos 4–7). Coronary angiography was performed showing normal coronary arteries (Supplementary Videos 1–3). A diagnosis of sintilimab associated myocarditis was considered. The patient received

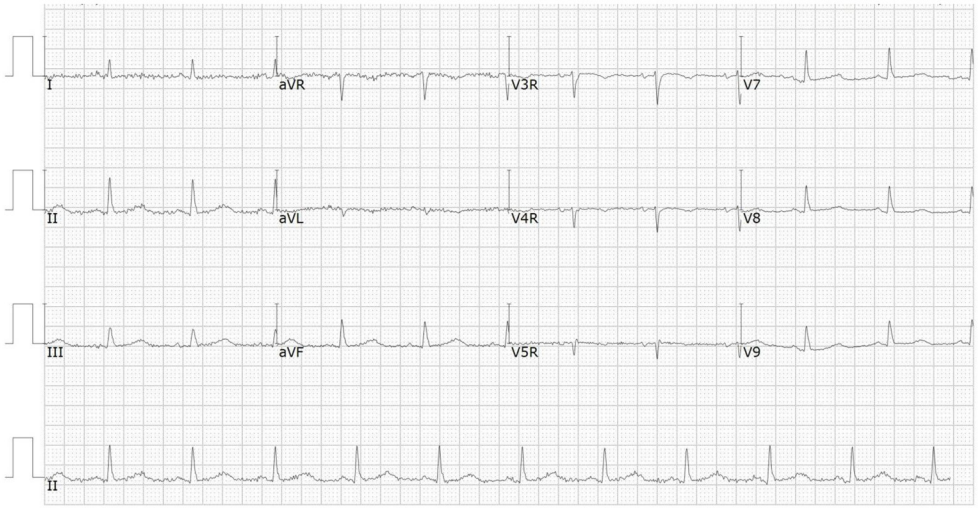

FIGURE 5
ECG at day 4 showed the elevated ST-segment in leads V7 through V9 had fallen back.

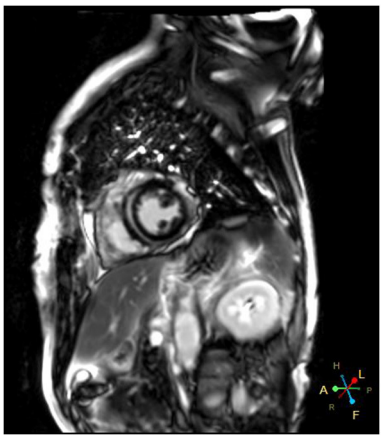

FIGURE 6
Cardiac magnetic resonance showed late gadolinium enhancement in left ventricular wall.

methylprednisolone (2 mg/kg) and immunoglobulin (0.4g/kg/d) intravenously for 7 days. At day 4, the ECG showed that the elevated ST-segment had fallen back (Figures 4, 5). At day 8, cardiac magnetic resonance was performed and showed late gadolinium enhancement in the mid layer of the septal segment and the subepicardial layer of the inferolateral wall (Figure 6), with an ejection fraction of 47% (Supplementary Video 11). Gradually, the patient's symptoms improved and his vital signs were stable. The lab tests showed persistent decrease of hs-cTnI, myocardial enzyme indexes (Table 1). Echocardiogram revealed improved left ventricular systolic function, with an ejection fraction of 52% (Supplementary Videos 8–10). The dose of

TABLE 1 The chronological changes of major parameters.

Days after sintilimab infusion	0	20	30
LVEF, %	65	35	52
TnI, ng/mL	0.02	9.4	0.42
NT-proBNP, pg/ml	28	8,290	1,265
CKMB, IU/L	13	109	24

CK, creatine kinase; LVEF, left ventricular ejection fraction; NT-proBNP, N-terminal pro-brain natriuretic peptide; hs-TnI, high-sensitivity Troponin I.

glucocorticoid therapy was gradually reduced. The patient was discharged 10 days after admission. He received oral prednisone tablets with gradually decreasing doses and regular follow-up.

Discussion

In recent years, Immune checkpoint inhibitors has become more widely used in clinical practice and improved the prognosis of patients with malignancy. In the meantime, ICI have been reported to induce cardiovascular toxicities, including myocarditis, pericarditis and vasculitis. The incidence of ICI related myocarditis has ranged from 0.27 to 1.14% (9), but it is often severe and life threatening. The reported incidence of ICIs-related myocarditis is low (<1%), it can be life threatening with a mortality rate up to 60 % (10, 11). Endomyocardial biopsy remains the gold standard for definitive diagnosis of ICI-induced myocarditis but it is not widely used because of its procedural risks and technical limitations. Cardiac magnetic resonance (CMR) has evolved as an standard noninvasive tool for the diagnosis and evaluation of

myocarditis. Late gadolinium enhancement (LGE) is associated with a poor prognosis in patients with ICI-induced myocarditis (12). Myocardial biopsy and CMR are often not available in the setting of an acute presentation. It has been demonstrated that 2D/3D speckle-tracking strain imaging echocardiography may be promising diagnostic and prognostic tool in acute myocarditis, even in patients with preserved left-ventricular ejection fraction (13). However, the major pitfalls of speckle-tracking are its dependency on image quality and its ability to define the endocardial and epicardial boundaries. Once diagnosed, treatment should be initiated immediately. However, due to the absence of high-level evidence studies, there are still no standard therapeutic strategies. Glucocorticoid treatment is recommended for ICI-associated myocarditis but the effective dosage and optimal duration of corticosteroid therapy are not precisely recommended. Due to limited clinical data, the utility of other immunosuppressive agents is not well established.

Sintilimab is a humanized monoclonal IgG4 antibody which was approved for the treatment of hematological cancers and several advanced solid tumors in China. The epitope of the sintilimab/PD-1 complex is located at the FG loop of PD-1, which is different from that of nivolumab or pembrolizumab Compared to nivolumab or pembrolizumab, sintilimab has a higher binding affinity with more PD-1 molecules on CD3+T cells, and has better T cell activating characteristics. Sintilimab exhibited good safety and tolerability in clinical studies (5–8). Compared to nivolumab or pembrolizumab, sintilimab has a higher binding affinity with more PD-1 molecules on CD3+T cells, and has better T cell activating characteristics. For sintilimab, the incidence of fatal treatment-related adverse events (TRAEs) ranges from 1 to 6.25%. The incidence of TRAEs for sintilimab monotherapy ranges from 0 to 2.5%. It seems to be higher than average (14). Four cases of sintilimab-induced myocarditis have been reported recently (15–18), but cardiac magnetic resonance imaging was not performed in all of these patients. In our case, the echocardiography showed that cardiac function was severely damaged with a LVEF of 35% on admission. A significant improvement of left ventricular systolic function with a LVEF of 52% was noted several days after treatment. However, cardiac MRI showed extensive myocardium fibrosis. Therefore, longer follow-up is warranted to determine whether myocardial fibrosis can fully regress and to observe the the long-term prognosis of the patient.

Data availability statement

The raw data supporting the conclusions of this article will be made available by the authors, without undue reservation.

Ethics statement

Written informed consent was obtained from the participant for the publication of this case report. Written informed consent was obtained from the individual(s) for the publication of any potentially identifiable images or data included in this article.

Author contributions

YL: contributed to the clinical care of the patient data analysis, writing of the article, and editing of the figure. XY: contributed to the literature search and clinical record collection. LC: contributed to study design and critical review of the article. All authors contributed to the article and approved the submitted version.

Funding

This study was financially supported by the funding for Top Hospital and Specialty Excellence of Fujian Province (grant no. 212790530102) and the Provincial Natural Science Foundation of Fujian (grant no. 2022J01253), China.

Conflict of interest

The authors declare that the research was conducted in the absence of any commercial or financial relationships that could be construed as a potential conflict of interest.

Publisher's note

All claims expressed in this article are solely those of the authors and do not necessarily represent those of their affiliated organizations, or those of the publisher, the editors and the reviewers. Any product that may be evaluated in this article, or claim that may be made by its manufacturer, is not guaranteed or endorsed by the publisher.

Supplementary material

The Supplementary Material for this article can be found online at: https://www.frontiersin.org/articles/10.3389/fcvm.2022.955527/full#supplementary-material

References

1. Zheng R, Zhang S, Zeng H, Wang S, Sun K, Chen R, et al. Cancer incidence and mortality in China, 2016. *J Natl Cancer Center*. (2022) 2:1–9. doi: 10.1016/j.jncc.2022.02.002

2. Liu SY, Wu YL. Tislelizumab: an investigational anti-PD-1 antibody for the treatment of advanced non-small cell lung cancer (NSCLC). *Exp Opin Invest Drugs*. (2020) 29:1355–64. doi: 10.1080/13543784.2020.1833857

3. Schneider BJ, Naidoo J, Santomasso BD, Lacchetti C, Adkins S, Anadkat M, et al. Management of immune-related adverse events in patients treated with immune checkpoint inhibitor therapy: ASCO guideline update. *J Clin Oncol*. (2021) 39:4073–126. doi: 10.1200/JCO.21.01440

4. Witteles RM, Neal JW, Nguyen P, Davis MM, et al. Immune checkpoint inhibitor cardiotoxicity: understanding basic mechanisms and clinical characteristics and finding a cure. *Annu Rev Pharmacol Toxicol*. (2021) 61:113–34. doi: 10.1146/annurev-pharmtox-010919-023451

5. Goody PR, Zimmer S, Öztürk C, Zimmer A, Kreuz J, Becher MU, et al. 3D-speckle-tracking echocardiography correlates with cardiovascular magnetic resonance imaging diagnosis of acute myocarditis—An observational study. *Int J Cardiol Heart Vasc*. (2022) 41:101081. doi: 10.1016/j.ijcha.2022.101081

6. Ren Z, Xu J, Bai Y, Xu A, Cang S, Du C, et al. Sintilimab plus a bevacizumab biosimilar (IBI305) versus sorafenib in unresectable hepatocellular carcinoma (ORIENT-32): a randomised, open-label, phase 2-3 study. *Lancet Oncol*. (2021) 22:977–90. doi: 10.1016/S1470-2045(21)00252-7

7. Tao R, Fan L, Song Y, Hu Y, Zhang W, Wang Y, et al. Sintilimab for relapsed/refractory extranodal NK/T cell lymphoma: a multicenter, single-arm, phase 2 trial (ORIENT-4). *Signal Transduc Targeted Ther*. (2021) 6:365. doi: 10.1038/s41392-021-00768-0

8. Randomized D. Phase 3 Study (Oncology pRogram by InnovENT anti-PD-1-11). *J Thorac Oncol*. (2020) 15:1636–46. doi: 10.1016/j.jtho.2020.07.014

9. Moslehi J, Lichtman AH, Sharpe AH, Galluzzi L, Kitsis RN. Immune checkpoint inhibitor-associated myocarditis: manifestations and mechanisms. *J Clin Invest*. (2021) 131:e145186. doi: 10.1172/JCI145186

10. Shalata W, Abu-salam A, Steckbeck R, Jacob BM, Massalha I, Yakobson A. Cardiac toxicity associated with immune checkpoint inhibitors: a systematic review. *Cancers*. (2021) 13:5218. doi: 10.3390/cancers13205218

11. Moslehi JJ, Salem JE, Sosman JA, Lebrun-Vignes B, Johnson DB. Increased reporting of fatal immune checkpoint inhibitor-associated myocarditis. *Lancet (London, England)*. (2018) 391:933. doi: 10.1016/S0140-6736(18)30533-6

12. Cadour F, Cautela J, Rapacchi SV, Habert P, Arnaud F, et al. Cardiac MRI Features and Prognostic Value in Immune Checkpoint Inhibitor-induced Myocarditis. *Radiology*. (2022) 2022:211765. doi: 10.1148/radiol.211765

13. Kostopoulos VS, Tryfou ES, Giannaris VD, Rodis IE, Olympios CD, et al. Subclinical left ventricular dysfunction and correlation with regional strain analysis in myocarditis with normal ejection fraction A new diagnostic criterion. *Int J Cardiol*. (2018) 259:116–21. doi: 10.1016/j.ijcard.2018.01.058

14. Zhang L, Lin W, Tan F, Li N, Xue Q, Gao S, et al. *Sintilimab for the treatment of non-small cell lung cancer*. *Biomark Res*. (2022) 10:23. doi: 10.1186/s40364-022-00363-7

15. Yang ZX, Chen X, Tang S, Zhan Q. Sintilimab-induced myocarditis overlapping myositis in a patient with metastatic thymoma: a case report. *Front Cardiovasc Med*. (2021) 8:797009. doi: 10.3389/fcvm.2021.797009

16. Tang Y, Zhang Y, Yang XY. Rare case of wide QRS tachycardia after sintilimab treatment for lung cancer. *Circulation*. (2022) 145:783–6. doi: 10.1161/CIRCULATIONAHA.121.058936

17. Xing Q, Zhang ZW, Lin QH, Shen LH, Wang PM, Zhang S, et al. Myositis-myasthenia gravis overlap syndrome complicated with myasthenia crisis and myocarditis associated with anti-programmed cell death-1 (sintilimab) therapy for lung adenocarcinoma. *Ann Transl Med*. (2020) 8:250. doi: 10.21037/atm.2020.01.79

18. Bi H, Ren D, Wang Q, Ding X, Wang H. Immune checkpoint inhibitor-induced myocarditis in lung cancer patients: a case report of sintilimab-induced myocarditis and a review of the literature. *Ann Palliat Med*. (2021) 10:793–802. doi: 10.21037/apm-20-2449

frontiers | Frontiers in Oncology

TYPE Case Report
PUBLISHED 27 October 2022
DOI 10.3389/fonc.2022.1018741

Check for updates

OPEN ACCESS

EDITED BY
Reto Asmis,
Wake Forest University, United States

REVIEWED BY
Chengming Fan,
Department of Cardiovascular Surgery, Central South University, China
Jun-Neng Roan,
National Cheng Kung University Hospital, Taiwan

*CORRESPONDENCE
Feixue Song
13639336037@139.com

SPECIALTY SECTION
This article was submitted to Cardio-Oncology, a section of the journal Frontiers in Oncology

RECEIVED 13 August 2022
ACCEPTED 14 October 2022
PUBLISHED 27 October 2022

CITATION
Tian K, Liu Y, Zhu H, Wang T, Chen T, Pei X and Song F (2022) A case report of primary cardiac angiosarcoma with *DNMT3A* gene mutation. *Front. Oncol.* 12:1018741. doi: 10.3389/fonc.2022.1018741

COPYRIGHT
© 2022 Tian, Liu, Zhu, Wang, Chen, Pei and Song. This is an open-access article distributed under the terms of the Creative Commons Attribution License (CC BY). The use, distribution or reproduction in other forums is permitted, provided the original author(s) and the copyright owner(s) are credited and that the original publication in this journal is cited, in accordance with accepted academic practice. No use, distribution or reproduction is permitted which does not comply with these terms.

A case report of primary cardiac angiosarcoma with *DNMT3A* gene mutation

Kun Tian, Yating Liu, Haiying Zhu, Tao Wang, Tianxing Chen, Xiaxia Pei and Feixue Song*

Department of Medical Oncology, Second Hospital of Lanzhou University, Lanzhou, China

Cardiac angiosarcoma is a rare disease with a high mortality rate despite its low incidence. Surgery is currently the mainstay treatment strategy for patients with this condition. Herein, we describe a case of primary cardiac angiosarcoma, including symptoms, examination findings, treatment strategy and prognosis. In 2020, the patient was admitted to our hospital, and Next-Generation Sequencing (NGS) revealed a mutation in the *DNMT3A* gene. Generally, *DNMT3A* mutations are most commonly seen in atherosclerosis and myeloid leukemia. To our knowledge, this is the first reported case of primary cardiac angiosarcoma with *DNMT3A* gene mutation.

KEYWORDS

cardiac angiosarcoma, *DNMT3A*, surgery, chemotherapy, cardiac tumor rupture

Introduction

Primary cardiac neoplasm is extremely rare, with an incidence of 0.001%-0.003%, among which only 25% of cases are classified as malignant (1). Primary cardiac angiosarcoma (PCAS) is the most common histological subtype (50%-75%) characterized by high malignancy and invasiveness. It originates from vascular endothelial cells and tends to invade the myocardium, valves, pericardium and even the coronary arteries. At the time of diagnosis, around 89% of patients reportedly have distant metastases (2, 3). PCAS patients have a poor prognosis in general, with the median overall survival (OS) estimated at around 16 months to as low as 2 months in advanced metastatic cases (4). In this case report, we present a unique case of PCAS induced by a mutation in the DNMT3 gene.

Case presentation

The patient is a 45-year-old middle-aged male, a farmer by profession, with no history of chronic diseases and no family history of tumors. He visited the Department of Orthopedics for "lumbago for a week" in early March 2020. CTimaging revealed bone destruction at the L3 vertebral level, with an abnormally low-density shadow (See Figure 1). The bone scan showed low uptake, but its properties remain to be determined. A biopsy was conducted, and pathological analysis revealed angiosarcoma (L3). Immunohistochemical (IHC) staining showed the following: CD31 (+), CD34 (+), Vimentin (+), CKp (-), S-100 (-), and 30% Ki-67-positive cells (See Figure 2). Considering that the angiosarcoma (L3) was metastatic, a whole-body CT scan was performed. Space-occupying lesions in the right atrium, liver segment S8, pericardium and bone (See Figure 3). Echocardiography (ECG) revealed: EF of 60% and FS of 31% in the Left ventricular ejection fraction (LVEF); a mean pulmonary arterial pressure (mPAP) of 17 mmHg; effusion in the pericardial cavity; pericardial thickening in the lateral right ventricular wall with the widest diameter measuring about 11 mm; and a hypoechoic lesion (6.4×5.7 cm) in the right atrial roof with inhomogeneous echogenicity causing compression of the atrium. During his hospital stay, the patient experienced pericardiac tamponade. Pericardiocentesis and pericardial drainage were performed, and 600 ml of hemorrhagic fluid was extracted and screened for cancer cells using cytology. After a period of symptomatic treatment, the patient felt better and discharge.

The patient was readmitted to the hospital in May 2022 with chest tightness, shortness of breath, and pain in the anterior chest region. A CT examination was performed and the right atrium and liver lesion were found to be significantly larger than before, as well as pericardial effusion, right pleural effusion and incomplete right lower lung distension were detected (See Figure 3). It was a challenge to determine the primary focus, for which we conducted a multidisciplinary discussion, and by reviewing the literature we found that angiosarcoma with primary origin in the heart accounted for 23.5%, while the percentage of primary in the liver and vertebral body was 7.4% and 4.4%. In addition, through imaging we found that the lesion in the liver was most likely due to direct invasion of the right atrial lesion into the liver (See Figure 4), so we judged that the primary lesion in this patient was the right atrium. Considering the risk of rupture of the cardiac tumor at any time, the patient was advised to remove the cardiac tumor and repair the wall of the right atrium, but the patient and his family refused the surgery considering the riskiness and cost of the procedure. Before starting treatment, we performed NGS of the L3 bone puncture specimen and found a 10.7% abundance of a missense mutation in exon 19 of the DNMT3A gene (p.Glu733Ala). There is no standard treatment option for patients with advanced

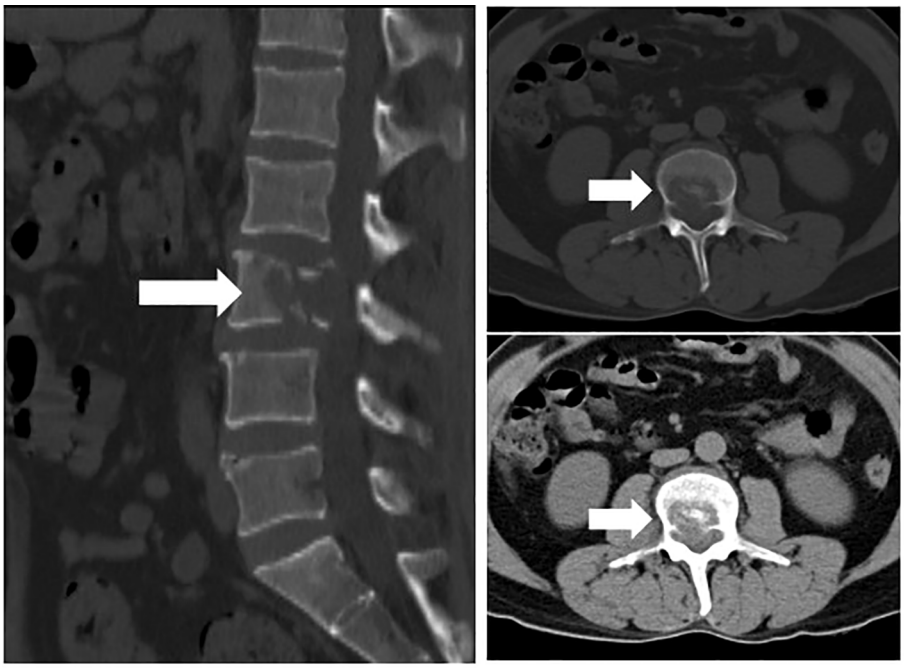

FIGURE 1
Bone destruction of the L3 vertebral body with abnormal low-density shadow within it(arrows).

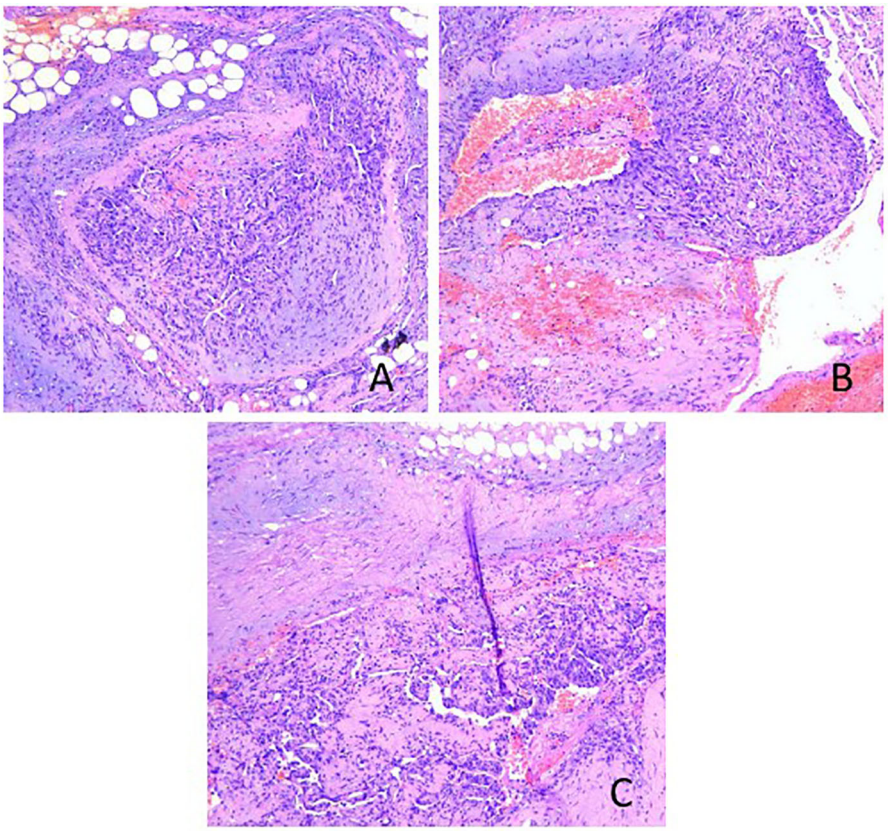

FIGURE 2
Hematoxylin & eosin staining of the L3 biopsy: **(A)** The tumor tissue consisted of well-differentiated vascular lumen, which grew infiltratively around; **(B)** the lumen was irregular in size and shape, communicating with each other to form anastomosis or communication, and erythrocytes were seen in the lumen; **(C)** the lumen was lined with monolayer, dark-stained endothelial cells, partly forming papillae in the lumen, and the tumor cells were heterogeneous with large, dark-stained, heterogeneous nuclei.

metastatic PCAS. Although we identified mutations in the DNMT3A gene, there are no corresponding targeted drugs; the TMB of this patient was 1.0 mutations/Mb, microsatellite stability(MSS) type, suggesting that immunotherapy may not be effective; meanwhile, the patient's tumor progressed too fast, the radiation treatment time was long, and there was a risk of acute cardiac rupture during the treatment, and the radiotherapy department evaluated and recommended 2 cycles of chemotherapy first to evaluate the efficacy before deciding whether to give radiotherapy. Therefore, we chose Gemcitabine (1.4 g, Day 1, 8) and Docetaxel (150 mg, Day 8) for two cycles starting May 2020. The Gemcitabine dose was then increased to 1.5 g in June and after 1 cycle, stable disease (SD) was achieved on CT scan (See Figure 3). However, in mid-July, the patient presented with acute chest pain, with blood pressure fluctuating between 80-90 and 40-50 mmHg. CT scan indicated significant pleural effusions (See Figure 5), and a routine blood test revealed an RBC of 2.69*10-12/L and HGB of 76 g/L. Combining the medical history, we hypothesize that the bleeding could have been caused by cardiac tumor rupture; and the patient subsequently died three days later.

Discussion

PCAS is a very rare malignant tumor. According to Epidemiological statistics there were 16 PCAS patients admitted to the Peking Union Medical College Hospital from January 1990 to June 2017, 40 PCAS patients at the French Sarcoma Group from 1977 to 2010, 16 PCAS patients at the British Columbia Cancer Agency from 1990 to 2006, and 9 PCAS patients at the Cleveland Clinic from 1988 to 2013. In addition, a total of 168 PCAS cases from 1973 to 2013 were documented in the SEER database. PCAS is a highly aggressive tumor that affects more males than females, with a mean age of onset of 44.4 ± 15.5 years old. The lungs, liver, brain, lymph nodes, bone, adrenal gland, and spleen are the most common sites of metastasis in the early stages. Besides, PCAS patients

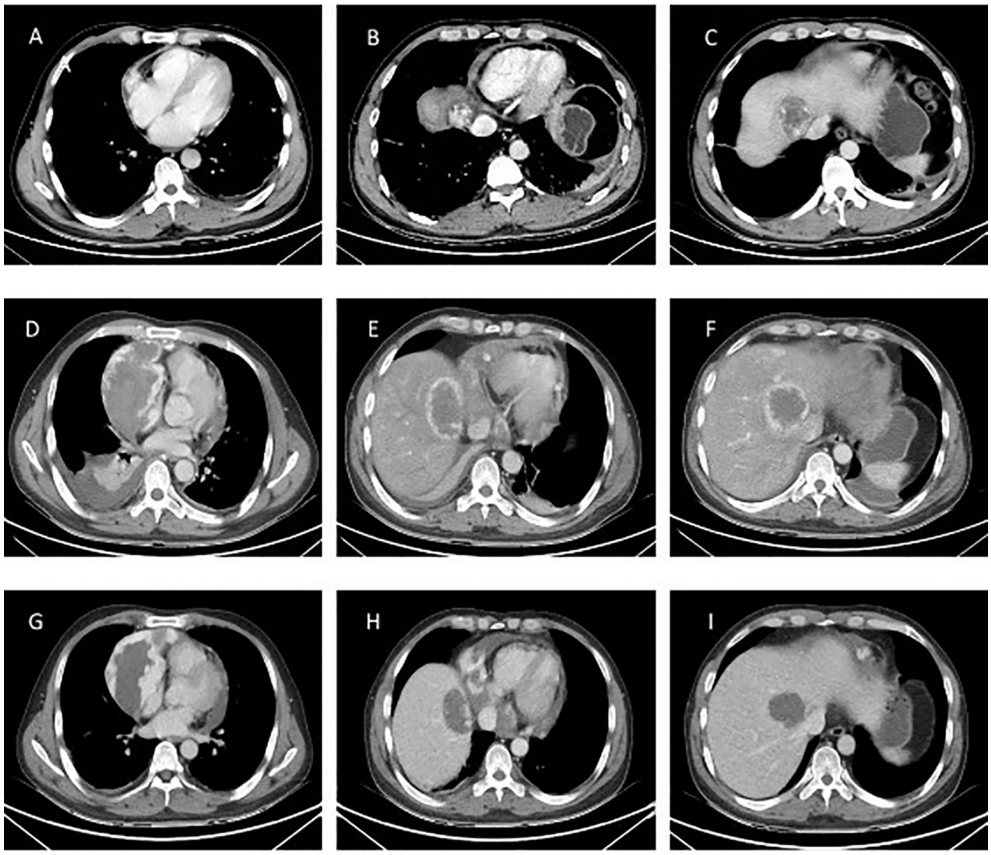

FIGURE 3
CT examination of the patient. **(A-C)** Patient's initial CT image in March 2020. Space-occupying lesions in the right atrium, liver segment S8, pericardium; **(D-F)** CT images at the time of the patient's readmission in May 2020. The right atrium and liver lesion were found to be significantly larger than before, as well as pericardial effusion, right pleural effusion and incomplete right lower lung distension were detected; **(G-I)** Efficacy evaluation after 1 cycle of chemotherapy with stable disease in June 2020.

have a short overall survival time, with a reported median of 12-14 months abroad and a median of 3 months in China (5–8). In most cases, PCAS originates from the right atrium, presenting with cough, chest tightness, shortness of breath, palpitation, fever or weakness in the early stage, as well as other non-specific symptoms such as dyspnea and chest pain in the later stages (9). Metastatic lesions can induce various symptoms, including lumbago, which was the initial presentation of our patient.

Imaging is a valuable tool for diagnosing and evaluating PCAS. The ECG is the most basic non-invasive diagnostic tool available that can be used to detect around 75% of primary cardiac malignancies. Additionally, it provides critical information on valve function, tumor site, and the relationship between the tumor and the heart wall. Furthermore, ECG can also be used to assess cardiac function (10). In contrast, CT scans are often used for cancer diagnosis by revealing the presence of a cardiac space-occupying lesion, lesion enhancement using a contrast agent, lesion attachment to the myocardium, central necrosis and uneven density of the tumor, pericardial effusion, local invasion, and distant metastasis. Positron emission computed tomography (PET) is a non-invasive preoperative test that can identify primary lesions and potential metastases *via* their hypermetabolic properties (SUV value: 3.5-9.4). On the other hand, Cardiac magnetic resonance (CMR) can clearly reveal tumor information, including the anatomical location, size, tissue characteristics and the adjacent structures, which serve as an important reference for surgical assessment (5–11). Angiosarcoma manifestations on CMR include inhomogeneous isointense or long T1/T2 signals, mild patchy enhancement within the lesion at first and predominantly inhomogeneous enhancement during the delayed phase.

Cytology and IHC are the golden standards for the diagnosis of PCAS. Microscopically, well-differentiated PCAS has irregular vessel lumens and blood sinusoids of different diameters that are interconnected to form a mesh-like pattern. The lumens are filled with red blood cells and the inner walls are covered with tumor endothelial cells, which present with varying morphologies (spindle-shaped or epithelioid), significant

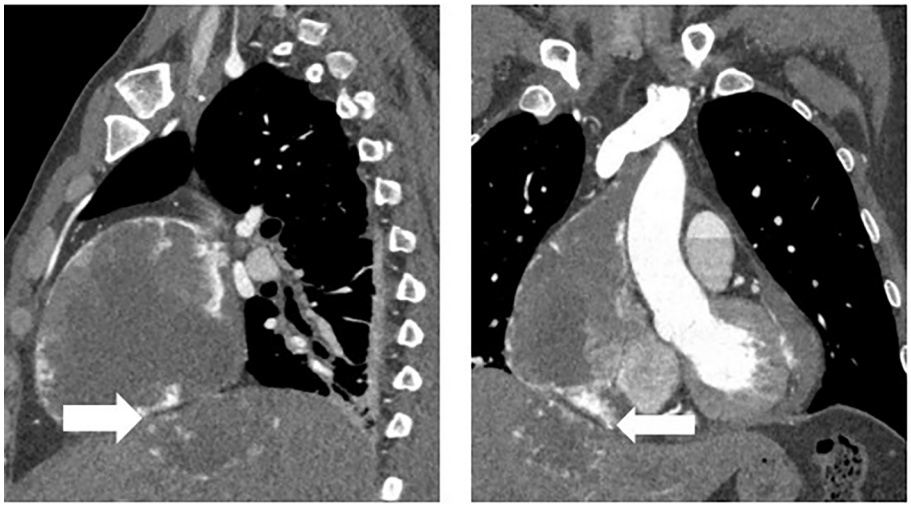

FIGURE 4
Direct invasion of the liver by a right atrial lesion(arrows).

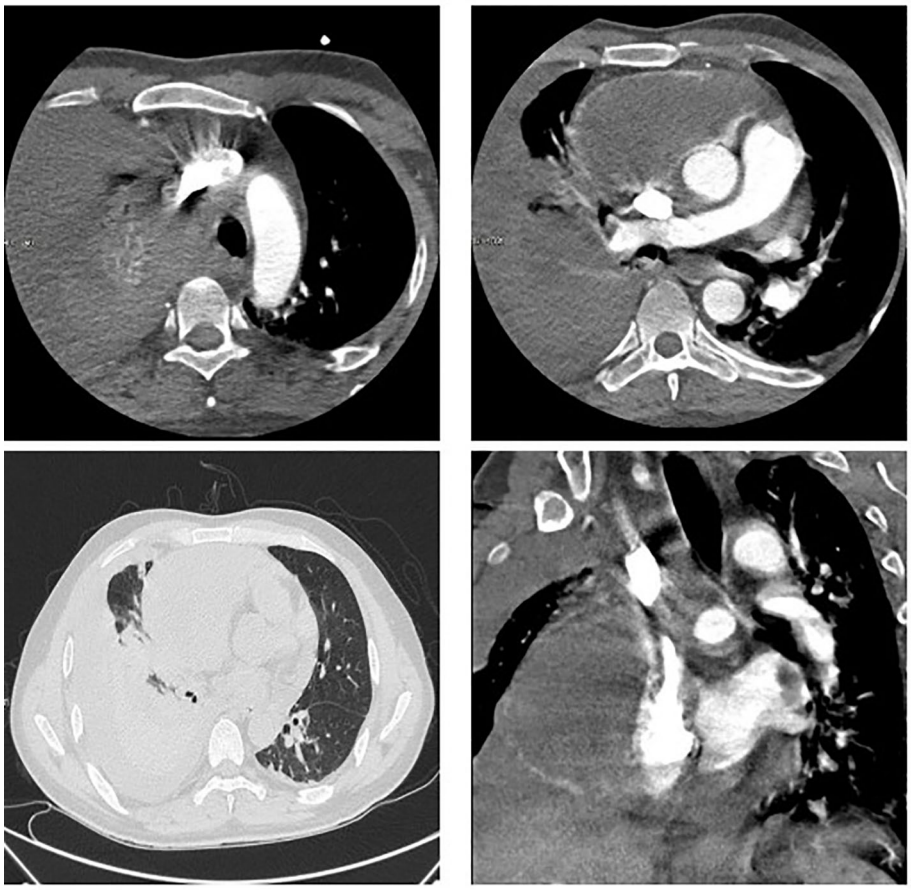

FIGURE 5
Massive pleural effusion, diagnosis of cardiac tumor rupture, but no exact bleeding point found.

atypia, abundant cytoplasm, large hyperchromatic nuclei with easily visible nuclear divisions (>10/10 HPF). In addition, local endothelial cells are hyperproliferative, manifesting as budding, protrusion or papilla. In contrast, poorly-differentiated PCAS presents with unremarkable vessel lumens with focal single-cell vessel lumen). The tumor cells are rounded or spindle-shaped, with a large nucleus and a prominent nucleolus, locally presenting with a spindle-shaped fibrosarcoma-like solid dense area. Meanwhile, surrounding tissues are infiltrated and damaged, partially involving the pericardium and accompanied by patchy hemorrhage and necrosis. Furthermore, IHC findings include diffuse enhancement of ERG, CD31, CD34, Vimentin, Fli-1 and FVIII, negative AE1/AE3, D2-40, SMA, MSA, MyoD1, Desmin, UEA-1, EMA, Myoglobin, Myosin, Calretinin, MC, WT-1, S-100 and HMB-45, and 30%-100% positive Ki-67 (12).

Given the small number of cases, there is no standardized treatment for PCAS to this date. Most medical facilities develop a personalized treatment regimen based on past experience. Therefore, there is an urgent need for evidence-based medicine. Surgery has been proven as an effective strategy to improve the prognosis of patients with localized PCAS. According to a British Columbia Cancer Agency analysis (4), the median OS in cases with resectable localized tumors is 25 months, which is substantially higher than the 6 months in non-resectable or non-R0 resections. Data from the French Sarcoma Group suggested that the median OS of localized PCAS patients receiving R0 resection, R1/R2 resection and those without surgical treatment was 38.8 months, 18.2 months and 11.2 months, respectively, with the extended survival attributed to tumor excision rather than adjuvant treatment (6). The Cleveland Clinic reported that the median OS was 67.6 months in surgical patients and 5.93 months in patients not undergoing surgery (7). In addition, the 1-, 3- and 5-year survival rates of angiosarcoma patients receiving surgical resection were 38.3%, 23.6% and 5.9%, respectively, compared to the 38.5%, 9.6% and 0% in patients not receiving surgical intervention (5). In some medical centers, heart transplantation is adopted as the main treatment strategy for PCAS; however, it was found that there was no significant superiority in terms of patient survival compared with palliative systemic therapy (9 months vs. 8 months) (13). Partial resection + extended resection + local reconstruction remains the standard procedure for PCAS. Nevertheless, R0 resection is difficult to achieve since neurovascular structures are often significantly affected by the tumor's invasiveness, posing a serious challenge to cardiac surgery.

Neoadjuvant chemotherapy (NAC) is a viable alternative in the treatment of locally advanced PCAS patients that cannot undergo surgical resection. Radulescu et al (14) found that PCAS patients who received Adriamycin-based NAC had a median progression-free survival (PFS) of 33 months due to enhanced tumor resectability. In a cohort study comprising of 32 primary cardiac sarcoma patients (24 PCAS patients) scheduled for surgical treatment in the University of Texas Health Science Center at Houston from 1990 to 2005, NAC was conducted using Adriamycin plus Ifosfamide and Gemcitabine or Docetaxel if not tolerated. The results showed that the median OS in patients with and without NAC was 20 months and 9.5 months, respectively (15). Comparatively, palliative chemotherapy's efficacy in advanced metastatic cases has yet to be validated by large-scale clinical trials. In the phase II ANGIOTAX trial (the only clinical trial on angiosarcoma), the objective remission rate (ORR) of patients (n=30) receiving Paclitaxel on a weekly regimen was 19%, the median PFS was 4 months and the median OS was 8 months (16). Apart from Paclitaxel, Anthracyclines, Gemcitabine, Ifosfamide, and Docetaxel are also clinically used alone or in combination. However, there were only a few case reports and retrospective studies and no randomized controlled trials to determine their efficacy. Furthermore, some targeted agents, primarily vascular endothelial growth factor (VEGF) -targeting agents such as Anlotinib, Bevacizumab, Sunitinib, and Pazopanib, are also used in PCAS treatment. Pazopanib was reportedly utilized in a case of metastatic PCAS, which resulted in complete remission following treatment (17). However, none of the agents have been subjected to large-scale clinical trials. In the present case, our patient received three cycles of Gemcitabine + Docetaxel and achieved SD. Notably, tumor markers such as CA125, NSE, and NT-proBNPa showed a consistent downward trend during treatment.

Due to the low incidence of angiosarcoma, large genomic studies have been challenging. Rosenbaum et al (18) performed genetic testing of 26 patients with angiosarcoma, the most common oncogenic or likely oncogenic abnormalities were TP53 alterations (27% of patients), MYC amplifications (23%), CRKL amplified (27%)and ATRX alterations (15%). Another genetic test that included the largest number of patients with angiosarcoma found the main mutation genes include TP53 (30%), KDR (26%), PIK3CA (21%), POT1 (19%), PLCG1 (17%), NF1 (13%), FAT1 (13%), NOTCH2 (13%), MYC (11%) and FGFR2, ATRX, BRAF, ARID1A, etc. (19). In addition, 33% of patients with angiosarcoma had recurrent amplification of the HOXA gene, which plays an important role in neovascularization and wound healing, suggesting a potential mechanism for HOXA amplification as an oncogene in angiosarcoma (20). Although more and more gene mutations have been found in angiosarcoma, but DNMT3A gene mutations have never been detected. The DNMT3A gene, located on chromosome 2p23, is made up of 26 exons and 25 introns and encodes a DNA methyltransferase that catalyzes the *de novo* transfer of methyl groups to specific CpG sites (21). DNMT3A is highly expressed by various hematopoietic stem cells and immune cells. Mutations in the DNMT3A gene can

promote the initiation and development of atherosclerosis by inducing inflammatory reactions, and they can also increase myeloid differentiation and malignant transformation of bone marrow hematopoietic stem cells (HSCs) by interfering with their ability to self-renew (22, 23). Primary cardiac tumors are extremely rare. Angiosarcoma is the most common histologic subtype and is characterized by its permeability and destructive nature. Herein, our patient presented with a mutation in the DNMT3A gene, which draws attention to the role of DNMT3A mutation in the initiation and development of PCAS. Furthermore, whether PCAS and atherosclerosis share some pathophysiological processes and whether cardiovascular drugs are effective in this rare disease warrant further investigation.

Conclusion

Primary cardiac angiosarcoma is an extremely uncommon tumor, to sum up. This is the first account of PCAS brought on by a DNMT3 gene mutation. It is frequently underdiagnosed or misdiagnosed due to its low prevalence and cryptic clinical appearance. Clinicians should include cardiac angiosarcoma in the initial differential diagnosis if there is even the slightest hint of suspicion. Due to its great sensitivity, echocardiography is one of the most effective diagnostic methods, and CT and MR scans are frequently utilized to determine whether metastases from other sites are present or not. Next-generation sequencing (NGS) and immunohistochemical staining are further diagnostic techniques. Contrarily, there aren't any uniformly accepted clinical standards or reliable preventative strategies. Surgery is still the preferred method of treatment. Patients with advanced disease may benefit from chemotherapy, targeted therapy, or immunotherapy, but these treatments have variable therapeutic outcomes and poor prognoses. As a result, selecting the optimum course of treatment to significantly increase patient survival and quality of life is still a difficult decision that merits additional research. Our study emphasizes how challenging it is to identify and treat this uncommon type of malignancy.

Data availability statement

The original contributions presented in the study are included in the article/Supplementary Material. Further inquiries can be directed to the corresponding author.

Ethics statement

Written informed consent was obtained from the individual for the publication of any potentially identifiable images or data included in this article.

Author contributions

KT, First authorship: contributed to editing, revising, and approving the manuscript. FS contributed to the writing and revision of the manuscript. YL, HZ, TW, TC, and XP contributed to collecting clinical data. All authors have read and approved the final manuscript.

Funding

This work obtained funding support from the Gansu Province Science and Technology Department Key R&D Program (21JR1RA121), China.

Conflict of interest

The authors declare that the research was conducted in the absence of any commercial or financial relationships that could be construed as a potential conflict of interest.

Publisher's note

All claims expressed in this article are solely those of the authors and do not necessarily represent those of their affiliated organizations, or those of the publisher, the editors and the reviewers. Any product that may be evaluated in this article, or claim that may be made by its manufacturer, is not guaranteed or endorsed by the publisher.

Supplementary material

The Supplementary Material for this article can be found online at: https://www.frontiersin.org/articles/10.3389/fonc.2022.1018741/full#supplementary-material

References

1. Butany J, Nair V, Naseemuddin A, Nair GM, Catton C, Yau T. Cardiac tumours: diagnosis and management. *Lancet Oncol* (2005) 6(4):219–28. doi: 10.1016/S1470-2045(05)70093-0

2. Antonuzzo L, Rotella V, Mazzoni F, Doni L, Bianchini D, Garbini F, et al. Primary cardiac angiosarcoma: a fatal disease. *Case Rep Med* (2009) 2009 (591512):1–4. doi: 10.1155/2009/591512

3. Zhang PJ, Brooks JS, Goldblum JR, Yoder B, Seethala R, Pawel B, et al. Primary cardiac sarcomas: a clinicopathologic analysis of a series with follow-up information in 17 patients and emphasis on long-term survival. *Hum Pathol* (2008) 39(9):1385–95. doi: 10.1016/j.humpath.2008.01.019

4. Truong PT, Jones SO, Martens B, Alexander C, Paquette M, Joe H, et al. Treatment and outcomes in adult patients with primary cardiac sarcoma: the British Columbia cancer agency experience. *Ann Surg Oncol* (2009) 16(12):3358–65. doi: 10.1245/s10434-009-0734-8

5. Zhang Z, Cheng Y, Gong X, Ge Y, Bai C, Wang X, et al. Characteristics and outcomes of primary angiosarcoma. *Chin J Oncol* (2019) 41(09):693–7. doi: 10.3760/cma.j.issn.0253-3766.2019.09.009

6. Isambert N, Ray-Coquard I, Italiano A, Rios M, Kerbrat P, Gauthier M, et al. Primary cardiac sarcomas: a retrospective study of the French sarcoma group. *Eur J Cancer* (2014) 50(1):128–36. doi: 10.1016/j.ejca.2013.09.012

7. Randhawa JS, Budd GT, Randhawa M, Ahluwalia M, Jia X, Daw H, et al. Primary cardiac sarcoma. *Am J Clin Oncol* (2016) 39(6):593–9. doi: 10.1097/COC.0000000000000106

8. Zhang C, Huang C, Zhang X, Zhao L, Pan D. Clinical characteristics associated with primary cardiac angiosarcoma outcomes: a surveillance, epidemiology and end result analysis. *Eur J Med Res* (2019) 24(1):1–10. doi: 10.1186/s40001-019-0389-2

9. Luo L, Zhao W, Wang Y, Liu K. Cardiac angiosarcoma: A case report and review of the literature. *Echocardiography* (2021) 38(12):2083–90. doi: 10.1111/echo.15221

10. Kupsky DF, Newman DB, Kumar G, Maleszewski JJ, Edwards WD, Klarich KW. Echocardiographic features of cardiac angiosarcomas: The Mayo clinic experience (1976-2013). *Echocardiography* (2016) 33(2):186–92. doi: 10.1111/echo.13060

11. Krishnan T, Pettersson G, Mukherjee R, Singhal N. Cardiac angiosarcoma: A diagnostic and therapeutic challenge. *J Cardiol cases* (2020) 22(2):90–3. doi: 10.1016/j.jccase.2020.04.010

12. Teng F, Chen D, Fang H, Shang J, Wu Y, Cui Y, et al. Clinicopathology analysis of 9 cases in primary cardiac angiosarcoma. *J Cardiovasc pulmonary Dis* (2016) 35(12):974–7. doi: 10.3969/j.issn.1007-5062.2016.12.011

13. Li H, Yang S, Chen H, Yang Z, Hong T, Hou Y, et al. Survival after heart transplantation for non-metastatic primary cardiac sarcoma. *J cardiothoracic Surg* (2016) 11(1):145. doi: 10.1186/s13019-016-0540-x

14. Radulescu D, Pripon S, Radulescu LI, Constantea NA, Gulei I. A rare case of primitive right atrium angio-sarcoma with favorable outcome, in a young female. *Case Rep literature review Rev Med Chile* (2008) 136(10):1311–6. doi: 10.4067/S0034-98872008001000012

15. Blackmon SH, Reardon MJ. Surgical treatment of primary cardiac sarcomas. *Texas Heart Institute J* (2009) 36(5):451–2.

16. Penel N, Bui BN, Bay JO, Cupissol D, Ray-Coquard I, Piperno-Neumann S, et al. Phase II trial of weekly paclitaxel for unresectable angiosarcoma: the ANGIOTAX study. *J Clin* (2008) 26(32):5269–74. doi: 10.1200/jco.2008.17.3146

17. Schur S, Hamacher R, Brodowicz T. Pazopanib in primary cardiac angiosarcoma of the right atrium: A case report. *Case Rep Oncol* (2016) 9 (2):363–7. doi: 10.1159/000447088

18. Rosenbaum E, Antonescu CR, Smith S, Bradic M, Kashani D, Richards AL, et al. Clinical, genomic, and transcriptomic correlates of response to immune checkpoint blockade-based therapy in a cohort of patients with angiosarcoma treated at a single center. *J Immunother Cancer* (2022) 10(4):e004149. doi: 10.1136/jitc-2021-004149

19. Painter CA, Jain E, Tomson BN, Dunphy M, Stoddard RE, Thomas BS, et al. The angiosarcoma project: enabling genomic and clinical discoveries in a rare cancer through patient-partnered research. *Nat Med* (2020) 26(2):181–7. doi: 10.1038/s41591-019-0749-z

20. Xie HM, Bernt KM. HOXA amplification defines a genetically distinct subset of angiosarcomas. *Biomolecules* (2022) 12(8):1124. doi: 10.3390/biom12081124

21. Cole CB, Russler-Germain DA, Ketkar S, Verdoni AM, Smith AM, Bangert CV, et al. Haploinsufficiency for DNA methyltransferase 3A predisposes hematopoietic cells to myeloid malignancies. *J Clin Invest* (2017) 127(10):3657–74. doi: 10.1172/jci93041

22. Cobo I, Tanaka T, Glass CK, Yeang C. Clonal hematopoiesis driven by DNMT3A and TET2 mutations: role in monocyte and macrophage biology and atherosclerotic cardiovascular disease. *Curr Opin Hematol* (2022) 29(1):1–7. doi: 10.1097/moh.0000000000000688

23. Guryanova OA, Shank K, Spitzer B, Luciani L, Koche RP, Garrett-Bakelman FE, et al. DNMT3A mutations promote anthracycline resistance in acute myeloid leukemia *via* impaired nucleosome remodeling. *Nat Med* (2016) 22(12):1488–95. doi: 10.1038/nm.4210

frontiers | Frontiers in Cardiovascular Medicine

TYPE Case Report
PUBLISHED 31 October 2022
DOI 10.3389/fcvm.2022.1001996

Check for updates

OPEN ACCESS

EDITED BY
Reto Asmis,
Wake Forest University, United States

REVIEWED BY
Chrystalle Katte Carreon,
Boston Children's Hospital and Harvard Medical School, United States
Hongzhou Duan,
Peking University, China
Hao Chen,
Fudan University, China

*CORRESPONDENCE
Chengwei Zou
zouchengwei@sdu.edu.cn
Gang Zhang
surgeonzg@outlook.com

†These authors have contributed equally to this work and share first authorship

SPECIALTY SECTION
This article was submitted to Cardio-Oncology, a section of the journal Frontiers in Cardiovascular Medicine

RECEIVED 24 July 2022
ACCEPTED 12 October 2022
PUBLISHED 31 October 2022

CITATION
Zhang S, Xu Z, Zou C and Zhang G (2022) Cardiac venous malformation concurrent with multiple hepatic venous malformations: A case report. *Front. Cardiovasc. Med.* 9:1001996. doi: 10.3389/fcvm.2022.1001996

COPYRIGHT
© 2022 Zhang, Xu, Zou and Zhang. This is an open-access article distributed under the terms of the Creative Commons Attribution License (CC BY). The use, distribution or reproduction in other forums is permitted, provided the original author(s) and the copyright owner(s) are credited and that the original publication in this journal is cited, in accordance with accepted academic practice. No use, distribution or reproduction is permitted which does not comply with these terms.

Cardiac venous malformation concurrent with multiple hepatic venous malformations: A case report

Shijie Zhang[1†], Zhenqiang Xu[1,2†], Chengwei Zou[1,2*] and Gang Zhang[1,2*]

[1]Department of Cardiovascular Surgery, Shandong Provincial Hospital, Shandong University, Jinan, China, [2]Department of Cardiovascular Surgery, Shandong Provincial Hospital, Shandong First Medical University, Jinan, China

A 50-year-old woman who had previously undergone right radical mastectomy presented with chest tightness and shortness of breath after physical activities. A cardiac mass and multiple hepatic lesions were successively detected. We first performed hepatic puncture biopsy. Histopathologic examination confirmed that the multiple hepatic lesions were venous malformations. Based on the imaging findings and previous reports in the literature, we boldly speculated that the cardiac mass was also a venous malformation. The cardiac venous malformation was successfully resected, and the postoperative pathology confirmed our suspicion.

KEYWORDS

cardiac, cardiac venous malformation, hepatic venous malformation, cardiac metastases, tricuspid regurgitation

Introduction

Cardiac cavernous hemangiomas, which should be now classified as venous malformations (VMs) (1), account for 5 to 10% of benign mass-forming cardiac lesions/tumors (2). Most cardiac VMs are solitary and concurrence at multiple locations is rarely reported (3). A literature review reveals cardiac VM coexisting VMs at other locations in the liver, lung, pleura, and thymus (4). Here, we report a rare right ventricular VM concurrent with multiple hepatic VMs. To our knowledge, only several cases of cardiac VMs have been reported coexisting with VMs in the liver (4–6). This case describes how we first identify the extracardiac VMs and then associate it with the intracardiac VM in a patient with breast cancer history. The diagnostic insight and experience are valuable for physician communication and learning.

Case presentation

A 50-year-old female patient was admitted with chest tightness and shortness of breath after activities. The patient denied previous cardiovascular antecedents and family history. She reported a history of right radical mastectomy performed 10 years ago. She did not receive radiotherapy, chemotherapy, or endocrine treatment after the operation. On admission, the patient's body temperature was normal (36.5°C) with a blood pressure of 139/70 mmHg, and a heart rate of 84 bpm. The patient was 158 cm tall and weighed 61.3 kg.

Physical examination revealed a grade III/VI systolic murmur at the left sternal margin. Jugular venous distention, generalized edema, and shifting dullness indicated severe right heart failure. The liver was enlarged, exceeding one transverse finger below the costal margin. By palpation, the liver edge felt slightly firm. There was no tenderness or rebound pain in the abdomen. The patient did not complain of other symptoms. The physical examination showed no positive signs of other systems.

Electrocardiography showed sinus rhythm, right axis deviation, and incomplete right bundle branch block (**Supplementary Figure 1**).

Laboratory examination

Routine blood examination: Hemoglobin level was 147 g/L; hematocrit level was 43.3%; and serum leukocyte and platelet levels were 3.93×10^9/L and 175×10^9/L, respectively. The biochemical investigation showed no alteration in the following serum levels: liver enzymes, albumin, urea, creatinine, potassium, glucose, and sodium. Direct and indirect bilirubin levels were elevated (20.89 and 33.88 μmol/L, respectively). Myocardial enzymes and myocardial markers including creatine kinase (CK), creatine kinase isoenzyme mass (CK-MB), myoglobin (MYO), and high-sensitivity troponin T (HS-TnT) were normal. B-type natriuretic peptide (BNP) level was 3,732.00 pg/mL. The blood tests for tumor markers were not evident except for an elevated CA125 level of 240 U/mL.

Imaging results

Echocardiography revealed a large solid mass (4.82 cm × 4.48 cm × 6.42 cm) (**Figure 1A**), with right ventricular outflow tract obstruction and secondary severe tricuspid regurgitation (Video 1). No abnormal echoes were detected in the pericardium or pericardial cavity. Computed tomography (CT) scan revealed right ventricular mass (**Figure 1B**), along with multiple occupancies in the liver. A diagnosis of breast cancer metastasis was suspected at first. Magnetic resonance imaging (MRI) was performed to further define the mass of these two organs. The cardiac mass (**Figure 1C**) showed iso-intensity on T1-weighted images and hyper-intensity on T2-weighted images compared with the normal myocardium of the right ventricle. The mass showed diffuse contrast uptake with gadolinium enhancement. Further, evaluation of the liver revealed multiple mass lesions with varied sizes showing progressive enhancement, indicating a typical VM (**Figure 1C**). Notably, the lesions of two organs were not detected in previous assessments of breast cancer.

Brain MRI and abdominal ultrasound revealed no other lesions. Coronary angiography (CA) revealed no obvious stenosis in the coronary arteries and no discernible tumor-feeding artery was detected.

Management

Although homologous multiorgan lesions were suspected, they were not determined as benign or malignant. The patient underwent hepatic puncture biopsy under ultrasound localization. Results of the pathological examinations revealed hepatic VM (**Figure 2A**). Given her medical history and imaging findings, the diagnosis of cardiac VM and multiple VMs was highly suspected. We decided to perform a resection of the cardiac mass.

Before surgery, our team administered diuresis, heart-rate reduction, and nutritional myocardial therapy. The patient's symptoms and cardiac function improved significantly. Complete excision of the cardiac mass (**Figure 2B**) was performed under standard cardiopulmonary bypass. The pedicle of the mass was attached to the interventricular septum, near the anterior wall of the right ventricle. The capsule was intact, and there was no adhesion or fusion with the tricuspid valve and chordae tendinae. We completely excised the pedicle from the myocardium while preserving the ventricular structure, as well as the free wall of the right ventricle. Upon exploration, the valve annulus of the tricuspid valve was enlarged. We believe that the cardiac lesion blocked the right ventricular outflow tract, causing dilatation of the right ventricle and enlargement of the valve annulus, resulting in functional tricuspid insufficiency. We used the 28 # Edwards tricuspid annuloplasty ring to perform tricuspid valvuloplasty. Pathological examination demonstrated thin-walled interanastomosing channels lined by endothelial cells. There is no atypia, necrosis or active mitosis (**Figure 2C**). By immunohistochemistry, the lining cells are positive for CD31 and CD34, confirming endothelial differentiation. Based on the histological and immunohistochemical features, we diagnosed the cardiac mass as a VM. The patient was discharged 6 days after the operation.

Although multiple VMs in the liver were also detected, they were small in size. Nonetheless, the patient complained of no abdominal symptoms. The liver enlargement disappeared, and her liver function was normal. We recommended a

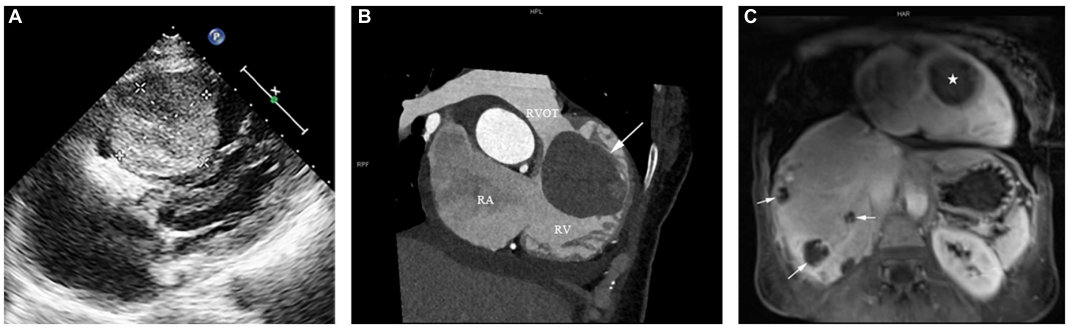

FIGURE 1
(A) Preoperative transthoracic echocardiography showing a large mass measuring 4.82 cm × 4.48 cm × 6.42 cm attached to the anterior wall of the right ventricle, with a moderate to strong and relatively homogeneous echo. **(B)** The computed tomography scan of the patient's chest showing a right ventricular mass (arrow) in the right ventricular outflow tract (RVOT). RA: right atrium; RV: right ventricle. **(C)** Reconstructed magnetic resonance imaging of the patient's chest and abdomen showed a cardiac mass concurrent with multiple hepatic lesions. The right ventricular mass and the multiple liver lesions are indicated by a star and three arrows, respectively.

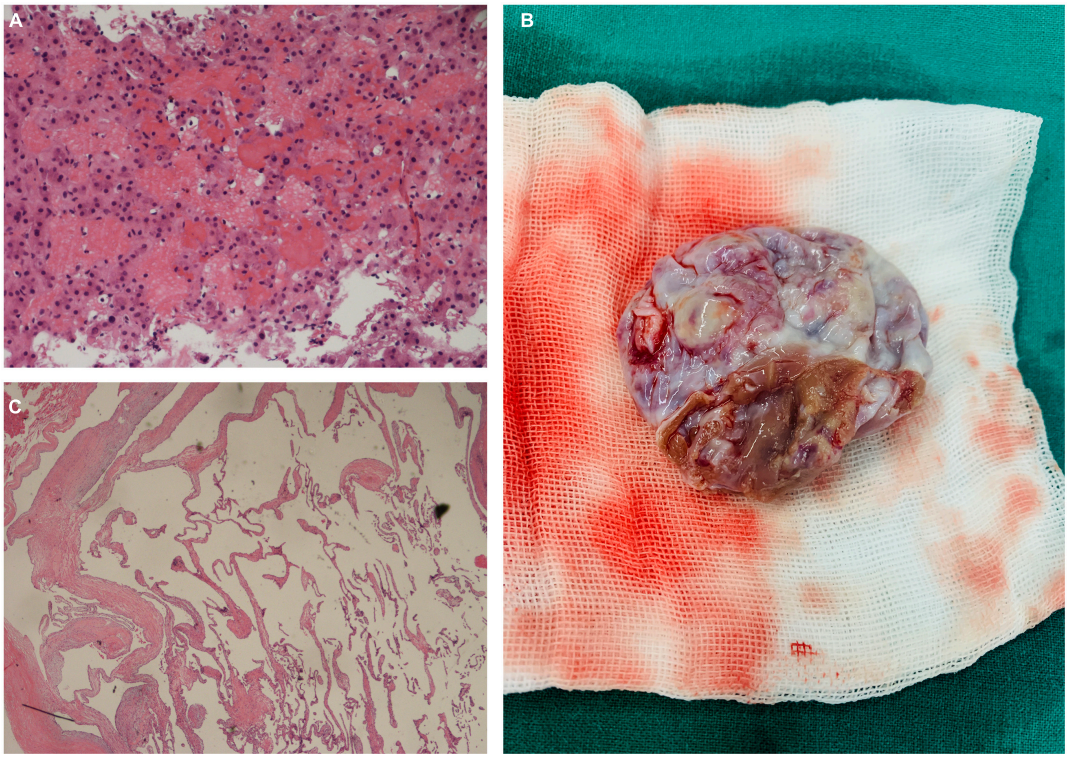

FIGURE 2
(A) Pathological examination of the liver mass showing multiple irregular dilatated vascular spaces and layers of endothelial cells without signs of malignancy (Hematoxylin and eosin, × 200). **(B)** Intraoperative photograph of the excised specimen appeared as a cystic mass with a broad base and intact capsule. **(C)** Pathological evaluation of the cardiac mass (Hematoxylin and eosin, × 100).

regular follow-up. A telephone follow-up was conducted 6 months and 1 year after surgery. The patient had no discomfort and her tolerance to activity was good. In addition, cardiac echocardiography revealed no tumor recurrence or tricuspid regurgitation. No significant progression of the hepatic VMs was detected.

Discussion

Diagnosis of the cardiac VM is aided by imaging techniques. Echocardiography has become an important tool for the initial identification of cardiac VMs. Contrast-enhanced myocardial echocardiography has evolved rapidly in recent

years and utilized in the diagnosis of cardiac vascular malformation (7). CT and MRI can be used to evaluate the size, location, extracardiac extension, and the degree of myocardial involvement of the malformation. In addition, MRI in this study suggested that the lesions were of vascular origin, which facilitated the diagnosis and differential diagnosis. Typically, cardiac VM shows isointense and high signal intensity compared with myocardium in T1- and T2-weighted images, respectively (5, 8, 9). Homogeneous enhancement after contrast infusion is another typical manifestation of cardiac VM (8–10). The high vascularity of cardiac VM is of great diagnostic value clinically. Besides, CA can be used to evaluate the presence of feeding vessels. However, imaging examination only provides limited diagnostic clues for cardiac VM. Biopsy is needed for a definitive diagnosis.

In this case, the patient was first diagnosed with a right ventricular mass, and further examination revealed concurrent multiple liver masses. Given that right ventricular occupying lesions are generally malignant, and both cardiac (11) and hepatic (12) metastases of breast cancer have been reported, it was initially believed that the cardiac mass, in this case, was malignant. However, as the diagnosis progressed, we assumed that the cardiac lesion was more likely to be benign. First, the mass was confined to the right ventricle, without obvious myocardial infiltration or invasion of other cardiac chambers, pericardium, or pericardial cavity. Both imaging and pathological findings showed that multiple liver lesions were VMs. The possibility of multiple metastases from breast cancer was ruled out. Finally, as mentioned above, cases of cardiac VM concurrent with hepatic VM have been reported in the literature. Despite the patient's history of breast cancer as a confounding factor, preoperatively, we believed that the cardiac mass was likely consistent with the nature of the lesions in the liver, which was also a VM. Total resection is possible in most cardiac VMs, but a few cases cannot be excised (10). The diagnosis of previously reported cases of cardiac VMs was almost established by biopsy of surgically excised specimens, suggesting that the benign or malignant nature of the lesion was uncertain before surgery. Our team first identified the multiple liver mass as VMs pathologically Combined with the imaging findings, the mass in the heart was suspected as a VM. The postoperative pathology confirmed our suspicion.

The cause of VMs remains unclear. Previous studies have shown that somatic mutations in TIE2, PIK3CA, MAP3K3 and other genes lead to VMs (13–17). Although abnormal veins are present at birth, deep lesions often grow within the body and remain undetected until symptoms appear (18). VMs can progress rapidly in response to changes in hormone levels (during puberty or pregnancy), infection, trauma, and inappropriate treatment (19, 20). However, the etiology of cardiac VMs is rarely reported. In our case, the lesions of two organs were not detected in previous assessments of breast cancer. The patient did not receive chemotherapy or endocrine therapy after surgery for breast cancer. We speculate that the progression of VMs may be related to her perimenopausal period.

In summary, we reported a rare case of right ventricular VM concurrent with multiple hepatic VMs. The decision to operate the patient was based on relatively clear diagnosis of the nature of the lesion. In addition to complete resection of the right ventricular VM, we also performed a successful repair of the tricuspid valve. Long-term follow-up is required, especially to evaluate recurrence and right heart function.

Despite its rarity, clinicians need to be aware that cardiac VMs are occasionally associated with extracardiac VMs. However, any underlying mechanism is unknown.

Patient perspective

"As a patient, I am glad that the cause of the disease has been found and solved. I underwent radical surgery for breast cancer 10 years ago. In recent years, I haven't seen my breast surgeon again. At first, I thought the breast cancer had returned and metastasized, which frightened me. Fortunately, both the cardiac and hepatic tumors were benign. I am very grateful to the doctors and nurses who treated me."

Data availability statement

The original contributions presented in the study are included in the article/**Supplementary material**, further inquiries can be directed to the corresponding author/s.

Ethics statement

Written informed consent was obtained from the individual(s) for the publication of any potentially identifiable images or data included in this article. Written informed consent was obtained from the patient for the publication of this case report.

Author contributions

SZ and ZX cared for the patient and wrote the final manuscript. CZ and GZ revised it critically. All authors read and approved the final version of the manuscript.

Funding

This study was supported by the Nature Science Foundation of Shandong Province (ZR2020MH044 to CZ).

Conflict of interest

The authors declare that the research was conducted in the absence of any commercial or financial relationships that could be construed as a potential conflict of interest.

Publisher's note

All claims expressed in this article are solely those of the authors and do not necessarily represent those of their affiliated organizations, or those of the publisher, the editors and the reviewers. Any product that may be evaluated in this article, or claim that may be made by its manufacturer, is not guaranteed or endorsed by the publisher.

Supplementary material

The Supplementary Material for this article can be found online at: https://www.frontiersin.org/articles/10.3389/fcvm.2022.1001996/full#supplementary-material

SUPPLEMENTARY FIGURE 1
The electrocardiography result.

References

1. Kunimoto K, Yamamoto Y, Jinnin M. ISSVA classification of vascular anomalies and molecular biology. *Int J Mol Sci.* (2022) 23:2358.

2. Sun, SB, Fan G, Farhaj Z, Hongxin L. A giant cardiac hemangioma encroaching on the right coronary artery. *Ann Thorac Surg.* (2022) S0003-4975(22)00470-2.

3. Burke A, Tavora F. The 2015 WHO classification of tumors of the heart and pericardium. *J Thorac Oncol.* (2016) 11:441–52.

4. Wang C, Chen H, Sun L, Mei Y. Cardiac cavernous hemangioma coexisting with pulmonary cavernous hemangiomas and giant hepatic hemangioma. *Ann Thorac Surg.* (2017) 103:e149–52. doi: 10.1016/j.athoracsur.2016.07.024

5. Shojaeifard M, Saedi S, Alizadeh Ghavidel A, Karimlu MR, Kasaei M, Reza Pouraliakbar H, et al. Concomitant cardiac and hepatic hemangiomas. *Echocardiography.* (2020) 37:462–4.

6. Kan CD, Yae CT, Yang YJ. Left ventricular haemangioma with papillary endothelial hyperplasia and liver involvement. *Heart.* (2004) 90:e49. doi: 10.1136/hrt.2004.040154

7. Xiachuan Q, Xuebin L, Yongjie W. Case of cardiac hemangioma diagnosed by myocardial contrast echocardiography. *Circ Cardiovasc Imaging.* (2019) 12:e008811.

8. Domoto S, Kimura F, Uwabe K, Koike H, Tabata M, Iguchi A, et al. Diagnostic features of cardiac cavernous hemangioma in the right ventricle on magnetic resonance imaging. *Gen Thorac Cardiovasc Surg.* (2017) 65:40–3. doi: 10.1007/s11748-015-0567-2

9. Hrabak-Paar M, Hübner M, Stern-Padovan R, Lušiæ M. Hemangioma of the interatrial septum: CT and MRI features. *Cardiovasc Intervent Radiol.* (2011) 34(Suppl. 2):S90–3. doi: 10.1007/s00270-010-0062-1

10. Li W, Teng P, Xu H, Ma L, Ni Y. Cardiac hemangioma: a comprehensive analysis of 200 cases. *Ann Thorac Surg.* (2015) 99:2246–52. doi: 10.1016/j.athoracsur.2015.02.064

11. Chae EY, Kim JE, Kim HH. Cardiac metastasis from breast cancer as an initial focus of recurrence. *Breast J.* (2015) 21:433–5. doi: 10.1111/tbj.12429

12. Disibio G, French SW. Metastatic patterns of cancers: results from a large autopsy study. *Arch Pathol Lab Med.* (2008) 132:931–9.

13. Castel P, Carmona FJ, Grego-Bessa J, Berger MF, Viale A, Anderson KV, et al. Somatic PIK3CA mutations as a driver of sporadic venous malformations. *Sci Transl Med.* (2016) 8:332ra42. doi: 10.1126/scitranslmed.aaf1164

14. Castillo SD, Tzouanacou E, Zaw-Thin M, Berenjeno IM, Parker VE, Chivite I, et al. Somatic activating mutations in Pik3ca cause sporadic venous malformations in mice and humans. *Sci Transl Med.* (2016) 8:332ra43.

15. Couto JA, Vivero MP, Kozakewich HP, Taghinia AH, Mulliken JB, Warman ML, et al. A somatic MAP3K3 mutation is associated with verrucous venous malformation. *Am J Hum Genet.* (2015) 96:480–6. doi: 10.1016/j.ajhg.2015.01.007

16. Limaye N, Kangas J, Mendola A, Godfraind C, Schlögel MJ, Helaers R, et al. Somatic activating PIK3CA mutations cause venous malformation. *Am J Hum Genet.* (2015) 97:914–21.

17. Limaye N, Wouters V, Uebelhoer M, Tuominen M, Wirkkala R, Mulliken JB, et al. Somatic mutations in angiopoietin receptor gene TEK cause solitary and multiple sporadic venous malformations. *Nat Genet.* (2009) 41:118–24. doi: 10.1038/ng.272

18. McCuaig CC. Update on classification and diagnosis of vascular malformations. *Curr Opin Pediatr.* (2017) 29:448–54.

19. Wassef M, Blei F, Adams D, Alomari A, Baselga E, Berenstein A, et al. Vascular anomalies classification: recommendations from the international society for the study of vascular anomalies. *Pediatrics.* (2015) 136:e203–14. doi: 10.1542/peds.2014-3673

20. Seront E, Vikkula M, Boon LM. Venous malformations of the head and neck. *Otolaryngol Clin North Am.* (2018) 51:173–84.

frontiers | Frontiers in Cardiovascular Medicine

TYPE Case Report
PUBLISHED 10 November 2022
DOI 10.3389/fcvm.2022.924538

Check for updates

OPEN ACCESS

EDITED BY
Jane Grande-Allen,
Rice University, United States

REVIEWED BY
Bruno Ramos Chrcanovic,
Malmö University, Sweden
Guoxia Yu,
Capital Medical University, China

*CORRESPONDENCE
Xiao-Li Hu
hxlblbg@sina.com
Lin-Sheng Zhao
Zlsh0@163.com

†These authors share first authorship

SPECIALTY SECTION
This article was submitted to Cardio-Oncology, a section of the journal Frontiers in Cardiovascular Medicine

RECEIVED 07 June 2022
ACCEPTED 19 October 2022
PUBLISHED 10 November 2022

CITATION
Zuo H-C, Huang J-Y, Hu X-L and Zhao L-S (2022) A case report of melanotic neuroectodermal tumor of infancy complicated with congenital heart disease and hypothyroidism.
Front. Cardiovasc. Med. 9:924538.
doi: 10.3389/fcvm.2022.924538

COPYRIGHT
© 2022 Zuo, Huang, Hu and Zhao. This is an open-access article distributed under the terms of the Creative Commons Attribution License (CC BY). The use, distribution or reproduction in other forums is permitted, provided the original author(s) and the copyright owner(s) are credited and that the original publication in this journal is cited, in accordance with accepted academic practice. No use, distribution or reproduction is permitted which does not comply with these terms.

A case report of melanotic neuroectodermal tumor of infancy complicated with congenital heart disease and hypothyroidism

Hua-Chu Zuo[1†], Jin-Yue Huang[2†], Xiao-Li Hu[1*] and Lin-Sheng Zhao[1*]

[1]Department of Pathology, Tianjin Children's Hospital (Tianjin University Children's Hospital), Tianjin, China, [2]Institute of Pediatrics, Tianjin Children's Hospital (Tianjin University Children's Hospital), Tianjin, China

To the best of our knowledge, thus far there are no reported cases of melanotic neuroectodermal tumor of infancy (MNTI) with multiple complications. In this case report, we describe the clinical phenotype of MNTI in a 9-month-old female infant associated with tetralogy of Fallot (TOF), a congenital heart defect, and congenital hypothyroidism (CH). Our study showed that the growth of MNTI was delayed by a lower dosage of levothyroxine (L-T4) that was prescribed to treat CH because of the presence of TOF, a severe congenital heart disease. However, the standardized dosage of L-T4 improved thyroid function but stimulated the rapid growth of MNTI. Our report demonstrated that treatment with L-T4 affects the progression of MNTI. Our findings demonstrated the role of thyroid hormone in MNTI growth and progression. Furthermore, our study suggested that the treatment of co-morbidities in children with MNTI requires careful consideration of their effects on the growth and progression of MNTI.

KEYWORDS

melanotic neuroectodermal tumor of infancy, congenital heart disease, hypothyroidism, case report, frequently encountered disease

Introduction

Melanotic neuroectodermal tumor of infancy (MNTI) is a rare, rapidly growing, benign, and pigmented tumor of neural crest origin that was first reported by Krombecher as congenital melanocarcinoma in 1918 (1). To date, nearly 500 MNTI cases have been reported worldwide. The mean age of onset for MNTI is 5 months and is mostly reported in male infants under 1 year of age (2). More than 90% of the MNTI lesions occur in the craniofacial region, especially in the maxillary (62.2%), cranial (15.6%), and mandibular (7.8%) regions; the other locations of MNTI lesions include the testes, epididymis, ovaries, uterus, and soft tissues of the extremities (3).

The histopathological features of MNTI lesions indicate the presence of small rounded neuroblast-like cellular areas surrounded by large areas of melanin-containing cells that include a combination of epithelial, neural, and melanocytic cells. The MNTI lesions show rapid, infiltrative growth. Surgical resection is the conventional treatment for MNTI. However, the recurrence rate is 10–60% because of anatomical limitations and incomplete excision to prevent damage to the adjacent tissues (4). The differential diagnosis of MNTI includes other small blue round cell tumors in children, such as neuroblastoma, Ewing's sarcoma, adenoid rhabdomyosarcoma, melanoma, and clear cell sarcoma (CCS) of soft tissue. Previously published studies mainly focused on the histopathological and immunohistochemical differences between the lesions in different anatomical sites, the scope of surgical resection treatment, and age-related characteristics (5, 6). However, so far, none of the reports have reported a variety of complications in the same case. Therefore, in this case report, we describe a 9-month-old female infant with a single, painless, non-ulcerated, pigmented, fast-growing, cranial (top of frontal) neoplasm with features that are as described previously for MNTI lesions. The patient was also diagnosed with TOF, a severe congenital heart disease, and CH after birth. Low-dose L-T4 treatment suppressed MNTI growth, but the tumor size increased significantly after cardiac surgery and standardized L-T4 treatment. This suggested that precautions and careful follow-up are necessary for treating MNTI patients with co-morbidities involving thyroid dysfunction and cardiac malformations. Moreover, genetic testing is recommended for cases with multiple organ diseases to determine the potential underlying genetic abnormalities. In cases without evidence of mechanisms promoting MNTI growth and development, our study suggested that medications reducing thyroid function may control tumor growth.

Case description

This case described the clinical characteristics of a 9-month-old girl with a 6-month history of growing mass in the left frontal cortex with faster growth in the recent 3 months. She was diagnosed with TOF and CH after birth and underwent radical surgery at the age of 6 months. The patient was given a reduced L-T4 dose for CH treatment because of the underlying TOF. After surgery, the dosage was gradually increased.

Physical examination of the melanotic neuroectodermal tumor of infancy

The tumor was present on the left forehead and showed basal fixation. It was hard, about 3 cm × 4 cm in size, and did not show any signs of neurologic involvement. The skull did not show asymmetry, cutaneous lesions, or inflammation. Neck mass was not observed. There were no symptoms of chronic hypoxia, such as paroxysmal cyanosis and clubbing fingers. The physical growth and development of the infant were normal and in range for her age group.

Brain computed tomography scan details

The brain CT scan showed irregular bone structure with mixed density mass on the left side of the cranial plate in the forehead, slightly reduced brain mass density in the bilateral parietal lobes, and wider ventricles and extracerebral spaces as shown in **Figure 1**.

Cardiac ultrasound characteristics

The postoperative cardiac ultrasound (**Figure 2**) showed that the inner diameter of the cardiac cavities was within the normal range. However, the motion amplitude of the ventricular septum was reduced. The ventricular septum and the left ventricular posterior wall were not thick. The left ventricular posterior wall showed normal motion. The atrial septum was continuous and complete. A strong patch echo was observed around the ventricular septum. The surrounding tissues did not show any obvious cracks. The morphological structure and the opening and closing movements of the valves were normal. The right ventricular outflow tract was not obstructed. A hypertrophic muscle bundle was not detected. The inner diameter of the pulmonary artery was normal (**Figure 2**). Doppler examination did not detect any shunt signal at the systolic ventricular level. The peak forward flow velocity of the pulmonary artery flow was 2.2 m/s (**Figure 2**).

Thyroid function tests

The thyroid function was normal at admission.

Surgical removal, histopathology, and immunohistochemical details of the melanotic neuroectodermal tumor of infancy

After admission, the left frontal tumor was resected under general anesthesia. After satisfactory anesthesia, the skin in the surgical area was routinely disinfected. An incision was made through the skin tissue, capillary tendon membrane, and the periosteum at the top of the frontal curvature to expose the skull. The skull in the surgical area was abnormally elevated, dark red

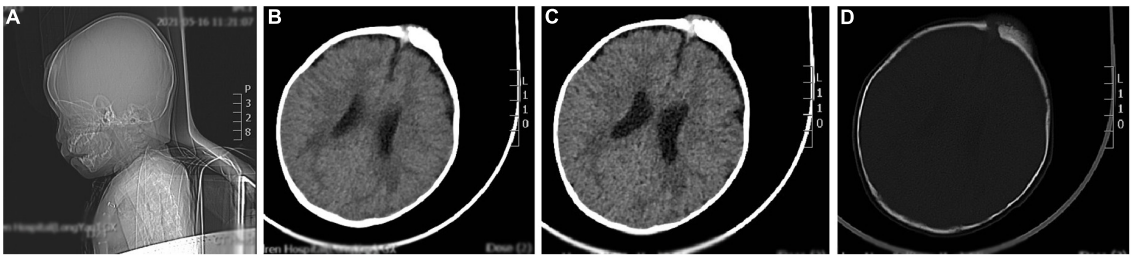

FIGURE 1
A representative image of the head CT scan shows the irregular bone structure with mixed density mass on the left side of the cranial plate in the median frontal area, slightly reduced density in the bilateral parietal lobes, widening of the ventricles and extracerebral space, and thickening of the septal sinus mucosa. **(A)** Sagittal view shows a mass in the frontal area. **(B,C)** Soft tissue window at the central level of the lateral ventricle show a high-density mass in the left frontal region. **(D)** Bone window at the central level of the lateral ventricle: the bony structure of the left cranial plate in the middle frontal region is irregular, and there is a mixed density mass shadow.

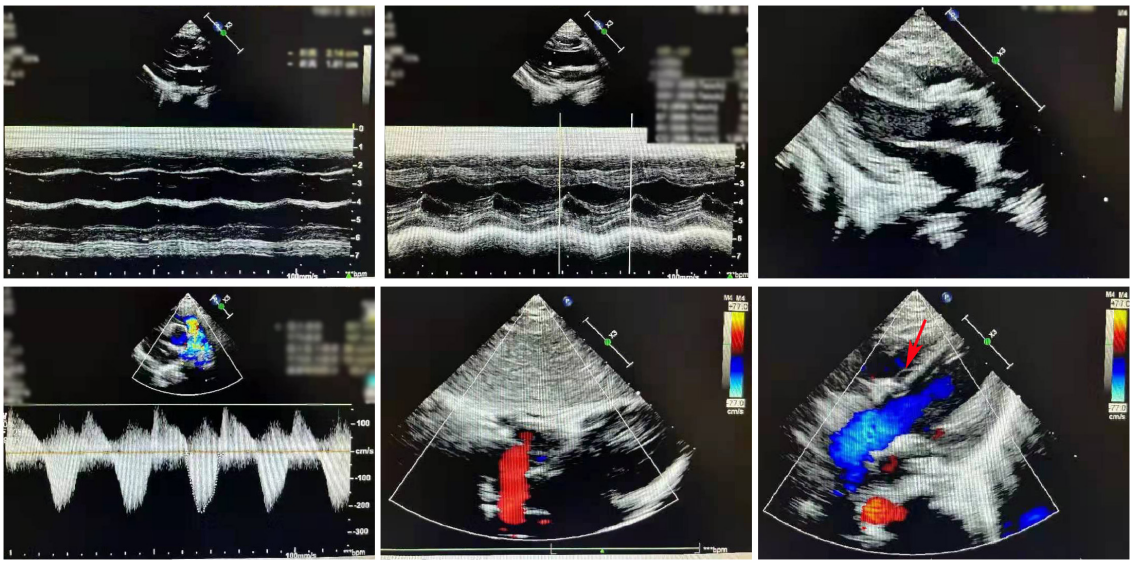

FIGURE 2
A representative image of the cardiac ultrasound (postoperative) shows the normal internal diameter of each chamber, low septal motion amplitude, and strong plaque echoes around the septum. The right ventricular outflow tract is not obstructed. The muscle bundles are not hypertrophic. The internal diameter of the pulmonary artery was normal.

in color, and poorly defined in comparison with the surrounding normal skull. Second, the abnormal skull was bitten, with a loose texture and poor blood supply. The abnormal skull was removed by grinding and drilling, and the cap-like aponeurosis, subcutaneous tissue, and skin were sutured. The wound was pressure dressed. The operation went smoothly without much bleeding. The patient was discharged after suture removal.

Under the postoperative pathological microscope (Figure 3), most of the lesion tissue was hyperplastic and fibrous with abundant new bone trabeculae. Few bone trabeculae showed osteoblasts. Irregular epithelioid cell clusters were scattered in the hyperplastic fibrous tissue. Melanin particles were observed in some cells. In between fibrous tissues, small blue cells with obvious multi-focal compression were observed.

Immunohistochemistry of the lesion showed cytokeratin (CK)-positive epithelial cells, synaptophysin (syn)-positive small blue cells, S-100-positive, HMB45-positive, CD99-negative, CD3-negative, NSE-positive, ERG-positive vascular endothelium, and 15% Ki67-positivity (Figure 4). Based on these findings, the lesion was diagnosed as MNTI.

The postoperative outcome of the patient was good and did not show any additional neurologic impairment. Chemotherapy and/or radiotherapy were not required. The timeline of the patient's clinical journey is shown in Figure 5. Brain MRI at the 12-month follow-up did not show any tumor recurrence.

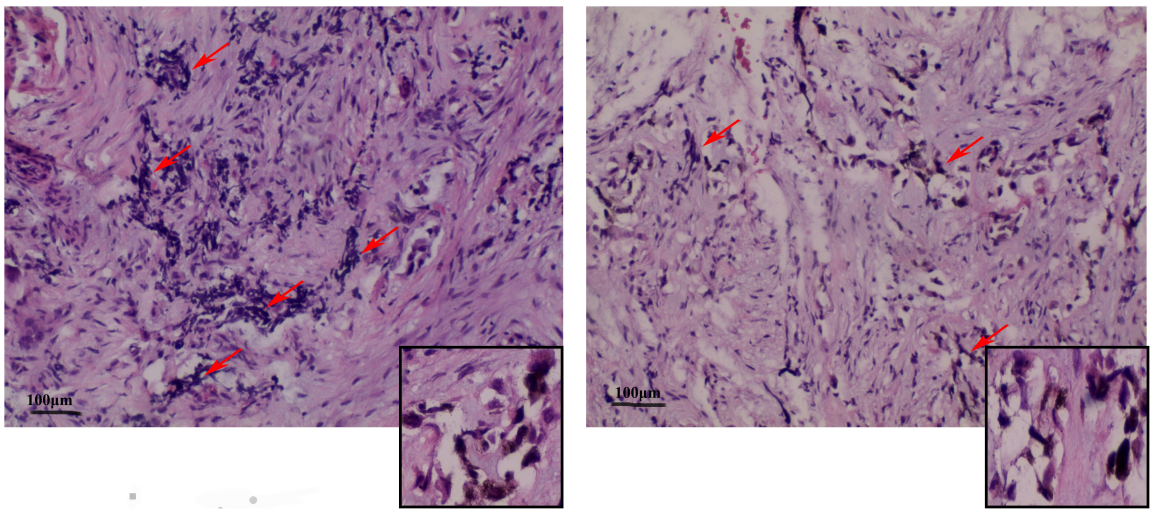

FIGURE 3
Representative image (× 100) shows the histopathological analysis of the tumor tissue. The tumor tissue consists mainly of neuroblastoma-like cells and melanin-containing epithelial cells. **(Left)** The small round or square and primitive neuroblastoma-like cells are large and contain melanin granules in the cytoplasm of the epithelial cells. The deep-stained and shrunken neuroblastoma-like cells are mostly arranged in nests with extruded nuclei. **(Right)** Pigmented epithelioid cells with vacuolated nuclei are observed in the large area surrounding the neuroblastoma-like cells. Some areas are mainly composed of pigmented epithelioid cells arranged in sheets, nests, or beam bundles, with dense fibrous connective tissue between the nests of cells, and some areas can be seen as bone trabeculae with visible nuclear schizograms (0–2 per 10 high magnification fields).

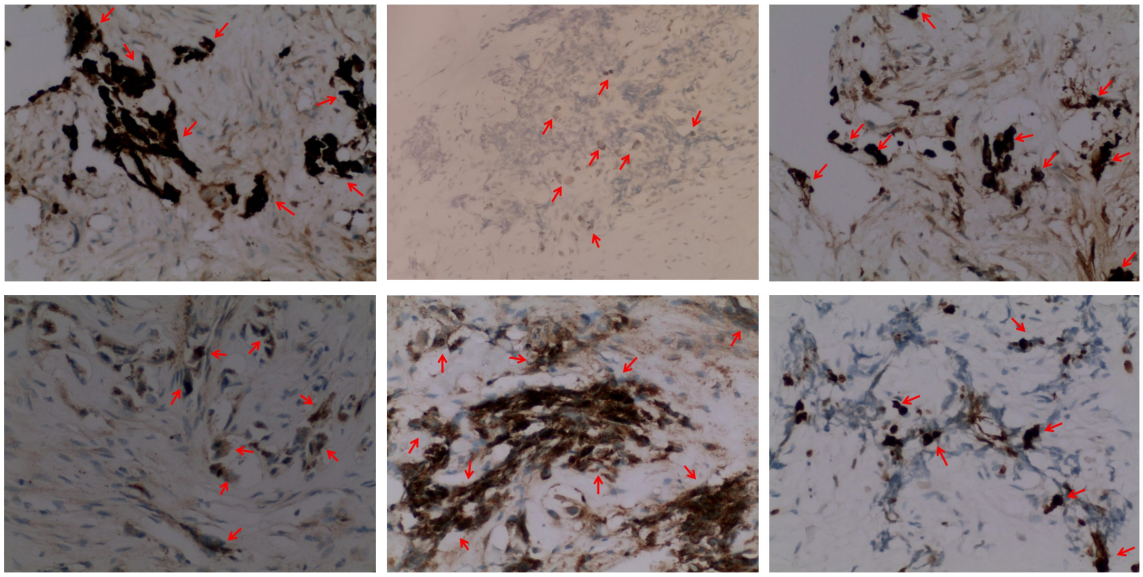

FIGURE 4
Representative immunohistochemical staining images (× 200) (from **left** to **right)** of the MNT1 tumor sections for cytokeratin (CK, epithelioid +), S-100 protein (epithelioid +), melanoma antibody (HMB45, epithelioid +), neuron-specific dilute alcoholase (NSE, small round cell +), synaptophysin (Syn, small round cell +), and Ki67. Nearly, 15% of the nuclei were Ki-67 positive.

Discussion

MNTI is a rare tumor of neural crest origin that is associated with increased urinary excretion of vanilloid acid (7). The biphasic population of melanocytes and primitive neuroectodermal cells in MNTI are both linked to the neural crest cells (NCCs), which are unique migratory pluripotent stem cells in the vertebrates that are required for the generation of

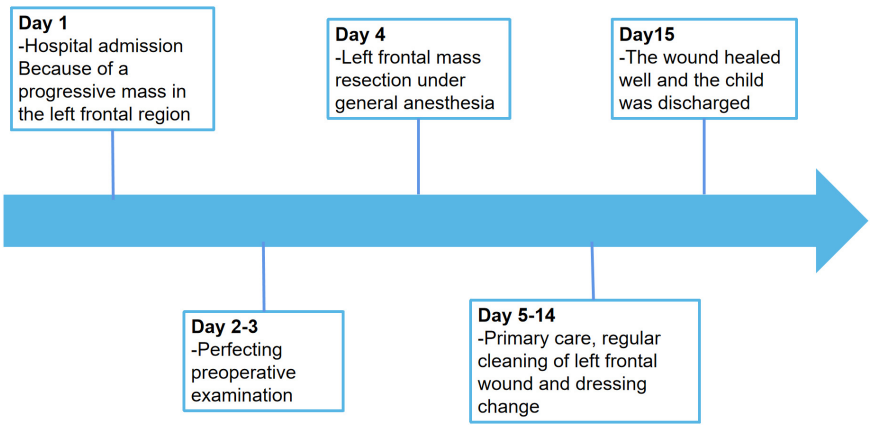

FIGURE 5
Timeline of the patient's clinical journey.

critical components of the craniofacial skeleton, melanocytes, and ganglia of the peripheral nervous system. The generation, migration, and differentiation of NCCs are tightly regulated. Therefore, aberrant development of the NCCs causes embryonic developmental abnormalities and is associated with a spectrum of disorders called neurocristopathies (NCPs). The majority of the known craniofacial developmental defects are associated with alterations in NCC development. Moreover, craniofacial birth defects account for almost one-third of all congenital birth defects reported in humans (8). Neuroblastoma is the most common cancer in infants who are younger than 1 year old and accounts for 1 in every 100,000 births (9). Reed (10) classified NCPs based on the presence or absence of accompanying tumors into developmental abnormalities (dysplasias), neoplasms, and combination of malformations and tumors. This classification was too simple and underestimated the incidence of neural crest disease because of the high variability of the NCPs and inaccurate diagnosis of the minor phenotypic malformations.

Clinically, MNTI is described as single, painless, non-ulcerated, pigmented, and fast-growing neoplasms. In this case-report, a fast-growing mass appeared in the left frontal cranial plate, after the child underwent radical surgery for TOF, a congenital heart disease, at the age of 6 months. This was consistent with the morphological characteristics of MNTI. The pre-operative CT image showed irregular bone structure and irregular soft tissue mass on the left side of the cranial plate in the middle of the forehead, and non-uniform density and "needle-like" periosteal reaction in the parietal bone (11). MNTI neoplasms are mainly composed of melanin-containing epithelial cells and small round neuroblastoma-like cells. MNTI is highly heterogeneous. Therefore, immunohistochemistry is an important tool for the diagnosis of MNTI. The epithelial-like cells in MNTI show higher levels of CK and HMB-45, and reduced S-100 protein levels. The small round neuroblastoma-like cells in MNTI lesions show high expression levels of CD56 and synaptophysin. The neuron-specific enolase is observed in both types of cells. In this study, the immunohistochemical staining data for the patient was consistent with previous reports. However, immunohistochemistry does not reflect the biological behavior of the tumor.

MNTI biopsies is susceptible to misdiagnosis as neuroblastoma. However, neuroblastoma lacks epithelial cells with melanin and is negative for CK and HMB45. The differential diagnosis of MNTI includes other small round blue cell tumors in children such as Ewing sarcomas, adenoid rhabdomyosarcomas, melanomas, and soft tissue CCSs. Ewing sarcoma shows varying degrees of neuroectodermal differentiation and includes morphologically similar small round blue cell tumors and common chromosomal translocations. The Ewing sarcoma family of tumors (ESFTs) are characterized by chromosomal translocations involving one of the several genes of the ETS family (*FLI1, ERG, ETV1, ETV4,* and *FEV*) and the *EWS* gene called *Ewing sarcoma breakpoint region 1* (*EWSR1*) on chromosome 22q12. The most commonly reported chromosomal translocation is t(11;22)(q24;q12), which involves the *EWS* and *FLI1* genes and is observed in 83% of cases with ESFTs. This occurs through an in-frame fusion of the *EWS* gene at 22q12 and the *FLI1* gene at 11q24 resulting in the formation of the *EWS-FLI1* fusion gene product (12). The tumors with the *EWS/FLI-1* fusion gene are characterized by small round cells that are arranged closely to form a Homer-Wright daisy-chain structure and the membrane-positive staining for the MIC gene product, CD99, in 90% of the cases. CD99 staining plays an important role in the diagnosis of Ewing sarcoma. However, Ewing sarcomas lack melanin-containing epithelial cells.

Adenoid rhabdomyosarcomas show morphological similarities with MNTI including adenoid or solid nested structures formed by naive small round cells with specific chromosomal abnormalities. The most common chromosomal translocation in adenoid rhabdomyosarcomas is the t(2;13)

(q35; q14) translocation that generates the *PAX3/FOXO1* fusion gene. The fusion proteins in adenoid rhabdomyosarcomas act as transcriptional activators and regulate myogenic differentiation by altering cellular growth, motility, differentiation, and apoptotic pathways that promote tumor development and metastasis. The nuclear schwannomas show diffused positivity for MyoD1 and myogenin and mostly negative staining for synaptophysin and NSE. In MNTI, transverse myoblast differentiation is occasionally seen, but not in small biopsies.

Since epithelial cells in MNTI neoplasms produce melanin, they need to be differentiated from melanomas. Melanomas are generally heterotypic and can be screened using the S-100 protein. However, the S-100 protein cannot be used as a confirmatory indicator because of its low specificity. Melan A, HMB45, and tyrosinase show higher specificity and varying sensitivity in melanomas, whereas CK and neuroendocrine markers are negative. Furthermore, in the melanomas, the Ki-67 positivity index and cyclin D1 expression levels were high and did not decrease with lesion depth. Therefore, for comprehensive diagnosis of MNTI, two or three of the above-mentioned markers are combined with the S-100 protein index (13).

A slow-growing painless tumor mass is characteristically observed in more than half of the patients with primary soft tissue CCS. In patients with CCS, immunohistochemistry analysis shows strong positivity for S-100, HMB45, melanA, and Vimentin. CCS is also associated with the t(12;22) (q13;q12) translocation and lack of neuroblastoma-like cells (14).

In this case, intraoperatively, the endplate of the milled bone flap showed a "pinprick-like" protrusion that was infiltrative and closely associated with the deep dura mater. This suggested that preoperative imaging was important for the diagnosis of MNTI to provide a reference for guiding the extent of surgical resection of the lesion and the surrounding tissues.

Surgical excision of the lesion is the treatment of choice for patients with MNTI. The prognosis for MNTI is generally good with a postoperative recurrence rate of approximately 15–45% mostly due to incomplete resection of the primary lesion (2). In 3% of MNTI cases, metastasis to the lymph nodes or the central nervous system has been documented (15, 16). Some studies suggest that the resection of the primary lesion should be expanded to remove the majority of the tumor that invades the surrounding tissues to decrease the rates of recurrence. However, it is difficult to determine the scope of expanding the resection site because the tumor originates mostly in the head and face and represents obstacles from anatomical structures (17). Adjuvant chemotherapy or combined radiotherapy is recommended as an alternative to surgery for patients with MNTI when total resection of the tumor is not possible or in cases with contraindications to surgery (18). Furthermore, age at diagnosis is a risk factor for recurrence. Infants diagnosed within the first 2 months of life have the highest likelihood of recurrence within 6 months and the shortest disease-free survival; infants diagnosed at 4.5 months or older have the lowest risk of recurrence; and those diagnosed between 2 and 4.5 months have an intermediate probability of recurrence (5). In this case, although the child was diagnosed at 6 months of age, the previous history of CH and congenital heart disease raised concerns regarding other co-morbidities and the risk of recurrence within 6 months. During the resection of the left frontal mass, we observed characteristic pigmentation of MNTI and localized "pinprick-like" reaction of the skull and adhesion of the tumor tissue on the dura mater. Although the resected tumor could have been frozen rapidly and sent for pathological examination, the extent and severity of surgical trauma would have affected the pathological findings. The tumor tissue was too close to the bone margin. Although the bone margin in the bone window did not show any obvious abnormality by visual observation, the skull was enlarged and 1 cm of tissue around the bone window was removed. The affected dura was also removed, and a dural patch was applied to repair the dural defect. The results of the 12-month postoperative follow-up showed that the child was in a good condition without any recurrence of the tumor mass *in situ* despite the choice to expand the surgical resection area, which increased the tissue trauma to the child. Therefore, although MNTI is a benign tumor, it is characterized by rapid growth and confers destructive effects on the adjacent tissues. The incomplete excision of the primary lesion because of anatomical constraints may lead to local recurrence. Therefore, early diagnosis and treatment are necessary. Moreover, the impact of other comorbidities or congenital developmental malformations needs to be observed during treatment and follow-up. The most effective treatment is complete resection of the lesion and the surrounding tissues that may be invaded by the tumor.

The aggressive course and poor prognosis of MNTI are based on the following prognostic indicators: nuclear schistosomes seen in more than 2 out of 10 high power fields (HPFs); greater than 25% Ki67 positive index; CD99 expression status; higher proportion of neuroblastoma-like cells compared to the epithelioid cells (6). In the present case, Ki67 positivity suggested rapid growth of the tumor and the risk of invasion. However, nuclear schistosomes in 0–2 out of 10 HPFs, negative CD99 staining, Ki-67 positive index of 15%, and appropriate ratio of the neuroblastoma-like cells to the epithelioid cells suggested a good prognosis for this child. The results of the 12-month postoperative follow-up showed the absence of *in situ* recurrences and confirmed the prognosis of the immunohistochemical index.

Characteristic cytogenetic or molecular abnormalities have not yet been identified in MNTI. The inhibition of Wnt and Shh signaling in the chicken embryos triggers craniofacial malformations and congenital heart disease by altering their migration and survival of NCCs and reducing the number of cranial and cardiac NCCs (19). Furthermore,

mutations in the mouse and human *Pax3* genes lead to a spotted (Splotch) mutant phenotype and Waardenburg type I syndrome, respectively; the pure Splotch embryos show severe neural crest cell (NCC) defects with complex phenotypes such as spina bifida, extracerebral malformations, and cardiac outflow tract abnormalities (20). Pax3 expression is upregulated in glioblastomas, neuroblastomas, melanomas, rhabdomyosarcomas, and gastric cancer (21). Liang et al. (22) reported that Pax3 overexpression promoted human glioma cell proliferation, survival, and cell cycle progression by altering the expression levels of Wnt signaling proteins, such as β-catenin, Myc, VEGF, cyclin D1, MMP7, and Wnt1. Several transcription factors and signaling pathways synergistically regulate the complex developmental process of the NCCs. Therefore, aberrations in any of these regulatory proteins can affect the formation, migration, and differentiation of the NCCs, and promote the generation of neural crest-like progenitors.

Tetralogy of Fallot is the most common form of cyanotic congenital heart disease that accounts for 3–5% of all congenital heart diseases; it has a worldwide prevalence of about 0.05% and is most common in Asia (23). The embryologic pathogenesis of the tetralogy of Fallot is complex and involves aberrant neural crest cell migration, mesenchymalization of endothelial cells, and cardiomyocyte differentiation. Notch l and Notch 2 are expressed in specific cell populations of the neural crest-derived outflow tract and the epicardium, and play a key role in the cell-autonomous growth and differentiation of the cardiac neural crest precursors into the SMCs; defects or differential changes in some of these loci can cause congenital heart defects (24). In patients with tetralogy of Fallot, *NOTCH1* gene mutations are detected in nearly 4.5% of cases and are considered the predominant causative gene; mutations in the *NOTCH1* and *JAG1* genes in the Notch signaling pathway are associated with congenital heart disease (25). In this case, MNTI was associated with the manifestation of congenital heart disease and CH. Therefore, mutations and abnormalities in the genetic regulation network (GRN) of the NCCs should be investigated in such cases. Genetic testing of the co-morbidities can add more clinical phenotypes to the spectrum of NCPs and related diseases.

CH is a common disorder of the endocrine system in newborns and infants that can severely impair mental and physical development in children. The worldwide prevalence of CH is 20–200 per 100,000 and 85% of these cases are caused by abnormal thyroid differentiation, migration, or growth (hypothyroidism), and resistance against the thyroid stimulating hormone (26). Thyroid development, differentiation, and migration to their final location in the fetal tissues are regulated by transcription factors such as the paired box gene 8 (PAX8), thyroid transcription factor 2 (TTF2, also known as FOXE1), and the NK2 homeobox 1 (NKX2.1) (27). Several genes implicated in thyroid dysplasia are also associated with abnormalities in other tissues and organ development. It has also been shown that the migration and differentiation of the NCCs are involved in the formation of endocrine glands such as the thyroid. The migration and differentiation of the NCCs are regulated by a variety of signaling proteins such as the retinoids, fibroblast growth factor (FGF), endothelins, and the members of the Wnt signaling family (28). During fetal and neonatal development, deficiency of thyroid hormones impaired proliferation, migration, and differentiation of the thyroid-sensitive neurons resulting in the development of CH that caused neurological impairment, growth retardation, and mental retardation. Children with CH exhibit significant lag in visual, language, and fine motor development, and the symptoms are irreversible. *DUOX2* gene mutations are the most common cause of thyroid hormone synthesis disorder in the Chinese population (27). In this case, a previous ultrasound examination showed a normal location of the thyroid gland and excluded ectopic factors. However, genetic testing was not performed in this case. Therefore, the clinical features and etiology of the congenital thyroid defect could not be clarified.

Once CH is diagnosed, treatment should be administered immediately. L-T4 is the first choice of treatment for CH. However, in patients with severe congenital heart disease, the initial dose of L-T4 should be reduced. In this case, TOF, severe congenital heart disease was diagnosed soon after birth in combination with CH. The MNTI tumor did not show any significant increase in size during reduced L-T4 therapy. However, the tumor size was significantly increased after cardiac surgery and standardized L-T4 treatment. This suggested that the reduction of L-T4 because of TOF affected the complete recovery from hypothyroidism but retarded the growth of the tumor. After congenital heart surgery, the standardized use of L-T4 improved the recovery of thyroid function but accelerated tumor growth. Age-related growth of the MNTI tumor cannot be ruled out in this case. However, this case also suggests that MNTI tumor growth may be associated with adequate treatment of CH. Future studies of MNTI cases at a later stage would shed more light on the potential dysmorphic syndromes or neurodevelopmental disorders associated with MNTI. Furthermore, advances in genetic and other biochemical tests would aid in early prenatal diagnosis and therapeutic management.

Conclusion

Congenital heart disease and/or congenital hypothyroidism are common complaints in children. However, their association with congenital neoplastic disorders is not clear. Our study shows that the growth and development of MNTI neoplasms require comprehensive and constant monitoring. Moreover, therapeutic interventions to co-morbidities may result in the progression of MNTI tumor growth. Genetic factors

are the major risk factors for NCPs. Furthermore, large phenotypic heterogeneity and etiological homogeneity of the NCPs can significantly challenge unraveling the underlying pathogenic mechanisms of NCC development. Therefore, precise elucidation of the pathogenic mutations in the NCPs will help the development of targeted therapeutic and preventive tools.

Data availability statement

The original contributions presented in this study are included in the article/supplementary material, further inquiries can be directed to the corresponding authors.

Ethics statement

The studies involving human participants were reviewed and approved by the Medical Ethics Committee of Tianjin Children's Hospital. It belongs to Tianjin Children's Hospital. Written informed consent to participate in this study was provided by the participants' legal guardian/next of kin. Written informed consent was obtained from the individual(s), and minor(s)' legal guardian/next of kin, for the publication of any potentially identifiable images or data included in this article.

Author contributions

H-CZ: methodology, formal analysis, investigation, and writing—original draft. J-YH: writing—original draft, resources, and visualization. L-SZ: resources, writing—review and editing, project administration, and funding acquisition. X-LH: conceptualization, data curation, writing—review and editing, and supervision. L-SZ and X-LH: responsible for the study described in this manuscript. All authors contributed to the article and approved the submitted version.

Funding

This work was supported by Science and Technology Project of Tianjin Health Committee. Detection of bone marrow micro metastases in children neuroblastoma based on artificial intelligence (ZC20155).

Conflict of interest

The authors declare that the research was conducted in the absence of any commercial or financial relationships that could be construed as a potential conflict of interest.

Publisher's note

All claims expressed in this article are solely those of the authors and do not necessarily represent those of their affiliated organizations, or those of the publisher, the editors and the reviewers. Any product that may be evaluated in this article, or claim that may be made by its manufacturer, is not guaranteed or endorsed by the publisher.

References

1. Krombecher E. Zur histogenese und morphologie der adamantinome und sonstiger kiefergeschwulste. *Beitr Pathol Anat Allg Pathol.* (1918) 64:165–97.

2. Soles BS, Wilson A, Lucas DR, Heider A. Melanotic neuroectodermal tumor of infancy. *Arch Pathol Lab Med.* (2018) 142:1358–63. doi: 10.5858/arpa.2018-0241-RA

3. Higashi K, Ogawa T, Onuma M, Usubuchi H, Imai Y, Takata I, et al. Clinicopathological features of melanotic neuroectodermal tumor of infancy: report of two cases. *Auris Nasus Larynx.* (2016) 43:451–4. doi: 10.1016/j.anl.2015.10.010

4. Rachidi S, Sood AJ, Patel KG, Nguyen SA, Hamilton H, Neville BW, et al. Melanotic neuroectodermal tumor of infancy: a systematic review. *J Oral Maxillofac Surg.* (2015) 73:1946–56. doi: 10.1016/j.joms.2015.03.061

5. Ebel F, Thieringer FM, Kunz C, Klein-Franke A, Scheinemann K, Guzman R, et al. Melanotic neuroectodermal tumor of infancy to the skull: case-based review. *Childs Nerv Syst.* (2020) 36:679–88. doi: 10.1007/s00381-020-04509-6

6. Pontes FSC, de Souza LL, Uchôa DCC, Joaquim AMC, do Nascimento LS, da Mata Rezende DDS, et al. Melanotic neuroectodermal tumor of infancy of the jaw bones: update on the factors influencing survival and recurrence. *Head Neck.* (2018) 40:2749–56. doi: 10.1002/hed.25514

7. Borello ED, Gorlin RJ. Melanotic neuroectodermal tumor of infancy:a neoplasm of neural crese origin. *Cancer.* (1966) 19:196–206. doi: 10.1002/1097-0142(196602)19:23.0.co;2-6

8. Bhattacharya D, Khan B, Simoes-Costa M. Neural crest metabolism: at the crossroads of development and disease. *Dev Biol.* (2021) 475:245–55. doi: 10.1016/j.ydbio.2021.01.018

9. Vega-Lopez GA, Cerrizuela S, Tribulo C, Aybar MJ. Neurocristopathies: new insights 150 years after the neural crest discovery. *Dev Biol.* (2018) 444(Suppl 1.):S110–43. doi: 10.1016/j.ydbio.2018.05.013

10. Reed RJ. Cutaneous manifestations of neural crest disorders (neurocristopathies). *Int J Dermatol.* (1977) 16:807–26. doi: 10.1111/j.1365-4362.1977.tb04299.x

11. Moreau A, Galmiche L, Minard-Colin V, Rachwalski M, Belhous K, Orbach D, et al. Melanotic neuroectodermal tumor of infancy (MNTI) of the head and neck: a French multicenter study. *J Craniomaxillofac Surg.* (2018) 46:201–6. doi: 10.1016/j.jcms.2017.12.001

12. Murugan P, Rao P, Tamboli P, Czerniak B, Guo CC. Primary ewing sarcoma / primitive neuroectodermal tumor of the kidney: a clinicopathologic study of 23 cases. *Pathol Oncol Res.* (2018) 24:153–9. doi: 10.1007/s12253-017-0228-0

13. Panel Members of Expert Consensus on Pathologic Diagnosis of Melanoma in China (2017 Edition). Expert consensus on standardized pathological diagnosis of melanoma in China (2017 edition). *Chinese J Pathol.* (2018) 47:7–13. doi: 10.3760/cma.j.issn.0529-5807.2018.01.003

14. Cornillie J, van Cann T, Wozniak A, Hompes D, Schöffski P. Biology and management of clear cell sarcoma: state of the art and future perspectives. *Expert Rev Anticancer Ther.* (2016) 16:839–45. doi: 10.1080/14737140.2016.1197122

15. Fernandes PM, Elias RA, Santos-Silva AR, Rocha AC, Vargas PA, Lopes MA. Melanotic neuroectodermal tumor of infancy: a clinicopathological case report. *Braz Dent J.* (2018) 29:400–4. doi: 10.1590/0103-6440201801787

16. Goel D, Qayoom S, Goel MM, Rawa J. Melanotic neuroectodermal tumor of infancy (MNTI)-A rare entity. *J Cancer Res Ther.* (2022) 18:784–7. doi: 10.4103/jcrt.JCRT_612_20

17. Sharma P, Yadav AK, Goyal S, Mandal AK. Melanotic neuroectodermal tumor of infancy: a rare entity. *J Oral Maxillofac Pathol.* (2019) 23:134–7. doi: 10.4103/jomfp.JOMFP_237_16

18. Lambropoulos V, Neofytou A, Sfougaris D, Mouravas V, Petropoulos A. Melanotic neuroectodermal tumor of infancy (MNT1) arising in the skull. Short review of two cases. *Acta Neurochir.* (2010) 152:869–75. doi: 10.1007/s00701-009-0472-5

19. Flentke GR, Baulch JW, Berres ME, Garic A, Smith SM. Alcohol-mediated calcium signals dysregulate pro-survival Snai2/PUMA/Bcl2 networks to promote p53-mediated apoptosis in avian neural crest progenitors. *Birth Defects Res.* (2019) 111:686–99. doi: 10.1002/bdr2.1508

20. Sudiwala S, Palmer A, Massa V, Burns AJ, Dunlevy LPE, de Castro SCP, et al. Cellular mechanisms underlying Pax3-related neural tube defects and their prevention by folic acid. *Dis Model Mech.* (2019) 12:dmm042234. doi: 10.1242/dmm.042234

21. Lv WL, Hu YY, Li ZN, Zhang W, Pan Q. PAX3 silencing suppresses gastric cancer proliferation and angiogenesis via MET/PI3K signaling. *Neoplasma.* (2020) 67:304–11. doi: 10.4149/neo_2019_190429N378

22. Liang X, Dong Z, Bin W, Dekang N, Xuhang Z, Shuyuan Z, et al. PAX3 promotes proliferation of human glioma cells by WNT/β-catenin signaling pathways. *J Mol Neurosci.* (2019) 68:66–77. doi: 10.1007/s12031-019-01283-2

23. van der Linde D, Konings EE, Slager MA, Witsenburg M, Helbing WA, Takkenberg JJ, et al. Birth prevalence of congenital heart disease worldwide: a systematic review and meta-analysis. *J Am Coll Cardiol.* (2011) 58:2241–7. doi: 10.1016/j.jacc.2011.08.025

24. High FA, Epstein JA. The multifaceted role of Notch in cardiac development and disease. *Nat Rev Genet.* (2008) 9:49–61. doi: 10.1038/nrg2279

25. Page DJ, Miossec MJ, Williams SG, Monaghan RM, Fotiou E, Cordell HJ, et al. Whole exome sequencing reveals the major genetic contributors to nonsyndromic tetralogy of fallot. *Circ Res.* (2019) 124:553–63. doi: 10.1161/CIRCRESAHA.118.313250

26. Cherella CE, Wassner AJ. Update on congenital hypothyroidism. *Curr Opin Endocrinol Diabetes Obes.* (2020) 27:63–9. doi: 10.1097/MED.0000000000000520

27. Sun F, Zhang JX, Yang CY, Gao GQ, Zhu WB, Han B, et al. The genetic characteristics of congenital hypothyroidism in China by comprehensive screening of 21 candidate genes. *Eur J Endocrinol.* (2018) 178:623–33. doi: 10.1530/EJE-17-1017

28. Liamlahi R, Latal B. Neurodevelopmental outcome of children with congenital heart disease. *Handb Clin Neurol.* (2019) 162:329–45. doi: 10.1016/B978-0-444-64029-1.00016-3

frontiers | Frontiers in Cardiovascular Medicine

TYPE Case Report
PUBLISHED 22 November 2022
DOI 10.3389/fcvm.2022.1060813

Check for updates

OPEN ACCESS

EDITED BY
Reto Asmis,
Wake Forest University, United States

REVIEWED BY
Kalliopi Keramida,
National and Kapodistrian University of Athens, Greece
Mario Enrico Canonico,
University of Naples Federico II, Italy

*CORRESPONDENCE
Christian Caglevic
christian.caglevic@falp.org

SPECIALTY SECTION
This article was submitted to Cardio-Oncology, a section of the journal Frontiers in Cardiovascular Medicine

RECEIVED 03 October 2022
ACCEPTED 03 November 2022
PUBLISHED 22 November 2022

CITATION
Ramos GE, Caglevic C, Bulnes JF, Panay SE, Zapata MI, Daniele AJ and Rodríguez ME (2022) Takotsubo cardiomyopathy Afatinib-related in a non-small cell lung cancer patient: Case report.
Front. Cardiovasc. Med. 9:1060813.
doi: 10.3389/fcvm.2022.1060813

COPYRIGHT
© 2022 Ramos, Caglevic, Bulnes, Panay, Zapata, Daniele and Rodríguez. This is an open-access article distributed under the terms of the Creative Commons Attribution License (CC BY). The use, distribution or reproduction in other forums is permitted, provided the original author(s) and the copyright owner(s) are credited and that the original publication in this journal is cited, in accordance with accepted academic practice. No use, distribution or reproduction is permitted which does not comply with these terms.

Takotsubo cardiomyopathy Afatinib-related in a non-small cell lung cancer patient: Case report

German E. Ramos[1,2], Christian Caglevic[3,4]*, Juan F. Bulnes[5], Sergio E. Panay[4,6], Mario I. Zapata[1,2], Andrés J. Daniele[7] and Manuel E. Rodríguez[1,2]

[1]Department of Cardiology, Instituto Oncológico Fundación Arturo López Pérez, Santiago, Chile, [2]Ehocardiography Laboratory, Instituto Oncológico Fundación Arturo López Pérez, Santiago, Chile, [3]Department of Cancer Research, Instituto Oncológico Fundación Arturo López Pérez, Santiago, Chile, [4]Clinical Trials Unit, Instituto Oncológico Fundación Arturo López Pérez, Santiago, Chile, [5]Department of Cardiology, Pontificia Universidad Católica de Chile, Santiago, Chile, [6]Department of Oncology, Instituto Oncológico Fundación Arturo López Pérez, Santiago, Chile, [7]Department of Cardio-Oncology, Institute of Oncology "Angel H. Roffo", Buenos Aires, Argentina

Endothelial Growth Factor Receptor (EGFR) mutations are frequently found among NSCLC patients. Second-generation Tyrosine Kinase Inhibitor (TKI) Afatinib is frequently used in this population of patients achieving better results than cytotoxic chemotherapy in terms of survival and progression. Afatinib-related cardiotoxicity has been rarely reported. Here we comment on a clinical case of a Takotsubo Cardiomyopathy Afatinib-induced in an NSCLC patient.

KEYWORDS

Takotsubo (stress) cardiomyopathy, Afatinib, EGFR mutation, tyrosine kinase inhibition, NSCLC

Clinical case

A 57-year-old woman with heavy active smoking history was hospitalized due to convulsive syndrome. A brain computed tomography (CT) scan showed an expansive lesion suggesting metastasis. A thorough workup in search of a primary malignancy including a thoracic CT scan reported a mass in the right lung upper lobe. Lung biopsy showed a squamous non-small cell lung cancer (NSCLC) with an Epidermal Growth Factor Receptor (EGFR) exon 19 deletion. The patient started treatment with Afatinib continuously, achieving partial clinical response according to Response Evaluation Criteria in Solid Tumors (RECIST) 1.1. Since the earliest cycles of Afatinib, the patient developed a mild skin rash. This situation is commonly observed among patients that are undergoing anti-EGFR treatments.

After 19 four-week cycles of Afatinib treatment, the patient was admitted due to a severe skin eruption that was considered secondary to Afatinib use, grade 3 according to

CTCAE V5.0 (1). The dermatologist's prescription indicated systemic steroidal therapy and, a multidisciplinary team confirmed that this severe cutaneous toxicity was related to Afatinib use, defining the interruption of this treatment, and achieving then the remission of the cutaneous syndrome. However, one week later after the hospitalization, the patient developed a rapid onset of upper extremity edema and dyspnea on minimal exertion. A thoracic CT showed progression of disease with a new mediastinal mass and superior vena cava thrombosis. Anticoagulation and a course of corticosteroids was started, with a good initial clinical response. By day 11 of hospitalization she presented an anxiety crisis followed by oppressive chest pain and dyspnea. Physical examination revealed tachycardia of 115 bpm, blood pressure 140/80 mm Hg, and oxygen saturation of 90% without oxygen support. The patient appeared to be in mild respiratory distress, with jugular vein distention, S3 gallop on cardiac auscultation, and crackles in both lower lung fields. Electrocardiogram showed ST segment elevation in anterior and septal walls (V2 and V3), with symmetrical T wave inversion in all anterior segments (DI, aVL, v4 to V6), and prolonged corrected QT interval (more than 500 ms). Electrocardiograms at TTS diagnosis, at day 2, and day 7 are shown in **Figures 1–3**, respectively. High-sensitivity troponin levels were raised (0.147 ng/mL, upper reference limit <0.03 ng/ml). A transthoracic echocardiogram (TTE) was performed, revealing akinesis of all middle and apical segments, basal anteroseptal hypokinesis and severe left ventricular systolic dysfunction with left ventricular ejection fraction (LVEF) of 30% (biplane Simpson method). Global longitudinal strain (GLS) – by speckle tracking technique – was severely reduced (−6.7%), displaying a circumferential pattern in the Bull's eye plot (**Figure 4**). These findings were highly suggestive of Takotsubo cardiomyopathy syndrome (TTS). Facing a poor clinical scenario due to a NSCLC metastatic disease, multidisciplinary team (oncologist, intensive care unit and cardiologist) considered that undergoing a coronary angiographic study was an extraordinary measure, so it was discarded. Nonetheless, patient was transferred to the intensive care unit. Medical therapy was initiated, including vasodilators and diuretics, and beta-blockers were introduced after relieving pulmonary congestion. The patient evolved with a prompt clinical and biochemical recovery. Echocardiographic follow up showed progressive improvement of initial findings, achieving complete recovery at three weeks after diagnosis, with no segmental motion abnormalities, a LVEF of 60%, and a peak GLS of −21% (**Figure 5**). A liquid biopsy showed the presence of the T790M resistance mutation, and Osimertinib was started. Unfortunately, the patient died a few months later due to progression of disease.

Discussion

Epidermal Growth Factor Receptors (EGFR) superfamily includes 4 subtypes of receptors currently named EGFR/ERbB1, ErbB2, ErbB3, and ERBb4. These tyrosine kinase EGFR groups have an important role in both embryological and postnatal development, including the cardiovascular system.

Endothelial Growth Factor Receptor (EGFR) amplification and mutations are involved in carcinogenesis, and among non-small cell lung cancer (NSCLC) patients show a high heterogeneity rate. Afatinib, a second-generation tyrosine kinase inhibitor (TKI), produces an irreversible covalent binding not only to EGFR but also to ErbB2, ErbB3, and ErbB4, achieving better results compared with gefitinib and cisplatin-doublet-based chemotherapy in NSCLC – EGFR mutated patients (2). Other EGFR-targeted treatments such as Gefitinib, Erlotinib, Cetuximab, and Panitumumab carry a very low risk of cardiotoxicity (3) and in the specific case of Afatinib-related cardiotoxicity mainly systolic dysfunction has only been sporadically reported (4).

The mechanism by which Afatinib may be involved with the development of cardiotoxicity is related to the "On/Off target" hypothesis. Tumor growth participates in the regulation of survival of cardiomyocytes by two different mechanisms that favor the development of cardiotoxicity. In the "on-target" mechanism the pharmacological target for the tyrosine kinase is similar in cardiomyocytes and in cancer cells and is involved in both proliferation and survival during tumorigenesis. In the "off-target" mechanism the TKI blocks a pathway or a specific kinase different from the original pharmacological target, carrying a risk of toxicity that depends on the inhibited pathway (5). Human epidermal growth factor receptor 2 (HER2) targeted treatment, such as Trastuzumab, triggers systolic dysfunction in approximately 10% of breast cancer patients that are exposed to this treatment (6). The mechanism of action of Afatinib includes not only inhibiting irreversibly both EGFR and HER 2 receptors. Based on the "on/off target mechanism," if saturation of the EGFR receptor occurs (clinically expressed in our patient as severe skin toxicity), afatinib would additionally inhibit HER 2 receptors, generating cardiotoxicity through a mechanism similar to Trastuzumab and other anti HER2 monoclonal antibodies.

Takotsubo syndrome (TTS) was first reported by Sato in 1991 (7). It consists of an acute and transient systolic dysfunction, affecting mainly postmenopausal women, and often preceded by a physical or emotional stressor. Although its exact pathophysiology is still a matter of debate, a catecholamine surge is thought to play a key role in the genesis of reversible myocardial stunning. Nonetheless, its transient nature, the acute phase of TTS could present serious cardiac complications such as acute heart failure and cardiogenic shock due to systolic dysfunction or to dynamic left ventricular outflow obstruction, and life threating ventricular arrhythmias, with in-hospital

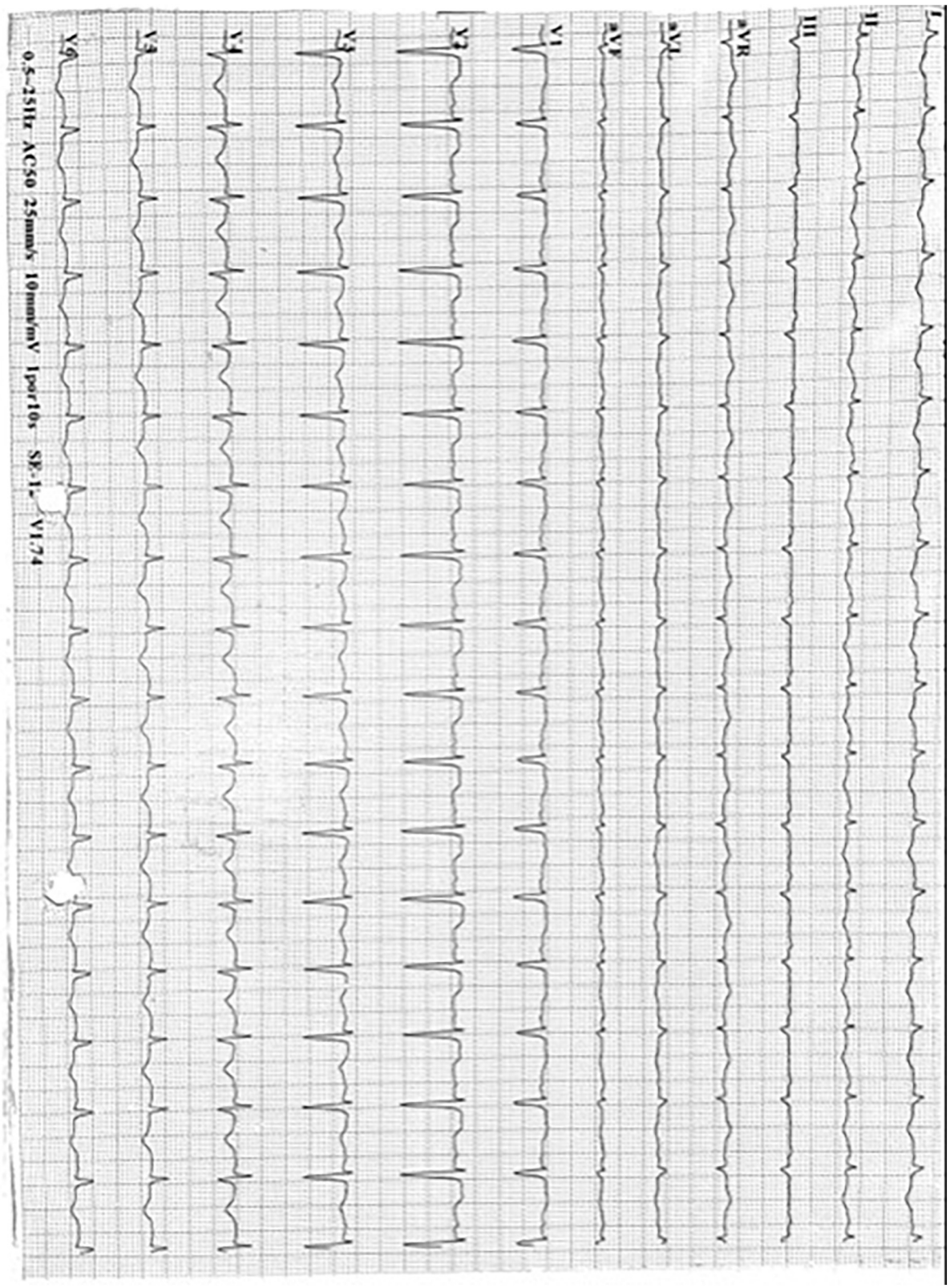

FIGURE 1
Electrocardiogram series. Shows the electrocardiogram at TTS diagnosis ST segment elevation in anterior and septal walls (V2 and V3), with symmetrical T wave inversion in all anterior segments (DI, aVL, v4 to V6), and prolonged corrected QT interval (more than 500 ms).

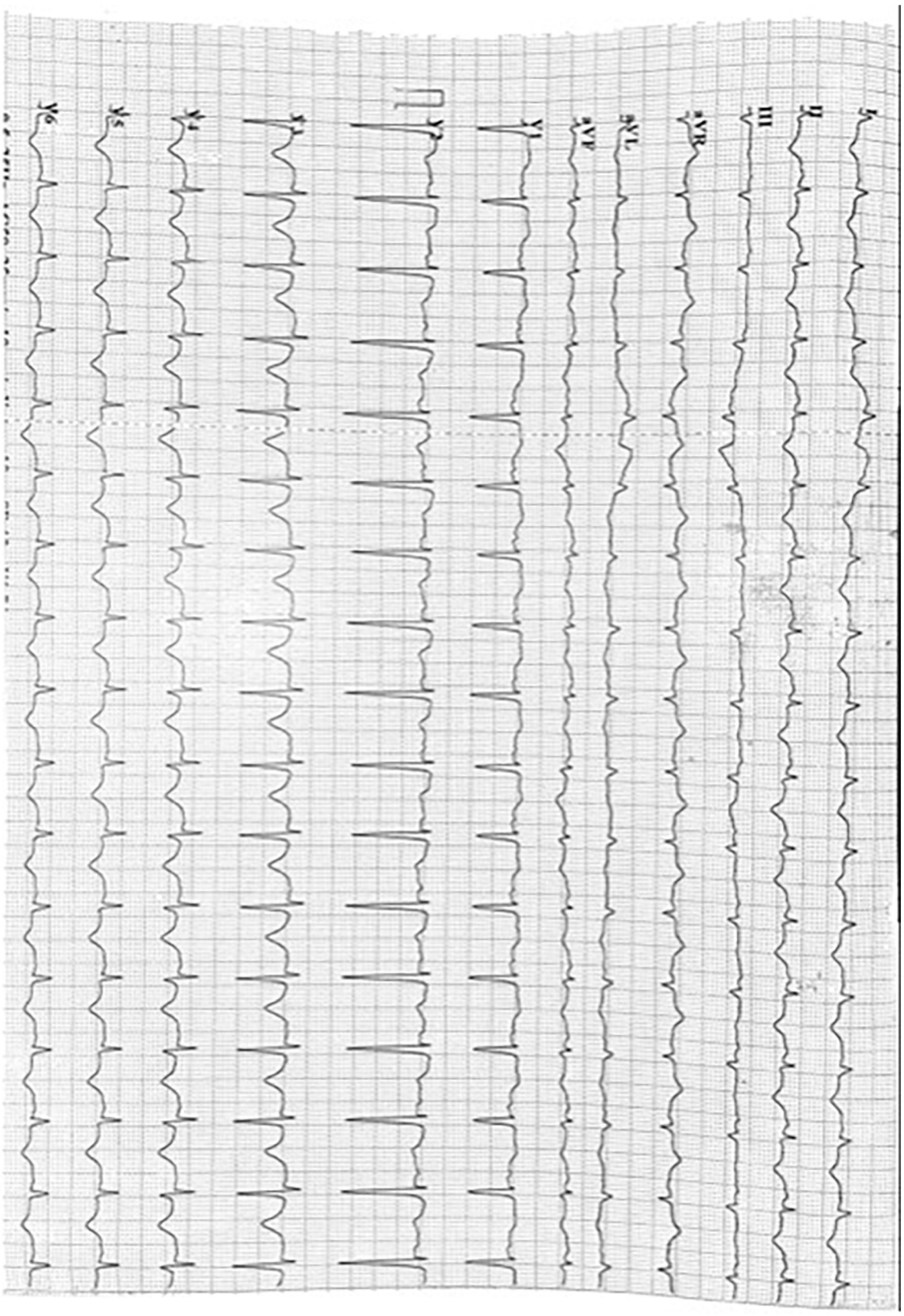

FIGURE 2
Electrocardiogram series. Shows electrocardiogram at day 2 since TTS diagnosis: A slight ST segment elevation (1 mm) in V1 is added compared with previous EKG.

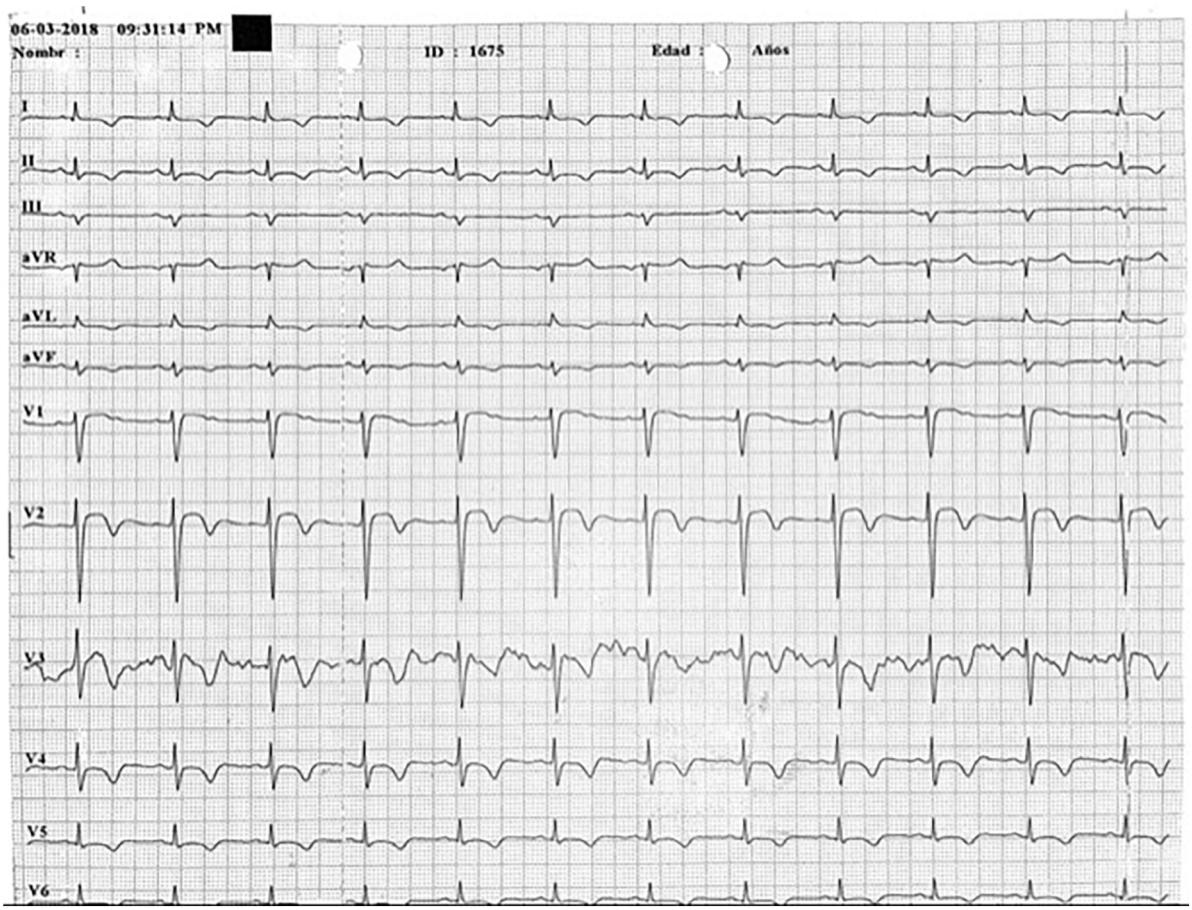

FIGURE 3
Electrocardiogram series. Shows electrocardiogram at day 7 since TTS diagnosis: A Wellens Pattern (type 1) is now observed in V2 and V3 leads t wave inversions and prolonged QT interval remains.

mortality of 4–5% (8). The InterTAK diagnostic criteria for TTS have been proposed, and have become a useful tool for the clinician, enabling a bedside diagnosis of this rare condition (9).

As the best of our knowledge this is the first published report of a case of TTS- Afatinib- related. There is no clear explanation for why our patient developed TTS, nevertheless, we may hypothesize that EGFR receptors were severely saturated by Afatinib and covalently bound adducts to plasma proteins, increasing the half-life of this drug that is known to be an ErbB irreversible blocker (10), giving a greater chance of acting on cardiomyocytes-EGFR receptors resulting in a TTS.

This relationship is based on remarkable and highly suggestive findings in the time line sequence:

- Clinical presentation, with a calculated Inter TAK score = 80 (female sex, emotional and physical stress, non-ST segment depression and prolonged QTc time), corresponding to an estimated 97.3% probability of TTSInitial echocardiographic evaluation suggesting typical, apical variant TTS: akinesis of the apical and middle segments, with a circumferential pattern in the GLS plot (apical ballooning).
- Patient's clinical recovery in a few weeks.
- Echocardiographic follow-up, with a complete regression of initial findings.
- For debate, the existence of drug related skin toxicity and the possible "EGFR saturation mechanism" of cardiotoxicity raised above.

Limitations

Despite the high clinical probability supporting TTS, ruling out coronary artery disease is often required for a definitive diagnosis. With coronary angiography ruled out, coronary computed tomography angiography (CCTA) was an excellent alternative to perform a non-invasive evaluation of coronary anatomy in this case, and has been suggested in patients at high risk of complications associated with

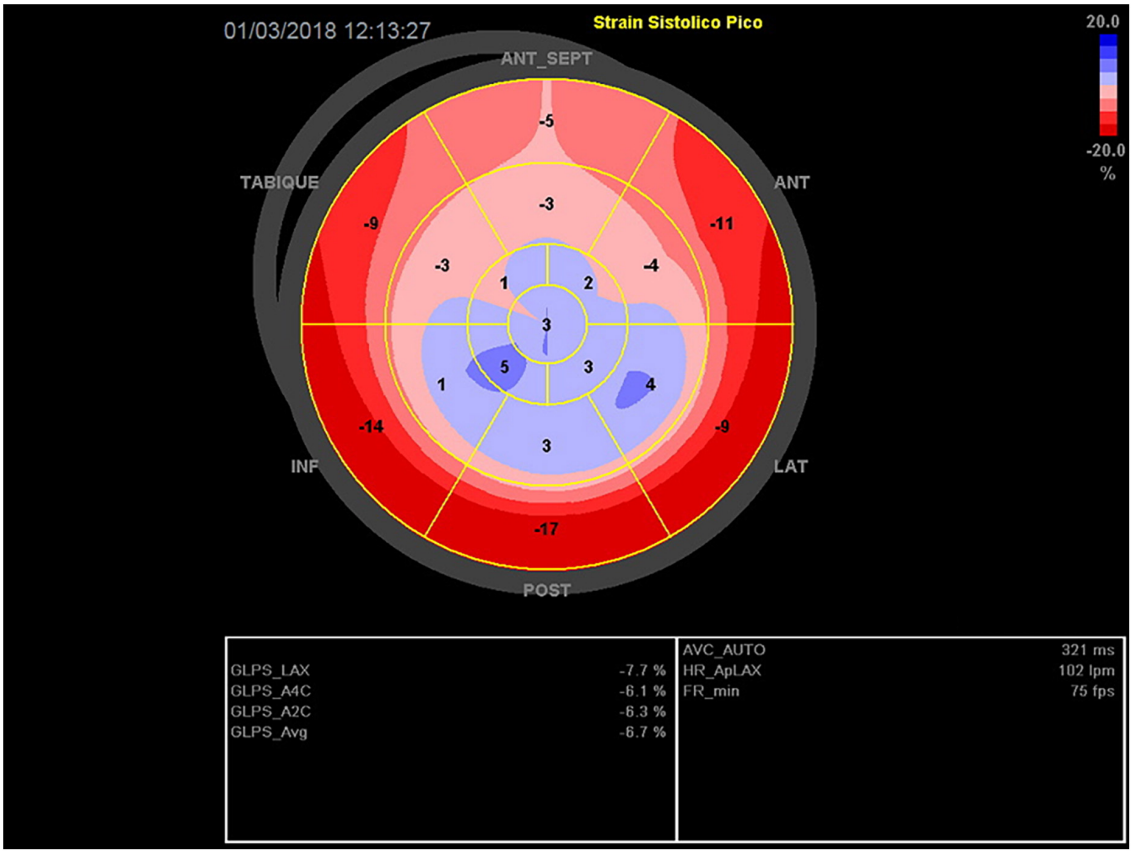

FIGURE 4
Global longitudinal strain (Bull's eye plot) at day 0. Akinesia of all middle and apical segments, with circumferential pattern. Global systolic function is severely compromised (GLS −7%).

formal coronary angiography, such as those with advanced oncological disease. Unfortunately in this patient, CCTA was initially not possible due to persistent tachycardia, and was later discarded due to progressive -and finally, complete- recovery of wall motion abnormalities demonstrated by TTE. A cardiac magnetic resonance would have been very useful, because its superior capacity for tissue characterization, being able to differentiate the presence of edema and absence of late gadolinium enhancement, from other fibrosis patterns suggestive of myocarditis or epicardial vasospasm (11).

Regarding the use of strain (GLS) technique as a key tool in the diagnosis of this patient, it is worth mentioning that In situations of acute heart failure, focused ultrasound (focus) is in first line of care (12). Although the usefulness of SGL in multiple pathologies is promising, there is still not enough evidence to justify its use as a first-line or gold standard diagnostic technique, especially in areas of uncertainty and where the technique has not been sufficiently validated to be incorporated into main heart disease clinical practice guidelines. Although its use in detecting cardiotoxicity in oncological patients acquires greater strength day by day, in acute HF (as in this case) its use is also doubtful, especially in the setting of the use of VAD and/or another circulatory assistance (13). Despite all the above limitations, and considering the lack of availability of other techniques, the echocardiogram and especially the use of GLS was a key element in the diagnosis.

An interesting point to comment on, and which could be a subject of debate in the future, will be the assessment of the need and usefulness of an echocardiogram prior to the use of this drug in selected patients. According to the recommendations published by the recent guidelines of the European Society of Cardiology (ESC), the use of echocardiography prior to the start of cancer treatment is reserved for high or very high-risk patients according to baseline stratification (class I-C recommendation). So far, the use of afatinib does not have a strong causal correlation with cardiotoxicity reported in the literature, especially in severe cases such as this one. More evidence is needed to allow, if it were the case, to reclassify this drug as a higher risk of cardiotoxicity, something that has not been consistently observed until now, as compared with other such as anthracyclines or trastuzumab (14).

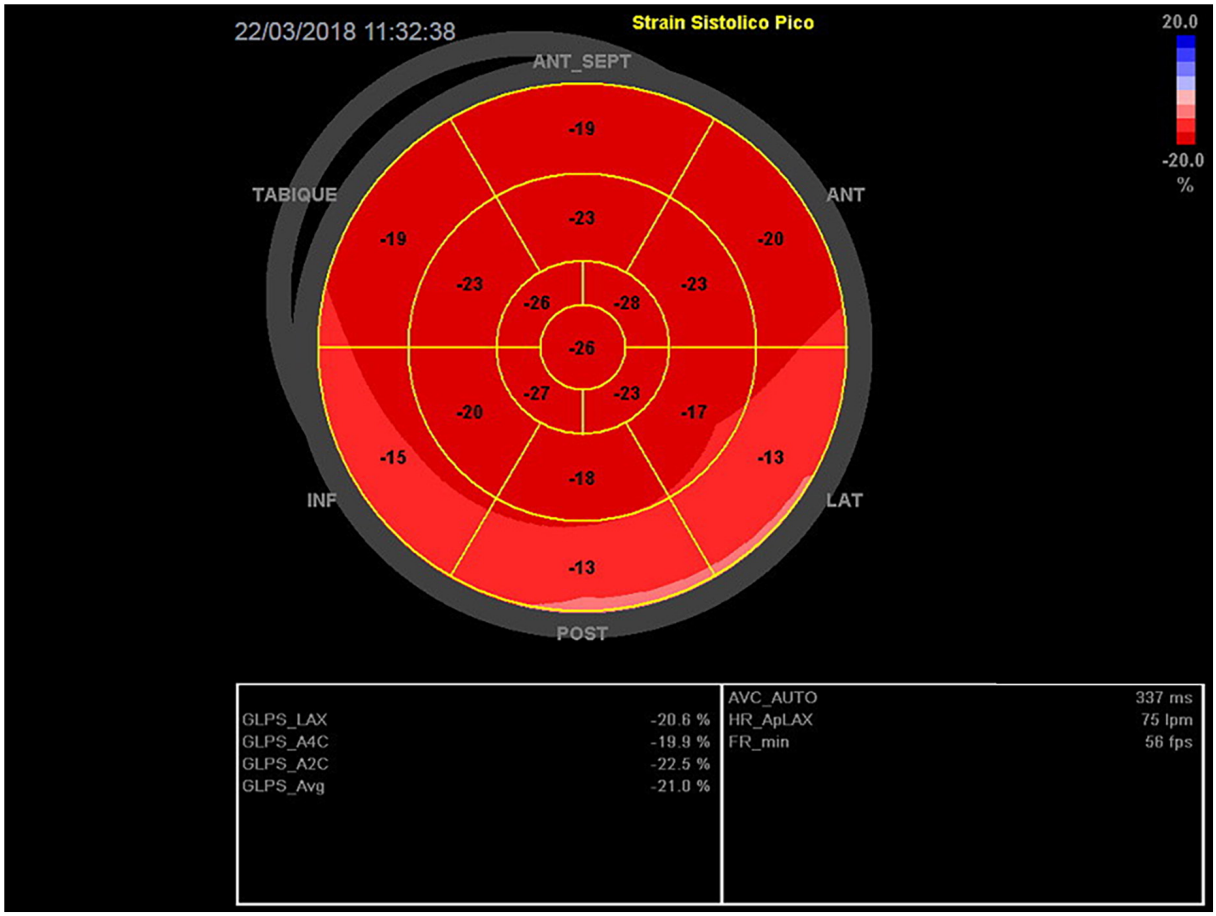

FIGURE 5
Global longitudinal strain (Bull's eye plot) at day 22. There is a remarkable, and practically complete, recovery from the severe initial compromise of the segmentary wall motion abnormalities observed on day 0. Global systolic function is preserved (GLS −21%).

Conclusion

So far, afatinib has been seldom associated with cardiovascular toxicity. We report a unique case of afatinib related-TTS in a patient with NSCLC, an association that must be confirmed by future reports. Given the existence of an important pathophysiological basis for cardiac damage, the cardiovascular and oncological communities should be aware of the potential cardiotoxic risk in patients that are under TKI treatments, including afatinib and other TKI that target EGFR.

Data availability statement

The datasets presented in this article are not readily available because this is a clinical case. Requests to access the datasets should be directed to corresponding author.

Ethics statement

Written informed consent was not required for this study in accordance with the local legislation and institutional requirements.

Author contributions

GR and CC: design, writing of the manuscript, revision of the literature, and approval of the article. JB: revision and writing of manuscript and approval of the article. SP: writing of case and approval of the article. MZ: providing images of basal and follow up echocardiograms, revision of manuscript, and approval of the article. AD: revision of the literature and approval of the article. MR: approval of the article. All authors contributed to the article and approved the submitted version.

Conflict of interest

CC: consulting–advisory MSD, Roche; speaker: MSD, Roche; Research: MSD, Medivation, Astra Zeneca, Roche, Astellas, Sanofi, BMS, GSK, Athenex. SP: speaker: MSD; traveling–accommodations and expenses Janssen, Merck.

The remaining authors declare that the research was conducted in the absence of any commercial or financial relationships that could be construed as a potential conflict of interest.

Publisher's note

All claims expressed in this article are solely those of the authors and do not necessarily represent those of their affiliated organizations, or those of the publisher, the editors and the reviewers. Any product that may be evaluated in this article, or claim that may be made by its manufacturer, is not guaranteed or endorsed by the publisher.

Supplementary material

The Supplementary Material for this article can be found online at: https://www.frontiersin.org/articles/10.3389/fcvm.2022.1060813/full#supplementary-material

SUPPLEMENTARY VIDEOS 1–3
Transthoracic apical views Echocardiography (Focus) at day 0. Apical view of 4, 2 and 3 chambers with apical and mid akinesia of all segments. Global systolic function is severely impaired.

References

1. U.S Department of Health and Human ServicesCommon Terminology. *Criteria for Adverse Events (CTCAE) Version 5.0*. U.S Department of Health and Human Services (2017). Available online at: https://ctep.cancer.gov/protocoldevelopment/electronic_applications/docs/ctcae_v5_quick_reference_5x7.pdf. (accessed November 1, 2022).

2. Ho GF, Chai CS, Alip A, Wahid MIA, Abdullah MM, Foo YC, et al. Real-world experience of first-line afatinib in patients with EGFR-mutant advanced NSCLC: a multicenter observational study. *BMC Cancer.* (2019) 19:896. doi: 10.1186/s12885-019-6107-1

3. Hervent A, De Keulenaer G. Molecular mechanisms of cardiotoxicity induced by ErbB receptor inhibitor cancer therapeutics. *Int J Mol Sci.* (2012) 13:12268–86. doi: 10.3390/ijms131012268

4. Nuvola G, Dall'Olio FG, Melotti B, Sperandi F, Ardizzoni A. Cardiac toxicity from afatinib in EGFR-mutated NSCLC: a rare but possible side effect. *J Thorac Oncol.* (2019) 14:e145–6. doi: 10.1016/j.jtho.2019.02.027

5. Cheng H, Force T. Why do kinase inhibitors cause cardiotoxicity and what can be done about it? *Prog Cardiovasc Dis.* (2010) 53:114–20. doi: 10.1016/j.pcad.2010.06.006

6. Jawa Z, Perez RM, Garlie L, Singh M, Qamar R, Khandheria BK, et al. Risk factors of trastuzumab-induced cardiotoxicity in breast cancer: a meta-analysis. *Medicine.* (2016) 95:e5195. doi: 10.1097/MD.0000000000005195

7. Dote K, Sato H, Tateishi H, Uchida T, Ishihara M. Myocardial stunning due to simultaneous multivessel coronary spasms: a review of 5 cases. *J Cardiol.* (1991) 21:203–14.

8. Citro R, Okura H, Ghadri JR, Izumi C, Meimoun P, Izumo M, et al. Multimodality imaging in takotsubo syndrome: a joint consensus document of the European Association of Cardiovascular Imaging (EACVI) and the Japanese Society of Echocardiography (JSE). *Eur Heart J Cardiovasc Imaging.* (2020) 21:1184–207. doi: 10.1093/ehjci/jeaa149

9. Ghadri JR, Cammann VL, Jurisic S, Seifert B, Napp LC, Diekmann J, et al. A novel clinical score (InterTAK Diagnostic Score) to differentiate takotsubo syndrome from acute coronary syndrome: results from the International Takotsubo registry. *Eur J Heart Fail.* (2017) 19:1036–42. doi: 10.1002/ejhf.683

10. Wind S, Schnell D, Ebner T, Freiwald M, Stopfer P. Clinical pharmacokinetics and pharmacodynamics of afatinib. *Clin Pharmacokinet.* (2017) 56:235–50. doi: 10.1007/s40262-016-0440-1

11. Haghi D, Fluechter S, Suselbeck T, Kaden JJ, Borggrefe M, Papavassiliu T. Cardiovascular magnetic resonance findings in typical versus atypical forms other acute apical ballooning syndrome (Takotsubo cardiomyopathy). *Int J Cardiol.* (2007) 120:205–11. doi: 10.1016/j.ijcard.2006.09.019

12. Čelutkienė J, Lainscak M, Anderson L, Gayat E, Grapsa J, Harjola VP, et al. Imaging in patients with suspected acute heart failure: timeline approach position statement on behalf of the Heart Failure- Association of the European Society of Cardiology. *Eur J Heart Fail.* (2020) 22:181–95. doi: 10.1002/ejhf.1678

13. Sanna GD, Canonico ME, Santoro C, Esposito R, Masia SL, Galderisi M, et al. Echocardiographic longitudinal strain analysis in heart failure: real usefulness for clinical management beyond diagnostic value and prognostic correlations? A comprehensive review. *Curr Heart Fail Rep.* (2021) 18:290–303. doi: 10.1007/s11897-021-00530-1

14. Lyon AR, López-Fernández T, Couch LS, Asteggiano R, Aznar MC, Bergler-Klein J, et al. 2022 ESC Guidelines on cardio-oncology developed in collaboration with the European Hematology Association (EHA), the European Society for Therapeutic Radiology and Oncology (ESTRO) and the International Cardio-Oncology Society (IC-OS). *Eur Heart J Cardiovasc Imaging.* (2022) 23:e333–465. doi: 10.1093/ehjci/jeac106

frontiers | Frontiers in Oncology

TYPE Case Report
PUBLISHED 07 December 2022
DOI 10.3389/fonc.2022.1011894

Check for updates

OPEN ACCESS

EDITED BY
Carlo Gabriele Tocchetti,
University of Naples Federico II, Italy

REVIEWED BY
Yuqin Song,
Beijing Cancer Hospital, Peking University, China
Xin Wang,
Shandong Provincial Hospital, China

*CORRESPONDENCE
Shuang Qu
shuangerqu@163.com
Kai-Yang Lin
lky7411@sina.com

†These authors have contributed equally to this work and share first authorship

SPECIALTY SECTION
This article was submitted to Cardio-Oncology, a section of the journal Frontiers in Oncology

RECEIVED 04 August 2022
ACCEPTED 21 November 2022
PUBLISHED 07 December 2022

CITATION
Xiang Y, Lin X, Cai X, Qu S and Lin K-Y (2022) Extranodal natural killer/T-cell lymphoma invading a patient's heart: A rare case report and literature review. *Front. Oncol.* 12:1011894. doi: 10.3389/fonc.2022.1011894

COPYRIGHT
© 2022 Xiang, Lin, Cai, Qu and Lin. This is an open-access article distributed under the terms of the Creative Commons Attribution License (CC BY). The use, distribution or reproduction in other forums is permitted, provided the original author(s) and the copyright owner(s) are credited and that the original publication in this journal is cited, in accordance with accepted academic practice. No use, distribution or reproduction is permitted which does not comply with these terms.

Extranodal natural killer/T-cell lymphoma invading a patient's heart: A rare case report and literature review

Yifei Xiang[1,2†], Xueqin Lin[1,2†], Xiaoling Cai[1,2], Shuang Qu[3*] and Kai-Yang Lin[1,2,4*]

[1]Department of Cardiology, Fujian Provincial Hospital, Shengli Clinical Medical College of Fujian Medical University, Fuzhou, China, [2]Fujian Provincial Key Laboratory of Cardiovascular Disease, Fujian Cardiovascular Institute, Fujian Provincial Center for Geriatrics, Fujian Clinical Medical Research Center for Cardiovascular Diseases, Fuzhou, China, [3]Department of Hematology, Fujian Provincial Hospital, Shengli Clinical Medical College of Fujian Medical University, Fuzhou, China, [4]Department of Hematology, Fujian Heart Failure Center Alliance, Fuzhou, China

Extranodal NK/T-cell lymphoma (ENKTL) is a rare but aggressive subtype of non-Hodgkin lymphoma, which is derived from NK cells or T cells. There are very few cases of ENKTL invading the heart. Only 12 cases of ENKTL invading the heart have been reported in the English literature. Due to the rarity of this lymphoma, an effective therapeutic strategy has not been defined. Here, we present a case of a 51-year-old Chinese male with extranodal NK/T-cell lymphoma invading the heart and review the literature. The patient received a chemotherapy regimen of PD1 monoclonal antibody (Sintilimab) in combination with first-line P-Gemox. The patient survived for 2 months after diagnosis.

KEYWORDS

extranodal natural killer/T-cell lymphoma, heart failure, poor prognosis, targeted therapy, PET-CT

Introduction

Extranodal NK/T-cell lymphoma is a rare non-Hodgkin lymphoma with dismal outcomes and limited treatment options. According to anatomic origin and clinical manifestations, ENKTL can be divided into nasal, non-nasal, and aggressive/leukemia subtypes. Of the three types, the non-nasal type has much lower survival rate (1). The incidence of this disease is higher in China than in Western countries, and the prognosis

Abbreviations: ENKTL, extranodal natural killer/T-cell lymphoma; MODS, multiple organ dysfunction syndrome; PET-CT, positron emission tomography - computed tomography; LVEF, left ventricular ejection fraction; LVOTG, left ventricular outflow tract gradient.

is poor with traditional treatments (2, 3). Improving the treatment is an urgent requirement.

Here we report a patient having ENKTL invading the heart. Initially, the patient's heart failure was thought to be due to pre-existing hypertrophic obstructive cardiomyopathy. Later, with the elevation of cardiac protein, rapid progression of heart failure and MODS, the patient was considered to have acute myocarditis, and finally ENKTL invading the heart was considered by biopsy of nodules found in the patient's body and whole-body PET-CT.

Case persentation

A 51-year-old man was admitted to our hospital with weakness and recurrent shortness of breath for almost a year, which was aggravated for two days. Two months prior to admission, a echocardiography showed left ventricular ejection fraction (LVEF) = 57% (Table 1). He was treated with alcohol ablation for hypertrophic obstructive cardiomyopathy 6 years ago. Laboratory tests after admission showed N-terminal pro-brain natriuretic peptide(NT-proBNP): 9077.00Pg/ml, Troponin T: 0.32ng/ml, ALT: 274U/L, AST: 432U/L, D dimer: 6.30mg/L. Therefore, acute heart failure is considered based on the patient's condition and laboratory tests. The patient's symptoms suddenly deteriorated two days after admission without any obvious cause, and laboratory tests found ALT: 1997U/L, AST: 2552U/L, D dimer:>35mg/L, LDH:2900U/L. The patient presenting acute heart failure combined with acute liver failure, MODS can be diagnosed. Thus, the patient was transferred to the ICU for further treatment.

After transferred to ICU, the patient's symptoms further deteriorate with oliguria and significantly increased NT-proBNP. Acute heart failure combined with acute kidney injury was taken into account. While in the ICU, a review of laboratory indicators indicated a rapid progression of NT-proBNP(25950Pg/ml), a sharp rise in troponin T(3.29ng/ml), and a progressive rise in ALT(2017U/L) and AST(2552U/L). By this time, the patient's pre-existing hypertrophic obstructive cardiomyopathy could no longer explain the patient's deteriorating condition. Consequently, fulminant myocarditis was taken into consideration. After administration of high dose methylprednisolone, the patient's symptoms were relieved. Echocardiography revealed significant thickening of the septum and left ventricular wall, pericardial effusion with decreased left ventricular myocardial contractility(LVEF=38%) (Table 1). The patient was treated with pericardiocentesis to drain the pericardial fluid and sent it for examination to determine its nature. And the nature of the pericardial fluid returned showed lymphoma cells. Meanwhile, because of the progression of an inadvertently discovered groin swelling, excision of the inguinal mass was performed, post-operative pathological return: moderate-sized lymphoid tumor cells showing diffuse infiltration with multifocal map-like necrosis. Immunohistochemistry showed: Ki-67(70%+), CD20 (–), CD79a(Focal weak +), PAX5(-), CD3(++), CD5(++), CD43(++), CD4(-), CD8(++), CD56(-), TIA-1 (++), EBER(+), CD30(-), ALKp80(-), TdT(-), CD123(-), CD68(-), CD10(-), BCL6(-), MUMI(++). Combined with the above results, the diagnosis of extranodal NK/T-cell lymphoma(ENKTL) was confirmed (Figure 1). Furthermore, PET-CT of the whole body demonstrated that multiple involvement of the heart, skin, blood vessels and muscles without nasal involvement (Figure 2). Hence, the patient was regarded as having ENKTL invading the heart. The patient's rapid progression of heart failure, myocardial injury and MODS were taken into account to be caused by the progressive myocardial infiltration of ENKTL. The palliative effect of glucocorticoids on the patient was considered to be due to the inhibition of the cytokine storm caused by ENKTL rather than inhibition of myocardial inflammation. The reason for this is that the effect of glucocorticosteroids on the patient is rapidly diminishing and the patient's cardiac function is not improving significantly.

After the patient's condition stabilized and all laboratory indicators improved, he was transferred to the hematology department for chemotherapy. The results of echocardiography were similar to the previous results. (LVEF=38%) and laboratory tests showed NT-proBNP: 10246.00Pg/ml, Troponin T: 0.84ng/ml. Considering the severity of the patient's disease, first-line P-Gemox regimen combined with PD-1 monoclonal antibody was administered. This regimen included sintilimab(200mg, day0), gemcitabine (1.8g, day1, day8), oxaliplatin(230mg, day1) and pegaspargase (3750U, day1). Taking into account the poor prognosis of ENKTL invasion of the heart combined with the patient's physical condition at the time, the dose used in this patient's chemotherapy regimen was adequate. During chemotherapy the patient's nodules did not improve, and chidamide(30mg, BIW) was given to improve the efficacy of the treatment. At the end of the current chemotherapy course, the patient's nodules did not improve and even new nodules appeared. In the meantime, the patient's heart function also did not show improvement, and laboratory results showed NT-proBNP: 10648.00Pg/ml, Troponin T: 0.25ng/ml. Finally, the patients decided to be discharged automatically. After automatic discharge, the

TABLE 1 Summary of patient echocardiographic changes.

Time of Echocardiography	LVEF	LVOTG
November 2015 (Pre-Alcohol Ablation)	64.8%	125mmHg
December 2015 (Post alcohol ablation)	64.4%	40mmHg
March 2018 (Post alcohol ablation review)	70.8%	26mmHg
June 2021 (Two months prior to admission)	57%	6.4mmHg
August 2021 (Transferred to ICU)	38%	4mmHg
September 2021 (Transferred to Hematology department)	38%	3.6mmHg

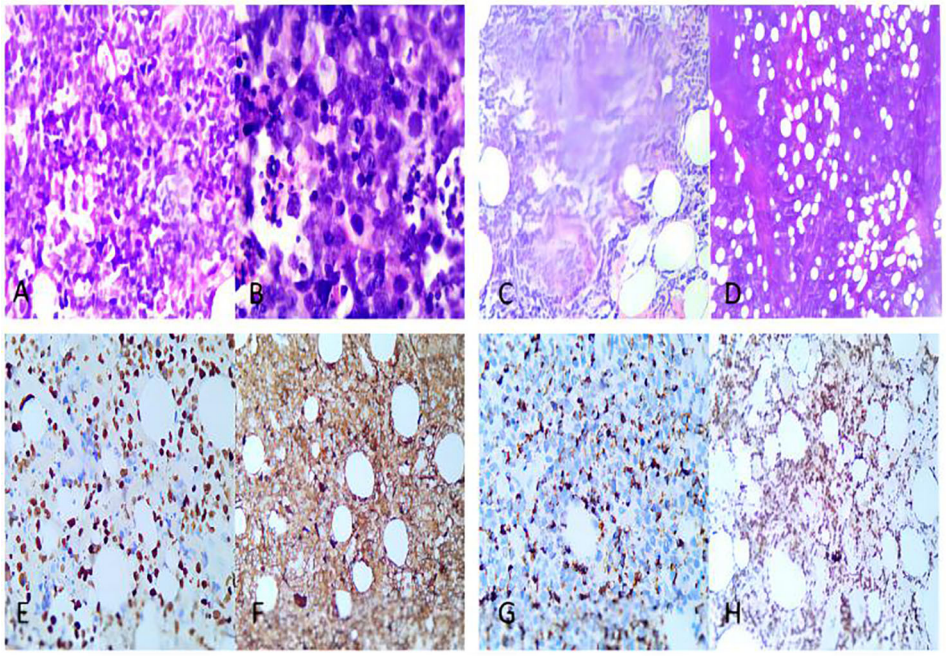

FIGURE 1
Pathological and immunohistochemical images of the patient. **(A, B)**. Obviously heterogeneous medium-sized tumor cells with apoptotic nuclear fragmentation. **(C)**. Tumor cells angiodestructive growth **(D)**. Subcutaneous interfatty infiltration with extensive necrosis. **(E)**. EBER positive. **(F)**. CD3-positive. **(G)**. TIA1-positive. **(H)**. Ki-67 positive, shows high value-added index.

patient's cardiac function deteriorated further, with symptoms of orthopnea, nocturnal paroxysmal dyspnea and edema of both lower limbs. Moreover, the patient's skin nodules were larger and more numerous than previously, and they were breaking down. In the end, the patient died at home on October 4, 2021.

Discussion

ENKTL is a kind of aggressive Epstein-Barr virus (EBV) infection-related NHL stemmed from mature NK cells and NK-Like T Cells, and shows highly-aggressive progression. Nevertheless, to our knowledge, there are only few cases of ENKTL invading the heart, and the non-nasal type accounts for the majority of these cases. The non-nasal ENKTL, which originates in rare sites like the eyes and skin, are more likely to invade the heart than the nasal type, which may partly account for its poor prognosis.

Not only is the number of cases rare, but patients with ENKTL invading the heart are also prone to misdiagnosis of myocarditis, heart failure and arrhythmias. Whole-body PET-CT with echocardiography is indispensable in the diagnostic process of such diseases. Moreover, this type of patient has poor prognosis, often with death as the clinical outcome (Table 2) (1, 4–14).

These features were also seen in our reported cases. However, unlike the previously reported cases, our case has its own characteristics: history of hypertrophic obstructive cardiomyopathy. Because of this feature, the patient's echocardiographic findings were not emphasized in the early stages. At the same time, because the history of heart disease was longer than the time of its nodal onset, it was thought to be a recurrence of hypertrophic obstructive cardiomyopathy triggering cardiac problems. These mislead clinicians about the diagnosis of the disease. In addition, to the best of our knowledge, this is the first case of ENKTL invading the heart in a patient with hypertrophic obstructive cardiomyopathy.

As ENKTL is one of the most difficult subtypes to treat and is associated with a poor prognosis, current treatment strategies have not been clear defined. Based on the only two surviving cases with successful chemotherapy, after successful chemotherapy for ENKTL invasion of the heart, significant improvements in various parameters such as echocardiography were observed, indicating that the results it caused could be reversed by chemotherapy (7, 8). Therefore, despite the adverse effects such as malignant arrhythmias that can occur in patients during chemotherapy, chemotherapy is still recommended as the preferred method once the diagnosis is confirmed. For the present, there is no standard chemotherapy regimen for ENKTL.

10.3389/fonc.2022.1011894

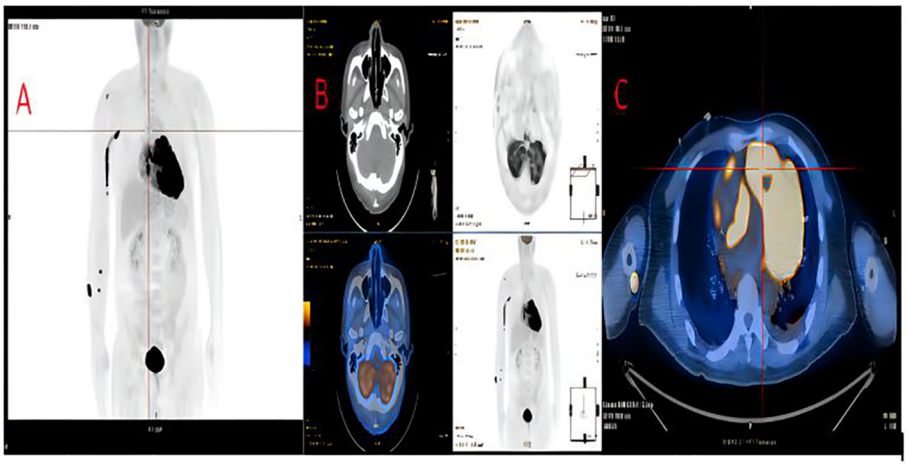

FIGURE 2
The whole pet-ct of this patient. **(A)**. Multiple involvement throughout the body, including the heart, blood vessels, muscles, and skin. **(B)**. No involvement of the nasal cavity. **(C)**. Cardiac involvement: including the LV as well as the funnel of the RV.

TABLE 2 Reported cases of ENKTL invading the heart and our case (1-12).

Case source	Type	Race	Age/ Sex	Cardiac manifestations	Results of chemotherapy	Clinical outcome
1	Non-nasal	Yellow	51/M	Heart failure	No improvement	Died
2. Asian Cardiovasc Thorac Ann. 2019. 27(3): 210-212.	Non-nasal	Yellow	38/M	Arrhythmia	Unknown	Unknown
3. Intern Med.2014. 53(20):2333-6.	Non-nasal	Yellow	23/M	Arrhythmia	Death due to cardiac arrhythmia during chemotherapy	Died
4. J Clin Oncol.2011.29(34): e833-6.	Non-nasal	Yellow	25/M	Myocarditis	Died without chemotherapy	Died
5.Hematol Rep.2011. 3(2): e9.	Non-nasal	White	54/M	Cardiac mass	No improvement after palliative chemotherapy	Died
6. 6. BMJ Case Rep. 2020.13(1).	Non-nasal	White	18/M	Myocarditis	Improvement	Alive
7. Acta Oncol. 2009.48(4):637-9	Nasal	Yellow	65/M	Arrhythmia	Improvement	Alive
8. ArqBras Oftalmol. 2012.75(6):430-2.	Non-nasal	White	33/F	Pericardial tamponade	Died without chemotherapy	Died
10. 9. Front Cardiovasc Med.2021. 8: 685736.	Nasal	Yellow	40/F	Myocarditis	Died without chemotherapy	Died
11. 10. Case Rep Hematol. 2016.2016: 2394809.	Non-nasal	White	62/M	Arrhythmia	Died without chemotherapy	Died
11.Leuk Lymphoa.2008. 49(5): 1008-11.	Non-nasal	Yellow	42/M	Arrhythmia	Death due to cardiac arrhythmia during chemotherapy	Died
12. Ocul Oncol Pathol. 2018. 4(6): 388-394.	Non-nasal	Black	53/M	Pericardial tamponade	Death during chemotherapy	Died
13.Hum Pathol.2003.34(3):290-2.	Non-nasal	Yellow	81/M	Myocardil hypertrophy	Died without chemotherapy	Died

In our case, we used the P-Gemox chemotherapy regimen, which has entered the National Comprehensive Cancer Network (NCCN) guidelines. In an oral presentation at ASH, the combination of Sintilimab and Chidamide was shown to have good antitumor activity in the treatment of patients with refractory or relapsed nasal ENKTL. In 36 refractory patients with evaluable efficacy, an overall efficacy rate of 58.3%, a complete remission rate of 44.4%, and an effective maintenance time of more than 9.2 months were achieved with a manageable safety profile (15). In contrast, the SMILE regimen used in successful cases has side effects that are so strong that patients may not tolerate them. Moreover, in a Japanese multicenter study, the SMILE regimen was reported to be ineffective in non-nasal type patients, with a 2-year overall survival of 34%, while it was more effective in nasal type patients, with a 2-year overall survival of 70% (16). Hence, the regimen we have adopted is already at the forefront of international regimens and is appropriate for the patient's condition. Despite this, the patient's skin nodules and heart failure continued to progress under this chemotherapy regimen. This makes us wonder about the refractory nature of ENKTL. Current considerations for the refractoriness and recurrence of ENKTL are due to immune evasion, some studies have shown that ENKTL cells avoid immune surveillance and the consequent killing of ENKTL, resulting in a poor outcome (17). This may be the reason why patients are resistant to Sintilimab. Such an outcome corresponds exactly to the poor prognosis of non-nasal ENKTL. This calls for further exploration of regimens for this disease.

Our case together with the summary of previous case reports illustrate (1). Non-nasal ENKTL is more likely to invade the heart and has a poorer prognosis than the nasal type (2). Our case is the first case of ENKTL invading the heart in a patient with hypertrophic obstructive cardiomyopathy (3). The regimen we used is already extremely cutting-edge clinically and has better efficacy and longer survival time for refractory recurrent ENKTL compared to the traditional SMILE regimen. Nonetheless, the results are still poor for our patients, which warrants for further exploration of chemotherapy regimens for this type of disease.

Data availability statement

The raw data supporting the conclusions of this article will be made available by the authors, without undue reservation.

Ethics statement

The studies involving human participants were reviewed and approved by Fujian Provincial Hospital ethics committee. Written informed consent for participation was not required for this study in accordance with the national legislation and the institutional requirements.

Author contributions

YX was responsible for the clinical design and conceptualization. YX and XL wrote the manuscript. XC was involved in the acquisition of the clinical data. SQ and K-YL conducted the clinical diagnosis. All authors discussed, read, and approved the submission of this manuscript to the journal.

Conflict of interest

The authors declare that the research was conducted in the absence of any commercial or financial relationships that could be construed as a potential conflict of interest.

Publisher's note

All claims expressed in this article are solely those of the authors and do not necessarily represent those of their affiliated organizations, or those of the publisher, the editors and the reviewers. Any product that may be evaluated in this article, or claim that may be made by its manufacturer, is not guaranteed or endorsed by the publisher.

References

1. Farfán-Leal F, Esteban A, Hinojar R, García-Cosío M, Contreras F. Primary cardiac natural killer/T-cell lymphoma, a very rare form of lymphoma. *Asian Cardiovasc Thorac Ann* (2019) 27(3):210–2. doi: 10.1177/0218492318798230

2. Tse E, Kwong YL. How I treat NK/T-cell lymphomas. *Blood* (2013) 121:4997–5005. doi: 10.1182/blood-2013-01-453233

3. Lee J, Suh C, Park YH, Ko YH, Bang SM, Lee JH, et al. Extranodal natural killer T-cell lymphoma, nasal-type: a prognostic model from a retrospective multicenter study. *J Clin Oncol* (2006) 24:612–8. doi: 10.1200/JCO.2005.04.1384

4. Baek YS, Shin SH, Yi HG, Kim DH, Woo SI, Park KS, et al. Cardiac involvement in CD56 negative primary pancreatic extranodal NK/T-cell lymphoma, nasal type, presenting with ventricular tachycardia during the early stages of chemotherapy. *Intern Med.* (2014) 53(20):2333–6.

5. Huang SH, Hsieh SC, Ko BS, Liu YB. Cardiac involvement of natural killer/T-cell lymphoma presenting with electrical storm after cardioverter-defibrillator implantation. *J Clin Oncol* (2011) 29(34):e833–6. doi: 10.1200/JCO.2011.36.7276

6. Lepeak LM, Yang DT, Chang JE. Extranodal NK/T-cell lymphoma presenting with primary cardiac involvement. *Hematol Rep* (2011) 3(2):e9. doi: 10.4081/hr.2011.e9

7. Leonor Lopez GL, Chaparro SV, Brozzi N, Badiye A. Heart failure enigma in young man: the acute onset of a frequently encountered condition with an unexpected cause. *BMJ Case Rep* (2020) 13(1):e233190. doi: 10.1136/bcr-2019-233190

8. Kanesvaran R, Tao M, Huat IT, Weng DT, Eng DN, Thye LS. Malignant arrhythmia: a case report of nasal NK/T-cell lymphoma with cardiac involvement. *Acta Oncol* (2009) 48(4):637–9. doi: 10.1080/02841860902740923

9. Abe RY, Pinto RD, Bonfitto JF, Lira RP, Arieta CE. Ocular masquerade syndrome associated with extranodal nasal natural killer/T-cell lymphoma: case report. *Arq Bras Oftalmol* (2012) 75(6):430–2. doi: 10.1590/S0004-27492012000600013

10. Zhang Z, Wang S, Liang Q, Peng D. Progressive heart failure and death as the initial manifestation of NK/T-cell lymphoma: A case report and literature review. *Front Cardiovasc Med* (2021) 8:685736. doi: 10.3389/fcvm.2021.685736

11. Li Y, Damjanov I. Extranodal NK/T cell lymphoma causing cardiorespiratory failure. *Case Rep Hematol* (2016) 2016:2394809. doi: 10.1155/2016/2394809

12. Kawasaki H, Shigeno Ohnishi K, Tsuchida T, Miura K, Kato T. A case of primary cutaneous natural killer/T-cell lymphoma, nasal type, directly invading to the heart. *Leuk Lymphoma* (2008) 49:1008–11.

13. Thompson AC, McCall CM, Proia AD. Beneath the retinal pigment epithelium: Histopathologic findings in metastatic extranodal natural Killer/T-cell lymphoma, nasal type. *Ocul Oncol Pathol* (2018) 4:388–94. doi: 10.1159/000487268

14. Kuwabara H, Tsuji M, Yoshii Y, Kakuno Y, Akioka T, Kotani T, et al. Nasal-type NK/T cell lymphoma of the orbit with distant metastases. *Hum Pathol* (2003) 34:290–2.

15. Gao Y HHQ, Wang XX ea. Anti-PD-1 antibody (Sintilimab) plus histone deacetylase inhibitor (Chidamide) for the treatment of refractory or relapsed extranodal natural Killer/T cell lymphoma, nasal type (r/r-ENKTL): preliminary results from a prospective, multicenter,single arm, phase Ib/II trial (SCENT). *Blood* (2020) 136(Supplement 1):39–40. doi: 10.1182/blood-2020-134665

16. Yamaguchi M, Suzuki R, Miyazaki K, Amaki J, Takizawa J, Sekiguchi N, et al. Improved prognosis of extranodal NK/T cell lymphoma, nasal type of nasal origin but not extranasal origin. *Ann Hematol*. (2019) 98(7):1647–55.

17. Li X, Cheng Y, Zhang M, Yan J, Li L, Fu X, et al. Activity of pembrolizumab in relapsed/refractory NK/T-cell lymphoma. *J Hematol Oncol* (2018) 11:15. doi: 10.1186/s13045-018-0559-7

frontiers | Frontiers in Cardiovascular Medicine

TYPE Case Report
PUBLISHED 08 December 2022
DOI 10.3389/fcvm.2022.1035569

Check for updates

OPEN ACCESS

EDITED BY
Carlo Gabriele Tocchetti,
University of Naples Federico II, Italy

REVIEWED BY
Nikhil Agrawal,
University of Texas Health Science Center at Houston, United States
Shui Lian Yu,
Guangzhou Medical University, China

*CORRESPONDENCE
Osnat Itzhaki Ben Zadok
osnat.itzhaki@gmail.com

SPECIALTY SECTION
This article was submitted to Cardio-Oncology, a section of the journal Frontiers in Cardiovascular Medicine

RECEIVED 02 September 2022
ACCEPTED 17 November 2022
PUBLISHED 08 December 2022

CITATION
Itzhaki Ben Zadok O, Shiyovich A, Hamdan A, Yeshurun M, Nardi Agmon I, Raanani P, Kornowski R and Shargian L (2022) Anti-immunoglobulin-like transcript 3 induced acute myocarditis—A case report.
Front. Cardiovasc. Med. 9:1035569.
doi: 10.3389/fcvm.2022.1035569

COPYRIGHT
© 2022 Itzhaki Ben Zadok, Shiyovich, Hamdan, Yeshurun, Nardi Agmon, Raanani, Kornowski and Shargian. This is an open-access article distributed under the terms of the Creative Commons Attribution License (CC BY). The use, distribution or reproduction in other forums is permitted, provided the original author(s) and the copyright owner(s) are credited and that the original publication in this journal is cited, in accordance with accepted academic practice. No use, distribution or reproduction is permitted which does not comply with these terms.

Anti-immunoglobulin-like transcript 3 induced acute myocarditis—A case report

Osnat Itzhaki Ben Zadok[1,2]*, Arthur Shiyovich[1,2], Ashraf Hamdan[1,2], Moshe Yeshurun[2,3], Inbar Nardi Agmon[1,2], Pia Raanani[2,3], Ran Kornowski[1,2] and Liat Shargian[2,3]

[1]Department of Cardiology, Rabin Medical Center, Petah Tikva, Israel, [2]Sackler Faculty of Medicine, Tel Aviv University, Tel Aviv, Israel, [3]Davidoff Cancer Center, Rabin Medical Center, Petah Tikva, Israel

To the best of our knowledge, this is the first published report of anti-immunoglobulin-like transcript 3 (ILT3)-induced myocarditis. A 48-year old female patient with refractory acute myeloid leukemia who was given a single dose of anti-ILT3 monotherapy presented with fever, hypotension, chest pain, and elevated cardiac biomarkers. Systolic bi-ventricular function was in normal limits. The patient was promptly treated with pulse dose steroids with a rapid hemodynamic and clinical improvement and declining levels of cardiac biomarkers. The diagnosis of acute myocarditis was confirmed using cardiac magnetic resonance imaging applying the revised Lake Lewis criteria. While larger-scale data are needed in order to assess the incidence, management and prognosis of anti-ILT-3 induced myocarditis, we believe a high level of suspicion for adverse non-target cardiac effects is required in patients receiving this novel class of drugs.

KEYWORDS

case report, anti-ILT-3 induced myocarditis, immunotherapy, acute myocarditis, cardio-oncology

Introduction

A 48-year-old female patient, BRCA-1 carrier, was diagnosed with triple negative breast carcinoma on age 44 and treated with neoadjuvant chemotherapy (adriamycin, carboplatin, and paclitaxel) followed by bilateral mastectomy and radiotherapy. As part of a clinical research protocol, she was also given pembrolizumab, an immune checkpoint inhibitor (ICI), both as neoadjuvant and maintenance therapy for another 12-months. On age 47, the patient presented with tri-lineage cytopenia and was diagnosed with myelodysplastic syndrome with excess of blasts. Cytogenetics revealed a monosomal complex karyotype with deletion of chromosomes 5 and 7 with no molecular aberration. The patient underwent allogeneic hematopoietic cell transplantation from a matched sibling with myeloablative treosulfan-based conditioning, with full donor chimerism on day 30. Due to an increased risk for relapse, maintenance therapy with azacytidine and venetoclax was initiated on day 60, however on day 180 the patient relapsed with overt-transformation to acute myeloid leukemia. The patient was then treated with salvage chemotherapy (FLAG-IDA protocol) combined with venetoclax for 7 days,

yet unfortunately she did not respond. Finally, the patient was recruited to a clinical immunotherapy trial in a different hospital.

Twelve-days after her first monotherapy treatment with humanized IgG4 anti immunoglobulin-like transcript 3 (ILT3) [MK-0482, MERCK (MSD)] (75 mg), the patient presented to the Hemato-Oncology Ambulatory Care Unit in the Davidoff Cancer Center, Rabin Medical Center (Israel) with fever and malaise (patient's presentation and management time-line is presented in Figure 1). Physical examination was unremarkable and vital signs were in normal range except for systemic fever (temperature 101.3 °F (38.5°C). Laboratory analysis demonstrated 2.1 K/micl leukocytes (normal-range values 4.5–11 K/micl) with 0.2 K/micl neutrophils (normal-range values 1.8–7.7 K/micl), hemoglobin 8.5 g/dL and platelets 12 K/micl. C-reactive protein was 17.3 mg/dL (normal-range values 0.0–0.5 mg/dL). Chest x-ray was normal and 12-leads electrocardiogram (ECG) revealed sinus rhythm with a T-wave inversion in aVL. On a working diagnosis of neutropenic fever, blood cultures were collected and empirical antibiotic (Meropenem) was initiated. COVID-19 status was negative. On day 2, the patient began complaining of a constant chest pain which exacerbated with breathing and was not relieved by oral analgesics. She denied any shortness of breath, palpitations or muscle pain. Blood pressure was 83/52 mmHg, pulse 107/min, oxygen saturation was 96% on room air, respiratory rate 20 breaths per minute. Repeated ECG was unchanged. Lungs were clear to auscultation bilaterally and heart sounds were rapid with no apparent new murmurs. The patient did not show signs of volume overload or pulmonary congestion. Neurologic examination was unremarkable. Troponin T level and NT pro-BNP level were 671 ng/L (normal-range values 0–14 ng/L) and 5,885 pg/ml (normal-range values below 125 pg/ml), respectively. Echocardiography demonstrated a lower limit of normal left ventricular systolic function (LVEF 55%) similar to her prior routine echocardiogram study performed 3 months earlier. Given her clinical presentation and recent novel immunotherapy treatment, the leading diagnosis was immunotherapy-induced acute myocarditis, and decisions were made to monitor her in the cardiac unit and to immediately initiate therapy with empirical pulse dose steroids (methylprednisolone 1 g for 3 days). Cardiac computed tomography revealed normal coronary arteries and ruled out acute pulmonary embolism. On day 3, the patient reported an improvement in her wellbeing and the amelioration of her chest pain. Blood pressure stabilized (103/85 mmHg) and laboratory analysis showed declining levels of cardiac biomarkers (Troponin T 224 ng/L and NT pro-BNP 5,815 pg/ml). The diagnosis of acute myocarditis was confirmed using cardiac magnetic resonance imaging (Figure 2) based on the updated Lake Louis criteria demonstrating subepicardial and mid-wall late gadolinium enhancement in the basal infero- and antero-lateral segments with increased values of native T1 time and T2 time revealing extensive diffuse myocardial edema. After the completion of 3 days of pulse steroid therapy, the patient was switched to oral high-dose (1 mg/Kg) prednisone treatment. Elaborated diagnostic work-up for infectious etiology which included blood cultures, inspiratory viral PCR panel and bacterial, rickettsial and viral serologies was unrevealing.

The patient was discharged home after a 5-day hospitalization with a favorable functional status. Her Troponin T and NT-proBNP levels at discharge were 110 ng/l and 3,812 pg/ml, respectively. A decision was made to discontinue investigational drug therapy.

Discussion

To the best of our knowledge, this is the first published report of anti-ILT3 monotherapy-induced acute myocarditis using the MK-0482 monoclonal antibody. ILT3, gene name LILRB4, is an inhibitory receptor expressed on myeloid-derived suppressor cells which is associated with immune tolerance within the tumor microenvironment. Anti-ILT3 were shown to abrogate myeloid immunosuppression and enable tumor killing (1). Moreover, antagonism of the ILT3 receptor may enhance the efficacy of immune checkpoint inhibitors (ICI) (2). Several phase 1 and phase 2 trials using these new class of drugs are currently ongoing worldwide in both solid and non-solid cancers. Data regarding both the efficiency and safety profile of these immunotherapy agents are still scarce, yet as recently presented in the American Society of Clinical Oncology annual meeting, the combined use of MK-0482 and pembrolizumab was associated with 2 cases of myositis, one of which was fatal (3). While cases of anti-ILT-3-induced myocarditis were not reported in this cohort, it is important to note that the co-existence of myositis and myocarditis is well-established with the use of ICIs (4). More data are needed in order to determine whether this clinical association also exists with the novel class of anti-ILT3 drugs.

Similarities between ICI-induced myocarditis and our presented case of anti-ILT-3 induced myocarditis are the short period of time between the first given dose of the antibody and the development of myocarditis [a median start of onset of 34 days of ICI-induced myocarditis (5–8)], the rise in troponin T which is evident in 94% of patients with ICI induced myocarditis (5, 9) and the presentation of acute myocarditis with normal left ventricular systolic function [found in 51% of patients with ICI-myocarditis (5–8)].

Due to the lack of published evidence regarding the treatment of anti-ILT-3-induced myocarditis and due to the similarities in the mechanism of action and clinical presentation to these two treatment modalities, we based

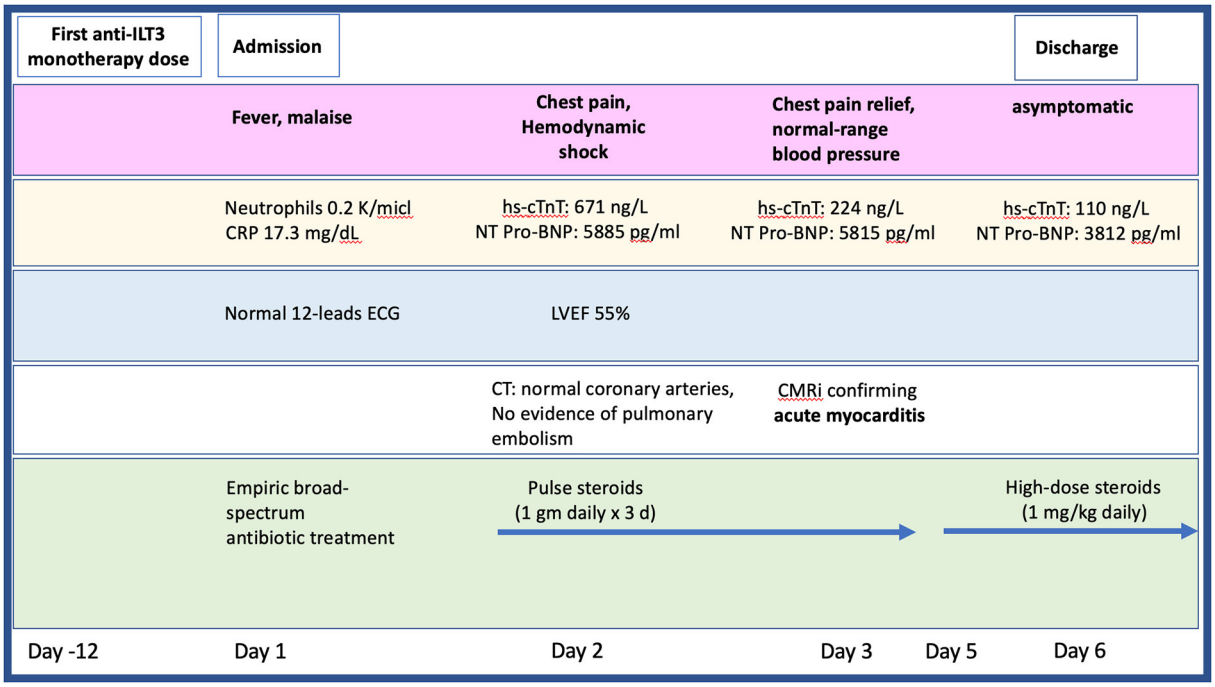

FIGURE 1
Timeline presenting the patient's clinical presentation, diagnostic findings, and treatment approach during hospitalization. CMR, cardiac magnetic resonance imaging; CT, computed tomography; ECG, electrocardiogram; hs-cTnT, high sensitive troponin; LVEF, left ventricular ejection fraction; NT pro-BNP, N-terminal pro-brain natriuretic peptide.

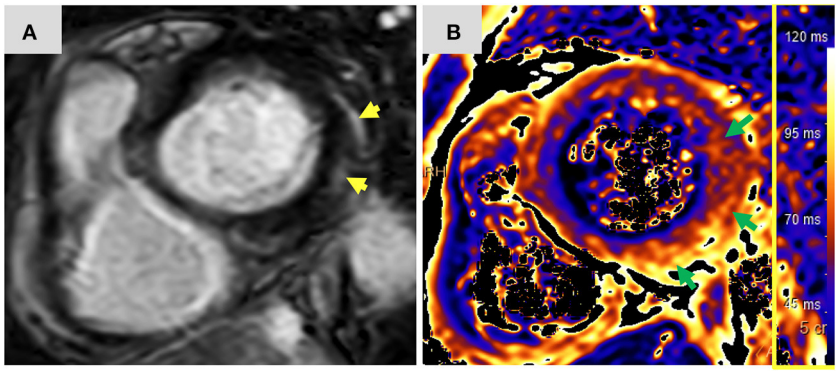

FIGURE 2
Magnetic resonance imaging findings: Short axis view **(A)** of late gadolinium enhancement illustrates sub-epicardial and mid-wall late gadolinium enhancement in the basal infero-lateral and antero-lateral segments (yellow arrows). The corresponding short axis view of T2 mapping **(B)** illustrates extensive diffuse interstitial myocardial edema (green arrows). Diffuse T2 value was 56.2 ms and focal T2 value in the infero-lateral segment was 61 ms (normal limit 55 ms). The presence of myocardial injury and extensive edema support the diagnosis of acute myocarditis according to the 2018 updated Lake Louise criteria. ms, miliseconds.

our management strategy on current published scientific literature and society-guideline recommendations for ICI-induced myocarditis (8, 10, 11). Endomyocardial biopsy was not performed due to patient's severe thrombocytopenia, yet cardiac magnetic resonance imaging allowed for a definite diagnosis of acute myocarditis with extensive diffuse edema (12). The patient was hemodynamically monitored and cardiac biomarkers' levels were regularly followed. Prompt treatment (<24 h from chest pain presentation) with high-dose steroids was given based on the recently published cardio-oncology society guidelines (8), as this was previously shown to improve patient's MACE and mortality (13). Due

to patient's rapid hemodynamic improvement and declining biomarkers' levels, we did not use immunosuppressive drugs other than high-dose steroids, which provided both clinical and laboratory improvement. Notably, it is critical to underscore the importance of a good collaboration between the hemato-oncology and cardio-oncology providers, which allowed for the patient's rapid evaluation, diagnosis and therapy initiation.

While larger-scale data are needed in order to assess the incidence, management and prognosis of anti-ILT-3 induced myocarditis, we believe a high level of suspicion for adverse non-target cardiac effects is required in patients receiving this novel class of drugs.

Data availability statement

The original contributions presented in the study are included in the article/supplementary material, further inquiries can be directed to osnatit@clalit.org.il.

Ethics statement

Written informed consent was obtained from the participant for the publication of this case report and any potentially identifiable images or data included in this article.

Author contributions

OI drafted the manuscript. AS, AH, MY, IN, PR, RK, and LS have reviewed and commented on the final draft. All authors contributed to the article and approved the submitted version.

Acknowledgments

We wish to deeply thank the patient for being an inspiration for us all.

Conflict of interest

The authors declare that the research was conducted in the absence of any commercial or financial relationships that could be construed as a potential conflict of interest.

Publisher's note

All claims expressed in this article are solely those of the authors and do not necessarily represent those of their affiliated organizations, or those of the publisher, the editors and the reviewers. Any product that may be evaluated in this article, or claim that may be made by its manufacturer, is not guaranteed or endorsed by the publisher.

References

1. Brandish PE, Palmieri A, Ayanoglu G, Baker J, Bueno R, Byford A, et al. Antibodies to ILT3 abrogate myeloid immunosuppression and enable tumor killing. *BioRxiv*. (2021) 2021:2021.12.18.472552. doi: 10.1101/2021.12.18.472552

2. Singh L, Muise E, Bhattacharya A, Grein J, Javaid S, Stivers P, et al. ILT3 (LILRB4) promotes the immunosuppressive function of tumor-educated human monocytic myeloid-derived suppressor cells. *Mol Cancer Res*. (2020) 19:molcanres.0622.2020. doi: 10.1158/1541-7786.MCR-20-0622

3. Gutierrez M, Spreafico A, Wang D, Golan T, Renouf D, Voskoboynik M, et al. Phase 1 first-in-human study of anti–ILT3 mAb MK-0482 as monotherapy and in combination with pembrolizumab in advanced solid tumors: dose escalation results. *J Clin Oncol*. (2022) 40(16_suppl):2505. doi: 10.1200/JCO.2022.40.16_suppl.2505

4. Pathak R, Katel A, Massarelli E, Villaflor VM, Sun V, Salgia R. Immune checkpoint inhibitor-induced myocarditis with myositis/myasthenia gravis overlap syndrome: a systematic review of cases. *Oncologist*. (2021) 26:1052–61. doi: 10.1002/onco.13931

5. Mahmood SS, Fradley MG, Cohen JV, Nohria A, Reynolds KL, Heinzerling LM, et al. Myocarditis in patients treated with immune checkpoint inhibitors. *J Am Coll Cardiol*. (2018) 71:1755–64. doi: 10.1016/j.jacc.2018.02.037

6. Lehmann LH, Cautela J, Palaskas N, Baik AH, Meijers WC, Allenbach Y, et al. Clinical strategy for the diagnosis and treatment of immune checkpoint inhibitor-associated myocarditis: a narrative review. *J Am Med Assoc Cardiol*. (2021) 6:1329–37. doi: 10.1001/jamacardio.2021.2241

7. Agrawal N, Khunger A, Vachhani P, Colvin TA, Hattoum A, Spangenthal E, et al. Cardiac toxicity associated with immune checkpoint inhibitors: case series and review of the literature. *Case Rep Oncol*. (2019) 12:260–76. doi: 10.1159/000498985

8. Lyon AR, López-Fernández T, Couch LS, Asteggiano R, Aznar MC, Bergler-Klein J, et al. 2022 ESC Guidelines on cardio-oncology developed in collaboration with the European Hematology Association (EHA), the European Society for Therapeutic Radiology and Oncology (ESTRO) and the International Cardio-Oncology Society (IC-OS): developed by the task force on cardio-oncology of the European Society of Cardiology (ESC). *Eur Heart J*. (2022) 43:4229–361. doi: 10.1093/eurheartj/ehac244

9. McDonagh TA, Metra M, Adamo M, Gardner RS, Baumbach A, Böhm M, et al. 2021 ESC Guidelines for the diagnosis and treatment of acute and chronic heart failure: developed by the Task Force for the diagnosis and treatment of acute and chronic heart failure of the European Society of Cardiology (ESC). With the special contribution of the Heart Failure Association (HFA) of the ESC. *Eur J Heart Fail*. (2022) 24:4–131. doi: 10.1093/eurheartj/ehab670

10. Thuny F, Alexandre J, Salem JE, Mirabel M, Dolladille C, Cohen-Solal A, et al. Management of immune checkpoint inhibitor-induced myocarditis: the French Working Group's plea for a pragmatic approach. *JACC CardioOncol*. (2021) 3:157–61. doi: 10.1016/j.jaccao.2020.12.001

11. Palaskas N, Lopez-Mattei J, Durand JB, Iliescu C, Deswal A. Immune checkpoint inhibitor myocarditis: pathophysiological characteristics, diagnosis, and treatment. *J Am Heart Assoc*. (2020) 9:e013757. doi: 10.1161/JAHA.119.013757

12. Bonaca MP, Olenchock BA, Salem JE, Wiviott SD, Ederhy S, Cohen A, et al. Myocarditis in the setting of cancer therapeutics: proposed case definitions for emerging clinical syndromes in cardio-oncology. *Circulation*. (2019) 140:80–91. doi: 10.1161/CIRCULATIONAHA.118.034497

13. Zhang L, Zlotoff DA, Awadalla M, Mahmood SS, Nohria A, Hassan MZO, et al. Major adverse cardiovascular events and the timing and dose of corticosteroids in immune checkpoint inhibitor-associated myocarditis. *Circulation*. (2020) 141:2031–4. doi: 10.1161/CIRCULATIONAHA.119.044703

frontiers | Frontiers in Cardiovascular Medicine

TYPE Case Report
PUBLISHED 09 December 2022
DOI 10.3389/fcvm.2022.993631

Check for updates

OPEN ACCESS

EDITED BY
Zaza Iakobishvili,
Clalit Health Services, Israel

REVIEWED BY
Hui Jiang,
Shenyang Northern Hospital, China
Andreea Calin,
Carol Davila University of Medicine and Pharmacy, Romania

*CORRESPONDENCE
A. Jamil Tajik
wi.publishing14@aah.org

SPECIALTY SECTION
This article was submitted to Cardio-Oncology, a section of the journal Frontiers in Cardiovascular Medicine

RECEIVED 13 July 2022
ACCEPTED 16 November 2022
PUBLISHED 09 December 2022

CITATION
Ashraf M, Jahangir A, Jan MF, Muthukumar L, Neitzel G and Tajik AJ (2022) Case report: Metastatic melanoma masquerading as apical hypertrophic cardiomyopathy. *Front. Cardiovasc. Med.* 9:993631. doi: 10.3389/fcvm.2022.993631

COPYRIGHT
© 2022 Ashraf, Jahangir, Jan, Muthukumar, Neitzel and Tajik. This is an open-access article distributed under the terms of the Creative Commons Attribution License (CC BY). The use, distribution or reproduction in other forums is permitted, provided the original author(s) and the copyright owner(s) are credited and that the original publication in this journal is cited, in accordance with accepted academic practice. No use, distribution or reproduction is permitted which does not comply with these terms.

Case report: Metastatic melanoma masquerading as apical hypertrophic cardiomyopathy

Muddasir Ashraf[1], Arshad Jahangir[1], M. Fuad Jan[1], Lakshmi Muthukumar[1], Gary Neitzel[2] and A. Jamil Tajik[1]*

[1]Aurora Cardiovascular and Thoracic Services, Aurora Sinai/Aurora St. Luke's Medical Centers, Advocate Aurora Health, Milwaukee, WI, United States, [2]Department of Pathology and Laboratory Medicine, Aurora St. Luke's Medical Center, Advocate Aurora Health, Milwaukee, WI, United States

Background: Cardiac tumors are usually metastatic. Melanoma is the tumor with the highest rate of cardiac metastasis. Clinicians need to be aware of the metastatic involvement of the left ventricular apex as a differential diagnosis of apical hypertrophic cardiomyopathy.

Case summary: A 74-year-old woman presented for evaluation of fatigue. The initial electrocardiogram and echocardiogram showed features of apical hypertrophic cardiomyopathy. The patient reported a lesion on her right forearm that had been present for many years, leading to its biopsy, which showed melanoma. Further evaluation with a chest-computed tomography (CT) scan showed left lung nodules and nodular thickening of the left ventricular apex. Positron emission tomography showed an increased uptake of fluorodeoxyglucose in the left lung nodule and left ventricular apex, suggestive of metastatic spread of the melanoma. A CT-guided biopsy of the left lung nodule revealed melanoma. The patient was treated with ipilimumab initially, followed by paclitaxel with poor response to treatment, and later passed under hospice care.

Conclusion: Metastatic tumors involving the left ventricular apex should be considered in the differential diagnosis of apical hypertrophic cardiomyopathy, especially in patients with a history of melanoma, and advanced cardiac imaging, including cardiac magnetic resonance imaging, CT, and/or positron emission tomography (PET) may help with narrowing down the differential diagnosis.

KEYWORDS

left ventricular apex, metastatic melanoma, tumor, case report, apical hypertrophic cardiomyopathy

10.3389/fcvm.2022.993631

Introduction

Cardiac tumors are usually metastatic, with a reported incidence 100 times higher than that of primary cardiac tumors. The reported incidence of cardiac metastasis is 0.7–3.5% in the general population, with rates up to 9.1% in patients diagnosed with metastatic cancer. Metastatic melanoma has a higher rate of metastasis to the heart than any other tumor (1). Metastatic melanoma should always be considered a differential diagnosis of apical hypertrophy cardiomyopathy, especially in patients with a history of melanoma. We present a 74-year-old woman who was initially diagnosed with apical hypertrophic cardiomyopathy, but further evaluation and diagnostic testing revealed metastatic involvement of the left ventricular apex due to melanoma.

Case summary

A 74-year-old female, who had a past medical history of chronic atrial fibrillation on daily warfarin, moderate pulmonary hypertension, and a pacemaker placement 4 years prior for complete heart block, came in for an evaluation of fatigue (**Table 1**). The initial 12-lead electrocardiogram showed demand ventricular pacing with underlying atrial fibrillation, left ventricular (LV) hypertrophy, and giant negative T waves in paced as well as normally conducted beats (**Figure 1A**), and a transthoracic echocardiogram (TTE) showed apical hypertrophy. Physical examination showed variable-intensity S1, normal intensity S2, point of maximal impulse non-displaced, grade I/VI systolic murmur along the left sternal border and apex, and an S3. A plaque-like 2.5 × 2 cm lesion was observed on the right forearm, which the patient said had been present for many years.

Differential diagnoses of apical wall thickening and T wave inversion in precordial leads considered are shown in **Supplementary Tables 1**, **2**, respectively.

Laboratory workup, including complete blood count, complete metabolic panel, pro-B-type natriuretic peptide, and ultrasensitive troponin, was unremarkable. Chest X-ray was normal. The subsequent 12-lead electrocardiograms showed a decreasing amplitude of T wave inversions and R waves over time in the paced beats (**Figures 1B,C**). A TTE showed an apical wall thickness of 19 mm (**Figure 2**; **Supplementary Videos 1–3**). The global longitudinal strain was reduced to −9% and the LV ejection fraction was 70%. A punch biopsy of the right forearm lesion showed nodular, amelanotic melanoma with Breslow tumor thickness of at least 2.2 mm and at least Clark level IV invasion. Subsequently, this was resected and considered T4B N0 M0, stage II-C melanoma. The chest computed tomography (CT) s162can showed nodular thickening of the LV apex and pulmonary nodules in the left lung, suggestive of metastatic disease (**Figures 3A,B**). A positron emission tomography (PET) scan revealed increased uptake of fluorodeoxyglucose (FDG) in the LV apex and left lung nodules (**Figure 3C**), suggestive of metastatic spread of the melanoma to the LV apex and left lung. CT-guided biopsy of the pulmonary nodule confirmed the metastatic spread of the melanoma to the lungs (see **Supplementary Figure 1**). Hematoxylin and eosin staining revealed a diffuse sheet of malignant epithelioid cells with moderately pleomorphic, hyperchromatic nuclei, and poorly defined cytoplasm without pigments. The tumor also expressed melanoma markers S100 and MART-1.

The patient was initially started on metoprolol succinate 25 mg daily for apical hypertrophic cardiomyopathy (ApHCM). Once the diagnosis of metastatic melanoma was confirmed, she was started on ipilimumab, a cytotoxic T-lymphocyte-associated protein 4 inhibitor. However, the patient's liver enzymes increased to greater than five times the normal, thus it was discontinued. PD-1 inhibitors were not approved by the Food and Drug Administration for metastatic melanoma at that time. The patient was subsequently started on paclitaxel, but the disease progressed, and the patient felt weaker with no significant improvement in her symptoms. The patient was actively involved in the decision-making. She did not

TABLE 1 Timeline of events.

Initial visit	The patient presented with fatigue and was diagnosed with apical hypertrophic cardiomyopathy based on an initial electrocardiogram and transthoracic echocardiogram.
One month later	The patient underwent punch biopsy of the right forearm lesion, which was positive for melanoma.
1.5 months later	Wide excision of the right forearm lesion and sentinel lymph node biopsy of right axilla done, and patient found to have Stage IIC melanoma.
20 months later	A computed tomography (CT) scan of the chest and a whole-body positron emission tomography (PET) scan were suggestive of metastatic spread of melanoma to the left ventricular apex and left lung. A CT-guided biopsy of the left pulmonary nodule confirmed metastatic melanoma.
21 months later	The patient was started on ipilimumab as she was negative for *BRAF V600* mutation.
23 months later	Ipilimumab was stopped due to a significant increase in liver enzymes.
24 months later	Patient started on paclitaxel.
32 months later	Repeat PET scan showed progressive disease. Patient started on hospice care and passed at a hospice facility.

Abbreviations: ApHCM, apical hypertrophic cardiomyopathy; CMR, cardiac magnetic resonance imaging; CT, computed tomography; FDG, fluorodeoxyglucose; LV, left ventricle/left ventricular; PET, positron emission tomography.

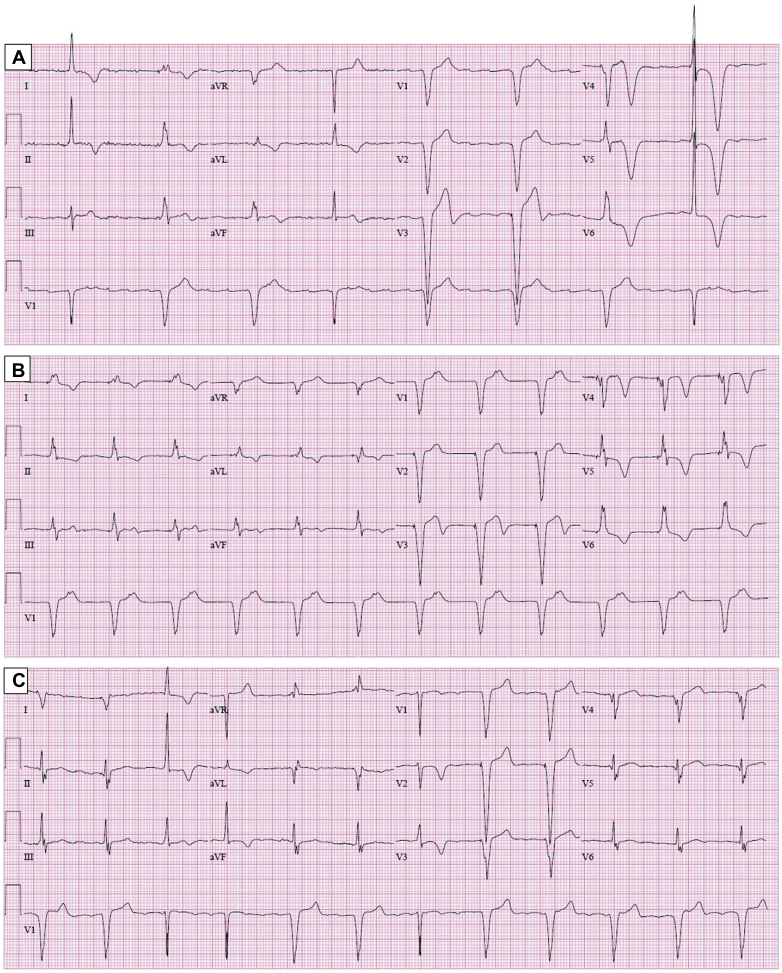

FIGURE 1
Electrocardiogram. Panel **(A)** shows tall R waves and giant-negative T waves in V4–V6. Panels **(B)** (8 months later) and **(C)** (24 months later) show a progressive decrease in the amplitude of the R waves and T wave inversions in the paced beats in precordial leads.

want any further treatment and was placed in hospice care, where she expired.

Discussion

In an autopsy study of patients with metastatic melanoma, 64% had cardiac metastases (2). The metastatic spread is usually through hematogenous dissemination (1). It usually involves the right atrium (3, 4). Apical involvement is rare (5, 6). Cardiac metastasis could be missed unless specific symptoms are present or specific imaging is performed.

Asymptomatic massive involvement of the myocardium in metastatic melanoma has been described as a "charcoal heart." The most common presenting symptom in patients with cardiac melanoma is shortness of breath, but chest pain, syncope, fatigue, and weakness have also been described.

Electrocardiographic changes suggestive of the ischemic pattern, including ST depression and T wave inversion, are more common in patients with cardiac metastasis. Cates et al. analyzed electrocardiograms obtained within 3 months prior to death in patients diagnosed with cancer premortem or postmortem and found an ischemic pattern in 40% of patients with cardiac metastasis compared to <1% in patients without cardiac metastasis (7). In the present case, the patient showed tall R waves and giant negative T waves in precordial leads. To our knowledge, this is the first case of cardiac melanoma with giant negative T waves mimicking the apical variant of hypertrophic cardiomyopathy. The patient's serial 12-lead electrocardiograms showed the resolution of giant negative T waves over 2 years. These serial changes in patients diagnosed with ApHCM may suggest additional processes, such as the progression of fibrosis, new myocardial infarction, or infiltrative disease.

A transthoracic echocardiogram is the most frequently used non-invasive test to evaluate benign and malignant

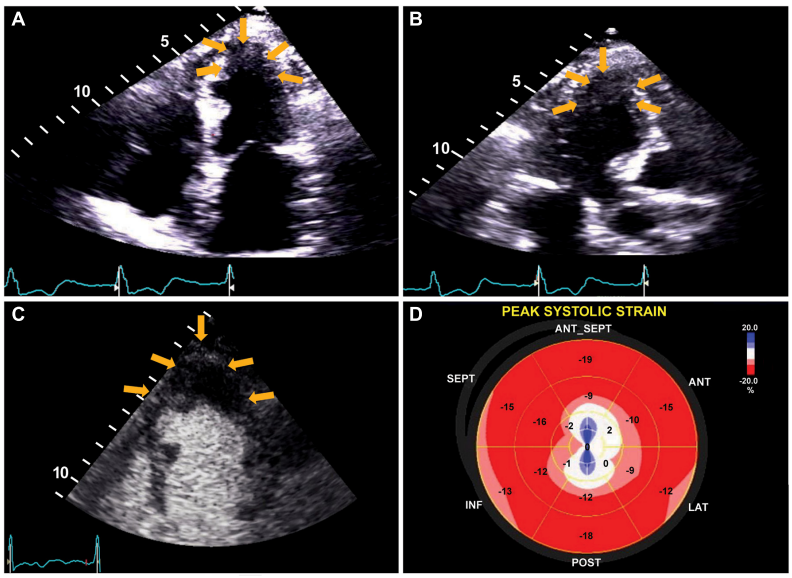

FIGURE 2
Transthoracic echocardiogram. The apical four-chamber view **(A)** (**Supplementary Video 1**), apical long-axis view **(B)** (**Supplementary Video 2**), and definity contrast echocardiogram **(C)** (**Supplementary Video 3**) show apical wall thickness (yellow arrows). Panel **(D)** shows strain analysis with markedly reduced peak systolic strain and evidence of dyskinesis in the apical segments.

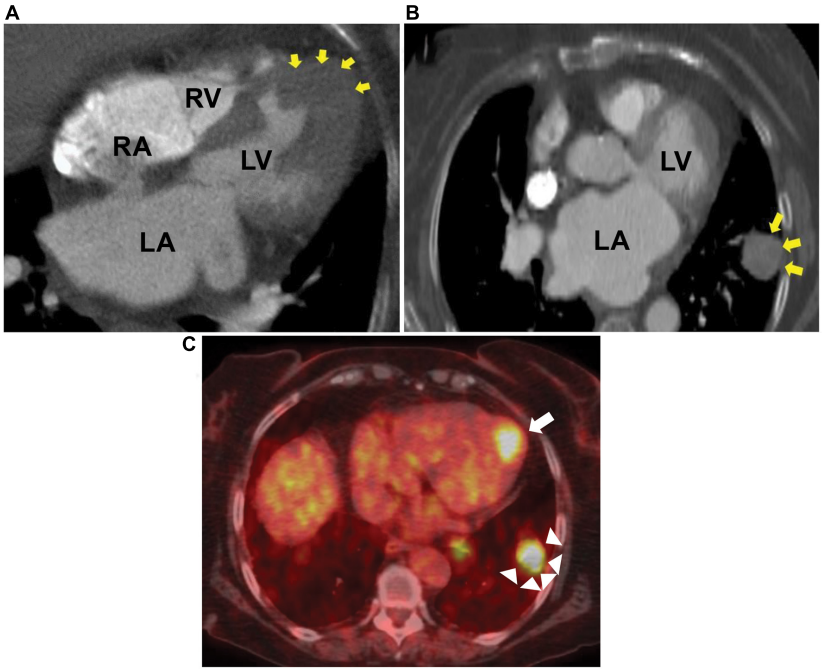

FIGURE 3
Chest CT and PET scan. Computed tomography (CT) showing metastatic melanoma involving the left ventricular apical wall **(A)**, left lung **(B)**, and positron emission tomography (PET) scan axial image **(C)** showing increased fluorodeoxyglucose uptake in the left ventricular apex (arrow) and left lung (arrow heads). LA, left atrium; LV, left ventricle; RA, right atrium; RV, right ventricle.

cardiac lesions and as a follow-up test for response to therapy. It can diagnose cardiac melanoma in up to 80% of cases (4).

The chest CT scan can help identify metastatic lesions in both cardiac and non-cardiac sites. Cardiac magnetic resonance imaging (CMR) is usually helpful in further characterizing these

lesions, but it could not be obtained in our patient owing to a pacemaker-dependent underlying complete heart block.

The PET scan helps identify increased metabolic activity in the regions affected by the tumor by measuring ^{18}F-FDG uptake by the tumor. It is more than 90% sensitive and specific in diagnosing malignant cardiac tumors (8).

The treatment of metastatic melanoma depends on the presence of a *BRAF*V600 mutation. Immune checkpoint inhibitors are used as the first-line treatment in patients who are negative for the mutation. The National Comprehensive Cancer Network recommends programmed cell death 1 (PD-1) inhibitors for these patients. Patients who harbor *BRAF*V600 mutation are usually treated with targeted therapies, including BRAF and MEK inhibitors (9). Median survival is 12 months after diagnosis, with poor prognosis in chemotherapy-resistant cases (4, 10).

Conclusion

The diagnosis of metastatic melanoma to the LV apex should be considered in patients with ApHCM, especially those with a history of melanoma. The resolution of negative T waves in the precordial leads in patients diagnosed with ApHCM should alert for additional processes, such as progression of fibrosis, new myocardial infarction, or infiltrative disease, such as cardiac metastasis involving the LV apex, as illustrated by this case. Cardiac imaging, including CMR, CT, and/or PET plays a vital role in narrowing down the differential diagnosis.

Data availability statement

The original contributions presented in this study are included in this article/**Supplementary material**, further inquiries can be directed to the corresponding author.

Ethics statement

Written informed consent was obtained from the individual(s) for the publication of any potentially identifiable images or data included in this article.

Author contributions

All authors listed have made a substantial, direct, and intellectual contribution to the work, and approved it for publication.

Acknowledgments

The authors acknowledge Sarah Kennedy and Jennifer Pfaff of Aurora Cardiovascular and Thoracic Services for editorial preparation of the manuscript and Brian Miller and Brian Schurrer of Aurora Cardiovascular and Thoracic Services for assistance with the figures.

Conflict of interest

The authors declare that the research was conducted in the absence of any commercial or financial relationships that could be construed as a potential conflict of interest.

Publisher's note

All claims expressed in this article are solely those of the authors and do not necessarily represent those of their affiliated organizations, or those of the publisher, the editors and the reviewers. Any product that may be evaluated in this article, or claim that may be made by its manufacturer, is not guaranteed or endorsed by the publisher.

Supplementary material

The Supplementary Material for this article can be found online at: https://www.frontiersin.org/articles/10.3389/fcvm.2022.993631/full#supplementary-material

References

1. Maleszewski J, Bois M, Bois J, Young P, Stulak J, Klarich K. Neoplasia and the heart: pathological review of effects with clinical and radiological correlation. *J Am Coll Cardiol.* (2018) 72:202–27. doi: 10.1016/j.jacc.2018.05.026

2. Glancy D, Roberts W. The heart in malignant melanoma: a study of 70 autopsy cases. *Am J Cardiol.* (1968) 21:555–71. doi: 10.1016/0002-9149(68)90289-0

3. Ali M, Adil A, Sawlani R, Jeffreys S, Cheema O, Galazka P, et al. Charcoal heart: metastatic melanoma mimicking right atrial myxoma. *JACC Case Rep.* (2021) 3:1545–50. doi: 10.1016/j.jaccas.2021.08.012

4. Tse C, Tan N, Idossa D, Click R. Cardiac melanoma: retrospective review of a rare disease at the mayo clinic (1988-2015). *Int J Cardiol.* (2017) 249:383–6. doi: 10.1016/j.ijcard.2017.08.077

5. Auer J, Schmid J, Berent R, Niedermair M. Cardiac metastasis of malignant melanoma mimicking acute coronary syndrome. *Eur Heart J.* (2011) 33:676. doi: 10.1093/eurheartj/ehr289

6. Schraml F, Yudt W, Gormley T, Ho V. Metastatic melanoma to the heart. *Eur J Nucl Med Mol Imaging.* (2005) 32:1349. doi: 10.1007/s00259-005-1884-y

7. Cates C, Virmani R, Vaughn W, Robertson R. Electrocardiographic markers of cardiac metastasis. *Am Heart J.* (1986) 112:1297–303. doi: 10.1016/0002-8703(86)90363-7

8. Meng J, Zhao H, Liu Y, Chen D, Hacker M, Wei Y, et al. Assessment of cardiac tumors by (18)F-FDG PET/CT imaging: histological correlation and clinical outcomes. *J Nucl Cardiol.* (2021) 28:2233–43. doi: 10.1007/s12350-019-02022-1

9. Dobry A, Zogg C, Hodi F, Smith T, Ott P, Iorgulescu J. Management of metastatic melanoma: improved survival in a national cohort following the approvals of checkpoint blockade immunotherapies and targeted therapies. *Cancer Immunol Immunother.* (2018) 67:1833–44. doi: 10.1007/s00262-018-2241-x

10. Ozyuncu N, Sahin M, Altin T, Karaoguz R, Guldal M, Akyurek O. Cardiac metastasis of malignant melanoma: a rare cause of complete atrioventricular block. *Europace.* (2006) 8:545–8. doi: 10.1093/europace/eul058

frontiers | Frontiers in Cardiovascular Medicine

TYPE Case Report
PUBLISHED 08 February 2023
DOI 10.3389/fcvm.2023.1001527

Check for updates

OPEN ACCESS

EDITED BY
Reto Asmis,
Wake Forest University, United States

REVIEWED BY
Ramesh Daggubati,
West Virginia University, United States
Yunling Lin,
Fujian Institute of Coronary Heart Disease, China

*CORRESPONDENCE
Cao Zou
✉ nkzc75@suda.edu.cn

SPECIALTY SECTION
This article was submitted to Cardio-Oncology, a section of the journal Frontiers in Cardiovascular Medicine

RECEIVED 23 July 2022
ACCEPTED 11 January 2023
PUBLISHED 08 February 2023

CITATION
Zhou J, Zhan C, Zhou J, Wei C and Zou C (2023) Case report: Persistent ST-segment elevation due to cardiac metastasis from lung cancer.
Front. Cardiovasc. Med. 10:1001527.
doi: 10.3389/fcvm.2023.1001527

COPYRIGHT
© 2023 Zhou, Zhan, Zhou, Wei and Zou. This is an open-access article distributed under the terms of the Creative Commons Attribution License (CC BY). The use, distribution or reproduction in other forums is permitted, provided the original author(s) and the copyright owner(s) are credited and that the original publication in this journal is cited, in accordance with accepted academic practice. No use, distribution or reproduction is permitted which does not comply with these terms.

Case report: Persistent ST-segment elevation due to cardiac metastasis from lung cancer

Jiawei Zhou[1,2], Chengchuang Zhan[1], Jing Zhou[1], Chao Wei[1] and Cao Zou[1]*

[1]Department of Cardiology, The First Affiliated Hospital of Soochow University, Suzhou, China, [2]Department of Echocardiography, The First Affiliated Hospital of Soochow University, Suzhou, China

Patients with secondary cardiac cancer occasionally show ST segment elevation that mimics acute coronary syndrome despite the absence of coronary artery occlusion. We herein describe a rare case of secondary cardiac cancer that presented with ST-segment elevation. An 82-year-old Chinese man was admitted to the hospital with chest discomfort. Electrocardiography (ECG) showed ST segment elevation in the precordial leads and low-voltage QRS complexes in limb leads without the development of *Q* waves. Unexpectedly, emergency coronary angiography showed no significant stenosis of the coronary arteries. However, fortunately, transthoracic echocardiography (TTE) revealed massive pericardial effusion and a mass at the apex of the ventricular myocardium. Coincidentally, contrast-enhanced chest computed tomography showed primary lung cancer in the left lower lobe, pericardial effusion, and myocardial metastasis at the ventricular apex. The pericardiac fluid contained blood with significantly increased CEA levels and exfoliated tumor cells. The lung histopathological report suggested squamous cell carcinoma. Two months later, the patient died. These findings suggested that the persistent ST-segment without the development of Q waves was associated with ventricular invasion by primary lung cancer and may indicate a poor prognosis. In conclusion, physicians should be aware of persistent ST-segment elevation mimicking myocardial infarction due to cardiac metastasis with a poor prognosis.

KEYWORDS

cardio-oncology, cardiac metastasis, lung cancer, ST-segment elevation, case report

Introduction

Cardiac tumors comprise primary tumors, including benign and malignant, metastatic tumors, and some other tumor-like camouflages (such as thrombosis) (1). Heart-related clinical manifestations often include dyspnea, arrhythmia, obstruction, heart failure, and systemic embolism. Related auxiliary examinations mainly include electrocardiogram (ECG), echocardiography, computed tomography (CT), cardiac magnetic resonance (CMR), and related laboratory tests. As a convenient, rapid, and intuitive examination, echocardiography often plays the primary role in finding lesions, confirming the extent of the lesions, and assessing cardiac function. Contrast-enhanced CT and cardiac magnetic resonance can further analyze the nature of the lesion, identify the tumor source, and display the extent of the invasion. Herein, we describe a case of cardiac metastasis from lung cancer accompanied by massive pericardial effusion, which was comprehensively evaluated by ECG, echocardiography, contrast-enhanced CT, laboratory tests, and histopathological assessment.

10.3389/fcvm.2023.1001527

Case description

On 9 October 2021, an 82-year-old man presented at the emergency department with an 8-h history of chest discomfort, nausea, vomiting, and orthopnea. He reported worsening chest discomfort during exertion accompanied by nausea, anorexia, and fatigue without any cough, chest pain, or edema of the lower limb for 20 days. His medical history included hypertension, hyperlipidemia, diabetes mellitus, and former tobacco use for 50 years.

On presentation, the patient's blood pressure was 123/72 mmHg, heart rate was 90 beats/min, oxygen saturation was 98%, and respiratory rate was 18 breaths/min. A cardiovascular physical examination showed a decreased S1 with no murmurs, rubs, or gallops. Respiratory and abdominal examinations were also within normal limits. ECG showed sinus tachycardia, ST segment elevation in precordial leads V1–V6, and low-voltage QRS complexes in limb leads (**Figure 1A**). Laboratory studies were notable for high sensitivity troponin T (hs-TnT) of 21.08 pg/ml (normal < 14 pg/ml) and *N*-terminal (NT)-pro hormone BNP (NT-proBNP) of 2,160 pg/ml (normal < 125 pg/ml). Acute precordial STEMI diagnosis was considered. We performed emergent coronary angiography, but there was no significant stenosis of coronary arteries (**Figures 1C, D**). Therefore, myocardial infarction of the non-obstructive coronary artery (MINOCA) was considered.

On day 2, a transthoracic echocardiogram (TTE) revealed massive pericardial effusion and a 6.5 × 3.1 cm-sized hypoechoic mass at the apex of left ventricular, septal, and right ventricular myocardium associated with hypokinesis and decreased absolute value of global longitudinal strain (**Figures 2A, B**). Contrast-enhanced chest CT showed scattered irregular iso-density shadow (the largest mass was 67 × 47 mm) with peripheral exudation in the left lower lobe and significant thickness at the ventricular apex with pericardial effusion (**Figures 2C–F**). Tumor marker levels were elevated as follows: CEA of 32.4 ng/ml (normal < 10 ng/ml), CA125 of 99.8 U/ml (normal < 35 U/ml), TPSA of 29.9 ng/ml (normal < 4 ng/ml), CYFRA211 of 57.4 ng/ml (normal < 3.07 ng/ml), and SCCA of 39.6 ng/ml (normal < 1.5 ng/ml).

On day 3, we performed pericardiocentesis. The pericardiac fluid contained blood with significantly increased CEA level (>1,000 ng/ml, normal < 5 ng/ml) and exfoliated tumor cells with CK7(+) and Ep-cam(+) (**Figures 3A–C**). When we obtained his medical history, his family provided an ECG performed 4 months before (**Figure 1B**), which demonstrated ST elevation and *T*-wave inversion similar to the ECG on this admission. These findings strongly suggested ventricular myocardial metastasis of primary lung cancer. We recommended that the patient should undergo a transbronchial lung biopsy to obtain a histopathological diagnosis, and he accepted it. One week later, he was transferred to the respiratory department. During hospitalization in the respiratory department, the patient underwent a percutaneous lung puncture. The lung histopathological report suggested squamous cell carcinoma. Immunohistochemical analyses showed CK5/6(+), P63(+), P40(+), and PD-L1 (22C3, about 60% +) (**Figures 3D–G**). Squamous cell carcinoma of the lungs at the stage of IVB (T3N1M1c) was considered a diagnosis. He was treated with immunotherapy by Sintilimab (PD-1 monoclonal antibody). Unfortunately, his cardiac function decreased with increased levels of hs-TNT and NT-proBNP (**Figures 4A, B**), and without any improvement. At the end of December 2021, he died of respiratory and heart failure. An autopsy could not be performed.

Discussion

Persistent ST-segment elevation (STE) newly found in patients should usually be considered STEMI. However, in our case, there was abnormal ST-segment elevation on precordial leads without the development of *Q* waves different from the typical ECG characteristics of STEMI. Several cases of cardiac metastasis mimicking STEMI have been reported (2–5). ECG findings of localized STE without *Q* waves have high specificity for myocardial tumor invasion (6).

In most cases of previously reported cardiac metastases with STE, cardiac enzymes have been normal (5), unlike in our patient. The present case was initially misdiagnosed as STEMI due to STE accompanied by an elevation in hs-TNT. However, emergent CAG did not reveal any significant coronary stenosis to explain the ECG and hs-TNT abnormalities. During hospitalization, the assessment of this patient also showed increased levels of hs-TNT and NT-proBNP due to aggravated myocardial injury for a long time because a previous ECG had demonstrated similar abnormal STE 4 months before admission.

The mechanism of STE in cardiac metastasis has not been fully understood. Some case reports describe STE caused by myocardial metastases (7–10), coronary artery invasion or direct compression, or pericardial involvement (11). The most frequent mode of metastasis is *via* the lymphatic pathway, followed by hematogenous spread (12). In our case, echocardiography was the initial imaging modality to detect pericardial effusion and the presence of cardiac metastasis. Then, contrast-enhanced chest CT revealed lung cancer in the left lower lobe and cardiac abnormality at the ventricular apex without any evidence of coronary artery invasion or direct compression. In addition, there were exfoliated tumor cells and significantly increased CEA levels in the patient's pericardiac fluid. Therefore, STE in this patient was due to myocardial injury caused by lung cancer metastases.

Lung cancer is the most frequent cause of cardiac metastatic tumors, with a reported incidence of up to 25% at autopsy, and squamous cell carcinoma is the most frequent cause of secondary cardiac cancer (13). In general, the pericardium is the most common cardiac site for metastasis *via* retrograde lymphatic extension from the lung to the heart (14, 15). In our patient, the lung histopathological report suggested squamous cell carcinoma, and echocardiography and chest CT detected massive pericardial effusion and myocardial metastatic lesions in the apical areas, respectively, which receive their blood supply from the left anterior descending artery. Therefore, our patient had STE in the precordial leads, which was similar to a case in which STE reflects the location of STEMI due to an obstruction of the left anterior descending artery.

Cardiac metastases have a poor prognosis. A myocardial metastatic lesion is often clinically silent, although it can cause malignant pericardial effusion with or without symptoms of pericarditis, arrhythmias, heart failure, and rarely acute myocardial infarction (14, 16, 17). This feature results in misdiagnosis or diagnosis delay in severe conditions. When the first ECG of our patient was recorded, STE was not treated. Four months later, he had symptoms and was admitted to our hospital. During hospitalization,

10.3389/fcvm.2023.1001527

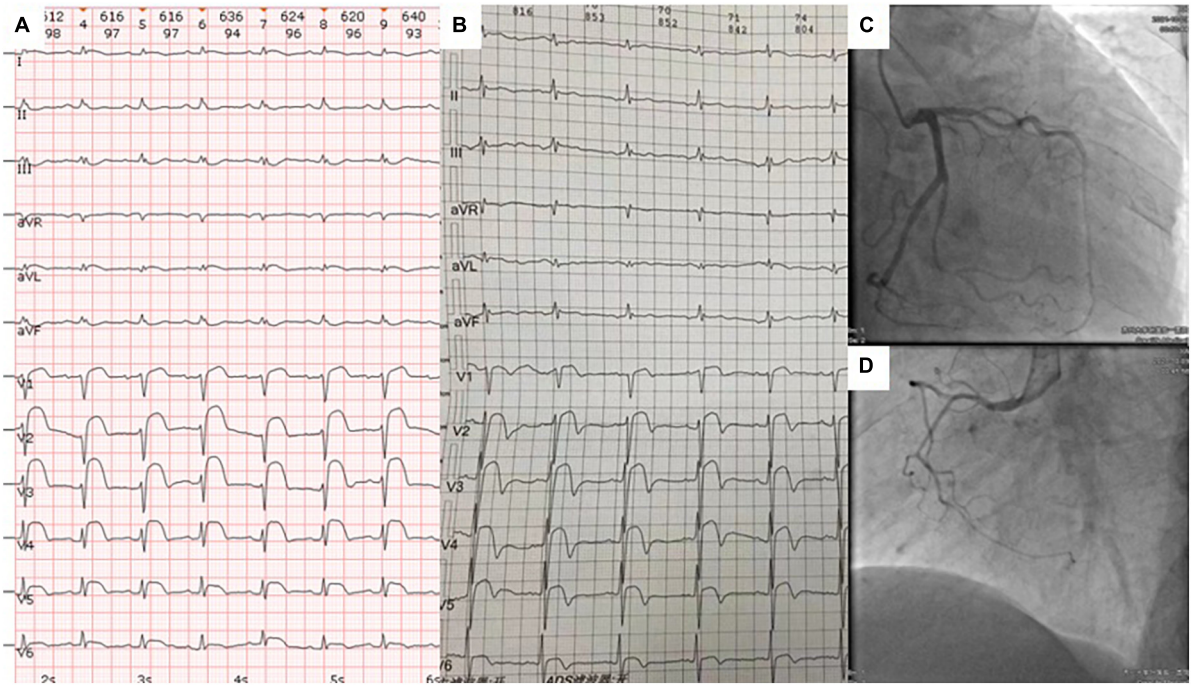

FIGURE 1
The ECG at admission **(A)** and 4 months prior to admission **(B)** showed abnormal ST segment elevations in leads V1–V6 and low-voltage QRS complexes in limb leads. Coronary angiography revealed no significant stenosis in the right coronary, left anterior descending, and circumflex coronary arteries **(C,D)**.

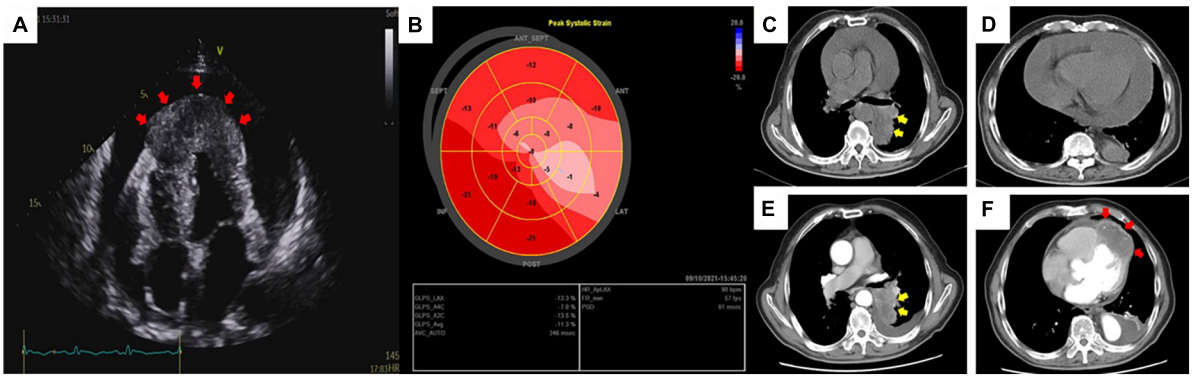

FIGURE 2
Transthoracic echocardiography **(A)** revealed massive pericardial effusion and a thickened and hypoechoic mass (red arrow) at the apex of the heart *via* an apical four-chamber view. Global longitudinal strain **(B)** showed a significantly decreased absolute value of strain in the area of the anterior and lateral walls of the heart. Routine chest CT at admission **(C,D)** and contrast-enhanced chest CT after pericardiocentesis **(E,F)** showed an irregular iso-density mass (yellow arrow) with peripheral exudation in the left lower lobe of the lung panels **(C,E)** and a myocardial mass (red arrow) located in the left and right ventricular apex emerging with reduced pericardial effusion panel **(F)**.

his condition worsened, his cardiac function decreased, and he died of respiratory and heart failure, although he received immunotherapy. Radical surgical resection, radiotherapy, and chemotherapy could be useful treatments for certain cardiac metastases. Unfortunately, our patient had no further choice.

The changes in ECG, such as STE that mimics acute coronary syndrome, caused by secondary cardiac cancer mentioned in this article, are not the first reported, and many related studies (2–8) have recognized this phenomenon before. However, this is not just another example of STEMI misdiagnosis. Our purpose of the case report was as follows. First, we aimed to stress the significance that our physicians should consider the possibility of cardiac metastasis in patients who are first diagnosed with acute coronary syndrome (ACS). Second, we wanted to show a complete diagnostic process of this case and list the relevant examination results.

It can be asked why coronary angiography was performed without echocardiography. Actually, it is a common phenomenon in China. The main reason is that emergency procedures are different. Once patients develop symptoms of significant chest tightness, pain accompanied by STE in precordial leads, including V1–V6, on ECG, and a significant increase in troponin, they will be diagnosed with ACS and undergo emergency percutaneous coronary intervention

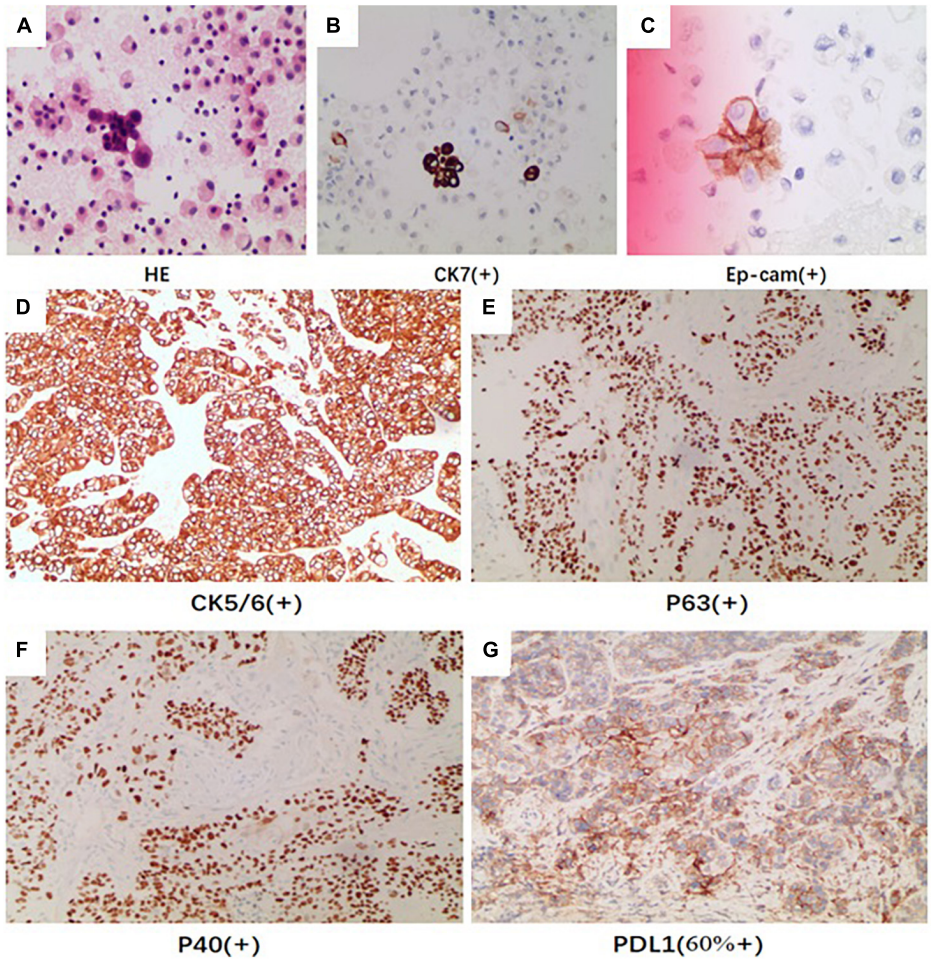

FIGURE 3
The pericardiac fluid by HE revealed **(A)** exfoliated tumor cells with **(B)** CK7 (positive) and **(C)** Ep-cam (positive). The immunohistochemical analysis of pathologic tissue by percutaneous lung puncture showed **(D)** CK5/6 (positive), **(E)** P40 (positive), **(F)** P63 (positive), and **(G)** PDL1 (positive).

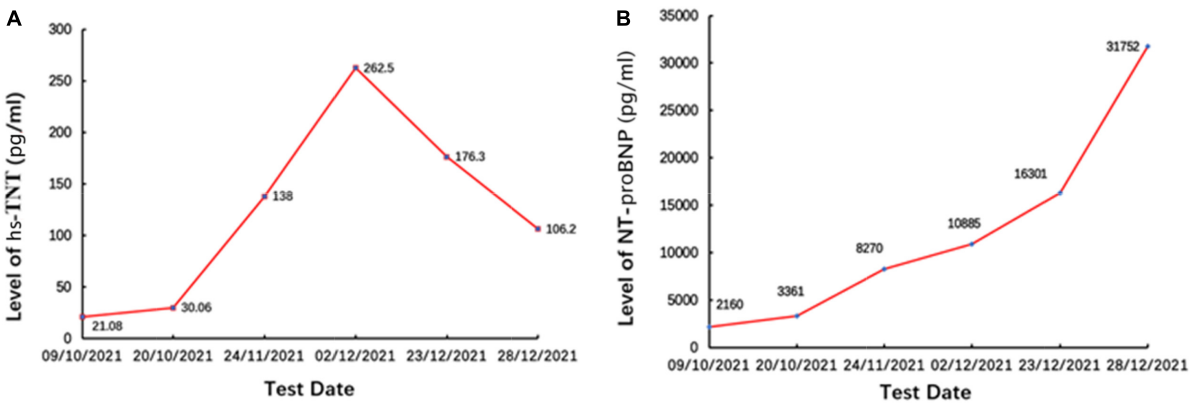

FIGURE 4
The levels of **(A)** hs-TNT and **(B)** NT-proBNP. Panel **(B)** were persistently increased, demonstrating decreased cardiac function.

(PCI) as quickly as possible. Echocardiography is often unnecessary in the first place. However, no severe stenosis was found during the operation; hence, MINOCA was considered. This is common sense in emergency procedures in China. Not all patients who are primarily diagnosed with ACS undergo echocardiography before emergency coronary angiography.

After we repeatedly confirmed the patient's physical signs, we did not find distention of the jugular veins but confirmed the distention of the inferior vena cava by echocardiography. This finding might be related to the chronic course of the disease rather than acute cardiac tamponade. Conversely, engorged jugular veins are normally more pronounced in older and leaner people without any discomfort.

Conclusion

When physicians treat patients with STE, they should first consider the diagnosis of ACS. However, when clinicians further evaluate the history and find that STE persists for a few days or more, especially with a history of tumor, they should consider the special situation described in this case report. Although the incidence of persistent STE due to cardiac metastasis is low, considering its possibility can help us broaden the horizon of the diagnosis process and head in the right direction quicker. We should also be aware of the poor prognosis of patients and try to inform patients and their families of the severity of the disease in advance. The significance of this case report lies in broadening our diagnostic thinking and providing a relatively complete and feasible diagnostic process for cardiac metastatic tumors.

Data availability statement

The original contributions presented in this study are included in the article/**Supplementary material**, further inquiries can be directed to the corresponding author.

Ethics statement

Written informed consent was obtained from the individual(s) for the publication of any potentially identifiable images or data included in this article. Written informed consent was obtained for the publication of this case report.

Author contributions

JiaZ and CZh were responsible for collecting case data, analyzing data, and writing manuscript. CZo was responsible for review, submission, and modification of manuscript. JinZ and CW were responsible for patient's diagnosis and treatment. All authors contributed to the article and approved the submitted version.

Conflict of interest

The authors declare that the research was conducted in the absence of any commercial or financial relationships that could be construed as a potential conflict of interest.

Publisher's note

All claims expressed in this article are solely those of the authors and do not necessarily represent those of their affiliated organizations, or those of the publisher, the editors and the reviewers. Any product that may be evaluated in this article, or claim that may be made by its manufacturer, is not guaranteed or endorsed by the publisher.

Supplementary material

The Supplementary Material for this article can be found online at: https://www.frontiersin.org/articles/10.3389/fcvm.2023.1001527/full#supplementary-material

References

1. Poterucha T, Kochav J, O'Connor D, Rosner G. Cardiac tumors: clinical presentation, diagnosis, and management. *Curr Treat Options Oncol.* (2019) 20:66. doi: 10.1007/s11864-019-0662-1

2. Chen T. Persistent ST-segment elevation due to cardiac metastasis. *BMJ Case Rep.* (2017) 2017:bcr2017220621. doi: 10.1136/bcr-2017-220621

3. Cincin A, Samedov F, Sari I, Sunbul M, Tigen K, Mutlu B, et al. Right ventricular metastasis of lung cancer. Persistent ST-segment elevation and constrictive physiology. *Herz.* (2014) 39:166–70. doi: 10.1007/s00059-013-3809-z

4. Zhou R, Prasada S, Roth M. A case report of an STEMI mimicker in a patient presenting with haemoptysis and chest pain with metastatic myocardial infiltration and left ventricular mural thrombi. *Eur Heart J Case Rep.* (2021) 5:ytaa546. doi: 10.1093/ehjcr/ytaa546

5. Jung HW. ST-segment elevation due to myocardial invasion of lung cancer mimicking ST elevation myocardial infarction: a case report. *Medicine.* (2021) 100:e26088. doi: 10.1097/MD.0000000000026088

6. Tandon V, Kethireddy N, Balakumaran K, Kim A. Metastatic squamous cell carcinoma to the heart: an unusual cause of ST elevation-a case report. *Eur Heart J Case Rep.* (2019) 3:ytz029. doi: 10.1093/ehjcr/ytz029

7. Astorri E, Fiorina P, Pattoneri P, Paganelli C. Persistent ST segment elevation in a patient with metastatic involvement of the heart. *Minerva Cardioangiol.* (2001) 49:81–5.

8. Konishi S, Kojima T, Ichiyanagi K, Kinihiko S, Yokoyama K, Taki J, et al. A case of double cancers with myocardial metastasis mimicking acute myocardial infarction both on an electrocardiogram and on Tc-99m-MIBI myocardial SPECT. *Ann Nucl Med.* (2001) 15:381–5. doi: 10.1007/BF02988248

9. Pan K, Wu L, Chung C, Chang S, Lin P, Hsu J. Misdiagnosis: cardiac metastasis presented as a pseudo-infarction on electrocardiography. *Int Heart J.* (2007) 48:399–405. doi: 10.1536/ihj.48.399

10. Paparoupa M, Aldemyati R, Theodorakopoulou M. Bilateral lung artery embolization mimicking an acute myocardial infarction. *Case Rep Med.* (2021) 2021:6616139. doi: 10.1155/2021/6616139

11. Shah S, Padaliya B, Mohan S. Noninfiltrating adenocarcinoma of the lung causing ST-segment elevation. *Tex Heart Inst J.* (2015) 42:381–4. doi: 10.14503/THIJ-14-4268

12. Kim K, Jeong M, Yoon H, Ahn Y, Cho J, Park J, et al. A case of myocardial involvement in lung cancer that mimics ST segment elevation in myocardial infarction. *Korean J Intern Med.* (2014) 29:525–8. doi: 10.3904/kjim.2014.29.4.525

13. Reynen K, Kockeritz U, Strasser R. Metastases to the heart. *Ann Oncol.* (2004) 15:375–81. doi: 10.1093/annonc/mdh086

14. Abe S, Watanabe N, Ogura S, Kunikane H, Isobe H, Yamaguchi E, et al. Myocardial metastasis from primary lung cancer: myocardial infarction-like ECG changes and pathologic findings. *Jpn J Med.* (1991) 30:213–8. doi: 10.2169/internalmedicine1962.30.213

15. Kline I. Cardiac lymphatic involvement by metastatic tumor. *Cancer.* (1972) 29:799–808.

16. Cates C, Virmani R, Vaughn W, Robertson R. Electrocardiographic markers of cardiac metastasis. *Am Heart J.* (1986) 112:1297–303. doi: 10.1016/0002-8703(86)90363-7

17. Matana A, Zaputovic L, Lucin K, Kastelan Z. Persistent and progressive ST segment elevation caused by myocardial metastasis. *Tumori.* (2006) 92:452–4. doi: 10.1177/030089160609200517

frontiers | Frontiers in Cardiovascular Medicine

TYPE Case Report
PUBLISHED 09 February 2023
DOI 10.3389/fcvm.2023.1089636

Check for updates

OPEN ACCESS

EDITED BY
Reto Asmis,
Wake Forest University, United States

REVIEWED BY
Abdallah Al-Mohammad,
Sheffield Teaching Hospitals NHS Foundation Trust, United Kingdom
Christian Cadeddu Dessalvi,
University of Cagliari, Italy

*CORRESPONDENCE
Haibo Xu
xuhaibo@whu.edu.cn
Jinping Liu
liujinping@znhospital.cn

†These authors have contributed equally to this work and share first authorship

SPECIALTY SECTION
This article was submitted to Cardio-Oncology, a section of the journal Frontiers in Cardiovascular Medicine

RECEIVED 04 November 2022
ACCEPTED 27 January 2023
PUBLISHED 09 February 2023

CITATION
Ye N, Lan L, Hu H, Liu J and Xu H (2023) Case report: The diagnostic challenge of primary cardiac intimal sarcoma.
Front. Cardiovasc. Med. 10:1089636.
doi: 10.3389/fcvm.2023.1089636

COPYRIGHT
© 2023 Ye, Lan, Hu, Liu and Xu. This is an open-access article distributed under the terms of the Creative Commons Attribution License (CC BY). The use, distribution or reproduction in other forums is permitted, provided the original author(s) and the copyright owner(s) are credited and that the original publication in this journal is cited, in accordance with accepted academic practice. No use, distribution or reproduction is permitted which does not comply with these terms.

Case report: The diagnostic challenge of primary cardiac intimal sarcoma

Naili Ye[1†], Lan Lan[1†], Huijuan Hu[1], Jinping Liu[2,3,4*] and Haibo Xu[1*]

[1]Department of Radiology, Zhongnan Hospital of Wuhan University, Wuhan, China, [2]Department of Cardiovascular Surgery, Zhongnan Hospital of Wuhan University, Wuhan, China, [3]Hubei Provincial Engineering Research Center of Minimally Invasive Cardiovascular Surgery, Wuhan, China, [4]Wuhan Clinical Research Center for Minimally Invasive Treatment of Structural Heart Disease, Wuhan, China

Primary cardiac intimal sarcoma, an extremely rare cardiac tumor subtype, is often mis-diagnosed owing to its rarity and non-specific clinical and radiological features. We report a case of cardiac intimal sarcoma mimicking atrial myxoma in which the clinical presentation and multimodality imaging are described in detail, and diagnostic challenges are highlighted.

KEYWORDS

intimal sarcoma, myxoma, cardiovascular magnetic resonance, CMR, multimodality imaging

Introduction

Primary cardiac intimal sarcoma is an extremely rare subtype of cardiac tumor, with only a few such cases having been reported (1–8). It often occurs in the left atrium, whereas it seldom originates in the right atrium and mitral valve (6, 8). Owing to its rarity and non-specific characteristics, cardiac intimal sarcomas are often mistaken for myxomas or thrombi. We report a case of cardiac intimal sarcoma of the left atrium and provide a detailed description of multimodality imaging aimed at highlighting pre-operative diagnostic challenges.

Case description

A 52-year-old woman was admitted to our hospital with a 3-month history of progressive cough and shortness of breath. On admission, laboratory findings and non-contrast thoracic computed tomography (CT) scan results were negative for infectious diseases. Her electrocardiogram was normal (heart rate, 76 bpm); however, transthoracic echocardiography revealed an irregularly shaped 4.8 × 6.7 mm hypoechoic mass in the left atrium that appeared broadly based and originating from the lateral atrial wall (**Figure 1**). The mass induced significant mitral stenosis through prolapsing toward the left ventricle during diastole.

The patient had undergone cervical cancer resection in 2014. No mass or mass-like lesion of the heart had been observed on contrast-enhanced thoracic CT during the follow-up period in 2019. However, possible cardiac metastasis was now suspected. Contrast-enhanced CT and cardiovascular magnetic resonance (CMR) imaging were performed for further characterization. CT images showed that the lobulated mass with homogeneous hypodensity almost occupied the left atrium and the left atrial appendage, extending to the orifice of the left superior pulmonary vein, and showing significantly inhomogeneous enhancement in the arterial phase. Contrast uptake decreased with a longer delay time (almost into the portal venous phase) (**Figure 2**).

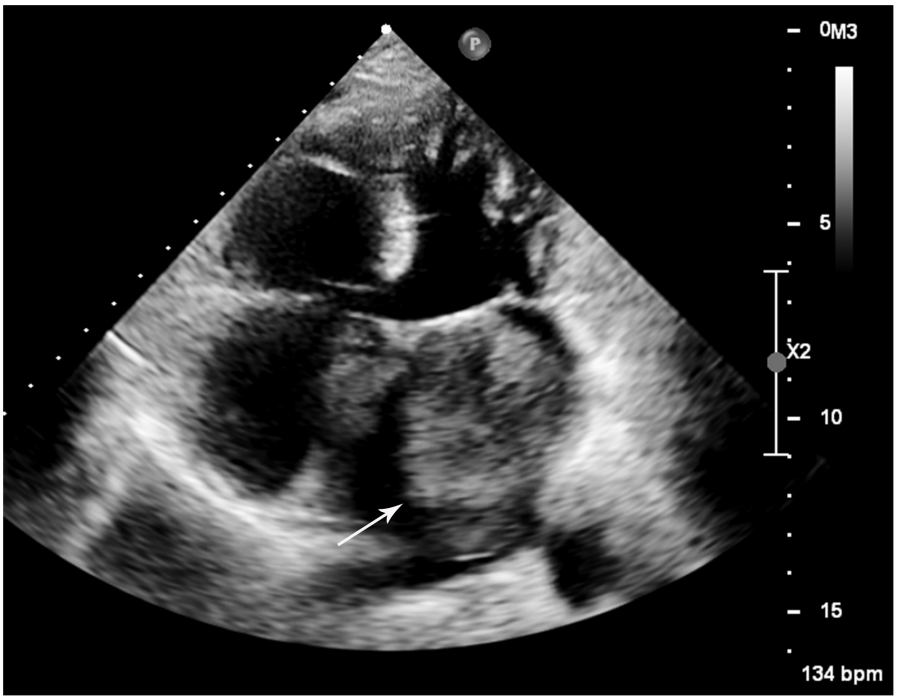

FIGURE 1
Transthoracic echocardiogram of the left mass. A large hypoechoic mass (white arrow) was revealed in the left atrium attaching to the lateral atrial wall *via* a broad base.

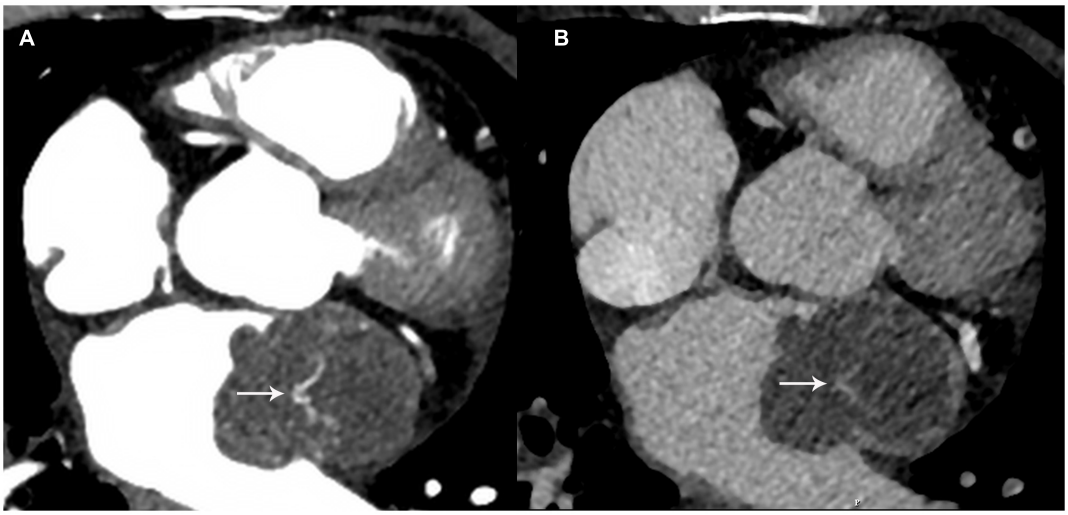

FIGURE 2
The mass showed heterogeneous enhancement at the arterial phase **(A)** white arrow and the contrast uptake decreased with a longer delay time **(B)** white arrow.

Regarding CMR imaging, compared with the myocardium, the lesion showed significantly elevated native T1 and T2 values on T1 and T2 mapping (Figure 3). Mildly increased regional perfusion was observed in the mass during first-pass perfusion imaging, as well as heterogeneous enhancement on late gadolinium-enhanced (LGE) imaging (Figure 4). No adjacent tissue infiltration was observed. Radiological findings suggested a possible diagnosis of atrial myxoma.

Surgical resection was then performed. Histopathological examination revealed spindle-shaped tumor cells with prominent atypia. Mitotic activity was frequent. Some stromal myxoid changes could also be observed in the tumor (Figure 5). Extensive immunohistochemical analyses showed that the cells were positive for vimentin, caldesmon, CDK4, Bcl-2, CD34 (focal), CK (focal), SMA (focal), TLE1 (focal), CD99 (focal) and negative for desmin, EMA, S-100, CD31, ERG, MDM-2, P16, SOX-10, MyoD1, myogenin, STAT6. The Ki-67 proliferative index was 40%. Pathological results supported the diagnosis of high-grade intimal sarcoma. At 4 months post-operatively, the patient was re-hospitalized and underwent systemic chemotherapy for a metastatic lesion of the left femur.

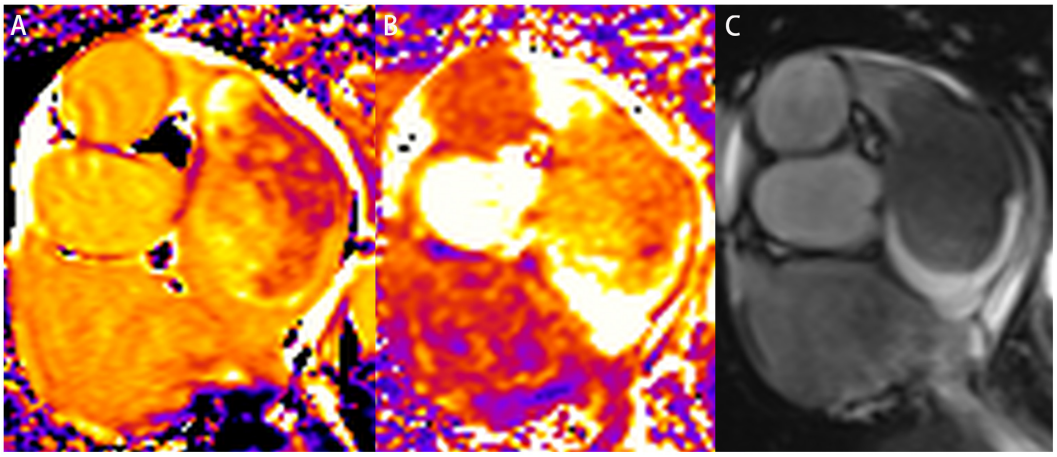

FIGURE 3
Characterization of the left atrial mass on cardiovascular magnetic resonance imaging. A slice of a short-axis view of left atrium was acquired on native T1 mapping **(A)**, T2 mapping **(B)**, and cine imaging **(C)**, respectively. The mass was heterogeneous on native T1 mapping and T2 mapping. The native T1 value ranged from 1,661 to 2,109 ms. The T2 value was also significantly elevated.

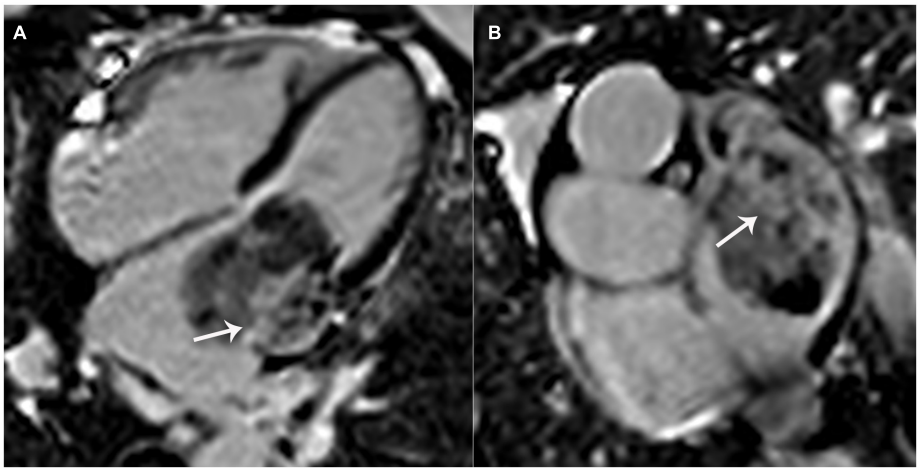

FIGURE 4
Left atrial mass on late gadolinium-enhanced (LGE) imaging. Significant patchy enhancement (white arrows) was observed on LGE images. **(A)** 4-chamber view; **(B)** a shot-axis view of left atrium.

Discussion

Non-invasive pre-operative assessment of cardiac tumors is vital for further management and could be an important predictor of prognosis. Echocardiography, CT, and magnetic resonance imaging (MRI) are common techniques used for diagnosis and monitoring. Owing to its wide availability and convenience, echocardiography is often used as the first imaging modality to confirm the presence of a cardiac mass and quantify the morphological characteristics, attachment, and mobility of the tumor. CT and MRI are optimal approaches for assessing tissue characterization, vascularity, adjacent infiltration, and extracardiac metastases (9–11). Considering the limitations of different imaging techniques, multimodality imaging of cardiac masses is required for determining treatment strategies.

Intimal sarcoma is a rare subtype of mesenchymal sarcoma that commonly originates in the great vessels with a predilection for the pulmonary arteries (12). The heart is rarely involved in intimal sarcomas, and only a few such case reports have been published (1–4)

Cardiac intimal sarcomas are frequently misdiagnosed as either atrial myxomas or thrombi. In this case, the diagnostic challenge has also been highlighted. Typical myxomas are well-defined, often located in the left atrium, and attached to the interatrial septum (9, 10, 13). The mass in our case originated from the atrial free wall, which was the less likely origin of myxomas, as shown in some reported cases (14). In terms of tissue characterization, regarding the similarity of histological components of myxomas and intima sarcomas (4), both may be characterized using isointense/hypointensity on T1-weighted imaging, hyperintensity on T2-weighted imaging and cine imaging, through comparison with the myocardium. Heterogeneous enhancement is often observed in LGE images (9, 10). One point of note is that on CT images, contrast uptake of myxomas is hardly observed in the arterial phase, whereas it significantly increases with a longer delay time (9, 15, 16). The mass in the reported case showed significant heterogeneous enhancement in the arterial phase, and the density decreased with a longer delay time, which is concerning for rich vascularity, an important characteristic of malignant lesions.

10.3389/fcvm.2023.1089636

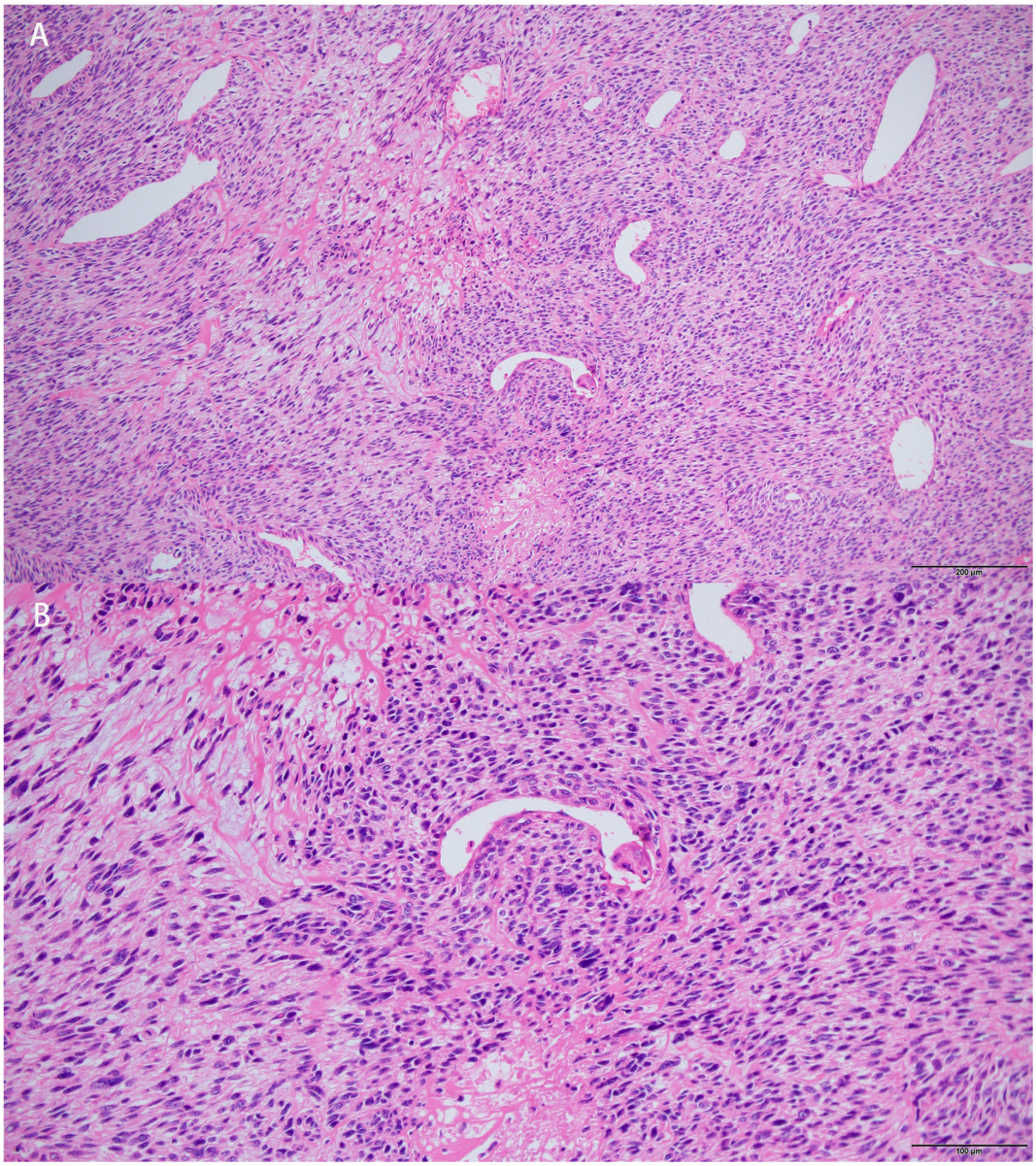

FIGURE 5
Histopathological features of the left atrial mass. Hematoxylin-eosin (HE) stained section showed that tumors cells were spindle-shaped, prominent atypical. Mitotic activity was frequent. Myxoid changes could be observed in stroma. [Bars: **(A)** 200 μm; **(B)** 100 μm].

TABLE 1 Comparison of imaging characteristics of cardiac intimal sarcomas and myxomas.

	Cardiac intimal sarcoma	Myxoma
Common location	Left atrium	Left atrium > right atrium
	Intracavitary	Intracavitary
Echocardiography	Mobile/Non-mobile mass with single or multiple separated sites of attachment to atrial wall (or atrial septum)	Highly mobile mass being attached to atrial septum (or atrial wall) by a stalk
Contrast-enhanced CT	Hypodensity Heterogeneous enhancement at arterial phase and the contrast uptake decreases with a longer delay time	Hypodensity Calcification may present No obvious arterial-phase contrast enhancement and heterogeneous enhancement is recognized with a longer delay time
CMR		
T1-weighted imaging*	Isointense/Hypointense	Isointense/Hypointense
T2-weighted imaging*	Hyperintense	Hyperintense
LGE imaging	Heterogeneous enhancement	Heterogeneous enhancement

*The signal intensity of T1- and T2- weighted imaging is relative to myocardium. CT, computed tomography; CMR, cardiovascular magnetic resonance.

In addition, a large mass with multiple separated sites of attachment should be considered as a sign of malignancy (1), although this was not observed in our case. Imaging characteristics of the two diseases were summarized in **Table 1**.

The mean survival of patients with cardiac intimal sarcoma ranges from 3 months to 1 year (11). Surgical resection is the only management strategy that is associated with prolonged survival (17). Chemotherapy is indicated in patients who cannot undergo surgery, although its benefits are limited.

Conclusion

Cardiac intimal sarcoma is a rare disease with specific characteristics. This case emphasizes the challenges of differential diagnosis and the importance of multimodality imaging for preoperative assessment.

Data availability statement

The original contributions presented in this study are included in this article/supplementary material, further inquiries can be directed to the corresponding authors.

Ethics statement

The studies involving human participants were reviewed and approved by Medical Ethics Committee of Zhongnan Hospital of Wuhan University. Written informed consent for participation was not required for this study in accordance with the national legislation and the institutional requirements.

Author contributions

LL conducted the draft writing and data analysis. NY was responsible for literature research and data acquisition. HH contributed to image postprocessing. HX and JL supervised the activities. All authors participated in concept development, revision of the manuscript, and read and approved the final manuscript.

Conflict of interest

The authors declare that the research was conducted in the absence of any commercial or financial relationships that could be construed as a potential conflict of interest.

Publisher's note

All claims expressed in this article are solely those of the authors and do not necessarily represent those of their affiliated organizations, or those of the publisher, the editors and the reviewers. Any product that may be evaluated in this article, or claim that may be made by its manufacturer, is not guaranteed or endorsed by the publisher.

References

1. Rehman M, El-Dabh A, Mandal S, Sattur S. A case report of a massive cardiac intimal sarcoma manifesting as syncope during a stress test. *Eur Heart J Case Rep.* (2021) 5:ytab258. doi: 10.1093/ehjcr/ytab258

2. Ho K, Yatham K, Seno R, Sultan O. A case report of primary cardiac intimal sarcoma presenting with atrial fibrillation and a left atrial mass. *Eur Heart J Case Rep.* (2021) 5:ytab410. doi: 10.1093/ehjcr/ytab410

3. Braams N, Kaffka Genaamd Dengler S, Rutten E, de Boer K. Left atrial spindle cell sarcoma: a case report. *Eur Heart J Case Rep.* (2019) 3:ytz005. doi: 10.1093/ehjcr/ytz005

4. Durieux R, Tchana-Sato V, Lavigne J, Radermecker M, Moonen M, Scagnol I, et al. Recurrent cardiac intimal sarcoma misdiagnosed as a myxoma or malignant transformation of a cardiac myxoma? *J Card Surg.* (2021) 36:357–62. doi: 10.1111/jocs.15200

5. Rahmouni K, Al Abri Q, Janelle M, Nguyen V, Sabapathy C, Bernier P. Intimal cardiac sarcoma in an adolescent presenting with sudden cardiogenic shock. *Pediatr Blood Cancer.* (2021) 68:e29083. doi: 10.1002/pbc.29083

6. Chen Y, Li Y, Lee J, Chen J. Staged surgery for advanced cardiac intimal sarcoma involving the right atrium and the inferior vena cava. *J Card Surg.* (2021) 36:3973–5. doi: 10.1111/jocs.15885

7. Muturi A, Kotecha V, Ruturi J, Muhinga M, Waweru W. High-grade spindle cell sarcoma of the heart: a case report and review of literature. *J Cardiothorac Surg.* (2015) 10:46. doi: 10.1186/s13019-015-0245-6

8. Todo S, Toba T, Okada K, Hirata KI. A rare manifestation of primary cardiac intimal sarcoma: mimicking non-bacterial thrombotic endocarditis with severe mitral regurgitation. *Eur Heart J Cardiovasc Imaging.* (2021) 22:e8. doi: 10.1093/ehjci/jeab026

9. Tyebally S, Chen D, Bhattacharyya S, Mughrabi A, Hussain Z, Manisty C, et al. Cardiac tumors: JACC CardioOncology state-of-the-art review. *JACC CardioOncol.* (2020) 2:293–311. doi: 10.1016/j.jaccao.2020.05.009

10. Motwani M, Kidambi A, Herzog B, Uddin A, Greenwood J, Plein S. MR imaging of cardiac tumors and masses: a review of methods and clinical applications. *Radiology.* (2013) 268:26–43. doi: 10.1148/radiol.13121239

11. Butany J, Nair V, Naseemuddin A, Nair G, Catton C, Yau T. Cardiac tumours: diagnosis and management. *Lancet Oncol.* (2005) 6:219–28. doi: 10.1016/S1470-2045(05)70093-0

12. Assi T, Kattan J, Rassy E, Moussa T, Nassereddine H, Honore C, et al. A comprehensive review on the diagnosis and management of intimal sarcoma of the pulmonary artery. *Crit Rev Oncol Hematol.* (2020) 147:102889. doi: 10.1016/j.critrevonc.2020.102889

13. Griborio-Guzman A, Aseyev O, Shah H, Sadreddini M. Cardiac myxomas: clinical presentation, diagnosis and management. *Heart.* (2022) 108:827–33. doi: 10.1136/heartjnl-2021-319479

14. Wang J, Wang B, Hu Y, Liu J, Liu B, Liu H, et al. Clinicopathologic features and outcomes of primary cardiac tumors: a 16-year-experience with 212 patients at a Chinese medical center. *Cardiovasc Pathol.* (2018) 33:45–54. doi: 10.1016/j.carpath.2018.01.003

15. Scheffel H, Baumueller S, Stolzmann P, Leschka S, Plass A, Alkadhi H, et al. Atrial myxomas and thrombi: comparison of imaging features on CT. *AJR Am J Roentgenol.* (2009) 192:639–45. doi: 10.2214/AJR.08.1694

16. Grebenc M, Rosado-de-Christenson M, Green C, Burke A, Galvin J. Cardiac myxoma: imaging features in 83 patients. *Radiographics.* (2002) 22:673–89. doi: 10.1148/radiographics.22.3.g02ma02673

17. Isambert N, Ray-Coquard I, Italiano A, Rios M, Kerbrat P, Gauthier M, et al. Primary cardiac sarcomas: a retrospective study of the French Sarcoma Group. *Eur J Cancer.* (2014) 50:128–36. doi: 10.1016/j.ejca.2013.09.012

frontiers | Frontiers in Cardiovascular Medicine

TYPE Case Report
PUBLISHED 15 February 2023
DOI 10.3389/fcvm.2023.984572

Check for updates

OPEN ACCESS

EDITED BY
John David Horowitz,
University of Adelaide,
Australia

REVIEWED BY
Mario Annunziata,
Hospital Antonio Cardarelli,
Italy
Laura N. Eadie,
South Australian Research and Development Institute,
Australia

*CORRESPONDENCE
Yuting Yuan
✉ yuanyuting@pkuih.edu.cn

SPECIALTY SECTION
This article was submitted to Cardio-Oncology, a section of the journal Frontiers in Cardiovascular Medicine

RECEIVED 02 July 2022
ACCEPTED 23 January 2023
PUBLISHED 15 February 2023

CITATION
Yuan Y, Wang C and Yao H (2023) A case report of sudden cardiac arrest and torsade de pointes induced by the second-generation tyrosine kinase inhibitor dasatinib combined with fluconazole.
Front. Cardiovasc. Med. 10:984572.
doi: 10.3389/fcvm.2023.984572

COPYRIGHT
© 2023 Yuan, Wang and Yao. This is an open-access article distributed under the terms of the Creative Commons Attribution License (CC BY). The use, distribution or reproduction in other forums is permitted, provided the original author(s) and the copyright owner(s) are credited and that the original publication in this journal is cited, in accordance with accepted academic practice. No use, distribution or reproduction is permitted which does not comply with these terms.

A case report of sudden cardiac arrest and torsade de pointes induced by the second-generation tyrosine kinase inhibitor dasatinib combined with fluconazole

Yuting Yuan[1]*, Chunjian Wang[2] and Hongying Yao[1]

[1]Department of Cardiology, Peking University International Hospital, Beijing, China, [2]Department of Hematology, Peking University International Hospital, Beijing, China

A-41-year-old man diagnosed with acute myeloid leukemia (AML) survived dasatinib + fluconazole drug-induced long QT syndrome, sudden cardiac arrest, and torsade de pointes. Drug features and interaction jointly contributed to the whole process. Therefore, appropriate attention to drug interaction and close ECG monitoring are highly recommended for hospitalized patients, especially for those undergoing multi-drug regimens.

KEYWORDS

dasatinib, fluconazole, drug-induced long QT syndrome, torsade de pointes, tyrosine kinase inhibitor, sudden cardiac arrest, case report

Introduction

Cardiac arrhythmia is an emerging and insufficiently recognized concern of anticancer drugs, resulting mostly from the use of an increasing number of targeted therapies, such as tyrosine kinase inhibitors (TKI) (1). In a World Health Organization pharmacovigilance study, 40 anticancer drugs, which were mostly kinase inhibitors (41%), were significantly associated with drug-induced long QT syndrome, which may deteriorate into morphologically distinctive polymorphic ventricular arrhythmia, torsade de pointes (Tdp), and sudden cardiac death (2). In this report, we present a patient with acute myeloid leukemia (AML) who, during hospitalization, survived Tdp and sudden cardiac arrest, which were caused by multiple factors, such as dasatinib and fluconazole co-administration and patient factors.

10.3389/fcvm.2023.984572

Case presentation

Timeline

Time point	Event
September 2021	Diagnosed with AML and treated with induction therapy (HAA)
October 2021	Diagnosed with invasive fungal disease and administered amphotericin B formulation and caspofungin acetate therapy
January 2022	Administered round 1 VEN + AZA
February 2022	Liver biopsy revealed *Candida* tropicalis infection
March 2022	Administered round 2 VEN + AZA
April 2022	Hospitalized due to fungal infection; antifungals, including micafungin, fluconazole, and antibacterial ceftazidime, were administered
Day 24 in hospital	100 mg dasatinib was administered orally
Day 25 in hospital	Sudden cardiac arrest and torsade de pointes occurred
Day 28 in hospital	Torsade de pointes and QTc resolved
Day 32 in hospital	Discharged from hospital
July 2022	Underwent chemotherapy in another hospital during follow-up

A 41-year-old man with a 6-month history of AML was admitted to our hospital for an invasive fungal infection of the lung, liver, and blood of a 4-month duration. In September 2021, the patient first presented to another hospital with fatigue and gingival bleeding. His complete blood count (CBC) was as follows: white blood cell, 4.48×10^9/L; hemoglobin, 71 g/dL; and platelets, 21×10^9/L. Bone marrow aspiration revealed the presence of blast cells (60%). Flow cytometry revealed 35% abnormal myeloid blasts expressing CD34, CD38, CD117, HLA-DR, CD13, CD33, and MPOdim. These abnormal myeloid blasts partially expressed CD19, CD15, and CD71, but lacked CD5, CD7, CD10, and CD14. Karyotype analysis showed 45,X,-Y,t(8,21)(q22;q22) in 20 analyzed metaphases. Next-generation sequencing revealed the presence of KIT (p.N822K). The diagnosis of AML [M2, ETO+, c-KIT (N 822+)] was made. Thereafter, the patient underwent induction chemotherapy, consisting of aclarubicin, homoharringtonine, and cytarabine. Then, 15 days later, the patient experienced diarrhea, fever, and pneumonia. The test results were suggestive of invasive fungal disease. Antifungal agents, including amphotericin B formulation and caspofungin acetate, were administered. In January and March 2022, the patient underwent two rounds of venetoclax (VEN) and azacitidine (AZA) chemotherapies separately. However, the infection was not thoroughly controlled; it gradually invaded the liver in the following months. Next-generation sequencing of a liver biopsy obtained in February 2022 confirmed *Candida* tropicalis infection. Thereafter, he was admitted to our hospital in April 2022. His medical and family histories were unremarkable.

On admission, echocardiography and electrocardiography findings were unremarkable. Antifungals, including micafungin, fluconazole, and antibacterial ceftazidime, were administered intravenously. Approximately 24 days after admission, 100 mg of dasatinib was administered orally. Thereafter, the patient complained of palpitations. Blood pressure was markedly elevated to 204/98 mmHg. The temperature, heart rate, and respiratory rate were 36.5°C, 42 beats per minute, and 15 breaths per minute, respectively. Electrocardiography showed remarkable sinus bradycardia, heart rate of 38 beats per minute, QT interval of 520 ms, and QT correction (QTc) interval of 482 ms (Figure 1). No ST segment deviation and T wave changes were observed. The complete blood count (CBC) was as follows: white blood cell, 7.53×10^9/L; hemoglobin, 115 g/dL; and platelets, 96×10^9/L. His full blood chemistry panel showed slight hypokalemia (3.22 mmol/L, reference level 3.5–5.5 mmol/L) and normal serum creatine and liver enzyme levels. NT-proBNP concentration was 434 pg./mL (reference level is ≤125 pg./mL), and the hyper-sensitive cardiac troponin T (hs-cTnT) level was 22.8 ng/L (reference level < 14 ng/L). The plasma magnesium level was 0.86 mmol/L (reference level = 0.75–1.02 mmol/L). Atropine was administered to increase the heart rate, whereas sodium nitroprusside was administered to decrease the blood pressure. Additionally, oral and intravenous potassium supplements were administered. On the second day, the potassium level increased to 3.68 mmol/L. At 1 p.m., the patient suddenly lost consciousness, and cardiopulmonary resuscitation was immediately initiated. The electrocardiography on the defibrillator showed ventricular fibrillation, and electrical cardioversion was performed simultaneously. The patient regained full consciousness and was transferred to the cardiac intensive care unit. Several episodes of torsade de pointes (Figure 1) were detected on cardiac telemetry monitoring; however, these episodes did not affect hemodynamic stability. Fluconazole and dasatinib were suspected to have induced these hemodynamic changes and were discontinued. Thereafter, intravenous isoproterenol was administered to elevate the heart rate to >90 beats per minute and shorten the QT interval. Aggressive potassium supplements were used to increase the potassium level to >4 mmol/L. Magnesium supplements, including magnesium sulfate and potassium magnesium aspartate, were added. The vicious arrhythmia abated, and the QTc interval gradually returned to 427 ms (QT interval returned to 366 ms) in the 3 days following the event. The longitudinal QT change is shown in Figure 2. Then, 5 days later, hs-cTnT and NT-proBNP levels were 23.4 ng/L and 162.1 pg./mL, respectively. Echocardiography revealed consistent normal left ventricular function. The patient was discharged after prolonged monitoring and duly educated about the prohibited use of certain drugs. Then, 2 months later during follow-up, the patient underwent chemotherapy in another hospital.

Discussion

The development of various anti-cancer therapeutics has improved the prognosis and increased the survival time of patients with different malignancies (3). However, associated cardiovascular adverse drug reactions, such as heart failure (4), acute myocardial infarction (5), myocarditis (6), vicious arrhythmia, and sudden cardiac death (1), have been the concern of clinicians. A drug-induced long-QT syndrome is an important adverse reaction of anti-tumor drugs, which can further deteriorate into Tdp, ventricular fibrillation, and sudden cardiac death. QTc prolongation refers to corrected QT prolongation > 450 ms in men and >470 ms in women (7) or an absolute increase of >60 ms above baseline. The risk of Tdp increases by 5%–7% for every 10-ms extension in the QTc interval (8), and QTc > 500 ms is considered to be remarkably associated with Tdp (9). However, the relationship between the changes in QT and Tdp widely varies. Tdp may occur when QTc is mildly prolongated, whereas, in some individuals, no events result from markedly prolonged QT (10). In this case, QTc was slightly elevated, which triggered Tdp and ventricular fibrillation. Herein, QT

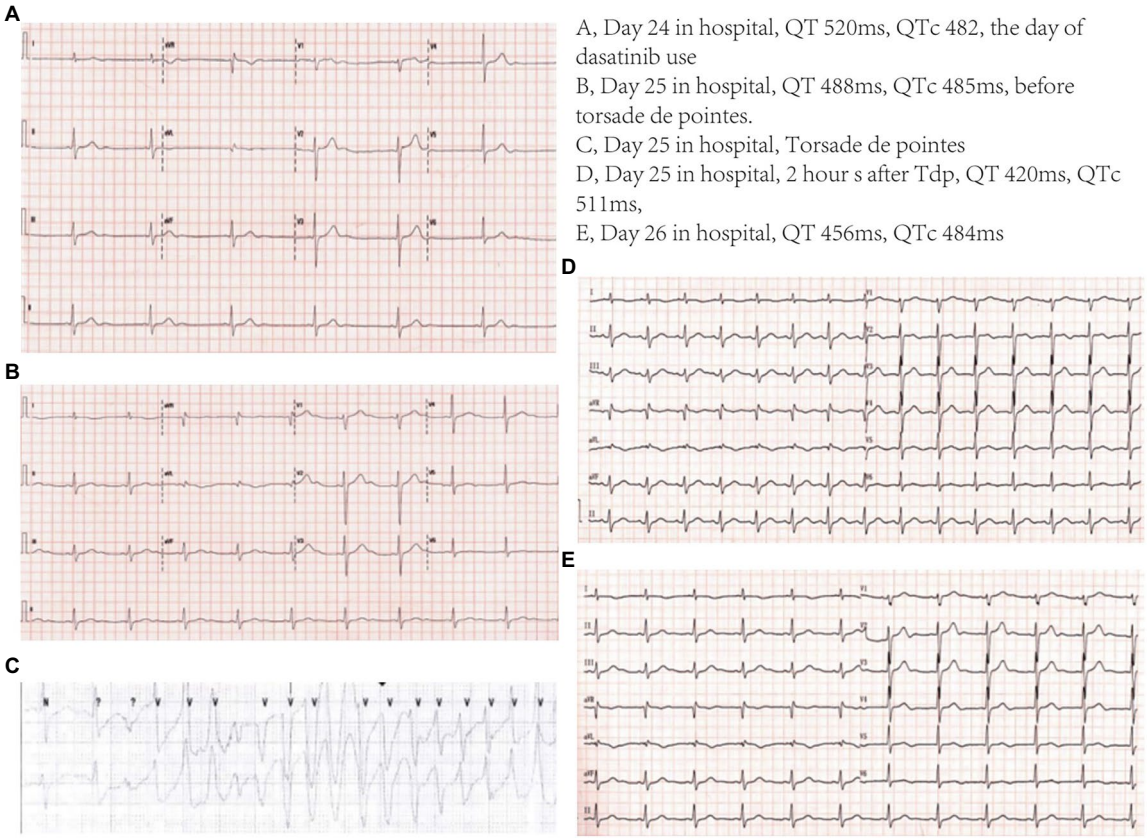

A, Day 24 in hospital, QT 520ms, QTc 482, the day of dasatinib use
B, Day 25 in hospital, QT 488ms, QTc 485ms, before torsade de pointes.
C, Day 25 in hospital, Torsade de pointes
D, Day 25 in hospital, 2 hour s after Tdp, QT 420ms, QTc 511ms,
E, Day 26 in hospital, QT 456ms, QTc 484ms

FIGURE 1
Electrocardiogram.

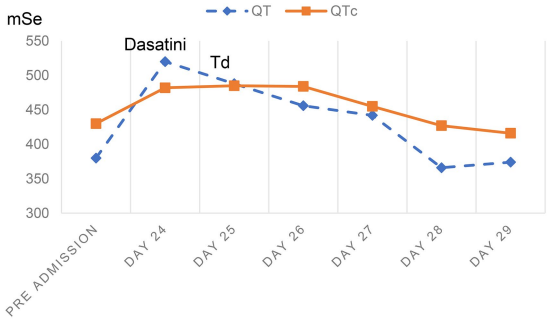

FIGURE 2
QT and QTc changes.

prolongation was not the cause of Tdp, but the manifestation of the increase in dispersion of repolarization, which provided the arrhythmogenic substrate and resulted in Tdp (11). Transmural dispersion of repolarization has been proven to be an indicator of this abnormality (12).

Dasatinib, the second-generation tyrosine kinase inhibitor, has been reported to suppress various types of kinases, including BCR-ABL1, FGFR2, c-KIT, PDGFRα, PDGFRβ, EPHA, and Src family (13, 14). Therefore, the drug is now being used to treat patients with leukemia having targeted chromosomal changes. This patient went through recurrent fungal and bacterial infections, which restricted the periodic administration of chemotherapy. After admission, his response to antifungal therapy was poor, and bone marrow aspiration revealed a possible AML relapse. Considering the role of c-KIT mutation in AML and the use of dasatinib, according to the NCCN 2022 guideline, in this kind of patient (15, 16), the hematologist decided to administer 100 mg of dasatinib, instead of chemotherapy, to target the c-KIT mutation. Dasatinib is rapidly absorbed, and at least 80% of the oral dose is deemed to be bioavailable. Dasatinib is eliminated through CYP3A4-mediated metabolism, with a relatively short half-life of approximately 5–6 h. Dasatinib pharmacokinetics are not influenced by age, race, and renal insufficiency. Clinicians need to be cautious of potential drug interactions between dasatinib and pH-modifying agents (17) and strong inducers/inhibitors of CYP3A (18).

According to the data extracted from adverse event reports recorded in the publicly available version of the United States Food and Drug Administration (FDA) Adverse Event Reporting System (FAERS) database, dasatinib can induce torsade de pointes/QT prolongation (at a relatively low rate) and pulmonary hypertension (19). Spechbach et al. (20) presented a case of dasatinib-induced reversible ventricular arrhythmia. Considering its pharmacokinetic characteristics, dasatinib is mostly metabolized by cytochrome P450 3A4 (CYP3A4). Hence, it is subjected to triazoles, and its risk of toxicity and half-life can be largely augmented when exposed simultaneously (18). Another tyrosine kinase inhibitor, osimertinib, when combined with *litsea cubeba*, has been reported to cause Tdp (21). Monitoring the plasma concentration of dasatinib may be helpful to determine the safe range. The safe concentration of dasatinib not causing pleural effusion has been determined (22), but data about Tdp are lacking.

Unfortunately, we are unable to determine TKI plasma concentrations in our hospital, so were unable to establish if dasatinib plasma concentration was elevated at the time when the patient developed TdP. Ongoing measurement of dasatinib plasma levels may have allowed the patient to safely continue dasatinib treatment following either a dose reduction or cessation of the interacting drugs.

Fluconazole is a triazole antifungal agent that inhibits the growth of fungi by inhibiting ergosterol production. It is commonly used to treat opportunistic fungal infections caused by *Candida*, *Cryptococcus*, and other fungal species. It has been proven to prolong the QT interval and endocardial ventricular action potential duration, increase transmural dispersion of repolarization, and induce early afterdepolarizations (EADs) in rabbit models (23). It was found to induce torsade de pointes in children (24) and adults, when administered singly or combined with other drugs, such as amitriptyline (25), fluoroquinolone (26), and arsenic trioxide (27). Acting as a potent inhibitor of cytochrome P450 3A4 (CYP3A4), fluconazole, may exhibit indefinite clinical effects due to drug interactions. In our case, the patient responded to fluconazole treatment only in the first 24 days but experienced sudden cardiac arrest when dasatinib was added. Herein, after excluding other possible factors, we suspected the reactions to be due to the drug features of dasatinib and its drug interactions with fluconazole.

Several risk factors contribute to the development of Tdp in hospitalized patients; they include QTc > 500 ms, QT-prolonging drug use, heart disease (congestive heart failure and myocardial infarction), advanced age, sex (woman), electrolyte disturbance (hypokalemia, hypomagnesemia, hypocalcemia, etc.), diuretic treatment, impaired hepatic drug metabolism (hepatic dysfunction or drug–drug interactions), bradycardia, and genetic polymorphisms (28). Particularly, drug interactions are easily neglected in clinical practice. Meanwhile, in our case, extracellular potassium increased, but intracellular potassium was unclear and potassium imbalance should be considered as one factor predisposing to arrhythmia. In clinical practice, QTc prolongation may occur without deteriorating into Tdp, as occurs with amiodarone use. Transmural dispersion of repolarization seems important but still lacks valid markers for monitoring and needs further investigation.

Conclusion

In this report, a 41-year-old man experienced sudden cardiac arrest and Tdp after dasatinib and fluconazole co-administration. Based on this case, clinicians should be cautious of the potential cardiac side effects of dasatinib and the possible drug interaction between dasatinib and CYP3A4 inhibitors. Additionally, the case accentuates the necessity for ECG monitoring during anticancer drug administration.

Ethics statement

Ethical review and approval was not required for the study on human participants in accordance with the local legislation and institutional requirements. The patients/participants provided their written informed consent to participate in this study and for the publication of this case report.

Author contributions

YY contributed to manuscript writing and data collection. CW and HY contributed to clinical management. All authors contributed to the article and approved the submitted version.

Funding

This study was funded by the Peking University International Hospital.

Conflict of interest

The authors declare that the research was conducted in the absence of any commercial or financial relationships that could be construed as a potential conflict of interest.

Publisher's note

All claims expressed in this article are solely those of the authors and do not necessarily represent those of their affiliated organizations, or those of the publisher, the editors and the reviewers. Any product that may be evaluated in this article, or claim that may be made by its manufacturer, is not guaranteed or endorsed by the publisher.

References

1. Alexandre, J, Moslehi, JJ, Bersell, KR, Funck-Brentano, C, Roden, DM, and Salem, JE. Anticancer drug-induced cardiac rhythm disorders: current knowledge and basic underlying mechanisms. *Pharmacol Ther*. (2018) 189:89–103. doi: 10.1016/j.pharmthera.2018.04.009

2. Salem, JE, Nguyen, LS, Moslehi, JJ, Ederhy, S, Lebrun-Vignes, B, Roden, DM, et al. Anticancer drug-induced life-threatening ventricular arrhythmias: a World Health Organization pharmacovigilance study. *Eur Heart J*. (2021) 42:3915–28. doi: 10.1093/eurheartj/ehab362

3. Arnold, M, Rutherford, MJ, Bardot, A, Ferlay, J, Andersson, TM, Myklebust, T, et al. Progress in cancer survival, mortality, and incidence in seven high-income countries 1995-2014 (ICBP SURVMARK-2): a population-based study. *Lancet Oncol*. (2019) 20:1493–505. doi: 10.1016/S1470-2045(19)30456-5

4. Moslehi, JJ. Cardiovascular toxic effects of targeted cancer therapies. *N Engl J Med*. (2016) 375:1457–67. doi: 10.1056/NEJMra1100265

5. Levis, BE, Binkley, PF, and Shapiro, CL. Cardiotoxic effects of anthracycline-based therapy: what is the evidence and what are the potential harms? *Lancet Oncol*. (2017) 18:e445–56. doi: 10.1016/S1470-2045(17)30535-1

6. Geraud, A, Gougis, P, Vozy, A, Anquetil, C, Allenbach, Y, Romano, E, et al. Clinical pharmacology and interplay of immune checkpoint agents: a yin-Yang balance. *Annu Rev Pharmacol Toxicol*. (2021) 61:85–112. doi: 10.1146/annurev-pharmtox-022820-093805

7. Goldenberg, I, Moss, AJ, and Zareba, W. QT interval: how to measure it and what is "normal". *J Cardiovasc Electrophysiol*. (2006) 17:333–6. doi: 10.1111/j.1540-8167.2006.00408.x

8. Trinkley, KE, Page, RL 2nd, Lien, H, Yamanouye, K, and Tisdale, JE. QT interval prolongation and the risk of torsades de pointes: essentials for clinicians. *Curr Med Res Opin*. (2013) 29:1719–26. doi: 10.1185/03007995.2013.840568

9. Yap, YG, and Camm, AJ. Drug induced QT prolongation and torsades de pointes. *Heart*. (2003) 89:1363–72. doi: 10.1136/heart.89.11.1363

10. Al-Khatib, SM, LaPointe, NM, Kramer, JM, and Califf, RM. What clinicians should know about the QT interval. *JAMA*. (2003) 289:2120–7. doi: 10.1001/jama.289.16.2120

11. Antzelevitch, C, and Shimizu, W. Cellular mechanisms underlying the long QT syndrome. *Curr Opin Cardiol*. (2002) 17:43–51. doi: 10.1097/00001573-200201000-00007

12. Di Diego, JM, Belardinelli, L, and Antzelevitch, C. Cisapride-induced transmural dispersion of repolarization and torsade de pointes in the canine left ventricular wedge preparation during epicardial stimulation. *Circulation*. (2003) 108:1027–33. doi: 10.1161/01.CIR.0000085066.05180.40

13. Druker, BJ. Translation of the Philadelphia chromosome into therapy for CML. *Blood*. (2008) 112:4808–17. doi: 10.1182/blood-2008-07-077958

14. Force, T, Krause, DS, and Van Etten, RA. Molecular mechanisms of cardiotoxicity of tyrosine kinase inhibition. *Nat Rev Cancer*. (2007) 7:332–44. doi: 10.1038/nrc2106

15. Boissel, N, Renneville, A, Leguay, T, Lefebvre, PC, Recher, C, Lecerf, T, et al. Dasatinib in high-risk core binding factor acute myeloid leukemia in first complete remission: a French acute myeloid leukemia intergroup trial. *Haematologica*. (2015) 100:780–5. doi: 10.3324/haematol.2014.114884

16. Paschka, P, Schlenk, RF, Weber, D, Benner, A, Bullinger, L, Heuser, M, et al. Adding dasatinib to intensive treatment in core-binding factor acute myeloid leukemia-results of the AMLSG 11-08 trial. *Leukemia*. (2018) 32:1621–30. doi: 10.1038/s41375-018-0129-6

17. Eley, T, Luo, FR, Agrawal, S, Sanil, A, Manning, J, Li, T, et al. Phase I study of the effect of gastric acid pH modulators on the bioavailability of oral dasatinib in healthy subjects. *J Clin Pharmacol*. (2009) 49:700–9. doi: 10.1177/0091270009333854

18. Johnson, FM, Agrawal, S, Burris, H, Rosen, L, Dhillon, N, Hong, D, et al. Phase 1 pharmacokinetic and drug-interaction study of dasatinib in patients with advanced solid tumors. *Cancer*. (2010) 116:1582–91. doi: 10.1002/cncr.24927

19. Cirmi, S, El Abd, A, Letinier, L, Navarra, M, and Salvo, F. Cardiovascular toxicity of tyrosine kinase inhibitors used in chronic myeloid leukemia: an analysis of the FDA adverse event reporting system database (FAERS). *Cancers*. (2020) 12:826. doi: 10.3390/cancers12040826

20. Spechbach, H, Morel, P, Ing Lorenzini, K, Besson, M, Gétaz, L, Sunthorn, H, et al. Reversible ventricular arrythmia induced by dasatinib. *Clin Case Rep*. (2013) 1:20–5. doi: 10.1002/ccr3.5

21. Zhang, XY, Wu, CB, Wu, CX, Lin, L, Zhou, YJ, Zhu, YY, et al. Case report: torsade de pointes induced by the third-generation epidermal growth factor receptor-tyrosine kinase inhibitor Osimertinib combined with Litsea Cubeba. *Front Cardiovasc Med*. (2022) 9:903354. doi: 10.3389/fcvm.2022.903354

22. Yu, H, Steeghs, N, Nijenhuis, CM, Schellens, JH, Beijnen, JH, and Huitema, AD. Practical guidelines for therapeutic drug monitoring of anticancer tyrosine kinase inhibitors: focus on the pharmacokinetic targets. *Clin Pharmacokinet*. (2014) 53:305–25. doi: 10.1007/s40262-014-0137-2

23. Wang, J, Wang, G, Quan, X, Ruan, L, Liu, Y, Ruan, Y, et al. Fluconazole-induced long QT syndrome via impaired human ether-a-go-go-related gene (hERG) protein trafficking in rabbits. *Europace*. (2017) 19:1244–9. doi: 10.1093/europace/euw091

24. Ünal Yüksekgönül, A, Ertuğrul, İ, and Karagöz, T. Fluconazole-associated QT interval prolongation and Torsades de pointes in a paediatric patient. *Cardiol Young*. (2021) 31:2035–7. doi: 10.1017/S1047951121001992

25. Dorsey, ST, and Biblo, LA. Prolonged QT interval and torsades de pointes caused by the combination of fluconazole and amitriptyline. *Am J Emerg Med*. (2000) 18:227–9. doi: 10.1016/S0735-6757(00)90027-5

26. Zeuli, JD, Wilson, JW, and Estes, LL. Effect of combined fluoroquinolone and azole use on QT prolongation in hematology patients. *Antimicrob Agents Chemother*. (2013) 57:1121–7. doi: 10.1128/AAC.00958-12

27. Naito, K, Kobayashi, M, Sahara, N, Shigeno, K, Nakamura, S, Shinjo, K, et al. Two cases of acute promyelocytic leukemia complicated by torsade de pointes during arsenic trioxide therapy. *Int J Hematol*. (2006) 83:318–23. doi: 10.1532/IJH97.05056

28. Drew, BJ, Ackerman, MJ, Funk, M, Gibler, WB, Kligfield, P, Menon, V, et al. Prevention of torsade de pointes in hospital settings: a scientific statement from the American Heart Association and the American College of Cardiology Foundation. *J Am Coll Cardiol*. (2010) 55:934–47. doi: 10.1016/j.jacc.2010.01.001

frontiers | Frontiers in Cardiovascular Medicine

TYPE Case Report
PUBLISHED 01 March 2023
DOI 10.3389/fcvm.2023.1115962

Check for updates

OPEN ACCESS

EDITED BY
Cezar Angi Iliescu,
The University of Texas MD Anderson Cancer Center, United States

REVIEWED BY
Teodora Donisan,
Mayo Clinic, United States
Efstratios Koutroumpakis,
The University of Texas MD Anderson Cancer Center, United States
Ankit Mangla,
Case Western Reserve University, United States

*CORRESPONDENCE
Andreea Blindaru
✉ blindaruandreea@gmail.com

†These authors have contributed equally to this work and share first authorship

SPECIALTY SECTION
This article was submitted to Cardio-Oncology, a section of the journal Frontiers in Cardiovascular Medicine

RECEIVED 04 December 2022
ACCEPTED 31 January 2023
PUBLISHED 01 March 2023

CITATION
Blindaru A, Vasilescu A, Danet A, Zimnicaru O, Cristu M, Tudorica S, Borjog T, Patrascu O and Badiu CC (2023) Surgical resection of a giant cardiac angiosarcoma and reconstruction of involved right heart structures: A case report.
Front. Cardiovasc. Med. 10:1115962.
doi: 10.3389/fcvm.2023.1115962

COPYRIGHT
© 2023 Blindaru, Vasilescu, Danet, Zimnicaru, Cristu, Tudorica, Borjog, Patrascu and Badiu. This is an open-access article distributed under the terms of the Creative Commons Attribution License (CC BY). The use, distribution or reproduction in other forums is permitted, provided the original author(s) and the copyright owner(s) are credited and that the original publication in this journal is cited, in accordance with accepted academic practice. No use, distribution or reproduction is permitted which does not comply with these terms.

Surgical resection of a giant cardiac angiosarcoma and reconstruction of involved right heart structures: A case report

Andreea Blindaru[1*†], Alexandru Vasilescu[1†], Andrei Danet[1], Oana Zimnicaru[1], Maximilian Cristu[1], Stefan Tudorica[2], Tudor Borjog[2], Oana Patrascu[3] and Catalin Constantin Badiu[1]

[1]Department of Cardiovascular Surgery, University Emergency Hospital Bucharest, Bucharest, Romania, [2]Department of Anesthesiology, University Emergency Hospital Bucharest, Bucharest, Romania, [3]Department of Anatomopathology, University Emergency Hospital Bucharest, Bucharest, Romania

We present the case of a young woman without a medical history who presented with a giant right atrial, transtricuspid, and right ventricular mass and in a severe clinical state. Multimodal imaging raised the suspicion of primary cardiac angiosarcoma. Due to rapid hemodynamic and respiratory deterioration, we were forced to perform surgical removal of the mass with a concomitant reconstruction of the involved right heart structures, only 48 h after presentation. The postoperative course was uneventful, and the patient was discharged from the intensive care unit 2 days later. Radical surgical resection with reconstruction of the resected heart structures was the only possible salvage option for giant angiosarcoma, which led to hemodynamic instability. Followed by chemotherapy, this radical approach may prolong survival.

KEYWORDS

cardiac angiosarcoma, surgery for cardiac angiosarcoma, primary cardiac tumor, surgical resection of giant cardiac angiosarcoma, angiosarcoma of the heart, case report

1. Introduction

Malignant cardiac tumors are scarce clinical entities with poor prognosis and a median survival time ranging from 6 months to a few years (1). Their occurrence in autopsy series varies between 0.001 and 0.28%, with angiosarcomas being the most common form (2). Aggressive local growth and metastasis are common features of angiosarcoma, and the primary site for metastases is represented by the lungs (3). Over the last decades, different treatment options have been proposed for dealing with angiosarcoma, unfortunately with poor results. This is likely related, on the one hand, to the complexity of the complete surgical resection of the tumor and the involved vital structures and, on the other hand, to the relative non-responsiveness of angiosarcomas to adjuvant therapies (1).

Abbreviations: ICU, intensive care unit; CT, computed tomography; MRI, magnetic resonance imaging; RV, right ventricle; LV, left ventricle; TEE, transesophageal echocardiography; CMR, cardiac magnetic resonance.

2. Case report

We report the case of an 18 years-old woman without a medical history who was admitted with symptoms of fatigue, dyspnea, and leg edema, which had started and worsened over the course of 3 weeks. The patient had no previous symptoms and no family history of malignancies. Upon admission, various diagnostic tests were conducted, including an electrocardiogram, echocardiography, computed tomography (CT), and magnetic resonance imaging (MRI). On admission, the patient's vital signs were normal (heart rate 95 bpm, blood pressure 110/60 mmHg, and oxygen saturation 98–99%). Laboratory results showed normochromic normocytic anemia (Hgb 11,7) and thrombocytopenia (PLT = 75.000 μL). The electrocardiogram revealed sinus tachycardia and a minor right bundle branch block. Physical examination showed dyspnea and leg edema, but no heart murmur and no jugular venous distension. Echocardiography revealed moderately impaired RV function, almost normal LV function, and a large mass occupying the right atrium and extending partially into both caval veins (**Supplementary Figure 1**). The mass was also expanding through the tricuspid valve into the RV, obstructing the RV inflow and outflow tract. The anterior and posterior tricuspid leaflets were engulfed in the tumoral mass (**Supplementary Video 1**). MRI confirmed the echocardiographic findings and further described the mass enclosing a part of the right coronary artery. The MRI appearance of the mass was highly suggestive of angiosarcoma (small intralesional foci with hyperintense T1 signal and hyperintense T2 signal compared to the myocardium, postcontrast heterogenous enhancement with gadolinophilic tissue areas, and intratumoral necrotic inclusions) (**Supplementary Figure 2** and **Supplementary Video 1**). A full body CT scan revealed multiple small pulmonary nodules, but no other secondary determinations.

Differential diagnosis of cardiac angiosarcoma must include hemangioendothelioma, intracardiac metastases (including metastatic angiosarcoma) as well as leiomyosarcoma, fibrosarcoma, or malignant fibrous histiocytoma.

To determine the therapeutic strategy, the patient was evaluated by a multidisciplinary team that included a cardiologist, oncologist, anesthesiologist, and thoracic and cardiovascular surgeon.

The patient was provided with psychological support to help her understand the severity of her diagnosis and the necessity of continuous treatment. It was our patient's decision to continue with the treatment.

Due to severe obstruction of the tricuspid valve, the patient developed a low cardiac output state, leading to severe hemodynamic instability, and therefore, we were forced to perform urgent surgical resection of the tumor. After sternotomy and adhesiolysis, a right femoro-femoral and concomitant distal cannulation of the superior vena cava was performed. Antegrade cardioplegia was administrated, and the right atrium was opened by resecting the entire free wall. Intraoperatively, we found a giant mass (11/10 cm) invading the entire right atrium, including the free wall, one-third of the right coronary artery, the anterior and posterior tricuspid valve leaflets, the basal part of the RV free wall, and a significant part of the RV cavity (**Supplementary Video 1**). The mass extended also to the proximal parts of both caval veins. Extensive tumoral resection was performed. Approximately 7 cm of the right coronary artery had also to be excised, and accordingly, a right coronary bypass graft was necessary. After complete macroscopic resection of the tumor (**Supplementary Video 1**), the reconstruction began with the implantation of a valvular prosthesis. As two-thirds of the annular circumference was resected, the bioprosthesis had to be fixed by pledged sutures to the endocardium of the RV free wall and to the septal leaflet (**Supplementary Video 1**). The right atrial wall was reconstructed using a generous bovine pericardial patch, which was directly sewn to the prosthetic valve ring, the interatrial septum, and the caval veins (**Supplementary Video 1**). Weaning from CPB was uneventful, and the aortic-cross-clamp time and CPB time were 115 and 239 min, respectively. The early postoperative course was uncomplicated, and our patient was discharged from the ICU 2 days later. The postoperative TEE showed a normofunctional bioprosthesis, with a mean diastolic gradient of 1.3 mmHg, moderate RV dysfunction (FAC 24%), and mild LV dysfunction (**Supplementary Video 1**).

The diagnosis of high-grade angiosarcoma was confirmed by the histopathologic and immunohistochemistry examinations, which were positive for CD31, CD34, ERG (erythroblast transformation-specific-related gene), and Ki67 (**Supplementary Figure 3**).

Due to the presence of lung metastases and the R1 resection, following surgery, the patient underwent chemotherapy with ifosfamide (3,000 mg) and mesna (2,800 mg). Starting from the second cure, the chemotherapy was extended with doxorubicin (40 mg). At 6 months of follow-up and after completing six sessions of chemotherapy, the patient presented in a stable clinical state NYHA I, with normal LV function and mild RV dysfunction. Furthermore, there was no evidence of tumor recurrence, and the small pulmonary nodules could not be identified anymore in the follow-up CT performed at 6 months. Unfortunately, 2 months later, a 20/19 mm intracranial metastasis was identified on the brain CT scan, and after 1 month, the patient underwent surgical resection and started radiotherapy. The chronological order of clinical events is shown in **Supplementary Table 1**.

3. Discussions

Cardiac angiosarcoma is a rare entity in clinical practice, and thus, there is a lack of consensus guidelines on the management of this pathology. Cardiac angiosarcoma is often found in the right atrium, but it can also invade the right ventricle, the tricuspid valve, and the right coronary artery.

Patients are asymptomatic only if the tumor is discovered in a very early stage. As the tumor mass grows, it may exhibit not only varied symptoms such as dyspnea or chest pain but also hemoptysis and embolic events (4). Early-stage diagnosis should be managed by immediate surgical therapy, as several studies have demonstrated the best long-term survival after complete resection in small angiosarcoma (1, 4, 5). Furthermore, as reported by different groups, a preoperative endomyocardial biopsy may lead to complications without being a very sensitive method for angiosarcoma diagnosis. Accordingly, this procedure should not be mandatory (6). Nevertheless, early-stage cardiac tumors are diagnosed incidentally or, unfortunately, often overlooked.

Due to rapid infiltrating growth, in patients with advanced right-sided angiosarcoma, the clinical presentation may be dominated by complications deriving from the massive tumor (7).

Right-sided tumors are bulky, infiltrative, and tend to metastasize early, but they do not usually present congestive heart failure until late in the disease (8, 9). To accurately characterize the tumor location and size, as well as its possible distant metastatic lesions, non-invasive imaging methods such as echocardiography, CT, and MRI contribute essentially. Thus, even if surgery may be often challenging, good imaging may improve preoperative planning and reduce the risk of operative mortality (10). Furthermore, imaging can even postpone surgery in some patients and prefer preoperative chemotherapy as a possibility of shrinking the tumor mass (11). This approach was used by Blackmon and Reardon who report their experience with 15 operated angiosarcomas in patients with no heart failure or imminence of heart failure. They started with preoperative chemotherapy to shrink the tumor, followed by surgical resection. In their case, median survival was 27 months, with the longest-surviving patient alive at 9.5 years. Our patient developed heart failure due to obstruction of the tricuspid valve, and such an approach was not possible at the time of presentation (5).

As described by Yadav and Mangla (8) in their study, surgical resection with an R0 margin is associated with the best outcomes. In situations where R0 resection is not achieved, chemotherapy and radiation therapy after surgical resection may improve results.

Nevertheless, technically feasible, surgical resection still represents the gold standard and an important prognostic factor for angiosarcoma treatment. In our case, surgery was necessary to achieve hemodynamic stability and relieve the life-threatening obstruction. Similar to other reports where R0 resection was achieved only in approximately 25% of cases, in our patient, an R0 resection has not been demonstrated by the histopathologic examination (10). Nevertheless, even in cases where R0 resection is possible, there still remains a high risk for local recurrence or even the appearance of postoperative metastatic lesions (12). As recommended by other authors, adjuvant chemotherapy should be considered in all patients (10). Even if there are no clear recommendations or clearly designed protocols for radiotherapy or targeted therapy as adjuvants to surgery, it has been reported that they may improve survival, especially in patients with R1 resection (10, 13).

In our case, the decision to offer immediate surgery and postpone chemotherapy was driven by the hemodynamic instability, even if several vital structures were infiltrated. The surgical judgment was based on the fact that complete resection of these structures may not severely influence the right heart function, especially as they were already affected by the tumor infiltration. Hence, right ventricular contractility was not severely affected by the ventricular wall resection as the excised area was already akinetic before surgery. Furthermore, the resected coronary artery could be replaced by a venous graft, as already described in the literature, without influencing the contractility of the remained RV (14). The replacement of the resected tricuspid valve offered a stable structure to rebuild the right atrioventricular groove and the right atrial wall using a heterologous pericardium. Hence, we advocate for complete surgical resection of the infiltrated right heart structure s in this malignant pathology whenever a sufficient part of the right ventricle remains functional.

Recently, a combination of proton beam therapy and chemotherapy followed by adjuvant chemotherapy has emerged as a promising approach for patients with R1 resection of right-sided angiosarcoma. Mangla et al. (15) reported a survival time of 18 months after treatment completion in a young man. Taxanes have been found to have similar efficacy compared to anthracyclines, however, without the cardiotoxicity associated with anthracyclines. Although survival after proton beam therapy is encouraging, it is not currently available at our institution (15).

4. Conclusion

Taking into account that cardiac angiosarcoma is associated with a very poor prognosis, an early-stage diagnosis should be immediately treated with surgical resection and a meticulous postoperative follow-up. In advanced cases, preoperative imaging should help plan aggressive resection and reconstruction of the involved structures. Multidisciplinary teams must establish the applications and benefits of postoperative adjuvant therapy, which may improve long-term survival.

Data availability statement

The original contributions presented in this study are included in this article/**Supplementary material**, further inquiries can be directed to the corresponding author.

Ethics statement

Written informed consent was obtained from the participant for the publication of this case report. Written informed consent was obtained from the individual(s) for the publication of any potentially identifiable images or data included in this article.

Author contributions

CB was part of the surgical team, reviewed and revised the manuscript critically for important intellectual content, contributed to the conception, and design and approved the final manuscript as submitted. AB was part of the surgical team, drafted the initial manuscript, contributed to the conception and design, and approved the final manuscript as submitted. AV was part of the medical team, reviewed and revised the manuscript, and approved the final manuscript as submitted. AD was part of the surgical team and contributed to data analysis and interpretation. OZ was the echocardiographist of the team and approved the final manuscript as submitted. MC was the video editor, reviewed and revised the manuscript, and approved the final manuscript as submitted. ST was part of the anesthesiological team and contributed to data analysis and interpretation. TB was part of the anesthesiological team and contributed to data analysis and interpretation. OP was the anatomopathologist and contributed to data analysis and interpretation. All authors contributed to the article and approved the submitted version.

Conflict of interest

The authors declare that the research was conducted in the absence of any commercial or financial relationships that could be construed as a potential conflict of interest.

Publisher's note

All claims expressed in this article are solely those of the authors and do not necessarily represent those of their affiliated organizations, or those of the publisher, the editors and the reviewers. Any product that may be evaluated in this article, or claim that may be made by its manufacturer, is not guaranteed or endorsed by the publisher.

Supplementary material

The Supplementary Material for this article can be found online at: https://www.frontiersin.org/articles/10.3389/fcvm.2023.1115962/full#supplementary-material

References

1. Randhawa J, Budd G, Randhawa M, Ahluwalia M, Jia X, Daw H. Primary cardiac sarcoma: 25-year cleveland clinic experience. *Am J Clin Oncol.* (2016) 39:593–9. doi: 10.1097/COC.0000000000000106

2. Bussani R, Castrichini M, Restivo L, Fabris E, Porcari A, Ferro F. Diagnosis, prognosis, and treatment. *Curr Cardiol Rep.* (2020) 22:169. doi: 10.1007/s11886-020-01420-z

3. Gaballah A, Jensen C, Palmquist S, Pickhardt P, Duran A, Broering G. Angiosarcoma: clinical and imaging features from head to toe. *Br J Radiol.* (2017) 90:20170039. doi: 10.1259/bjr.20170039

4. Simpson L, Kumar S, Okuno S, Schaff H, Porrata L, Brukner J. Malignant primary cardiac tumors: review of a single institution experience. *Cancer.* (2008) 112:2440–6. doi: 10.1002/cncr.23459

5. Blackmon S, Reardon M. Surgical treatment of primary cardiac sarcomas. *Tex Heart Inst J.* (2009) 36:451–2.

6. Rettmat K, Stierle U, Sheikhzadeh A, Diederich K. Primary angiosarcoma of the heart. report of a case and review of literature. *Jpn Heart J.* (1993) 34:667–83. doi: 10.1536/ihj.34.667

7. Chaves V, Pereira C, Andrade M, von Hafe P, Almeida J. Cardiac angiosarcoma: from cardiac tamponade to ischaemic stroke – a diagnostic challenge. *Eur J Case Rep Intern Med.* (2019) 6:001079. doi: 10.12890/2019_001079

8. Yadav U, Mangla A. Primary pericardial angiosarcoma: case report and review of treatment options. *Ecancermedicalscience.* (2020) 14:1056.

9. Leja M, Shah D, Reardon M. Primary cardiac tumors. *Tex Heart Inst J.* (2011) 38:261–2.

10. Hasan S, Witten J, Collier P, Tong M, Pettersson G, Smedira G. Outcomes after resection of primary cardiac sarcoma. *JTCVS Open.* (2021) 8:384–90. doi: 10.1016/j.xjon.2021.08.038

11. Abu Saleh W, Ramlawi B, Shapira O, Al Jabbari O, Ravi V, Benjamin R. Improved outcomes with the evolution of a neoadjuvant chemotherapy approach to right heart sarcoma. *Ann Thorac Surg.* (2017) 104:90–6. doi: 10.1016/j.athoracsur.2016.10.054

12. Uemura K, Sano H, Takaoka H, Okita Y. Cardiac angiosarcoma in the right ventricle treated by surgical resection. *BMJ Case Rep.* (2021) 14:e238736. doi: 10.1136/bcr-2020-238736

13. Yada M, Tara Y, Sato S, Sekine Y, Nishina T, Yamanaka K. A case of primary cardiac angiosarcoma with surgical resection and reconstruction. *J Cardiol Cases.* (2021) 25:103–5. doi: 10.1016/j.jccase.2021.07.012

14. Kwon Y, Park S, Kim H, Kim J. Complete resection of cardiac angiosarcoma invading right heart and right coronary artery. *Ann Thorac Surg.* (2020) 110:e501–3. doi: 10.1016/j.athoracsur.2020.04.026

15. Mangla A, Gupta A, Mansur DB, Abboud S, Rothermel L, Oliveira G. Right atrial cardiac angiosarcoma treated with concurrent proton beam therapy and paclitaxel: a novel approach to a rare disease. *Thorac Cancer.* (2021) 12:1131–3. doi: 10.1111/1759-7714.13895

frontiers | Frontiers in Cardiovascular Medicine

TYPE Case Report
PUBLISHED 14 March 2023
DOI 10.3389/fcvm.2023.1135233

Check for updates

OPEN ACCESS

EDITED BY
Reto Asmis,
Wake Forest University, United States

REVIEWED BY
Chiara Lestuzzi,
Santa Maria degli Angeli Hospital Pordenone, Italy
Marcello Chiocchi,
University of Rome Tor Vergata, Italy

*CORRESPONDENCE
Philippe Garot
✉ pgarot@angio-icps.com

SPECIALTY SECTION
This article was submitted to Cardio-Oncology, a section of the journal Frontiers in Cardiovascular Medicine

RECEIVED 31 December 2022
ACCEPTED 28 February 2023
PUBLISHED 14 March 2023

CITATION
Bohbot Y, Garot J, Danjon I, Thébert D, Nahory L, Gros P, Salerno F and Garot P (2023) Case report: Diagnosis, management and evolution of a bulky and invasive cardiac mass complicated by complete atrioventricular block.
Front. Cardiovasc. Med. 10:1135233.
doi: 10.3389/fcvm.2023.1135233

COPYRIGHT
© 2023 Bohbot, Garot, Danjon, Thébert, Nahory, Gros, Salerno and Garot. This is an open-access article distributed under the terms of the Creative Commons Attribution License (CC BY). The use, distribution or reproduction in other forums is permitted, provided the original author(s) and the copyright owner(s) are credited and that the original publication in this journal is cited, in accordance with accepted academic practice. No use, distribution or reproduction is permitted which does not comply with these terms.

Case report: Diagnosis, management and evolution of a bulky and invasive cardiac mass complicated by complete atrioventricular block

Yohann Bohbot[1], Jérôme Garot[1], Isabelle Danjon[2], Dominique Thébert[2], Louis Nahory[1], Philippe Gros[3], Fiorella Salerno[1] and Philippe Garot[1]*

[1]Institut Cardiovasculaire Paris Sud, Hôpital Privé Jacques CARTIER, Ramsay Santé, Massy, France, [2]Intensive Care Unit Department, Hôpital Privé Jacques CARTIER, Ramsay Santé, Massy, France, [3]Department of Pathology, Praxea Diagnostics, Massy, France

Introduction: Cardiac lymphoma is a rare but serious disease that is usually located in the right heart. The symptoms (dyspnea, respiratory distress, fatigue, syncope…) are not specific and depend on the mass location. Cardiac magnetic resonance has a crucial role in the diagnostic strategy but biopsy is mandatory to confirm the diagnosis.
Case presentation: We report the case of a 63-yeart old man who presented with severe dyspnea and complete atrioventricular block (AVB). A bulky and invasive mass was found in the left atrium extending to the right atrium through the interatrial septum. A cardiac lymphoma was suspected by cardiac magnetic resonance (CMR) imaging and confirmed by transvenous biopsy. The patient was treated with urgent chemotherapy (R-CHOP) and pacemaker implantation. After 4 cycles of R-CHOP the patient was in complete remission with total disappearance of the mass and return of a spontaneous sinus rhythm.
Conclusion: lymphoma is a therapeutic emergency as appropriate treatment can lead to complete remission even when the mass is extensive and invasive. Complete AVB is a potentially reversible complication of cardiac lymphoma, and the decision to implant a pacemaker must be carefully weighed.

KEYWORDS
lymphoma, atrioventicular block, cardiac magnet resonance imaging (CMR), biopsy, chemotherapy

Introduction

Multimodality imaging, and in particular cardiac magnetic resonance (CMR), plays a key role in the diagnostic strategy of cardiac masses (1, 2). However, when a malignancy is suspected, a cardiac biopsy is necessary to distinguish sarcoma from lymphoma, as the treatments are diametrically opposed (1). Lymphomas are most often located in the right heart and rarely involves the left side, but few cases of left heart localization have been reported (3, 4). To our knowledge, we report the first case of a large left-sided cardiac lymphoma complicated by complete atrioventricular block (AVB) that was diagnosed by transvenous imaging-guided biopsy through its extension across the interatrial septum. Our case also illustrates that cardiac lymphoma is a therapeutic emergency, as a rapid intravenous bolus of corticosteroids and chemotherapy can result in rapid regression of

the mass even when the mass is extensive and invasive, and that complete AVB is a potentially reversible complication of cardiac lymphoma.

Case presentation

In March 2022, a 63-year-old man without notable past medical history presented with rapidly progressive exertional dyspnea associated with night sweats. The electrocardiogram revealed complete atrioventricular block (AVB) with a heart rate of 40 beats per minutes and narrow QRS complexes. Lab tests showed anemia with hemoglobin at 9 g/dl, normal renal function and a biological inflammatory syndrome with CRP at 181 mg/L (normal upper limit: 4 mg/L) and the patient was transferred to the intensive care unit with Isoprenaline infusion. The initial workup included a bedside transthoracic echocardiography, which revealed a heterogeneous left atrial mass, measured at 50 × 60 mm, infiltrating the inter-atrial septum with an extension into the right atrium measured at 43 × 26 mm. This mass seemed to be implanted in the lateral wall of the left atrium and prolapsed into the mitral valve causing moderate mitral regurgitation and significant mitral stenosis with a mean gradient ranging from 7 to 14 mmHg. Then, a thoracic, abdominal and pelvic CT scan was performed and showed the cardiac mass associated with a mild pericardial effusion, hilar and mediastinal lymphadenopathy and bilateral moderate pleural effusion (**Figure 1**). The workup was completed by a cardiac magnetic resonance imaging (CMR) study to better characterize the mass. CMR confirmed the presence of a bulky mass with a "cauliflower" appearance, extending throughout the entire left atrium, infiltrating the interatrial septum and the right atrium as well as the basal inferior and inferolateral walls of the left ventricle (**Figure 2A**). This mass appeared isointense on black blood spin echo T1-weighted imaging, slightly hyperintense on fat saturated T2-weighted imaging with a heterogeneous enhancement on late gadolinium enhancement (LGE) sequences (**Figures 2B,C**), suggestive of a malignant tumor. In order to distinguish between cardiac lymphoma or sarcoma, for which initial treatments are diametrically opposed (i.e., urgent chemotherapy vs. surgical resection) (1), a myocardial biopsy guided by transesophageal echocardiography was performed. Four endomyocardial fragments were collected from the right atrial side of the interatrial septum *via* a femoral venous access. Given the persistence of complete AVB at day 7, a VVI single lead transvenous pacemaker was implanted. Prompt pathological analysis revealed the presence of a diffuse large B-cell lymphoma classified as germinal center B cell type (CD10+, BCL6+, MUM1+), with a double expression of MYC/BCL2 (**Figure 3**). Urgent treatment was initiated as soon as the pathology results were obtained, 10 days after the biopsy, with corticosteroids (1 mg/kg) associated with chemotherapy including rituximab, cyclophosphamide, doxorubicin, vincristine, and prednisone (R-CHOP). Six cycles of R-CHOP were completed within 6 months, allowing a clear improvement of the dyspnea and of the overall condition. CT-scan after the fourth cycle of R-CHOP showed complete remission of the lymphoma (2). After setting the MR conditional pacemaker to DOO mode, follow-up CMR revealed complete disappearance of the cardiac mass (**Figures 2D–F**). Because the patient was in spontaneous sinus rhythm at the last visit and the stimulation rate dropped from 100% to 26% after the third R-CHOP cycle, an evaluation by the cardiac electrophysiologist was scheduled 3 months later to assess the percentage of RV pacing for possible pacemaker removal. Written informed consent was obtained from the patient for the publication of any potentially identifiable images or data included in this article.

Discussion

Cardiac lymphoma is a rare disease accounting for only 1.3% of all cardiac tumors and 0.5% of lymphomas (1, 3). There is a male predominance and the mean age at diagnosis is 63 years as in the current case (3). The tumor is most often located in the right heart (atrium or ventricle) and rarely involves the left side, but few cases of left heart localization have been reported (3, 4). The symptoms are not specific and depend on the location of the mass. They may include dyspnea with possible respiratory distress, syncope related

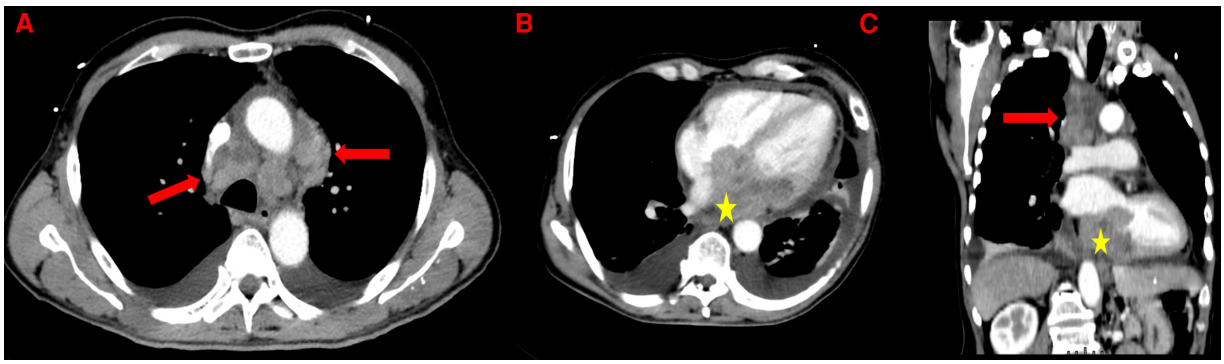

FIGURE 1
Thoracic CT-scan showing mediastinal lymphadenopathies (red arrows) and the left atrial mass (yellow stars) in axial view (A and B) and in coronal view (C). Presence of a bilateral pleural effusion and a thickened pericardium (B).

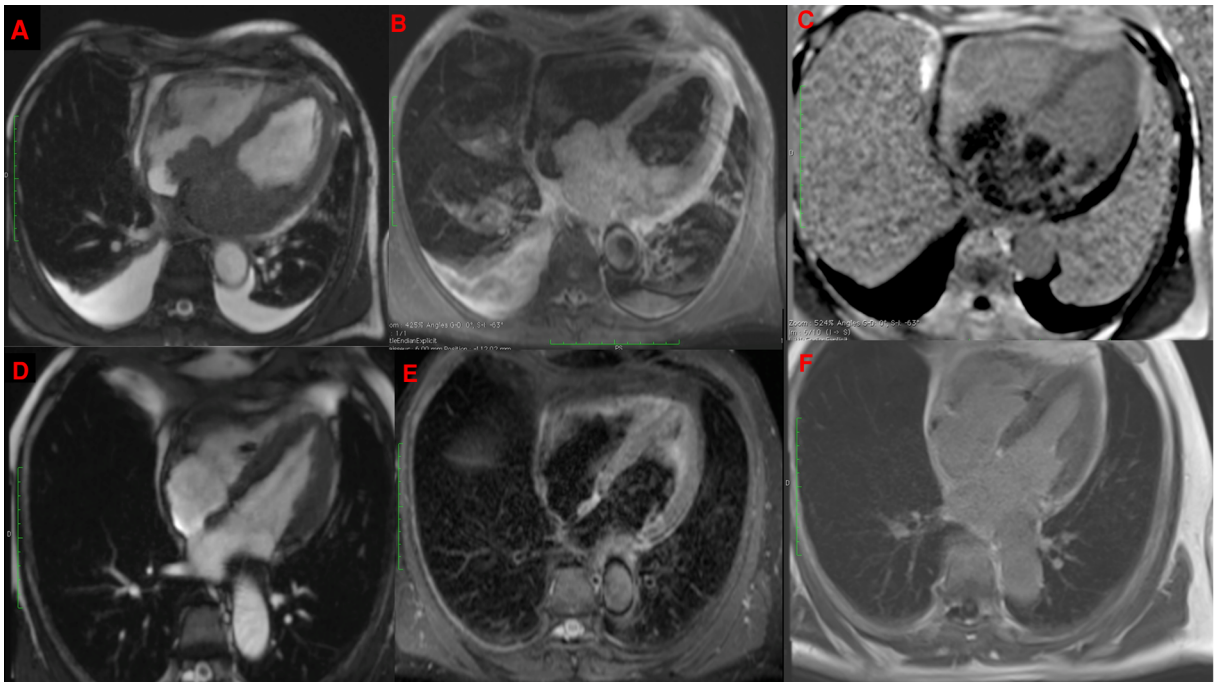

FIGURE 2
CMR showing a bulky mass extending throughout the left atrium, infiltrating the interatrial septum and right atrium, on cine imaging sequence (A), slightly hyperintense on fat-saturated T2-weighted imaging (B) with heterogeneous enhancement on late gadolinium enhancement sequences (C) with complete disappearance after 6 cycles of R-CHOP in the same sequences (D–F).

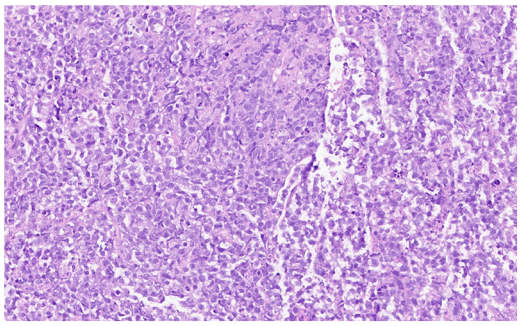

FIGURE 3
Hematoxylin and eosin stain: large lymphocytes cells with moderately abundant cytoplasm and oval nuclei containing several nucleoli corresponding to centroblasts.

to cardiac rhythm or conduction disorders, superior vena cava syndrome as well as altered overall condition and fatigue (3). In our patient's case, the dyspnea was most likely related to the obstructive nature of the tumor through the mitral valve resulting in mitral stenosis and to the complete AVB due to conduction pathway infiltration.

Cardiac masses include benign tumors, primary and secondary malignancies, and other diagnoses (e.g., thrombus, pericardial cyst, and Lambl's excrescences). Multimodality imaging, and in particular CMR, plays a key role in the diagnostic strategy (1) Beyond the localization and mass aspect, T1 and T2 weighted imaging and LGE sequences are crucial to distinguish between benign from malignant tumors (1, 5). Lymphoma generally appears isointense on T1- and T2-weighted imaging (or mildly T2-hyperintense due to diffuse edema) and may or may not show enhancement on LGE sequences. Sarcomas also appear isointense on T1-weighted imaging but show hyperintensity on T2-weighted imaging and heterogeneous enhancement on LGE sequence (1, 5). Because of the slight T2 hyperintensity in our patient, both diagnoses were possible. Nevertheless, the distinction between these two entities is mandatory, because the treatments and outcomes are totally different. Complete surgical resection, that is often difficult and damaging to the cardiac structures is the best option for sarcomas, whereas corticosteroid therapy and chemotherapy should be initiated promptly for cardiac lymphoma (1). Corticosteroids can be started promptly without waiting for the biopsy results if there is a strong clinical suspicion of lymphoma in order to improve the patient's symptoms (6). Surgery is not indicated in the management of cardiac lymphoma except for pathological documentation when transvenous biopsy is not feasible (1). Indeed, histological documentation is required and essential to establish the correct diagnosis and to start the appropriate treatment without delay. Fortunately for our patient, the mass had invaded the right atrium through the interatrial septum and an imaging-guided transfemoral biopsy was possible, which is rarely the case for left heart masses.

Primary cardiac lymphoma in immunocompetent patients –as in this case– are infrequent, accounting for only 1.3% of primary

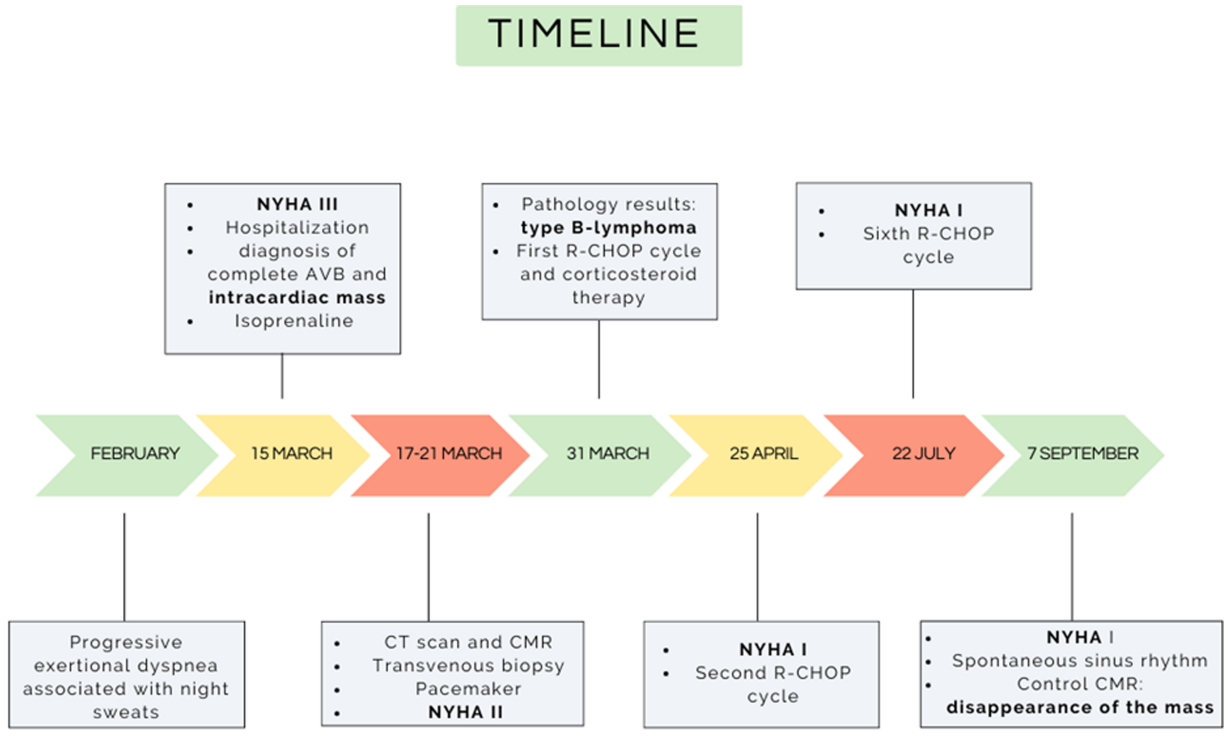

FIGURE 4
Timeline of the case. AVB, atrioventricular block; CMR, cardiac magnetic resonance; CT, computed tomography; NYHA, New York Heart Association.

cardiac tumors (1, 7). The vast majority of cardiac lymphomas are aggressive B-cell lymphomas carrying a poor prognosis, with more than 60% of patients dying within 2 months of diagnosis (1, 8). Predictors of unfavorable outcome include immune status, presence of extracardiac disease, left ventricular involvement, and arrhythmia (3). However, the response rates to chemotherapy ranged between 79% and 87% and unlike cardiac sarcomas, numerous other cases of complete remission have been reported in cardiac lymphomas (9). Most cases of complete remission of cardiac lymphoma involve the right heart, but some cases involving the left side, diagnosed and treated rapidly as in the present one, have also been reported (4, 9).

Complete AV block is a known complication of cardiac tumors, and few cases have been reported in cardiac lymphomas (10, 11). In most of the reported cases, these patients benefited from pacemaker implantation but the conduction disorders improved under chemotherapy, raising the question of the need for permanent pacemaker implantation in this case (10, 11). If the patient is clinically stable, it may be reasonable to delay the pacemaker implantation until evaluation of the clinical response to chemotherapy or to use a temporary pacemaker in the meantime (10). Subramanyam et al. proposed an algorithm for the management of cardiac conduction abnormality in patients with cardiac lymphoma (11). They suggest, in the absence of hemodynamic instability, to wait until performing CMR to assess the extent of cardiac involvement by the tumor before placing the temporary pacemaker. Then, two decisions should be taken: the duration of the temporary pacing before the implantation of a definitive pacemaker and the type of pacemaker to be implanted (i.e., transvenous or leadless) (11). Transition to a permanent pacemaker should be considered in cases of persistent complete AVB with extensive lesions impacting cardiac conduction that are not expected to resolve in a few weeks, as in our patient's case (11) There are no recommendations on the type of pacemaker that should be implanted and, if dual chamber pacing is not required, a leadless pacemaker could be considered in these patients who are at high risk of infection (11). However, no study has yet compared transvenous and leadless pacemakers in cancer patients in terms of complication rates. Thus, the management of cardiac conduction disorders associated with lymphoma is complex and requires close coordination between cardiology and oncology teams. In our patient's case, the pacing rate dropped from 100% to 26% after the third cycle of R-CHOP, and a reevaluation by the cardiac electrophysiologist was planned to discuss possible removal of the device.

Despite the complete remission, the patient will be followed closely by cardiac and thoracic imaging with rigorous hematological monitoring because recurrence risk (often extracardiac) estimated at 55% (9).

Conclusions

A prompt cardiac biopsy, ideally percutaneous and guided by imaging should be performed if a malignant cardiac tumor is

suspected in order to select the appropriate treatment. Cardiac lymphoma should be considered as a therapeutic emergency, since prompt intravenous bolus of corticosteroids and chemotherapy can provide rapid regression of the mass and ultimately complete remission even when the mass is extensive and invasive. Complete AVB is a potentially reversible complication of cardiac lymphoma, and the decision to implant a pacemaker must be carefully weighed (**Figure 4**).

Data availability statement

The original contributions presented in the study are included in the article/Supplementary Material, further inquiries can be directed to the corresponding author.

Ethics statement

Ethical review and approval was not required for the study on human participants in accordance with the local legislation and institutional requirements. The participants provided their written informed consent to participate in this study and written informed consent was obtained from the participants for the publication of this case report. Written informed consent was also obtained from the patient for the publication of any potentially identifiable images or data included in this article.

Author contributions

Drafting of the manuscript: BY, GJ and GP; Critical revision for important intellectual content: all authors. All authors contributed to the article and approved the submitted version.

Conflict of interest

The authors declare that the research was conducted in the absence of any commercial or financial relationships that could be construed as a potential conflict of interest.

Publisher's note

All claims expressed in this article are solely those of the authors and do not necessarily represent those of their affiliated organizations, or those of the publisher, the editors and the reviewers. Any product that may be evaluated in this article, or claim that may be made by its manufacturer, is not guaranteed or endorsed by the publisher.

References

1. Tyebally S, Chen D, Bhattacharyya S, Mughrabi A, Hussain Z, Manisty C, et al. Cardiac tumors: jACC CardioOncology state-of-the-art review. *JACC CardioOncol*. (2020) 2:293–311. doi: 10.1016/j.jaccao.2020.05.009

2. Younes A, Hilden P, Coiffier B, Hagenbeek A, Salles G, Wilson W, et al. International working group consensus response evaluation criteria in lymphoma (RECIL 2017). *Ann Oncol*. (2017) 28:1436–47. doi: 10.1093/annonc/mdx097

3. Petrich A, Cho SI, Billett H. Primary cardiac lymphoma. *Cancer*. (2011) 117:581–9. doi: 10.1002/cncr.25444

4. Chin JY, Chung MH, Kim JJ, Lee JH, Kim JH, Maeng IH, et al. Extensive primary cardiac lymphoma diagnosed by percutaneous endomyocardial biopsy. *J Cardiovasc Ultrasound*. (2009) 17:141. doi: 10.4250/jcu.2009.17.4.141

5. Pazos-López P, Pozo E, Siqueira ME, García-Lunar I, Cham M, Jacobi A, et al. Value of CMR for the differential diagnosis of cardiac masses. *JACC Cardiovasc Imaging*. (2014) 7:896–905. doi: 10.1016/j.jcmg.2014.05.009

6. Lestuzzi C, Spina M, Martellotta F, Carbone A. Massive myocardial infiltration by HIV-related non-hodgkin lymphoma: echocardiographic aspects at diagnosis and at follow-up. *J Cardiovasc Med (Hagerstown)*. (2012) 13:836–8. doi: 10.2459/JCM.0b013e3283511fa7

7. Gowda RM, Khan IA. Clinical perspectives of primary cardiac lymphoma. *Angiology*. (2003) 54:599–604. doi: 10.1177/000331970305400510

8. Lamba G, Frishman WH. Cardiac and pericardial tumors. *Cardiol Rev*. (2012) 20:237–52. doi: 10.1097/CRD.0b013e31825603e7

9. Carras S, Berger F, Chalabreysse L, Callet-Bauchut E, Cordier JF, salles G. Primary cardiac lymphoma: diagnosis, treatment and outcome in a modern series. *Hematol Oncol*. (2017) 35:510–9. doi: 10.1002/hon.2301

10. Crisel RK, Knight BP, Kim SS. Reversible, complete atrioventricular block caused by primary cardiac lymphoma in a nonimmunocompromised patient. *J Cardiovasc Electrophysiol*. (2012) 23:1386–9. doi: 10.1111/j.1540-8167.2012.02343.x

11. Subramanyam P, Mahmood SS, Dinsfriend W, Pastore RD, Martin P, Chan AT, et al. Infiltrative lymphoma-associated bradycardia and cardiac conduction abnormalities. *JACC CardioOncol*. (2020) 2:135–8. doi: 10.1016/j.jaccao.2020.01.002

frontiers | Frontiers in Cardiovascular Medicine

TYPE Case Report
PUBLISHED 19 April 2023
DOI 10.3389/fcvm.2023.1020082

Check for updates

OPEN ACCESS

EDITED BY
Carlo Gabriele Tocchetti,
University of Naples Federico II, Italy

REVIEWED BY
Zoltan Varga,
Semmelweis University, Hungary
Iris Parrini,
Hospital Mauritian Turin, Italy

*CORRESPONDENCE
Mohammadbagher Sharifkazemi
dr.sharifkazemi@gmail.com

SPECIALTY SECTION
This article was submitted to Cardio-Oncology, a section of the journal Frontiers in Cardiovascular Medicine

RECEIVED 15 August 2022
ACCEPTED 24 March 2023
PUBLISHED 19 April 2023

CITATION
Sharifkazemi M, Elahi M and Sayad M (2023) Case report: Early acute myocarditis after radiation therapy for breast cancer: A case presentation and review of literature. Front. Cardiovasc. Med. 10:1020082. doi: 10.3389/fcvm.2023.1020082

COPYRIGHT
© 2023 Sharifkazemi, Elahi and Sayad. This is an open-access article distributed under the terms of the Creative Commons Attribution License (CC BY). The use, distribution or reproduction in other forums is permitted, provided the original author(s) and the copyright owner(s) are credited and that the original publication in this journal is cited, in accordance with accepted academic practice. No use, distribution or reproduction is permitted which does not comply with these terms.

Case report: Early acute myocarditis after radiation therapy for breast cancer: A case presentation and review of literature

Mohammadbagher Sharifkazemi[1]*, Mahsa Elahi[2] and Masoud Sayad[3]

[1]Department of Cardiology, Nemazee Hospital, Shiraz University of Medical Sciences, Shiraz, Iran, [2]Radiation Oncology Department, Nemazee Hospital, Shiraz University of Medical Sciences, Shiraz, Iran, [3]Cardio-Oncology Department, Rajaie Heart Hospital, Iran University of Medical Sciences, Tehran, Iran

Breast cancer is the most commonly diagnosed cancer in women worldwide, and with the increased survival of patients by novel treatments, the frequency of complications of cancer treatments rises. Radiotherapy, especially on the chest wall, can damage different cardiac structures. Radiotherapy-induced cardiomyopathy mainly occurs over 10 years after breast cancer treatment; however, there is a gap in the literature on acute myocarditis following radiotherapy. Here, we present a 54-year-old woman who developed acute myocarditis shortly after 25 sessions of radiotherapy with 50 Gy of radiation, successfully diagnosed with the use of speckle tracking echocardiography (STE) and cardiac magnetic resonance (CMR), and responded to the medical treatment with relative clinical improvement until the final follow-up. This case suggests the necessity of detailed examination of patients after radiotherapy, not only for chronic occurrence of cardiomyopathy but also for acute myocarditis. Although STE and CMR resulted in accurate diagnosis, in this case, further studies are required to determine the diagnostic accuracy of these two imaging methods compared with other imaging modalities in such patients and investigate the best diagnostic tool and therapeutic approach for these patients.

KEYWORDS
radiation-induced, cardiomyopathies, acute myocarditis, myocarditis, breast cancer

Introduction

Cardiovascular diseases (CVDs) and cancers are the top causes of death worldwide, and female breast cancer is the most diagnosed cancer with an increasing trend (1). With the advances in early diagnostic and new treatment approaches, the survival of patients improves, resulting in the increased occurrence of cancer treatment complications (2). Certain types of chemotherapy can lead to cardiovascular complications because of their cardiotoxic effects (3). Radiotherapy (RT) can also result in coronary artery disease (by the induction and acceleration of atherosclerosis through endothelial damage), as well as fibrotic damage to the valves, pericardium, and myocardium, with an estimated incidence of 10%–30%, occurring 5–10 years after treatment, known as radiation-induced heart disease (RIHD) (4).

Cardiomyopathy, induced by RT, is mainly silent (without clinical symptoms) with minor electrocardiography (ECG) changes, and the diagnosis is usually made by the

abnormal findings of transthoracic echocardiography (TTE) and cardiac magnetic resonance imaging (CMR) (5). Furthermore, RT-induced cardiomyopathy generally develops over 10 years after RT, when the patient does not refer to the physician regularly, which increases the chance of missed diagnosis (6). However, the acute development of cardiomyopathy and other RIHDs should also be considered (7). Here, we present a case with the occurrence of acute myocarditis after RT for breast cancer, successfully diagnosed with the use of speckle tracking echocardiography (STE) and CMR and responded to the medical treatment until the final follow-up.

Case presentation

A 54-year-old woman, with known case of diabetes mellitus (DM, controlled with oral hypoglycemic pills) and ischemic heart disease (left main and advanced three-vessel disease), presented to our center with complaints of dyspnea on exertion and orthopnea, with neither feverishness, sputum production, nor chest pain. She was a nonsmoker, had a body mass index of 23 kg/m^2, her blood pressure was 105/64 mmHg, heart rate was 110 bpm, and respiratory rate was 28/min. She had no family history of cardiomyopathy. She had been on daily oral long-acting nitrate (nitrocontin 2.6 mg twice a day), 6.25 mg carvedilol thrice a day, 80 mg aspirin once a day, and 20 mg rosuvastatin once a day. Six months before her referral, left breast cancer was diagnosed for the patient (invasive ductal cell carcinoma, T1BN0M0, positive estrogen receptor), and she underwent a left-sided mastectomy (R0 resection) and conventional RT, which included 25 courses of 50-Gy external beam RT with a compact machine (6 MV photon 3D conformal therapy), delivered within 5 weeks. Computed tomography (CT) simulation was done before planning. The clinical target volume was 185.7 and the planned target volume was 548.3; we did not have gross tumor volume (GTV) because the patient underwent surgery, and the gross tumor was resected surgically. Organs at risk (OAR) included the heart, the left and right lung, and the cord. For sparing OARs, the patient was initially immobilized in the treatment position, with immobilization devices (supine breast boards); and posterior jaw was set at zero to half-beam block/beam split to minimize dose of lung and heart. Gantry angle, collimator angle, and table angle were adjusted to optimize coverage of desired targets, while minimizing normal tissue inclusion within the field. Three-dimensional (3D) treatment planning was done for delineation of the breast, heart, lungs, and the cord. All of these organs received radiotherapy less than their tolerant dose. In this plan, mean dose of the heart was 541.7 cGy. The dose–volume histogram is provided in the **Supplementary Figure**. After RT, the patient developed the symptoms mentioned earlier, which resulted in the referral of the patient to the physician. She remained afebrile in several visits. On physical examination, she had tachycardia and tachypnea; on auscultation, third and fourth heart sound (S3 and S4) and lung crackle were detected.

In the history, the patient was under cardiac follow-up because of the right ventricular outflow tract tachycardia (RVOT VT) with the impression of idiopathic type, left ventricular (LV) ejection fraction (EF) of 49%, and negative single-photon emission computed tomography (SPECT) for more than 2 years. Also, 24-h ECG Holter recordings showed sinus tachycardia, in addition to nonspecific ST-T changes in the precordial leads with premature ventricular complexes (PVC) of 24%, for which medical treatment with 40 mg verapamil thrice a day was prescribed 2 years ago. Four months later, with 14.7% PVC count and a drop in LV EF to 31%, the patient was scheduled for PVC ablation. However, because of the demonstration of calcified coronaries in fluoroscopy, she underwent diagnostic angiography, which determined left main and three-vessel disease, according to which the treatment strategy shifted to coronary artery bypass grafting (CABG). After the surgery, LV EF improved to 48%, and PVC count reached <1% in serial ECG Holter follow-up.

Before mastectomy, TTE evaluation (performed for estimation of surgical risk) showed an LV EF of 42% and a global longitudinal strain (GLS) of −18.2% (**Figures 1**, **2A**) with mild ischemia in the apex on SPECT. Before RT, PVC was 6% in the 24-h ECG Holter monitoring. After RT, the frequency of PVCs during 24-h Holter monitoring raised to 13.8%, accompanied by a drop of LV EF to 29% (from 42%) and GLS to −11.2% (from 18.2%, **Figures 2B**, **3**). LV EF was measured by 2D TTE and was calculated using Simpson's method. She did not receive any course of chemotherapy at all.

The results of serum tests showed a high sensitivity troponin I level six times above the normal limit (up to 14 ng/L), evaluated using high sensitivity (hs) troponin I assay technique, high level of lactate dehydrogenase (LDH), creatine phosphokinase (CPK), aspartate aminotransferase (AST), estimated sedimentation ratio (ESR), C-reactive protein (CRP), and mild elevated total white blood cell (WBC) count (about 12,000), as well as elevated N-terminal pro-B-type brain natriuretic peptide (NT pro-BNP) (six times above the normal limit). Serum lipids were within normal limits (cholesterol = 162 mg/dl, LDL = 58 mg/dl, HDL = 41 mg/dl, and triglyceride = 166 mg/dl). The viral antibody markers were negative, which include Coxsackie virus group B, human immunodeficiency virus (HIV), cytomegalovirus, Epstein–Barr virus, hepatitis virus family, and influenza virus.

The patient did not accept to undergo endomyocardial biopsy. CMR was performed using a Siemens Skyra 3 T MRI scanner with the application of real-time cine images of LV, short inversion time inversion-recovery (STIR) T2-weighted image (T2WI), T2 mapping, native and postcontrast T1 mapping, and delayed postcontrast images. The results of CMR showed diffuse myocardial inflammation in T1 mapping and extracellular volume (ECV) map of LV, mid-wall late gadolinium enhancement (LGE) in basal segments of the interventricular septum (IVS), and subepicardial delayed enhancement in the basal inferolateral segments of LV without an ischemic pattern of myocardial injury (**Figure 4**). The regions marked as LGE on MRI refer to the presence of fibrosis in the patient. Matching the patient's clinical signs and symptoms with the European guideline for clinically suspected myocarditis, the diagnosis was considered as active myocarditis.

The prescribed medications included: carvedilol (12.5 mg twice a day), spironolactone (25 mg once a day), furosemide

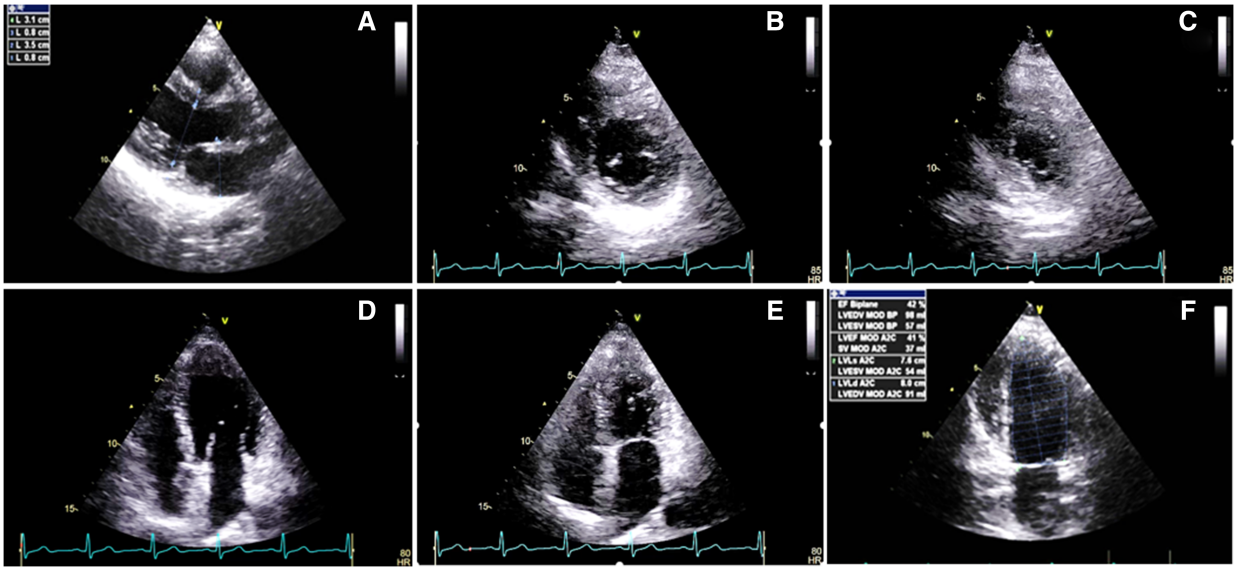

FIGURE 1
Two-dimensional transthoracic echocardiography 1 week before the radiotherapy course (A–F), illustrating the normal thickness of the left and right ventricular walls, in addition to global mild left ventricular systolic dysfunction: (A) PLAX view. (B) PSAX in the end-diastole. (C) PSAX in the end-systole. (D) A4C view in the end-diastole. (E) A4C view in the end-systole. (F) LV EF = 42% by Simpson's method. PLAX, parasternal long axis view; PSAX, parasternal short axis view; A4C, apical four chamber view.

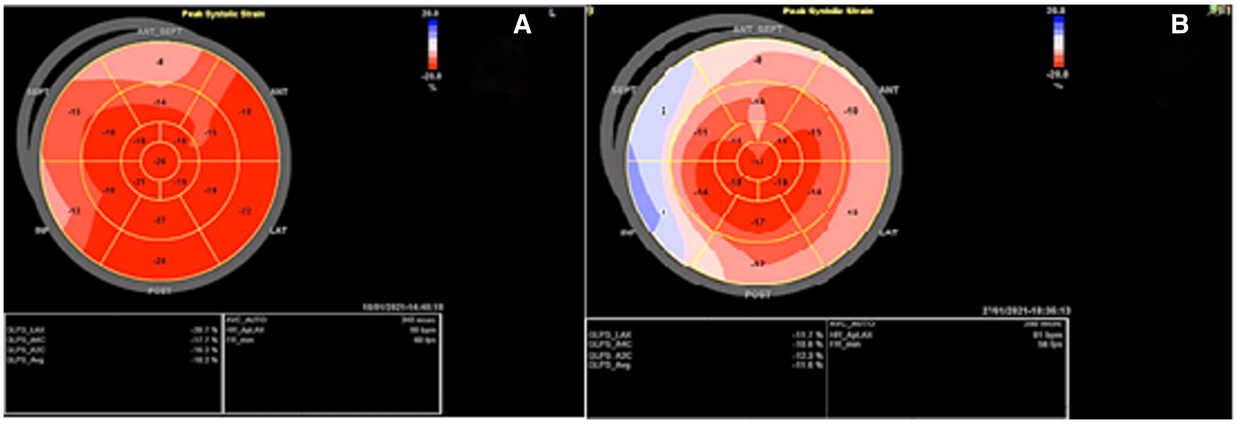

FIGURE 2
Speckle tracking echocardiography before and after the radiotherapy course: (A) Before radiotherapy, which showed a global longitudinal strain of –18.2% with myocardial performance impairment in the bases of inferior, septal, and anteroseptal walls a week. (B) After radiotherapy, which showed GLS: –11.2% with evidence of severe myocardial performance impairment accompanied by relative apical sparing.

(40 mg twice a day), rosuvastatin (20 mg once a day), and prednisolone (10 mg once a day). Prednisolone and other medications were prescribed for improving cardiac function based on the available evidence (8, 9). Statin was prescribed considering the LDL level <60 mg/dl. At follow-up visit (2 weeks later), the patient was clinically stable without improvement of echocardiographic or STE findings: LV EF = 33% with normal LV size and focal increased myocardial thickness in the mid to apical lateral segments of the LV. Also, CT angiography at follow-up (10 months after RT) showed patent coronary grafts.

The timeline of the signs, symptoms, and diagnostic and therapeutic procedures are shown in Table 1, arranged in chronological order. On arrival, at the first cardiologist's visit (after the radiotherapy), her symptoms were classified as New York Heart Association (NYHA) class III; after the treatment, it reduced to NYHA class I. The patient gave consent for all steps of the diagnostic procedure and cooperated with the physician. The cardiologist in charge was open to listen to the patient's opinion and reflected them in the medical records. Comparison between the values measured at the baseline and at the follow-up is provided in Table 2.

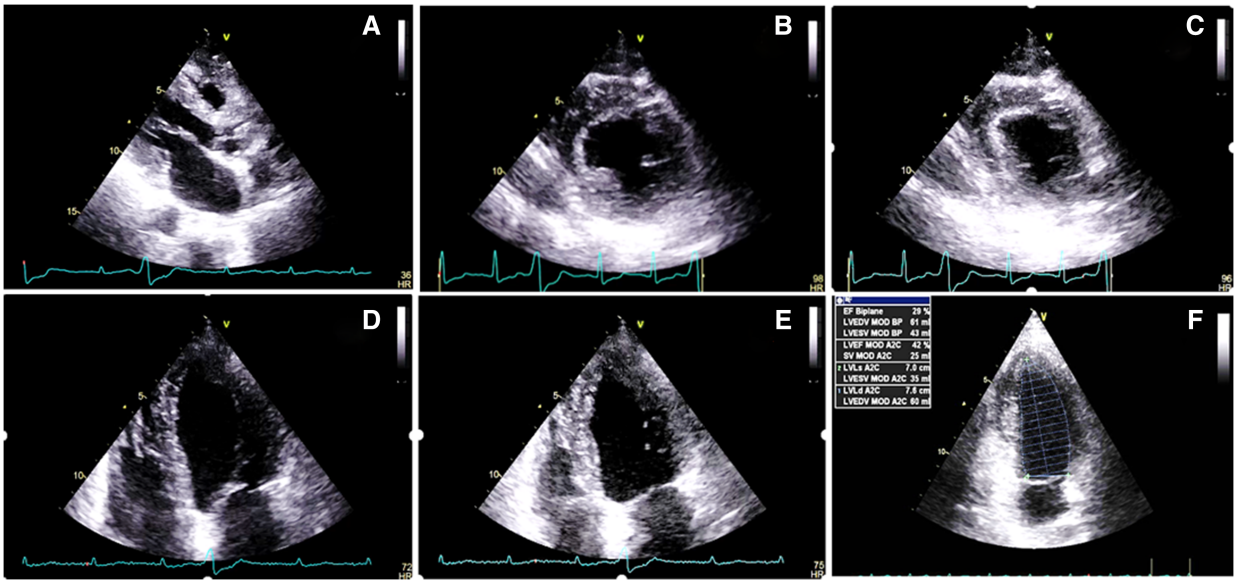

FIGURE 3
Two-dimensional transthoracic echocardiography 1 month after the radiotherapy course (A–F), illustrating a marked increase in the thickness of the left and right ventricular walls (15 and 7 mms, respectively), in addition to severe left ventricular systolic dysfunction. (A) PLAX view. (B) PSAX in the end-diastole. (C) PSAX in the end-systole. (D) A4C view in the end-diastole. (E) A4C view in the end-systole. (F) LV EF = 28% by Simpson's method. PLAX, parasternal long axis view; PSAX, parasternal short axis view; A4C, apical four chamber view.

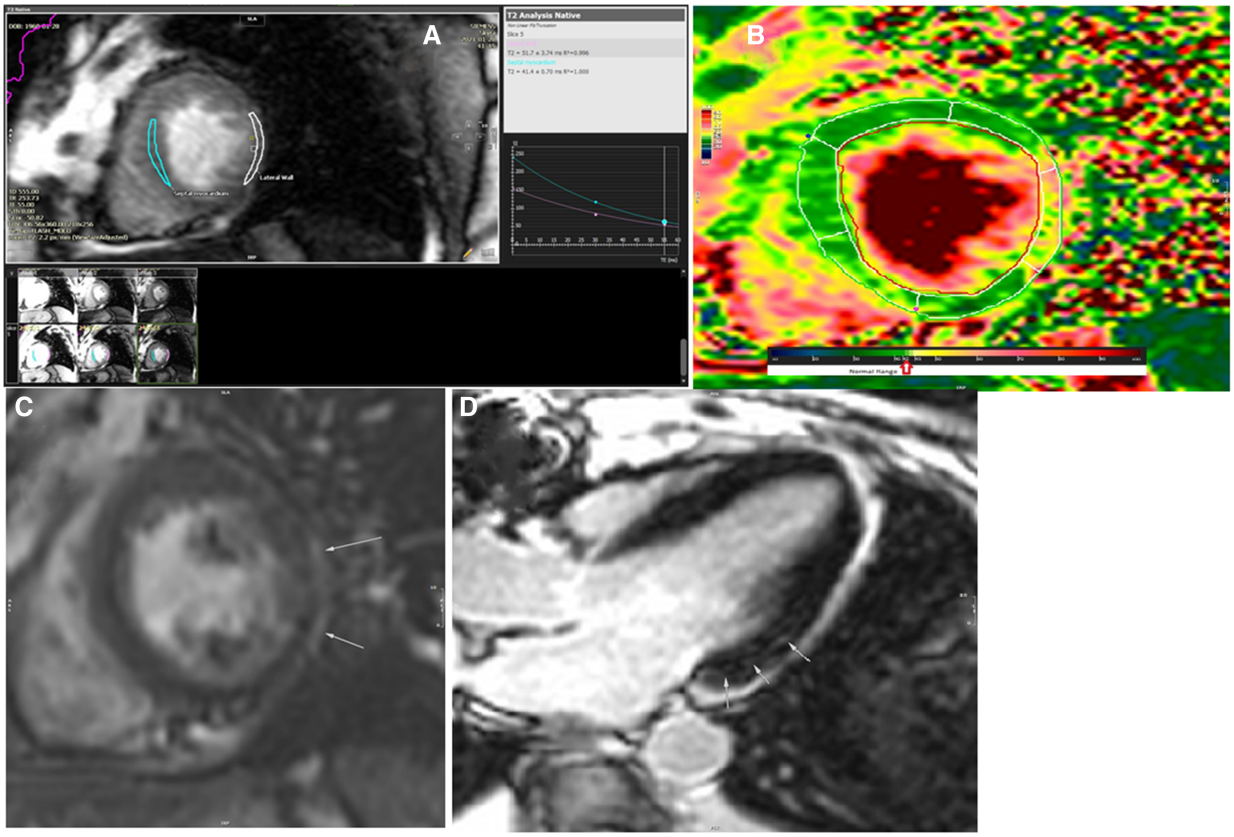

FIGURE 4
The results of cardiac magnetic resonance imaging after the radiation (A–D). (A) T2 analysis of mid-septal and mid-lateral segments of the left ventricle revealed prolongation of T2 relaxation time in the mid to apical segments of the lateral wall (52 ms). (B) T2 map image of the left ventricle in short axis view showed abnormal T2 value in the mid-lateral segment of the left ventricle. (C) Delayed postcontrast image of the left ventricle in short axis view showed a subepicardial rim of late gadolinium enhancement on the lateral wall of the left ventricle. (D) Delayed postcontrast image of the left ventricle in long axis three-chamber axis view revealed small focal subepicardial to mid-wall patches of late gadolinium enhancement in the basal inferolateral segment.

TABLE 1 Timeline of the presenting symptoms, diagnostic, and therapeutic procedures.

6 months before referral to our clinic	Coronary artery bypass graft surgery.
9 weeks before referral to our clinic	Transthoracic and STE (performed before surgery for estimation of surgical risk) showed LV EF of 42% and GLS of −18.2%, with mild ischemia in apex on single-photon emission computed tomography.
7 weeks before referral to our clinic	Mastectomy.
5 weeks before referral to our clinic	Radiotherapy for 25 days.
Day 0	The last fraction of radiation therapy.
Day 10	Symptoms that lasted for 10 days before referral to our clinic: dyspnea on light exertion and two-pillow orthopnea. Her symptoms were classified as New York Heart Association functional class III heart failure. Signs: Heart rate =110 bpm, respiratory rate =28 /min, and blood pressure =105/64 mmHg. On heart auscultation, she had S3 and S4, lung rales and crackle. A 12-lead electrocardiogram exhibited sinus tachycardia accompanied by nonspecific ST-T changes in the precordial leads. Premature ventricular count was 13.8% during 24-h Holter monitoring, accompanied by LV EF of 29% and global longitudinal strain of −11.2%.
Day 11	The results of serum tests showed a high sensitivity troponin I level 6 times above the normal limit (up to 14 ng/L), high levels of lactate dehydrogenase, creatinine phosphokinase, aspartate aminotransferase, C-reactive protein, and mild elevated total white blood cell count, as well as elevated NT pro-brain natriuretic peptide (6 times above the normal limit). Viral markers were negative.
Day 11	The results of cardiac magnetic resonance showed diffuse myocardial inflammation in T1 mapping, mid-wall late gadolinium enhancement in basal segments of interventricular septum, and subepicardial delayed enhancement in basal inferolateral segments.
Day 25	The patient was clinically stable without improvement of echocardiographic or STE findings (LV EF = 33%, global longitudinal strain =−11.9%).

LV EF, left ventricular ejection fraction; STE, speckle tracking echocardiography; GLS, global longitudinal strain.

TABLE 2 Transthoracic and speckle tracking echocardiographic findings: Baseline and postradiotherapy.

Dimensions	Baseline	Post-RT (day 10)
LVIDD (mm)	46	57
LVIDS (mm)	34	44
LVPW (D) (mm)	8	9
IVS (D) (mm)	8	9
LVPW (S) (mm)	10	10
IVS (S) (mm)	10	10
LVED volume (ml)	50.0	62
LVES Volume (ml)	24.8	44
LVEF (Simpson's) (%)	42	29
GLS (Average) (%)	−18.2	−11.2
RVIDD (Base) (mm)	33	32
TAPSE (mm)	13	13
IVC dimension (mm)	15	14
Left atrium (ES) (mm)	30	32
LAVI (ml/m^2)	32	33
Sinus of Valsalva (mm)	31	31
AorticrRoot (mm)	29	30
Lateral e' (cm/s)	8	7
Septal e' (cm/s)	7	6
Mitral E/A	0.67	0.61

LVIDD, left ventricular internal dimension in diastole; LVIDS, left ventricular internal dimension in systole; LVPW, left ventricular posterior wall; LVED, left ventricular end diastole; LVES, left ventricular end systole; RVIDD, right ventricular internal dimension in diastole; TAPSE, tricuspid annular plane systolic excursion; IVC, inferior vena cava; ES, end systole; LAVI, left atrial volume index; IVS, interventricular septum; LV EF, left ventricular ejection fraction; GLS, global longitudinal strain.

Discussion

Our case developed acute myocarditis after completing RT sessions. Pre-radiotherapy cardiac examinations, including ECG, echocardiography, and SPECT nuclear scan, were negative; therefore, the patient did not have any diagnosed coronary as well bypass graft failure in blood supply to the heart before radiation. Matching the postradiation clinical signs and results of cardiac examinations (reduced LV EF, reduced GLS, increased frequency of PVC complexes, and increased serum levels of inflammatory markers) with the European guideline of diagnosis of myocarditis guided the physician toward RIHD (10); diagnosis could be proved by biopsy analysis, but our patient refused to undergo cardiac biopsy. Therefore, CMR was performed for the patient, which showed acute myocarditis without an ischemic pattern. With the prescribed medications, the patient's clinical symptoms and signs improved and she had stable echocardiographic manifestations until the last follow-up.

Although the cardiotoxic effects of RT is a known quantity, the frequency and severity of myocardial damage are not parallel in all patients and depend on several factors, including the site of action, radiation dose, the method of administration, and patients' characteristics, such as underlying CVDs or their risk factors, and the current or previous use of other antineoplastic therapies (11). Because of the proximity of the breast to the heart, RIHD can damage the heart and increase the risk of valvular heart disease, coronary artery disease, cardiomyopathy, congestive heart failure, and acute myocardial infarction, and pericarditis is higher in those with left-sided breast cancer (12, 13). Also, in the acute phase, most patients demonstrate ECG changes, such as abnormal heart rate, poor R wave progression and septal ST changes, RT-associated bundle branch block, and rarely complete heart block (14). The mechanism of RIHD is related to the microvascular ischemia that can disrupt the capillary endothelial framework (increase the capillary permeability) and cause hypoxia and injury to differentiated myocytes that result in the deposition of collagen and fibrosis (14, 15).

Patients with an underlying CVD and/or other diseases, including hypertension and DM, have also a higher vulnerability to the RT-induced endothelial damage and are thus at a higher risk of RIHD (11, 16); our patient also had a positive history of three-vessel disease and CABG 2 years before her mastectomy plus RT. The history of DM also predisposed the patient to endothelial dysfunction and systemic inflammatory reaction that could pave the path for the cardiotoxic effects of RT (16, 17). It is thus important to differentiate the RIHD from the cardiac

diseases, such as cardiomyopathy or ischemic heart disease, the patient had before RT or developed after RT due to other causes. History of RT and the clinical signs and symptoms, suggested by the European guideline, can help with the diagnosis (10). It is worth mentioning that the combination of cancer treatment with chemotherapy has also been shown to increase the risk of RIHD in these patients (12, 18), but our patient had received no chemotherapy course at all.

Considering the high prevalence of breast cancer and the risk of damage to the adjacent organs, a high incidence has been reported for RIHD within 2 years of RT (11). Accordingly, several modifications have been suggested for sparing the heart from the toxic effects of RT, such as more accurate mapping by three-dimensional methods, additional maneuvers for displacing the heart from the radiation field, and advanced radiation methods (19), like intensity- and volumetric-modulated radiation therapy, to decrease the dose of radiation delivered to the heart, defined as the mean heart dose (MHD) (20). Also, the risk of RIHD has been shown to be positively associated with the radiation dose and increased per Gy of radiation (21). The cumulative risk of acute coronary event is reported to increase by 16.5% per Gy; the volume of the left ventricle receiving 5 Gy is identified as the most important prognostic dose–volume parameter (7). Despite the recommendations to reduce the MHD, some areas of the heart are exposed to higher radiation doses, which result in the occurrence of cardiac damage, even in small doses of radiation (16). 20–30 Gy has been considered as a high dose (6) and patients with a mediastinal radiation of ≤30 Gy had no increased risk for RIHD, while those >30 Gy reported a 3.5-fold increased risk. Of note, the radiotherapy dose in the case presented here did not pass 30 Gy (22). Thus, severe RIHD is not anticipated in this patient, although long-term follow-up should be performed for evaluating this issue. In addition to the above-mentioned factors, other patient-related risk factors, such as age at diagnosis, also influence the risk of RIHD development (7).

Pericardial fibrosis is caused by collagen deposition in the interstitium and parietal region of the thickened pericardium. Collagen deposition in the cardiac tissue results in RT-induced myocardial fibrosis that replaces cardiomyocytes (6). The oxidative injury and release of proinflammatory cytokines, altered coagulation and platelet activity, and altered permeability of cell membranes finally result in fibrosis and myocardial cell death (23, 24), which justifies the increased serum levels of inflammatory markers in the patient presented here. The cardiac biomarkers, hs Troponin I and NT pro-BNP, elevated in the patient presented here, have also been suggested as valuable serum biomarkers for early prediction of RIHD in patients with breast cancer (25, 26). Therefore, these markers have been suggested as available and easy methods to be used for the early screening of patients after RT (27). However, there is a lack of evidence-based literature for screening the presence and intensity of cardiac damage (28).

Abnormalities observed on ECG, such as arrhythmia, ST segment depression, and conduction block, can help diagnosis, but are not always present, and multimodality imaging techniques are suggested to be used for accurate diagnosis (29). Our patient also demonstrated an increased rate of PVCs on 24-h Holter ECG monitoring. Another issue concerning diagnosis is that the RT-induced myocardial fibrosis is mainly silent, and half of the cases that develop myocardial perfusion defects have no clinical signs and symptoms, sometimes found incidentally by TTE (11). In the case presented here, the patient had no clinical signs but showed reduced LV EF compared with that before mastectomy. However, our patient was a known case of CVD, and thus cardiac examination was performed for the patient, while diagnosis may be missed in patients with the late occurrence of cardiac damage, which includes most of the cases (30). One of the novelties of the case presented here is the occurrence of myocardial damage shortly after RT.

Although ECG and TTE are suggested as the preferred tools used for the assessment of the cardiovascular damage induced by RT, they may not be sensitive for the detection of myocardial fibrosis (27). Accordingly, CMR has been recommended for reflection of global and regional function, such as myocardial function and diagnosis of fibrosis (31). As STE has also been suggested as an appropriate tool for early diagnosis of RT-induced LV dysfunction (32), in the present study, we examined the myocardial strain using both CMR and STE, which helped the physician achieve the final diagnosis for the patient. The histopathological examination (and direct observation of myocardial cell degeneration) could have resulted in a definite diagnosis (31), not performed in our patient because of the lack of patient's consent.

The general therapeutic strategies suggested for RT-induced myocardial injury include antioxidants and anti-inflammatory agents, statins, and angiotensin-converting enzyme inhibitors; however, the treatment strategy is mainly selected individually based on the identified myocardial pathology and underlying diseases (33). In our case, the prescription of beta-blockers, mineralo recetore antagonist (MRA), furosemide, rosuvastatin, and low-dose oral steroid therapy resulted in clinical stability of the patient without changes in cardiac function (LV EF = 33%). Because of the lack of evidence on the best therapeutic approach in patients with acute myocarditis following RT, more studies are required to determine the best therapeutic approach for such patients.

Conclusion

The case presented here suggested the necessity of detailed examination of patients after radiotherapy, not only for chronic occurrence of cardiomyopathy but also for the early occurrence of acute myocarditis. The three layers of the endocardium, myocardium, and epicardium can be affected by the RT, both at early and late phases. It has to be kept in mind that RIHD can also occur in the early phase, resulting in acute diseases, which can be of great significance. Therefore, it is suggested to pay greater attention to the risk factors of RIHD that can help the physician in the identification of patients with a higher risk. Also, the literature suggests that the available screening methods,

such as serum tests, ECG, and TTE, can help with the diagnosis in some cases. However, the screening methods cannot result in a definite diagnosis. Here, we showed that STE and CMR could accurately diagnose LV dysfunction and myocarditis in a patient. However, further studies are required to determine the diagnostic accuracy of these two imaging methods compared with other imaging modalities in such patients in order to determine the best diagnostic tool for these patients. Also, the follow-up examination of the patient showed the appropriateness of the treatment strategy used for this patient, while there are no specific guidelines for the most appropriate treatment approach for such patients, and more studies are required in this regard.

Data availability statement

The raw data supporting the conclusions of this article will be made available by the authors, without undue reservation.

Ethics statement

Ethical review and approval was not required for the study on human participants in accordance with the local legislation and institutional requirements. The patients/participants provided their written informed consent to participate in this study. Written informed consent was obtained from the individual(s) for the publication of any potentially identifiable images or data included in this article.

Author contributions

MS (first author): Cardiologist in charge who performed the acquisition, description, and interpretation of 2D and STE echocardiograms; contributed to data collection, original draft preparation, literature search, manuscript editing, and critically reviewed the manuscript for important intellectual content, and approved the final version. ME and MS (third author): MD in charge who extracted the data from the patient's file and checked and added them in the manuscript, contributed to gathering data, critically reviewed the manuscript for important intellectual content, and approved the final version. All authors contributed to the article and approved the submitted version.

Conflict of interest

The authors declare that the research was conducted in the absence of any commercial or financial relationships that could be construed as a potential conflict of interest.

Publisher's note

All claims expressed in this article are solely those of the authors and do not necessarily represent those of their affiliated organizations, or those of the publisher, the editors and the reviewers. Any product that may be evaluated in this article, or claim that may be made by its manufacturer, is not guaranteed or endorsed by the publisher.

Supplementary material

The Supplementary Material for this article can be found online at: https://www.frontiersin.org/articles/10.3389/fcvm.2023.1020082/full#supplementary-material.

SUPPLEMENTARY FIGURE
Dose volume histogram of the radiation.

References

1. Sung H, Ferlay J, Siegel RL, Laversanne M, Soerjomataram I, Jemal A, et al. Global cancer statistics 2020: GLOBOCAN estimates of incidence and mortality worldwide for 36 cancers in 185 countries. *CA Cancer J Clin*. (2021) 71:209–49. doi: 10.3322/caac.21660

2. Miller KD, Nogueira L, Mariotto AB, Rowland JH, Yabroff KR, Alfano CM, et al. Cancer treatment and survivorship statistics, 2019. *CA Cancer J Clin*. (2019) 69:363–85. doi: 10.3322/caac.21565

3. Gegechkori N, Haines L, Lin JJ. Long-term and latent side effects of specific cancer types. *Med Clin North Am*. (2017) 101:1053–73. doi: 10.1016/j.mcna.2017.06.003

4. Wang H, Wei J, Zheng Q, Meng L, Xin Y, Yin X, et al. Radiation-induced heart disease: a review of classification, mechanism and prevention. *Int J Biol Sci*. (2019) 15:2128–38. doi: 10.7150/ijbs.35460

5. Mahabadi AA, Rischpler C. Cardiovascular imaging in cardio-oncology. *J Thorac Dis*. (2018) 10:S4351–S66. doi: 10.21037/jtd.2018.10.92

6. Zou B, Schuster JP, Niu K, Huang Q, Rühle A, Huber PE. Radiotherapy-induced heart disease: a review of the literature. *Precis Clin Med*. (2019) 2:270–82. doi: 10.1093/pcmedi/pbz025

7. van den Bogaard VA, Ta BD, van der Schaaf A, Bouma AB, Middag AM, Bantema-Joppe EJ, et al. Validation and modification of a prediction model for acute cardiac events in patients with breast cancer treated with radiotherapy based on three-dimensional dose distributions to cardiac substructures. *J Clin Oncol*. (2017) 35:1171–8. doi: 10.1200/JCO.2016.69.8480

8. Chen HS, Wang W, Wu SN, Liu JP. Corticosteroids for viral myocarditis. *Cochrane Database Syst Rev*. (2013) 2013:CD004471. doi: 10.1002/14651858.CD004471.pub3

9. Sinagra G, Anzini M, Pereira NL, Bussani R, Finocchiaro G, Bartunek J, et al. Myocarditis in clinical practice. *Mayo Clin Proc*. (2016) 91:1256–66. doi: 10.1016/j.mayocp.2016.05.013

10. Caforio AL, Pankuweit S, Arbustini E, Basso C, Gimeno-Blanes J, Felix SB, et al. Current state of knowledge on aetiology, diagnosis, management, and therapy of myocarditis: a position statement of the European Society of Cardiology Working Group on myocardial and pericardial diseases. *Eur Heart J*. (2013) 34:2636–48. doi: 10.1093/eurheartj/eht210

11. Rygiel K. Cardiotoxic effects of radiotherapy and strategies to reduce them in patients with breast cancer: an overview. *J Cancer Res Ther*. (2017) 13:186–92. doi: 10.4103/0973-1482.187303

12. Rehammar JC, Jensen M-B, McGale P, Lorenzen EL, Taylor C, Darby SC, et al. Risk of heart disease in relation to radiotherapy and chemotherapy with anthracyclines among 19,464 breast cancer patients in Denmark, 1977–2005. *Radiother Oncol*. (2017) 123:299–305. doi: 10.1016/j.radonc.2017.03.012

13. McGale P, Darby SC, Hall P, Adolfsson J, Bengtsson N-O, Bennet AM, et al. Incidence of heart disease in 35,000 women treated with radiotherapy for breast

cancer in Denmark and Sweden. *Radiother Oncol*. (2011) 100:167–75. doi: 10.1016/j.radonc.2011.06.016

14. Yusuf SW, Venkatesulu BP, Mahadevan LS, Krishnan S. Radiation-induced cardiovascular disease: a clinical perspective. *Front Cardiovasc Med*. (2017) 4:66. doi: 10.3389/fcvm.2017.00066

15. Lee MS, Finch W, Mahmud E. Cardiovascular complications of radiotherapy. *Am J Cardiol*. (2013) 112:1688–96. doi: 10.1016/j.amjcard.2013.07.031

16. Díaz-Gavela AA, Figueiras-Graillet L, Luis ÁM, Salas Segura J, Ciérvide R, Peñalver E, et al. Breast radiotherapy-related cardiotoxicity. When, how, why. Risk prevention and control strategies. *Cancers*. (2021) 13:1712. doi: 10.3390/cancers13071712

17. Koutroumpakis E, Palaskas NL, Lin SH, Abe J-i, Liao Z, Banchs J, et al. Modern radiotherapy and risk of cardiotoxicity. *Chemotherapy* (2020) 65:65–76. doi: 10.1159/000510573

18. Cho H, Lee S, Sim SH, Park IH, Lee KS, Kwak MH, et al. Cumulative incidence of chemotherapy-induced cardiotoxicity during a 2-year follow-up period in breast cancer patients. *Breast Cancer Res Treat*. (2020) 182:333–43. doi: 10.1007/s10549-020-05703-5

19. Shah C, Badiyan S, Berry S, Khan AJ, Goyal S, Schulte K, et al. Cardiac dose sparing and avoidance techniques in breast cancer radiotherapy. *Radiother Oncol*. (2014) 112:9–16. doi: 10.1016/j.radonc.2014.04.009

20. Zhang N, Liu X, Tao D, Wang Y, Wu Y, Zeng X. Optimal radiotherapy modality sparing for cardiac valves in left-sided breast cancer. *Ann Transl Med*. (2023) 11:46. doi: 10.21037/atm-22-6633

21. Piroth MD, Baumann R, Budach W, Dunst J, Feyer P, Fietkau R, et al. Heart toxicity from breast cancer radiotherapy. *Strahlenther Onkol*. (2019) 195:1–12. doi: 10.1007/s00066-018-1378-z

22. Giza DE, Iliescu G, Hassan S, Marmagkiolis K, Iliescu C. Cancer as a risk factor for cardiovascular disease. *Curr Oncol Rep*. (2017) 19:1–8. doi: 10.1007/s11912-017-0564-y

23. Lewis GD, Farach A. Cardiovascular toxicities of radiation therapy. *Methodist Debakey Cardiovasc J*. (2019) 15:274–81. doi: 10.14797/mdcj-15-4-274

24. Liu LK, Ouyang W, Zhao X, Su SF, Yang Y, Ding WJ, et al. Pathogenesis and prevention of radiation-induced myocardial fibrosis. *Asian Pac J Cancer Prev*. (2017) 18:583–87. doi: 10.22034/APJCP.2017.18.3.583

25. D'Errico MP, Grimaldi L, Petruzzelli MF, Gianicolo EA, Tramacere F, Monetti A, et al. N-terminal pro-B–type natriuretic peptide plasma levels as a potential biomarker for cardiac damage after radiotherapy in patients with left-sided breast cancer. *Int J Radiat Oncol Biol Phys*. (2012) 82:e239–46. doi: 10.1016/j.ijrobp.2011.03.058

26. Tian S, Hirshfield KM, Jabbour SK, Toppmeyer D, Haffty BG, Khan AJ, et al. Serum biomarkers for the detection of cardiac toxicity after chemotherapy and radiation therapy in breast cancer patients. *Front Oncol*. (2014) 4:277. doi: 10.3389/fonc.2014.00277

27. Ma C-X, Zhao X-K, Li Y-D. New therapeutic insights into radiation-induced myocardial fibrosis. *Ther Adv Chronic Dis*. (2019) 10:2040622319868383. doi: 10.1177/2040622319868383

28. Meattini I, Poortmans PM, Aznar MC, Becherini C, Bonzano E, Cardinale D, et al. Association of breast cancer irradiation with cardiac toxic effects: a narrative review. *JAMA Oncol*. (2021) 7:924–32. doi: 10.1001/jamaoncol.2020.7468

29. Desai MY, Jellis CL, Kotecha R, Johnston DR, Griffin BP. Radiation-associated cardiac disease: a practical approach to diagnosis and management. *JACC Cardiovasc Imaging*. (2018) 11:1132–49. doi: 10.1016/j.jcmg.2018.04.028

30. Chang H-M, Moudgil R, Scarabelli T, Okwuosa TM, Yeh ET. Cardiovascular complications of cancer therapy: best practices in diagnosis, prevention, and management: part 1. *J Am Coll Cardiol*. (2017) 70:2536–51. doi: 10.1016/j.jacc.2017.09.1096

31. Mukai-Yatagai N, Haruki N, Kinugasa Y, Ohta Y, Ishibashi-Ueda H, Akasaka T, et al. Assessment of myocardial fibrosis using T1-mapping and extracellular volume measurement on cardiac magnetic resonance imaging for the diagnosis of radiation-induced cardiomyopathy. *J Cardiol Cases*. (2018) 18:132–5. doi: 10.1016/j.jccase.2018.06.001

32. Anthony FY, Ho AY, Braunstein LZ, Thor ME, Chuy KL, Eaton A, et al. Assessment of early radiation-induced changes in left ventricular function by myocardial strain imaging after breast radiation therapy. *J Am Soc Echocardiogr*. (2019) 32:521–8. doi: 10.1016/j.echo.2018.12.009

33. Wang B, Wang H, Zhang M, Ji R, Wei J, Xin Y, et al. Radiation-induced myocardial fibrosis: mechanisms underlying its pathogenesis and therapeutic strategies. *J Cell Mol Med*. (2020) 24:7717–29. doi: 10.1111/jcmm.15479

frontiers | Frontiers in Cardiovascular Medicine

TYPE Case Report
PUBLISHED 25 April 2023
DOI 10.3389/fcvm.2023.1124276

Check for updates

OPEN ACCESS

EDITED BY
Reto Asmis,
Wake Forest University, United States

REVIEWED BY
Mohammad Sheibani,
Iran University of Medical Sciences, Iran
Adele Stewart,
Florida Atlantic University, United States

*CORRESPONDENCE
Hirotaka Suto
hirotaka.suto@jfcr.or.jp
Makiko Suto
maki1129@hotmail.co.jp

RECEIVED 15 December 2022
ACCEPTED 11 April 2023
PUBLISHED 25 April 2023

CITATION
Suto H, Suto M, Inui Y and Okamura A (2023) Late-onset doxorubicin-induced congestive heart failure in an elderly cancer survivor: A case report.
Front. Cardiovasc. Med. 10:1124276.
doi: 10.3389/fcvm.2023.1124276

COPYRIGHT
© 2023 Suto, Suto, Inui and Okamura. This is an open-access article distributed under the terms of the Creative Commons Attribution License (CC BY). The use, distribution or reproduction in other forums is permitted, provided the original author(s) and the copyright owner(s) are credited and that the original publication in this journal is cited, in accordance with accepted academic practice. No use, distribution or reproduction is permitted which does not comply with these terms.

Late-onset doxorubicin-induced congestive heart failure in an elderly cancer survivor: A case report

Hirotaka Suto[1,2]*, Makiko Suto[3]*, Yumiko Inui[2] and Atsuo Okamura[2]

[1]Department of Medical Oncology, The Cancer Institute Hospital of Japanese Foundation for Cancer Research, Tokyo, Japan, [2]Department of Medical Oncology/Hematology, Kakogawa Central City Hospital, Hyogo, Japan, [3]Department of Cardiovascular Medicine, Takarazuka City Hospital, Hyogo, Japan

Background: Recently, the survival rate of patients with cancer has improved annually due to advancements in cancer diagnosis and treatment technologies. Meanwhile, late-onset complications associated with cancer treatment significantly affect survival and quality of life. However, different from pediatric cancer survivors, there is no unified view on the follow-up of late complications in elderly cancer survivors. We reported a case of congestive heart failure as a late-onset complication of doxorubicin (DXR) in an elderly cancer survivor.

Case report: The patient is an 80-year-old woman with hypertension and chronic renal failure. She received six cycles of chemotherapy for Hodgkin's lymphoma that started in January 201X-2. The total dose of DXR was 300 mg/m^2, and a transthoracic echocardiogram (TTE) performed in October 201X-2, showed good left ventricular wall motion (LVWM). In April 201X, she suddenly developed dyspnea. Upon arrival at the hospital, a physical examination revealed orthopnea, tachycardia, and leg edema. A chest radiograph showed cardiac enlargement and pleural effusion. A TTE showed diffusely reduced LVWM and a left ventricular ejection fraction in the 20% range. After close examination, the patient was diagnosed with congestive heart failure due to late-onset DXR-induced cardiomyopathy.

Conclusion: Late-onset DXR-induced cardiotoxicity is considered high-risk from 250 mg/m^2 or higher. Elderly cancer survivors are at higher risk of cardiotoxicity than non-elderly cancer survivors and may require closer follow-up.

KEYWORDS

doxorubicin, cardiotoxicity, onco-cardiology, cancer survivor, elderly, troponin I, global longitudinal strain

1. Introduction

Recently, advancements in cancer diagnosis and treatment techniques have improved the survival rate of patients with cancer, including those with Hodgkin's lymphoma, annually (1, 2). On the other hand, late-onset complications associated with cancer treatment significantly affect survival and quality of life (3). In particular, doxorubicin (DXR) cardiotoxicity, which affects survival, is speculated to impair DXR-induced mitochondrial function, ultimately leading to cardiomyocyte death, and correlates with cumulative DXR dosage (4). The incidence of DXR-induced congestive heart failure is as high as 16% when the cumulative dose of DXR exceeds 500 mg/m^2 and is a critical problem for patients receiving DXR (5). Therefore, the Japanese DXR's package insert

includes a dose limit of up to 500 mg/m^2 of cumulative dosage. However, since a history of radiation therapy to the heart and long-term survival after DXR administration are risks for the development of DXR cardiotoxicity, the European Society of Cardiology guidelines recommend risk-based monitoring such as echocardiography and troponin I (TnI) for pediatric cancer survivors with risk factors, even if the cumulative dose of DXR is lower than 500 mg/m^2 (6–8). Furthermore, the efficacy of dexrazoxane as prophylaxis for DXR cardiotoxicity has been reported, but effective treatment for DXR cardiotoxicity remains unclear (9, 10). Thus, late-onset complications are considered a problem in oncology for children, adolescents and young adults, and adults, and guidelines have been developed for cancer survivors, including methods for long-term follow-up (6, 11–14). However, there is no unified view on late complications in elderly cancer survivors, who are at risk of cardiac complications, and most of the survivors remain unrecognized. In this study, we reported a case of congestive heart failure as a late-onset complication of DXR in an elderly Hodgkin's lymphoma survivor.

TABLE 1 Patient's laboratory results at the emergency room.

Blood components	Patient		Normal range
Complete blood count			
White blood cell	11,440	/μl	3,300–8,600
Red blood cell	305×10^4	/μl	$386–492 \times 10^4$
Hemoglobin	8.7	g/dl	11.6–14.8
Hematocrit	29.3	%	35.1–44.4
Mean corpuscular volume	96.0	fL	83.6–98.2
Platelet	37.4×10^4	/μl	$158–348 \times 10^4$
Neutrophil	49.9	%	40.0–70.0
Lymphocyte	43.2	%	20.0–50.0
Monocyte	4.7	%	0.0–10.0
Eosinocyte	1.9	%	1.0–5.0
Basocyte	0.3	%	0.0–1.0
Coagulation test			
Activated partial thromboplastin time	30.9	sec	26.0–38.0
Prothrombin time	90.0	%	70.0–130.0
D-dimer	0.9	μg/ml	0.0–1.0
Biochemistry			
Total protein	7.3	g/dl	6.6–8.1
Albumin	3.6	g/dl	4.1–5.1
C-reactive protein	0.80	mg/dl	0.00–0.14
Aspartate aminotransferase	34	IU/L	13–30
Alanine aminotransferase	14	IU/L	7–23
Alkaline phosphatase	444	IU/L	106–322
Total bilirubin	0.5	mg/dl	0.4–1.5
Lactate dehydrogenase	205	IU/L	124–222
Blood urea nitrogen	28.9	mg/dl	8.0–20.0
Creatinine	1.48	mg/dl	0.46–0.79
Na (sodium)	139	mEq/L	138–145
K (potassium)	5.3	mEq/L	3.6–4.8
Cl (chlorine)	106	mEq/L	101–108
Creatine kinase	59	IU/L	41–153
Creatine kinase-myocardial band	4	IU/L	0–25
Amylase	81	IU/L	44–132
Glucose	216	mg/dl	73–109
Hemoglobin A1c	5.2	%	4.9–6.0
Troponin I	0.08	ng/ml	0.00–0.014
B-type natriuretic peptide	1,155	pg/ml	0.0–18.4
Thyroid-stimulating hormone	5.71	μIU/ml	0.34–4.22
Free thyroxine	1.38	ng/dl	0.77–1.59
Arterial blood gas analysis (under 5 L of oxygen administration)			
pH	7.351		7.35–7.45
pO_2 (partial pressure of oxygen)	284.4	mmHg	80–100
pCO_2 (partial pressure of carbon dioxide)	38.6	mmHg	35.0–45.0
sO_2 (oxygen saturation)	99.4	%	95–99
HCO_3^- (bicarbonate)	20.9	mmol/L	22–26
Lactate	3.2	mmol/L	0.4–1.8
Base excess	−4.3	mmol/L	−3–3

2. Case description

The patient was an 80-year-old woman with coexisting hypertension, dyslipidemia, and chronic renal failure (CRF). She routinely took enalapril 5 mg once per day and atorvastatin 10 mg once per day. She had no smoking history and no family history of cardiac disease. A transthoracic echocardiogram (TTE) performed in December 201X-3, showed a left ventricular (LV) ejection fraction (LVEF) of 63.4%. She received six cycles of DXR, bleomycin, vinblastine, and dacarbazine (ABVD) for Hodgkin's lymphoma (Lugano classification, stage III) that started in January 201X-2. The total dose of DXR was 300 mg/m^2, and a TTE performed on October, 201X-2, showed good LV wall motion (LVEF, 65.4%) and no evidence of heart failure. Subsequently, the patient did not experience any recurrence of Hodgkin's lymphoma. In April 201X, the patient suddenly developed dyspnea and was rushed to the emergency room. Upon arrival at the hospital, a physical examination revealed the following: body temperature, 36.9°C; heart rate, 144 beats/min; blood pressure, 160/114 mmHg; respiratory rate, 25 breaths/minute; and oxygen saturation, 98% (under 5 L of oxygen administration). The patient's consciousness was also impaired [Glasgow Coma Scale score, 13 (E3V4M6); Japan Coma Scale score, 10], and her eyelid and conjunctiva were pale. The patient had no heart murmur and no chest pain, but she had mild wheezing, orthopnea, and bilateral leg pitting edema. Blood test results (**Table 1**) revealed markedly elevated B-type natriuretic peptide (BNP) (1,155 pg/ml) level and slightly increased TnI level (0.08 ng/ml). The patient's hemoglobin (Hb) A1c, free thyroxine, and D-dimer levels were within the normal ranges. The patient also showed decreased Hb level (8.7 g/dl) and increased serum creatinine level (1.48 mg/dl), but these two values had not changed over time for more than a year. An electrocardiogram (ECG) showed sinus tachycardia (**Supplementary Figure S1**). A chest radiograph showed an enlarged heart and pleural effusion. A TTE showed a diffusely reduced LV wall motion and an LVEF of 21.6% (**Figure 1**). The

Dimension	
LVDd	53.1 mm
LVDs	46.0 mm
FS	13.4%
LAD	44.9 mm
AoD	20.7 mm

IVC	11.2 mm
TR-PG	26.7 mmHg
ECG	sinus rhythm

Simpson	
EF	21.6%

LV inflow	
E/A	0.9
DcT (E)	141.6 ms

	Valve	
Regurgitation	AR	mild
	MR	mild~moderate
	TR	mild
	PR	mild

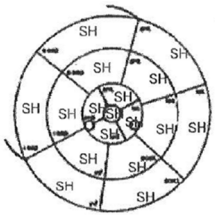

FIGURE 1
Transthoracic echocardiogram findings at the emergency department visit. LVDd, left ventricular internal dimension in diastole; LVDs, left ventricular internal dimensions in systole; FS, fractional shortening; LAD, left atrial dimension; AoD, aortic root diameter; IVC, inferior vena cava; TR-PG, tricuspid regurgitation peak gradient; ECG, electrocardiogram; EF, ejection fraction; LV, left ventricle; E/A, early-to-late transmitral velocity; DcT, deceleration time; AR, aortic regurgitation; MR, mitral regurgitation; TR, tricuspid regurgitation; PR, pulmonary regurgitation; SH, severe hypokinesis.

patient was diagnosed with clinical scenario 1 acute heart failure (15) and underwent close examination and treatment in the intensive care unit. Thallium-201 myocardial perfusion scintigraphy showed transient ischemic dilatation and old myocardial infarction (OMI) of the left circumflex artery. LV perfusion, LV wall motion, and LV end-diastolic volume results were consistent with tachycardia-induced cardiomyopathy (**Figure 2**, **Supplementary Figure S2**). No chest symptoms or significant ECG changes appeared at the time of loading. Since the patient had no evidence of progressive anemia, exacerbation of chronic renal failure, arrhythmia, or acute coronary syndrome and the cumulative dose of DXR was 300 mg/m^2, the patient

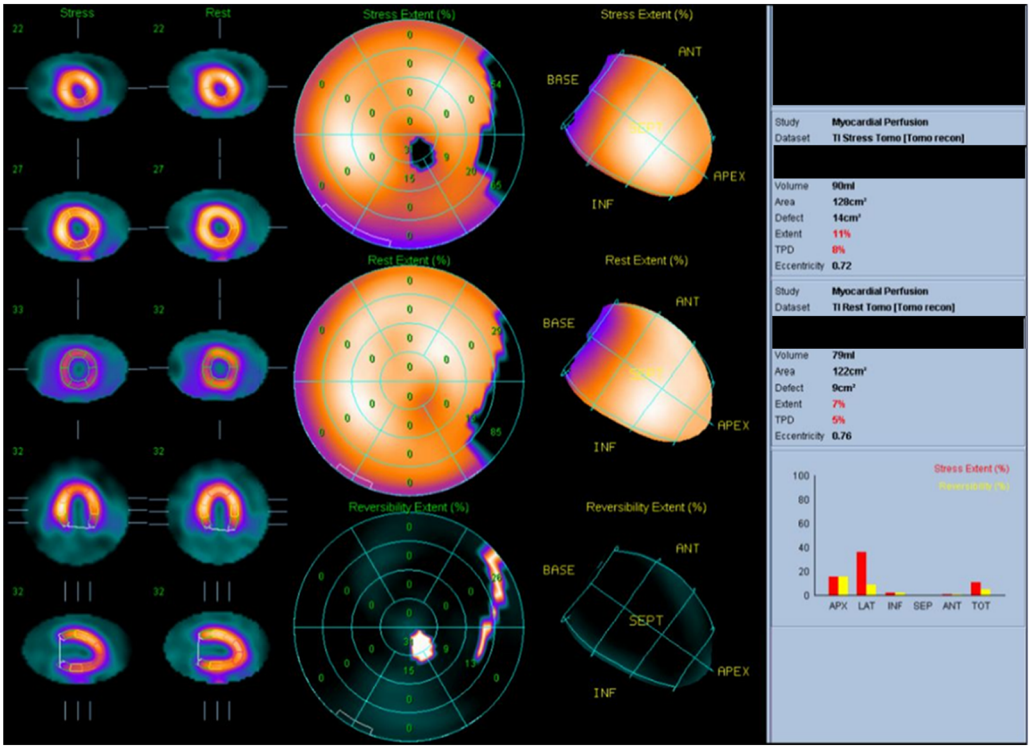

FIGURE 2
Thallium-201 myocardial perfusion: transient ischemic dilatation and old myocardial infarction of the left circumflex artery.

was diagnosed with congestive heart failure due to late-onset DXR-induced cardiomyopathy.

3. Clinical course of treatment

We administered furosemide (1 mg/h) and nitroglycerin (2 mg/h) in the hyperacute phase and added bisoprolol (2.5 mg/day) in the early phase. After the patient's congestive heart failure improved, we continued bisoprolol and added spironolactone (50 mg/day) and azosemide (60 mg/day). After treatment, symptoms, such as leg edema, tachycardia, and orthopnea, disappeared, BNP level decreased to 75.7 pg/ml, and the patient's LVEF improved to 51.2% on TTE in September 201X (**Figure 3**).

4. Discussion

We presented a case of an elderly cancer survivor with late-onset DXR-induced heart failure, whose cardiac function improved with therapeutic intervention.

DXR is a key drug in Hodgkin's and non-Hodgkin's lymphomas and breast and endometrial cancers (16–19). A previous study demonstrated that the 6-year overall survival rate for previously untreated patients with stage III or IV classic Hodgkin lymphoma was 89.4% in the ABVD group (16). Another study reported a 5-year survival rate of 86%–90% for adjuvant chemotherapy containing DXR for recurrent high-risk breast cancer (18).

Pediatric cancer survivors who receive anthracyclines, including DXR, have a persistent risk of developing cardiovascular disease over time. However, the risk of cancer recurrence decreases over time (20, 21). This trend is also evident in adult patients with Hodgkin's lymphoma and breast cancer (22). Patients with breast cancer, even the elderly, reported more deaths from cardiovascular disease than breast cancer 10 years after diagnosis (23).

One potential mechanism for this persistent DXR cardiotoxicity is that DXR accumulates in the mitochondria of cardiomyocytes (24). Accumulated DXR increases the concentration of iron in the mitochondria and produces reactive oxygen species (ROS). ROS may cause myocardial damage, which is a possible reason why the iron chelator dexrazoxane is effective in protecting against DXR-induced myocardial damage (9, 25). Furthermore, topoisomerase IIβ expressed in the myocardium is a key molecular mediator of DXR-induced cardiotoxicity and is thought to impair myocardial repair and irreversibly reduce cardiac function (26–28). Other mechanisms associated with DXR cardiotoxicity include calcium hemostasis imbalance inducing DNA damage and disruption of the neuroglial/ErbB signaling pathway resulting in apoptosis and mitochondrial dysfunction (4). There were recent reports of an association between cardiac syndrome X and DXR-induced endothelial cell damage (29). DXR-induced endothelial cell damage triggers the onset and progression of cardiomyopathy by reducing the release and activity of critical endothelial factors and inducing endothelial cell death. That may be an important mechanism for microvascular angina development in young patients without risk factors or comorbid conditions. The present case was out of the characteristics of DXR-induced cardiac

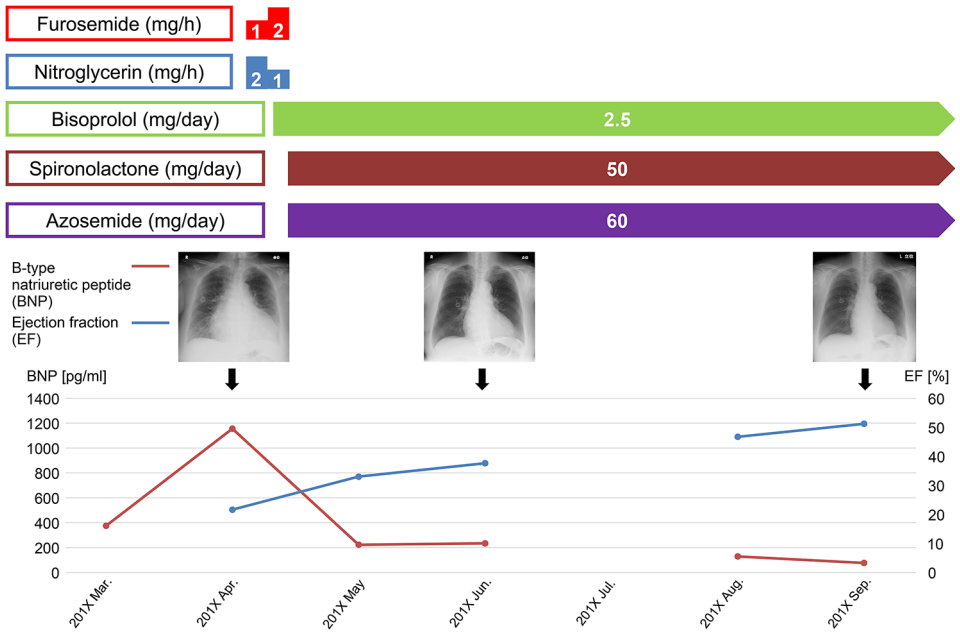

FIGURE 3
The clinical course of congestive heart failure.

syndrome X due to the presence of OMI, hypertension, and CRF, as well as the patient's advanced age.

DXR-induced cardiotoxicity is dose-dependent, with LV dysfunction occurring in 3%–5% of patients at a cumulative dose of 400 mg/m^2 compared to 7%–26% at a dose of 550 mg/m^2 (28, 30). Therefore, the Japanese package insert states that the cumulative dose of DXR should be up to 500 mg/m^2, but for late cardiotoxicity, DXR has a higher risk starting at 250 mg/m^2 or higher (6, 31). The risk of cardiovascular disease would be higher in DXR-treated patients aged over 65 years compared to those aged under 65 years (5, 6). In addition, the average life expectancies for Japanese women are 15.6 years at age 75 years and 11.4 years at age 80 years, and follow-up for late complications is necessary even in elderly patients (32). Therefore, elderly patients receiving DXR should be followed up more closely than non-elderly patients, paying attention to late complications. The patient in this case report also received ABVD regimen for Hodgkin's lymphoma at age 78 years, with a cumulative dose of 300 mg/m^2. Therefore, the risk of late-onset DXR-induced heart failure is high, and close follow-up is necessary.

Although DXR-induced cardiotoxicity is generally considered irreversible, there have been reports of improved cardiac function with early therapeutic interventions with β-blockers, angiotensin-converting enzyme inhibitors, angiotensin receptor blockers, and diuretics (28, 33–35). In the present case, early diuretic and β-blockers administration improved cardiac function with the improvement of sinus tachycardia and reduction of cardiothoracic ratio associated with congestive heart failure (**Figure 3**, **Supplementary Figure S1**). Thus, the early diagnosis and treatment of late-onset DXR-induced heart failure may have effectively improved patients' outcomes.

Recently, there have been reports on the prediction of the risk of developing DXR-induced cardiovascular disease based on genes and the value of global longitudinal strain and TnI for the early detection of DXR-induced cardiotoxicity (36, 37).

In conclusion, elderly cancer survivors with an estimated life expectancy of 5–10 years or more are at higher risk of cardiovascular disease and other late complications than non-elderly cancer survivors. Therefore, elderly cancer survivors with a history of DXR treatment may benefit from closer follow-up with BNP and TnI testing and early detection and treatment of DXR-induced heart failure.

Data availability statement

The original contributions presented in the study are included in the article/**Supplementary Material**, further inquiries can be directed to the corresponding authors.

Ethics statement

Ethical review and approval was not required for the study on human participants in accordance with the local legislation and institutional requirements. The patients/participants provided their written informed consent to participate in this study.

Author contributions

Conceptualization: HS, MS, and AO. Methodology: HS and MS. Investigation: HS, MS, YI, and AO. Data curation: HS, MS, YI, and AO. Writing—original draft preparation: HS. Writing—review and editing: HS, MS, YI, and AO. Supervision: MS and AO. All authors contributed to the article and approved the submitted version.

Acknowledgments

The authors would like to thank Editage (www.editage.com) for English language editing.

Conflict of interest

The authors declare that the research was conducted in the absence of any commercial or financial relationships that could be construed as a potential conflict of interest.

Publisher's note

All claims expressed in this article are solely those of the authors and do not necessarily represent those of their affiliated organizations, or those of the publisher, the editors and the reviewers. Any product that may be evaluated in this article, or claim that may be made by its manufacturer, is not guaranteed or endorsed by the publisher.

Supplementary material

The Supplementary Material for this article can be found online at: https://www.frontiersin.org/articles/10.3389/fcvm.2023.1124276/full#supplementary-material.

References

1. Siegel RL, Miller KD, Fuchs HE, Jemal A. Cancer statistics, 2022. *CA Cancer J Clin*. (2022) 72:7–33. doi: 10.3322/caac.21708

2. Welch HG, Kramer BS, Black WC. Epidemiologic signatures in cancer. *N Engl J Med*. (2019) 381:1378–86. doi: 10.1056/NEJMsr1905447

3. Kadowaki H, Akazawa H, Ishida J, Komuro I. Cancer therapeutics-related cardiac dysfunction—insights from bench and bedside of onco-cardiology. *Circ J*. (2020) 84:1446–53. doi: 10.1253/circj.CJ-20-0467

4. Sheibani M, Azizi Y, Shayan M, Nezamoleslami S, Eslami F, Farjoo MH, et al. Doxorubicin-induced cardiotoxicity: an overview on pre-clinical therapeutic approaches. *Cardiovasc Toxicol*. (2022) 22:292–310. doi: 10.1007/s12012-022-09721-1

5. Swain SM, Whaley FS, Ewer MS. Congestive heart failure in patients treated with doxorubicin: a retrospective analysis of three trials. *Cancer*. (2003) 97:2869–79. doi: 10.1002/cncr.11407

6. Lyon AR, López-Fernández T, Couch LS, Asteggiano R, Aznar MC, Bergler-Klein J, et al. 2022 Esc guidelines on cardio-oncology developed in collaboration with the European hematology association (eha), the European society for therapeutic radiology and oncology (ESTRO) and the international cardio-oncology society (IC-OS). *Eur Heart J*. (2022) 43:4229–361. doi: 10.1093/eurheartj/ehac244

7. Bates JE, Howell RM, Liu Q, Yasui Y, Mulrooney DA, Dhakal S, et al. Therapy-related cardiac risk in childhood cancer survivors: an analysis of the childhood cancer survivor study. *J Clin Oncol*. (2019) 37:1090–101. doi: 10.1200/JCO.18.01764

8. Lipshultz SE, Lipsitz SR, Sallan SE, Dalton VM, Mone SM, Gelber RD, et al. Chronic progressive cardiac dysfunction years after doxorubicin therapy for childhood acute lymphoblastic leukemia. *J Clin Oncol*. (2005) 23:2629–36. doi: 10.1200/JCO.2005.12.121

9. Lipshultz SE, Rifai N, Dalton VM, Levy DE, Silverman LB, Lipsitz SR, et al. The effect of dexrazoxane on myocardial injury in doxorubicin-treated children with acute lymphoblastic leukemia. *N Engl J Med*. (2004) 351:145–53. doi: 10.1056/NEJMoa035153

10. Chow EJ, Aggarwal S, Doody DR, Aplenc R, Armenian SH, Baker KS, et al. Dexrazoxane and long-term heart function in survivors of childhood cancer. *J Clin Oncol*. (2023):Jco2202423. doi: 10.1200/JCO.22.02423

11. Plana JC, Galderisi M, Barac A, Ewer MS, Ky B, Scherrer-Crosbie M, et al. Expert consensus for multimodality imaging evaluation of adult patients during and after cancer therapy: a report from the American society of echocardiography and the European association of cardiovascular imaging. *J Am Soc Echocardiogr*. (2014) 27:911–39. doi: 10.1016/j.echo.2014.07.012

12. Armenian SH, Lacchetti C, Barac A, Carver J, Constine LS, Denduluri N, et al. Prevention and monitoring of cardiac dysfunction in survivors of adult cancers: american society of clinical oncology clinical practice guideline. *J Clin Oncol*. (2017) 35:893–911. doi: 10.1200/JCO.2016.70.5400

13. Armenian SH, Armstrong GT, Aune G, Chow EJ, Ehrhardt MJ, Ky B, et al. Cardiovascular disease in survivors of childhood cancer: insights into epidemiology, pathophysiology, and prevention. *J Clin Oncol*. (2018) 36:2135–44. doi: 10.1200/JCO.2017.76.3920

14. Curigliano G, Lenihan D, Fradley M, Ganatra S, Barac A, Blaes A, et al. Management of cardiac disease in cancer patients throughout oncological treatment: esmo consensus recommendations. *Ann Oncol*. (2020) 31:171–90. doi: 10.1016/j.annonc.2019.10.023

15. Mebazaa A, Gheorghiade M, Piña IL, Harjola VP, Hollenberg SM, Follath F, et al. Practical recommendations for prehospital and early in-hospital management of patients presenting with acute heart failure syndromes. *Crit Care Med*. (2008) 36 (1):S129–39. doi: 10.1097/01.CCM.0000296274.51933.4C

16. Ansell SM, Radford J, Connors JM, Długosz-Danecka M, Kim WS, Gallamini A, et al. Overall survival with brentuximab vedotin in stage III or IV hodgkin's lymphoma. *N Engl J Med*. (2022) 387:310–20. doi: 10.1056/NEJMoa2206125

17. Tilly H, Morschhauser F, Sehn LH, Friedberg JW, Trněný M, Sharman JP, et al. Polatuzumab vedotin in previously untreated diffuse large B-cell lymphoma. *N Engl J Med*. (2022) 386:351–63. doi: 10.1056/NEJMoa2115304

18. Miller KD, O'Neill A, Gradishar W, Hobday TJ, Goldstein LJ, Mayer IA, et al. Double-blind phase III trial of adjuvant chemotherapy with and without bevacizumab in patients with lymph node-positive and high-risk lymph node-negative breast cancer (E5103). *J Clin Oncol*. (2018) 36:2621–9. doi: 10.1200/JCO.2018.79.2028

19. Nomura H, Aoki D, Michimae H, Mizuno M, Nakai H, Arai M, et al. Effect of taxane plus platinum regimens vs doxorubicin plus cisplatin as adjuvant chemotherapy for endometrial cancer at a high risk of progression: a randomized clinical trial. *JAMA Oncol*. (2019) 5:833–40. doi: 10.1001/jamaoncol.2019.0001

20. van der Pal HJ, van Dalen EC, van Delden E, van Dijk IW, Kok WE, Geskus RB, et al. High risk of symptomatic cardiac events in childhood cancer survivors. *J Clin Oncol*. (2012) 30:1429–37. doi: 10.1200/JCO.2010.33.4730

21. Armstrong GT, Kawashima T, Leisenring W, Stratton K, Stovall M, Hudson MM, et al. Aging and risk of severe, disabling, life-threatening, and fatal events in the childhood cancer survivor study. *J Clin Oncol*. (2014) 32:1218–27. doi: 10.1200/JCO.2013.51.1055

22. Sturgeon KM, Deng L, Bluethmann SM, Zhou S, Trifiletti DM, Jiang C, et al. A population-based study of cardiovascular disease mortality risk in US cancer patients. *Eur Heart J*. (2019) 40:3889–97. doi: 10.1093/eurheartj/ehz766

23. Patnaik JL, Byers T, DiGuiseppi C, Dabelea D, Denberg TD. Cardiovascular disease competes with breast cancer as the leading cause of death for older females diagnosed with breast cancer: a retrospective cohort study. *Breast Cancer Res*. (2011) 13:R64. doi: 10.1186/bcr2901

24. Ichikawa Y, Ghanefar M, Bayeva M, Wu R, Khechaduri A, Naga Prasad SV, et al. Cardiotoxicity of doxorubicin is mediated through mitochondrial iron accumulation. *J Clin Invest*. (2014) 124:617–30. doi: 10.1172/JCI72931

25. Jones RL, Wagner AJ, Kawai A, Tamura K, Shahir A, Van Tine BA, et al. Prospective evaluation of doxorubicin cardiotoxicity in patients with advanced soft-tissue sarcoma treated in the announce phase III randomized trial. *Clin Cancer Res*. (2021) 27:3861–6. doi: 10.1158/1078-0432.CCR-20-4592

26. Zhang S, Liu X, Bawa-Khalfe T, Lu LS, Lyu YL, Liu LF, et al. Identification of the molecular basis of doxorubicin-induced cardiotoxicity. *Nat Med*. (2012) 18:1639–42. doi: 10.1038/nm.2919

27. Vejpongsa P, Yeh ET. Topoisomerase 2β: a promising molecular target for primary prevention of anthracycline-induced cardiotoxicity. *Clin Pharmacol Ther*. (2014) 95:45–52. doi: 10.1038/clpt.2013.201

28. Ewer MS, Ewer SM. Cardiotoxicity of anticancer treatments. *Nat Rev Cardiol*. (2015) 12:547–58. doi: 10.1038/nrcardio.2015.65

29. Avagimyan A, Mkrtchyan L, Abrahomovich O, Sheibani M, Guevorkyan A, Sarrafzadegan N, et al. Ac-mode of chemotherapy as a trigger of cardiac syndrome x: a case study. *Curr Probl Cardiol*. (2022) 47:100994. doi: 10.1016/j.cpcardiol.2021.100994

30. Zamorano JL, Lancellotti P, Rodriguez Muñoz D, Aboyans V, Asteggiano R, Galderisi M, et al. 2016 Esc position paper on cancer treatments and cardiovascular toxicity developed under the auspices of the esc committee for practice guidelines: the task force for cancer treatments and cardiovascular toxicity of the European society of cardiology (esc). *Eur J Heart Fail*. (2017) 19:9–42. doi: 10.1002/ejhf.654

31. Armenian SH, Hudson MM, Mulder RL, Chen MH, Constine LS, Dwyer M, et al. Recommendations for cardiomyopathy surveillance for survivors of childhood cancer: a report from the international late effects of childhood cancer guideline harmonization group. *Lancet Oncol*. (2015) 16:e123–36. doi: 10.1016/S1470-2045(14)70409-7

32. Iwamoto M, Nakamura F, Higashi T. Estimated life expectancy and risk of death from cancer by quartiles in the older Japanese population: 2010 vital statistics. *Cancer Epidemiol*. (2014) 38:511–4. doi: 10.1016/j.canep.2014.07.005

33. Cardinale D, Colombo A, Lamantia G, Colombo N, Civelli M, De Giacomi G, et al. Anthracycline-induced cardiomyopathy: clinical relevance and response to pharmacologic therapy. *J Am Coll Cardiol*. (2010) 55:213–20. doi: 10.1016/j.jacc.2009.03.095

34. Cardinale D, Colombo A, Bacchiani G, Tedeschi I, Meroni CA, Veglia F, et al. Early detection of anthracycline cardiotoxicity and improvement with heart failure therapy. *Circulation*. (2015) 131:1981–8. doi: 10.1161/CIRCULATIONAHA.114.013777

35. Ohtani K, Fujino T, Ide T, Funakoshi K, Sakamoto I, Hiasa KI, et al. Recovery from left ventricular dysfunction was associated with the early introduction of heart failure medical treatment in cancer patients with anthracycline-induced cardiotoxicity. *Clin Res Cardiol*. (2019) 108:600–11. doi: 10.1007/s00392-018-1386-0

36. Visscher H, Ross CJ, Rassekh SR, Barhdadi A, Dubé MP, Al-Saloos H, et al. Pharmacogenomic prediction of anthracycline-induced cardiotoxicity in children. *J Clin Oncol*. (2012) 30:1422–8. doi: 10.1200/JCO.2010.34.3467

37. Cardinale D, Iacopo F, Cipolla CM. Cardiotoxicity of anthracyclines. *Front Cardiovasc Med*. (2020) 7:26. doi: 10.3389/fcvm.2020.00026

frontiers | Frontiers in Cardiovascular Medicine

TYPE Case Report
PUBLISHED 20 April 2023
DOI 10.3389/fcvm.2023.1103918

Check for updates

OPEN ACCESS

EDITED BY
Reto Asmis,
Wake Forest University, United States

REVIEWED BY
Petr Peichl,
Institute for Clinical and Experimental Medicine (IKEM), Czechia
Donald Hagler,
Mayo Clinic, United States
Jingquan Zhong,
Shandong University, China

*CORRESPONDENCE
Xiaohong Pan
✉ heartpanxh@zju.edu.cn

SPECIALTY SECTION
This article was submitted to Cardio-Oncology, a section of the journal Frontiers in Cardiovascular Medicine

RECEIVED 21 November 2022
ACCEPTED 29 March 2023
PUBLISHED 20 April 2023

CITATION
Zhu J, Zhang N, Ma Q, Jin L and Pan X (2023) Intracardiac echocardiographic-guided biopsy of cardiac tumors: Case reports. Front. Cardiovasc. Med. 10:1103918. doi: 10.3389/fcvm.2023.1103918

COPYRIGHT
© 2023 Zhu, Zhang, Ma, Jin and Pan. This is an open-access article distributed under the terms of the Creative Commons Attribution License (CC BY). The use, distribution or reproduction in other forums is permitted, provided the original author(s) and the copyright owner(s) are credited and that the original publication in this journal is cited, in accordance with accepted academic practice. No use, distribution or reproduction is permitted which does not comply with these terms.

Intracardiac echocardiographic-guided biopsy of cardiac tumors: Case reports

Jinyun Zhu[1], Ning Zhang[2], Qunchao Ma[1], Luhang Jin[1] and Xiaohong Pan[1]*

[1]Department of Cardiology, Second Affiliated Hospital, College of Medicine, Zhejiang University, Hangzhou, China, [2]Department of Cardiology, the Affiliated Hangzhou First People's Hospital, College of Medicine, Zhejiang University, Hangzhou, China

Background: Primary cardiac tumors are very rare, and about 20–30% of them are malignant tumors. Since early signs of cardiac tumors are non-specific, diagnosis can be challenging. There is a lack of the recommended guidelines or standardized strategies for diagnosis and optimal treatment for this disease. As the definite diagnoses of most tumors are made by pathologic confirmation, biopsied tissue is essential in determining the treatment for patients with cardiac tumors. Recently, intracardiac echocardiography (ICE) has been introduced to assist biopsy procedures of cardiac tumors and it provides high-quality imaging.
Case Description: Due to its low prevalence and variable presentation, cardiac malignant tumors usually are easily missed. Hereby, we report three cases of patients who presented with non-specific signs of cardiac disorder and was initially suspended diagnosis as lung infection or cancer. Under the guidance of ICE, cardiac biopsies were successfully on cardiac masses, giving critical data for diagnosis and treatment planning. No procedural complications were obtained in our cases. These cases are intended to highlight the clinical value and importance of ICE-guided biopsy of intracardiac mass.
Conclusions: The diagnosis of primary cardiac tumors relies on the histopathological results. In our experience, using ICE for biopsy of an intracardiac mass is an attractive tool to increase diagnostic results and reduce the risk of cardiac complications associated with inadequate targeting of the biopsy catheters.

KEYWORDS

intracardiac echocardiography, endomyocardial biopsy, primary cardiac tumor, case reports

Introduction

Primary cardiac tumors are extremely uncommon, and the majority of them are benign. It was reported that the prevalence of primary cardiac tumors is between 0.001 to 0.28% in autopsy series (1). About 40% of malignant tumors are angiosarcomas, which make up the majority of sarcomas. Cardiac angiosarcomas are a rare group of soft tissue sarcomas, characterized by aggressive local growth and early spread. The majority develop in the right atrium, and can infiltrate into neighboring structures and spread distantly (2). Another uncommon hemangioma that develops from pre-endothelial or vascular endothelial cells is cardiac epithelioid hemangioendothelioma (EHE). Its biological behavior is between benign hemangioma and malignant angiosarcoma, and it has local invasiveness and metastatic potential (3). It is difficult to diagnosis due to the initial nonspecific symptoms.

Multimodality imaging and atrial biopsy of a cardiac mass should be performed early as a diagnostic approach (4). Although cardiac biopsy is not a common procedure, tissue diagnosis is crucial for the treatment strategy because the prognosis of cardiac tumors varies greatly depending on the underlying disease. In a patient suspected of having a malignant cardiac tumor who does not have access to curative surgical treatment, histopathological confirmation is a necessary option next to treatment approach. Several methods have been used to replace thoracotomy such as transvenous biopsy, ultrasound-guided transesophageal biopsy and transthoracic biopsy guided by ultrasonography or CT. Intracardiac echocardiography (ICE) is ideally suited to imaging structures in the right heart (5). Although it needs local anesthesia and venous puncture with relatively large catheter, it can provide us a good guidance during the biopsy of cardiac tumors.

Until now, only a few case studies have demonstrated the use of ICE in directing biopsy of cardiac tumor (6–8). Here, we present three cases of right atrium masses treated by biopsy of cardiac masses under ICE guidance. Our cases demonstrated the difficulty in diagnosing cardiac masses due to initial nonspecific symptoms such as dyspnea and shortness of breath. They also highlighted the importance of multimodality imaging and ICE guided atrial biopsy in the early diagnosis of rare cardiac tumors. We hope to provide practical evidence for the use of ICE guided biopsy in the diagnosis of suspected intracardiac mass.

Case presentation

We herein show three cases of ICE-guidance for biopsy of cardiac masses being used to diagnose cardiac tumor. This study was approved by our institutional review board.

Case 1

A 70-year-old man presented with progressive dyspnea and weakness for one month. His physical examination, including the cardiovascular examination, was unremarkable. He had low-grade pyrexia of 37.8°C, with no cough and sputum. Oxygen saturations were 97% on room air. Blood tests showed normocytic anemia (90 g/L), elevated C-reactive protein (CRP) (33.4 mg/L), leucocyte count (12.7×10^9/L), pro-Brain natriuretic peptide level 406 pg/ml, D-dimer of 9840 ug/L, and tumor marker CA125 (312.1 U/ml). Chest X-ray (**Figure 1A**) and computed tomography (**Figures 1B,C**) revealed striking extensive pulmonary lesions, a large soft tissue mass in the right atrium (RA), and pleural effusion. He had persistent bilateral bloody

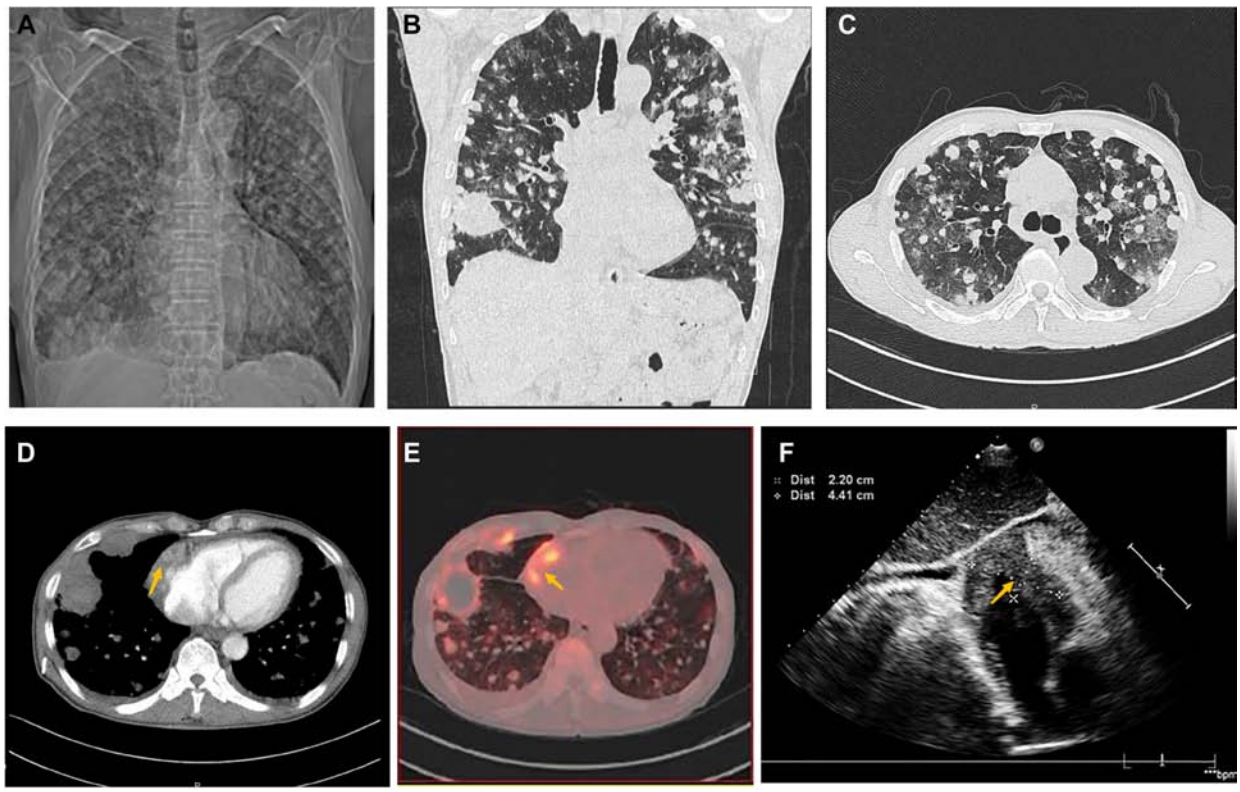

FIGURE 1
Chest computed tomography demonstrated cardiac mass of Case1. (**A**) Chest x-ray and Chest CT images in axial (**B**) and coronal planes (**C**) showed remarkable extensive pulmonary lesions. (**D**) Contrast-enhanced CT showed a hypodense oval filling contrast defect (arrow) at the right atrium (RA). (**E**) 18F-fluorodeoxyglucose positron emission tomography/CT (18F-FDG PET/CT) showed more uptake in the RA mass (arrow), lung, and pleura. (**F**) Echocardiography depicted an oval-shaped mass (22 × 41 mm) (arrow) in the RA at the level of the superior vena cava ostium.

pleural fluid. Thoracentesis removed bloody exudative fluid without malignant cells. Superficial lymph nodes ultrasonography revealed left subclavian lymphadenopathy. Pathological results of lung biopsy and lymph nodes were nondiagnostic. Contrast-enhanced CT showed a hypodense oval filling contrast defect at the right atrium (RA) (**Figure 1D**) 18F-fluorodeoxyglucose positron emission tomography/CT revealed focal uptake in the RA mass (with SUVmax of 5.8), and scattered uptake in lung and pleura metastatic (**Figure 1E**). Echocardiogram showed a large mass (22 × 41 mm) in the RA invading the superior vena cava (**Figure 1F**). Ultrasonographical guided right atrial biopsy was performed. An 11F sheath containing an intracardiac ultrasonography catheter (Biosense Webster, Johnson & Johnson, USA) was inserted into the right atrium through the right femoral vein while under local anesthesia with 1% lidocaine. By crossing the tricuspid annulus, the mass' size and extent could be clearly seen. Under the guidance of ICE, a cardiac biopsy forceps (Argon, USA) was inserted into the right atrium *via* the right internal jugular vein and clamped atrial tissue. The RA mass was visualized and five biopsies were performed (**Figure 2A,B**, **Supplementary Appendix Video S1-2**). Of those samples, 3 were mixtures of necrotic myocardium, and 2 were diagnostic for EHE. Histopathology results (**Figures 2C–F**) revealed a spindle cell tumor, staining with CD34, CD31, and ERG expression, confirming the diagnosis of cardiac epithelioid hemangioendothelioma (EHE). A multidisciplinary team (oncologists, cardiologists, and respiratory doctors) evaluated this patient and recommended chemotherapy and targeted therapy with no mass resection. Unfortunately, the patient's condition deteriorated quickly due to aggressive pulmonary lesions (**Figures 2G–I**), and he had severe dyspnea. The patient made the decision to receive hospice care.

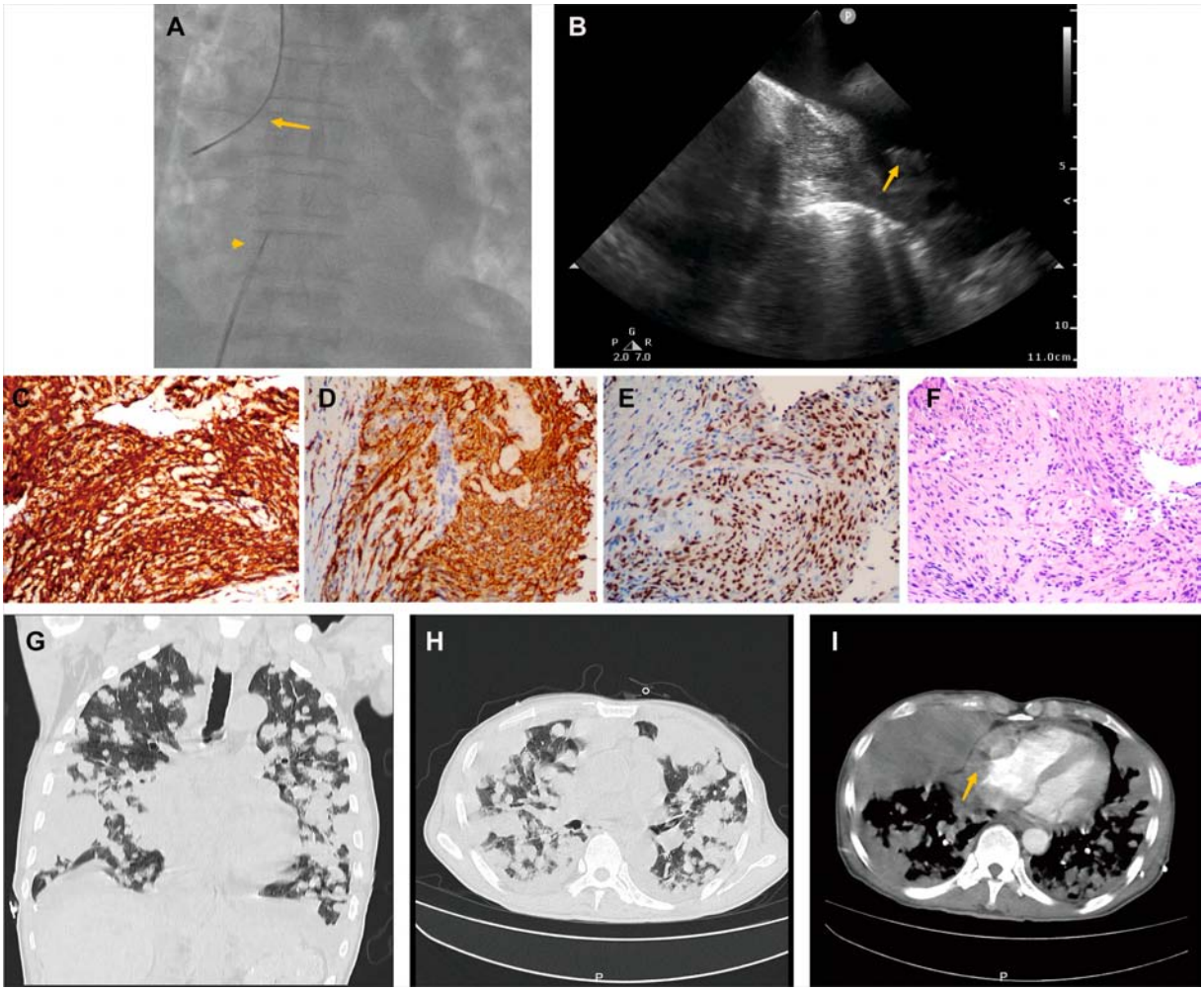

FIGURE 2
Histological endomyocardial biopsy specimen of the right atrium and lung rapid deterioration of Case1. (**A**) Catheter for intracardiac echocardiography (arrowhead) and cardiac bioptome (arrow). (**B**) The intracardial echocardiography demonstrates the mass of the right atrium and well-targeted biopsy catheter (arrow) on the mass. (**C**–**F**) The representative histologic aspect of the mass. Immunohistochemical staining for CD31(**C**), CD34 (**D**), and ERG (**E**) marker in cytoplasmic. (**F**) Cells displaying epithelioid morphology, large nuclei, and ample cytoplasm (hematoxylin and eosin). (Original magnification 40X). (**G**,**H**) Axial and coronal contrast-enhanced CT scans showed rapid progression of lung metastases, and (**I**) recurrent bloody pleural effusion one month after hospitalization. The arrow indicates progressive RA mass.

Case 2

A 50-year-old woman, who had been experiencing shortness of breath and chest tightness for four months, was admitted to a nearby hospital. A chest computed tomography (CT) revealed enlarged heart with pericardial effusion as well as multiple lesions in lungs with suspected infection. CT-guided needle biopsy of pulmonary lesions was performed. Only heterozygous cells were found in the necrosis, and the pathological findings of the lung biopsy were unremarkable. After a few days, the patient gradually felt dyspnea and weakness. She was transferred to our cardiology department for a conclusive diagnosis. Blood testing showed high level of the C-reactive protein (CRP) (16.6 mg/L), pro-Brain natriuretic peptide level of 224 pg/mL, D-dimer of 2050 ug/L, and tumor marker CA125 (60.1 U/ml). Her chest x-ray (**Figures 3A,B**) and chest CT (**Figures 3C,D**) revealed multiple lung lesions. Enhanced chest CT showed an oval hypodense contrast filling defect in the right atrium wall. The size is about 55mm × 28mm × 36 mm (**Figure 3E**). Transthoracic echocardiography (**Figure 4A**) and contrast-enhanced Cardiac magnetic resonance (CMR) imaging (**Figure 4B**) confirmed a large irregular mass (55.2 × 38.1 × 33.9 mm) in the right atrium (RA) invading the superior vena cava. We suspected that this was a cardiac malignant tumor with extensive lung metastases, and then performed an ICE-guided right atrial biopsy (**Figures 4C,D**, **Supplementary**

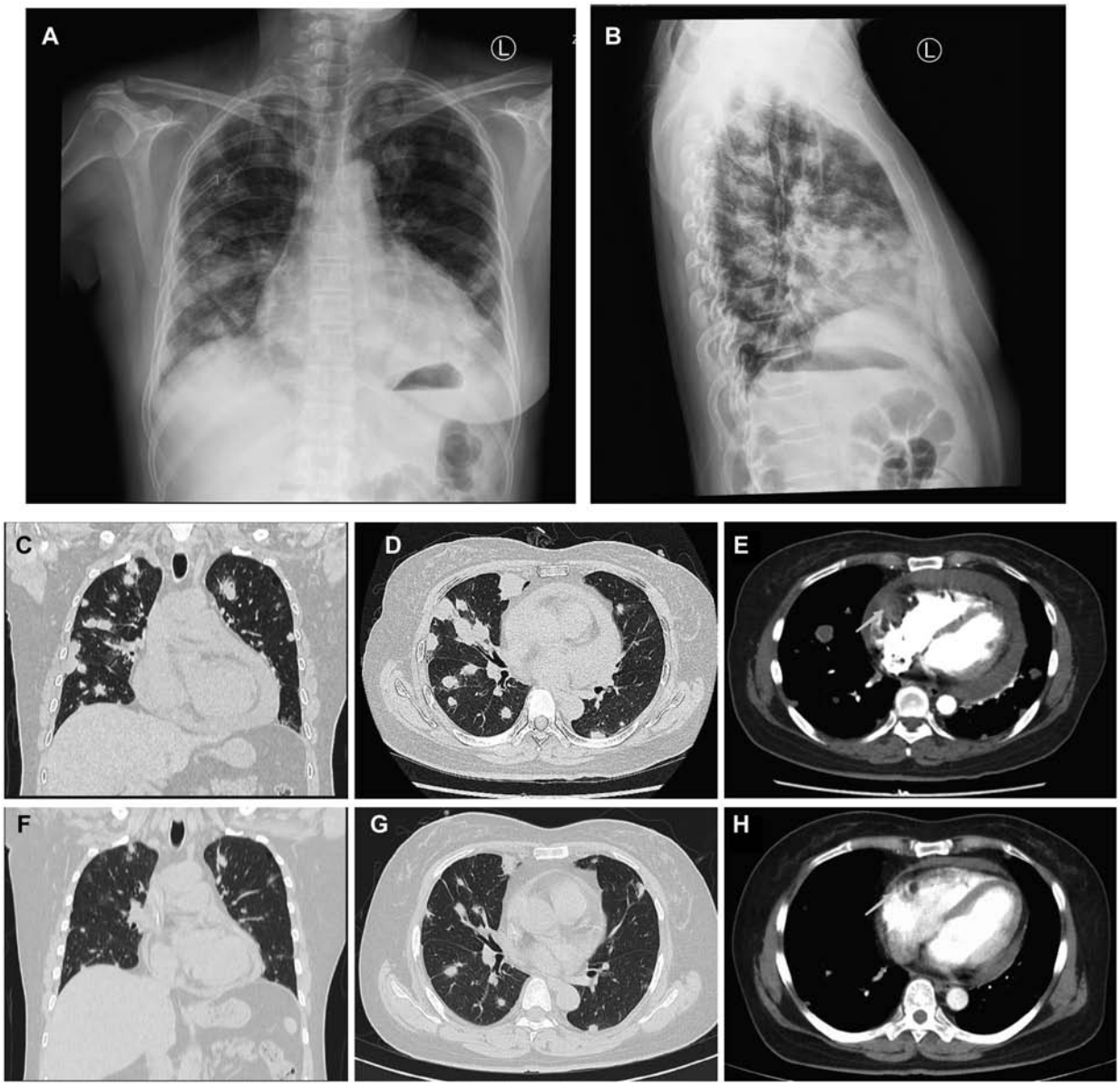

FIGURE 3
Comparison of lung metastases and cardiac mass before and after chemotherapy of Case2. (**A**,**B**) Frontal and lateral Chest x-ray demonstrated extensive pulmonary lesions. (**C**) Chest CT at coronal view and (**D**) axial view revealed severe lung metastases. (**E**) Contrast-enhanced Chest CT reveals a mass lesion (arrow) along the superior and posterior right atrial wall without enhancement. After 5 courses of chemotherapy, the number of lung metastases (**F**,**G**) was less than before (**C**,**D**), and the lateral wall of the RA (**H**) has no occupied (arrow) compared to earlier (**E**).

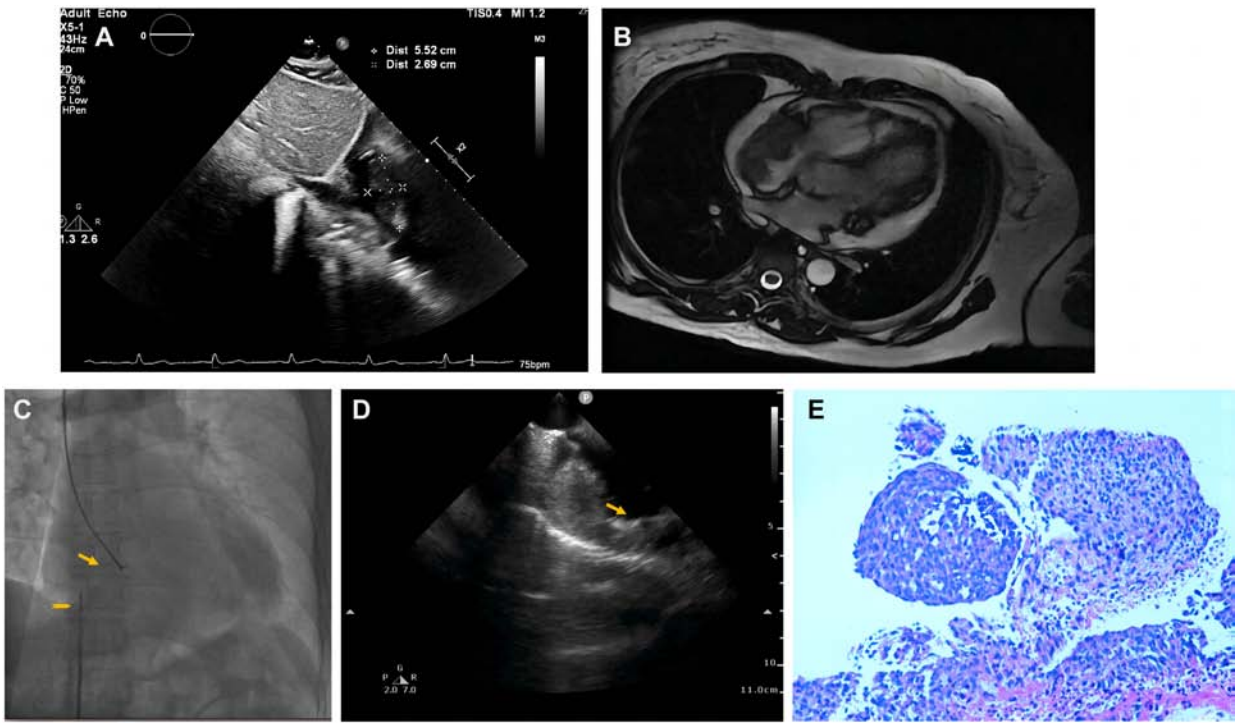

FIGURE 4
Multimodality images and intracardiac echocardiography-guided biopsy of cardiac tumors of Case2. (A) Transthoracic echocardiography showed a huge mass lesion in the RA. (B) Cardiac enhanced-MRI revealed a large irregular mass (55.2 × 38.1 × 33.9 mm) with a rounded appearance in the RA and connected with the right atrium. (C) Catheter for intracardiac echocardiography (arrowhead) and cardiac bioptome(arrow). (D) The intracardial echocardiography demonstrates thickness mass of the right atrium and well-targeted biopsy catheter (arrow) on the mass. (E) Histopathological diagnosis revealed cardiac angiosarcoma, with spindle tumor cells.

Appendix Videos S3-4). Histopathological results (Figure 4E) confirmed the diagnosis of cardiac angiosarcoma, with spindle tumor cells staining positively for CD34, CD31, Fli-1, and ERG, with ki-67 proliferation index reached 60%. After being transferred to the oncology unit, this patient was advised to undergo chemotherapy and targeted therapy without having a mass removed. The patient was treated with chemotherapy (Paclitaxel 207 mg/m^2 day1, liposomal doxorubicin 30 mg/m^2 day1, and Anlotinib day1–14 for targeted therapy). After 5 courses of chemotherapy, the lateral wall of the right atrium has no occupied, and the number of lung metastases was less than before (Figures 3F–H).

Case3

A 62-year-old man was transferred from local hospital to our cardiology department for chest tightness and recurrent pericardial effusion for two months. More than two months ago, the patient experienced chest tightness. When the patient went to the local hospital's emergency room, chest CT showed enlarged cardiac shadow and massive pericardial effusion with interstitial pulmonary edema in the lower lobe of right lung.

Pericardiocentesis was used to treat his bloody pericardial effusion and drain it. In order to treat the symptoms, diuretics and antihypertensives were given. After one month, the patient once more experienced a significant increase in pericardial effusion along with obvious chest tightness. The patient then went to the emergency department for pericardial effusion drainage. Unexpectedly, his chest tightness and dyspnea immediately got worse. He was admitted to our hospital for further diagnosis. A second pericardiocentesis was carried out, producing 900 ml of bloody fluid in total. Blood tests performed shortly after admission revealed high levels of the C-reactive protein (CRP) (25.4 mg/L), pro-Brain natriuretic peptide (660 pg/ml), D-dimer (3,560 ug/L), and tumor marker CA125 (87 U/ml). Echocardiography showed a hyperechoic mass at the right ventricle lateral wall junction (Figure 5A). Enhanced-CMR and chest CT clearly confirmed that a mass (38mm × 23 mm) was located at the junction of the right atrium and ventricle and had a modest amount of pericardial effusion (Figures 5B,C). Pathological analysis of the pericardial effusion revealed sporadic mesothelial cells and inflammatory cells but no tumor cells. For further diagnosis, we carried out an atrial biopsy under the guidance of the ICE (Supplementary Appendix Videos S5–6). The biopsy technique was the same as above without complications (Figure 5D,E). This result revealed small vascular lumen formed by single cell (Figure 5F). and considered as an intermediate or low-grade malignant vascular tumor with positive CD34, CD31, Fli-1, and ERG expression, confirming the diagnosis of cardiac epithelioid hemangioendothelioma (EHE). With the pericardial effusion's rapid progression and significant dyspnea, the patient eventually discontinued getting treatment.

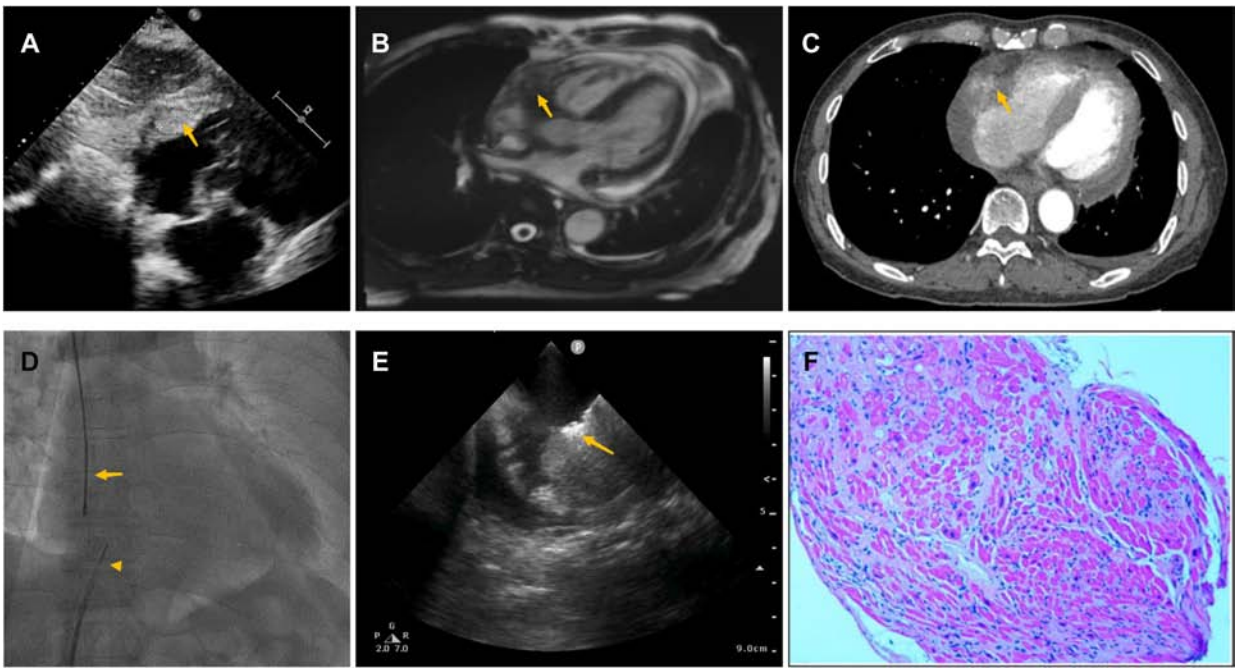

FIGURE 5
Multiple investigations for diagnosis of Case3. (A) Transthoracic echocardiography showed cardiac mass lesion (arrow) in the RA. (B) Chest enhanced CT, and (C) Cardiac enhanced-MRI revealed a large mass (arrow) at the junction of the RA and RV. (D) Catheter for intracardiac echocardiography (arrowhead) and cardiac bioptome (arrow). (E) The intracardial echocardiography demonstrates well-targeted biopsy catheter (arrow) on the mass. (F) Histopathological imaging revealed small vascular lumen formed by single cell, and cardiac epithelioid hemangioendothelioma (EHE) was diagnosed.

All procedures performed in this study were in accordance with the ethical standards of the institutional and/or national research committee(s) and with the Helsinki Declaration (as revised in 2013). Written informed consent was obtained from the patient for publication of these case reports and accompanying images.

Discussion

Primary cardiac tumors are rare, with incidences ranging from 0.001% to 0.030% at autopsy series (9). Among them only 20% are malignant. The malignant primary cardiac tumors are extremely uncommon, whereas metastatic cardiac tumors occur more frequently. Due to the nonspecific nature of the initial symptoms, diagnosis is frequently challenging and delayed (10).

Cardiac angiosarcoma is an uncommon subset of soft tissue sarcomas, and because of its aggressiveness, high rates of local recurrence, and systemic metastases, it is linked to a poor prognosis (11). Because the earliest symptoms of cardiac angiosarcoma are vague and associated with massive pulmonary metastases, our cases illustrated how challenging it is to diagnose this type of cardiac tumor. It implies in the prognosis that more than 50% of these individuals have metastases at the time of diagnosis (12). There is presently no established treatment strategy for this rare condition. When localized, surgery appears to lead to the best outcomes, but this can be technically challenging and not always feasible. Furthermore, some individuals may not be candidates for surgery due to the disease's rapid progression. Cardiac epithelioid hemangioendothelioma (EHE) is a malignant vascular neoplasm, characterized by significant heterogeneity in both clinical presentation and prognosis. Its biological behavior is between benign hemangioma and malignant angiosarcoma, and it has local invasiveness and metastatic potential (13). Metastases and mortality can occur in about 25% and 15% of EHE, respectively (14). Because of its low prevalence and inconsistent presentation, cardiac EHE is frequently overlook.

However, the conclusive diagnosis and gold standard are cytology and immunohistochemistry. Open heart surgery, mediastinoscopy, and metastatic mass exploration are more invasive methods that require general anesthesia. Percutaneous transvenous biopsy of cardiac tumor can be done under the guidance of transesophageal echocardiography (TEE). But for this treatment, general anesthesia is also required. Given these tumors are often located in higher risk areas for perforation (atrial or right ventricular free wall), fluoroscopy alone is insufficient for bioptome guidance, and an additional imaging modality is required to guide the procedure. The use of intracardiac echocardiography (ICE) in cardiac procedures has continuously increased since it was first brought into clinical practice many years ago (15).

Currently, ICE is used for more than just electrophysiologic procedures, transcatheter aortic valve insertion, and percutaneous device closures (16). The operator can adjust the catheter for the

position, orientation and angle to acquire the optimal views. Without the use of general anesthesia, ICE can give us clearer cardiac imaging, and it is more practical and patient-friendly (17). ICE can reduce fluoroscopy times, resulting in less radiation exposure and procedural duration. The ICE differs from a CT and an MRI since it uses real-time imaging while being performed.

In this report, we showed the feasibility of the ICE during targeting of the biopsy catheter, and confirmed that use of ICE guided diagnostic myocardial biopsy is safe and accurate for tissue localization. The patients underwent cardiac biopsies without any complications. It can be used for the biopsy of the mass from right-side of the heart, especially in patients with high risk for anesthesia. The experiences for the left heart biopsy will be improved in the future when this approach is combined with trans-septal puncture and intracoronary sinus ICE (18). The conventional chemotherapeutic drugs paclitaxel, docetaxel, and doxorubicin are still in use today. Additionally, angiogenesis inhibitors, such as bevacizumab, sunitinib, and sorafenib, have been used to prevent the proliferation of endothelial cells. There are some studies showed many of these metastatic patients die within a few months after diagnosis (19, 20). Therefore, we must understand how crucial early diagnosis is for cardiac tumors.

However, there have been several technical challenges or limitations in the cardiac biopsy. The fluoroscopy provides very limited information in spatial information. As a result, ensuring precise location and depth in sample acquisition is insufficient. Image temporal resolution is also required because heart beats, respiration and blood flow can all affect target movement. As the wall thickness varies, the operator should be cautious of perforation (especially in left atrium). It is currently used less frequently in left atrial masses and can be combined with other more refined techniques.

Conclusions

In our cases, heart tumors present with the patient's initial nonspecific symptoms. Multiple investigations should be carried out early on in these patients, and diagnoses must be systematically taken into account. Additionally, ICE-guided atrial biopsies are a reliable and efficient diagnostic technique.

Data availability statement

The original contributions presented in the study are included in the article/**Supplementary Material**, further inquiries can be directed to the corresponding author/s.

Ethics statement

The studies involving human participants were reviewed and approved by Human Research Ethics Committee of the Second Affiliated Hospital, Zhejiang University School of Medicine.. The patients/participants provided their written informed consent to participate in this study.

Author contributions

JZ contributed to collecting clinical data. JZ and NZ contributed to editing, revising, and approving the manuscript. LJ contributed to interpreting the data. QM and XP contributed to the writing and revision of the manuscript. All authors contributed to the article and approved the submitted version.

Funding

Youth Program of National Natural Science Foundation of China (No. 81902002 for JYZ).

Conflict of interest

The authors declare that the research was conducted in the absence of any commercial or financial relationships that could be construed as a potential conflict of interest.

Publisher's note

All claims expressed in this article are solely those of the authors and do not necessarily represent those of their affiliated organizations, or those of the publisher, the editors and the reviewers. Any product that may be evaluated in this article, or claim that may be made by its manufacturer, is not guaranteed or endorsed by the publisher.

Supplementary material

The Supplementary Material for this article can be found online at https://www.frontiersin.org/articles/10.3389/fcvm.2023.1103918/full#supplementary-material.

References

1. Poterucha TJ, Kochav J, O'Connor DS, Rosner GF. Cardiac tumors: clinical presentation, diagnosis, and management. *Curr Treat Options Oncol.* (2019) 20 (8):66. doi: 10.1007/s11864-019-0662-1

2. Krishnan T, Pettersson G, Mukherjee R, Singhal N. Cardiac angiosarcoma: a diagnostic and therapeutic challenge. *J Cardiol Cases.* (2020) 22(2):90–3. doi: 10.1016/j.jccase.2020.04.010

3. Stacchiotti S, Miah AB, Frezza AM, Messiou C, Morosi C, Caraceni A, et al. Epithelioid hemangioendothelioma, an ultra-rare cancer: a consensus paper from the community of experts. *ESMO Open.* (2021) 6(3):100170. doi: 10.1016/j.esmoop.2021.100170

4. Marsico S, Orellana-Fernandez R, Tizon-Marcos H, Mas-Stachurska A, Solano A, Zuccarino F. Multimodality imaging evaluation of a primary cardiac epithelioid hemangioendothelioma. *Acta Cardiol.* (2022) 77(6):557–9. doi: 10.1080/00015385.2021.1908704

5. Ooms JF, Hirsch A, Von der Thüsen JH, Michels M, Van Mieghem NM. Intracardiac echocardiography-guided biopsy in the work-up of an unexplained cardiac mass. *JACC Cardiovasc Interv.* (2021) 14(21):e297–e9. doi: 10.1016/j.jcin.2021.08.009

6. Zanobini M, Dello Russo A, Saccocci M, Conti S, De Camilli E, Vettor G, et al. Endomyocardial biopsy guided by intracardiac echocardiography as a key step in intracardiac mass diagnosis. *BMC Cardiovasc Disord.* (2018) 18(1):15. doi: 10.1186/s12872-018-0749-9

7. Park KI, Kim MJ, Oh JK, Lee JH, Park JH, Choi SW, et al. Intracardiac echocardiography to guide biopsy for two cases of intracardiac masses. *Korean Circ J.* (2015) 45(2):165–8. doi: 10.4070/kcj.2015.45.2.165

8. Mitchell AR, Timperley J, Hudsmith L, Neubauer S, Bashir Y. Intracardiac echocardiography to guide myocardial biopsy of a primary cardiac tumour. *Eur J Echocardiogr.* (2007) 8(6):505–6. doi: 10.1016/j.euje.2006.08.005

9. Maraj S, Pressman GS, Figueredo VM. Primary cardiac tumors. *Int J Cardiol.* (2009) 133(2):152–6. doi: 10.1016/j.ijcard.2008.11.103

10. Simpson L, Kumar SK, Okuno SH, Schaff HV, Porrata LF, Buckner JC, et al. Malignant primary cardiac tumors: review of a single institution experience. *Cancer* (2008) 112(11):2440–6. doi: 10.1002/cncr.23459

11. Patel SD, Peterson A, Bartczak A, Lee S, Chojnowski S, Gajewski P, et al. Primary cardiac angiosarcoma—a review. *Med Sci Monit.* (2014) 20:103–9. doi: 10.12659/MSM.889875

12. Chen Y, He X, Shang J, Zhang N, Li X, Liu J, et al. CT Findings of pulmonary metastases from primary cardiac angiosarcoma. *Curr Med Imaging.* (2021) 17 (10):1216–20. doi: 10.2174/1573405617666210521151753

13. Rosenberg A, Agulnik M. Epithelioid hemangioendothelioma: update on diagnosis and treatment. *Curr Treat Options Oncol.* (2018) 19(4):19. doi: 10.1007/s11864-018-0536-y

14. Marchiano D, Fisher F, Hofstetter S. Epithelioid hemangioendothelioma of the heart with distant metastases. A case report and literature review. *J Cardiovasc Surg (Torino).* (1993) 34(6):529–33. PMID: 8300722

15. Prejean SP, Ahmed MK, Salama AY, Akdogan RE, Hull MS, Watts TE, et al. Use of echocardiography as an essential tool for targeted transcatheter biopsy of cardiac masses. *Echocardiography* (2019) 36(11):2086–9. doi: 10.1111/echo.14512

16. Gianni C, Sanchez JE, Della Rocca DG, Al-Ahmad A, Horton RP, Di Biase L, et al. Intracardiac echocardiography to guide catheter ablation of atrial fibrillation. *Card Electrophysiol Clin.* (2021) 13(2):303–11. doi: 10.1016/j.ccep.2021.03.009

17. Alkhouli M, Hijazi ZM, Holmes DR Jr., Rihal CS, Wiegers SE. Intracardiac echocardiography in structural heart disease interventions. *JACC Cardiovasc Interv.* (2018) 11(21):2133–47. doi: 10.1016/j.jcin.2018.06.056

18. Yokoyama Y, Yamagata K, Kanzaki H, Kusano K. Left ventricular endomyocardial biopsy guided by intracardiac echocardiography via a trans-septal approach. *BMJ Case Rep.* (2021) 14(7):1–3. doi: 10.1136/bcr-2021-243176

19. Agaimy A, Rösch J, Weyand M, Strecker T. Primary and metastatic cardiac sarcomas: a 12-year experience at a German heart center. *Int J Clin Exp Pathol.* (2012) 5(9):928–38. PMC ID: PMC3484490

20. Lau C, Leonard JR, Schwann AN, Soletti G, Abouarab AA, Munjal M, et al. A 20-year experience with resection of primary cardiac tumors and metastatic tumors of the heart. *Ann Thorac Surg.* (2019) 107(4):1126–31. doi: 10.1016/j.athoracsur.2018.10.023

frontiers | Frontiers in Cardiovascular Medicine

TYPE Case Report
PUBLISHED 02 May 2023
DOI 10.3389/fcvm.2023.1115870

Check for updates

OPEN ACCESS

EDITED BY
Reto Asmis,
Wake Forest University, United States

REVIEWED BY
Yung-Wei Chi,
University of California, Davis, United States
Fabian Linden,
Heidelberg University, Germany

*CORRESPONDENCE
Agnes S. Kim
akim@uchc.edu

RECEIVED 04 December 2022
ACCEPTED 12 April 2023
PUBLISHED 02 May 2023

CITATION
Zeman J, Kompella R, Lee J and Kim AS (2023) Case report: Non-thrombotic iliac vein lesion: an unusual cause of unilateral leg swelling in a patient with endometrial carcinoma. Front. Cardiovasc. Med. 10:1115870. doi: 10.3389/fcvm.2023.1115870

COPYRIGHT
© 2023 Zeman, Kompella, Lee and Kim. This is an open-access article distributed under the terms of the Creative Commons Attribution License (CC BY). The use, distribution or reproduction in other forums is permitted, provided the original author(s) and the copyright owner(s) are credited and that the original publication in this journal is cited, in accordance with accepted academic practice. No use, distribution or reproduction is permitted which does not comply with these terms.

Case report: Non-thrombotic iliac vein lesion: an unusual cause of unilateral leg swelling in a patient with endometrial carcinoma

Jan Zeman[1], Ritika Kompella[1], JuYong Lee[1,2] and Agnes S. Kim[1,2]*

[1]Department of Internal Medicine, University of Connecticut Health Center, Farmington, CT, United States, [2]Calhoun Cardiology Center, University of Connecticut Health Center, Farmington, CT, United States

81-year-old female presented with subacute right lower extremity edema due to iliac vein compression by a markedly enlarged external iliac lymph node later identified as newly relapsed metastatic endometrial carcinoma. The patient underwent a full evaluation of the iliac vein lesion and cancer and had an intravenous stent placed with complete resolution of symptoms post-procedure.

KEYWORDS

peripheral edema, cancer, imaging, vascular disease, intravascular ultrasonography (IVUS)

History of presentation and medical history

An 81-year-old Caucasian female with a history of stage IB high-grade undifferentiated endometrial carcinoma diagnosed 2 years prior and paroxysmal atrial fibrillation (AF) on anticoagulation presented with a two-week history of right leg swelling (**Table 1**). The edema extended to her knee and was not relieved by conservative measures, including compression stockings. Of note, the patient's endometrial carcinoma was initially treated with hysterectomy, bilateral salpingo-oophorectomy, vaginal brachytherapy, and 6 cycles of chemotherapy with Carboplatin and Paclitaxel. The patient had since been in remission. Her family history was significant for breast cancer and dementia in her mother, atrial fibrillation (AF) and leukemia in her father, and unspecified cancer in her brother. The patient had multiple risk factors for AF—family history of AF, sedentary lifestyle, obesity, hypertension, left atrial enlargement, and previous exposure to carboplatin. She had no significant smoking, alcohol, or illicit drug history. She retired from accounting 20 years ago.

Learning objectives

- To broaden the differential diagnosis of unilateral peripheral edema in a patient with a history of cancer.
- To understand the comprehensive evaluation and treatment of NIVL.

Abbreviations
(NIVL), Non-thrombotic iliac vein lesion; (RHC), right heart catheterization; (CT), computed tomography; (PET), positron emission tomography; (IVUS), intravascular ultrasound; (DVT), deep vein thrombosis; (MTS), May-Thurner Syndrome; (LAD), lymphadenopathy.

TABLE 1 Timeline of the events.

DATE	EVENT
January 2018	Endometrial biopsy after complaints of severe abdominal pain and vaginal spotting
May 18, 2018	Laparoscopic hysterectomy with bilateral salpingo-oophorectomy for staging purposes after abnormal endometrial biopsy showing endometrial carcinoma
June 15, 2018	Initiation of chemotherapy with Carboplatin and Paclitaxel as well as vaginal brachytherapy for pathologically confirmed stage IB high-grade undifferentiated endometrial carcinoma
November 2018	Completion of chemo-radiation therapy; CT abdomen pelvis showed no evidence of disease
February 2019	Initial diagnosis of atrial fibrillation after an evaluation of sudden onset shortness of breath; started on anticoagulation
June 25, 2020	The patient initially noticed significant right leg swelling
July 8, 2020	Cardiology visit for evaluation of new-onset unilateral leg edema
July 31, 2020	Ultrasound examination of the right lower extremity showed right external iliac vein compression, transthoracic echocardiogram showed normal LVEF, left atrial enlargement, and moderate mitral regurgitation
August 18, 2020	Right iliac vein venogram and right heart catheterization performed
September 2, 2020	Stent was placed in the right iliac vein to relieve the compression
September 21, 2020	Laparoscopy with lymph node biopsy confirmed cancer invasion in the wall of the right iliac vein and the right ureteral wall
April 5, 2023	Ultrasonographic evaluation of the venous stent showed patency.

Differential diagnosis

The differential diagnosis of unilateral leg edema includes deep vein thrombosis, cellulitis, Baker's cyst, lower extremity trauma, lymphedema, venous insufficiency, and May-Thurner syndrome.

Investigations

The first step in the patient's diagnostic work-up was a venous Duplex ultrasound test of the right lower extremity, which revealed marked right external iliac vein narrowing with abnormal Doppler waveforms, suggestive of a hemodynamically significant obstructive lesion secondary to external compression. A transthoracic echocardiogram revealed normal left ventricular size and systolic function, mild left atrial dilation, grade 1 diastolic dysfunction, moderate mitral regurgitation, and an elevated estimated right atrial pressure based on the dilated inferior vena cava. To measure the intracardiac pressures, rule out pulmonary hypertension, and better characterize the iliac vein stenosis, the patient underwent right heart catheterization (RHC) with iliac venography. The iliac venogram revealed severe stenosis of the right external iliac vein (**Figure 1A**), while RHC showed normal intracardiac pressures (normal RAP, mean PAP, and PCWP).

Given her history of endometrial carcinoma, the possibility of extrinsic compression of the iliac vein by tumor was considered. Thus, a computed tomography (CT) scan of the abdomen/pelvis with and without intravenous (IV) contrast was obtained. The results indicated a markedly enlarged and necrotic right external iliac lymph node ($2.5 \times 3.2 \times 2.7$ cm) which was causing external compression of, and likely invading, the right iliac vein (**Figure 1B**). Significant compression of the right ureter associated with severe right-sided hydronephrosis (**Figure 1C**) and right pelvic sidewall lymphadenopathy were seen as well. Next, a full-body PET scan was ordered for staging purposes, demonstrating metabolic activity in the right external iliac lymph node and an area of increased activity in the left adrenal gland (**Figures 1D, E**). After a multidisciplinary discussion, the patient was offered an endovascular intervention of the iliac vein with stenting to improve her refractory right lower extremity edema.

Management

Since there was a high probability of cancer invading the vessel wall and the right ureter, a decision was made for palliative endovascular stent placement to provide symptomatic relief and to avoid the risks of an open surgical approach, including intra-operative and post-operative bleeding. The patient was taken to the cardiac catheterization laboratory, where an intravascular ultrasound (IVUS) was performed to visualize the lesion and to measure the lesion length and the reference diameter for choosing the correct size of the stent. After the lesion was crossed with a 0.035 angled glide guide wire, the patient underwent right external iliac vein balloon angioplasty followed by the successful placement of a VICI 14×90 mm stent, VENITI, INC., Fremont, CA. Post-dilation was done with a 10×60 mm balloon at 8 atmospheres and a 14×60 mm balloon at 4 atmospheres. The follow-up IVUS showed a re-canalized iliac vein with normal venous flow and 100 mm^2 of luminal gain at the previously occluded point. The re-canalization was additionally re-demonstrated on an abdominal/pelvic CT scan (**Figures 2A, B**).

Follow-up

The patient's right lower extremity edema completely resolved after the intervention. The patient was started on aspirin 81 mg daily for three months to prevent stent thrombosis and allow its endothelization. A few weeks later, the patient underwent laparoscopy with retroperitoneal lymph node biopsy and tumor debulking. The surgeon released the ureteral compression but was unable to remove the obstructing lymph node, as it was invading the iliac vein wall with a high risk of bleeding. The patient was followed by interventional cardiology every six months with Doppler imaging, with vein patency noted during two years of follow-up.

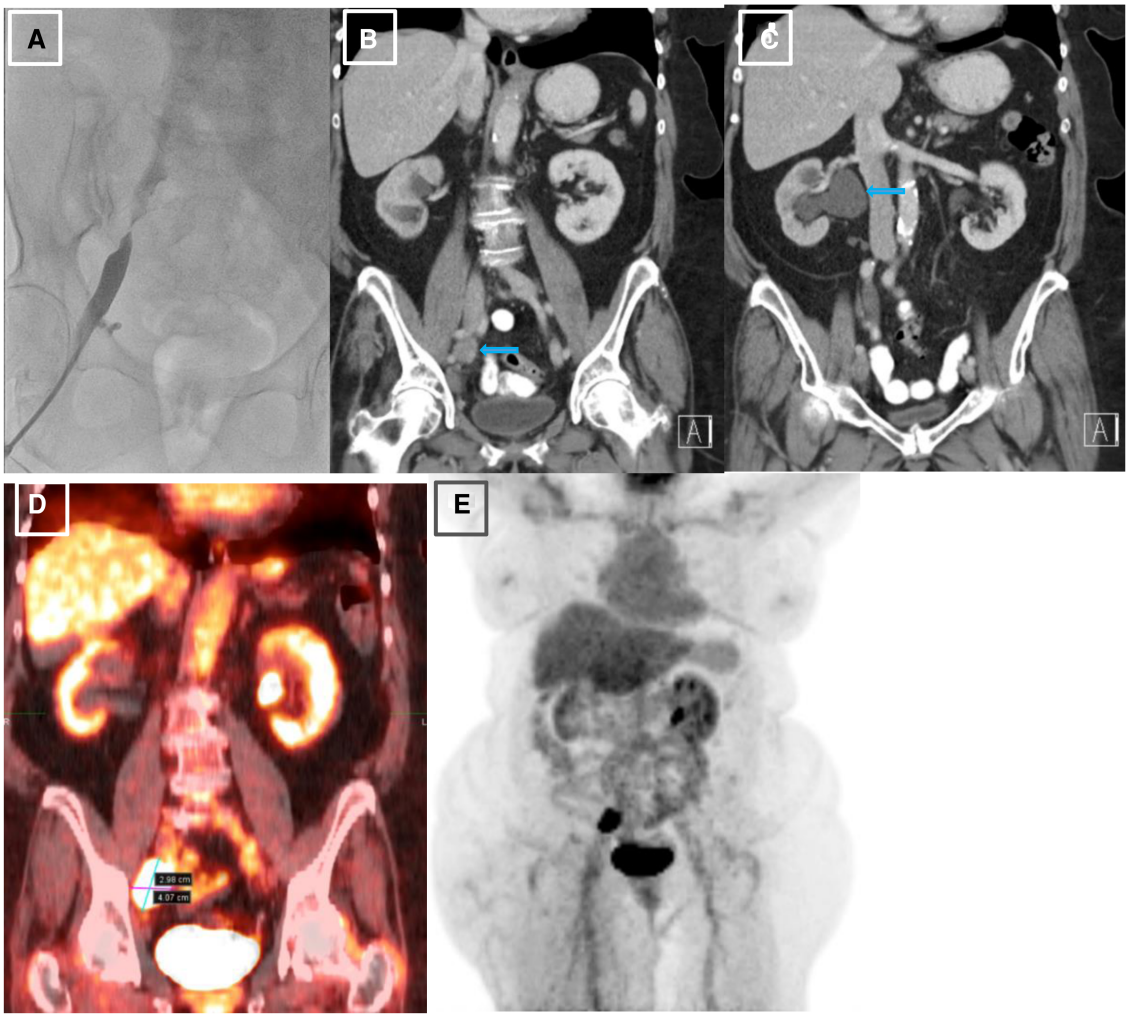

FIGURE 1
Initial venography, CT and PET imaging of the right external iliac vein. (**A**). Iliac venography demonstrating severe stenosis of right external iliac vein. (**B**). CT abdomen pelvis revealing right external iliac lymphadenopathy (LAD), measuring 2.5 × 3.2 × 2.7 cm, marked by blue arrow. (**C**). CT abdomen pelvis demonstrating severe right sided hydronephrosis due toR ureteral external compression by mass burden, marked by blue arrow. (**D**, **E**). PET scan redemonstrating R external iliac LAD.

Discussion

The development of lower extremity edema, as other types of edema, occurs by three main mechanisms, all of which are caused by fluid shifts from the intravascular to the interstitial space: an increase in intravascular hydrostatic pressure, a decrease in hydrostatic oncotic pressure or increased capillary permeability. The diagnostic work-up for leg swelling depends on the time of onset and its laterality. As seen in this patient, the development of an acute or subacute unilateral lower extremity edema can occur over the span of hours or weeks, and the differential diagnosis includes deep vein thrombosis (DVT), musculoskeletal injury, ruptured popliteal cyst, or venous compression (1). Patients with cancer have a high risk of developing venous thromboembolism (VTE) for several reasons: cancer is associated with high a pro-inflammatory and hypercoagulable state, tumor mass can cause venous external compression, and certain anticancer drugs can increase the risk of VTE. Anticancer drugs that have been reported to increase VTE risk include Thalidomide, Lenalidomide, and Bevacizumab (2). These medications are linked to an increased risk of VTE including DVT and arterial events (2). Thalidomide, particularly when used with dexamethasone, has been associated with up to 28% DVT rates, with additional risk factors including combined use with Doxorubicin, newly diagnosed disease, and Chromosome 11 abnormalities (2). Lenalidomide may have VTE rates as high as 75% (2). Bevacizumab, an anti-angiogenic, has been linked to an increased risk of arterial and venous events (2). Platinum-based compounds, such as cisplatin and carboplatin, can also cause arterial and venous thromboembolism (3). In patients with unprovoked DVT, age-appropriate cancer screening should follow the treatment of DVT. In the case of bilateral lower extremity edema in a patient with cancer, the differential diagnosis should also include thrombosis within, or extrinsic compression of, the inferior vena cava.

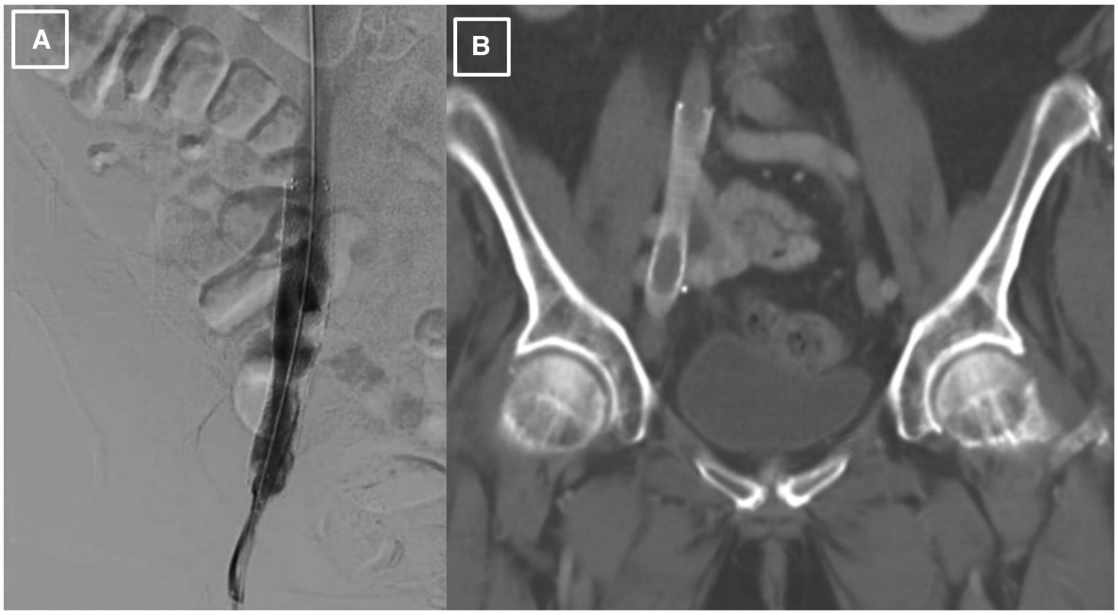

FIGURE 2
Post-procedural imaging of the stented right external iliac vein. (**A**). Iliac venography status post IVUS-guided visualization and right external iliac vein balloon-angioplasty with successful placement of VICI 14 × 90 mm stent and resultant patency. (**B**). CT abdomen pelvis demonstrating presence of stent within the R external iliac vein prior to abdominal debulking procedure.

Iliac vein compression syndrome, a subtype of NIVL, also known as May-Thurner syndrome (MTS) is a condition mostly seen in young women who present with left leg swelling due to the compression of the left common iliac vein by the right common iliac artery at the level of the lumbar spine. The prevalence of MTS is estimated to be between 15%–30% based on autopsy data. The vast majority of these patients remain asymptomatic with only 2%–5% of patients developing a DVT. Long-standing MTS often results in chronic venous disease (4). In contrast to MTS, NIVL can occur in any segment of the iliac vein caused by other etiologies such as extrinsic compression by tumor, mass, spine spurs, or calcified atherosclerotic iliac arteries (5).

The first-line imaging modality used in diagnosing NIVL or evaluating unilateral leg swelling in patients with cancer is Doppler ultrasound of the iliac and other lower extremity veins. The test is noninvasive, easily accessible, and readily available. However, its diagnostic value may be limited in lesions with lower severity or in patients with obesity due to technical limitations. For typical MTS, CT pelvis with IV contrast is not sensitive enough to diagnose the compressed iliac vein due to limited visibility, but it is a good modality for ruling out extrinsic compression as in NIVL. CT venography with contrast is useful to further differentiate thrombotic from non-thrombotic intravenous lesions (6). Invasive venography is a useful diagnostic tool for identifying occlusion or severe stenosis of iliac veins, as demonstrated in our case. However, its effectiveness may be limited in detecting luminal narrowing, resulting in potentially missed diagnoses of NIVL due to its low sensitivity in this regard. Specifically, the diagnostic quality may be compromised in cases of non-occlusive or partially narrowed iliac vein lesions. Therefore, in instances where clinical indications strongly suggest NIVL, such as in our case, the use of intravascular ultrasound (IVUS) is warranted for a more accurate diagnosis as IVUS can provide a 360° view within the vessel itself, which provides greater anatomic detail of the affected region (7). In fact, it has been demonstrated to approximate the morphology of the lesion, affording greater predictive value for stent sizing compared with the CT venogram alone (8, 9). IVUS was found to have a diagnostic sensitivity of > 90% for lesion detection when compared with CT venography, which has a 68% sensitivity (6).

The spectrum of treatments available for NIVL largely depends on the severity and persistence of the patient's symptoms. Conservative management includes compression stockings with leg elevation and calf muscle exercises. In refractory cases, endovascular repair with stent placement is pursued (10). Many studies have demonstrated an overall improvement in the quality of life and reduction in symptom severity with the use of venous stenting, such that it is nearly considered to be the gold standard for patients with high symptom burden (5, 9, 11).

A specific subgroup of NIVL called cancer-associated vein obstruction (CAVO) has recently garnered attention (12). A few studies have shown that percutaneous intervention is effective in reducing symptoms of swelling and discomfort with a low risk of complications (13). One group studied the efficacy of treating CAVO with an endovascular venous stent combined with linear Iodine-125 radioactive seeds strand. The new technique yielded longer patency of the stent and lower symptom burden without affecting survival (14).

Conclusions

In patients with cancer, DVT is the most likely cause of acute or subacute unilateral leg edema and should be ruled out first before considering other less common etiologies, such as NIVL. The latter condition may not be widely recognized by general providers. The recommended diagnostic workup consists of a duplex ultrasound of the deep iliac venous system, which often demonstrates abnormal venous Doppler waveforms, and a CT venogram of the pelvis to potentially visualize the iliac vein compression. It is important to remember that a negative CT venogram does not rule out NIVL due to its low diagnostic sensitivity. When there is a high index of suspicion for NIVL, invasive iliac venography with IVUS evaluation is instrumental in leading to the correct diagnosis and offering the option of therapeutic endovascular venous stenting. After multidisciplinary discussion and shared decision-making with the patient, endovascular intervention vs. surgical approach vs. medical management is chosen depending on the clinical situation.

Data availability statement

The original contributions presented in the study are included in the article, further inquiries can be directed to the corresponding author.

Ethics statement

Written informed consent was obtained from the individual for the publication of any potentially identifiable images or data included in this article.

Author contributions

JZ, RK—writting sections of the article equally JL—revision and editing mainly of the interventional part of the article and the discussion AK—supervision of the composition of the whole manuscript, editing the article, consulting with other authors during this process. All authors contributed to the article and approved the submitted version.

Funding

The article publishing charge has been funded by the Letts O'Brien Fund for Breast Cancer Research.

Conflict of interest

The authors declare that the research was conducted in the absence of any commercial or financial relationships that could be construed as a potential conflict of interest.

Publisher's note

All claims expressed in this article are solely those of the authors and do not necessarily represent those of their affiliated organizations, or those of the publisher, the editors and the reviewers. Any product that may be evaluated in this article, or claim that may be made by its manufacturer, is not guaranteed or endorsed by the publisher.

References

1. Gasparis AP, Kim PS, Dean SM, Khilnani NM, Labropoulos N. Diagnostic approach to lower limb edema. *Phlebology*. (2020) 35(9):650–5. doi: 10.1177/0268355520938283

2. Qureshi W, Ali Z, Amjad W, Alirhayim Z, Farooq H, Qadir S, et al. Venous thromboembolism in cancer: an update of treatment and prevention in the era of newer anticoagulants. *Front Cardiovasc Med*. (2016) 3:24. doi: 10.3389/fcvm.2016.00024

3. Grover SP, Hisada YM, Kasthuri RS, Reeves BN, Mackman N. Cancer therapy-associated thrombosis. *Arterioscler Thromb Vasc Biol*. (2021) 41(4):1291–305. doi: 10.1161/ATVBAHA.120.314378

4. Raju S, Neglen P. High prevalence of nonthrombotic iliac vein lesions in chronic venous disease: a permissive role in pathogenicity. *J Vasc Surg*. (2006) 44(1):136–44. doi: 10.1016/j.jvs.2006.02.065

5. Radaideh Q, Patel NM, Shammas NW. Iliac vein compression: epidemiology, diagnosis and treatment. *Vasc Health Risk Manag*. (2019) 15:115–22. doi: 10.2147/VHRM.S203349

6. Liu Z, Gao N, Shen L, Yang J, Zhu Y, Li Z, et al. Endovascular treatment for symptomatic iliac vein compression syndrome: a prospective consecutive series of 48 patients. *Ann Vasc Surg*. (2014) 28(3):695–704. doi: 10.1016/j.avsg.2013.05.019

7. McLafferty RB. The role of intravascular ultrasound in venous thromboembolism. *Semin Intervent Radiol*. (2012) 29(1):10–5. doi: 10.1055/s-0032-1302446

8. Montminy ML, Thomasson JD, Tanaka GJ, Lamanilao LM, Crim W, Raju S. A comparison between intravascular ultrasound and venography in identifying key parameters essential for iliac vein stenting. *J Vasc Surg Venous Lymphat Disord*. (2019) 7(6):801–7. doi: 10.1016/j.jvsv.2019.03.015

9. Neglén P, Raju S. Intravascular ultrasound scan evaluation of the obstructed vein. *J Vasc Surg*. (2002) 35(4):694–700. doi: 10.1067/mva.2002.121127

10. Razavi MK, Black S, Gagne P, Chiacchierini R, Nicolini P, Marston M, et al. Pivotal study of endovenous stent placement for symptomatic iliofemoral venous obstruction. *Circ Cardiovasc Interv*. (2019) 12(12):e008268. doi: 10.1161/CIRCINTERVENTIONS.119.008268

11. Chen Z, Zhang XC, Sun Y, Xu M. Diagnosis and treatment of nonthrombotic right iliac vein compression syndrome. *Ann Vasc Surg*. (2019) 61:363–70. doi: 10.1016/j.avsg.2019.05.033

12. Xiao L, Tong JJ, Shen J. Endoluminal treatment for venous vascular complications of malignant tumors. *Exp Ther Med*. (2012) 4(2):323–8. doi: 10.3892/etm.2012.589

13. O'Sullivan GJ, Waldron D, Mannion E, Keane M, Donnellan PP. Thrombolysis and iliofemoral vein stent placement in cancer patients with lower extremity swelling attributed to lymphedema. *J Vasc Interv Radiol*. (2015) 26(1):39–45. doi: 10.1016/j.jvir.2014.10.010

14. Wu B, Yin G, He X, Chen G, Zhao B, Song J, et al. Endovascular treatment of cancer-associated venous obstruction: comparison of efficacy between stent alone and stent combined with linear radioactive seeds strand. *Vasc Endovascular Surg*. (2020) 54(7):565–72. doi: 10.1177/1538574420939747

frontiers | Frontiers in Cardiovascular Medicine

TYPE Case Report
PUBLISHED 10 May 2023
DOI 10.3389/fcvm.2023.1130237

Check for updates

OPEN ACCESS

EDITED BY
Xiang Wei,
Huazhong University of Science and Technology, China

REVIEWED BY
JunMing Zhu,
Capital Medical University, China
Alan Soo,
University Hospital Galway, Ireland

*CORRESPONDENCE
Liu Kexiang
email@uni.edu
kxliu64@hotmail.com

RECEIVED 23 December 2022
ACCEPTED 21 April 2023
PUBLISHED 10 May 2023

CITATION
Ran W, Cuilin Z, Hulin P and Kexiang L (2023) Case report: Successful treatment of mediastinal unicentric castleman disease using cardiopulmonary bypass.
Front. Cardiovasc. Med. 10:1130237.
doi: 10.3389/fcvm.2023.1130237

COPYRIGHT
© 2023 Ran, Cuilin, Hulin and Kexiang. This is an open-access article distributed under the terms of the Creative Commons Attribution License (CC BY). The use, distribution or reproduction in other forums is permitted, provided the original author(s) and the copyright owner(s) are credited and that the original publication in this journal is cited, in accordance with accepted academic practice. No use, distribution or reproduction is permitted which does not comply with these terms.

Case report: Successful treatment of mediastinal unicentric castleman disease using cardiopulmonary bypass

Wei Ran, Zhu Cuilin, Piao Hulin and Liu Kexiang*

Dept Cardiovasc Surg, Second Hosp Jilin Univ, Changchun, China

Unicentric Castleman disease (UCD) is a rare, benign lymphoproliferative disorder. Mediastinal UCD has tumors with no clear boundaries that are highly vascularized. Resection surgery results in bleeding, leading to further challenges. Mixed-type UCD is rare. We report the case of a 38-year-old asymptomatic patient with mixed-type UCD; the tumor measured 7.8 cm in size and had unclear boundaries. The tumor was successfully resected by performing a cardiopulmonary bypass on the beating heart; the patient recovered uneventfully.

KEYWORDS

castleman's disease, middle mediastinal tumor, mixed pathology, cardiopulmonary bypass, surgery

Introduction

Castleman disease (CD), first reported by Castleman and Towne in 1954, is a rare, benign lymphoproliferative disorder (1). CD can be divided into two categories: unicentric Castleman disease (UCD) and multicentric Castleman disease (MCD). Mediastinal UCD is a common type of UCD that is accompanied by prominent feeding vessels. Owing to the lack of typical clinical signs, CD is difficult to diagnose. Herein, we report the case of a 38-year-old asymptomatic patient with mixed-type UCD; the tumor measured 7.8 cm in size and had unclear boundaries. The tumor was successfully resected by performing a cardiopulmonary bypass (CPB) on the beating heart.

Case presentation

A 38-year-old man with no obvious symptoms was found to have a mediastinal tumor during a physical examination. The patient had no significant medical history except having diabetes mellitus for a year. He was referred to our hospital for medical treatment. No pathologic signs were found through other physical examinations. His laboratory test results were all within the normal limits, except for the lymphocyte count (13.1%), which was lower than the normal range. The levels of tumor markers alpha-fetoprotein, human chorionic gonadotropin, and lactate dehydrogenase were all normal. The thoracic computed tomography (CT) scan revealed a huge soft tissue density shadow of 72 × 48 mm in the mediastinum. The tumor was compressed near the main pulmonary artery bifurcation and extended along the right pulmonary artery and did not have clear boundaries (**Figure 1**). His cardiac ultrasonography revealed a huge pericardial effusion, approximately 28 mm. Considering the location of the tumor and the risk of bleeding, we

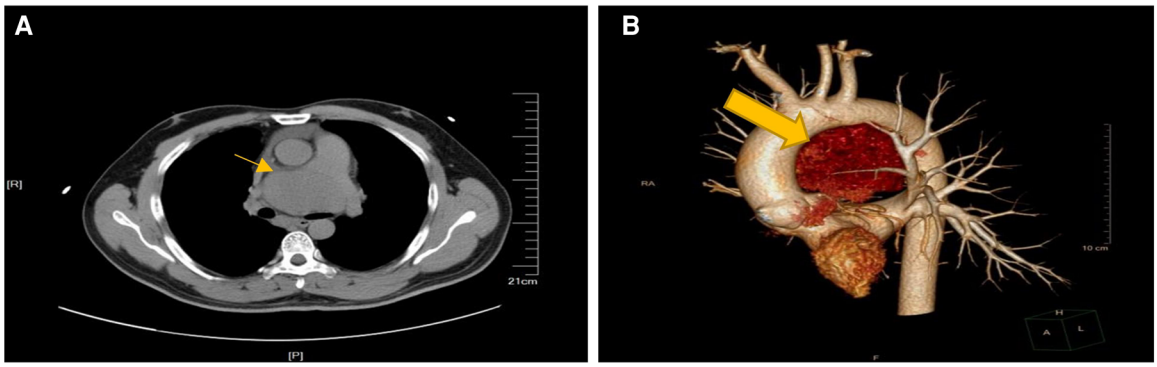

FIGURE 1
Preparative computed tomography scan of the chest showing in the anterior mediastinum. (A) The mass close to the main pulmonary artery bifurcation and extended along the right pulmonary artery. (B) Lateral view of 3-D computerized tomography showing the mass between aortic arch and pulmonary artery.

did not schedule a biopsy for him. The tumor was planned for resection via median sternotomy.

After sternotomy, the tumor was observed to occupy the area within the aorta-pulmonary window, which also severely compressed the cardiac left atrium. The tumor was vascularized and thus was highly susceptible to bleeding. Disassociation of the pulmonary arteries and the left atrium was essential for successful and complete resection of the tumor. The tumor was huge, and dissection of the tumor was attempted from the pulmonary artery and the left atrium, but the patient was hemodynamically unstable. To guarantee the safety of the patient, the surgical team decided to complete the surgery by performing CPB on the beating heart as an adjunct surgical support. CPB was performed via cannulation of the femoral artery and superior and inferior vena cava. The pressure in the pulmonary artery and heart was reduced through CPB. The aorta and pulmonary artery were pulled away to expose the tumor completely, and then, the tumor was meticulously dissected along the margins from the surrounding tissues. Before dissociation, the area of strong adhesion was gently peeled off and the borders of the blood vessels and the surrounding tissue were carefully confirmed. Electrocoagulation was used to control bleeding from tiny bleeding spots, whereas ligation was done when bigger blood vessel branches were found. The tumor was completely resected after a CPB duration of 165 min. After recovery of stable hemodynamics, CPB was discontinued. The remainder of the surgery was smooth, including hemostasis and chest closure.

On gross inspection, the resected tumor measured 7.8 cm in size (Figure 2). Microscopic examination demonstrated preserved lymph node architecture with a capsule, surrounded by peripheral lymphocytes in concentric circles, interfollicular vascular proliferation with perivascular hyalinization, plasma cells, and macrophage infiltration (Figure 3). Immunohistochemical staining showed the following: CD20 (+), CD3 (+), PAX5 (+), CD5 (+), CyclinD1 (−), CD10 (−), Bcl6 (−), CD21 (FDC +), Kappa (+), Lambda (+), IgD (weak +), Ki67 (positive rate 15%), CD23 (FDC +), CD38 (+), CD30 (scattered +), MUMI (partial +), CD34 (vascular +), HHVV8 (−), and CD123 (−). Based on the pathology slides, the final diagnosis of this patient was mixed-type UCD.

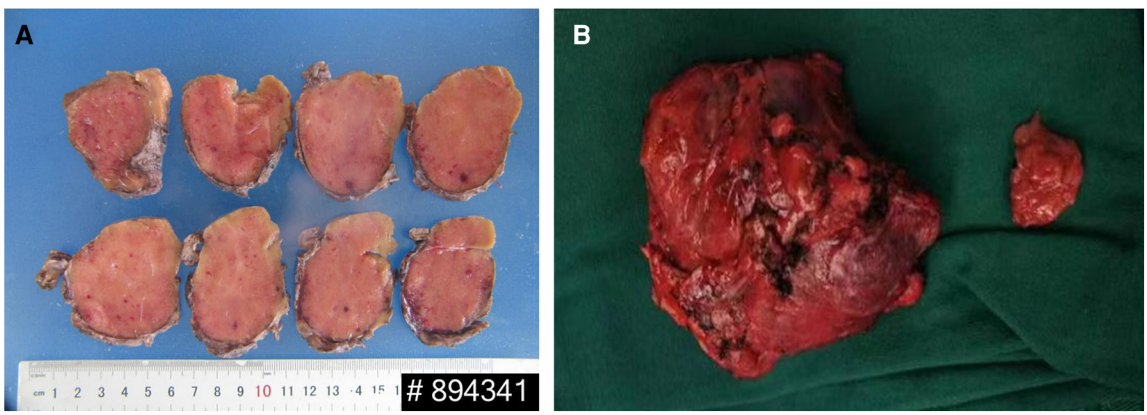

FIGURE 2
(A) The cut surface showing a solid, homogeneous, and gray mass. (B) Gross appearance of the mass.

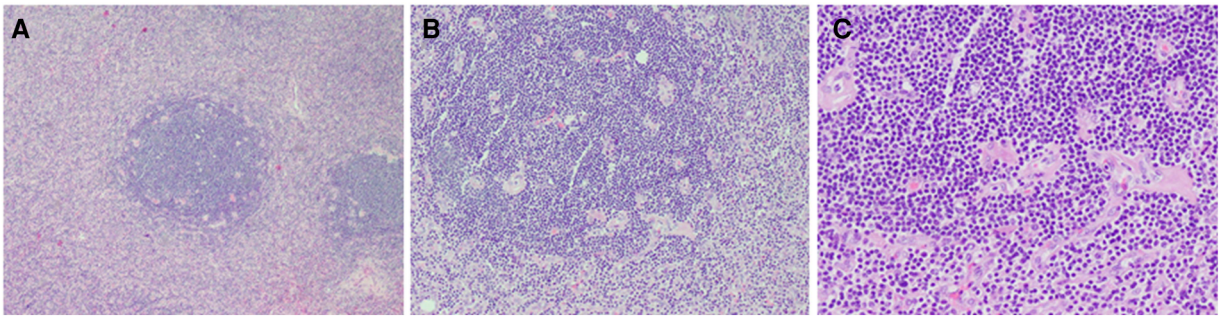

FIGURE 3
Histopathological examination showed (A) preserved lymph node architecture with a capsule, (B) surrounded by peripheral lymphocytes in concentric circles, (C) interfollicular vascular proliferation with perivascular hyalinization and plasma cells and histiocytes infiltration.

The patient had an uneventful postoperative course and was discharged on postoperative day 21. The patient was continuously followed up; he was doing well 1 year postoperatively. The 1-year CT scan showed no residual tumor and no recurrence of the tumor (**Figure 4**). Regular annual CT imaging follow-up was advised for the patient.

Discussion

CD is a rare, benign lymphoproliferative disorder of unknown etiology and is also called follicular lymph node hyperplasia. Pathologically, it can be divided into hyaline vascular type, plasma cell type, or mixed type. Clinically, single lymph node region enlargement is defined as UCD and multiple lymph node region enlargement as MCD. UCD is mostly hyaline vascular type, MCD is mostly plasma cell type and mixed type, and mixed-type UCD is rare (2). Our patient had mixed-type UCD, which is rare.

UCD is mostly asymptomatic, and chest tightness, dyspnea, cough, and dysphagia can occur when the tumor increases in size and starts oppressing the surrounding tissues and organs. UCD often occurs in the mediastinum and needs to be differentiated from thymoma, lymphoma, metastatic tumor, and neurogenic tumor. Pericardial effusion is associated with CD (3, 4), possibly due to the generalized inflammatory syndrome related to plasma cell histology. The pathological type of our patient was categorized as mixed type, and pericardial effusion is not a common clinical manifestation of mixed type. To the best of our knowledge, this is the first case of mixed-type UCD presenting with pericardial effusion as a clinical manifestation.

Surgical excision of the tumor is both a diagnostic and therapeutic procedure. The gold standard of diagnosis is pathological examination (5). Although ultrasound and CT can be used as diagnostic tools, ultrasound-guided penetration has the risk of causing hemorrhage because UCD is densely packed with blood vessels (6). Our team believes that preoperative puncture has a high risk of bleeding; thus, biopsy during surgery was considered to be safer. Therefore, in our case, we did not perform penetration before surgery.

Mediastinal UCD is treated with surgical resection, which includes open surgery and video-assisted thoracoscopy. A

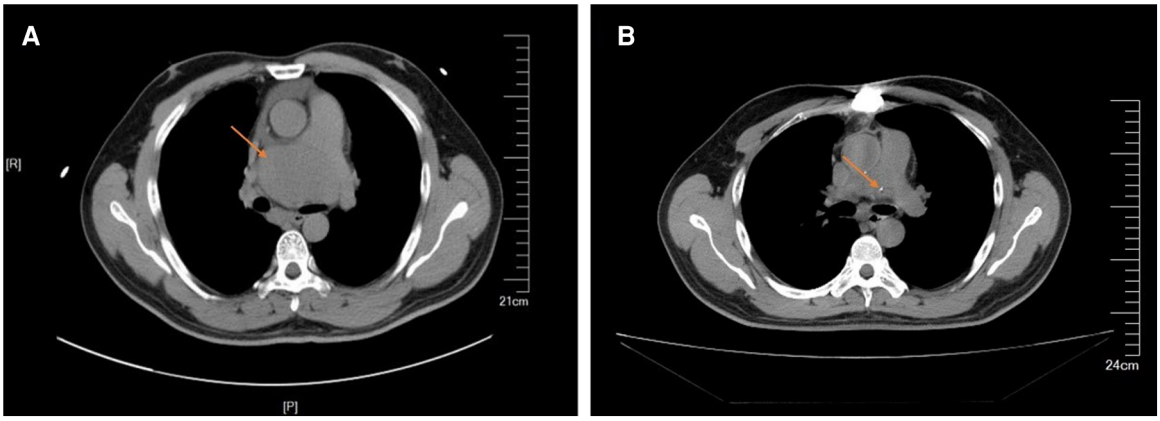

FIGURE 4
(A) Preparative computed tomography scan showed that the mass close to the main pulmonary artery bifurcation and extended along the right pulmonary artery. (B) Postoperative computed tomography scan showed no residual and no recurrence of the tumor.

previous study has shown video-assisted thoracoscopy to be not useful (7). However, there have been cases of effective thoracoscopic resection in recent years (8, 9). Video-assisted thoracoscopy is a good option for UCD that is located in the anterior mediastinum or upper mediastinum and has distinct boundaries and does not oppress the heart or blood vessels. The tumor in our case was near the pulmonary arteries and left atrium with no clear boundaries. Therefore, VATS was not used in our case; we believed that median sternotomy was safer for the patient.

Surgical resection of UCD is complicated by excessive blood loss because CD is highly vascularized. Preoperative embolization can be used as an adjunct to avoid intraoperative bleeding (10). In our case, we used CPB to guarantee complete resection of the tumor and the safety of the patient. The application of CPB is of great contribution to intraoperative dynamic stability and meticulous surgical bleeding control. Moreover, to reduce the chances of rupture during operation, the pressure on the pulmonary and cardiac arteries can be relieved by CPB. In our case, the patient did not require any blood transfusion. Thus, our experience supports the application of CPB as a safe and effective technique for the successful surgical treatment of UCD.

Conclusion

CD is a rather uncommon condition. Pathological diagnosis is the gold standard, as radiographic examination is not specific. For UCD, surgical resection is the treatment of choice. The application of CPB is a useful and effective technique for successful surgical treatment.

Data availability statement

The original contributions presented in the study are included in the article, further inquiries can be directed to the corresponding author/s.

Ethics statement

The studies involving human participants were reviewed and approved by the ethics Committee of the second hospital of jilin university. The patients/participants provided their written informed consent to participate in this study. Written informed consent was obtained from the individual(s) for the publication of any potentially identifiable images or data included in this article.

Author contributions

WR, CL, and LX: contributed to the conception of the manuscript. WR and PL: organized the data collection. All authors contributed to the article and approved the submitted version.

Conflict of interest

The authors declare that the research was conducted in the absence of any commercial or financial relationships that could be construed as a potential conflict of interest.

Publisher's note

All claims expressed in this article are solely those of the authors and do not necessarily represent those of their affiliated organizations, or those of the publisher, the editors and the reviewers. Any product that may be evaluated in this article, or claim that may be made by its manufacturer, is not guaranteed or endorsed by the publisher.

References

1. Castleman B, Iverson L, Menendez VP. Localized mediastinal lymph-node hyperplasia resembling thymoma. *Cancer*. (1956) 9(4):822–30. doi: 10.1002/1097-0142(195607/08)9:4<822::AID-CNCR2820090430>3.0.CO;2-4

2. Keller AR, Hochholzer L, Castleman B. Hyaline-vascular and plasma-cell types of giant lymph node hyperplasia of the mediastinum and other locations. *Cancer*. (1972) 29(3):670. doi: 10.1002/1097-0142(197203)29:3<670::AID-CNCR2820290321>3.0.CO;2-#

3. Mihăilă M, Herlea V, Dobrea C. An unusual presentation of plasma cells—castleman disease: a case report. *Rom J Intern Med*. (2016) 54(2):129–33. doi: 10.1515/rjim-2016-0014

4. Nicolosi AC, Almassi GH, Komorowski R. Cardiac tamponade secondary to giant lymph node hyperplasia: castleman's Disease. *Chest*. (1995) 105(2):637–9. doi: 10.1378/chest.105.2.637

5. Arlet J-B, Hermine O, Darnige L, Ostland V, Westerman M, Badoual C, et al. Iron-deficiency anemia in castleman disease: implication of the interleukin 6/hepcidin pathway. *Pediatrics*. (2010) 126(6):e1608. doi: 10.1542/peds.2010-1123

6. Madan R, Chen JH, Trotman-Dickenson B, Jacobson F, Hunsaker A. The spectrum of Castleman's disease: mimics, radiologic pathologic correlation and role of imaging in patient management. *Eur J Radiol*. (2012) 81(1):123–31. doi: 10.1016/j.ejrad.2010.06.018

7. Talat N, Belgaumkar AP, Schulte KM. Surgery in Castleman's disease: a systematic review of 404 published cases. *Ann Surg*. (2012) 255:677–84. doi: 10.1097/SLA.0b013e318249dcdc

8. Wang YQ, Li SQ, Guo F. Video-assisted thoracoscopic surgery is a safe and effective method to treat intrathoracic unicentric Castleman's disease. *BMC Surg*. (2020) 20:127. doi: 10.1186/s12893-020-00789-6

9. Amano Y, Takai D, Ohishi N, Shinozaki-Ushiku A, Fukayama M, Akahane M, et al. Successful treatment of mediastinal unicentric Castleman's disease using video-assisted thoracoscopic surgery with preoperative embolization. *Case Rep Med*. (2013) 2013:354507. doi: 10.1155/2013/354507

10. Safford SD, Lagoo AS, Mahaffey SA. Preoperative embolization as an adjunct to the operative management of mediastinal castleman disease. *J Pediatr Surg*. (2003) 38(9):E21–3. doi: 10.1016/S0022-3468(03)00421-4

frontiers | Frontiers in Cardiovascular Medicine

TYPE Opinion
PUBLISHED 15 September 2023
DOI 10.3389/fcvm.2023.1259620

Check for updates

OPEN ACCESS

EDITED BY
Luigi Tarantini,
IRCCS Local Health Authority of Reggio Emilia, Italy

REVIEWED BY
Alessandra Ghigo,
University of Turin, Italy

*CORRESPONDENCE
Carlo Gabriele Tocchetti
✉ cgtocchetti@gmail.com

†These authors share first authorship

RECEIVED 16 July 2023
ACCEPTED 04 September 2023
PUBLISHED 15 September 2023

CITATION
Iengo M, Topa E, Cuomo A, Marone G, Poto R, Varricchi G, Cristinziano L, Galdiero MR, Ferrara AL, Loffredo S, Formisano L, Troiani T, Mercurio V and Tocchetti CG (2023) The broad spectrum of cardiotoxicities from immunotherapies.
Front. Cardiovasc. Med. 10:1259620.
doi: 10.3389/fcvm.2023.1259620

COPYRIGHT
© 2023 Iengo, Topa, Cuomo, Marone, Poto, Varricchi, Cristinziano, Galdiero, Ferrara, Loffredo, Formisano, Troiani, Mercurio and Tocchetti. This is an open-access article distributed under the terms of the Creative Commons Attribution License (CC BY). The use, distribution or reproduction in other forums is permitted, provided the original author(s) and the copyright owner(s) are credited and that the original publication in this journal is cited, in accordance with accepted academic practice. No use, distribution or reproduction is permitted which does not comply with these terms.

The broad spectrum of cardiotoxicities from immunotherapies

Martina Iengo[1†], Ester Topa[1†], Alessandra Cuomo[1], Giancarlo Marone[2], Remo Poto[1,3], Gilda Varricchi[1,3,4,5], Leonardo Cristinziano[1], Maria Rosaria Galdiero[1,3,4], Anne Lise Ferrara[1,5], Stefania Loffredo[1,3,4,5], Luigi Formisano[6,7], Teresa Troiani[8], Valentina Mercurio[1,7,9] and Carlo Gabriele Tocchetti[1,4,7,9]*

[1]Department of Translational Medical Sciences, Federico II University, Naples, Italy, [2]Department of Pharmacy, Moscati Hospital Pharmacy, Aversa, Italy, [3]World Allergy Organization (WAO) Center of Excellence, Naples, Italy, [4]Center for Basic and Clinical Immunology Research (CISI), Federico II University, Naples, Italy, [5]Institute of Experimental Endocrinology and Oncology (IEOS), National Research Council, Naples, Italy, [6]Department of Medicine and Surgery, Federico II University, Naples, Italy, [7]Interdepartmental Center of Clinical and Translational Sciences (CIRCET), Federico II University, Naples, Italy, [8]Medical Oncology, Department of Precision Medicine, University of Campania Luigi Vanvitelli, Naples, Italy, [9]Interdepartmental Hypertension Research Center (CIRIAPA), Federico II University, Naples, Italy

KEYWORDS

cardio-oncology, immunotherapy, cardiotoxicity, detection, management

Introduction

Cancer immunotherapies have revolutionized antineoplastic treatments. CTLA-4, PD-1, and PD-L1 are crucial regulators of the immune response and play a central role in the maintenance of self-tolerance (1). Monoclonal antibodies directed against CTLA-4, PD-1, and PD-L1 block these immune checkpoints and unleash anti-tumor immunity, leading to tumor cell death through cytolytic molecules. Unfortunately, these immune checkpoint inhibitors (ICIs) either alone or in combination, can lead to imbalances in immunologic tolerance resulting in a broad spectrum of immune-related adverse events (irAEs) (2–4). The true incidence of cardiac irAEs due to ICIs is unknown; current estimates suggest less than 1% of patients (2).

The largest case series of 122 subjects with ICI-associated myocarditis had early symptoms (median of 30 days after initial exposure to ICI), and up to 50% died (5). Late cardiovascular (CV) events (>90 days) are not well characterized but usually show higher risk of non-inflammatory heart failure (HF), progressive atherosclerosis, hypertension, and mortality rates (6). Other CV toxicities described during ICI therapy are MI, Atrio-Ventricular (AV) block, supraventricular and ventricular arrhythmias, sudden death, Takotsubo-like syndrome (TTS), hypercholesterolaemia, pericarditis, pericardial effusion, ischaemic stroke, and VTE (7, 8). Conditions related with high baseline ICI-related CV toxicity risk include dual ICI therapy (e.g., ipilimumab and nivolumab), combination ICI therapy with other cardiotoxic therapies, and patients with ICI-related non-CV events or prior cancer therapy-related cardiac dysfunction (CTRCD) or cardiovascular disease (CVD) (**Figure 1**) (9–11).

More recently, engineered T cells with chimeric antigen receptors (CAR-T cells) are being used for acute lymphocytic leukaemia and aggressive B-cell lymphomas (12). There is a growing recognition of the association between CAR-T therapy and cancer therapy-

10.3389/fcvm.2023.1259620

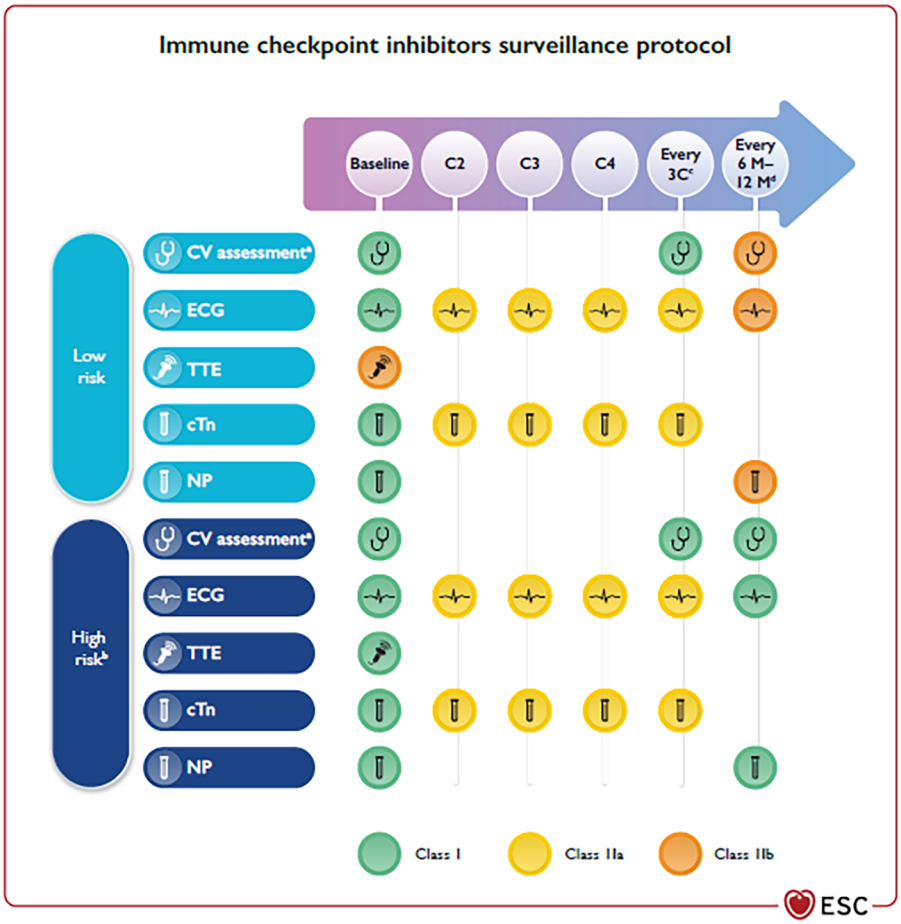

FIGURE 1
(reproduced with permission from 9). Cardiovascular surveillance in patients treated with immune checkpoint inhibitors. BNP, B-type natriuretic peptide; BP, blood pressure; C, chemotherapy cycle; cTn, cardiac troponin; CV, cardiovascular; CVD, cardiovascular disease; CTRCD, cancer therapy-related cardiac dysfunction; CTR-CVT, cancer therapy-related cardiovascular toxicity; CVRF, cardiovascular risk factors; ECG, electrocardiogram; HbA1c, glycated haemoglobin; ICI, immune checkpoint inhibitors; M, months; NP, natriuretic peptides (including BNP and NT-proBNP); NT-proBNP, N-terminal pro-B-type natriuretic peptide; TTE, transthoracic echocardiography; AF, atrial fibrillation. [a]Including physical examination, BP, lipid profile, and HbA1c. [b]Dual ICI, combination ICI-cardiotoxic therapy, ICI-related non-CV events, prior CTRCD or CVD. [c]Every three cycles until completion of therapy to detect subclinical ICI-related CV toxicity. [d]In patients who require long-term (>12 months) ICI treatment.

related cardiovascular toxicity (CTR-CVT), including left ventricular dysfunction (LVD), HF, cardiac arrhythmias, pericardial effusion, TTS, and cardiac arrest (13–18). The majority of the described CV toxicities have been shown to be associated with cytokine release syndrome (CRS) (12, 19), a systemic inflammatory response due to the widespread release of cytokines.

Broad spectrum of cardiotoxicities

Acknowledging the revolutionary advances in cancer obtained with immunotherapies (and unfortunately also their toxicities), it is noteworthy that this Special Issue contains several papers that describe toxicities from immunologic therapies. Su and Colleagues (20) report a case of head and neck squamous cell carcinoma treated with pembrolizumab, a humanized monoclonal IgG4 antibody, that binds to programmed death receptor-1 (PD-1) and blocks its interaction with programmed death ligand-1 (PD-L1). The authors report that pembrolizumab-induced atrioventricular block complicated by myocarditis, successfully treated with glucocorticoids within 24 h after initial symptoms. Although left ventricular ejection fraction (LVEF) was normal, speckle tracking echocardiography revealed a slightly decreased left ventricular global longitudinal strain (GLS).

Nivolumab (anti-PD-1) and Pembrolizumab were probably the cause of immune related pericarditis, pericardial effusion and tamponade in two cases described by Chye and coworkers, who underlined the importance of monitoring and follow-up of selected patients for rechallenge with ICI after full recovery from immune-related pericardial disease (21) The two patients were suffering from advanced non-small cell lung cancer (NSCLC).

Sintilimab is a humanized monoclonal IgG4 antibody approved for the treatment of hematological cancers and several advanced solid tumors in China. Lin and collaborators presented a sintilimab related decrease of LVEF at echocardiography (22) in

a patient with advanced lung adenocarcinoma. Echocardiography showed severely impaired heart function with a LVEF of 35% on admission. A significant improvement of LVEF to 52% was noted several days after treatment with methylprednisolone and immunoglobulin. However, cardiac magnetic resonance (CMR) showed extensive myocardium fibrosis. Therefore, longer follow-up is warranted to determine whether myocardial fibrosis can fully regress and to observe the long-term prognosis of the patient (Lin et al.).

Toripalimab is a PD-1 monoclonal antibody approved by the National Medical Products Administration of China in 2018. A phase I trial registered with U.S. National Library of Medicine (identifier NCT03474640) is underway in the USA. Luo and coworkers describe a case presenting with polymyositis, myocarditis, and myasthenia gravis after toripalimab used for treatment of metastatic thymoma. Toripalimab can provoke diffuse inflammation of myocytes from striated muscles to Myocardial cells, worsened in case of thymic epithelial tumors, because of the alteration of T cells immune tolerance (23).

Another manuscript shows acute pericardial effusion with cardiac tamponade with CAR-T therapy (24) in a patient with diffuse large B-cell lymphoma. Specifically, the Authors evidenced that a rapid introduction of immunosuppressive therapy can reduce the need of pericardiocentesis.

Discussion

The conditions and toxicities described in the above-mentioned papers of this Special Issue are well recognized by the first ESC 2022 Cardio-Oncology Guidelines, which recommend that all patients on ICI treatment should have an ECG and troponin assay at baseline (**Figure 1**) (9). In addition, high-risk patients should undergo trans-thoracic echocardiography (TTE). Once started on therapy, ECG, cTn, and NP should be checked (9). In high-risk patients, and in those with high baseline cTn levels, TTE monitoring may be considered. Subjects with new ECG abnormalities, biomarker changes, or cardiac symptoms at any time, need to be promptly evaluated by cardio-oncologists, including a TTE for the assessment of LVEF and GLS, and CMR if myocarditis is suspected (9). Cessation of ICI treatment is recommended with ICI-associated myocarditis; patients should be admitted to hospital with continuous ECG monitoring. CV complications should be treated as per specific ESC Guidelines (HF (25), tachyarrhythmias (26), AV block (27, 28) or pericardial effusion (29)). Methylprednisolone 500–1,000 mg i.v. once daily for the first 3–5 days should be started as soon as possible (9).

Baseline CV evaluation including ECG, NP, and cTn is also recommended in patients who are to be treated with CAR-T. Baseline TTE should also be considered, especially in subjects with pre-existing cardiovascular risk factors (CVRF) and CVD. CRS should be suspected if a subject develops fever, with or without tachypnoea, tachycardia, hypotension, hypoxia, and/or other end-organ dysfunction hours to days after treatment. A high index of suspicion is necessary to diagnose CRS and to distinguish it from other conditions that occur in these settings (infections, HF, drug reactions, and PE) (9). A rise in cTn can be frequently observed in subjects with CRS and is linked to a higher risk for subsequent CV events (13). CAR-T was associated with tachyarrhythmias (atrial fibrillation, AF, the most common, followed by ventricular arrhythmias), cardiomyopathy, and pleural and pericardial diseases (16). Globally, the fatality rate of CV and pulmonary adverse events was 30.9% (30). Early cardiac evaluation in patients with cTn increase should include NP, ECG, and TTE (9). When suspected, a resting 12-lead ECG, continuous ECG monitoring, TTE, and cTn and NP are recommended. In severe cases admission to ICU is recommended because of the risk of malignant cardiac arrhythmias, circulatory collapse, and multiorgan system failure (9).

The above-mentioned surveillance strategies of acute fulminant myocarditis brought to the recognition of more subtle forms of heart inflammation, spanning from smouldering myocarditis to asymptomatic rises in serum troponin I (31–34). Hence, chronic (lasting for >12 weeks after ICI discontinuation) irAEs are increasingly detected, and can affect up to 40% of patients (35). Chronic irAEs are mostly endocrine or rheumatological, but may also affect other organs and systems (31). Extrapolating from non-ICI-associated myocarditis, it may be expected that subjects who recover from ICI-associated myocarditis would also experience chronic consequences related to residual cardiomyopathy as a long-term sequela (36). This brings to a fundamental long-term implication of irAEs, whether patients who experienced some benefit but also severe toxicities from ICI treatment should be rechallenged upon resolution of the irAE. Retrospective studies suggest that recurrence of irAEs occurs in approximately 25%–50% of patients rechallenged with ICIs (31, 37, 38). De-escalation of therapy (such as de-escalation from combination anti-PD-1–anti-CTLA4 antibodies to anti-PD-1 monotherapy) appears to be linked with a lower risk of irAE recurrence (18% in one series, 38). Determining which patients bring the highest risk of recurrent irAEs is challenging; colitis, pneumonitis and hepatitis seem to recur more frequently on rechallenge than do other irAEs, with older age also being associated with irAE recurrence (37). It is not fully understood whether a longer delay between discontinuation and rechallenge would also decrease the risk of recurrent toxicities. When evaluating the reintroduction of an ICI-based therapy, both the type and severity of the irAE, as well as the clinical need for rechallenge should be taken into account. If rechallenge is undertaken, patients should undergo close clinical and/or laboratory monitoring should in order to assess for possible irAE recurrence (31).

Author contributions

MI: Writing – original draft. ET: Writing – original draft. AC: Writing – original draft. GM: Writing – original draft. RP: Writing – original draft. GV: Writing – review & editing. LC: Writing – original draft. MG: Writing – review & editing. AF: Writing – original draft. SL: Writing – review & editing. LF: Writing – review & editing. TT: Writing – review & editing. VM: Writing –

review & editing. CT: Conceptualization, Funding acquisition, Investigation, Methodology, Project administration, Supervision, Validation, Visualization, Writing – review & editing.

Funding

The author(s) declare financial support was received for the research, authorship, and/or publication of this article.

CGT is supported by two grants from the Italian Ministry of Health (PNRR-MAD-2022-12376632 and RF-2016-02362988). ALF and LF are supported by a grant from the Italian Ministry of Health (PNRR-MAD-2022-12376632). LF is supported by MFAG 21505 – 2018 grant. MRG is supported by MIUR-PRIN 2017M8YMR8_005 and AIRC under MFAG 2020 (grant number 25123).

Conflict of interest

CT reports honoraria or consultation fees from VivaLyfe, Univers Formazione, Solaris, Summeet, Astra Zeneca, Myocardial Solutions; funding from Amgen and MSD, outside the submitted work; and is listed as an inventor of two patents related to HF. GV reports research support from AstraZeneca International. LF reports support from Lilly. TT reports support from Novartis BMS, Pfizer, Amgen, Merck, Sanofi, MSD.

The remaining authors declare that the research was conducted in the absence of any commercial or financial relationships that could be construed as a potential conflict of interest.

The reviewer AG declared past co-authorships with the authors CGT, VM, AC, GV, and, RM to the handling editor.

The author(s) declared that they were an editorial board member of Frontiers, at the time of submission. This had no impact on the peer review process and the final decision.

Publisher's note

All claims expressed in this article are solely those of the authors and do not necessarily represent those of their affiliated organizations, or those of the publisher, the editors and the reviewers. Any product that may be evaluated in this article, or claim that may be made by its manufacturer, is not guaranteed or endorsed by the publisher.

References

1. Hu JR, Florido R, Lipson EJ, Naidoo J, Ardehali R, Tocchetti CG, et al. Cardiovascular toxicities associated with immune checkpoint inhibitors. *Cardiovasc Res.* (2019) 115(5):854–68. doi: 10.1093/cvr/cvz026

2. Johnson DB, Balko JM, Compton ML, Chalkias S, Gorham J, Xu Y, et al. Fulminant myocarditis with combination immune checkpoint blockade. *N Engl J Med.* (2016) 375(18):1749–55. doi: 10.1056/nejmoa1609214

3. Tocchetti CG, Ameri P, de Boer RA, D'Alessandra Y, Russo M, Sorriento D, et al. Cardiac dysfunction in cancer patients: beyond direct cardiomyocyte damage of anticancer drugs: novel cardio-oncology insights from the joint 2019 meeting of the ESC working groups of myocardial function and cellular biology of the heart. *Cardiovasc Res.* (2020) 116(11):1820–34. doi: 10.1093/cvr/cvaa222

4. Zimmer L, Goldinger SM, Hofmann L, Loquai C, Ugurel S, Thomas I, et al. Neurological, respiratory, musculoskeletal, cardiac and ocular side-effects of anti-PD-1 therapy. *Eur J Cancer.* (2016) 60:210–25. doi: 10.1016/j.ejca.2016.02.024

5. Salem JE, Manouchehri A, Moey M, Lebrun-Vignes B, Bastarache L, Pariente A, et al. Spectrum of cardiovascular toxicities of immune checkpoint inhibitors: a pharmacovigilance study. *Lancet Oncol.* (2018) 19(12):1579–89. doi: 10.1016/S1470-2045(18)30608-9

6. Dolladille C, Ederhy S, Allouche S, Dupas Q, Gervais R, Madelaine J, et al. Late cardiac adverse events in patients with cancer treated with immune checkpoint inhibitors. *J Immunother Cancer.* (2020) 8(1):e000261. doi: 10.1136/jitc-2019-000261

7. D'Souza M, Nielsen D, Svane IM, Iversen K, Rasmussen PV, Madelaire C, et al. The risk of cardiac events in patients receiving immune checkpoint inhibitors: a nationwide Danish study. *Eur Heart J.* (2021) 42(16):1621–31. doi: 10.1093/eurheartj/ehaa884

8. Kondapalli L, Neilan TG. Immune checkpoint inhibitors and cardiovascular events among patients with cancer: a window into the critical role of the immune system in cardiovascular biology. *Eur Heart J.* (2021) 42(48):4978–80. doi: 10.1093/eurheartj/ehab708

9. Lyon AR, López-Fernández T, Couch LS, Asteggiano R, Aznar MC, Bergler-Klein J, et al. 2022 ESC guidelines on cardio-oncology developed in collaboration with the European hematology association (EHA), the European society for therapeutic radiology and oncology (ESTRO) and the international cardio-oncology society (IC-OS). *Eur Heart J Cardiovasc Imaging.* (2022) 23(10):e333–465. doi: 10.1093/ehjci/jeac106

10. Zamami Y, Niimura T, Okada N, Koyama T, Fukushima K, Izawa-Ishizawa Y, et al. Factors associated with immune checkpoint inhibitor-related myocarditis. *JAMA Oncol.* (2019) 5(11):1635–7. doi: 10.1001/jamaoncol.2019.3113

11. Zhang L, Reynolds KL, Lyon AR, Palaskas N, Neilan TG. The evolving immunotherapy landscape and the epidemiology, diagnosis, and management of cardiotoxicity: JACC: cardioOncology primer. *Cardio Oncol.* (2021) 3(1):35–47. doi: 10.1016/j.jaccao.2020.11.012

12. Frey N, Porter D. Cytokine release syndrome with chimeric antigen receptor T cell therapy. *Biol Blood Marrow Transplant.* (2019) 25(4):e123–7. doi: 10.1016/j.bbmt.2018.12.756

13. Alvi RM, Frigault MJ, Fradley MG, Jain MD, Mahmood SS, Awadalla M, et al. Cardiovascular events among adults treated with chimeric antigen receptor T-cells (CAR-T). *J Am Coll Cardiol.* (2019) 74(25):3099–108. doi: 10.1016/j.jacc.2019.10.038

14. Fradley MG, Damrongwatanasuk R, Chandrasekhar S, Alomar M, Kip KE, Sarnaik AA. Cardiovascular toxicity and mortality associated with adoptive cell therapy and tumor-infiltrating lymphocytes for advanced stage melanoma. *J Immunother.* (2021) 44(2):86–9. doi: 10.1097/CJI.0000000000000341

15. Ghosh AK, Chen DH, Guha A, Mackenzie S, Walker JM, Roddie C. CAR T cell therapy–related cardiovascular outcomes and management: systemic disease or direct cardiotoxicity? *Cardio Oncol.* (2020) 2(1):97–109. doi: 10.1016/j.jaccao.2020.02.011

16. Goldman A, Maor E, Bomze D, Liu JE, Herrmann J, Fein J, et al. Adverse cardiovascular and pulmonary events associated with chimeric antigen receptor T-cell therapy. *J Am Coll Cardiol.* (2021) 78(18):1800–13. doi: 10.1016/j.jacc.2021.08.044

17. Lefebvre B, Kang Y, Smith AM, Frey NV, Carver JR, Scherrer-Crosbie M. Cardiovascular effects of CAR T cell therapy: a retrospective study. *Cardio Oncol.* (2020) 2(2):193–203. doi: 10.1016/j.jaccao.2020.04.012

18. Salem JE, Ederhy S, Lebrun-Vignes B, Moslehi JJ. Cardiac events associated with chimeric antigen receptor T-cells (CAR-T): a VigiBase perspective. *J Am Coll Cardiol.* (2020) 75(19):2521–3. doi: 10.1016/j.jacc.2020.02.070

19. Ganatra S, Redd R, Hayek SS, Parikh R, Azam T, Yanik GA, et al. Chimeric antigen receptor T-cell therapy-associated cardiomyopathy in patients with refractory or relapsed non-hodgkin lymphoma. *Circulation.* (2020) 142(17):1687–90. doi: 10.1161/CIRCULATIONAHA.120.048100

20. Su L, Liu C, Wu W, Cui Y, Wu M, Chen H. Successful therapy for myocarditis concomitant with complete heart block after pembrolizumab treatment for head and neck squamous cell carcinoma: A Case Report with literature review. *Front Cardiovasc Med.* (2022) 9:898756. doi: 10.3389/fcvm.2022.898756

21. Chye AM, Nordman IIC, Sverdlov AL. Successful immune checkpoint inhibitor rechallenge after immune-related pericarditis: Clinical case series. *Front Cardiovasc Med.* (2022) 9:964324. doi: 10.3389/fcvm.2022.964324

22. Lin Y, Yuan X, Chen L. Immune myocarditis related to sintilimab treatment in a patient with advanced lung adenocarcinoma: A case report. *Front Cardiovasc Med.* (2022) 9:955527. doi: 10.3389/fcvm.2022.955527

23. Luo YB, Tang W, Zeng Q, Duan W, Li S, Yang X, et al. Case Report: The neuromusclar triad of immune checkpoint inhibitors: a Case Report of myositis, myocarditis, and myasthenia gravis overlap following toripalimab treatment. *Front Cardiovasc Med*. (2021) 8:714460. doi: 10.3389/fcvm.2021.714460

24. Moriyama S, Fukata M, Yokoyama T, Ueno S, Nunomura T, Mori Y, et al. Case Report: Cardiac tamponade in association with cytokine release syndrome following CAR-T cell therapy. *Front Cardiovasc Med*. (2022) 9:848091. doi: 10.3389/fcvm.2022.848091

25. McDonagh TA, Metra M, Adamo M, Baumbach A, Böhm M, Burri H, et al. 2021 ESC guidelines for the diagnosis and treatment of acute and chronic heart failure. *Eur Heart J*. (2021) 42(36):3599–726. doi: 10.1093/eurheartj/ehab368

26. Brugada J, Katritsis DG, Arbelo E, Arribas F, Bax JJ, Blomstrom-Lundqvist C, et al. 2019 ESC guidelines for themanagement of patients with supraventricular tachycardia. *Eur Heart J*. (2020) 41(5):655–720. doi: 10.1093/eurheartj/ehz467

27. Glikson M, Nielsen JC, Kronborg MB, Michowitz Y, Auricchio A, Barbash IM, et al. 2021 ESC guidelines on cardiac pacing and cardiac resynchronization therapy. *Eur Heart J*. (2021) 42(35):3427–520. doi: 10.1093/eurheartj/ehab364

28. Zeppenfeld K, Tfelt-Hansen J, De Riva M, Winkel BG, Behr ER, Blom NA, et al. 2022 ESC guidelines for the management of patients with ventricular arrhythmias and the prevention of sudden cardiac death. *Eur Heart J*. (2022) 43(40):3997–4126. doi: 10.1093/eurheartj/ehac262

29. Adler Y, Charron P, Imazio M, Badano L, Barón-Esquivias G, Bogaert J, et al. 2015 ESC guidelines for the diagnosis and management of pericardial diseases. *Eur Heart J*. (2015) 36(42):2921–64. doi: 10.1093/eurheartj/ehv318

30. Ragoonanan D, Khazal SJ, Abdel-Azim H, McCall D, Cuglievan B, Tambaro FP, et al. Diagnosis, grading and management of toxicities from immunotherapies in children, adolescents and young adults with cancer. *Nat Rev Clin Oncol*. (2021) 18(7):435–53. doi: 10.1038/s41571-021-00474-4

31. Johnson DB, Nebhan CA, Moslehi JJ, Balko JM. Immune-checkpoint inhibitors: long-term implications of toxicity. *Nat Rev Clin Oncol*. (2022) 19(4):254–67. doi: 10.1038/s41571-022-00600-w

32. Bonaca MP, Olenchock BA, Salem J-E, Wiviott SD, Ederhy S, Cohen A, et al. Myocarditis in the setting of cancer therapeutics: proposed case definitions for emerging clinical syndromes in cardio-oncology. *Circulation*. (2019) 140(2):80–91. doi: 10.1161/CIRCULATIONAHA.118.034497

33. Norwood TG, Westbrook BC, Johnson DB, Litovsky SH, Terry NL, McKee SB, et al. Smoldering myocarditis following immune checkpoint blockade. *J Immunother Cancer*. (2017) 5(1):91. doi: 10.1186/s40425-017-0296-4

34. Waliany S, Neal JW, Reddy S, Wakelee H, Shah SA, Srinivas S, et al. Myocarditis surveillance with high-sensitivity troponin I during cancer treatment with immune checkpoint inhibitors. *Cardio Oncol*. (2021) 3(1):137–9. doi: 10.1016/j.jaccao.2021.01.004

35. Patrinely JR Jr, Johnson R, Lawless AR, Bhave P, Sawyers A, Dimitrova M, et al. Chronic immune-related adverse events following adjuvant anti-PD-1 therapy for high-risk resected melanoma. *JAMA Oncol*. (2021) 7(5):744–8. doi: 10.1001/jamaoncol.2021.0051

36. Ammirati E, Frigerio M, Adler ED, Basso C, Birnie DH, Brambatti M, et al. Management of acute myocarditis and chronic inflammatory cardiomyopathy: an expert consensus document. *Circ Heart Fail*. (2020) 13(11):e007405. doi: 10.1161/CIRCHEARTFAILURE.120.007405

37. Dolladille C, Ederhy S, Sassier M, Cautela J, Thuny F, Cohen AA, et al. Immune checkpoint inhibitor rechallenge after immune-related adverse events in patients with cancer. *JAMA Oncol*. (2020) 6(6):865–71. doi: 10.1001/jamaoncol.2020.0726

38. Santini FC, Rizvi H, Plodkowski AJ, Ni A, Lacouture ME, Gambarin-Gelwan M, et al. Safety of resuming anti-PD-1 in patients with immune-related adverse events (irAEs) during combined anti-CTLA-4 and anti-PD1 in metastatic melanoma. *Ann Oncol*. (2018) 29(1):250–5. doi: 10.1093/annonc/mdx642

39. Pollack MH, Betof A, Dearden H, Rapazzo K, Valentine I, Brohl AS, et al. Safety of resuming anti-PD-1 in patients with immune-related adverse events (irAEs) during combined anti-CTLA-4 and anti-PD1 in metastatic melanoma. *Ann Oncol*. (2018) 29(1):250–5. doi: 10.1093/annonc/mdx642

Frontiers in Cardiovascular Medicine

Innovations and improvements in cardiovascular treatment and practice

Focuses on research that challenges the status quo of cardiovascular care, or facilitates the translation of advances into new therapies and diagnostic tools.

Discover the latest Research Topics

See more →

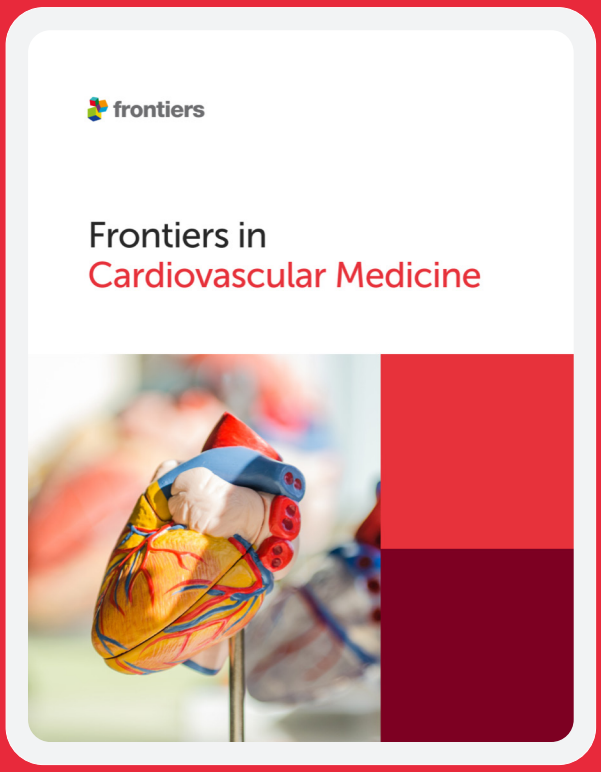

Frontiers

Avenue du Tribunal-Fédéral 34
1005 Lausanne, Switzerland
frontiersin.org

Contact us

+41 (0)21 510 17 00
frontiersin.org/about/contact